2008 Annual Report

“Emergence of Adaptive Motor Function through Interaction among the Body, Brain and Environment - A Constructive Approach to the Understanding of Mobiligence - ”

Project Leader: Hajime Asama (The University of Tokyo)

March, 2009

Area No. 454
Under Grant-in-Aid for Scientific Research
on Priority Area
from the Japanese Ministry of Education, Culture, Sports, Science and Technology

Academic Year from 2005 to 2009

2008 Annual Report

“Emergence of Adaptive Motor Function through Interaction among the Body, Brain and Environment - A Constructive Approach to the Understanding of Mobiligence - ”

Project Leader: Hajime Asama (The University of Tokyo)

March, 2009

Area No. 454
Under Grant-in-Aid for Scientific Research
on Priority Area
from the Japanese Ministry of Education, Culture, Sports, Science and Technology

Academic Year from 2005 to 2009

Contents

Introduction of the *Mobiligence* Program

Emergence of Adaptive Motor Function through Interaction among the Body, Brain and Environment - A Constructive Approach to the Understanding of *Mobiligence* -

Hajime Asama
Director of the *Mobiligence* Program
The University of Tokyo

1. Introduction

The *Mobiligence* program is a five-year program started from 2005[1], which was accepted as a program of Scientific Research on Priority Areas of Grant-in-Aid Scientific Research sponsored by the Japanese Ministry of Education, Culture, Sports, Science and Technology (MEXT). Currently, 40 subjects are being carried out (11 subjects for planned research group, 20 subjects for applied research group, and one subject for operation). The first and second international symposium on *mobiligence* was held in December of 2005[2] and July of 2007[3] respectively, in which we discussed mainly the research results obtained in the *mobiligence* program and the research plans.

In this report, the outline of the program including the objective and the organization is presented. The concept of *mobiligence*, which can be defined as intelligence for generating adaptive motor function which emerges by mobility, and the approach to understand the mechanisms that generate the adaptive behaviors are explained, and a part of the current research outcome is introduced.

2. Program Objective of the *Mobiligence* Program

All the life forms such as humans, animals, and insects, can behave adaptively even in diverse and complex environment in various types of behaviors, such as locomotive behaviors in the form of swimming, flying, and walking, manipulation behaviors such as reaching, capturing, and grasping by using hands and arms, social behaviors to the other subjects, etc. The intelligent sensory-motor functions to generate adaptive behaviors are considered most essential and indispensable for them to survive.

It is known that such function for adaptive behaviors is disturbed in patients with neurological disorders. Parkinson disease is a typical example of such disorders on adaptive motor function, and autism or depression can also be considered as a disorder on social adaptive function. Recently, due to aging or environmental change of society, the population of people who are suffering from these diseases is growing rapidly, and it has become urgent to cope with this problem. However, the mechanisms of generating such adaptive behaviors are not thoroughly known yet. With this background, the objective of the program is set to understand the mechanism that generates the adaptive behaviors.

3. Concept of *Mobiligence*

Such an adaptive function is considered to emerge by the active mobility of the cognitive subject. In the subject is in the stationary state, there is not so much interaction among body, brain, and environment. However, once the subject starts to move, the signals to move the body are transmitted from the brain to the body. As the result of the motion of the body, the physical interaction between the body and environment are made, and due to the interaction, the information from environment is input to the brain directly or fed back to the brain via the body as somatosensory signals. Namely, the motion of the subject accelerates the interaction among body, brain, and environment, which is considered essential for the subject to behave adaptively. Based on the consideration, we built up a working hypothesis that the adaptive function emerge from the interaction among the body, brain and environment, which requires actions or motions of the subject, and defined *mobiligence* as intelligence for generating adaptive motor function which emerges by mobility.

The information which can be acquired by mobility can be listed as follows:

1. Diverse information by changing location of the subject
2. Dynamical information by motion
3. Experience accumulated in the subject

There is difference in the concept of the conventional robotics and *mobiligence*, which are compared in fig. 1.

In the conventional robotics, which discusses intelligence for mobility, the first step is perception and cognition. The subject recognizes the environment based on the information perceived by sensors, then plans the motions by applying knowledge which should be implemented in advance, and behaves by controlling the actuators, namely, moves the body, which causes the interaction to the environment, as shown in fig. 1-(a). On the other hand, in the concept of *mobiligence* which investigates intelligence emerged by mobility, the first step is behavior as shown in fig. 1-(b). The perception is initiated by the behavior. As a result of the behavior, rich information can be acquired by the interaction between the body and the environment, and input to the brain. The information can be accumulated in the brain, and utilized concurrently to generate adaptive behaviors in real time. The combination of the two concepts derives the tight and continuous loop between cognition and

behavior or among body, brain, and environment, which is considered quite important to understand the intelligence of living systems that behave adaptively or to design the intelligence of the autonomous artificial robots.

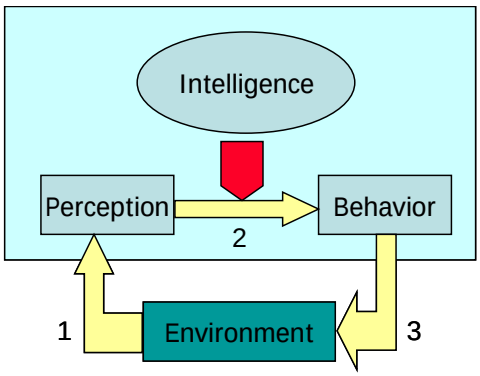

(a) Concept of conventional robotics

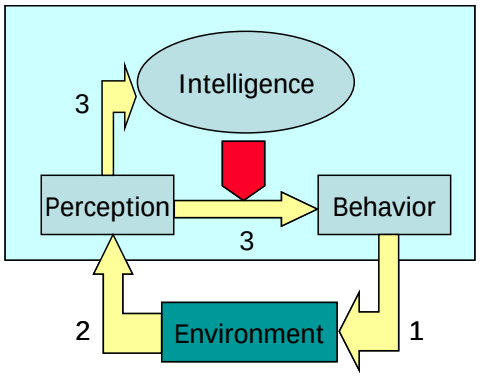

(b) Concept of Mobiligence

Fig. 1. Comparison of the concepts of conventional robotics and *mobiligence*

4. Collaborative Research of Biology and Engineering

It is typical to use animal experiments in the conventional biological research. By this analytical approach, large amount of knowledge and findings have been obtained so far, such as the structure and function of various neural networks, neural transmitters/modulators, etc. However, there is also limitation in this conventional analytical approach based on animal experiments. The animal experiments are usually made with animals in the fixed conditions, and they can reveal only the simple brain function in a stationary state. For the *mobiligence* research, where it is required to investigate the complex function which emerges through interaction among brain, body, and environment in a dynamic state, the mechanisms that generate adaptive behaviors are hardly able to be elucidated only by the conventional analytical approach.

To overcome the problem, a new approach was introduced to tackle this problem in the *mobiligence* program. Based on the knowledge of biological research, such as neurophysiology, neuroethology, clinical medicine, cognitive science, microbiology, physiological models are to be derived. To these biological models, dynamic system modeling technology is applied to derive biological system models, which can be implemented on simulators or actual robot systems. By constructing the adaptive function on the simulators or actual robots based on the models, we can verify the models, evaluate the effects of the various parameters, and introduce new hypotheses to the biological scientists. In the *mobiligence* program, this approach is called a constructive approach by collaborative research of biology and engineering.

In the *mobiligence* program, three methodologies for collaborative research of biology and engineering have been proposed and in practice so far:

A. System Biomechanics

By neurophysiological research, we can derive models for nervous systems. On the other hand, by engineering and anthropological research, musculoskeletal models can be derived. By integrating the nervous system models and musculoskeletal models, dynamic system models can be introduced, and can be implemented on simulators or actual robots. As the results of experiments using the simulators or actual robots, we can verify the models or hypotheses, produce new possible hypotheses on the mechanisms which generates the adaptive behaviors, and feed them back to the biological scientists, or provide robotic scientists with design principle to realize adaptive artificial systems. This methodology for collaborative research is shown in figure 2-(a).

B. Synthetic Neuroethology

From neurophysiological research, enormous independent pieces of physiological knowledge are acquired in diverse levels from chemical reaction to cellular and behavioral (individual or social) level. Multiple pieces of the knowledge in multi-levels can be synthesized by technologies in robotics or engineering to derive dynamic system models, which represent the hypotheses of the mechanisms that generate adaptive behaviors. The behavior or performance of the models which should be implemented on simulators or actual robots can be compared with the behavior or performance of the actual living systems, and the models or hypotheses can be verified in ethological manner. This methodology for collaborative research is shown in figure 2-(b).

C. Brain-Machine Integrated System

Biology can provide us with biological body components, such as brains, limbs, organs etc. Engineering or robotics can provide us with mechanical body parts, such as sensor devices, actuators, processors, etc. By integrate these body parts, we can construct brain-machine integrated systems, which can also be called *cyborg*. By analyzing the behavior and function of the integrated system, we can investigate the function of the biological

components or systems, and can provide robotics scientists with the methodologies to realize artificial systems that can behave adaptively. This methodology for collaborative research is shown in figure 2-(c).

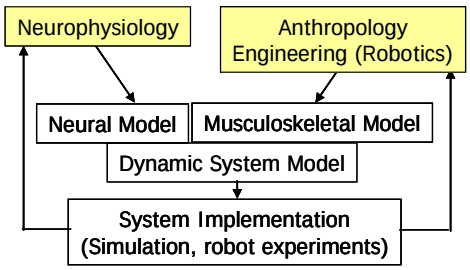

(a) System Biomechanics

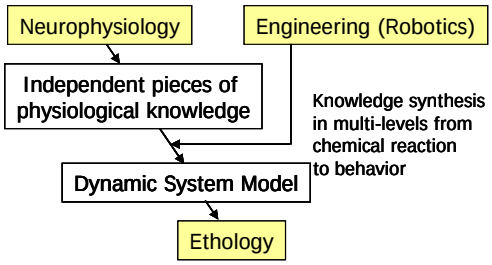

(b) Synthetic Neuroethology

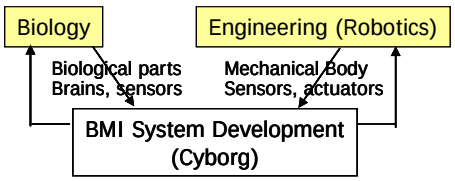

(c) Brain-Machine Integrated System

Fig. 2. Methodologies for collaborative research of biology and engineering

5. Research Subjects and Groups

In the *mobiligence* program, we focused on the following three aspects to investigate the mechanisms that generate adaptive behaviors, and organized three research groups for each aspect:

Group A (Adaptation to the environmental change)

Investigation of mechanism to generate the information adaptively based on cognition of the environmental change

Group B (Physical Adaptation)

Investigation of mechanism to control the motion of the body adaptively according to the environment

Group C (Social Adaptation)

Investigation of mechanism to select the behaviors adaptively to the other subjects and the society

The researchers in these three groups conduct their respective research on specific subjects, such as cognition, learning, motion generation, and body control, focusing on specific life forms, such as humans, animals, and insects in individual level and social level. However, another important target of this program is to clarify the universal and common principle underlying the mechanism of *mobiligence*, and establish the design principle for adaptive systems. We organized the fourth group to understand the common principle:

Group D (Common Principle)

Investigation of common principle on dynamics in generating adaptive behaviors

6. Recent Research Outcome

In the *mobiligence* program, many collaborative research subjects have been initiated, and various valuable research outcome have been obtained so far by the intensive specific research in the group A, B, and C. In parallel to the specific research, some common structures and features have been extracted as the common principle on the structural dynamics or information creation of the mechanisms for adaptation. Followings are a part of the recent research outcome:

In the research of group A, which focuses on cognition to the environmental change, adaptation to dynamic environments in reaching movements as shown in Fig. 3 has been investigated by Ito, et. al[4]. Two types of force fields, namely velocity-dependent force field for internal model adaptation and divergent force field for impedance adaptation, have tested, in which the subject should learn to reach the targets. It was proved that the subjects can learn to generate the optimal hand force patterns in both cases, and can adapt even when that force field was changed in the middle of the motion. As a result of the experiments, it can be assumed that the impedance and internal-model controls can be programmed in a feedforward manner in adaptation to the contexts of dynamic environments. This function is called anticipatory adaptation. Yano, et. al. investigated real time adaptation mechanisms on a feedforward structure, especially mechanisms on generating real time constraints as *Minashi* (abductive) information, taking an example of olfactory computation in slug brain[5]. As a result of experiments, it was found that the initial signals to move the body, which is considered to correspond to

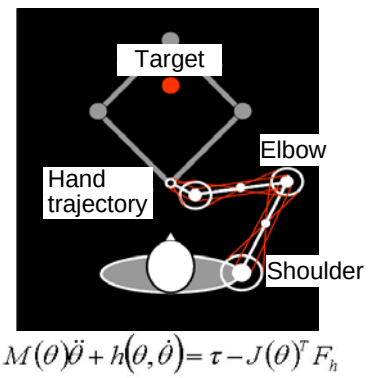

Fig. 3. Reaching behavior

emotional behavior, precedes about 40-60[msec] to the memory accessing signal flow, which is considered to correspond to interpretation of the perceived information.

In the research of group B, which focuses on physical adaptation, namely adaptation in the individual level, emergence and control in adaptive locomotion under changing environment has been investigated by system biomechanics approach, namely systematic approach based on neural and musculoskeletal models. Takakusaki, et. al. investigated function of basal ganglia, cerebral cortex, brainstem, spinal cord, thalamus, limbic system, and cerebellum on locomotion, and discovered a detail structure on the signal flow in the neural networks[6]. Especially, Nakajima, et. al. investigated how cortical motor areas (M1, SMA, PMd) in primates contribute to the gait control by using Japanese (Macaque) monkey[7]. As a result of experiments on recording the firing pattern of cortical neurons during locomotion of macaque monkeys on moving treadmill, it was found that the discharge frequency drastically increased when the monkey converted its locomotor pattern from quadrupedal to bipedal. A block diagram on the locomotion was derived as a physiological model for locomotion, where it was also indicated that the postural control system is activated earlier than the movement control system, and sends feedforward signals to movement control system. On the other hand, Tsuchiya, Ogihara, et. al. developed a musculoskeletal model of Japanese monkey based on anatomical data and CT data by anthropological and engineering approaches[8], which is shown in fig. 4. It is expected to integrate the physiological model and the musculoskeletal model to enable simulation on dynamic locomotion of Japanese monkey by constructive approach for further investigation in near future.

In the research of group C, which focuses on social adaptation, namely adaptation in the social (multi-agent) level, cognition of other agents and selection of adaptive behaviors to other agents or society have been investigated by synthetic neuroethology approach. Aonuma, et. al. focused on fighting behaviors between male crickets as shown in fig. 5. As a result of experimental investigation, new physiological knowledge were obtained such that aggressiveness increases by inhibition of NO/cGMP cascade, OA level in the brain decreases by NO and fighting behavior, and the decrease level depends on the results of fights (win or lose)[9]. Fujiki, Asama, et. al. implemented a mathematical model of the neural mechanism by reaction diffusion equations[10], and Ashikaga and Ota, et. al. implemented a mathematical model of interaction between male crickets by finite automaton[11]. By integrating both models, the behavior selection of male cricket can be simulated from chemical reaction level in the brain to the social interaction level. As a result of simulation results, it was suggested that the different types of the society emerge depending on the density, namely the number of individuals per unit area. Figure 6 is the simulation results on aggressiveness of male crickets depending on the density. The graph shows that all the individuals become aggressive in low density (large field size) condition, while only small number of individuals become aggressive in high density (small field size) condition. It is pointed out in the ethological research that this simulation results fits the behaviors of actual make crickets very well, and from these consideration, the models we derived are proved to be reasonable.

In the research of group C, Kanzaki, et. al. have investigated the adaptive brain function of silk moth by brain-machine integrated system approach[12]. A mobile robot integrated with insect brain, which is shown in fig. 7 has been developed, where the robot can be controlled

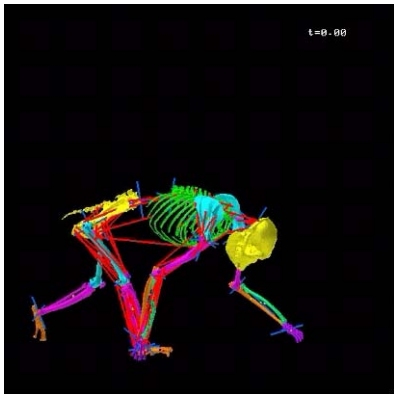

Fig. 4. Musculoskeletal model of Japanese monkey

Fig. 5. Fighting behavior of male crickets

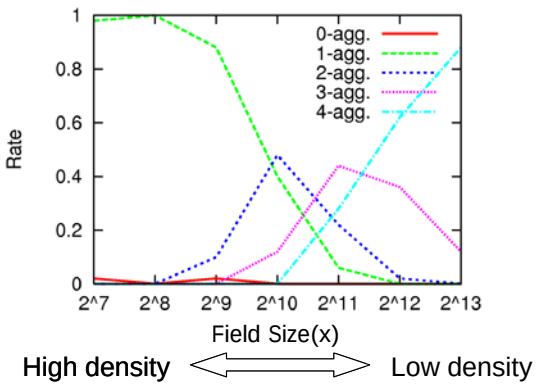

Fig. 6. Simulation results on aggressiveness depending on density

by the embedded insect brain signals. As a result of pheromone source localization experiments with this robot, it was found that the silk moth brain can successfully control the robot body and localize the pheromone source even if the control gain of the right wheel and the left wheel were differentiated. This result verified the plasticity of the silk moth brain. By changing body dynamics, control gain or other parameters of the body, it is expected to investigate the adaptive function of the silk moth brain and neural systems more in detail.

In the research of group D, which focuses on common principle, balance dynamics in mechanical properties and information processing in control has been investigated from the viewpoint of physical constraints, because it is considered that the balance between mechanical embodiment and neural control system is considered very important for realization of adaptive function. The main concern of this group is what kind of balance mechanisms exist in living systems, and how this should be designed in autonomous artificial systems. Osuka, et. al. have focused on adaptive function in passive dynamic walking, and discovered a stabilization mechanism by implicit feedback structure in body dynamics[13]. Ishiguro, et. al. have developed a modular robot system "Slimebot" based on collective behavioral approach as mimesis of slime mould (amoeba), which is shown in fig. 8[14]. The robot system employs a fully decentralized control by exploiting embodied coupled nonlinear oscillators, and passivity by s spontaneous inter-modular connectivity control mechanism. As a result of actual robot experiments, it was discovered that a certain passivity can significantly increases its adaptiveness.

From the research outcome obtained so far in the *mobiligenc*e program, there found a common characteristic in the mechanisms that generate adaptive behaviors as shown in fig. 9. The perceived sensory information is dimensionally compressed in environment cognition. However, the information which can be obtained is not always sufficient to generate motion. In such situation, *Minashi* (abductive) information is generated in real time, which is equivalent to constraints for control of redundant degrees of freedom in the physical body. The motion is not always generated or switched in a reactive manner (such as impedance adaptation). The internal models learned and formed in the brain through experience are quite essential to generate adaptive behaviors effectively according to the context. The motion generation complexity depends much on the embodiment. If the body is well organized, the active mechanism to control the body can be simplified.

7. Expected Impact of the *Mobiligence* Program

By the *mobiligence* program, various types of mechanisms that generate adaptive behaviors in various living systems, such as humans, animals, and insects, are expected to be elucidated as well as common principle. Although the main contribution will be brought to biological field, huge impacts to other fields are expected as well. To the medical field, the results of our research will contribute to the discovery of a method to improve motor impairment and develop rehabilitation systems. To the engineering field, the results of our research will contribute to the derivation of the design principles of artificial intelligence systems. By the *mobiligence* program, the new research discipline is expected to be explored, and a new research organization that integrates biology and engineering is expected to be established, where new programs or curriculums are implemented to foster young engineering scientists and biologists to conduct collaborative and interdisciplinary research between biological and engineering research, respectively.

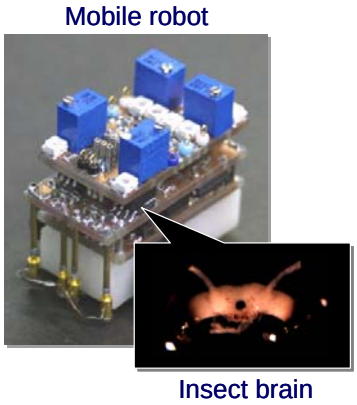

Fig. 7. Mobile robot integrated with silk moth brain

Fig. 8. Modular robot system "Slimebot"

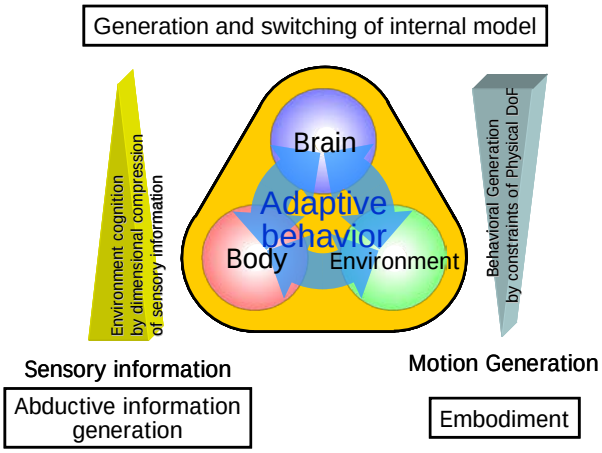

Junior Academy of the *mobiligence* program was established, and tutorials, workshops, and seminars have been carried out for the young researchers in *mobiligence* program. The academy is now working on editing the terminology related to the *mobiligence* research.

8. Conclusion

The *mobiligence* program was introduced, which started from 2005 in Japan as a five-year program of Scientific Research on Priority Areas of Grant-in-Aid Scientific Research sponsored by the Japanese Ministry of Education, Culture, Sports, Science and Technology (MEXT). The concept of *mobiligence* was explained, which can be defined as intelligence for generating adaptive motor function which emerges by mobility. The objective of the program and the constructive approach by collaborative research of biology and engineering for the *mobiligence* research were mentioned as well as the subjects and organization of the program. Finally, a part of the current research outcome was introduced.

The outline of the program including the objective and the organization was presented. The concept of *mobiligence*, which can be defined as intelligence for generating adaptive motor function which emerges by mobility, and the approach to understand the mechanisms that generate the adaptive behaviors were explained. A part of the recent research outcome was introduced.

Detail and other research outcome was presented in AMAM ’08 (Fourth International Symposium on Adaptive Motion of Animals and Machines), in the workshop of IROS ’08 (2008 IEEE/RSJ International Conference on Intelligent Robots and Systems), DARS ’08 (2008 International Symposium on Distributed Autonomous Robotic Systems), and will be presented in Mobiligence ’09 (Third International Symposium on Mobiligence), which will be held in Awaji, Japan, in Nov., 2009.

Acknowledgment

The concept of Mobiligence and the organization of the Mobiligence program were established through the discussion with Prof. Kazuo Tsuchiya (Doshisha Univ.), Prof. Koji Ito (Tokyo Inst. of Tech.), Prof. Masafumi Yano (Tohoku Univ.), Prof. Kaoru Takakusaki (Asahikawa Medical Col.), Prof. Ryohei Kanzaki (The Univ. of Tokyo), Prof. Jun Ota (The Univ. of Tokyo), Akio Ishiguro (Tohoku Univ.), Hitoshi Aonuma (Hokkaido Univ.), Koichi Osuka (Kobe Univ.), and the other planned research group members. I thank all these members for their valuable contributions. I thank also all the reviewers of the mobiligence program for valuable comments on program organization and research directions, who are Prof. Sten Grillner (Karolinska Inst.), Prof. Avis H. Cohen (Univ. of Maryland), Prof. Rolf Pfeifer (Univ. of Zurich), Prof. Shigemi Mori (National Inst. for Physiological Sci.), Prof. Ryoji Suzuki (Kanazawa Inst. of Tech.), and Prof. Shinzo Kitamura (Kobe Univ.).

References

[1] http://www.arai.pe.u-tokyo.ac.jp/mobiligence/index_e.html

[2] Proceedings of 1st international symposium on mobiligence, Sapporo, Japan, Dec. 2005.

[3] Proceedings of 2nd international symposium on mobiligence, Awaji, Japan, July 2007.

[4] K. Ito, M. Doi, T. Kondo: “Feed-Forward Adaptation to a Varying Dynamic Environment During Reaching Movements”, Journal of Robotics and Mechatronics, vol. 19, no. 4, pp. 474-481, 2007.

[5] Y. Makino, H. Makinae, T. Obara, H. Miura and M. Yano: “Observations of Olfactory Information Flows within Brain of the Terrestrial Slug, Inciralia fruhstorferi”, Proc. of 2006 International Joint Conference on Neural Networks , pp. 7605-7612, 2006.

[6] K. Takakusaki, “Forebrain control of locomotor behaviors”, Brain Res. Rev., vol. 57, pp. 192-198, 2008.

[7] K. Nakajima, F. Mori, C. Takasu, M. Mori, K. Matsuyama and S. Mori: "Biomechanical constraints in hindlimb joints during the quadrupedal versus bipedal locomotion of M-fuscata", Progress in Brain Research, vol. 143, pp.183-190, 2004.

[8] N. Ogihara: “Synthetic Study of Quadrupedal/Bipedal Locomotion in the Japanese Monkey”, Fourth International Symposium on Adaptive Motion of Animals and Machines (AMAM ’08), Cleveland, USA, June 2008.

[9] H. Aonuma and K. Niwa: “Nitric Oxide Regulates the Levels of cGMP Accumulation in the Cricket Brain”, Acta Biologica Hungarica, vol. 55, pp. 65-70, 2004.

[10] T. Fujiki, K. Kawabata, H. Asama: "Adaptive Action Selection of Body Expansion Behavior in Multi-Robot System using Communication", Journal of Advanced Computational Intelligence and Intelligent Informatics, vol.11, no.2, pp. 142-148, 2007.

[11] M. Ashikaga, M. Kikuchi, T. Hiraguchi, M. Sakura, H. Aonuma and J. Ota: “Foraging Task of Multiple Mobile Robots in a Dynamic Environments Using Adaptive Behaviors in Crickets”, Journal of Robotics and Mechatronics, vol. 19, no. 4, pp. 466-473, 2007.

[12] S. Emoto, N. Ando, H. Takahashi, R. Kanzaki: “Insect-Controlled Robot –Evaluation of Adaptation Ability–“, Journal of Robotics and Mechatronics, vol. 19, no. 4, pp. 436-443, 2007.

[13] M. Iribe, K. Osuka: “Design of the Passive Dynamic Walking Robot by Applying its Dynamic Properties”, Journal of Robotics and Mechatronics, vol. 19, no. 4, pp. 402-408, 2007.

[14] A. Ishiguro, M. Shimizu, T. Kawakatsu: “A Modular Robot That Exhibits Amoebic Locomotion”, Robotics and Autonomous Systems, vol. 54, pp. 641-650, 2006.

Steering Committee Report on the *Mobiligence* Program

Hajime Asama*[1], Kazuo Tsuchiya*[2], Koji Ito*[3], Masafumi Yano*[4], Koichi Osuka*[5], Kaoru Takakusaki*[6], Ryohei Kanzaki*[1], Hitoshi Aonuma*[7], Akio Ishiguro*[8], Jun Ota*[1]

*[1]The University of Tokyo, *[2]Kyoto University, *[3]Tokyo Institute of Technology, *[4]Tohoku University, *[5]Kobe University, *[6]Asahikawa Medical College, *[7]Hokkaido University, *[8]Nagoya University

1. Missions

The missions of the steering committee are as follows:

- Establish goals for the *Mobiligence* Program
- Plan and coordinate research
- Evaluate research progress and consult
- Determine the procedures for the public invitation of proposed topics
- Organize symposia and research meetings for the purpose of developing related research
- Plan publicity of research results
- Encourage close collaboration among researchers, i.e., information exchange, mutual understanding, and communication
- Plan international research and lectures by members of academic societies and announce interim and ex post evaluations of progress
- Devise programs to encourage fused collaboration among biologists and engineering scientists and establish a research center and research organization

2. Summary of 2008 Activities of the Steering Committee

Research subjects were coordinated in each group to facilitate the fused collaboration between biologists and engineering scientists, which characterizes this program, and joint group meetings and open group meetings were organized to promote the inter-group collaboration effectively. Following events were organized; a domestic open workshop, a domestic open symposium, a domestic closed symposium for internal review, an open symposium, a closed symposium, tutorials, workshops, and seminars. The internal review to the research activities of each project was performed. Many organized sessions are organized at international and domestic conferences. A new brochure to introduce the *mobiligence* program was publicized, which includes new projects accepted from 2008. The homepage for publicity and the database to record the activities in the program were maintained and updated. Research report was edited and published. Junior Academy of the *mobiligence* program was established and their activities were supported.

3. Steering Committee Meetings and WGs

The following Steering Committee meetings and its WG meetings were held:

- 1st Steering Committee Meeting
  Oct. 21st, 2008, 12:20-13:40
  at RCAST in Komaba Campus of the University of Tokyo
- 2nd Steering Committee Meeting
  Mar. 4th, 2008, 12:00-13:30
  at Hotel Taikanso in Matsushima
- 1st WG Meeting
  Oct. 13th,2008, 20:00-22:00
  at Awaji Yumebutai International Conference Center
- 2nd WG Meeting
  Mar. 4th, 2009, 13:30-15:30
  at Hongo Campus of the Univ. of Tokyo

4. Publication Committee Meetings and WGs

- 1st Publication Committee Meeting
  Feb. 24th, 2009, 15:00-17:30
  at Hongo Campus of the Univ. of Tokyo
- 1th WG Meeting
  Apr. 26th, 2008, 10:00-12:30
  at Hongo Campus of the Univ. of Tokyo
- 2nd WG Meeting
  May 26th, 2008, 14:00-16:00
  at Hongo Campus of the Univ. of Tokyo
- 3rd WG Meeting
  July 23rd, 2008, 10:00-12:00
  at RIES in Hokkaido Univ.
- 4th WG Meeting
  Aug. 29th, 2008, 10:00-12:30
  at Hongo Campus of the Univ. of Tokyo
- 5th WG Meeting
  Oct. 13th, 2008, 13:00-18:00,
  Oct. 14th, 2008, 9:00-12:00
  at Awaji Yumebutai International Conference Center

5. Organization of Symposia

5.1 Domestic Open Workshop

The domestic open workshop on New Trend in Mobiligence was held in the University of Tokyo on Apr. 25, 2008. Eight presentations on the research topics and plans, which were accepted from 2008, were made by each project leader followed by an introductory speech by the program director. Total number of participants was 57.

5.2 Domestic Open Symposium

The 2nd domestic open symposium on Mobiligence tackled by integrative approach of living and artificial systems was held RCAST in Komaba Campus of the University of Tokyo on Oct. 21th, 2008. At first, the objective of the project was introduced by the director of the project. Prof. Atsuko Takamatsu, Prof. Daisuke Kurabayashi, Prof. Yoshio Sakurai, Prof. Takafumi Suzuki, Dr. Naotaka Fujii, Prof. Hiroshi Yokoi, and Dr. Tetsunari Inamura presented their recent research outcome as representatives of Group A, B, C, and D. Dr.

Hideaki Koizumi (Hitachi Ltd.) gave an invited talk entitled “Mobiligence and Brain Functional Imaging”. Total number of participants was 80. The presentations and discussions were recorded and edited, which can be seen at [1].

5.3 Domestic Closed Symposium

A symposium for internal evaluation was held in Hotel Taikanso in Matsushima, Japan, on Mar. 2-4, 2009. Oral and poster presentations on the research progress in 2008 of all the subjects in the *Mobiligence* program were made by each research leader and members. They were all reviewed by the review committee members and the steering committee members. Dr. Hidenori Kimura (RIKEN) gave an invited talk. A night session was also organized by Junior Academy of the *Mobiligence* program. Total number of participants was 118.

6. Publicity

6.1 Organization of Special Issues of Journals

A special issue on Mobiligence was organized in the Advanced Robotics, International Journal, Vol.22, No.15, in which 5 papers were included. It was published in December of 2008.

6.2 Session Organization in Conferences

Sessions on Mobiligence were organized in the following international conferences:

- IEEE International Conference on Robotics and Systems (IROS2008), Nice, September (2008), workshop, 12 papers
- The 9th International Symposium on Distributed Autonomous Systems, Tsukuba, November. (2008), organized session, 3 papers
- SICE Annual Conference 2008, Chofu, organized session, 5 papers
- Fourth International Symposium on Adaptive Motion of Animals and Machines, Ohio, 2008, 11 papers

Sessions on Mobiligence were organized in the following international conferences:

- 2008 JSME Robotics and Mechatronics Division Annual Conference, Nagano, Japan, June 2008, 11 posters
- 2008 RSJ Annual Conference, Kobe, Japan, Sep. 2008, 4 papers
- SICE System Integration Division Annual Conference, Gifu, Japan, Dec. 2008, 8 papers
- SICE Decentralized Autonomous Systems Symposium, Tottori, Japan, Jan. 2009, 6 papers

6.3 Other Publicity Activities

The home page of the *Mobiligence* program was updated accordingly[1], database on research achievements[2] and activity records was maintained and presented on the web site.

The brochure of the *Mobiligence* program including subscribed research groups was published and distributed as well as call for proposals for the new subscribed research. The report, this volume, on the research activities of the *Mobiligence* program in 2007 was edited and published. The concept of the Mobiligence and current research outcome were broadcasted through an internet TV program, Netrush[3].

7. Organization of Tutorials and Seminars

To accelerate the fused collaboration and to foster young scientists and students who are doing *mobiligence* research, one workshop, one tutorial, and two seminars were arranged and held:

- Tutorial “From Cognition to Emergence of Motion and Behaviors”
  June 5th, 2008, 10:00-16:00 in 2008 JSME Robotics and Mechatronics Division Annual Conference, Nagano, Japan
- Workshop “Research on Adaptive Behaviors of Super-individuals by collaboration of robotics and biology ”
  Aug. 23rd, 2008, 12:00-14:30 in 2008 Annual Meeting for the Society of Evolutionary Studies, Tokyo, Japan
- Tohoku University RIEC workshop on “Motion control of Animals”
  Dec. 19th, 2008, 13:30-17:50 at RIEC, Tohoku University, Sendai, Japan
- Mobiligence seminar on “Ecological and Physiological Studies about Sociality of Insects”
  Jan. 12th, 2009, 13:00-17:00 at School of Human Science and Environment of University of Hyogo, Himeji, Japan

8. Review

In the domestic closed symposium mentioned above, steering committee members in addition to the three domestic reviewers who are Prof. Shinzo Kitamura (Kobe University), Prof. Shigemi Mori (National Institute for Physiological Sciences), and Prof. Ryoji Suzuki (Kanazawa Institute of Technology), reviewed the research progress and grade of collaboration between biology and robotics. The review results are fed back to the research leaders toward successful research execution in future.

9. Activity Support for Junior Academy of the *Mobiligence* program

The steering committee supported the following activities of the Junior Academy of the *mobiligence* program:

- Joint Meeting of Junior Academy of the Mobiligence project & JSCPB 2008
- Creating Glossaries (ongoing project)

References

[1]http://www.robot.t.u-tokyo.ac.jp/mobiligence/index_e.html
[2]http://www.robot.t.u-tokyo.ac.jp/mobiligence/act/index.html
[3]http://www.netrush.jp/science_top.htm

Group A: Adaptation to Environment
Annual Report

Koji ITO
Tokyo Institute of Technology, Japan

I. RESEARCH PROJECT

The aim of Group A is 1) to clarify the brain-nervous mechanisms for creating appropriate hypothesis to constrain behaviors based on the accumulated experiences under unpredictable environments, 2) to analyze the motor control mechanisms producing adaptive behaviors corresponding to dynamical environments, and 3) to construct mathematical models of the adaptive sensorimotor coordination mechanism composed of the brain, body and environment. To perform the above aim, the group hangs the following research subjects.

Research subject A01: Modeling of intra-cerebral mechanisms for motor adaptation to unknown environments.

In order to generate adaptive behaviors in various environments, it is necessary to integrate the redundant degrees of freedom in the brain, body and environment based on changing contexts of situation. The research subject aims to elucidate the brain mechanisms of the sensorimotor coordination corresponding to the dynamic environments by the experimental, constructive and systematic approaches.

Research subject A02: Anticipatory adaptation of sensorimotor coordination.

To understand the sensorimotor coordination mechanism for environment cognition and appropriate motor adaptation, behavioral contexts and intrinsic factors (e.g., anticipation, intention, attention, affection, etc.) of subjects should be considered. The research subject aims to clarify the relationship between these intrinsic factors and sensorimotor adaptation under unfamiliar environments.

II. RESEARCH GROUPS

Group A consists of two planned and seven subscribed research groups. The research groups are reformed in this year based on the middle evaluation.

- Planned Research Groups

1) A01-01 Koji Ito (Tokyo Institute of Technology)

   Modeling of intra-cerebral mechanisms for motor adaptation to unknown environments

2) A01-02 Toshiyuki Kondo (Tokyo University of Agriculture and Technology)

   Anticipatory adaptation of sensorimotor coordination

- Subscribed Research Groups

3) A01-11 Toshiya Matsushima (Hokkaido University)

   Optimal motor investments: algorism of instantaneous gain rate computation

4) A01-12 Yasuharu Koike (Tokyo Institute of Technology)

   Learning and control model in consideration of inconsistency between vision and tactile

5) A01-13 Tadashi Ogawa (Kyoto University)

   The role of the prefrontal cortex in advancing cognitive adaptation under unknown circumstances

6) A01-14 Yasuji Sawada (Tohoku Institute of Technology)

   Study of optimization for the cooperative adaptation between motions of two persons by mutual tracking experiments

7) A01-15 Akira Murata (Kinki University, School of Medicine)

   Brain mechanisms for recognition of bodily self and others

8) A01-16 Tetsunari Inamura (National Institute of Informatics)

   Multimodal sensorimotor integration and behavior induction between other and self based on mirror neuron model

9) A01-17 Jun Tani (Brain Science Institute, RIKEN)

   Understanding "Organic Compositionality" in cognitive brain mechanisms

III. RESEARCH RESULTS

A. Cooperative mechanisms of internal model control and impedance control in force fields (A01-01 Koji Ito)

When performing the arm movements under the dynamical environments (ex. object manipulation and tool-use), CNS needs to combine internal model control and impedance control in a feedforward manner. Recently, in the area of human motor control and computational neuroscience, many experiments which investigate motor adaptation of human arm movements under the dynamical environments have been performed. However, the mechanism which CNS combines two control strategies (internal model control and impedance control) has not been clarified.

In our research, we setup the mixed force field '$V+P$' by composing the velocity-dependent force field 'V' and position-dependent force field 'P' and analyze motor adaptation of arm movements under the force field. The experimental results show that the subjects did not learn the internal model of $V+P$ accurately and they compensated for the load by using impedance control.

B. Simultaneous learning of conflicting visuomotor rotations (A01-02 Toshiyuki Kondo)

Humans can learn appropriate internal models for compensating two unfamiliar and conflicting visuomotor transformations simultaneously. We used a rotated computer mouse paradigm in where the cursor's motion is rotated clockwise or counterclockwise by 90 degrees. We focused on the effect of successive experiences during simultaneous learning of conflicting tasks. It had been reported that simultaneous learning of two opposing force fields with a random order was significantly better than training with alternating order, even with the same total number of experiences. We assumed that this was because the alternating training schedule gave no chance to retry the same rotational transformation successively. To test this assumption, we compared three training conditions: alternating every trial, alternating every two trials, and changed at random.

Experimental results suggested that providing the chance of successive trials to the subjects had a small positive effect on simultaneous learning compared with alternating every trial. However, the subjects trained under the random condition still showed a significant advantage in comparison with those trained under the other conditions.

IV. MEETING AND OTHERS

- 1st. Meeting of Group A (Joint meeting with Group D).

  Date: Jul. 23 13:00-17:30, 2008.

  Place: Lecture hall 2, Research Institute for Electronic Science, Hokkaido University.

  Attendee: 30 members of group A and D.

  Presenters:

  1) Prof. T.Matsushima, Hokkaido University,

  2) Prof. Y.Koike, Tokyo Institute of Technology,

  3) Prof. Y.Sawada, Tohoku Institute of Technology.

- Full Day Workshop on the 2008 IEEE/RSJ International Conference on Intelligent Robots and Systems (IROS2008).

  Date: Sep. 26, 9:00 – 18:00, 2008.

  Place: Acropolis Convention Center, Nice, France.

  Attendee: 50.

  Contents: The workshop, proposed by Dr. Kondo and I consisted of 12 invited talks from the ***Mobiligence*** project, and 6 papers of them was related with the group A.

  1) Internal Model Control and Impedance Control in Human Voluntary Movements (Prof. K.Ito, Tokyo Institute of Technology),

  2) Effect of Successive Trials during Simultaneous

  Learning of Conflicting Visuomotor Transformation Tasks (Dr. T.Kondo, Tokyo University of Agriculture and Technology),

  3) Bimanual interactions in humans and humanoid robots (Prof. P.G.Morasso, University of Genova),

  4) Specificity of Motor Learning (Prof. D.Ostry, McGill University),

  5) Preliminary investigation on how humans perform a video controlled pointing task under visual and kinesthetic combined disturbances (Dr. L.Masia, Italian Institute of Technology),

  6) Adaptation of Reaching Movements to Assistive Forces (Dr. V.Novakovic, University of Genova).

- 2nd. meeting of Group A.

  Date: Nov. 6, 13:00 – Nov. 7, 15:30, 2008.

  Place: Meeting room 1208, National Center of Sciences Bldg. National Institute of Informatics.

  Attendee: 30 members of group A.

  Contents: Reports on 13 research results by group A members, two invited talks, and the general discussions on adaptation to environments.

  Invited speakers:

  1) Dr. Hiroyuki Nakahara, Brain Science Institute, RIKEN

  2) Dr. Jun Izawa, Johns Hopkins University

- Organized Session on "Mobiligence" in Division Symposium of System Integration (SICE- SI2008).

  Date: Dec. 5, 10:00 – 12:00, 2008.

  Place: Nagaragawa Convention Center, Gifu.

  Attendee: 40.

  Number of Presentation: 8.

Modeling of Intra-cerebral Mechanisms for Motor Adaptation to Unknown Environments

Koji Ito, Manabu Gouko (Tokyo Institute of Technology)

I. INTRODUCTION

Even if we situated in unfamiliar environments with any kinematic and/or dynamic transformations, we can adapt to them in several trials-and-errors. As a consequence of the motor learning process, we can acquire a neural representation of the relation between motor command and the movement, i.e. *internal model* of the environment. However, it is still open question to explain the neural representation, i.e. how the internal models are represented in our brains.

For instance, we can instantly manipulate any objects by using any tools even though there are a number of combinational possibilities. In addition, we can select an appropriate internal model according to the contextual information of the environments. It implies that there is an intrinsic prediction and motor adaptation mechanisms in the motor area of our brain.

The A01-01 group aims to clarify the intra-cerebral mechanisms to recognize unfamiliar environments and to generate suitable motor commands, through psychophysical experiments and computational modeling of human movement learning. Additionally, a rehabilitation system for the stroke patient based on the motor adaptation mechanisms is also developed.

In this report we explain about our recent research topics entitled "Cooperative mechanisms of internal model control and impedance control in force fields", "Coordinate frame for bilateral movement" and "Electroencephalogram (EEG) and Functional Electrical Stimulation (FES) system for Rehabilitation of Stroke Patient."

II. COOPERATIVE MECHANISMS OF INTERNAL MODEL CONTROL AND IMPEDANCE CONTROL IN FORCE FIELDS

When performing the arm movements under the dynamical environments (ex. object manipulation and tool-use), CNS needs to combine internal model control and impedance control in a feedforward manner. Recently, in the area of human motor control and computational neuroscience, many experiments which investigate motor adaptation of human arm movements under the dynamical environments have been performed [1]. However, the cooperative mechanism of two control strategies (internal model control and impedance control) has not been clarified.

In this study, we investigated the cooperative mechanism, through psychophysical experiments of human arm-reaching movement learning. In this research, we set up the mixed force field 'V+P' by composing the velocity-dependent force field 'V' and position-dependent force field 'P', then we analyzed motor adaptation of arm movements under the force field. The experimental results show that the subjects did not learn the internal model of V+P accurately and they compensated for the load by using impedance control [2].

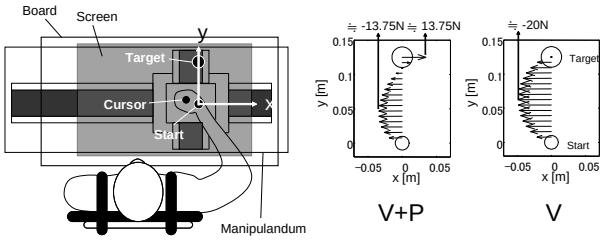

(a) Robotic manipulandum (b) Force fields

Fig.1 Experimental setup

A. Experimental protocol

15 students participated in the experiment. As a experimental apparatus, we used the robotic manipulandum (x and y axes) shown in Fig.1(a). The subject was seated on the chair in front of the manipulandum and learned point-to-point arm movements to eight targets located radially from a central start position. The movement distance was 0.125 m. The subject was instructed to reach the target from the initial position within 300±50 ms. The hand, start and target positions were indicated on the screen. During the reaching movements, visual feedback of the hand position was suppressed and the entire hand pass was shown after the movements were terminated.

During the movement, the external load called 'force field' was applied to the hands by the manipulandum. In the experiment, we used two types of force fields as follows.

$$\mathbf{V}: \quad \mathbf{F} = \mathbf{B}\dot{\mathbf{x}}, \tag{1}$$

$$\mathbf{V+P}: \quad \mathbf{F} = \mathbf{B}\dot{\mathbf{x}} + \mathbf{K}\mathbf{x}, \tag{2}$$

where $\mathbf{x}$ ($\mathbf{x}=[x,y]^T$) is the hand position, and $\mathbf{F}$ ($\mathbf{F}=[F_x,F_y]^T$) is the load acting in the horizontal plane. The coefficient matrix B equals [0 -25;25 0], and K equals [0 110;-110 0]. The equation (1) represents the velocity-dependent force field 'V' which applied the load to the hand proportional to the hand velocity. The equation (2) represents the mixed force field 'V+P' which applied the load proportional to the hand velocity and hand position. Fig.1(b) shows load patterns of two force fields. V+P generates a force to the left depending on the hand velocity, and then the direction of the force is reversed to the right depending on the hand position.

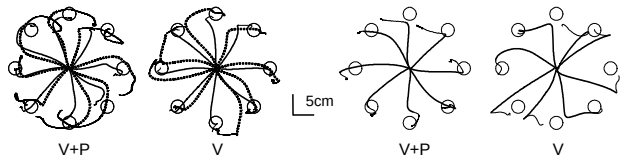

(a) Before and after learning (b) After effects

Fig.2 Hand trajectories

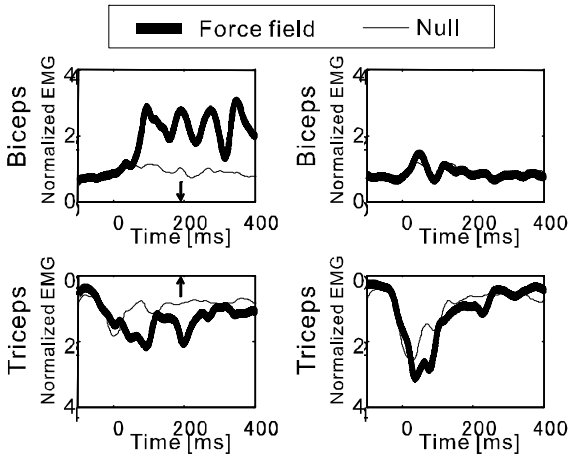

(a) V+P (b) V

Fig.3 EMG

The subjects were randomly assigned to one of two groups. First, all subjects practiced point-to-point arm movement during which no force field was applied (200 trials). This condition is called the 'null field'. After the practice, group 1 learned the V+P (200 trials) and group 2 learned the V (200 trials).

B. Experimental result

Fig.2(a) shows the hand trajectories of typical subjects in each field. The dotted lines represent the trajectories before learning. The solid lines represent the trajectories after learning. Before learning, the subjects were not able to perform straight reaching movements in both fields. After learning, the trajectories of the both subjects became straighter, which indicates the subjects learned to compensate for the load. However, the V+P trajectories were not perfectly straight. Fig.2(b) shows after effect movements of typical subjects in each field, i.e. the movements when the force field was unexpectedly removed in selected trials after learning. The after effect movements in V were curved to the opposite direction of the loads generated by V, which indicates that the subject learned to produce the opposing force necessary to predictively compensate for the force field. In contrast, the after effect movements in V+P deviated very little. This indicates that the subject did not learn to produce the opposing force accurately (i.e., the subject did not learn the internal model control in V+P accurately). Fig.3 shows the EMG patterns (the biceps and the triceps) of typical subjects after learning. The movement direction is 'y-axis' direction. In V+P, the biceps and the triceps were co-contracted during the movement. Thus, the subject compensated for the load by increasing the arm impedance (using impedance control) instead of using the internal model control. There were significant differences in all data shown above.

Our results suggest that humans use impedance control when internal models become inaccurate because of the complexity of the external dynamics. This finding infers that the CNS has a mechanism that combines two control strategies adaptively in various environments and that the two control strategies are complementary.

In the future, we plan to construct an accurate computational model of the musculo-skeletal system that describes arm behaviors in dynamical environments.

III. COORDINATE FRAME FOR BILATERAL MOVEMENT

Human's hemispheres control mainly contralateral body parts and human can coordinate bilateral ones skillfully. Previous studies on bilateral movements reported some evidences. 1: Connection between right and left control systems, for example callous corpus, occurs interhemispheric interaction. 2: Interhemispheric interaction contributes coordination stability. 3: Coordination stability depends on bilateral symmetry (i.e. muscle activation pattern). Generally, symmetric movements are more stable than asymmetric movements. In our study, we focused on interhemispheric interaction which is important to make the coordination stability. The aim of our study is to reveal the coordinate frame related to control the interhemispheric interaction. In particular, we assume two coordinate frames. First, intrinsic coordinate frame discussed in many previous studies such as the coordinate frame represents internal information, for example, muscle activation. Second, external coordinate frame which represents movement direction in external space, for example. That is, we investigated whether or not symmetrical property of bilateral movement and congruence of bilateral movement directions are related to interhemispheric interaction.

A. Experimental protocol

Fig.4 shows the experimental conditions to examine the 2 coordinate frames. We asked subjects to perform cyclical flexion-extension movements by using bilateral index fingers. At a certain point during the movements, subjects needed to modify the amplitude of right index finger voluntarily with left finger amplitude constant. Then, we could observe unconscious change of left finger amplitude when subjects modified the right finger amplitude. We defined the unconscious response of left finger as effect of interaction between right and left finger control systems and we estimated the effect in each condition.

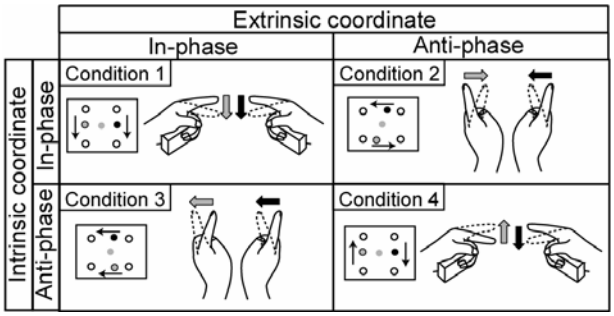

Fig.4 Relative phase between both fingers based on intrinsic and extrinsic coordinate frame.

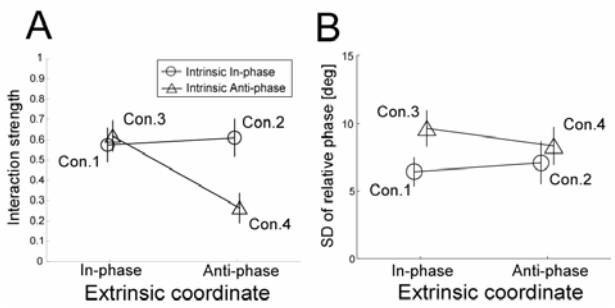

Fig.5 Interaction strength (A) and coordination stability (B) of each condition.

B. *Experimental result*

Fig. 5A shows interaction strength in each condition. Each value shows amount of amplitude change of left finger normalized by that of right finger. Left finger movement is affected strongly except for condition 4. Previous studies suggested that symmetrical movement works strong coupling between bilateral control systems and also from our study symmetrical movements could observe the strong interaction. Therefore, our results in condition 1 and 2 agree with the previous contentions. However, despite the asymmetric movement in condition 3, the interaction is very strong as well as condition 1 and 2. These results indicate that in addition to intrinsic coordinate frame, extrinsic coordinate frame was used to modify the interhemispheric interaction.

To affect the contralateral movements means that hemispheres have strong interaction. In condition 1 and 2, bilateral control systems could have the same motor commands because subjects activated the same muscles at the same time. On the other hand, in condition 1 and 3, these systems could have the same motor planning in external space because both finger's movement direction is congruent. If the brain has a sharing information mechanism, interaction might occur by sharing or referring the congruent information in contralateral hemisphere. This mechanism would contribute to decreasing the signal processing load. According to previous studies, brain activity is asymmetry during symmetric movements. The results in our study suggested that the functional mechanism between hemispheres works on multiple coordinate frame.

In addition, if the interaction influences the stability, the stability could also relate to these coordinate frames. Figure 5B shows the results of the stability in each condition. The stability was estimated by standard deviation (SD) of relative phase. High SD of relative phase means low stability. Unlike with interaction features, the stability depended on only intrinsic factor (movement symmetrical property). In condition 3, although the interaction is strong, stability is low. The results suggest that these interactions which based on two coordinate frames are generated in different level. The extrinsic and intrinsic coordinate frames would represent higher and lower information respectively, for example motor planning and motor command.

We have to investigate more concrete brain function by using fMRI imaging. Many studies focused on supplemental motor area and primary motor area as the important brain area to control the bilateral movements. These areas have strong connections toward the same site of contralateral hemisphere and we expect that these areas related to interaction discussed in our study. A further study about the function of each area's connection should be conducted.

IV. Electroencephalogram (EEG) and Functional Electrical Stimulation (FES) system for Rehabilitation of Stroke Patient

Stroke is the leading cause of adult disability. Impairments due to a stroke create functional deficits in motor control that interfere with peoples' daily lives. Recent evidence showed that motor recovery in the acute stages can minimize the effects of stroke. Therefore, most stroke survivors will need training to enhance their recovery and minimize disability.

Motor recovery is an important aspect of motor learning, which is used in stroke rehabilitation. The signal flow in a motor control system is as follows. A motor signal emerges from the motor area, goes through the spinal cord and finally activates specific muscles. After muscles contract, sensory feedback is conveyed to the somatosensory area in the cerebrum. This flow makes a sensorimotor closed loop. Healthy subjects can learn motor ability by repeating this flow, but stroke patients have difficulty learning specific motions because the loop is damaged.

We propose a rehabilitation method that combines the brain computer interface (BCI) and functional electrical stimulation (FES) systems (Fig.6). The system uses event-related desynchronization (ERD) to reflect motor intentions. FES stimulates the corresponding muscles, which return sensory feedback to the brain creating a pseudo motor-loop.

This section explains two pilot studies which we carried out. One is the study on the check of motor imagery training, because many patients cannot extract ERD without imagery training. In another study, we investigated the effect of sensor feedback on ERD.

A. *Experimental protocol*

10 healthy subjects participated in the motor imagery task. This task was to show the cursor movement (real-time) on the computer screen which is induced by the detection of ERD. The task continues 1 hour per day and we did this experiment for 3 days. At the end of each day, motor imagery and relaxed states EEG were measured without feedback, and this datasets were used for the evaluation of training effect [3].

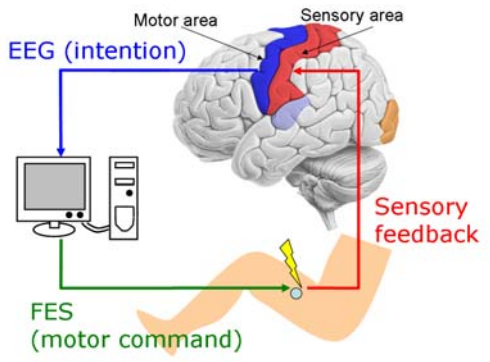

Fig.6 EEG-FES system for stroke patients

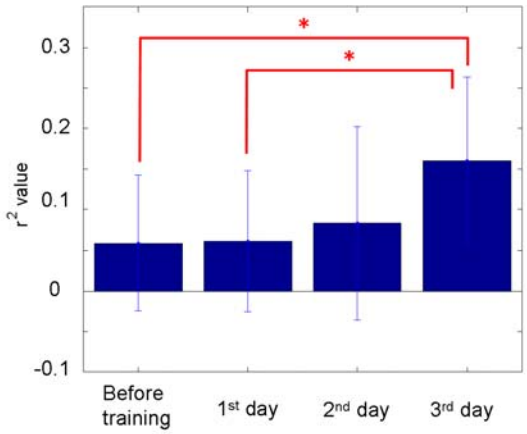

Fig.7 Imagery training effect (r^2 value : 10 subjects' average and variance)

17 healthy subjects participated in the FES feedback task. EEG was measured while FES was impressed on the both quadriceps. The FES condition was 'FES normal' that subjects' knee angle extended 30 degrees and 'FES 1/3' that was the 1/3 intensity of FES normal. And we also changed the leg condition as 'leg free' and 'leg fixed' condition. In this experiment, we investigated which sensation mainly affects ERD [4].

As a quantitative measure of the difference between presence and absence of motor imagery, we used the r^2 value method (equation(3), (4)), which is a well-known BCI research technique In the motor imagery task, x and y indicate each class frequency segment data (for example, x : motor imagery (26-28Hz), y : no motor imagery (26-28Hz)) and n_x, n_y indicate the quantity of data.

$$r^2(x,y)=\frac{(\sum x)^2/n_x+(\sum y)^2/n_y-G}{\sum x^2+\sum y^2-G} \qquad (3)$$

$$G=(\sum x+\sum y)^2/(n_x+n_y) \qquad (4)$$

The r^2 value was used to calculate within and between variances of each class. Increase in the r^2 value indicates a greater difference, i.e. greater ERD.

B. *Experimental result*

Fig.7 shows r^2 value in the motor imagery task. The result shows that it is effective even if the training is short time (three days).

The fig.8 shows comparison of each r^2 value (FES normal and FES 1/3, leg free and leg fixed). The results show significant differences. These suggest that muscular and articular sensation mainly affect ERD on motor area [4].

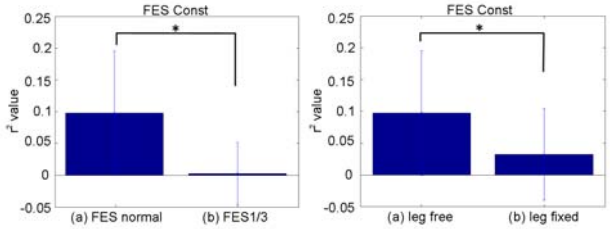

Fig.8 FES effect for ERD(r^2 value : 17 subjects' average and variance)

V. CONCLUSION

In the paper, we shortly reported our recent research results; "Decomposition of internal models in arm movements under mixed force fields", "Simultaneous learning of mouse operation with conflicting visuomotor transformation" and "Electroencephalogram (EEG) and Functional Electrical Stimulation (FES) system for Rehabilitation of Stroke Patient."

Next year, we continue to clarify the intra-cerebral mechanisms for recognizing unfamiliar environments and/or generating suitable motor commands, through psychophysical motor learning experiments and computational modeling of human movement. And we also are planning the check of the effect of the rehabilitation system by a stroke patient.

REFERENCES

[1] R.Shadmehr and S.P.Wise: The Computational Neurobiology of Reaching and Pointing, The MIT press, 2005

[2] N.Tomi, M.Gouko, T.Kondo and K.Ito: Inaccuracy of internal models in force fields and complementary use of impedance control, Transactions of the Society of Instrument and Control Engineers, 44(11), 896/904, 2008 (in Japanese)

[3] M. Takahashi, M.Gouko, K. Ito: Electroencephalogram(EEG) and Functional Electrical Stimulation (FES) System for Rehabilitation of Stroke patients, Proc. of 21st IEEE International Symposium on Computer-Based Medical System (CBMS2008), 53/58, 2008.

[4] M. Takahashi, M.Gouko, K. Ito: Functional Electrical Stimulation (FES) Effects for Event Related Desynchronization (ERD) on Foot Motor Area, 44(9), 699/704, 2008 (in Japanese).

Anticipatory adaptation of sensorimotor coordination

Toshiyuki Kondo
Tokyo University of Agriculture and Technology

I. Introduction

Learning is an essential feature of living creatures, especially humans. Even though we are situated in unfamiliar environments that have kinematic and/or dynamic visuomotor transformations, we can probably adapt to them within several episodes of trial and error. As a consequence of these active motor learning processes, our brain acquires neural representations of the relationship between our motor commands and body movements, i.e., *internal models* of various environments [1], [2], [7]. For instance, motor learning of arm reaching movements under unfamiliar force fields has been widely and intensively studied in psychophysics and neuroscience research fields [3]. In addition, we can flexibly select an appropriate motor command according to the context of internal states and/or surrounding environments. However, it is still not clear how the internal models are structured or represented in our brains.

To investigate human motor learning and appropriate selection of internal models, it is worth that paying attention to the *interference* among the identified internal models during motor learning. Thus, we focused on the problem of simultaneous learning of conflicting visuomotor transformations and contextual switching of the internal models [4], [5], [6], [9].

To verify whether humans can obtain appropriate internal models that compensate for two unfamiliar and conflicting visuomotor transformations simultaneously, we investigated a psychophysical visuomotor learning experiment using a rotated computer mouse paradigm [8]. In the experiment, human subjects were asked to move a cursor to a target emerging randomly on a screen as quickly and directly as they could using a computer mouse; however, there were one of two possible rotational transformations between the cursor and mouse movements, clockwise or counterclockwise by 90 degrees, respectively.

Our previous study [10] confirmed that these two visuomotor rotations can result in a conflict in the subjects. Thus, a preceding color cue corresponding to each rotational transformation was displayed on the screen before starting each trial. The subjects were expected to learn to compensate for the two rotational transformations (i.e., create internal models) and to bind each internal model to a corresponding color cue to distinguish them.

In the paper, we focused particularly on the effect of successive experiences on simultaneous learning of conflicting visuomotor rotations. It has been reported that simultaneous learning of two conflicting visuomotor transformation tasks presented in random order was significantly better than the training with alternating order, even if the total number of experiences was the same in each case [6]. However, it remains unclear why the random training schedule aids simultaneous learning of conflicting tasks. In this study, we assumed that the alternating training schedule gave no opportunity to experience the same rotational transformation successively. To test this assumption, we compared three training conditions; the encountered rotational transformation type was (1) alternating with every trial (ALT1), (2) alternating with every two trials (ALT2), and (3) changed at random (RAND).

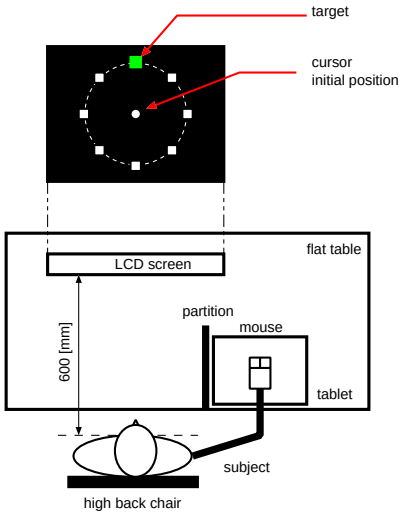

Fig. 1. Experimental setup.

II. Methods

A. Subjects

Twelve subjects (eight males and four females, 21.0±2.0 years old, mean±SD) participated in the experiment with informed consent, but they know nothing about the purpose of the experiment. All subjects were right-handed and relatively experienced with the operation of a computer mouse.

B. Experimental setup and task

The experimental setup is illustrated in Fig. 1. In the experiment, the subjects were seated on a height-adjustable high-back chair. An LCD screen (Hewlett-Packard, hp2035) was placed on a flat table in front of the subjects. The distance between the subjects and the screen was approximately 600 mm. A computer mouse with a pen tablet apparatus (WACOM, PTZ-631W) was located at the right-hand side on the table.

As shown in the figure, a mouse cursor and a target were displayed on the screen. The cursor was a small solid white circle (diameter approximately 4.0 mm) on a black

background. During a trial, the subjects could see the cursor at all times, but their hand movements were hidden by a partition. The target was displayed on the screen as a small solid green square (approximately 6.5 mm on a side). At each trial, the target appeared at a position randomly selected from eight peripheral candidates at 45-degree intervals illustrated in Fig. 1.

In the experiment, subjects were asked to move the computer mouse to shift the cursor to the target as quickly as possible. However, the cursor position (X_c, Y_c) was determined by the displacement of the computer mouse (x, y) with the following rotational transformation:

$$\begin{pmatrix} X_c \\ Y_c \end{pmatrix} = \kappa \begin{pmatrix} \cos\theta & \sin\theta \\ -\sin\theta & \cos\theta \end{pmatrix} \begin{pmatrix} x \\ y \end{pmatrix} \qquad (1)$$

where κ corresponds to an amplification of the mouse's motion. Before starting the experiment, each subject was asked to adjust the parameter regarding cursor movement to be as usual. Also, θ is a rotation angle of -90, 0, or 90 degrees. A clockwise rotation is assumed to be positive.

Fig. **??** schematically shows the three rotational transformations between mouse and cursor movements. The lower row indicates mouse movements and the upper one represents the corresponding cursor movements. In the following, NULL, CW90, and CCW90 stand for no transformation and clockwise and counterclockwise 90-degree rotations, respectively.

Trials proceeded as follows (see Fig. 2).

1) The subject was asked to place the mouse device at the initial position indicated on the tablet.
2) At that time, the background of the screen was filled with blue (RGB #000080) or red (RGB #800000) in accordance with the rotational transformation presented in the next trial (i.e., CW90 or CCW90, respectively).
3) The subject clicked the mouse button. At the same time, one of the eight targets chosen randomly was displayed on the screen. Immediately, the subject started to move the mouse to direct the cursor toward the target.
4) When the cursor reached the target, the trial was terminated with the message, "Please return the mouse device to the home position."
5) The process was repeated until a series of trials was completed.

In the experiment, one *set* consisted of 32 trials ($N_S = 32$). Thus, the eight targets were randomly chosen four times each in a set; however, the same target was not presented consecutively.

C. Performance criteria

In the experiments, all subjects were instructed to move the cursor quickly on a straight trajectory to the target. To assess each subject's performance, the time required to reach the target (reaching time; T_i [sec]) and accumulated directional error (E_i [rad]) measured in a trial were used (subscript i denotes the trial number). The accumulated directional error E_i was defined as

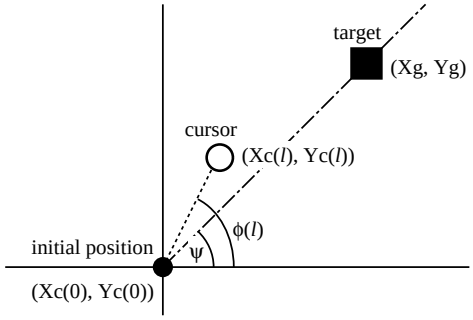

Fig. 3. Directional error criterion.

$$E_i = \sum_{l=1}^{L_i} |\phi(l) - \psi| \,,$$

$$\psi = \arctan\left[\frac{Y_g - Y_c(0)}{X_g - X_c(0)}\right],$$

$$\phi(l) = \arctan\left[\frac{Y_c(l) - Y_c(0)}{X_c(l) - X_c(0)}\right],$$

where X_g and Y_g represent the target coordinates, and $X_c(l)$ and $Y_c(l)$ denote the cursor coordinates sampled at discrete time step n (see Fig. 3). Thus, $X_c(0)$ and $Y_c(0)$ correspond to the initial cursor position. L_i is the total number of time steps in the i-th trial.

D. Training procedures

Before starting the simultaneous training experiment, all subjects were asked to accustom themselves to the task without visuomotor rotation (i.e., in the NULL condition). After familiarization, subjects executed one set in the NULL condition to determine baseline performance of each subject.

Subsequently, we started the simultaneous training experiment. During the training, the subjects were exposed to one of two conflicting visuomotor rotations, CW90 or CCW90, depending on their training schedules. As specified in Table I, the subjects were randomly assigned to three groups; (1) Group ALT1 with a visuomotor rotation alternating every trial ($n = 4$), (2) Group ALT2 with a visuomotor rotation alternating every two trials ($n = 4$), and (3) Group RAND with a visuomotor rotation randomly selected at every trial ($n = 4$). The training iteration consisted of two sessions of 10 sets each, with a 90-minute rest interval between the sessions.

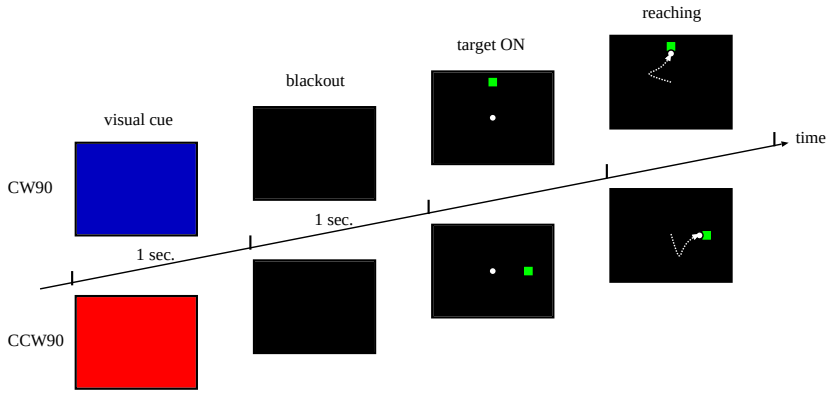

Fig. 2. Procedure of a trial.

TABLE I

TRAINING PROCEDURE OF THE EXPERIMENT.

	ALT1 ($N = 4$)	ALT2 ($N = 4$)	RAND ($N = 4$)
first half (1st-10th)	alternating (trial by trial)	alternating (every two trials)	random
rest	90 min.		
second half (11th-20th)	alternating (trial by trial)	alternating (every two trials)	random

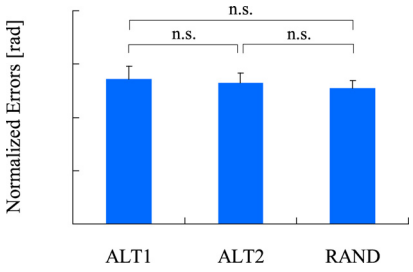

Fig. 4. Baseline performances of each group of subjects. The accumulated directional errors measured in a NULL set were divided by the corresponding reaching time, and the normalized directional errors were averaged across trials. ANOVA revealed no significant differences among the groups ($F_{2,9} = 0.695, p = 0.524$).

III. RESULTS

A. Baseline performance

To evaluate the baseline performance of the subjects, the accumulated directional error measured in each trial (E_i^{BSL}) was divided by the corresponding reaching time (T_i^{BSL}), and we obtained the normalized directional error averaged across trials for each subject.

$$\bar{E}^{BSL} = \sum_{i=1}^{N_S} \frac{E_i^{BSL}/T_i^{BSL}}{N_S}.$$

Normalized directional errors averaged across trials were evaluated for each group with the analysis of variance (ANOVA). As Fig. 4 shows, no significant differences with respect to baseline performance were found among the subjects in the three groups ($F_{2,9} = 0.695, p = 0.524$).

B. Learning performance

To assess the learning curve of each subject in the training sets, the accumulated directional error in each trial (E_i) was normalized by each subject's baseline performance ($\bar{E}^{BSL}$). The performance index, here referred to as *error rate* (R_i) was calculated as $R_i = E_i/\bar{E}^{BSL}$.

Since each training set includes the same number of CW90 and CCW90 trials, we averaged them separately within the set.

In addition, Fig. 5 compares the average error rates between the first and last five training sets for each training group and rotation type. As the figure shows, the error rates seem to decrease in all cases through the training.

To clarify whether the subjects could learn the two conflicting visuomotor rotations simultaneously, we analyzed the decrement in the averaged error rates between the first and last five training sets separately in the case of CW90 or CCW90. The error rates were also averaged across the subjects in each group.

According to the results of ANOVA, we confirmed that the error rates were decreased significantly in all cases (training groups $\times$ rotation types), ALT1 group (CW90: $F_{1,38} = 5.95, p = 0.0195$; CCW90: $F_{1,38} = 6.01, p = 0.0190$), ALT2 group (CW90: $F_{1,38} = 36.2, p < 0.001$; CCW90: $F_{1,38} = 13.8, p < 0.001$), and RAND group (CW90: $F_{1,38} = 23.3, p < 0.001$; CCW90: ($F_{1,38} = 22.7, p < 0.001$).

From another perspective, we analyzed the error rates among the training groups by ANOVA separately for each stage (i.e., the first or last five sets) and rotation type (CW90 or CCW90). Fig. 6 shows the comparison.

No significant differences appeared in the early stage (i.e., the first five sets) of CW90 ($F_{2,57} = 2.58, p = 0.0844$) and CCW90 ($F_{2,57} = 2.68, p = 0.0770$). Note that the level of significance was $p = 0.05$.

In contrast, significant differences were confirmed in the

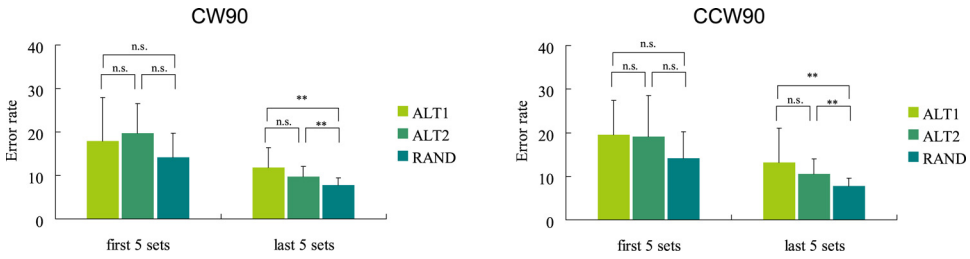

Fig. 6. Change in the average error rates between the first and last five sets under the three training conditions. (Left: averaged across CW90 trials. Right: averaged across CCW90 trials)

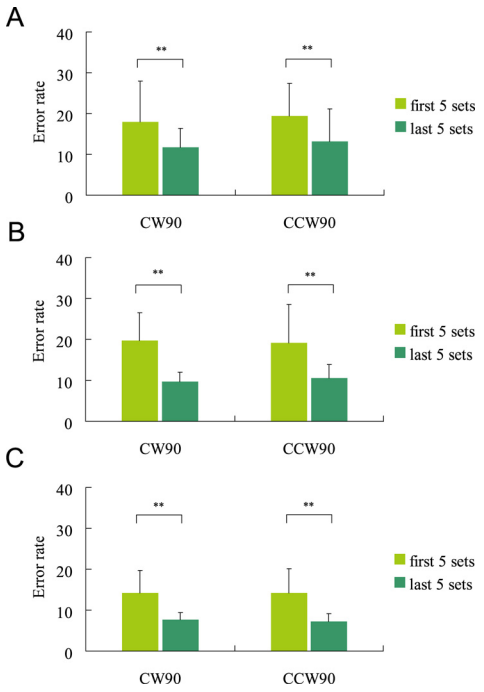

Fig. 5. Comparison of the error rates averaged within CW90 (or CCW90) trials between the first and last five training sets for each training group (**a**: ALT1 group, **b**: ALT2 group, and **c**: RAND group).

later stage (i.e., the last five sets) of both rotation types; CW90 ($F_{2,57} = 7.73, p = 0.00107$) and CW90 ($F_{2,57} = 6.31, p = 0.00334$). Accordingly, we executed multiple comparisons (*Bonferroni-Dunn* tests) with regard to the cases.

The results of the multiple comparison were as follows: CW90 (ALT1 vs. ALT2: $p = 0.0948$, ALT1 vs. RAND: $p = 0.00161$, ALT2 vs. RAND: $p = 0.00554$), CCW90 (ALT1 vs. ALT2: $p = 0.212$, ALT1 vs. RAND: $p = 0.00506$, ALT2 vs. RAND: $p = 0.000733$). The significance level used here was $p = 0.0167 (= 0.05/3)$.

From these results, we confirmed a significant difference between the ALT1 or ALT2 and RAND groups, even though there were no significant differences in the early stage.

IV. Conclusions

In this paper, we demonstrated that humans can learn appropriate internal models for compensating two unfamiliar and conflicting visuomotor transformations simultaneously. We used a rotated computer mouse paradigm in where the cursor's motion is rotated clockwise or counterclockwise by 90 degrees.

We focused on the effect of successive experiences during simultaneous learning of conflicting tasks. It had been reported that simultaneous learning of two opposing force fields with a random order was significantly better than training with alternating order, even with the same total number of experiences. We assumed that this was because the alternating training schedule gave no chance to retry the same rotational transformation successively. To test this assumption, we compared three training conditions: alternating every trial, alternating every two trials, and changed at random.

Experimental results suggested that providing the chance of successive trials to the subjects had a small positive effect on simultaneous learning compared with alternating every trial. However, the subjects trained under the random condition still showed a significant advantage in comparison with those trained under the other conditions.

References

[1] M. Ito, *The Cerebellum and Neural Control*, Paven Press, 1984.
[2] M. Kawato, *Internal models for motor control and trajectory planning*, *Current Opinion in Neurobiology*, **9**, pp.718–727 1999.
[3] R. Shadmehr and F. A. Mussa-Ivaldi, *Adaptive representation of dynamics during learning of a motor task*, *J. Neuroscience*, **14**, pp.3208–3223, 1994.
[4] A. Karniel and F. A. Mussa-Ivaldi, *Sequence, time, or state representation: how does the motor control system adapt to variable environments?*, *Biological Cybernetics*, **89**, 1, pp.10–21, 2003.
[5] J. W. Krakauer, M.-F. Ghilardi, and C. Ghez, *Independent learning of internal models for kinematic and dynamic control of reaching*, *Nature neuroscience*, **2**, 11, pp.1026–1031, 1999.
[6] R. Osu, H. Hirai, T. Yoshioka, and M. Kawato, *Random presentation enables subjects to adapt to two opposing forces on the hand*, *Nature neuroscience*, **7**, pp.111–112, 2004.
[7] K. Ito, T. Imai and T. Kondo, *Motor Adaptation to Dynamic Environments in Arm Reaching Motions*, *Proc. of XVIII IMEKO WORLD CONGRESS*, 2006.
[8] H. Imamizu, S. Miyauchi, T. Sasaki, R. Takino, B. Puetz, T. Yoshioka, and M. Kawato, *Human cerebellar activity reflecting an acquired internal model of a novel tool*, *Nature*, **403**, pp.192–195, 2000.
[9] H. Imamizu, N. Sugimoto, R. Osu, K. Tsutsui, K. Sugiyama, Y. Wada and M. Kawato, *Explicit contextual information selectively contributes to predictive switching of internal models*, *Experimental Brain Research*, **181**-3, pp.395–408, 2007.
[10] T. Kondo and Y. Kobayashi, Simultaneous learning of computer mouse operation with conflicting rotational transformations, *Proc. of The 3rd. International Symposium on Measurement, Analysis and Modeling of Human Functions*, pp.93–100, 2007.

Mobiligence for optimal investment
: toward the computational algorithm of instantaneous gain rate

Toshiya Matsushima, Animal Behavior and Intelligence, Department of Biology, Faculty of Science, Hokkaido University

***Abstract*—Do animals have mind? Do non-mammalian vertebrate animals in particular have mental processes similar to ours? The issue of "animal mind" has long been unchallenged simply because it was ill-defined. Recent progresses in behavioral studies in birds, however, revealed that they have cognitive process analogous to ours. In this report, we will show data obtained from a series of experimental psychological studies using chicks of domestic chickens as subjects. Basic assumption is that selection pressure has shaped economically rational (i.e., features linked to maximization of own benefit; or greedily ego-centric decision maker hypothesis) as evolutionary adaptive traits. Common selection pressure therefore could have shaped basically identical cognitive processes in taxonomically distinct groups of animals, such as mammals (including human) and birds. The evolutionary explanation will make sense, if animals show optimal behaviors in a variety of different situations. Guided by this strategy, we have accomplished (in the academic year of 2008) the following series of experimental studies. (1) We compared risk sensitivity in two distinct conditions; one in which the amount was at risk (i.e., the associated amount of food reward varied among trials) and another in which the proximity was at risk (i.e., the associated delay to the food reward varied among trials at equal probabilities). Chicks showed risk aversion in amount, and risk proneness in delay, in favor of the dissociated internal representation of amount and delay. In order to reveal the difference, however, we had to apply Bayesian estimation (or statistical analysis of behavioral data by using hierarchical Bayesian models). (2) Developmental facilitation of impulsiveness by competitive foraging was experimentally confirmed in behavioral titration experiment using inter-temporal choice paradigm. Study of characteristic gene expression patterns in telencephalone is now underway by using cDNA microarray analysis. (3) Patch use behavior was experimentally reproduced by using a feeder of gradually diminishing return. The mean residence time proved to follow Poisson process, whereas the underlying decision was based on retrospective time perception, or the interval of two successive food delivery in the immediate past, in a clear contrast to the binary choices that were based on anticipatory (prospective) sense of time. Furthermore, pharmacological experiments have suggested that the serotonergic system in the medial striatum played a critical role both in the anticipatory (prospective) and experienced (retrospective) foods, however in opposite manners. These results support the idea that; (i) Foraging choices follow a complex evaluation function with multiple factors such as amount, delay, consumption cost, and risk, and (ii) These multiple factors are dissociable in different regions in the brain.**

Toshiya Matsushima, Department of Biology, Faculty of Science, Hokkaido University (corresponding author), phone & fax: +81-11-706-3523; e-mail:matusima@mail.sci.hokudai.ac.jp).

I. Introduction

RECENT progress in behavioral studies of birds suggested that they have cognitive processes analogous to ours, humans. Pepperberg [1] reported that African Grey Parrots are able to communicate with human in English (a natural language of *Homo*). Clayton [2] has studied food storing behaviors and assumed that blue jays (corvids in general) could have episodic-like memory. Furthermore, Emery [3] has suggested that jays organize their behaviors based on assumption of other individuals' cognitive process, indicative of "theory of mind" in birds. All these cases were successful in showing that the birds have cognitive processes similar to primates. Does it mean that the they have "mind" that is identical to ours?

This issue of the animal mind is however, terribly ill-defined, simply because many topics and concepts remain highly *polysemic*; without specifying them, we are unable to precisely argue the "similarity". It is also highly controversial whether elementary brain processes in animals (and humans) mind process can be categorized in the same fashion. Purely materialistic approaches have limited applicability to the issue of mind.

In this report, I will introduce some of the experimental psychology of domestic chicks as subjects. The idea is that the ecological backgrounds of foraging choice can be related to the neural bases and cognitive processes. Through viewing the issue in both ecology and neuroscience, we will be prepared to discuss the issue of animal mind (or evolution of intelligence) with minimal assumptions.

Due to phenomenal convergence, a given "equation" often yields a diverging spectrum of "solutions." Neuroscience has been a powerful tool, because we could disregards those "solutions" that were physiologically unrealistic. Similarly, through filtering the possible "solutions" by ecological / evolutionary means, we will be given additional constraints, thus making our arguments on animal minds more tractable (i.e., requiring fewer lines of assumption) than it used to be. The present series of study thus aims at the foundation of *system neuro-ecology*.

II. Optimal Foraging Theory

Based on insect behaviors, Charnov [4] proposed two classical models for foraging behaviors based on foraging behaviors, both of which are quantitatively formulated and are highly sensitive to experimental verifications; they are,

optimal diet menu model (or optimal prey menu model) and ***optimal patch use model*** (or optimal patch stay time model). Both of these two models assume that rational decision makers adopt the optimization strategy, so that animal behaviors are designed toward maximization of subjective long-term gain rate.

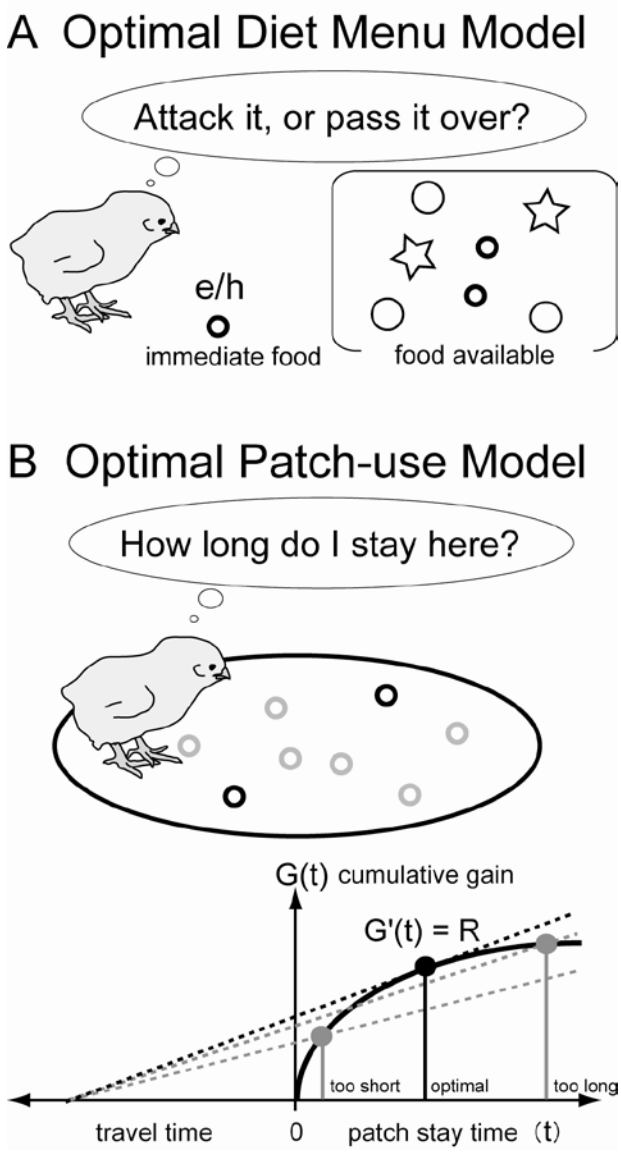

Fig.1 Optimal menu model (A) and patch-use model (B)
A: Assume a forager that encounters one of *n* different kinds of food items. The forager decides to attack the food, or to pass it over in search for an alternative, or lost opportunity. B: Assume a situation in which food resources are unevenly scattered in a patchy manner, and the forager encounters one of these patches. As the forager continues to forage in the patch, naturally the resource will be exhausted, making the instantaneous gain rate gradually decrease. At a marginal point ($G'(t)=R$), in which the instantaneous gain rate reaches maximum, optimal forager should leave the patch of food.

Let us assume a forager that encounters a food item while foraging. The environment contains food items of several different types. The forager is omniscient and knows the gain (e) and handling time (h) for each food type. However, the encounter is randomized, and the subject forager does not know what food type he will find next. Attack will give rise to a certain gain at the expense of the handling time; passing over will, on the other hand, gives rise to the food item that is potentially available, or the lost opportunity.

Natural condition is actually much more complicated. Food items are often scattered in a patchy fashion, and forager must move from a patch to another without explicit information on the location and quality of food patches. Once subject encounters a patch, he will collect the food items. In the initial phase of patch use, the gain rate is high, because the patch is fresh with a certain amount of food. Subsequently, as the forager stays longer, the food density decreases, making the instantaneous gain rate monotonically decreasing. Optimal forager must leave the patch before the food is exhausted. At certain point of time, the lost opportunity (the gain available in the next patch) will exceed the immediate gain, making the move an economically rational decision. The law of "diminishing return" holds true also in the animal economics.

Ecological / ethological studies in insects, birds and fish basically proved validity of these two models, as they are successful in predicting some of the foraging behaviors [5]. The ***molar*** properties of foraging behaviors thus follow general rules irrespective of evolutionary backgrounds. What behavior and cognition at the ***molecular*** level are responsible?

III. Choice Theory

Birds do not learn aerodynamics in order to fly. Similarly, economical decision makers do not need to learn economics in order to achieve the optimal foraging. The point is whether the decision leads to the long-term gain, irrespective of the immediate consequences.

It should be noted that both of these models could be explained by a unifying scheme as shown in **Fig.2**. Here, the choices are between "small-but-immediate reward" (immediate food or the food available within reach) and "large-but-delayed food" (lost opportunity). In psychological framework for human behaviors, the former is referred to as ***impulsive***, while the latter ***self-control***. Clearly in human society, we have an agreement that the self-control choice is "adaptive" and the impulsive choice is "maladaptive" nature.

When viewed from the ecological standpoint, however, the terms seem somehow misleading. Actually, in many situations, foraging animals show a certain level of impulsiveness in foraging decisions, suggesting that the distance (spatial proximity) or delay (temporal proximity) is critical. Why?

Under natural condition, the immediate food is often available for a short period of time. The food item may flee, or snatched by others, making the self-control decision makers less profitable. In this situation, on the other hand, impulsive decision makers may even maximize the long-term gain rate.

Depending on the food resources, level of impulsiveness must be appropriately kept elevated to a certain point.

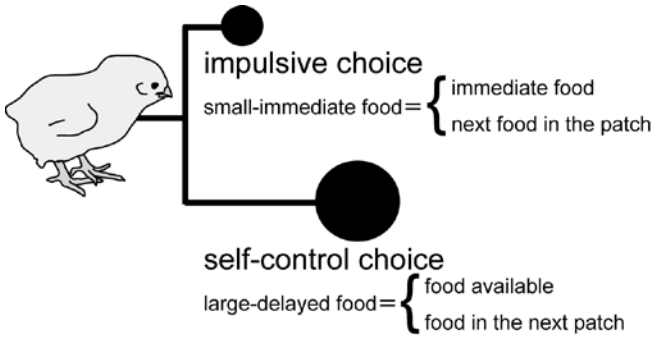

Fig.2 Inter-temporal choice scheme as a unifying framework for the two models of optimal foraging theory

IV. Diminishing Return, Serotonin, Time Perception and Decision Making

In this report, we will focus on the issue of chicks' decision to leave the food patch of gradually decreasing gain rate. We tried to reconstruct the natural foraging situation in laboratory apparatus shown in **Fig.3A**.

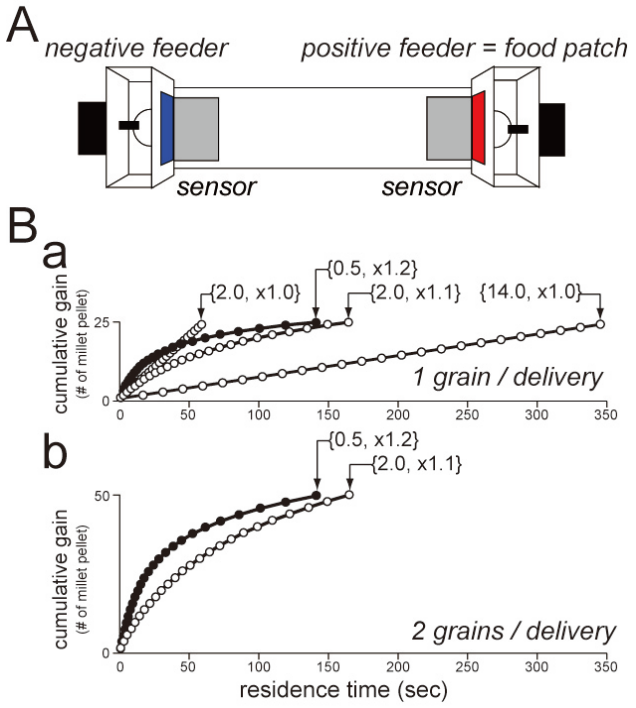

Fig.3 I-shaped maze and feeding patterns.

A: Sensor placed on each feeder detects the chick approach to the positive feeder (red), and triggers the programmed feeding patters shown in B. The program is interrupted when the chick approached to the opposite negative feeder. In this situation, chicks soon learn to actively shuttle between the two feeders to gain food from the positive one. B: Control parameters are the initial interval (0.5 sec or 2.0 sec) and the increment rate (x1.1 or x1.2). In two other groups of chicks, the instantaneous gain rate was doubled by delivering two grains at a time, whereas the temporal patterns of feeding was identical. Factors of time and amount were thus dissociated.

Residence time was measured in these 6 different conditions (each containing 6 chicks without overlaps, and each chick was examined three times, each containing 20 shuttles). Variance of the residence time was approximately square of the mean in each chick, suggesting that exponential distribution fits. Most probably, the underlying process is simply Poisson-based. We therefore represented each chick by the mean, as an inverse of the mean probability to leave.

Further detailed analysis of the instance of patch leave, we found that the decisions were made based on the retrospective time perception, rather than the prospective time. As a measure of the retrospective time, we adopted the leave-point interval or the interval of the latest two delivery just before the leaving point (**Fig. 4**).

Fig. 4 Leave points from the positive feeder reveal distinction between retrospective and prospective time perception

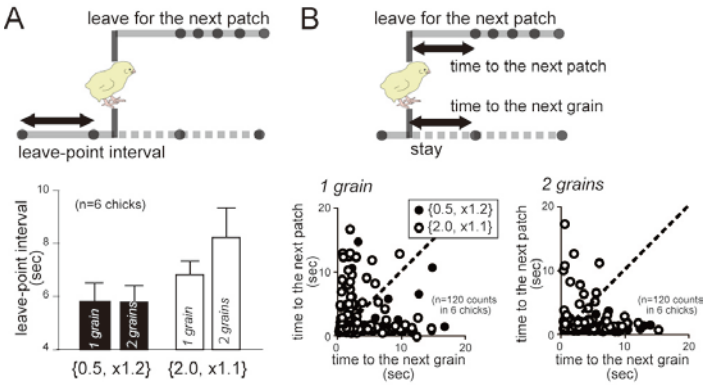

As shown in **Fig.4A**, chicks left the feeder at a certain level of the leave-point interval irrespective of the amount of food (1 or 2 grains per delivery); in contrast to our initial prediction, no significant effects of the amount factor was found after statistical tests using two-way ANOVA (data not shown). On the other hand, as shown in **Fig. 4B**, the time to the next food (i.e., the time to the next patch (anticipated food of the leave option) and the time to the next grain (anticipated food of the stay option) were not correlated with the chick decisions. Clearly, chicks cared the immediate past, but not the food to be gained in the future.

These results suggest that the unifying scheme (**Fig. 2**) is not applicable to chicks. It rather suggested that the two models in the optimal foraging theory are accomplished by distinct time perception; namely, the diet menu model by the prospective time (food anticipation) and the patch use model by the retrospective time (food experience in the immediate past).

Pharmacological action on serotonin (5-HT) also revealed distinction between the two models. As reported previously (in 2007 report), selective serotonin reuptake inhibitor (SSRI,

fluvoxamine (flu) was used in this study) proved to suppress impulsiveness in inter-temporal choice paradigm, and the acutely treated chicks shifted their choices toward a larger but more delayed food reward. Actually, as shown in **Fig. 5**, systemic injection of flu selectively (but not specifically) enhanced the extracellular concentration of 5-HT in the medial striatum, which has been shown to be involved in choices based on anticipated food reward.

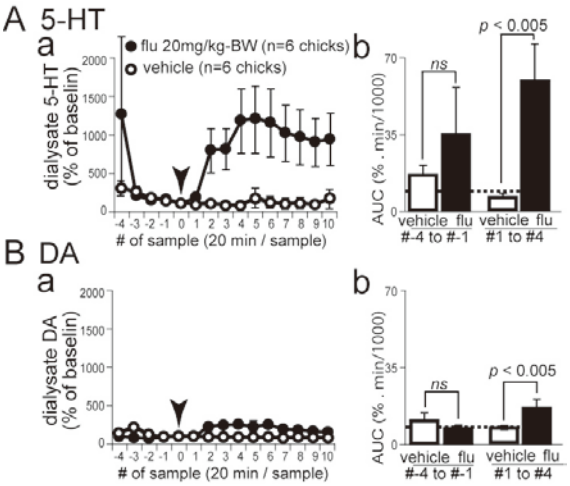

Fig. 5 *In vivo* microdialysis from freely behaving chicks revealed selective increase in 5-HT in the medial striatum after the injection of fluvoxamine (arrows).

The unifying scheme shown in **Fig. 2** suggested that flu injection caused chicks less impulsive (or more self-controlled), thus making the move to the new patch (larger and distant food) more frequently. Flu could have decrease the patch residence time, making chicks to leave the feeder when the instantaneous gain rate was yet considerably high. In reality, however, chicks injected with flu showed a longer residence time. It is to be noted, however, that both of the prospective and retrospective time perception are influenced by localized lesions to the medial striatum – nucleus accumbens [8,9].

V. Conclusions

1. Classical foraging theory has proposed two different models, "optimal diet menu model" and "optimal patch use model". These two models can be unified, as a single scheme of inter-temporal choice could explain these two.
2. Results of behavioral and psychopharmacological studies were not in concert with the idea of unified theory.
3. It is suggested that the menu model is based on the anticipation of immediate future reward (or the prospective time perception), whereas the patch use model is based on the experience in the immediate past (or the retrospective time perception).

References

[1] Pepperberg, I.M. The Alex Studies. Cambridge, Massachusetts: Harvard University Press, 1999.

[2] Clayton, N. & Dickinson, A. Episodic-like memory during cache recovery by scrub jays. Nature, 395, 272-274, 1998.

[3] Emery, H.J. & Clayton, N. Effects of experience and social context on prospective cashing strategies by scrub jays. Nature, 414, 443-446, 2001.

[4] Charnov, E.L. Optimal foraging: the marginal value theorem. Theoretical Population Biology, 9, 129-136, 1976.

[5] Stephens, D.W. & Krebs, J.R. Foraging Theory. Princeton, New Jersey: Princeton University Press. 1986.

[6] Mazur, J.E. Learning and memory (5th ed.). Prentice Hall. 2002.

[7] Matsushima, T. *et al.* Neuro-economics in chicks: foraging choices based on delay, cost and risk. Brain Research Bulletin, 76: 245-252, 2008.

[8] Izawa, E.-I. *et al*. Localized lesion of caudal part of lobus parolfactorius caused impulsive choice in the domestic chick: evolutionarily conserved function of ventral striatum. *Journal of Neuroscience* 23: 1894-1902, 2003.

[9] Ichikawa, Y.*et al*. Excitotoxic lesions of the medial striatum delay extinction of a reinforcement color discrimination operant task in domestic chicks; a functional role of reward anticipation. *Cognitive Brain Research*, 22: 76-83. 2004

Recalibration of time to contact

Yasuharu Koike
Tokyo Institute of Technology

***Abstract*— In order to elucidate the mechanism of predicting the timing of contact.We examined an experimental investigation of the adaptation process that shifts in the timing of the visual and tactile. Visual stimulus was the falling ball in 9.8 $\mathrm{m/s^2}$ acceleration for any tactile stimuli and the tactile stimuli was shifted 60 msec. The subject repeated the ball catch task with shifted condition. As a result, the subjects did not aware the timing shift, but they change the timing of tactile contact with the estimated time. This means that the simultaneity was also shifted about 60 msec after the adaptation task.**

I. Introduction

We are born without adapting to the natural environment on Earth, and have been adapting to the environment by learning. To recognize the environment, especially visually, its color, shape and texture as well as external features, or to study the physical characteristics such as weight and softness. This capability not only be acquired by sight, touch and manipulation of the object give us some information about the dynamics of it. To manipulate the object, brain needs to generate a motor command to control the movement of arms. Moreover, the brain can estimates the future state[5].

The pathway of two cortical systems provide 'vision for action' and 'vision for perception', respectively [4].

We can assume two hypotheses for explaining this phenomena in fig. 1. One is that the subject learned the different timing by using visual stimuli (1). They would become to estimate the different TTC with same visual stimuli as they learned the different acceleration. The other one is that the subject learned the delay between the motor command and muscle tension (2). It is known that the delay between muscle activation and force exertion is about 100 msec, and the delay between motor cortex and muscle is about 20 msec. Usually, we don't aware of this delays during motor tasks. We probably learned this delay and send the motor command beforehand to compensate these delay.

There are some researches which has been focused on the sense of the time difference between two modalities in both physical transmission time and sensory processing time. Visual signals to reach the brain behind times, so the scene what we are looking now is in the past[1]. However, for a variety of different sense of time delay, some mechanism is needed to ignore it[2]. Thus, the time difference between the auditory and visual are investigated. In this study, the time difference between visual and tactile were examined. Also the stimuli was not passive.

P & I Laboratory, Tokyo Institute of Technology, R2-15, 4259, Nagatsuta-cho, Midori-ku, Yokohama, 226-8503 koike@pi.titech.ac.jp

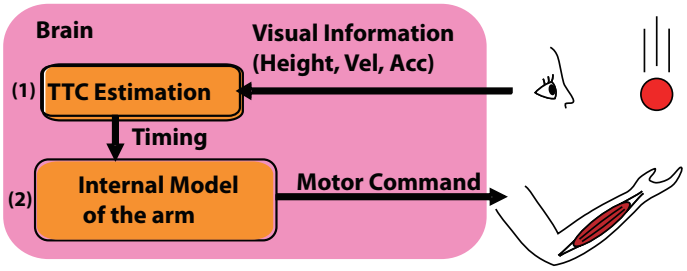

Fig. 1. Two hypotheses for learning this task

II. Method

A. VR environment

We use a haptic device "SPIDAR" which use four motors (Maxon DC motor, RE25) to strain by strings for applying the force to a hand [3]. This device can be measure the position by measuring the length of the strings by rotary encorder in 1 kHz sampling.

We also measure Electromyographic (EMG) signals (Bagnoli-16 system Delsys inc.) for measuring a intention for catching, because EMG signals activate about 100 msec before exerting a force. Active electrode was put on palmaris longus and EMG signals was sampled at 2 kHz with 16bit. In order to show the visual stimuli to the subject, plasma display (PDP503-CMX, 50 inches, Pioneer) was used. Virtual ball was falling from 80 [cm] height with 0 [m/sec] initial velocity, was same color and size, and applied 4.9 [N] force to right hand for 1.1 sec for different perturbation conditions.

B. Ball catching task

Subjects were asked to catch the ball at the initial position. At the beginning of the trial, beep signal sounded and after a random delay ranging from 2.5 to 3.5 sec, the virtual ball was falling with 0 m/s initial velocity and 9.8 $\mathrm{m/s^2}$ acceleration.

In experiment 1, the participants judged the simultaneity of vision and haptic stimuli presented with various time lag from -200 msec to 200 msec. One condition was that the visual stimuli was fixed to 9.8 $\mathrm{m/s^2}$ and the haptic stimuli was shifted from -200 ms to 200 ms randomly. Other condition was that the haptic stimuli was fixed to 9.8 $\mathrm{m/s^2}$ condition (about 400 ms) and the vision stimuli

Fig. 2. Experimental environment.

was changed from about $4.4\ \mathrm{m/s^2}$ to $20.0\ \mathrm{m/s^2}$. A trial consisted of pairs of stimuli presented at one of 15 physical stimuli onset asynchronies (SOA), which were randomly interleaved within a method of constant stimuli. In this study, positive SOAs always refer to a visual lead and negative always to a tactile lead. Each experiment contained 20 presentations at each SOA.

In experiment 2, subjects performed two different experiments. In each experiment, the force timing was different, and the timing was selected from 2 conditions, -60 or 60 msec. In 60 msec delayed condition, the force signal was applied after 60 msec in visually contact.

Subject caught the ball with constant time lag condition and repeated 100 trials for adaptation without any judgment.

After the adaptation phase, the subject did the same experiment for time lag judgment as same as experiment 1. In the experiment, the subject made an unspeeded temporal order judgment task as to "which stimuli came first." The subject was forced to choose the tactile or the vision stimulus which was preceded.

III. Result

A. Experiment 1

In experiment 1, the subject performed two different conditions. The vision stimuli was the ball trajectory of $9.8\ \mathrm{m/s^2}$ acceleration and the tactile stimuli was shifted from

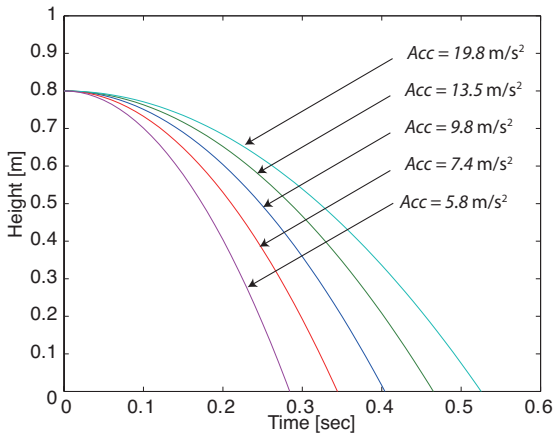

Fig. 3. Ball trajectories for different acc conditions.

-200 to 200 ms (blue dot). Other condition was the tactile stimuli was constant at $9.8\ \mathrm{m/s^2}$ acceleration timing. The vision stimuli was shifted from $6\ \mathrm{m/s^2}$ to $20\ \mathrm{m/s^2}$ (red dot).

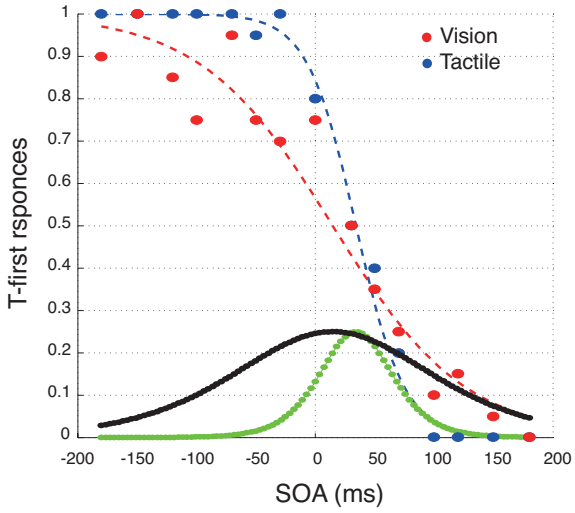

Fig. 5. Psychometric functions for visuotactile pairing

Psychometric functions can be seen in Fig. 5. The corresponding to the 50% response level on the psychometric function was about 30 msec and the sensitivity of SOA was height for tactile condition. This because that it is difficult to judge the difference of visual stimuli and the subject would estimate the same timing as $9.8\ \mathrm{m/s^2}$ conditions.

B. Experiment 2

In experiment 2, after the adaptation, the vision stimuli was the ball trajectory of $9.8\ \mathrm{m/s^2}$ acceleration and the tactile stimuli was shifted from -200 to 200 ms in Fig. 6(red dot).

As a result, the simultaneity was also shifted to about 60 msec and it was the same time lag of the adaptation. From

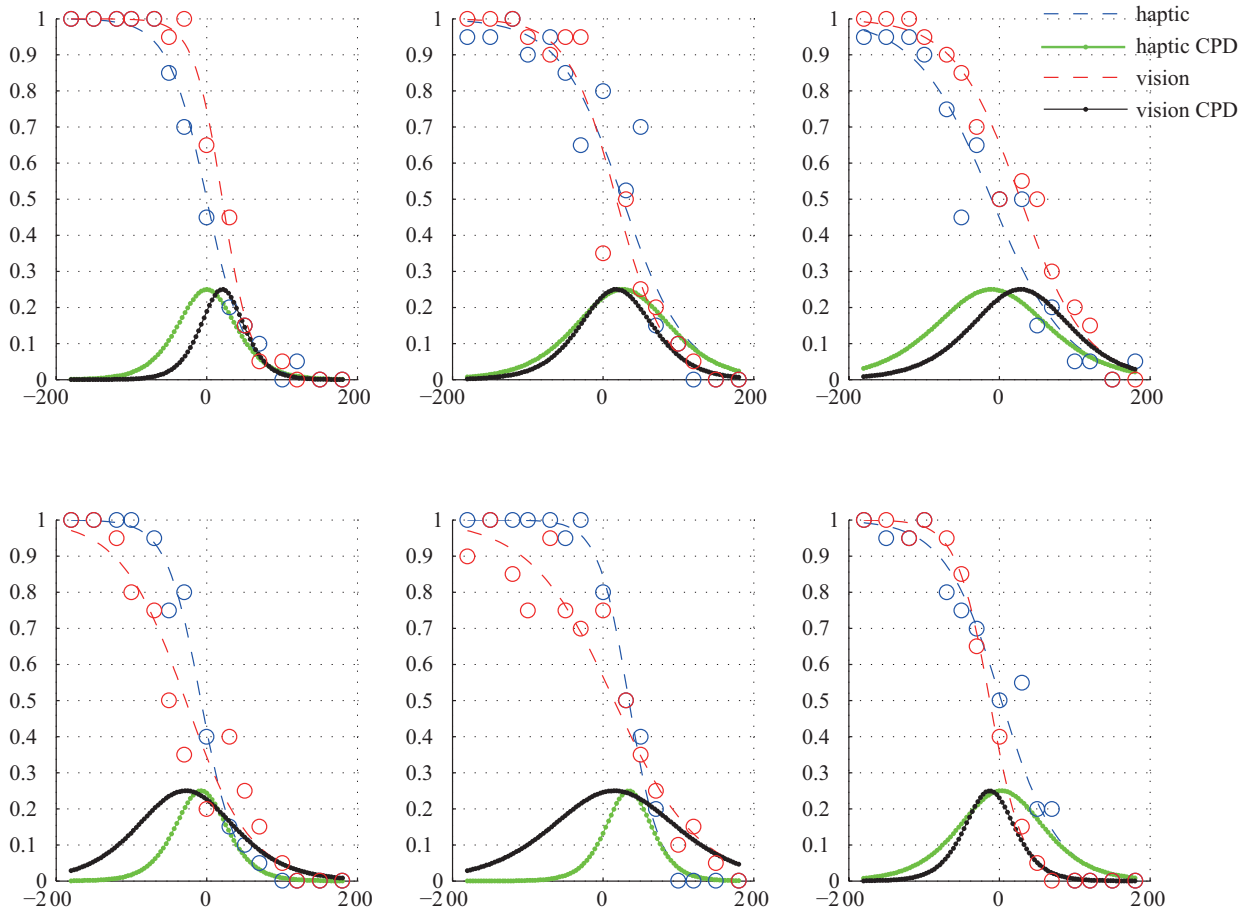

Fig. 4. Psychometric functions for visuotactile pairing for all subject

previous some experiments, we found that the onset of EMG activities before the time to contact. So motor planing or the state estimation of the ball was affected and also the judgement was shifted.

IV. MRI COMPATIBLE HAPTIC DEVICE

In fMRI room, in order to apply the force feedback, we can not use conventional electric motor. So we have been developing the new haptic device which is controlled by ultrasonic motor. This device is controlled by the equiriblium point and stiffness which were estimated from EMG signals.

The schematic picture is shown in Fig. 7. In this figure, two muscles are represented as spring and the model parameters of muscle are estimated by equiriblium posture which was calculated from surface EMG signals. The joint stiffness is also estimated using same model parameters.

Figure 9 shows the controlled device using ultrasonic motor. The prothetic arm is controlled from estimated posture. This posture is quite similar to the real posture woth no delay. Also the force can be produced.

The joint torques are estimated from this equation.

$$\boldsymbol{\tau}(\boldsymbol{u},\boldsymbol{\theta};\boldsymbol{v}) = \boldsymbol{v_{10}} + \boldsymbol{v_2 u} + \boldsymbol{u}^{\mathrm{T}} \boldsymbol{V_3 u} + (\boldsymbol{v_{40}} + \boldsymbol{v_5 u})\,\boldsymbol{\theta} \quad (1)$$

$$\tau = v_{10} + \boldsymbol{v}_2 \boldsymbol{u} + \boldsymbol{u}^{\mathrm{T}} V_3 \boldsymbol{u} + (v_{40} + \boldsymbol{v}_5 \boldsymbol{u})\,\theta \quad (2)$$

where, $\boldsymbol{v}_j = (v_{j1}, v_{j2})\ \ (j = 2, 3, 5)$, $V_3 = \mathrm{diag}(v_{31}, v_{32})$, $\boldsymbol{u} = (u_1, u_2)^{\mathrm{T}}$ respectively. v_{ji} are esimation value and are represent from a_i, k_{ji} and l_{ji} $(i = 1, 2)$.

Figure 8 shows the estimated results of equiriblium posture and joint torque. As shown in this picuture, not only the joint torque and also equiriblium posture are estimated precisely.

V. CONCLUSION

Visual stimulus was followed the normal gravitational environment and only the timing of force was changed. In this condition, the subjects could learn the proper timing of catching task. This means that the subject predict the timing of contact from the adaptation task. Also the subject shifted the simultaneity of vision and tactile stimuli.

Moreover the subject could adjust the timing of not only the static tactile environment, but also dynamic environment such as ball catching task.

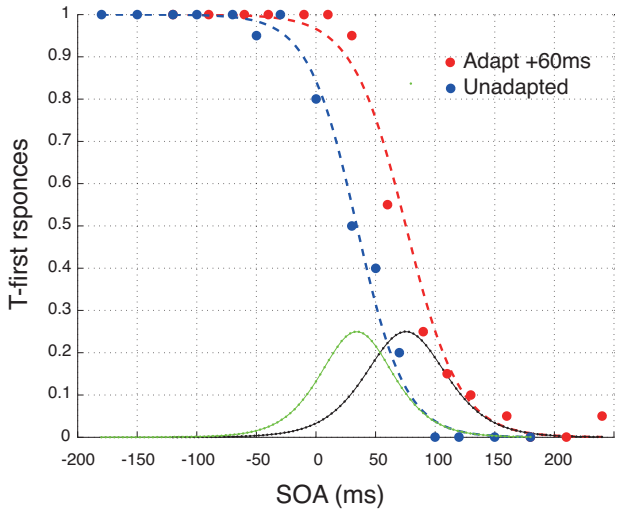

Fig. 6. Psychometric functions after adaptation

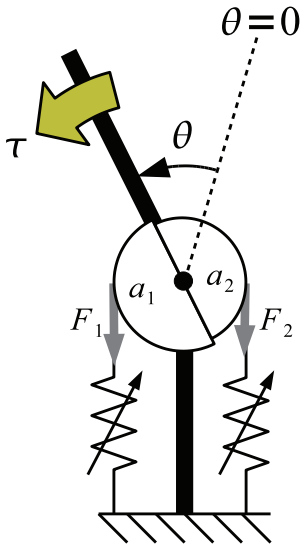

Fig. 7. Wrist model

REFERENCES

[1] W. Bair, J.R. Cavanaugh, M.A. Smith, and J.A. Movshon. The timing of response onset and offset in macaque visual neurons. *J Neurosci*, 22(8):3189–205, 2002.

[2] W. Fujisaki, S. Shimojo, M. Kashino, and S. Nishida. Recalibration of audiovisual simultaneity. *Nat Neurosci*, 7(7):773–8, 2004.

[3] Masahiro Ishii and Makoto Sato. A 3d spatial interface device using tensed strings. *Presence*, 3:81–86, 1994.

[4] A.D. Milner and M.A. Goodale. Two visual systems re-viewed. *Neuropsychologia*, 46(3):774–85, 2008.

[5] Miall Wolpert. Forward models for physiological motor control. *Neural Netw*, 9(8):1265–1279, 1996.

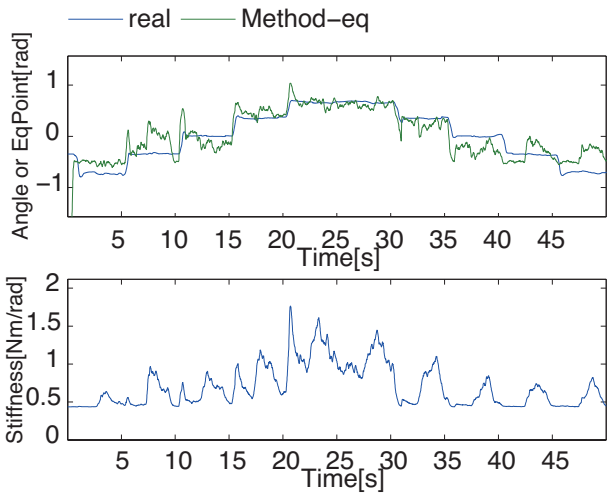

Fig. 8. Estimation result

Fig. 9. Haptic Device

Condition-dependent and condition-independent target selection in the macaque posterior parietal cortex

Tadashi Ogawa

***Abstract*— During a visual search, information about the visual attributes of an object as well as associated behavioral requirements is essential for discriminating a target object from others in the visual field. On the other hand, information about the object's position appears to be more important when orienting the eyes toward the target. To understand the neural mechanisms underlying such a transition (i.e., from nonspatial- to spatial-based target selection), we examined the dependence of neuronal activity in the macaque posterior parietal cortex (PPC) on visual sensory properties and ongoing task demands. We found that a subset of PPC neurons significantly discriminated the target from other stimuli only when the target was defined by a particular stimulus dimension and had specific stimulus features (condition-dependent target selection), while another subset did so irrespective of the stimulus features and the target-defining dimension (condition-independent target selection). A great deal of variety in the neural representations specifying the locus of the target suggests the PPC may be situated at the level where the transition from nonspatial- to spatial-based target selection takes place [25].**

I. Introduction

During a visual search, information about the visual sensory properties of individual objects and the ongoing behavioral requirements is essential for discriminating an object of interest from others in the visual field. On the other hand, information about the locus of the target is more important when shifting covert spatial attention and overt eye movement toward it. This information flow may correspond to the transition from nonspatial- to spatial-based target selection processes.

Several lines of evidence suggest the importance of the posterior parietal cortex (PPC) in the transition from nonspatial- to spatial-based target selection. On the one hand, area 7a and the lateral intraparietal area (LIP), which are visual-motor areas [1]-[3], play crucial roles in target selection [6], [9], [21], [23] spatial attention and anticipation [5], [7], [8] [10] and saccade planning [20]. On the other hand, the activity of PPC neurons can directly reflect visual sensory attributes, such as the color and shape of a stimulus [11], [15], [18], [19], [22]. Thus, the PPC may be situated such that it is able to play a key role in the transition from nonspatial- to spatial-based target selection.

To obtain insight into the neural mechanism underlying such a transition process during target selection, we examined the dependence of neuronal activity in the PPC of the macaque on visual sensory properties and ongoing task demands.

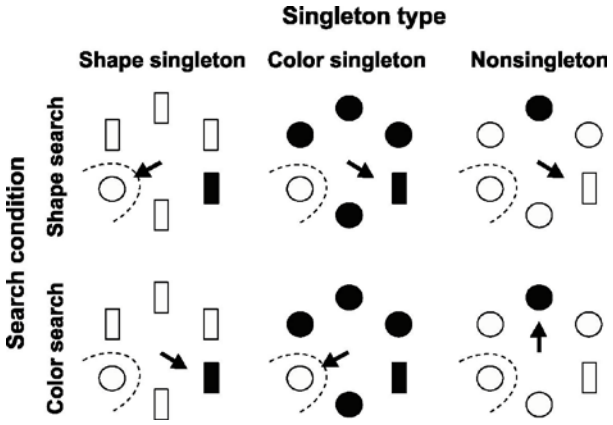

Fig. 1. Stimulus conditions for the experiment. Two singleton stimuli, one unique in the color dimension, the other in the shape dimension, were presented simultaneously with four additional identical stimuli. Open and filled symbols correspond to cyan and yellow, respectively. Monkeys had to make a saccade (*arrows*) to one of the singleton stimuli, depending upon the instructed target-defining dimension. In the shape search (*upper row*), the shape singleton was the target and the color singleton was the distractor. In the color search (*bottom row*), the shape singleton was the distractor and the color singleton was the target. The nonsingleton stimulus never became the target (nontarget). Examination of the two search conditions was conducted in separate blocks. The ongoing target-defining dimension was signaled by the color of the fixation spot.

II. Methods

The monkeys were required to perform a multidimensional visual search task (Fig. 1). In each array, two singletons, one unique in the shape dimension (shape singleton), the other in the color dimension (color singleton), were presented with four additional identical stimuli (nonsingleton). Each stimulus was made from two possible shapes (bar and circle) and two possible colors (cyan and yellow). One of the singletons served as a target and the other as a distractor, depending on the ongoing target-defining dimension, which was indicated by the color of the fixation spot (shape search, red; color search, blue). In the shape search, the shape singleton was the target, and the color singleton was the distractor (upper row in Fig. 1), and the opposite was the case in the color search

Tadashi Ogawa, Dept of Integrative Brain Science, Graduate School of Medicine Kyoto University, Sakyo-ku 606-8501, Kyoto, Japan (tel: +81-75-753-4678, e-mail: togawa@brain.med.kyoto-u.ac.jp)

Original manuscript was received July 28, 2008, accepted in final form December 4, 2008 and published in February from *Journal of Neurophysiology*[25]. This work was supported by grants from the Japan Society for the Promotion of Science and by a Grant-in-Aid for Scientific Research on Priority Areas. "Emergence of Adaptive Motor Function through Interaction between Body, Brain and Environment" from the Japanese Ministry of Education, Culture, Sports, Science, and Technology

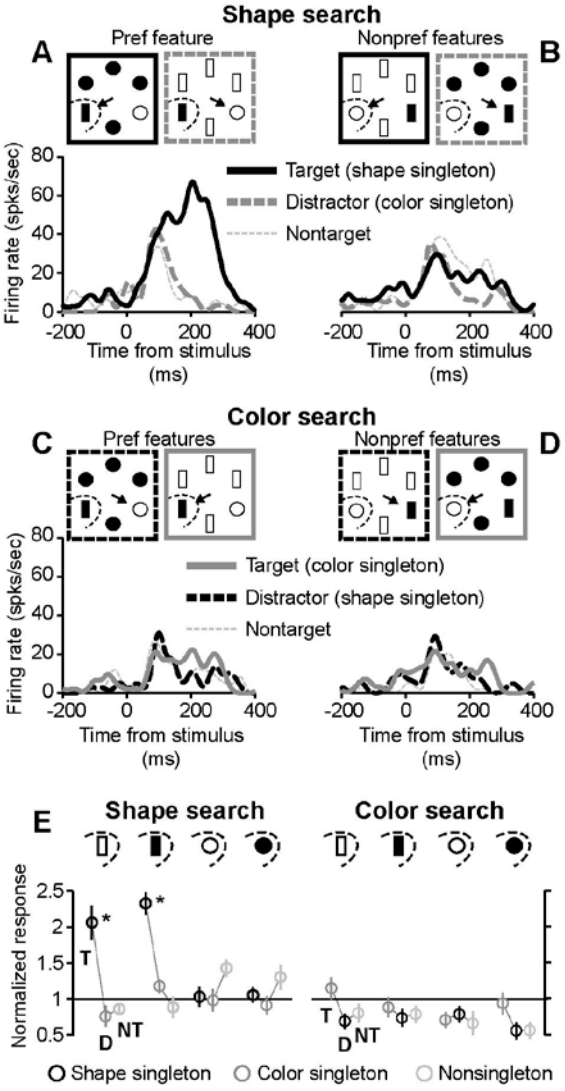

Fig. 2. A parietal neuron showing dependence on stimulus features and the target-defining dimension
(A-D) Spike density functions during the multidimensional visual search task. Thick black and gray lines indicate the responses to the shape and color singleton stimuli appearing in the receptive field. Dotted thin gray lines indicate the responses to a nontarget (nonsingleton) stimulus. Solid and dashed lines respectively indicate that the stimulus in the receptive field was the target or distractor. The responses are temporally aligned at the onset of the stimulus array. (E) Normalized mean responses (with SE) of the same neuron for the entire set of 24 trial conditions, which were calculated by dividing the responses to the 24 different stimulus conditions by their average. Upper insets indicate the stimulus features in the receptive field in the shape search (left) and the color search (right). In each set, three connected circles respectively indicate from left to right that the stimulus in the receptive field was the target (T), distractor (D) or nontarget (NT). Asterisks indicate significant difference from the two other responses in each set (Mann-Whitney U test, $p < 0.01$).

(lower row in Fig. 1). A nonsingleton never became the target under either search condition (this stimulus condition will be referred to as nontarget, in contrast to the target and distractor conditions).

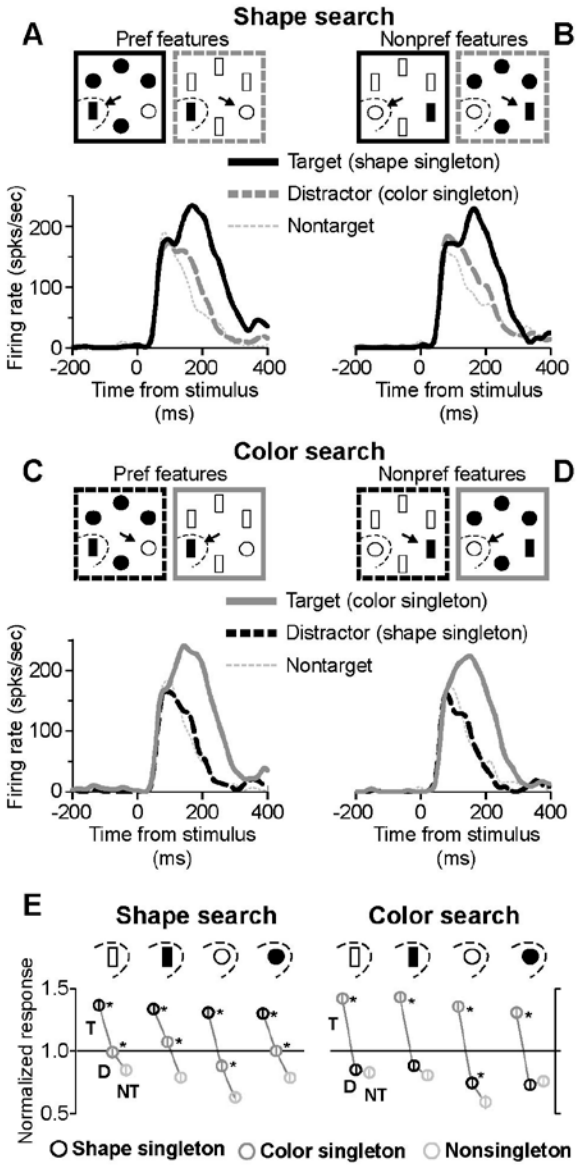

Fig. 3. A parietal neuron showing no dependence on stimulus features or the target-defining dimension
The activity of this neuron always exhibited significant discrimination of the target from the other stimuli, irrespective of the stimulus features and target-defining dimension. Conventions are the same as in Fig. 2.

III. Results

Activity of posterior parietal neurons in the multidimensional visual search task

Figure 2 shows one representative neuron. The response patterns elicited in this cell by the target stimulus varied greatly, depending on the stimulus features and the target-defining dimension. This neuron showed the greatest activity when the target was a yellow bar and the target-defining dimension was the shape dimension (black trace in Fig. 2A). Under those conditions, the activity significantly discriminated the target from the distractor and

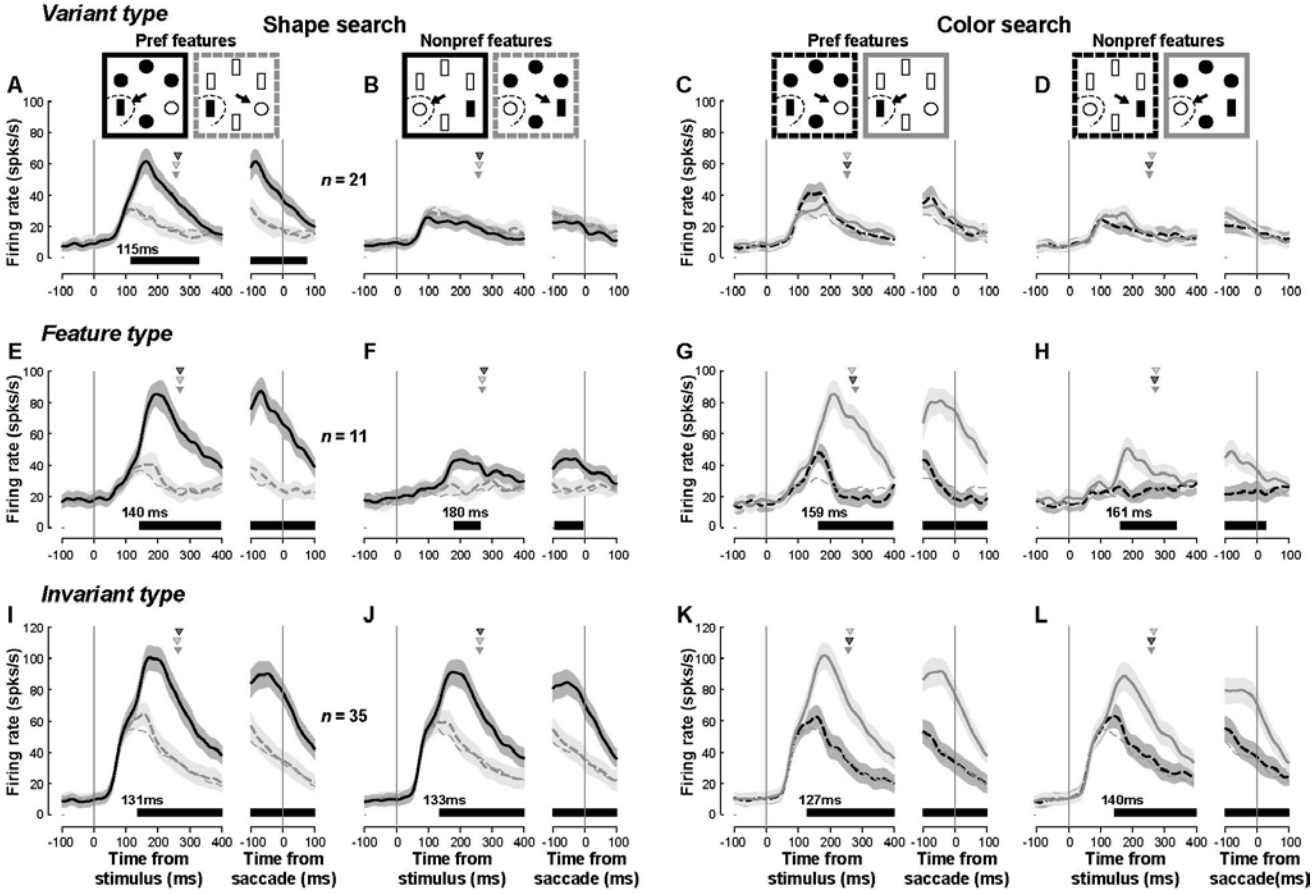

Fig. 4. Time course of the population responses

Average population responses of the variant type neurons (n =21) in the shape search (A, B) and the color search (C, D). For clarity, only neurons that preferred the shape dimension are shown. The stimulus shown in the receptive field had either the preferred (A, C) or nonpreferred (B, D) stimulus features. Traces in each panel are aligned at the time of array presentation (left panel) or saccade initiation (right panel). Thick solid, thick dashed and thin dotted lines indicate the population responses to the target, distractor and nontarget stimuli, respectively. Black, gray and blue lines respectively correspond to the responses to a shape, color and non singleton stimuli. Shaded areas indicate 1 SE. Black, gray and blue triangles respectively denote mean saccade reaction times when a shape, color, or non singleton stimulus was presented within the receptive field. Horizontal black lines below the spike density functions indicate the period during which the target was significantly discriminated from the distractor and nontarget stimuli (permutation test, $p < 0.01$). The number above this horizontal line indicates the first time after the stimulus onset that target discrimination became significant and continued for at least 50 ms. (E-H) Time course of the population responses of the feature type neurons (n = 11) are shown in the same format as in A-D. (I-L) Time course of the population responses of the invariant type neurons (n = 35).

nontarget stimuli (Mann-Whitney U test, $p < 0.001$). By contrast, when the stimulus features of the target were changed from a yellow bar to a cyan circle (black trace in Fig. 2B), when the target-defining dimension was changed from the shape dimension to the color dimension (gray trace in Fig. 2C), or when both the stimulus features and the target-defining dimension were changed (gray trace in Fig. 2D), the magnitude of the activity elicited by the target stimuli were significantly less than the maximal response (Mann-Whitney U test, $p < 0.001$) and were no longer sufficient to significantly discriminate the target (Mann-Whitney U test, $p > 0.05$).

Figure 2E shows the normalized responses for the entire set of 24 trial conditions (two shapes × two colors × three behavioral relevance × two search dimensions). This neuron only exhibited significant target discrimination when the target was a bar stimulus and was defined in the shape dimension (Mann-Whitney U test, $p < 0.001$). Thus, the activity related to target discrimination was highly selective for the combination of the stimulus features and the target-defining dimension.

Figure 3 shows another representative neuron whose response profile is very different from that of neuron in Fig. 2, in that the activity elicited by the target was much less dependent on the stimulus features and the target-defining dimension during the visual search. Figure 3E shows that under all eight target conditions the responses to the target were significantly larger than those to the distractor and nontarget stimuli (Mann-Whitney U test, $p < 0.001$), irrespective of the stimulus features and the target-defining dimension.

Time course of neural representation of target

information

Figures 4A-D show activity averaged across the variant type neurons. For clarity, only the neurons that preferred the shape dimension were considered (n=21). The response was significantly larger when the target stimulus in the receptive field had the preferred stimulus features and was defined in the shape dimension (black solid trace in Fig. 4A) than when the identical stimulus was the distractor or the nontarget (gray dashed and gray dotted thin traces in Fig. 4A). However, when the stimulus features of the target were changed to the nonpreferred ones (black trace in Fig. 4B) or when the target was defined in the color dimension (gray traces in Figs. 4C and D), there was no evident increase in the response to the target, and the significant target discrimination disappeared (permutation test, $p > 0.01$).

Figures 4E-H show the activity averaged across the feature type neurons (n=11). When the target had the preferred features in the shape search (black trace in Fig. 4E) or in the color search (gray trace in Fig. 4G), the activity significantly discriminated the target from the other stimuli. However, when the stimulus features of the target were changed to the nonpreferred ones (black trace in Fig. 4F and gray trace in Fig. 4H), the magnitude of the increase in activity elicited by the target was substantially diminished, but the average population responses still significantly discriminated the target from the other stimuli (permutation test, $p < 0.01$) around 160-180 ms after array presentation.

Figures 4I-L show activity averaged across the invariant type neurons (n=35). Irrespective of the stimulus features and the target-defining dimension, the target discrimination became significant around 130-140 ms after array presentation (permutation test, $p < 0.01$) and remained significant throughout the trials.

IV. Discussion

We found that the neural representation specifying the locus of a target showed a great deal of variability in PPC neurons. At one extreme was a subset of neurons that exhibited significantly enhanced activity only when the target had the preferred stimulus features and was defined in the preferred stimulus dimension (variant type, Figs. 4A-D). An intermediate subset of neurons showed strongly increased activity when the target had the preferred stimulus features (feature type, Figs. 4E-H). Finally, a subset of neurons at the other extreme invariably exhibited enhanced activity when the target was in the receptive field, irrespective of the stimulus features and target-defining dimension (invariant type, Figs. 4I-L). Such a wide variety of condition-dependent and condition-independent target selection processes suggests that the PPC may be one of the sites in the cortex where the transition from nonspatial- to spatial-based target selection processes takes place.

References

[1] Andersen RA, Asanuma C, Essick G, and Siegel RM. Corticocortical connections of anatomically and physiologically defined subdivisions within the inferior parietal lobule. J Comp Neurol 296: 65-113, 1990.

[2] Barash S, Bracewell RM, Fogassi L, Gnadt JW, and Andersen RA. Saccade-related activity in the lateral intraparietal area. I. Temporal properties; comparison with area 7a. J Neurophysiol 66: 1095-1108, 1991a.

[3] Barash S, Bracewell RM, Fogassi L, Gnadt JW, and Andersen RA. Saccade-related activity in the lateral intraparietal area. II. Spatial properties. J Neurophysiol 66: 1109-1124, 1991b.

[4] Bichot NP, Rossi AF, and Desimone R. Parallel and serial neural mechanisms for visual search in macaque area V4. Science 308: 529-534, 2005.

[5] Bisley JW and Goldberg ME. Neuronal activity in the lateral intraparietal area and spatial attention. Science 299: 81-86, 2003.

[6] Buschman TJ and Miller EK. Top-down versus bottom-up control of attention in the prefrontal and posterior parietal cortices. Science 315: 1860-1862, 2007.

[7] Bushnell MC, Goldberg ME, and Robinson DL. Behavioral enhancement of visual responses in monkey cerebral cortex. I. Modulation in posterior parietal cortex related to selective visual attention. J Neurophysiol 46: 755-772, 1981.

[8] Colby CL, Duhamel JR, and Goldberg ME. Visual, presaccadic, and cognitive activation of single neurons in monkey lateral intraparietal area. J Neurophysiol 76: 2841-2852, 1996.

[9] Constantinidis C and Steinmetz MA. Neuronal responses in area 7a to multiple-stimulus displays: I. neurons encode the location of the salient stimulus. Cereb Cortex 11: 581-591, 2001.

[10] Duhamel JR, Colby CL, and Goldberg ME. The updating of the representation of visual space in parietal cortex by intended eye movements. Science 255: 90-92, 1992.

[11] Durand JB, Nelissen K, Joly O, Wardak C, Todd JT, Norman JF, Janssen P, Vanduffel W, and Orban GA. Anterior regions of monkey parietal cortex process visual 3D shape. Neuron 55: 493-505, 2007.

[12] Hamker FH. A dynamic model of how feature cues guide spatial attention. Vision Res 44: 501-521, 2004.

[13] Itti L and Koch C. A saliency-based search mechanism for overt and covert shifts of visual attention. Vision Res 40: 1489-1506, 2000.

[14] Koch C and Ullman S. Shifts in selective visual attention: towards the underlying neural circuitry. Hum Neurobiol 4: 219-227, 1985.

[15] Konen CS and Kastner S. Two hierarchically organized neural systems for object information in human visual cortex. Nat Neurosci 11: 224-231, 2008.

[16] Ogawa T and Komatsu H. Neuronal dynamics of bottom-up and top-down processes in area V4 of macaque monkeys performing a visual search. Exp Brain Res 173: 1-13, 2006.

[17] Ogawa T and Komatsu H. Target selection in area V4 during a multidimensional visual search task. J Neurosci 24: 6371-6382, 2004.

[18] Sereno AB and Amador SC. Attention and memory-related responses of neurons in the lateral intraparietal area during spatial and shape-delayed match-to-sample tasks. J Neurophysiol 95: 1078-1098, 2006.

[19] Sereno AB and Maunsell JH. Shape selectivity in primate lateral intraparietal cortex. Nature 395: 500-503, 1998.

[20] Snyder LH, Batista AP, and Andersen RA. Coding of intention in the posterior parietal cortex. Nature 386: 167-170, 1997.

[21] Thomas NW and Pare M. Temporal processing of saccade targets in parietal cortex area LIP during visual search. J Neurophysiol 97: 942-947, 2007.

[22] Toth LJ and Assad JA. Dynamic coding of behaviourally relevant stimuli in parietal cortex. Nature 415: 165-168, 2002.

[23] Wardak C, Olivier E, and Duhamel JR. Saccadic target selection deficits after lateral intraparietal area inactivation in monkeys. J Neurosci 22: 9877-9884, 2002.

[24] Wolfe JM. Guided search 2.0: A revised model of visual search. Psychonomic Bulletin & Review 1: 202-238, 1994.

[25] Ogawa T and Komatsu H, Condition-dependent and condition-independent target selection in the macaque posterior parietal cortex. J Neurophysiol. 101: 721-736, 2009

Study of Cooperative Optimization Problems between Two Humans by Mutual Tracking

Y. Sawada and Y. Hayashi, Tohoku Institute of Technology
sawada@tohtech.ac.jp

1. The condition of successful communication

Verbal communication is essential for human society and human civilization. Non-verbal communication, on the other hand, is more widely used not only by human but also other kind of animals, and the content of information is estimated even larger than the verbal communication.

Among the non-verbal communication mutual motion is the simplest and easiest to study experimentally and analytically. The preliminary data of the mutual tracking experiment is shown in Fig.1 and Fig.2

Fig.1 shows the mutual correlation function of the velocities of two subjects in the reactive tracking experiment, that is, the subject is asked to track as accurate as possible but not to pass the marker of the other subject. Fig.2 shows the same in proactive tracking experiment, that is, the subject is asked to track as accurate as possible but not to be passed by the marker of the other subject. The graphs show that the simultaneous correlation (the value for τ =0) is high for proactive tracking and that it is low for reactive tracking. If we consider that the high mutual correlation is good communication, the data shows that proactive control is important for communication.

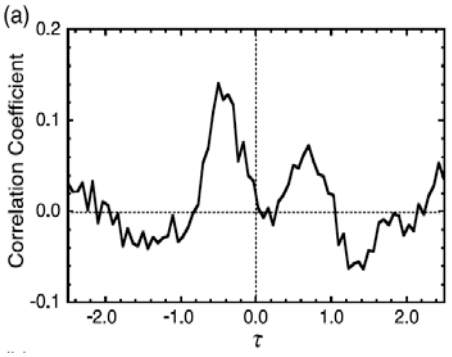

Fig.1. Mutual velocity correlation function in reactive trackingexperiment

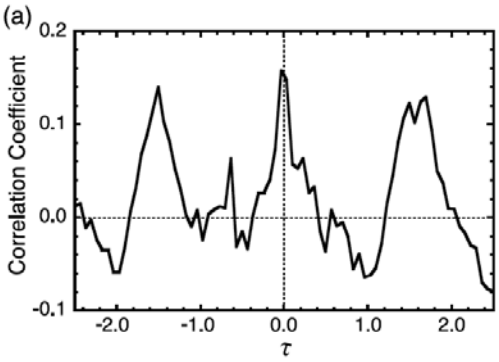

Fig.2 Mutual velocity correlation function in proactive tracking experiment

2. Importance of proactive control

Predictive function is important for human and other animals to adapt for the constantly changing environment and to communicate smoothly with other members of the society(1,2,4). The “real time” response cannot be realized without this function by humans and other animals which is not equipped with the fast response system of milliseconds

which modern robots easily achieve.

Proactive response is widely observed in the human life, such as in driving a car in a curved road(2). Proactive control to move the hands preceding the target is realized by over-predicting and over-compensating the delay. The advantage of moving the body preceding the change of environment exists in the statistical reduction of the error of the body motion.(1,2,3) Optimization of the dynamic error realized by proactive control, thus consists one of the important principle of the MOBILIGENCE.

3. The unsolved problems of predictive function in proactive control

The model (1,3,4) we proposed for proactive control consists of an ordinary feedback term and a feedforward term which is the target velocity multiplied by an unknown factor γ slightly greater than unity. Both terms are expressed at t $-\delta$、where δ is the delay time necessary for perception and information processing to drive muscles. Although the model explains the main part of the experimental observation, there remained unsolved problems.

(1) What is γ in the model?
(2) The model failed to explain the missing proaction in the low frequency region (f<0.3Hz) for the harmonic motion in a linear orbit.
(3) How one recognizes the speed of the target expressed in the model?
(4) Why the feedback term and feedforward term is added to drive muscle?

4. The purpose of the present research

We have made research to solve the problems cited above, especially in this work we focused on a problem why some rhythmic component appears in the velocity spectrum when the hand is proactive. The experimental research we have pursued so far in this project suggested that mainly 2f component rhythmic motion always appears when the hand motion is proactive. We hoped this might give a solution to unsolved problem (3).

5. Experimentals

1)Tracking in a straight linear orbit and the velocity power spectrum

This experiment was undertaken to clarify the difference between the tracking characteristics of circular orbit and linear orbit. Target velocity; 3m/37.5sec. Distance of the screen from the subject;4m Maximum vision angle ~80degree

2)Blind tracking and the velocity power spectrum

Target is not shown, but the orbit is always shown (linear or circular). In this paper experiments was performed only for a circular orbit. f=0.1Hz

3)Intermittent blind tracking and the velocity power spectrum

The circular orbit was constructed by two target –hidden regions (each 30%, at the top and the bottom) and two target－shown regions (each 20%, at the right and the left ends)

6. The results and discussions

1) Tracking in a straight linear orbit

Fig 3 shows a typical example of the

power spectrum of the hand velocity in this condition. The spectrum is not far from a Gaussian with its peak around 1Hz and the half width of 1Hz. The power spectrum is close to what was observed for a circular orbit (Fig4), except the fact that the spectrum for the circular orbit has a longer tail. The difference is discussed in the next section.

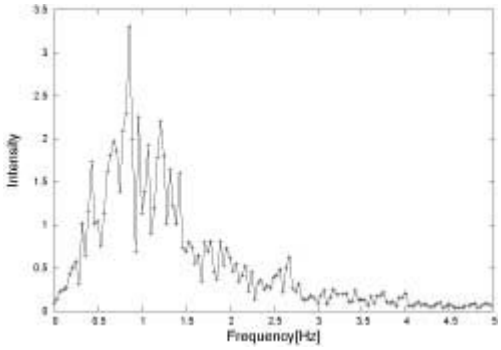

Fig. 3 Power spectrum of tracking velocity in a straight linear orbit

2) Blind tracking in a circular orbit

Fig.5 shows a typical example of the power spectrum of hand velocity of the blind tracking in a circular orbit. The spectrum has a long tail with no peak, and clearly different from Fig.3 and Fig.4 This interesting results seem to show

1)The spectrum in blind tracking represent lateral error correction from the orbit. It is necessary in near future to verify the results in a linear orbit.

2)The spectrum of tracking in a circular orbit(Fig.4) may be understood as being composed of the authentic tracking spectrum(Fig.3) and the lateral orbit correction spectrum(Fig5)

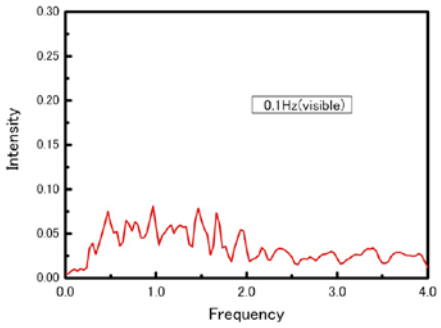

Fig.4. Power spectrumof tracking velocity in a circular orbit at f=0.1Hz

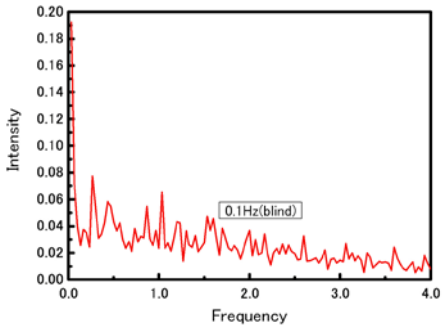

Fig.5 Power spectrum of blind tracking velocity in a circular orbit at f=0.1Hz

1) Intermittent blind tracking

Fig.6 and Fig.7 illustrate the power spectra of intermittent blind tracking (red lines) at f=0.1Hz and f=0.7Hz, respectively. Black lines show the normal tracking at the same frequencies. The results seem to show that

1) Only the feed-back mechanism seems to operate when there is no structure on the orbit.
2) The rhythm components of f and 2f (f is the target frequency) appears even at the low frequency f=0.1Hz when there is a structure on the orbit.
3) Fig 7 shows that rhythmic components appear when the target speed is high, whether or

not the orbit has a structure. The reason for this result may be understood that the whole symmetry of circle was lowered by the preferential axis of eye motion and/or muscle motion. This situation would be special to a circular orbit because no rhythmic motion can be expected in a linear orbit other than the broad feed-back spectrum shown in Fig 3.

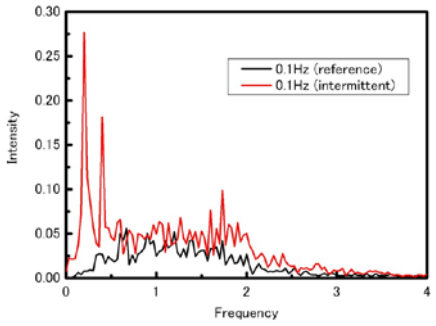

図 6　Power spectrum of　tracking velocity in an intermittent circular orbit at f=0.1Hz (red line). Power spectrum of an ordinary tracking velocity (black line)is shown for comparison for the same frequency

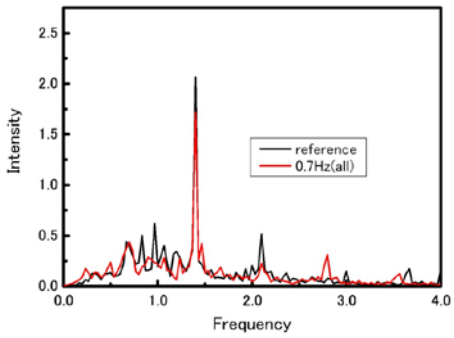

図 7 Power spectrum of　tracking velocity in an intermittent circular orbit at f=0.7Hz (red line). Power spectrum of an ordinary tracking velocity (black line)is shown for comparison.

7. Conclusive remarks

We measured the power spectrum of the hand velocity in various conditions and clarified the following points on the feed-back and feed- forward mechanism as basic knowledge to understand the condition of good communication.

1) The spectrum of tracking error correction (feed-back term)is a broad Gaussian type with its peak at ~1Hz and half width of ~1Hz.
2) The spectrum of lateral error correction from the orbit is a long tail type with no peak.
3) The feed-forward mechanism seems to function by creating and remembering a rhythmic component in the velocity which reflects some structure available in the orbit. Proactive control and good communication seem to work when this mechanism functions to a sufficient level.

Reference

1）”Human hand moves proactively to the external stimulus; An evolutional strategy for minimizing transient error”, F.Ishida and Y.Sawada, Physical Review Letters, 96, 168105(2004)

2) 高齢運転者のカーブ走行時運転挙動特性について―ドライビングシミュレーターによる走行実験分析― (in Japanese)
高地康弘、村岡一信、沢田康次、太田博雄
人間工学　44(2008)、165-170

3）”Semi-analytical transient solution of a delayed differential equation and its application to the tracking motion in the sensory-motor system”, F.Ishida and Y.Sawada, Physical Review E 75, 9,12901(2007)

4) 予測と行為 ー主体的行為はいかにして可能かー(in Japanese)
沢田康次、石田文彦
計測と制御　48 (2009), 60-65

Representation of self and other in the parieto-premotor network

Murata A and Ishida H., Department of Physiology, Kinki University School of Medicine

Abstract— **It is well known that parietal cortex is much concerned with self body representation by integrating visual and somatosensory input. Furthermore, it is claimed that other is represented in the brain with self. Mirror neuron is one example. These neurons represent image of other's behavior on own motor representation. This suggests shared representation of self body and other's body in the brain. We found that some of parietal bimodal neurons were concerned with representation of both self and other's body. In 2008, the paper reported these neurons has been accepted to J. Cog Neuroscience[2]. Then we also report the results of information analysis of spike frequency of single neurons of area AIP and F5 with collaboration of University of Electro-communication.**

I. REPRESENTATION OF OTHER'S BODY IN THE BRAIN

THE parietal cortex is much involved in self body representation. For corporeal awareness, integration of visual-somatosensory is very important. Actually in the parietal association cortex, there are several areas where multimodal neurons are found, for example visual-tactile bimodal neurons. In these areas, properties of area VIP have been well studied[3]. The tactile receptive fields of the neurons are usually located on the face, head or sometimes limbs and the visual receptive fields are in the locations congruent with the tactile receptive fields. In many cases, the visual receptive fields are located very close to the body, namely in the peripersonal space. These neurons may encode body parts centered frame of reference.

On the other hand, self and other are encoded in the brain on the same neuronal bases. For example mirror neurons represent other's visual action on own motor representation[4]. The function of these neurons is considered to be related to action recognition. Existence of mirror neurons suggests that there are some mechanisms for recognition of other's body in the brain. For moment, it is not clear how the brain represent other's body. In the imitation of other's action, matching own body and other's body seems to be necessary. Decety et al. suggested that self body and other's body were represented in the shared brain network[5]. Further, it was reported a female subject for whom the observation of another person being touched was experienced as tactile stimulation on the equivalent part of own body[6]. In addition, the case of an anosognosic patient who denied another patient's paralysis has suggested the importance of own body representations for perception of others' bodies[7]. Accordingly, we suggest that the process of corporeal awareness share the mechanisms to percept self and other's body. In this paper, we will report neuronal activity that is related to both self and other bodily perception. We expect that other's body map in the brain may exist on one's own body map. We studied neuronal activity in area VIP whether these neurons would be related to other's body representation. The paper concerned the results has been accepted to J Cog.Neuroscience[2] and also reported at the meeting of FENS2008[8].

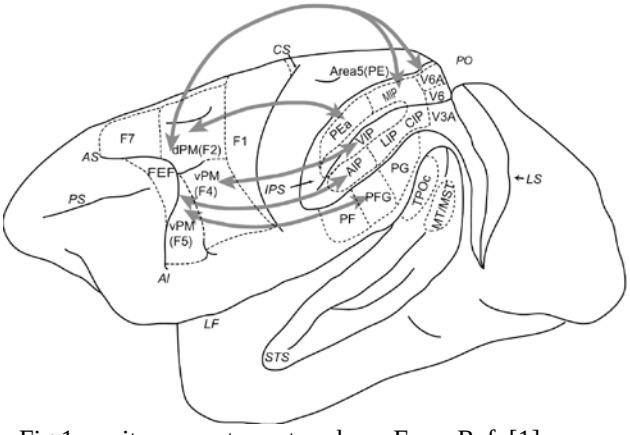

Fig.1 parito-premotor networks From Ref. [1]

1. Materials and methods

Single neurons in the ventral intraparietal area and area 7b (PF/PFG) were recorded from four hemispheres of three Japanese monkeys. The electrode was inserted from the lateral convexity of the inferior parietal cortex, then went inside of the medial or lateral bank of the intraparietal sulcus, The border of VIP was functionally recognized on the basis of distribution of tactile and visual receptive fields (RFs). Neurons in area VIP showed tactile RFs principally located on the face and visual RFs, limited to the peripersonal space, in register with the tactile ones.

Once a cell was isolated, we tested with a standard battery of tactile and visual stimuli. Somatosensory stimuli consisted of hair bending, touch of the skin, gentle pressure of the tissue, manipulation of the joint. Somatosensory RFs were plotted by repeated presentation of the most effective of these stimuli. Somatosensory responses were tested while the eyes were covered. Visual stimuli consisted of three-dimensional real objects. Geometrical solids, food and various objects found at hand in the laboratory were used. No obvious differences were observed between these stimuli in determining neuronal responses. A quantitative study of preferences of neurons for different stimuli was not carried out in the present study, however.

In order to investigate the RFs of neurons, stimuli were moved by hand towards the animal from different angles and distance. The procedure was repeated again and again until the borders of the visual RFs were defined. Especially, we were very careful for the extension in the depth of the RFs.

After mapping of the tactile and visual RFs, an experimenter confronted with the monkey. To ensure that bimodal neurons also responded to stimuli within other's peripersonal space, visual stimuli were presented vicinity of the experimenter's body parts and explored visual RFs.

Additionally, when the monkey observed visual stimuli near the experimenter's body parts, the experimenter kept regular distance 120cm from the monkey. The reason of this regulation was to exclude the possibility of a false interpretation that the neuronal response merely due to simple visual response within the visual RFs in the extrapersonal space. Since previous studies suggested that the extension in the depth of visual RFs in VIP was 5cm to 50cm from the surface of body: we set the distance between the monkey and experimenter more than twice of that.

2. Results

We recorded 541 visuo-tactile bimodal neurons from VIP and 7b (PF/PFG). Tactile RFs were mostly located on a single body part (n =451, 83%), that is, on the face (n = 294), forearm, hand, digit (n = 131; visual-tactile, n = 68;visual-joint, n = 63), or trunk or leg (n = 26). Another 13% (n = 69) were located on multiple body parts including the hemibody, with the majority on the face, upper limb, or trunk (n = 50). RFs of almost all of these neurons (96%) tended to be spatially congruent in the both modalities. Most RFs were located on the contralateral side of the body (66%), though some were also found bilaterally or centrally (25%) or ipsilaterally (4%). The remaining RFs could not be placed in any of these categories. .

Forty-eight bimodal neurons also responded to the visual stimuli presented near the experimenter's body parts. In these neurons, 23 neurons were studied distribution of RFs in detail. Remarkably, visual RFs surround the experimenter's body parts of these neurons corresponded with location of bimodal RFs on the monkey's body parts. As shown in Fig.2, the neuron showed tactile RFs particularly on the left cheek of the monkey and visual RFs extended within 30 cm from the cheek. Furthermore, when the monkey observed visual stimuli moving close to experimenter's left cheek, the neuron particularly discharged. This neuron showed strong directional selectivity, that is, preferred to rightward movement with respect to the monkey's perspective. Importantly, the visual RF around the experimenter's face was in a mirror image position with respect to the monkey's visual RF. As a result, 23 of 10 neurons showed this mirror image matching of the RFs.

In addition, we found other type of distribution of RFs. For example, bimodal RFs located in the center of monkey's face. The neuron discharged when the monkey observed visual stimuli moving close to the center of the experimenter's face. This type also involved some neurons that showed RFs on the bilateral body parts (ex. both hands). We found that 10

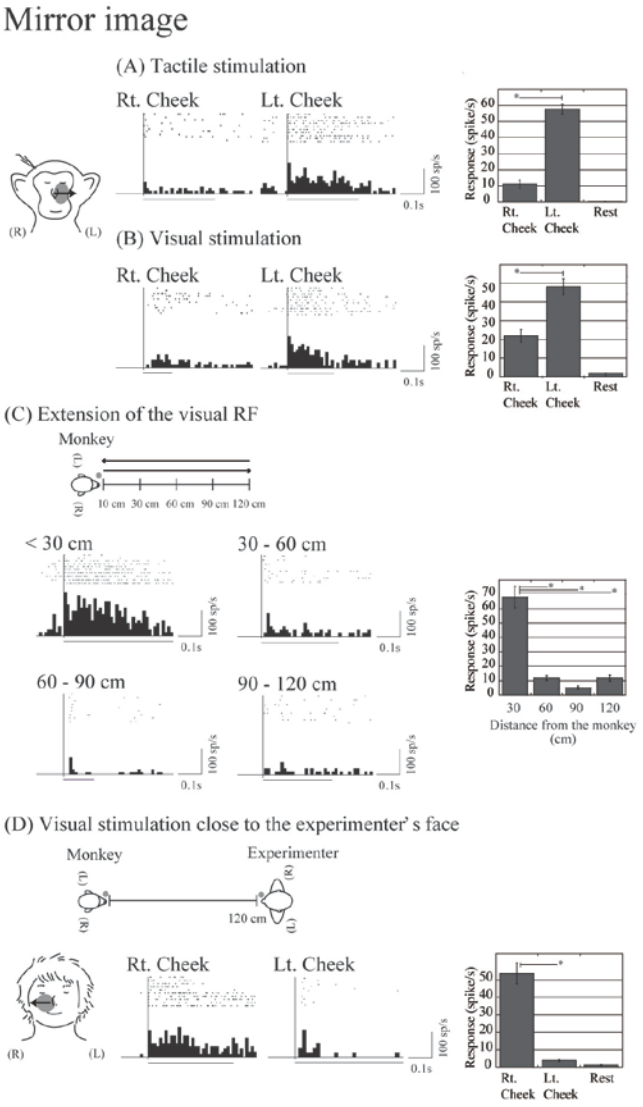

Fig.2 Tactile (A) and visual RF (B) were on the left cheek of the monkey. Visual RF was within 30cm from the body. The same neuron had RF on the confronted experimenter' s right cheek. From Ref. [2]

neurons showed this center matching or bilateral mating of RFs.

In contrast with mirror image, despite the experimenter confronted with the monkey, location of RFs matched anatomically with the same side of the body each other (left to left). Of 23 neurons, three neurons have this kind of an anatomical correspondence.

In seven of these neurons, we also studied the extension of visual RFs in between the monkey and experimenter to ensure that visual RFs just anchored on the experimenter's peripersonal space, visual stimuli were presented each position between the monkey and experimenter. All these seven neurons only responded when stimuli were within approximately 30cm from the monkey and experimenter's body surface respectively. The neurons did not respond

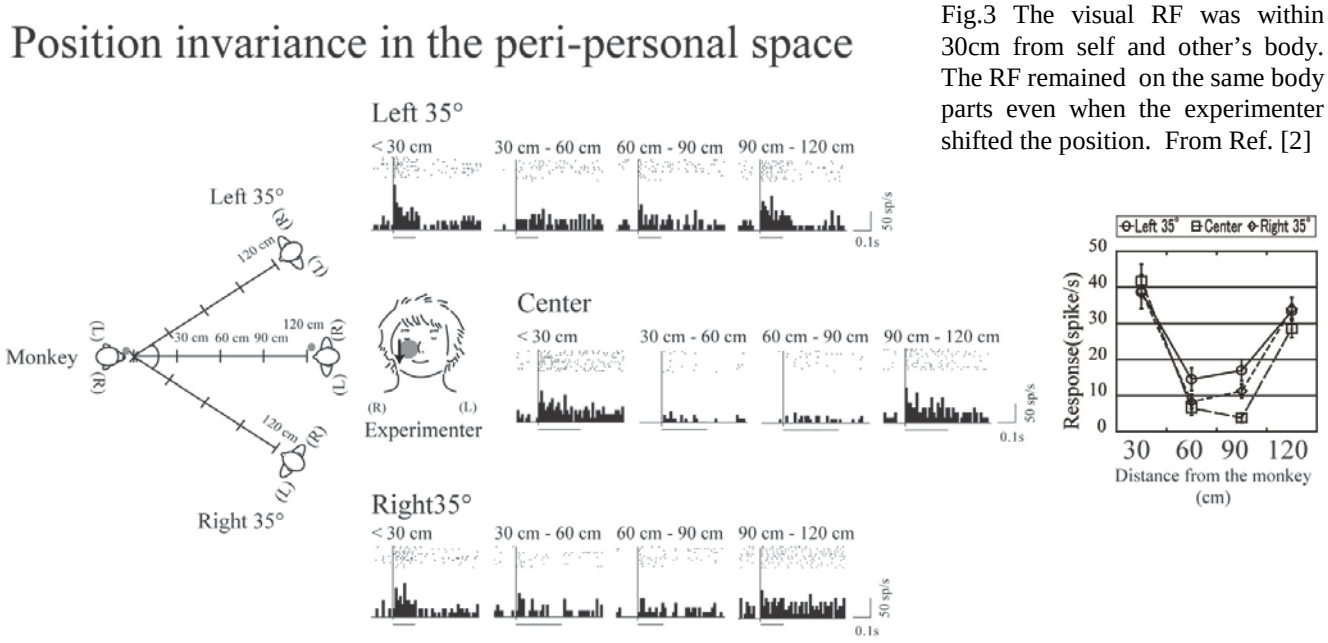

Fig.3 The visual RF was within 30cm from self and other's body. The RF remained on the same body parts even when the experimenter shifted the position. From Ref. [2]

outside of the peripersonal space in between the monkey and experimenter.

Furthermore, to elucidate reliability of visual RFs on the experimenter's body, we investigated activity of two of these neurons when the experimenter shifted the sitting position to the left or right side of the monkey maintaining 1.2m distance. As shown in Fig 3, the RFs were on the monkey left cheek and experimenter's right cheek. The RFs was within peripersonal space (<30cm) of both the monkey and experimenter, and when stimuli were presented in the intermediate space between both bodies, the neurons was less active. Furthermore, the RFs remained on the same body part.

Taken together, activities of these VIP bimodal neurons were independent of position of the experimenter (the other) and may be represented self and others body parts independently from egocentric spatial position.

3. conclusion

These results suggest that other's body parts is encoded in the same area that is related to one's own body parts, and a map of self body parts is referred for recognition of other's body. For the adaptive behavior in the robotics, it is a big issue how the system recognizes other's body. In the imitation, the system should superimpose other's body onto one's own. Our data will provide important idea for matching system between one's own body and other's.

The response properties of these neurons may appear to be associable with those of mirror neurons. These mirror neurons have been proposed to play important roles in action recognition and imitation learning. For these cognitive functions, representation of other's body is necessary in one's own brain. It is noteworthy that VIP has much connection with PF/PFG in which mirror neurons were recorded. It is possible that VIP send other's body representations to the mirror neuron.

II. INFORMATION ANALYSIS FOR HAND MANIPULATION RELATED ACTIVITY OF AIP AND F5 NEURONS

In a previous study, information analysis has been applied to neuronal activity of face neurons in inferior temporal cortex. The study revealed that the neurons encoded global information of the face in early phase of processing and then fine information of the face was conveyed later. Of course, this information analysis could be adopted in other all spike data. For example, if it is applied to the spike data in motor control system, it might be possible to reveal dynamics of intra and/or inter areas in temporal sequence.

The connection between parietal cortex and premotor cortex is concerned with sensory motor control. In this study, information analysis was adapted to investigate functional properties of each area. Real neuronal spike data recorded from inferior parietal area and ventral premotor cortex (provided from a group of Parma University) that concern to precise distal hand movement was analyzed. The study has been done by collaboration with Sakaguchi's group in University of Electro-Communications [9].

The data was recorded from monkey parietal (area AIP) and ventaral premotor cortex (F5) that was well known to be related to precise control of distal hand movement. In the recording session, the monkeys were required to manipulate an object with guidance of LED spot (hand manipulation task). The monkey was asked to fixate on the object and then reach and grasp it. The neurons in this area were classified into five types according activity for motor component and visual stimuli. Visual-motor neurons showed less activity during manipulation in the dark than in the light. Visual dominant neurons were not active during manipulation in the dark. Motor dominant neurons did not show any difference of activity in the dark and the light. The neurons with visual input

were also subdivided into object type which showed visual response to the objects, and non-object type which did not show[10]. In the recording experiment, six different objects, plate, ring, cube, cylinder, cone and sphere were adopted for grasping and the activity of these neurons was selective to these 3D properties. The information analysis was applied to spike data of these hand manipulation neurons from F5 and AIP. Mutual information (MI) was calculated between spike frequency of single neurons and various combinations among 6objects. Analysis for each type of neurons was done separately. The calculation was performed with a following function in each 50 ms during task trials.

$$I(S;R) = H(S) - H(S \mid R)$$
$$= \sum_{s} -p(s)\log p(s) - \langle \sum_{s} -p(s \mid r)\log p(s \mid r) \rangle_{r} \quad (1)$$

In this function, *H* indicates entropy. *S* and R are sets of the objects and number of spikes, respectively. The conditional entropy $H(S \mid R)$ is the uncertainty about *S* after observing spikes. In this study, MI was calculated using activities of 122 single neurons in all possible combination of two groups of six objects. Then relationship between the timing of peak and the task phase (i.e., fixation of the object, reaching , and grasping) was examined in each types of neurons.

It was revealed that there was much difference among type of neurons and between recorded areas. Visual-motor neurons object type in AIP showed faster latency of MI peak value in the fixation period than in F5. On the other hand, In visual-motor neurons object type of F5, MI increased gradually in this period. As for motor dominant neurons of AIP, peak value of MI was found in the phase of preshaping before grasping the object and similar tendency found also in visual-motor neurons in F5. MI changed with temporal sequence in the task then also showed different latency between two areas.

As in the following figure, AIP has strong connection with F5 in the ventral premotor cortex. Our previous study suggested that AIP received visual information about 3D objects and this information was sent to F5, then appropriate motor pattern was selected in F5, while the copy of this motor information returned to AIP in which matching with visual information occurred. The early peak latency in the fixation period may reflect to object information, while F5 builet-up activity in F5 may concern to visuo-motor transformation. Analyze of MI using spike data may reveal stream of

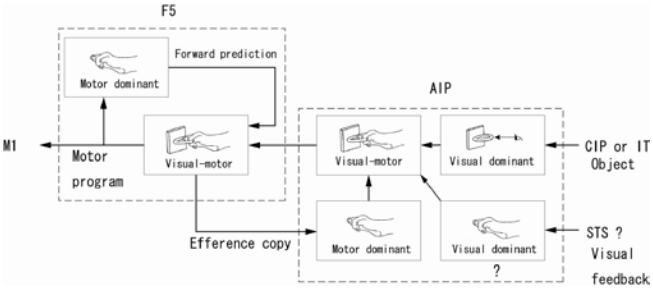

information in the temporal sequence. This is not only useful dynamics in the cortical motor control system, but also functional model of mirror neuron system and body recognition system, since motor control system are shared with these systems.

ACKNOWLEDGMENT

The MI analysis mainly has been done by Mr. Takashi Shimizu and Dr. Fumihiko Ishida with leadership of Prof. Yutaka Sakaguchi in University of Electro-Communications. We gratefully acknowledge the collaboration.

REFERENCES

1. Murata, A. and H. Ishida, Representation of bodily self in the multimodal parieto-premotor network, in Representation and Brain, S. Funahashi, Editor. 2007, Springer. p. 151-176.
2. Ishida, H., et al., Shared mapping of own and others' bodies in visuo-tactile bimodal area of the monkey parietal cortex. J Cog Neurosci, 2009 in press.
3. Colby, C.L., J.R. Duhamel, and M.E. Goldberg, Ventral intraparietal area of the macaque: anatomic location and visual response properties. J Neurophysiol, 1993. **69**(3): p. 902-14.
4. Rizzolatti, G., et al., Premotor cortex and the recognition of motor actions. Brain Res Cogn Brain Res, 1996. **3**(2): p. 131-41.
5. Decety, J. and J.A. Sommerville, Shared representations between self and other: a social cognitive neuroscience view. Trends Cogn Sci, 2003. **7**(12): p. 527-33.
6. Blakemore, S.J., et al., Somatosensory activations during the observation of touch and a case of vision-touch synaesthesia. Brain, 2005. **128**(Pt 7): p. 1571-83.
7. Ramachandran, V.S. and D. Rogers-Ramachandran, Denial of disabilities in anosognosia. Nature, 1996. **382**(6591): p. 501.
8. Ishida, H., M. Inase, and A. Murata. Shared representation of self ad other's body parts in visuo-tactile bimodal area of the monkey parietal cortex. in FENS Forum 2008. 2008. Geneva, Switzerland.
9. 石田文彦, 村田哲, 阪口豊, 手操作運動中のサルF5-AIP野神経活動の情報量解析. 電子情報通信学会技術研究報告書, 2008. **108**(264): p. 43-48.
10. Murata, A., et al., Selectivity for the shape, size, and orientation of objects for grasping in neurons of monkey parietal area AIP. J Neurophysiol, 2000. **83**(5): p. 2580-601.

Estimation of other's sensor pattern based on dialogue and abstract phase space of sensorimotor patterns

Tetsunari INAMURA and Keisuke OKUNO

***Abstract*— We propose an adaptive acquisition method to infer model of others' sensorimotor patterns, using mimesis model, which is our previous work. The model abstracts others' motion patterns and links to a primitive symbol representation based on self body configuration. It, however, doesn't concern the structural difference between self and other. Furthermore, unobservable inner sensory information such as torque cannot be treated. We utilize symbol communication to solve these problems. Through experiments on virtual environments, we have confirmed the feasibility of our proposed method.**

I. INTRODUCTION

Inamura *et al* have proposed *proto-symbol space* based on *mimesis theory* as an abstract representation of sensorimotor patterns for humanoid robots.[1][2][3]. The proto-symbol space describes relationship between abstracted representation of sensorimotor patterns based on Hidden Markov Models. The space is constructed by distance information between the abstracted representations using Kullback-Leibler divergence and multi-dimensional scaling method. In this proto-symbol space, motion patterns are able to be transformed into static state points, that is proto-symbols, even though an input motion pattern is unknown. In the method, interpolation and extrapolation of motion patterns are realized with creating internal/external dividing points between two positions of the proto-symbols. Motion imitation, that is combination of recognition and generation of motion patterns, has been realized with integrating these two calculation, even though the original motion patterns are unknown and novel.

In the previous works, motion imitation was discussed between human beings and humanoid robots, however, a problem has been remained that abstract representation of others' sensorimotor patterns was not considered. There was an assumption that the same physical condition was shared by learner and performer even if the one was human being and the other was humanoid robot. To clear the problem, a mimesis model that can estimate other's sensor pattern should be realized, by establishment of connection between other's proto-symbol space and self proto-symbol space as shown in Fig.2.

In this paper, we propose an extended model of our previous method to estimate other's sensor patterns with consideration of difference of physical conditions between self and other. Especially, we focus on gradual acquisition strategy to estimate unobservable other's sensor pattern with making communication between self and other.

Fig.1 shows a process flow of the conventional imitation. Fig.2 shows a flow of the proposed method by two proto-symbol spaces of self and other.

Tetsunari INAMURA: National Institute of Informatics(NII) Assoc. Prof.inamura@nii.ac.jp

Keisuke OKUNO: The Graduate University for Advanced Studies(SOKENDAI) k-okuno@nii.ac.jp

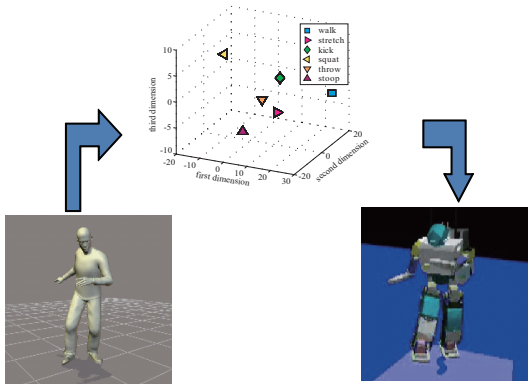

Fig. 1. Conventional mimesis model that uses sole proto-symbol space

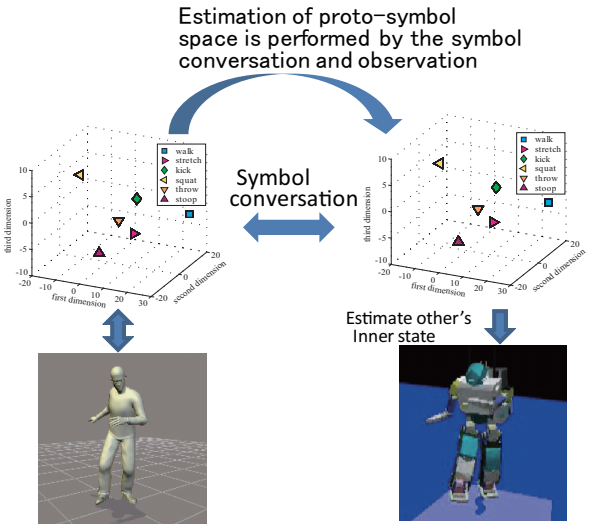

Fig. 2. Proposed mimesis model that consists of two proto-symbol spaces

II. ACQUISITION OF ESTIMATION MODEL OF OTHER'S SENSORIMOTOR PATTERNS

As shown in Fig.2, two different proto-symbol spaces should be used for other and self to realize imitation with consideration of sensor patterns. However, a problem should be solved that other's motion patterns cannot input to self proto-symbol space where we realize motion imitation with

a style shown in Fig.2. Additionally, since other's sensor pattern is unobservable, a certain estimation function from observable motion pattern to the sensor pattern is also required. We therefore consider a strategy in which the *self* has estimation model of the other's proto-symbol space as well as the self proto-symbol space.

To simplify the explanation, we use PSS_{self} as a self proto-symbol space, PSS_{other} as a proto-symbol space of other's, $\hat{PSS}_{other}$ as an estimation model of other's proto-symbol space owned by self. Since other's sensor patterns are unobservable, a sensorimotor pattern database D_{other} which is used to construct $\hat{PSS}_{other}$ should be set by a copy of D_{self} which is used to construct the PSS_{self}. In the acquisition phase, the following procedures are repeated.

1) Consider an objective motion pattern that can be shared between self and other. Estimate an expected sensor pattern that should be felt by other using $\hat{PSS}_{other}$.
2) Detect a difference between estimated sensor pattern and actual sensor pattern with conversation between self and other.
3) Modify the estimated sensor pattern based on the result of dialogue, then input the modified sensor pattern into database D_{other} to be used for the construction of $\hat{PSS}_{other}$.

Estimated other's proto-symbol space $\hat{PSS}_{other}$ will be getting closer to the proper proto-symbol space $\hat{PSS}_{other}$ with repetition of above procedures.

III. Acquisition of Proto-Symbol Space Based on Dialogue

A. Basic strategy of the acquisition

In the concrete, consider an experiment in which a humanoid robot R_1 try to estimate sensorimotor pattern of another robot R_2 whose physical condition is different from R_1. Let a sequence of joint angle vector be an example of objective motion pattern that can be shared between self and motion, a torque pattern be an unobservable sensor pattern. D a database of sensorimotor pattern consists of m motion patterns $\boldsymbol{M} = (M_1, M_2, \cdots, M_m)$ as sequence of joint angle vector and m sensor sensor patterns $\boldsymbol{S} = (S_1, S_2, \cdots, S_m)$ as torque vector for each joint. The problem could be regarded as an acquisition of a proto-symbol space $\hat{PSS}_{R_2}$ based on the database D.

Here, the following procedure is used for the acquisition of $\hat{PSS}_{R_2}$

1) Consider a database D_{R_2} that is used by R_1 to estimate R_2's proto-symbol space $\hat{PSS}_{R_2}$. Let the initial state of D_{R_2} be copy of D_{R_1} that is set of $\boldsymbol{M}$ and $\boldsymbol{S}$ of R_1. In other words, the initial state of $\hat{PSS}_{R_2}$ is PSS_{R_1}.
2) Input a motion pattern M_i, which is stored in the database D_{R_2}, into $\hat{PSS}_{R_2}$ to calculate a sensor pattern $\hat{S}_i$. This procedure corresponds to estimation of R_2's sensorimotor pattern by R_1
3) R_2 performs the motion pattern M_i by its own body, then transfers the felt sensor pattern S into a symbol index k_{R_2}.

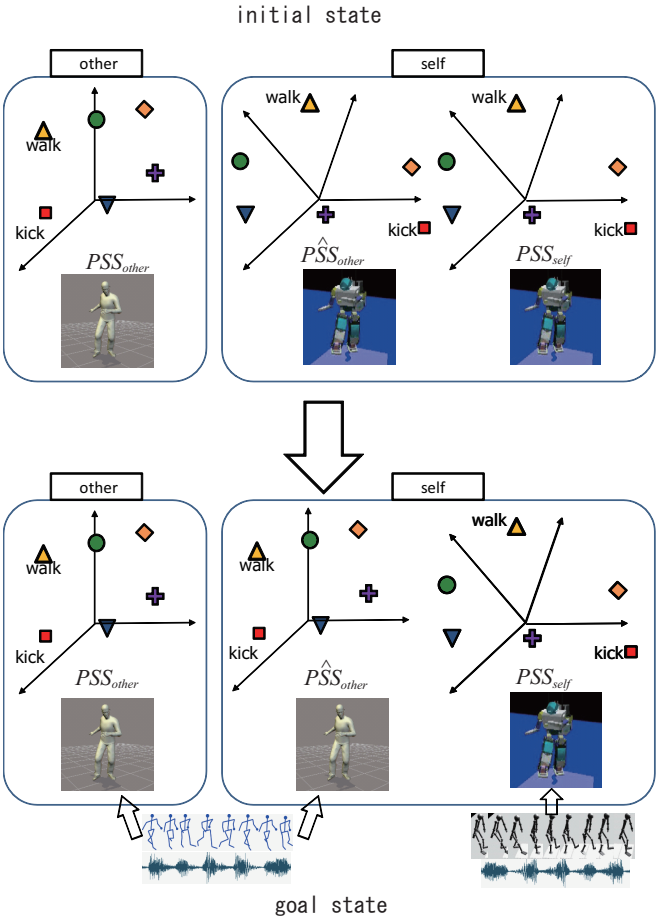

Fig. 3. Concept of the acquisition of other's proto-symbol space

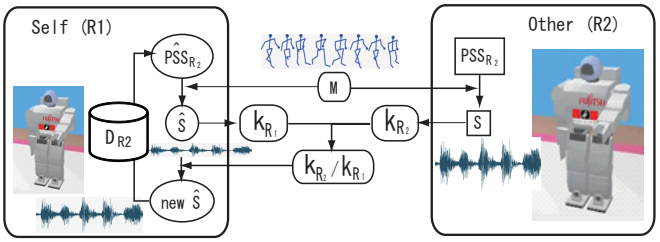

Fig. 4. Block diagram of the revision of estimated proto-symbol space

4) R_1 also transfers the estimated sensor pattern $\hat{S}_i$ into a symbol index k_{R_1} to detect difference between estimated sensor pattern $\hat{S}_i$ and actual sensor pattern S. After that, R_1 starts a dialogue to confirm whether the two symbol indexes are the same or not.
5) Modify the estimated sensor pattern $\hat{\boldsymbol{S}}$ according to the difference between k_{R_1} and k_{R_2}. A corresponding pattern in the database D_{R_2} will be replaced with the modified $\hat{\boldsymbol{S}}$. $\hat{PSS}_{R_2}$ is re-constructed by the modified database.
6) Repeat the above procedures to acquire $\hat{PSS}_{R_2}$.

An outline of the above process is depicted in Fig.4.

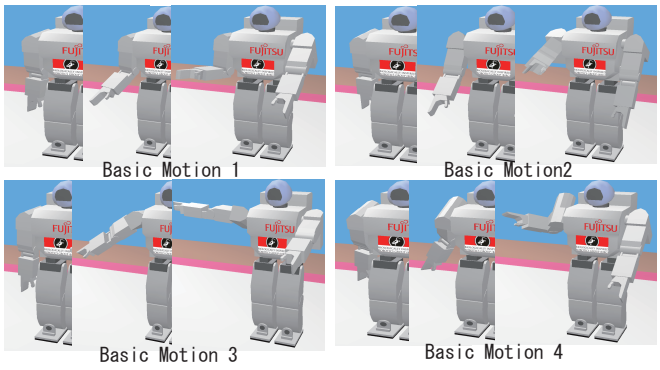

Fig. 5. Four basic motion patterns : M

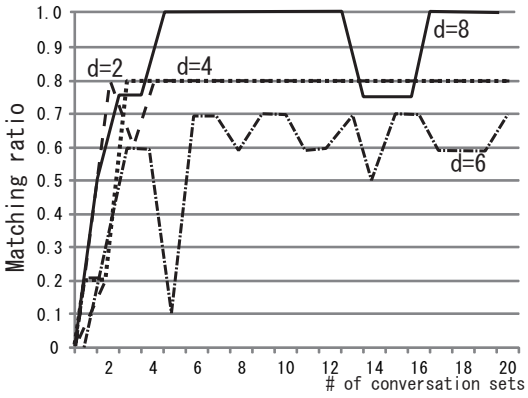

Fig. 6. A result of matching ratio through conversation

B. Experiment and Evaluation

In the experiment, two virtual humanoid robot R_1 and R_2 are used in a simulator environment. Structure of both of the robots is same as HOAP-2 produced by Fujitsu Corp; however weight of R_1 is 2.4[kg] and the one of R_2 is 4.8[kg]. An experiment is performed with torque pattern on the right hand for four motion patterns shown in Fig.5.

First of all, a proto-symbol space $PSS_{R_i}(i = 1, 2)$ is created by the four basic motion patterns and measured sensor pattern by R_1 and R_2, where let torque value for the right elbow, pitch and roll rotation torque on the right shoulder $[\ _1\ \ _2\ \ _3]$ is set as $\boldsymbol{S}$. Joint angle for the same joint rotation $[\ _1\ \ _2\ \ _3]$ is set as $\boldsymbol{M}$. $_i and\ _i$ are time-series data.

Symbol indexes k used in the dialogue is calculated by the following procedure.

- Let $_{MAX}$ as the maximum torque value measured by R_2. Consider a normalized torque value defined by

$$g = \frac{1}{T}\int_0^T \frac{|\ _1(t)| + |\ _2(t)| + |\ _3(t)|}{_{MAX}} dt \qquad (1)$$

  is calculated, where T is time length of the $_i(t)$, $_{MAX}$ is constant value as 0.4[Nm].
- Dividing an interval of the g into d segments equally. Several symbol indexes k are assigned following to the Table.1.

TABLE I

RELATION BETWEEN EXPRESSION AND DENSITY OF THE EXPRESSION

k	d=2	d=4	d=6	d=8
1	light	light	very light	quite light
2	heavy	bit light	light	very light
3	-	bit heavy	bit light	light
4	-	heavy	bit heavy	bit light
5	-	-	heavy	bit heavy
6	-	-	very heavy	heavy
7	-	-	-	very heavy
8	-	-	-	quite heavy

When the sensor pattern S_i in the database should be modified following to the result of dialogue, amplitude of S_i is amplified by k_{R_2}/k_{R_1}, that is ratio between k_{R_1} and k_{R_2} Perform the modification against four basic motion patterns. If at least one sensor pattern were modified, the proto-symbol space would be revised by the modified database.

To evaluate the performance of the estimation of proto-symbol $\hat{PSS}_{R_2}$, the following evaluation criteria are considered against N unknown motion patterns $M_i^{'}(i = 1, \cdots, N)$

a) Concordance ratio of the symbol indexes: Ratio that the symbol indexes $k_{i_{R_1}}$ and $k_{i_{R_2}}$ are concordant among $\boldsymbol{M_i^{'}}$.

b) Difference between symbol indexes: This criteria indicates degree of unlikeness between each symbol indexes defined by:

$$k_{diff} = \frac{1}{N}\sum_i^N \frac{|k_{i_{R_1}} - k_{i_{R_2}}|}{d}. \qquad (2)$$

Here, the interval of k_{diff} is $0 \leq k_{diff} \leq 1$ from the above definition.

c) Estimated torque error: This criteria is difference between estimated torque by R_1 and actual torque observed by R_2 using

$$e = \frac{1}{N}\sum_i^N |\hat{g}_i - g_i|, \qquad (3)$$

where $\hat{g}_i$ is normalized torque value of estimated torque by R_1 with Eq.(1) against motion pattern M_i, g_i is normalized torque value actually observed by R_2.

C. Experimental results

Fig.6 shows evaluation result for the criteria of concordance ratio. Horizontal axis indicates the number of loop described in section III-A. (We call the number of loop as the number of dialogue.) Vertical axis indicates concordance ratio between k_{R_1} and k_{R_2} for 10 unknown motion patterns. We have performed in 4 kinds of situation where the number of expressions are different ($d = (2, 4, 6, 8)$) The concordance ratio was getting higher with the repetition of the dialogue, even though the target motion patterns were unknown.

In Fig.6, the concordance ratio indicated partially low in the case of $d = 6$ and $d = 8$; however the estimated torque were not inconsequent. Let's consider the criteria of difference between symbol indexes. Fig.7 indicate the criteria of difference between symbol indexes defined by

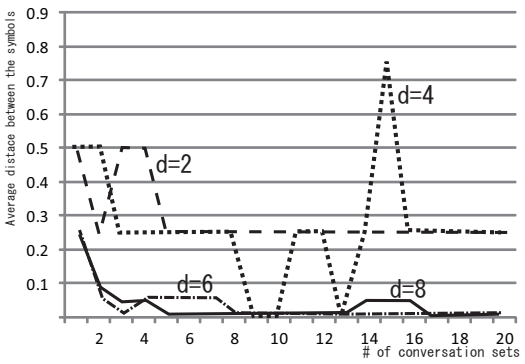

Fig. 7. Difference of the symbol index for basic motion patterns

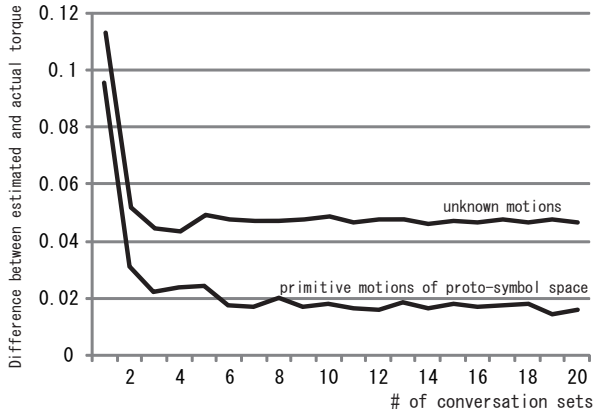

Fig. 8. Difference between estimated torque and actual torque by 6 words (d=6)

Eq.(2) with the repetition of dialogue. When $d = 4$, the band of fluctuation was little wide. But in case of $d = 6, 8$, differences were suppressed. The result shows that the difference of the symbol indexes are little when many expressions were used, that is density of the expression was fine.

Next, we confirmed the criteria of estimated torque error with repetition of dialogue. Fig.8 shows progression of estimated torque e calculated by Eq.(3). In the graph, $d = 6$ is used. torque values for both of motion pattern $\boldsymbol{M}$ in database D_{R_2} and unknown motion pattern $\boldsymbol{M}'$ for test evaluation were depicted. Error between estimated torque value and true torque value was about 0.05[Nm] at most. Estimated torque value from $\boldsymbol{M}'$ were about from 0.2 to 0.25[Nm]. Therefore, the error was suppressed within about 10% for known motion pattern in database D_{R_2}. Even if the target motion patterns were unknown, the error was surpressed within 20%〜25%.

Fig.9 shows a superposition of Fig.8 for four case of $d = 2, 4, 6, 8$. Since the estimated torque error was within about 20%, the capability of stable torque estimation was shown. The result have close relationship between the result by Fig.7. The one result backs up the another result.

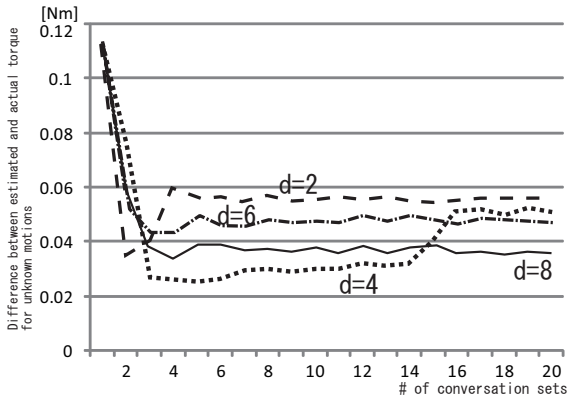

Fig. 9. Error of estimated torque for unkown motions

IV. Conclusion and Discussion

In this research, we focuse on the remained problem of our previous works, that is proto-symbol space that can be abstract sensorimotor patterns between both of self and other even though the two subjects have different physical conditions. The approach is estimation of other's proto-symbol space through repetition of dialogue. Specifically, design a dialogue protocol based on symbol index to express the inner sensor patters, and approximation method with modification of sensorimotor patterns based on dialogue, are proposed. We have also performed quantitative experiments to evaluate the proposed method and performance of the estimation of other's proto-symbol space.

A problem has been still remained that how to design the symbol index from sensor patterns. On current state, average value (normalized torque value) calculated by Eq.(1) was adopted, however the definition should be modified adaptivelly according to type of task, context, situation and so on. Another problem is that the symbol indexes are not concerned with proto-symbols defined by the phase space structure. As a ultimate goal, symbolization should be performed with unified rule. We are planning to update our method to fit the concept of proto-symbol space not only the abstract of sensorimotor patterns, but also design of dialogue between human beings and robots.

References

[1] Tetsunari Inamura, Yoshihiko Nakamura, Iwaki Toshima, and Hiroaki Tanie. Embodied symbol emergence based on mimesis theory. *International Journal of Robotics Research*, Vol. 23, No. 4, pp. 363–378, 2004.

[2] Tetsunari Inamura, Hiroaki Tanie, and Yoshihiko Nakamura. From stochastic motion generation and recognition to geometric symbol development and manipulation. In *International Conference on Humanoid Robots*, 2003. (CD-ROM).

[3] Tetsunari Inamura, Tomohiro Shibata. Motion Pattern Synthesis based on Geometric Symbol Manipulation –Synthesis of motion patterns which have different time length–. Proc. of the 13th Robotics Symposia, pp. 457–462, 2008. (in Japanese)

[4] Ryunosuke Yokoya, Tetsuya Ogata, Jun Tani, Kazunori Komatani, and Hiroshi G. Okuno. Discovery of other individuals by projecting a self-model through imitation. In *Proc. 2007 IEEE/RSJ International Conference on Intelligent Robots and Systems (IROS'07)*, pp. 1009–1014, 2007.

Research on the Functional Hierarchy in the Cognition and Generation of Skilled Behavior

Hiroaki Arie
RIKEN Brain Science Institute

Shigeki Sugano
Science & Engineering,
Waseda University

Jun Tani
RIKEN Brain Science Institute

***Abstract*— The present study examines the possible roles of cortical chaos in generating novel actions for achieving specified goals. The proposed neural network model consists of a sensory-forward model responsible for parietal lobe functions, a chaotic network model for premotor functions and prefrontal cortex model responsible for manipulating the initial state of the chaotic network. Experiments using humanoid robot were performed with the model and showed that the action plans for satisfying specific novel goals can be generated by diversely modulating and combining prior-learned behavioral patterns at critical dynamical states. Although this criticality resulted in fragile goal achievements in the physical environment of the robot, the reinforcement of the successful trials was able to provide a substantial gain with respect to the robustness.**

I. Introduction

Why some cognitive acts entail explicit consciousness but many others undergo unconsciously? For example, we can grasp a coffee mug without paying much attention to the action, while consciously talking with others. Some neuroscience researchers have considered that consciousness is deeply involved with prefrontal lobe activity. It is well known that prefrontal lesion patients often have problems in generating new plans to achieve novel given goals even though they seemingly have no problems in generating everyday's skilled actions such as reaching for a mug and grasping it[1], [2]. The former case involves the conscious and deliberate manipulation of mental images in planning the novel goal-directed actions which presumably require prefrontal activity. On the other hand, the latter case seems to proceed automatically with having less activities in the prefrontal lobe. How can we model the underlying mechanisms accounting for these phenomena?

The current study attempts to look at this problem by using a dynamical system approach[3], [4], [5] combined with robotics synthetic experiments. In particular, we focus on the possible roles of cortical chaos in generating "creative" behaviors. We have shown that certain compositional structures can be self-organized in the internal neuro-dynamic memories as regularities hidden in the sensory-motor interactive experience are consolidated[4], [6], [7]. The current study will attempt to extend this line of thought to the problem of how novel action imagery[8] can be "created" from the memory dynamics of consolidated.

II. Model

Figure1 shows the overall schematics of how each part of the brain functions and interacts with other parts in the proposed model.

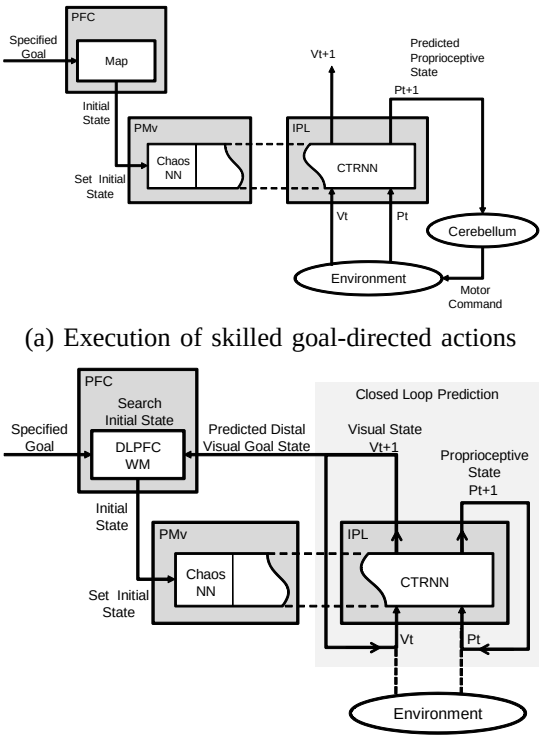

(a) Execution of skilled goal-directed actions

(b) Searching for a novel goal-directed action plan

Fig. 1. Correspondences of the model to the brain anatomy where the execution of skilled goal-directed actions in (a) and searching for action plans for novel goal states in (b)

A. Generation of well-trained actions

Firstly, let's look at the case of generating well-trained goal-directed actions, as shown in Figure1 (a). We have considered that the trajectories of different goal-directed behaviors can be generated depending on the initial states given to a particular neural dynamical system by means of the initial sensitivity characteristics of the nonlinear systems[9]. When a goal to be achieved is specified from well-trained ones, its corresponding initial state is set to PMv by remembering it. Both of the PMv and IPL are implemented by a continuous time recurrent neural network (CTRNN) model[10], [11]. The CTRNN dynamics in the PMv is designed to be chaotic with pre-wired synaptic connectivity. The synaptic weights inside the chaotic network are designed such that the maximum Lyapunov exponent becomes positive. On the other hand, the synaptic connectivity in the IPL is determined through the learning processes.

By having connectivity between these two networks, the IPL learns the details of the visuo-proprioceptive (VP) patterns by predicting the VP state at the next step (V_{t+1}, P_{t+1}) from the previous one (V_t, P_t), while the PMv tends to combine and modulate those patterns memorized by IPL through interacting with it. The central assumption in the current model is that brains might utilize cortical chaos in enhancing diversity of the behavioral patterns generated by utilizing its initial sensitivity characteristics. The initial state in terms of the neural activation states in the chaotic neural network is manipulated in order to generate different goal-directed actions.

The training of IPL is conducted using BPTT algorithm[12] by utilizing the VP sequences acquired as input to the IPL through the tutor guidance of the robot. The error signal is back-propagated among IPL to PMv by which the synaptic weights in the IPL network are tuned. It is important to note that the learning proceeds with accompanying the pre-wired chaotic dynamics such that different initial states of the chaotic network initiate trajectories of different trained goal-directed actions. In our proposed learning scheme these initial states as well as the synaptic weights in IPL are self-determined in the course of training with a set of goal-directed action trajectories. The time constant of the chaos dynamics in PMv is set relatively to be larger than the one in IPL such that two levels of functions dealing with abstract plan scenarios and primitive behavioral pattern details can emerge. In the recent study of our group Yamashita and Tani[7] showed that such functional decomposition can emerge in the neural network model of multiple time scales RNN (MTRNN).

B. Generation of novel actions

Next, we consider how brains can generate novel combinations of action programs for achieving novel goals. One possibility is to utilize stochastic noise to combine parts of learned trajectories into novel ones. The current paper, however, investigates an alternative possibility, in which deterministic chaos plays an essential role in generating novel combinations. If the forward model is learned as being associated with certain networks whose dynamics is characterized by chaos, the mapping can become complex by means of the strong initial sensitivity of the chaos. In such situations, the forward model can generate diverse imagery of novel sequences by combining and modulating the prior-learned temporal patterns depending on the initial state. Then, it might be possible to search for the initial state, which leads to the generation of novel action programs satisfying newly given goals.

Let's see the ideas by looking at Figure1 (b). Firstly, the goal specified externally is stored in the working memory assumed in the dorsolateral prefrontal cortex (DLPFC). Then the distal goal image which is generated by the forward dynamics with a particular initial state is matched with the specified goal image in the working memory. This is performed in the so-called closed-loop mode without the actual execution of motor acts in which the consequences of one's own actions are mentally simulated[4], [13], [14] . The forward dynamics is conducted without the actual sensory input but with the sensory imaginary loop utilizing its own prediction as shown by the dotted lines in Figure1 (b). If matching the specified goal image and the generated one fails, another initial state is examined. This search continues until perfect match is achieved. If perfect match is obtained with a certain initial state, the actual movement is initiated by setting this initial state to PMv in the same way as described in Figure1 (a).

III. Experiment

A. Implementation in a humanoid robot

The experiment was carried out by using a small-scale humanoid robot named HOAP3. The robot has a head, which is equipped with a stereo camera, and two arms, each of which has 4 rotational joints. Our neural model receives the following sensory-input from the robot, namely the proprioception P_t (an 8-dimensional vector representing the angles of the arm joints), the direction of the camera on the head V_t^d (a 2-dimensional vector representing the rotational angle of the neck joints), and the visual perception V_t^v (16×12 dimensional vector representing the retinal image). The direction of the camera is controlled by a PID controller which is programmed to track a red-colored object to be centered in the retina image. Receiving the current VP state (P_t, V_t^d, V_t^v), the neural network generates the next step prediction of them as $P_{t+1}, V_{t+1}^d, V_{t+1}^v$. Then, the robot arm is moved toward P_{t+1} as target joint angles with a PID controller.

The sensory-inputs of the proprioception, the direction of the eyes and the visual perception are initially processed by the corresponding TPMs. The mathematical details are described in the paper written by Yamashita and Tani[7].

B. Task design

The robot was fixed to a chair, and a workbench base was set up in front of the robot. A movable rectangular solid object which is painted half blue and half red was placed on the base immediately in front of the robot. Also, a low height pedestal was fixed to the base behind the object.

The robot was tutored for five operational actions, which are shown in Figure2: (a) move the standing object to the left, (b) hold up the standing object and put it onto the pedestal, (c) knock over the standing object to lie, (d) move the lying object to the right, (e) hold up the lying object and put it onto the pedestal. The object was placed in the center in front of the robot in actions (a-c) and in the left-hand side in actions (e,f). For each operational action, the robot was tutored 3 times with changing the initial object position as 2cm left of the original position, the original one and 2cm right of the original one. Therefore, a total of 15 VP sequences were sampled for the training of the network.

After the training, two types of the robot behavior generations were examined. The first one was simply regenerate the 5 trained goal-directed actions. The network was set with

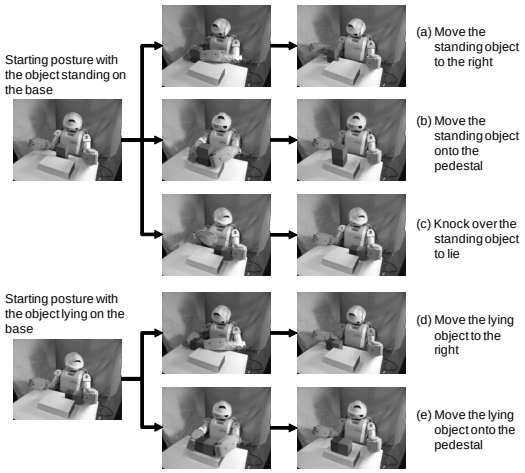

Fig. 2. Five types of goal-directed actions

the corresponding initial state values which had been self-determined for each goal state with the case of the original object position in the training phase and then the robot was started to move. The robot movement was tested for the left, the original and the right object position cases for each goal-directed action.

The second one is to plan and to generate a novel goal-directed action. The goal state is given as the visual state of the object lying on the pedestal with the condition that the object is initially standing on the base in front of the robot. Note that this combination of the goal state and the object initial position is novel for the robot, i.e., the robot has to generate novel motor-act sequences of firstly knocking down the object to lye on the base and then holding up this onto the pedestal. In this experiment, action plans are generated by searching for the initial state which can bring the best match between the specified goal state and the predicted one in the distal step by the sensory-forward model. The search is iterated 100 times with a 0.1 grid in the two-dimensional initial state space in the range between 0.05 and 0.95 for each dimension. Then, the plan of the best match is enacted by the robot in the physical environment with activating the network forward dynamics with the corresponding initial state values.

C. Results

1) Regeneration of the trained goal-directed actions: All three Kohonen networks were pre-adapted before the training of the MTRNN utilizing the sensory patterns acquired for the 15 tutoring sequences. The networks after the training were tested to regenerate the trained actions by the robot. Each goal-directed action is tested with varying the object position among the left, the original, and the right ones. Each trial was repeated for three times. The results of the experiment show that the robot could regenerate 15 actions (3 positions $\times$ 5 actions) with a success rate of about 70%. The details are shown in the Table1. As shown in this table, the success rate was 93% when the object was placed in the original position. The score becomes lower when the object is located in the left or right positions. It can be said that in most

TABLE I

THE NUMBER OF SUCCESSFUL TRIALS WITHIN THREE TRIALS IN REGENERATION OF THE TRAINED ACTIONS.

Specified goal-directed action	Position of the object		
	2cm left	original	2cm right
(a) standing object to right	3	2	2
(b) standing object onto the pedestal	0	3	1
(c) standing object to lying	3	3	3
(d) lying object to right	0	3	2
(e) lying object onto the pedestal	3	3	0

cases the trained actions can be regenerated successfully. We found that the instability of light reflection on the colored object in the visual sensation caused certain fluctuations in the MTRNN dynamics during the task execution.

2) Planning and generating actions for achieving the specified novel goal state: In this experiment, imaginary VP sequences were generated utilizing closed-loop operation, in which predicted sensory values serve as virtual sensory feedback, so the network can generate imaginary VP sequences without generating physical movements of the robot. As a result of searching the best match VP imaginary sequences with varying the initial state for 100 times, only one VP sequence was found to satisfy the specified goal state in its distal step image. The initial state of the successful sequence was (0.35, 0.95).

The upper part of figure3 shows the generated sequence of the visual imagery in the retina and the direction of the head camera represented as its corresponding TPM in the lower part of the figure, starting with the best match initial state (0.35, 0.95). It is seen that when the two-colored object is

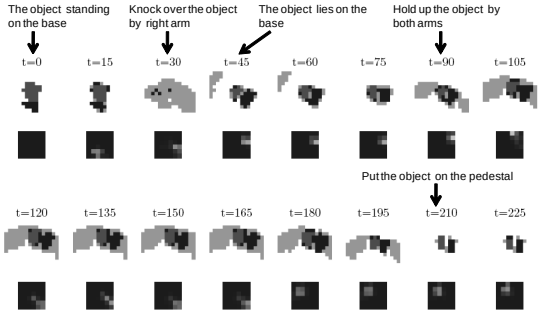

Fig. 3. Imaginary sequence generated with the initial state (0.35, 0.95) where the upper part shows the retinal image and the lower part does for the TPM population coding for the camera head direction.

standing on the base at the 0th step, the object is knocked down by the right arm of the robot at the 30th step, the object is lying on the base with the left hand of the robot is in the air at the 45th step, the object is held up at the 90th step, then the object is put on the pedestal by both arms, and finally the object is lying on the pedestal after both arms release the object. It should be noted that the TPM population coding for the direction of the head camera is different between the two situations where the object is lying on the base at the 45th step and that where it is lying

on the pedestal at the 210th step. Therefore, this imagery is regarded as a sequential combination of knocking over the object and then holding up the lying object onto the pedestal.

Next, we investigated whether the robot can physically achieve the specified goal state successfully by setting the initial state with (0.35, 0.95) of which plan was found to be the best match. However, it was found that the robot could not achieve the goal with this initial state values. Next, the robot actions were generated repeatedly with varying the initial state within the found grid of (0.3-0.4, 0.9-1.0). It was found that successful accomplishment occurred in only two out of 40 trials. The VP sequence of one successful case is shown in Figure4. It was also found that the same initial

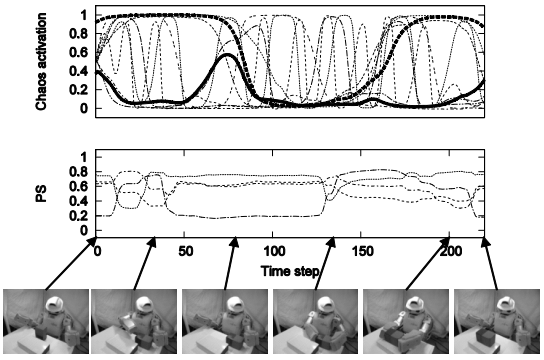

Fig. 4. Actual performance of the robot to achieve the given novel goal state. The upper graph shows the activation of chaos network units. The bottom graph shows the proprioceptive state (PS) for four joint angles in the right arm. Bottom pictures show the actual state of the robot at specific time steps.

state of one time successful case hardly repeats the same behavior patterns of the robot. It can be concluded that both the plans and their enactions for the given novel goal state are substantially sensitive to the initial state as well as to the external noise in the environment as compared to the cases of regenerating the well-trained ones.

3) Additional reinforcement of effective actions generated: Next, we examined whether the novel effective actions generated by chance in the previous section could be reinforced such that they could be regenerated in more stably. Two successful VP sequences which had been generated by the robot for achieving the specified novel goal were added to the original 15 VP sequences for additional incremental training.

It was observed that the novel goal-directed actions turned to be skilled ones with gaining their robustness after their reinforcement in our experiments. When the novel plans were enacted by setting the initial state, the robot was able to achieve the specified novel goal state with more than 70% success rate. This experimental result suggests that the reinforcement of successful trials by chance can increase the stability of regenerating them.

IV. Conclusion

The current study proposed a synthetic model of representing how well-skilled actions as well as novel ones can be generated in goal-directed ways by utilizing neurodynamical systems characteristics. Our experiments using a small humanoid robot implemented with the model showed that (1) all of tutored goal-directed actions can be regenerated robustly by setting each corresponding initial state obtained in the learning phase, that (2) the robot was able to create actional imaginaries of achieving the specified novel goal state with the consolidated memory at the critical regions of the initial state space, that (3) enactions of such generated plans brought potential instability in achieving the goal and however that (4) the reinforcements of some effective trials generated by chance gained the stability in regenerating those trials.

This result suggests that generation of novel or "creative" behaviors require two prerequisites for cognitive systems. One is that a good amount of sensory-motor experiences had been consolidated with self-organizing certain relational structures in distributed memories. The other is an existence of intrinsic cortical chaos which could enhance the criticality of the dynamic structure of the consolidated memory for generating diverse actional imaginaries. The continuous iterations of experiencing, consolidating and meditating would lead to developments of truly open-ended human-like intelligence.

References

[1] A. R Luriia. *Higher cortical functions in man.* Basic Books, New York, 1966.

[2] W. Penfield and J. Evans. The frontal lobe in man: A clinical study of maximum removals. *Brain*, (65):115–133, 1935.

[3] R.D. Beer. A dynamical systems perspective on agent-environment interaction. *Artificial Intelligence*, 72(1):173–215, 1995.

[4] Jun Tani. Model-based learning for mobile robot navigation from the dynamical systems perspective. *IEEE Trans. on SMC (B)*, 26(3):421–436, 1996.

[5] T. Ziemke. On 'parts' and 'wholes' of adaptive behavior: Functional modularity and diachronic structure in recurrent neural robot controllers. In *From animals to animats 6*, pages 171–180, Cambridge, MA, 2000. MIT Press.

[6] J. Tani, R. Nishimoto, and R. Paine. Achieving "organic compositionality" through self-organization: Reviews on brain-inspired robotics experiments. *Neural Networks*, 21:584–603, 2008.

[7] Yuichi Yamashita and Jun Tani. Emergence of functional hierarchy in a multiple timescale neural network model: a humanoid robot experiment. *PLoS Computational Biology*, 4(11), 2008.

[8] Marc Jeannerod. The representing brain: Neural correlates of motor intention and imagery. *Behavioral and Brain Sciences*, 17(2):187–245, 1994.

[9] Ryunosuke Nishimoto, Jun Namikawa, and Jun Tani. Learning multiple goal-directed actions through self-organization of a dynamic neural network model: A humanoid robot experiment. *Adaptive Behavior*, 16(2-3):166–181, 2008.

[10] Ronald J. Williams and David Zipser. A learning algorithm for continually running fully recurrent neural networks. *Neural Computation*, 1(2):270–280, 1989.

[11] Kenji Doya and Shuji Yoshizawa. Memorizing oscillatory patterns in the analog neuron network. In *Proc. of 1989 int. joint conf. on neural networks*, volume 1, pages 27–32, Washington, D.C., 1989.

[12] David E. Rumelhart, Geoffrey E. Hinton, and Ronald J. Williams. *Learning internal representations by error propagation*, volume 1 of *Parallel distributed processing: explorations in the microstructure of cognition.* MIT Press, Cambridge, 1986.

[13] Jun Tani. An interpretation of the "self" from the dynamical systems perspective: a constructivist approach. *Journal of Consciousness Studies*, 5(5-6):516–42, 1998.

[14] G. Hesslow. Conscious thought as simulation of behaviour and perception. *Trends in Cog. Sci.*, 6(6):242–247, 2002.

Group B: Research Report

Kazuo Tsuchiya
Faculty of Science and Engineering, Doshisha University

I. Research Brief

Animal skillful behaviors emerge through dynamical interactions between brain, nervous system, and musculoskeletal system. So far, biomechanical studies have investigated the mechanical and dynamical characteristics of animal behaviors and neurophysiological studies have examined neural activities and evaluated their functional roles. They individually conduct their studies. Group B consists of biologists who study exercise physiology and engineers who study biomechanics and robotics and conduct cooperative research. They use constructive approach toward understanding the mechanisms by integrating biomechanics and neurophysiology (System Biomechanics), where they conduct numerical simulations by constructing anatomically based whole-body musculoskeletal model and neurophysiologically based nervous system model and develop robots to investigate in the real world. This group aims to clarify not only the functional roles of information processed in various nervous systems but also the design principles to produce the mechanical systems, "soft machinery", that adapt themselves to environmental variations.

II. Research Organization

This research group consists of planned and subscribed research groups. The research subject of each group is as follows:

- B01-01 Neuronal mechanisms of generating and selection of adaptive behaviors (Kaoru Takakusaki, Asahikawa Medical College)
- B01-02 Exploration of the principle mechanism of generating adaptive locomotion on the basis of neurophysiological findings (Naomichi Ogihara, Kyoto University)
- B01-03 Realization of adaptive locomotion based on dynamic interaction among the body, brain, and environment (Koh Hosoda, Osaka University)
- B01-11 Reflex walk modeling for physically changed person (Hiroshi Yokoi, The University of Tokyo)
- B01-12 Study on brain adaptation using rat-machine fusion systems and multifunctional neural electrodes (Takafumi Suzuki, The University of Tokyo)
- B01-13 Analysis of relation between neuronal coding and body movement using BMI (Yoshio Sakurai, Kyoto University)
- B01-14 Exploration of reinforcement learning and motivation mechanism in the brainstem-midbrain-basal ganglia circuits (Yasushi Kobayashi, Osaka University)
- B01-15 Neural correlates of muscle synergy in hand movement (Kazuhiko Seki, National Institute for Physiological Sciences)

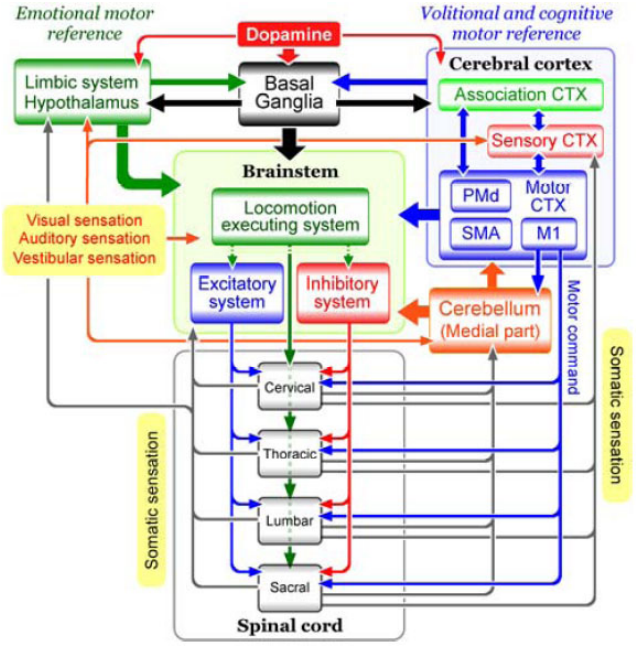

Fig. 1. Multi-tiered organization of CNS for locomotor behaviors

- B01-16 Movement control by the basal ganglia (Atsushi Nanbu, National Institute for Physiological Sciences)
- B01-17 Quantitative evaluation of movement disorders in muscle space for patients with cerebellar degeneration or Parkinson's disease (Shinji Kakei, Tokyo Metropolitan Organization for Medical Research)
- B01-18 Understanding of adaptive mechanisms of gait by combining neuroimaging, electrophysiology and computational methods (Takashi Hanakawa, National Center of Neurology and Psychiatry)

III. Research Achievement

This report shows the representative studies of this group. Further details are shown in the report of each subgroup.

A. Regulation of muscle tone during movements at the level of spinal cord (B01-01 Kaoru Takakusaki, Asahikawa Medical College)

This group aimed at elucidating the mechanisms of integration of postural and locomotor synergies and suggested the multi-tiered organization of CNS for locomotor behaviors (Fig. 1). Basic mechanisms of controlling muscle tone and locomotion exist in the brainstem and spinal cord. Signals from the supraspinal motor centers and sensory signals would be integrated at the level of spinal cord. We investigated how descending muscle tone inhibitory system controls spinal reflexes and how sensory afferents modulates the activity of muscle tone control system and identified the interneurons mediating muscle tone suppression at the level of spinal

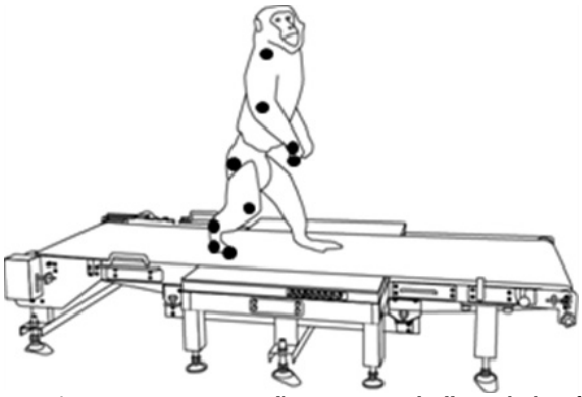

Fig. 2. A Japanese mocaque walking on a treadmill in which a force platform was embedded

Fig. 3. Biped robot with biarticular muscles

cord. Reciprocal inhibitory interaction between the inhibitory system and FRA system was revealed. Since interneurons in flexion reflex afferents (FRA) partly operate as locomotor rhythm generating system, we propose that this interaction may be involved in the muscle tone regulation during locomotion.

B. Locomotion analysis using musculoskeletal model (B01-02 Naomichi Ogihara, Kyoto University)

This group has been biomechanically analyzing adaptive locomotor phenemena observed in actual bipedal locomotion in the Japanese monkey (*Macaca fuscata*) using an anatomical whole-body musculoskeletal model (Fig. 2). This year, we dynamically reconstructed bipedal walking of the Japanese monkey by computer simulation based on the biologically relevant musculoskeletal modeling to biomechanically evaluate causal relationships among musculoskeletal morphology, locomotor kinematics, and energetics. We constructed a two-dimensional musculoskeletal model of the bipedal Japanese monkey consisting of seven links, where the parameters were determined based on the 3D musculoskeletal model. The desired joint trajectories were created based on the 3D kinematic data. The simulation suggests that the Japanese monkey adaptively alters its locomotor kinematics depending on its walking velocity to minimize the metabolic cost of transport.

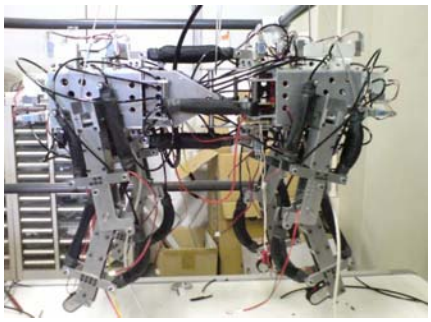

Fig. 4. Quadruped robot driven by pneumatic artificial muscles

Fig. 5. Snake-like robot with pneumatic actuators

C. Realization of adaptive locomotion based on dynamic interaction between body, brain, and environment (B01-03 Koh Hosoda, Osaka University)

An animal has complicated structure consisting of many bones connected with muscles and ligaments that works antagonistically and/or synergistically. Redundancy provided from such complicated mechanism effectively contributes to the hierarchical system consisting of a lower layer devoted to rhythm generation and a higher layer devoted to purposive behavior. This group develops robots driven by artificial pneumatic muscles and clarify the contribution of the joint elasticity on the adaptive locomotion.

(1) Biped robot with biarticular muscles

A biped robot with biarticular muscles is developed to investigate their roles on dynamic locomotion (Fig. 3). We conducted jumping experiment from standstill, landing experiment, and bouncing experiment to investigate the role of the biarticular muscles.

(2) A feasibility study on stability of gait patterns with changeable body stiffness using pneumatic actuators in a quadruped robot

A quadruped robot with pneumatic artificial muscles is developed (Fig. 4). The muscle tone of the robot on the pitching motion at the trunk is changeable by using the changeable elasticity of the pneumatic actuators. The stability of quadruped locomotion in walk and trot patterns with changeable body stiffness was evaluated with numerical simulations and hardware experiments.

(3) Realization of snake-like locomotion and observation of a real snake

We develop a snake-like robot and several sensors required for the adaptive locomotion (Fig. 5) and analyze influence of viscoelasticity on locomotion performance. As the result, very simple control can exhibit three types of locomotion (lateral undulation, sidewinding, and rectilinear) smoothly.

B01; Regulation of Muscle Tone during Movements at the Level of Spinal Cord

Kaoru Takakusaki[1], Futoshi Mori[2], Katsumi Nakajima[3], Dai Yanagihara[4], Taizo Nakazato[5], Kenji Yoshimi[5], Shigeru Kitazawa[5], Masahiko Inase[3], Kiyoji Matsuyama[6], Yoshimasa Koyama[7], Toshikatsu Okumura[8].

Abstract: To generate adaptive movements, an integration of supraspinal and sensory signals is essential. Because all movements of limbs and trunk are evoked through the operation of spinal reflex arcs, we examined how muscle tone control system interacted with the somatosensory systems at the level of spinal cord. An interaction between inhibitory reticulospinal system and flexion reflex pathways may play crucial roles in the integrative process of muscle tone and movements so that goal-directed behaviors can be performed.

I. Introduction

Sensory information is important to initiate, execute and regulate movements. However knowledge has not been enough to understand how sensory signals are involved in the process of integrating postural muscle tone and movements. To clarify this process, thorough examination of spinal mechanisms of controlling posture and movements is necessary because limb and trunk movements are induced through the activation of various spinal reflex arcs [1]. Appropriate postural muscle tone is required to produce adaptive locomotor movements. Basic mechanisms of controlling muscle tone and locomotion exist in the brainstem and spinal cord. Therefore signals from the supraspinal motor centers, such as the cerebral cortex, the limbic system, the basal ganglia and the cerebellum, and those from sensory signals in the muscles, skin and joint afferents would be integrated at the level of spinal cord, particularly at interneuronal level [1]. Spinal interneurons are also involved in the rhythm generation (central pattern generators; CPGs) [2]. Accordingly quite important is to elucidate the integrative mechanisms of signals from supraspinal motor centers and those from sensory afferents at the level of spinal cord in terms of regulation of muscle tone during ongoing movements.

The purpose of this study was to clarify following two points. First, how does descending muscle tone inhibitory system control spinal reflexes? Second, how does sensory afferents modulate the activity of muscle tone control systems? For this purpose electrophysiological studies were performed using decerebrate cat preparation. Functional role of the interaction between the muscle tone inhibitory system and the sensory signals was discussed with respect to the regulation of muscle tone during goal-directed behaviors.

1. Department of Physiology, Asahikawa Medical College.
2. Department of Physiology, Veterinary Medicine, Yamaguchi University.
3. Department of Physiol. School of Medicine, Kinki University.
4. Graduate School of Arts and Science, Tokyo Univ.
5. Department of Physiology, Graduate School of Medicine, Juntendo University.
6. Department of Occupational Therapy, School of Health Science, Sapporo Medical University
7. Faculty of Symbolic System Science, Fukushima University
8. Department of General Medicine, Asahikawa Medical College

II. Materials and Methods

1) Animals; Adult cats with either sex (body weight 2.8-3.5kg) were employed. All procedures are according to the Guide for the Care and Use of Laboratory Animals （NIH Guide; revised at 1996）
2) Operation; All surgical procedures are performed under halothane -nitrous oxide gas anesthesia. Laminectomy was made to expose L5-S2 segments. Left ventral roots (VR) of L5-S1 segments and a part of dorsal root (DR) of L7-S1 segments were dissected and recording electrodes were attached to their central ends. Stimulating electrodes were attached to left muscle and skin nerves. Moreover, a cuff-style stimulating electrode was attached to L1 spinal segment. Surgical decerebration was made at precollicular-postmammillary level (Fig.1A). The cats were then fixed to the stereotaxic apparatus.
3) Stimulation and recording; Microelectrode was inserted in the brainstem, and rectangular pulses of stimuli (3 pulses, 5 ms interval 20-50 μA) were applied to the muscle tone inhibitory region in the medulla (Fig.1B). The effective sites were located in the nucleus reticularis gigantocellularis (NRGc). Medullary stimulus effects upon motoneurons, interneurons and primary (sensory) afferents were examined at L5-S1 levels. Cord dorsum potential (CDP) was recorded at the surface of L7 segment. Motoneurons were intracellularly recorded and identified by the presence of antidromic spikes evoked from VR stimulation. Their innervations were determined by the patterns of Ia EPSPs. Intra- and extra-cellular activities of interneurons were recorded from L6-L7 segments. They lacked antidromic responses evoked from the VR and L1 segment. Muscle and skin afferents to each interneuron were determined. Afferent volleys were expressed by multiples of threshold (T) of emerging CDP. Coming volleys evoked by 1.0-1.3 T and 1.4-2.4 T were induced by group Ia and Ib muscle afferents, respectively. Coming volleys induced by stimuli more than 2.5 T were induced by flexion reflex afferents (FRA) [1]. Ventral and dorsal root potentials (VRP and DRP) were recorded from VR and DR at L7, respectively.
4). Spike-triggered averaging was performed to determine synaptic connections between the subject and target neurons. Membrane potential of target neurons was averaged 1000-4000 times by the firing of spinal interneurons as a time reference.

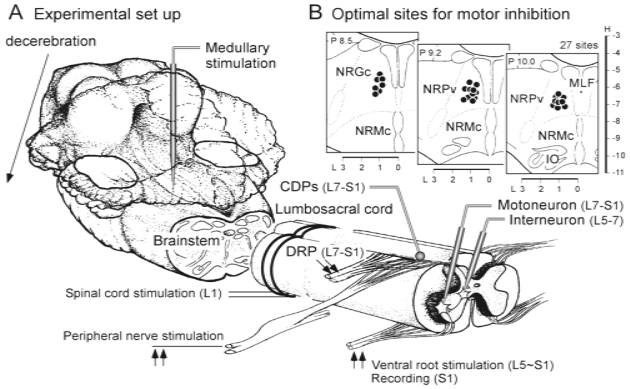

Figure 1 Experimental setup

Schematic illustration of brainstem-spinal cord preparation in decerebrate cat. A. Arrangements of electrodes. B. Stimulus sites in the medulla.

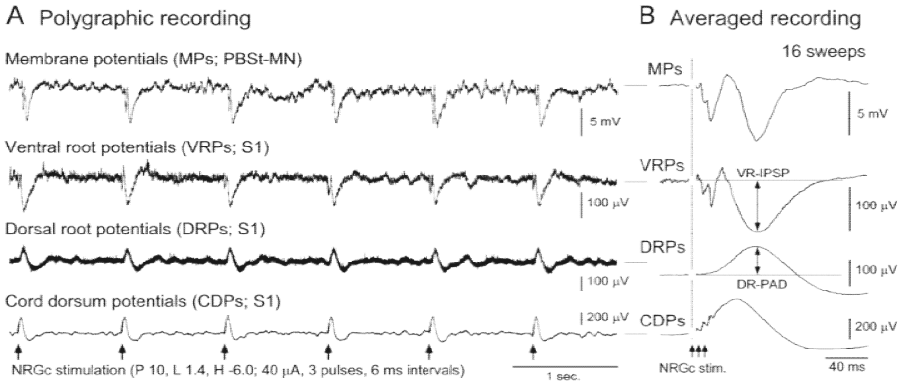

Figure 2. Medullary stimulus effects upon spinal reflex arcs

A. From upper to bottom; membrane potentials of posterior biceps semitendinosus motoneuron (PBSt-MN), ventral root potentials (VRPs), dorsal root potentials (DRPs), and cord dorsum potentials (CDPs). Upward arrows indicate stimulation of the NRGc. Hyperpolarization was observed in the MN and the VRPs. Depolarization was induced in the DRPs. B. Averaging of each potential. Late latency potentials were obvious in the MN, VRPs (hyperpolarization) and DRPs (depolarization). See text for further explanations.

III. Results

1. Muscle tone inhibitory system and spinal reflexes

We stimulated the NRGc and examined its effects upon VRP, DRPs and motoneurons. The NRGc stimulation hyperpolarized a motoneuron and VRP, and depolarized DRP (Fig.2A). Time course was examined by averaging these potentials (Fig.2B). There were early (~20 ms) and late (30~70 ms) inhibitory effects in the motoneuron and the VRP (upper two traces). The effects were due to inhibitory post-synaptic potentials (IPSP). On the other hand, primary afferent depolarization (PAD) was observed only in the late latency in the DR (third trace). The PAD was induced by presynaptic inhibition [1]. The late inhibitory effects in the VRP and the DRP were exclusively induced from the NRGc. These results suggest that NRGc stimulation, an activation of the muscle tone inhibitory system, blocks the entry of sensory signals and reduces excitability of motoneurons. Post- and pre-synaptic inhibitions are considered to be induced by glycinergic and GABAergic interneurons [1]. These effects were induced by stimuli applied to the medial part of the NRGc bilaterally (Fig.3AB). In addition there are strong positive correlation in the amplitude between the VRP and the DRP (Fig.3C).

Both inhibitory effects were blocked by the activation of FRA. As shown in Fig.4A, NRGc stimulation induced VR-IPSP and DR-PAD. Volleys in group II muscle afferents of the plantar muscles induced Ia reflex in the VR and PAD in the DR (Fig.4B). Conditioning volleys in the FRA greatly reduced the NRGc-induced VR-IPSP and DR-PAD (Fig.4C). These findings suggest that interneurons responsible for IPSP and those for PAD receive inhibition from volleys in FRA. Possibly a particular group of common interneurons that receive inhibition from FRA may responsible for the post- and the pre-synaptic inhibition.

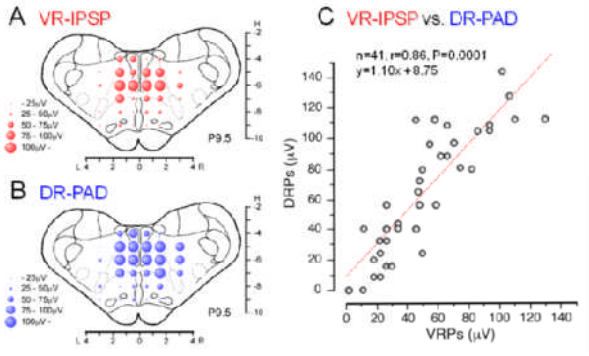

Figure 3 Medullary areas subserving the VR-IPSP and DR-PAD

Location of effective sites where electrical stimulation induced VR-IPSP (A) and DR-PAD (B). Both sites were mainly distributed to the medial medullary reticular formation corresponding to the nucleus reticularis gigantocellularis (NRGc). Sites from which large effects were induced are indicated large circles. C. There are positive correlation in the amplitude between the VR-IPSP and DR-PAD.

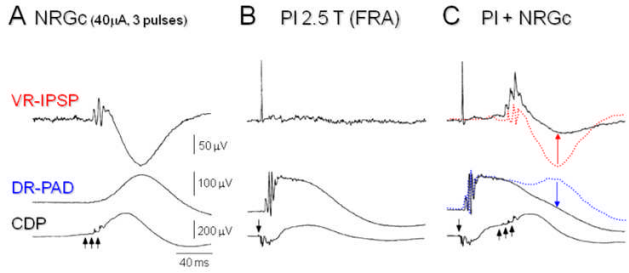

Figure 4 Volleys in FRA modulated the medullary inhibitory effects

A. VR-IPSP (upper) and DR-PAD (middle) induced by NRGc stimulation which is indicated by upward arrows. A bottom trace is CDP. B. An activation of group II muscle afferents from the plantar (Pl) muscle induced excitation via stretch reflex in VR and PAD in DR. C. Conditioning volleys in FRA in Pl nerve largely suppressed the NRGc-induced IPSP and DRP.

2. Neuronal activities in the spinal reflex arcs

Effects induced by the muscle tone inhibitory system upon neuronal elements in various reflex arcs were precisely examined. Major findings are shown in Fig.5. Stimulation of the NRGc induced late-IPSPs in α- (A) and γ- motoneurons (B). The inhibitory effects were observed in interneurons mediating reciprocal Ia inhibition (C), recurrent (Renshaw) inhibition (D), flexion reflex (E) and skin reflex (F). It should be noticed that time course of the IPSPs was mostly identical in motoneurons and interneurons. The NRGc stimuli induced PAD in Ia and skin afferents (G-H). Although data were not shown, volleys in FRA greatly reduced the inhibitory effects. Figure 6A summarized the NRGc-effects on spinal neurons. The IPSP was observed in 98% of motoneurons, and the PAD was induced in 78% of primary afferent fibers. Inhibitory and excitatory effects were induced the interneurons. Twenty-nine percent of interneurons received excitatory effects from the NRGc, whereas 35% cells were inhibited. More than one-thirds of cells (36%) did not respond to the NRGc stimulation.

The NRGc stimulation effectively activated inter-

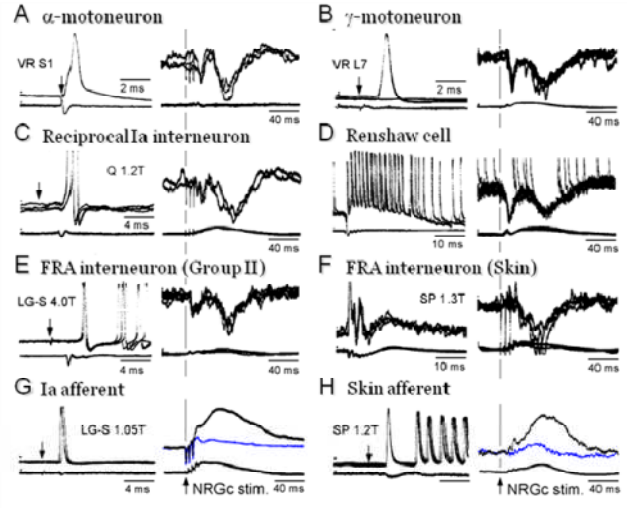

Figure 5 NRGc stimulus effects upon intracellular membrane potentials in motoneurons, interneurons and sensory afferents

Intracellular recording from lateral gastrocnemius motoneuron (A), γ-motoneuron (B), reciprocal Ia inhibitory interneuron (C), Renshaw cell (D) and interneurons mediating group II reflex (E) and skin reflex (F). NRGc stimulation induced IPSPs in these neurons. NRGc stimulation induced PAD in Ia muscle afferent (G) and skin afferent (H).

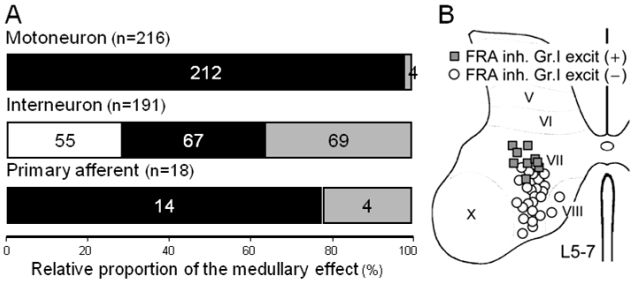

Figure 6 NRGc stimulus effects upon spinal neurons in reflex arcs

A. NRGc stimulus effects upon motoneurons (top), interneurons (middle) and primary (sensory) afferents (bottom). Neurons inhibited and excited by the NRGc stimuli were denoted by black and white colors. Neurons denoted by gray did not respond to the stimuli. B. Location of interneurons excited from the NRGc. All cells were inhibited from FRA. Interneurons receiving monosynaptic group I inputs were denoted by gray squares, while those without monosynaptic group I inputs were indicated by open circles.

neurons located in the lamina VII of Rexed (Fig.6B). A representative example was shown in Fig.7. Stimulation of the NRGc exerted early (monosynaptic) excitation and late excitation which induced action potentials (Fig.7A, B). This cell receives strong inhibition from volleys in skin afferent or FRA. Most of NRGc-excited interneurons received inhibitory effects from FRA (45/55=82%). A part of these cells also receive monosynaptic excitation from Gr. I muscle afferents. These findings suggest that the inhibitory reticulospinal system suppresses the activities constituents of spinal reflex arcs, sensory afferents, interneurons in reflex pathways and motoneurons, to reduce the level of muscle tone. Moreover a group of interneurons satisfying the following characteristics possibly mediate the inhibitory effects. They receive 1) late excitatory effects from the muscle tone inhibitory region (NRGc), and 2) inhibitory effects from volleys in FRA. 3) A part of cells receive monosynaptic Gr. I muscle afferents. 4) They are located in the lamina VII.

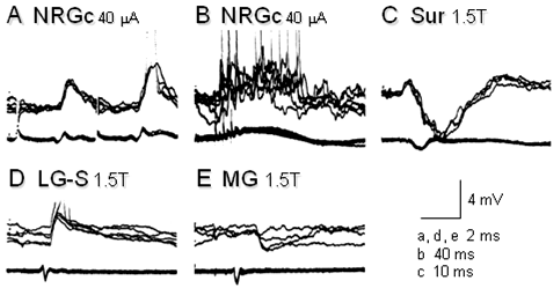

Figure 7 An interneuron that was excited from the NRGc

Monosynaptic (A) and late (B) EPSPs evoked from the NRGc. Volleys in skin afferents of sural nerve (Sur) induced IPSPs (C). Monosynaptic Ia EPSP (D) and disynaptic (E) Ia IPSP evoked from lateral gastrocnemius-soleus muscles (LG-S) and medial gastrocnemius muscles (MG), respectively.

3. IDENTIFICATION OF INTERNEURONS MEDIATING MUSCLE TONE SUPPRESSION

Then the question is whether the interneurons satisfying above criteria are involved in the inhibition of spinal reflex arcs? This was examined by spike-triggered averaging. In Fig. 8, the plausible interneurons induced IPSPs in an LG-S motoneuron (A) and a group II interneuron, and a PAD in a Ia afferent (C). Inhibitory connections to hindlimb motoneurons were precisely examined. Several interneurons inhibited plural motoneurons. However, no interneurons inhibited motoneurons with antagonistic relationship.

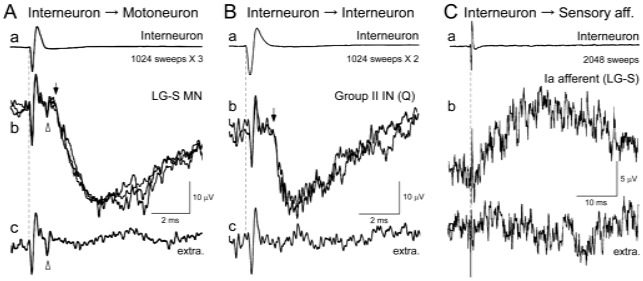

Figure 8 Inhibitory connections revealed by spike-triggered averaging

Plausible inhibitory interneurons inhibited monosynaptic IPSPs in an LG-S motoneuron (A) and a group II interneuron of quadriceps (Q) muscles (B). The same group of the interneuron induced primary afferent depolarization (PAD) in a group Ia afferent of LG-S muscles (C). From top to bottom, an action potential of the interneuron as a time reference, intracellular membrane potentials and extracellular control of each neuron. Three and two averaged recordings were superimposed in (A) and (B), respectively

IV. DISCUSSION

1. HOW DOES MUSCLE TONE INHIBITORY SYSTEM MODULATE THE EXCITABILITY OF SPINAL REFLEX ARCS?

Based on findings so far including the present study, we schematically summarize the muscle tone inhibitory system in the brainstem and spinal cord. This system is arising from the cholinergic neurons in the pedunculopontine tegmental nucleus (PPN), which subsequently excite pontine reticular neurons, medullary reticulospinal neurons in the NRGc and spinal inhibitory interneurons. Consequently this system exerts postsynaptic inhibition of α– and γ–motoneurons and interneurons mediating reflex pathways, and presynaptic

inhibition of primary afferents. Spinal reflexes can be therefore suppressed at the levels of sensory afferents (input stage), interneurons (integration stage) and motoneurons (output stage). It follows that suppression of muscle tone are due to the inhibition of spinal reflex arcs.

Then how does this system control muscle tone during movements? Interneurons in FRA partly operate as locomotor rhythm generating system, CPG [3]. Because reciprocal inhibitory interaction between the inhibitory system and FRA system was revealed in this study (Figs. 4, 5, 7), we propose that this interaction may be involved in the muscle tone regulation during locomotion. Moreover, plausible inhibitory interneurons in the inhibitory system partly receive group I muscle afferents, indicating that the inhibitory system may control muscle tone as a negative feedback system.

2. Control of Muscle Tone During Various Movements

A part of the present findings is schematically illustrated in Fig.10A. Reticulospinal neurons in the NRGc, brainstem output of the muscle tone inhibitory system activate plausible interneurons, which in turn inhibit either extensor or flexor muscles. The inhibitory interneurons receive inhibitory effect from volleys in FRA. Because large numbers of the NRGc-reticulospinal neurons project to the whole spinal neuraxis, the inhibitory system may simultaneously modulate the activity of motoneurons in the whole spinal segments. Because NRGc-reticulospinal neurons are possibly active during rapid eye movement (REM) sleep, the inhibitory system may exert generalized motor inhibition, resulting in muscular atonia. During REM sleep, FRA pathways were inactive (Fig.10B). Interneurons in the FRA pathways are alternately active during locomotion depending on step cycles. The alternate FRA activity may therefore inhibit the plausible inhibitory interneurons in a cyclic manner. This disinhibitory process may alternatively activate motoneurons in the left and right motoneurons in the lumbosacral spinal segments (Fig. 10C). Excitation of interneurons in FRA pathways in addition to flexor motoneurons innervating hand and digit muscles by the corticospinal tract is necessary to grip something. In this case, muscle tone inhibitory system may disinhibit because of FRA pathways, resulting in assisting excitation of flexor motoneurons. However other motoneurons that lack corticospinal inputs may not excite (Fig.10D).

In conclusion, we propose that interaction between muscle tone inhibitory system and FRA pathways at the level of spinal cord may play critical role in the real-time regulation of muscle tone during the ongoing various movements.

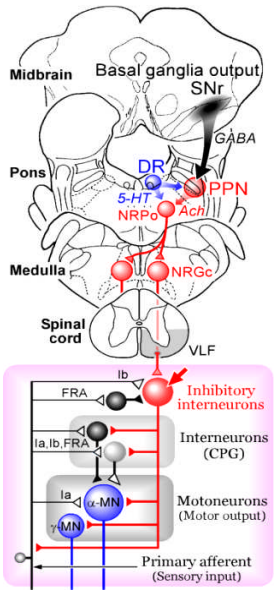

Figure 9 Muscle tone inhibitory system

Muscle tone inhibitory system inhibits sensory afferents, interneurons in reflex pathways and motoneurons, resulting in suppression of muscle tone. This system receives excitatory projections from the cerebral cortex, limbic system and the cerebellum at the level of the brainstem. The pedunculopontine tegmental nucleus (PPN) receives GABAergic projections from the substantia nigra pars reticulata (SNr), one of the basal ganglia output nuclei, indicating that the basal ganglia output inhibits this system. Serotonergic input from the DR inhibits this system.

ACh; acetylcholine; CPG; central pattern generator, DR; dorsal raphe nucleus, GABA; γ-amino-butylic acid, Ia and Ib Ia and Ib afferents, MN; motoneurons, NRGc; the nucleus reticularis gigantocellularis, NRPo; the nucleus reticularis pontis oralis, VLF; ventrolateral funiculus, 5- HT; serotonin.

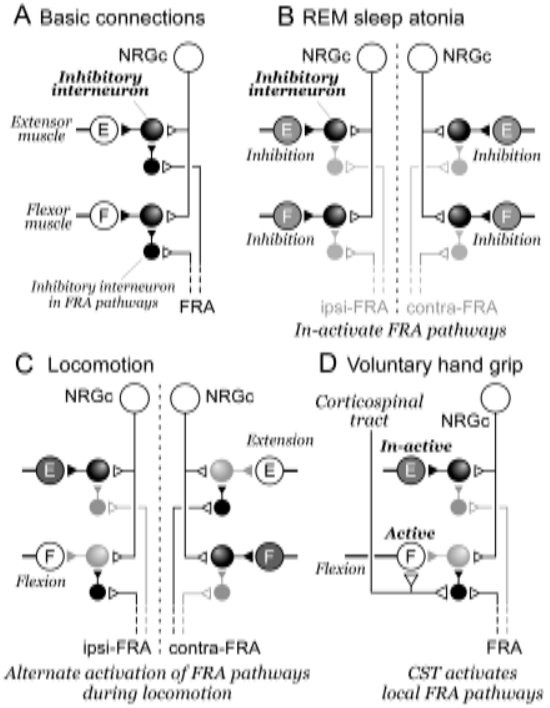

Figure 10 Interaction between muscle tone inhibitory system and FRA pathways during various movements

A. Basic neural connections between the muscle tone inhibitory system and FRA system at the level of spinal cord. Hypothetical models of muscle tone regulation during REM sleep (B), locomotion (C) and precise hand-digits movements. In each, muscle tone can be regulated by the inhibition from the FRA pathways to inhibitory interneurons in the muscle tone inhibitory system. See text for detail explanations. E and F; extensor and flexor motoneurons, ipsi-; ipsilateral, contra-; contralateral.

References

[1] E. Jankowska,, 1992 Interneuronal relay in spinal pathways from proprioceptors. Prog Neurobiol. 38, 335-378, 1992.

[2] S. Grillner, 2003. The motor infrastructure: from ion channels to neuronal networks. Nat. Rev. Neurosci., 4, 573-586, 2003

[3] Grillner, S., 1981. Control of locomotion in bipeds, tetrapods, and fish. In: Brooks, V.B. (Ed.), The Nervous System II, Am. Physiol. Soc. Press, Bethesda, pp 1179-1236.

[4] K. Takakusaki, K. Saitoh, S. Nonaka, T. Okumura, N. Miyokawa, Y. Koyama, "Neurobiological basis of state-dependent control of motor behavior", Sleep Biol. Rhyth., vol. 4, pp. 87-104, 2006

System Biomechanics of locomotion in the Japanese macaque: Exploration of principal mechanism for generating adaptive locomotion based on a neuro-musculoskeletal model

Naomichi Ogihara, Shinya Aoi, Yasuhiro Sugimoto, Masato Nakatsukasa, and Kazuo Tsuchiya

I. INTRODUCTION

Animals are capable of generating locomotion adaptive to diverse environments by coordinately controlling complex musculoskeletal systems. Mechanisms underlying the emergence of such intelligent adaptive behavior have conventionally been attributed to the sophisticated control mechanism of a biological sensorimotor nervous system. However, the suggestion has recently been made that animals achieve such adaptive yet efficient locomotion by exploiting intrinsic designs and properties of the musculoskeletal structures acquired through evolutionary history. A fundamental limitation may thus exist in attempts to clarify how the nervous system adaptively functions during locomotion based solely on neurophysiological studies; towards elucidating the mechanisms, the mechanisms of information processing emerging from appropriate dynamic interactions among the neuro-control system, musculoskeletal system and environment must be thoroughly investigated.

For this reason, our group has been biomechanically analyzing adaptive locomotor phenomena observed in actual bipedal locomotion in the Japanese monkey (*Macaca fuscata*) using an anatomical whole-body musculoskeletal model. Furthermore, we try to construct a biologically plausible computer simulation of Japanese monkey locomotion by integrating physiological findings from the locomotor nervous system and the anatomy and biomechanics of the musculoskeletal system, with the aim of illuminating the dynamic principles underlying the emergence of adaptive locomotion in animals. Herein we report current progress in our system biomechanics study of bipedal locomotion in the Japanese monkey, i.e., three-dimensional gait analysis and forward dynamic simulation based on the anatomically based whole-body musculoskeletal model.

II. 3D KINEMATICS OF LOCOMOTION

Two Japanese monkeys (KA = 12.3 kg; KU = 9.2 kg) walking bipedally on a treadmill at 3, 4, and 5 km/h was filmed using 4 high-speed cameras (Nac Image Technology, HotShot 1280) and locomotor kinematics was analyzed. Frame rate and shutter speed are set to 125 frame/sec and 1/250 sec, respectively. The treadmill (Maruyasu Kikai, MMX300-FG-140) was specially designed so that a force platform (Kyowa Dengyo, EFP-S-1.5KNSA13) can be embedded, and we synchronously measured vertical component of ground reaction force acting on right foot during bipedal walking. From the motion images, well-recorded bipedal sequences were manually digitized frame-by-frame using three-dimensional (3D) motion analysis software and the coordinates of markers were calculated. A total of 16 reflexive markers (8 on one side) were digitized at: 1) head of 5th metatarsal; 2) lateral malleolus of fibula; 3) lateral epicondyle of femur; 4) greater trochanter; 5) acromion; 6) lateral epicondyle of humerus; 7) styloid process of ulna; and 8) head of 5th metacarpal (Fig. 1).

If our anatomically-based whole-body musculoskeletal model of Japanese monkey (with 20 segments and 41 joint degrees of freedom) could be matched to the temporal history of digitized marker coordinates, all body skeletal motion could be reconstructed [1]. For this, the musculoskeletal model was firstly scaled to the size of the monkey in the video based on segment lengths, and the joint angles were adjusted frame-by-frame to minimize the sum of distances between corresponding markers while minimizing deviations of joint angles from the anatomically natural position (midpoints of the ranges of joint rotations). The quasi-Newtonian method was used to solve this minimization problem. Figure 2 illustrates a result of matching, indicating that the whole-body kinematics of a Japanese monkey walking on a treadmill was successfully reconstructed using an anatomically based musculoskeletal model and the model-based matching technique. By introducing kinematc constraints defined by joint morphology, the present study yielded anatomically reasonable, natural skeletal motion from a limited number of external markers.

Based on this estimated 3D skeletal kinematics, hip, knee and ankle joint angles were calculated and changes in the joint angle profiles with increasing walking velocity were investigated. It was found that 1) the femur is abducted with respect to the pelvis throughout the gait cycle and is laterally rotated at the time of foot-contact but medially rotated at the

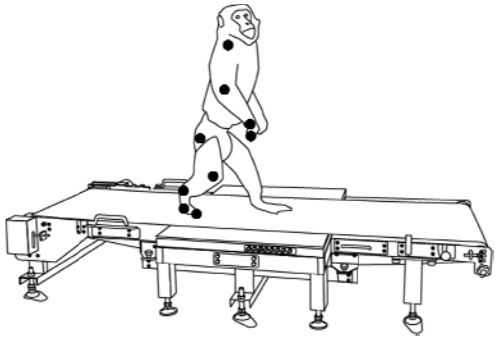

Fig. 1. A Japanese macaque walking on a treadmill in which a force platform was embedded.

N. Ogihara and M. Nakatsukasa are with Laboratory of Physical Anthropology, Graduate School of Science, Kyoto University, Kitashirakawa-oiwakecho, Sakyo, Kyoto 606-8502, Japan (e-mail: {ogihara, nakatsuk}@anthro.zool.kyoto-u.ac.jp).

S. Aoi is with Department of Aeronautics and Astronautics, Graduate School of Engineering, Kyoto University, Yoshida-honmachi, Sakyo, Kyoto 606-8501, Japan (e-mail: shinya_aoi@kuaero.kyoto-u.ac.jp).

Y. Sugimoto is with Department of Mechanical Engineering, Graduate School of Science and Technology, Kobe University, Rokkodai, Nada, Kobe City, Hyogo 657-8501, Japan (e-mail: yas@osukalab.mech.kobe-u.ac.jp).

K. Tsuchiya is with Faculty of Science and Engineering, Doshisha University, Tatara Miyakodani, Kyotanabe City, Kyoto 610-0394, Japan (e-mail: katsuchi@mail.doshisha.ac.jp).

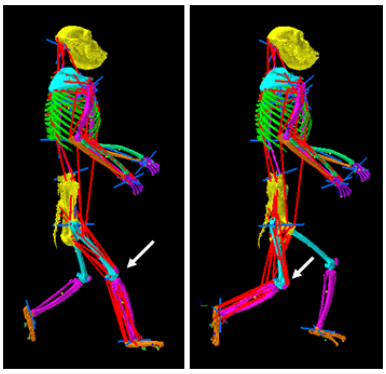

Fig. 2. Reconstruction of whole-body kinematics of bipedal walking in the Japanese macaque using a model-matching method. At the time of foot-contact (right) and toe-off (left).

time of toe-off; and 2) with increasing walking velocity, the hip joint is more extended at the toe-off and the knee joint is more flexed in the mid-stance phase. This indicates that gait pattern is adaptively altered depending on velocity; the velocity was not controlled by simple tuning of step frequency of the locomotor rhythm generated by a neuronal network. The comparison of the ground reaction force confirmed that the vertical force profiles were single-peaked; the double-peaked curve that is seen in humans was not observed [2]. Besides, this study demonstrated that the vertical force profile is also altered with walking velocity; its peak value gets larger with the velocity increases.

III. METABOLIC COST OF TRANSPORT

In human walking, there is optimal speed of locomotion at which the metabolic cost of transport is minimized. Human natural walking is generated approximately at this speed. Is there similar optimal speed for bipedal walking in the Japanese macaque? To answer this question, we investigated the metabolic cost of transport with different walking velocities. Two Japanese macaques (Subject 1 = 12 kg; Subject 2 = 5.5 kg) walked bipedally at different velocities on a treadmill that is placed in an airtight chamber, and we measured time rate of change in carbon dioxide concentration (CO_2 ppm/sec) in the chamber using an infrared gas analyzer (Shimadzu Corp., CGT-7000) [3,4]. We then calculated CO_2 production rate by multiplying it by the volume of the chamber, and converted it to O_2 consumption rate, assuming respiratory quotient is equal to 0.85. We obtained metabolic energy consumption rate by using the factor of 20.1 J/ml O_2 [5] and estimated the cost of transport by dividing the metabolic energy consumption rate by the treadmill speed and the body mass.

Figure 3 shows the variations of the metabolic cost of transport with walking speed for the two Japanese macaques.

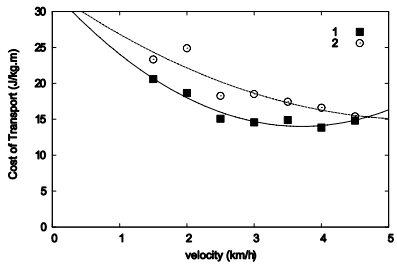

Fig. 3. Metabolic cost of transport of bipedal walking in the Japanese macaque plotted against walking velocity.

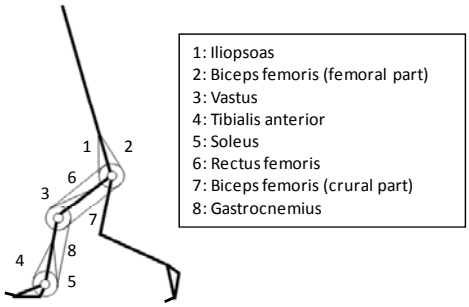

Fig. 4. Two-dimensional musculoskeletal model of Japanese macaque.

The cost of transport for human walking is a U-shaped profile, but that for the Japanese macaques does not exhibit a clear U-shaped profile; the cost of transport is almost constant or decreases gradually as the speed increases. This discrepancy may be attributable to adoption of a running mechanics (spring-mass mechanism in which tendons and ligaments store elastic energy in the early stance (breaking) phase and release it for moving the body forward in the late stance (propulsive) phase) at a relatively slower speed in the Japanese macaque, even though its duty ratio is above 0.5. The cost of transport for human running shows a gradual decrease with an increase in speed [6]. Because the corresponding curve for macaque running is located at a relatively lower position, a clear humanlike U-shaped profile might not have been experimentally observed for the macaque bipedalism.

IV. SIMULATION OF BIPEDAL LOCOMOTION

If bipedal walking of the Japanese macaque is dynamically reconstructed by computer simulation based on biologically relevant musculoskeletal modeling, predictive study of locomotion becomes possible. This would enable biomechanical evaluation of causal relationships among musculoskeletal morphology, locomotor kinematics, and energetics, allowing examination of hypotheses and scenarios of the origin and evolution of human bipedalism. Therefore, we developed a dynamic simulation of bipedal locomotion in the Japanese macaque based on a PD feedback control.

We constructed a two-dimensional musculoskeletal model of the bipedal Japanese macaque consisting of seven links and eight principal muscles (Figure 4). Both inertial parameters of the limb segments and muscle parameters were determined based on the 3D musculoskeletal model [1]. The foot segment is represented by two parts: tarsometatarsal part modeled by a rigid body and massless phalangeal part. Metacarpophalangeal joint is assumed to be kinematically prescribed.

Generation of locomotion was achieved by the following method. First, desired joint trajectories of bipedal walking were created based on the 3D kinematic data measured previously. Specifically, the experimentally obtained 3D coordinates of the five hindlimb and trunk markers and a newly digitized point at distal phalanx of the foot were projected onto the sagittal plane, and average 2D displacements of the six coordinates were then calculated for each walking speed (3, 4 and 5 km/h) to obtain the desired joint trajectories. The kinematic data used for this calculation are those of KA because body dimensions of this individual were very similar to that of the model used here.

The displacement of the hip joint in the sagittal plane is essentially a sinusoidal curve. Thus, the hip displacement was

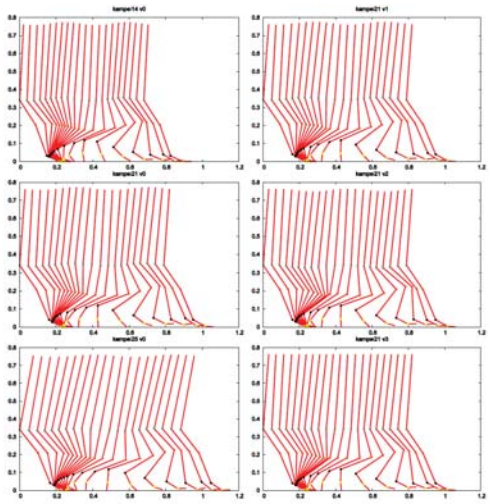

Fig. 5. Gait kinematics used for the simulation. A-C: Measured gait patters at 3, 4, 5 km/h (condition 1). D-F: Virtual gait patterns (4 km/h) based on the condition 2, 3 and 4..

approximated by the following sinusoidal function using least square fitting.

$$z = a\cos[4\pi(\frac{x}{s} - \theta)] + b \quad (1)$$

where (x,z) is the coordinate of the hip joint, s is the stride length, $a,b,\ \theta$ are the coefficients representing the amplitude, height above the ground, and phase, respectively. Here we altered these three coefficients to generate virtual walking trajectories for predictive simulation. In this study, the following four trajectories of the hip joint were generated for each of the walking speeds: 1) no changes in the three coefficients thus the trajectory corresponds to the measured data; 2) the phase θ is altered to that of human value; 3) the phase θ is altered to that of human value and a is multiplied by -1; and 4) a is zero. The positions of the knee and ankle joints and the acromion were subsequently modified under the condition that the movement of the phalangeal part of the foot segment was kinematically prescribed based on the corresponding measured data. Figure 5A-C illustrate three gait patterns calculated based on the condition 1 for the speeds of 3, 4, 5 km/h, respectively. These gait patterns corresponds to the actually measured locomotion. Figure 5 D-F show three virtual gait patterns for the speed of 4 km/h calculated based on the conditions 2, 3, and 4, respectively. These three virtual gait patterns correspond to walking with humanlike trunk displacement, with that of reversed phase, and with no vertical trunk displacement, respectively.

A total of 12 gait patters (4 conditions × 3 speeds) were calculated and the desired joint trajectories and then the trajectories of the desired muscle length generated. Motor command sent to the m th muscle a_m is generated using two oscillators and a PD feedback control low as [7]:

$$\begin{aligned} \dot{\phi}_L &= \omega - K\sin(\phi_L - \phi_R - \pi) \\ \dot{\phi}_R &= \omega - K\sin(\phi_R - \phi_L - \pi) \\ a_m &= \kappa(\xi_m - \xi^*_m(\varphi)) + \sigma\dot{\eta}_m \end{aligned} \quad (2)$$

where φ_L and φ_R are the oscillatory phases of left and right legs ($0 \le \varphi_L, \varphi_R, \le 2\pi$), ω is the parameter defining the frequency of the oscillator ($2\pi/T$), T is the gait cycle, and K is a gain parameter, ξ_m and η_m is the normalized muscle length and contractile velocity, ξ^*_m is the desired normalized muscle length

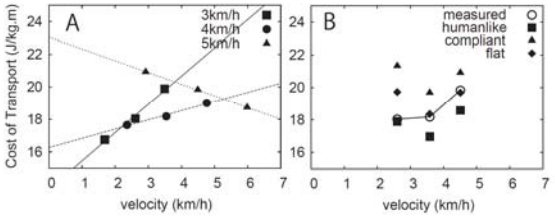

Fig. 6. Cost of transport of generated locomotion vs. walking velocity.

(expressed as a function of φ), and κ and σ are the gain parameters, respectively. The magnitude of the muscle force is modeled to be proportional to the motor command a_m ($a_m = 0$ if $a_m < 0$). The muscle generates its maximum force when $a_m = 1$.

The energetic cost of the generated locomotion is estimated based on the calculation of mechanical energy of the muscles:

$$E = \frac{1}{e} \cdot \int \sum_m |F_m v_m| dt \quad (3)$$

where E is the estimated metabolic cost of locomotion, v is the contractile velocity of the muscle, e is the efficiency of conversion from metabolic to mechanical energy (0.25) [8,9],.

To investigate the effects of change in the gait cycle on the cost of transport of bipedal walking in the Japanese macaque, we emulated locomotion using the desired trajectories based on the condition 1 with changing the gait cycle by multiplying the measured average cycle by 0.75, 1, and 1.5. These alterations of the gait cycle represent approximately 1.3, 1.0, and 0.7-fold changes in walking velocity without changing gait kinematics. Figure 6A plotted the cost of transport of the generated locomotion against walking velocity. If the velocity is low, the 3km/h gait pattern is most economical whereas the 5 km/h gait pattern is most efficient in fast-moving locomotion; in the middle range, the 4 km/h gait pattern is cheapest. Thus, the Japanese macaque adaptively alters its locomotor kinematics depending on its walking velocity. It was also observed that the cost of transport increases with increasing walking velocity for the 3 and 4 km/h gait patterns, but it decreases for the 5 km/h gait pattern, suggesting 5 km/h gait pattern is mechanically running despite the fact the duty factor is above 0.5.

Comparisons of the cost of transport of the virtual gait patterns (Figure 6B) suggest that the humanlike gait pattern (condition 2) was the most economical, indicating that humanlike fluctuation of the body's center of mass actually contributes for generation of efficient walking. However, the Japanese macaque does not acquire this humanlike efficient walking pattern particularly when walking velocity is higher, probably due to its anatomical constraints. However, this simulation does not take the elastic elements into consideration and the cost of transport for the fast-moving gaits might be overestimated. The effect of the elastic recoil must be investigated in future studies.

V. SIMULATION OF ADAPTIVE LOCOMOTION

In the above simulation based on a feedback control low, we must have assumed unrealistically high values for the gain parameters to make it work. Furthermore, the system obviously destabilizes if we introduce transport delays in the nervous system. It was therefore anticipated that animals utilize some sort of feedforward control strategy to generate locomotion for adaptively coping with various changing environments.

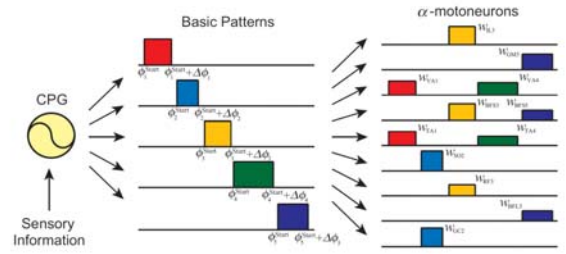

Fig. 7.Basic muscle activity patterns are constructed by a combination of five principal waveforms.

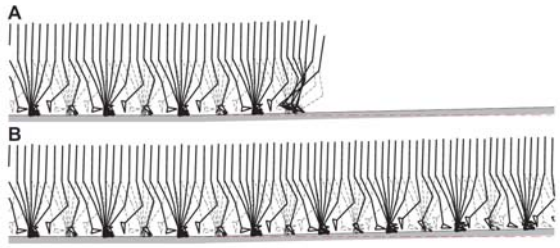

Fig. 8. Autonomous adaptation of locomotion on a slope. A: without, B: with thephase resetting mechanism.

Ivanenko et al. analyzed electromyographic activity patterns of muscles in human leg during walking using principal component analysis and found that activation patterns of muscles can be decomposed into a combination of five principal waveforms [10-11]. These invariant synergistic muscle activation patterns are considered to be created by a functional module located in the spinal cord, and control of this combination patterns alters muscle activity, and hence movement [12]. In this study, we assume that appropriate combinations of such basic muscle activation patterns are prescribed in the spinal cord level to form feedforward muscle activity for locomotion, and a new neuro-control model was constructed (Figure 7). Specifically, each of the principal waveforms, represented by a square wave, is assumed in the spinal module and each of the muscle activities is generated as a linear summation of the principal waveforms. The motor commands are sent out to muscles in a feedforward manner based on this phase signal. Recent studies suggested that a CPG consists of two layers: a rhythm generator (RG) that generates oscillatory signal, and a pattern generator (PG) that generates muscle activity patterns based on the phase signal from the RG [13-14]. The five principal waveforms are generated by the RG and they are combined to generate the basic muscle activities in the PG. In addition, feedback control mechanisms are modeled to autonomously maintain the posture of the trunk segment and the walking velocity. We also incorporated a phase-resetting mechanism based on foot-contact information.

We emulated human bipedal walking using a 2D musculoskeletal model [15,7] and this nervous model. The generated locomotion was confirmed to be autonomously adaptable to a certain degree of external force perturbation, sudden increase in the trunk mass, and slope (Figure 8). We plan to apply this locomotor nervous model for dynamic simulation of bipedal locomotion in the Japanese macaque using the anatomically based whole-body musculoskeletal model.

VI. CONCLUSION

Herein we report our system biomechanics studies of bipedal locomotion in the Japanese macaque based on an anatomically based musculoskeletal model, importance of which has gained particular emphasis in recent years for truly elucidating adaptive mechanisms of locomotion in animals. The final goal of our project is to understand the dynamic principles underlying the emergence of adaptive locomotor phenomena to the extent that we can quantitatively reproduce them in a computer using biologically relevant models. To this end, we further investigate adaptive strategies of locomotion in Japanese macaques by biomechanical analyses of locomotion in response to perturbations (such as weighted locomotion and locomotion on a split-belt treadmill) and by synthesizing such adaptive behaviors using mathematical models.

REFERENCES

[1] N. Ogihara, H. Makishima, S.Aoi, Y. Sugimoto, K.Tsuchiya, and M. Nakatsukasa, “Development of an Anatomically Based Whole-Body Musculoskeletal Model of the Japanese Macaque (Macaca fuscata)”, American Journal of Physical Anthropology, in press.

[2] N. Ogihara, E. Hirasaki, H. Kumakura and M. Nakatsukasa, “Ground-reaction-force profiles of bipedal walking in bipedally-trained Japanese monkeys”, Journal of Human Evolution, vol. 53, pp.302-308, 2007.

[3] M. Nakatsukasa, N. Ogihara, Y. Hamada, Y. Goto, M. Yamada, T. Hirakawa and E. Hirasaki, “Energetic costs of bipedal and quadrupedal walking in Japanese Macaques”, American Journal of Physical Anthropology, vol. 124, pp.248-256, 2004.

[4] M. Nakatsukasa, E. Hirasaki, and N. Ogihara, “Energy expenditure of bipedal walking is higher than that of quadrupedal walking in Japanese macaques”, American Journal of Physical Anthropology, vol. 131, pp.33-37, 2006.

[5] K. Schmidt-Nielsen, Animal Physiology: Adaptation and Environment. Cambridge: Cambridge University Press, 1997.

[6] D.R. Carrier, “The energetic paradox of human running and hominid evolution”, Current Anthropology, vol. 25, pp.483-495, 1984.

[7] S.Aoi, N. Ogihara, Y. Sugimoto, and K.Tsuchiya, “Simulating adaptive human bipedal locomotion based on phase resetting using foot-contact information”, Advanced Robotics, vol. 22, pp.1697-1713, 2008.

[8] R.A. Ferguson, D. Ball, P. Krustrup, P. Aagaard, M. Kjaer, A.J. Sargeant, Y. Hellsten and J. Bangsbo, “Muscle oxygen uptake and energy turnover during dynamic exercise at different contraction frequencies in humans”, Journal of Physiology, vol. 536, pp.261-271, 2001.

[9] N.C. Heglund and G.A. Cavagna, “Efficiency of vertebrate locomotory muscles”, Journal of Experimental Biology, vol. 115, pp.283-292, 1985.

[10] Y.P. Ivanenko, R.E. Poppele and F. Lacquaniti, “Motor control programs and walking”, Neuroscientist, vol. 12, pp.339-348, 2006.

[11] Y.P. Ivanenko, R.E. Poppele and E. Lacquaniti, “Five basic muscle activation patterns account for muscle activity during human locomotion”, Journal of Physiology, vol. 556, pp.267-282, 2004.

[12] A. d'Avella, P. Saltiel and E. Bizzi, “Combinations of muscle synergies in the construction of a natural motor behavior”, Nature Neuroscience, vol. 6, pp.300-308, 2003.

[13] M. Lafreniere-Roula and D.A. McCrea, “Deletions of rhythmic motoneuron activity during fictive locomotion and scratch provide clues to the organization of the mammalian central pattern generator”, Journal of Neurophysiology, vol. 94, pp.1120-1132, 2005.

[14] I.A. Rybak, N.A. Shevtsova, M. Lafreniere-Roula and D.A. McCrea, “Modelling spinal circuitry involved in locomotor pattern generation: insights from deletions during fictive locomotion”, Journal of Physiology, vol. 577, pp.617-639, 2006.

[15] N. Ogihara and N. Yamazaki, “Generation of human bipedal locomotion by a bio-mimetic neuro-musculo-skeletal model”. Biological Cybernetics, vol. 84, pp. 1-11, 2001.

Group B-3: Realization of Adaptive Locomotion based on Dynamic Interaction between Body, Brain, and Environment

Koh Hosoda, Osaka University
Hiroshi Kimura, University of Electro-Communications
Katsuyoshi Tsujita, Osaka Institute of Technology
Kousuke Inoue, Ibaraki University
Takashi Takuma, Osaka Institute of Technology

***Abstract*— Behavior of an agent is emerged from the interaction between body, control, and environmental dynamics. The research group B-3 aims to design body and control dynamics for emerging adaptive locomotion. We investigate three types of locomotion, biped, quadruped, and snake-like and developed robots. In 2008, our achievement is (1) conducting jumping experiments by a monopod with anthropomorphic muscular-skeletal system, (2) investigating walking stability of a pneumatic-driven quadruped robot by changing its body compliance, and (3) developing several sensors required for adaptive locomotion of the snake-like robot, analyzing influence of viscoelasticity on locomotion performance, and conducting measurement of locomotion of a living snake.**

I. Introduction

The research program entitled Emergence of Adaptive Motor Function through Interaction between Body, Brain, and Environment - Understanding of Mobiligence by Constructive Approach - started in 2005, as a MEXT Grant-in-Aid for Scientific Research on Priority Areas. One of the main goals of the project is to find a principle of emergence of adaptive locomotion. To approach the issue from the constructivist viewpoint, our research group B-3 aims to develop locomotive agents with various modalities based on dynamic interaction between body, control and environment. In 2008, our achievement is (1) conducting jumping experiments by a monopod with anthropomorphic muscular-skeletal system, (2) investigating walking stability of a pneumatic-driven quadruped robot by changing its body compliance, and (3) developing several sensors required for adaptive locomotion of the snake-like robot, analyzing influence of viscoelasticity on locomotion performance, and conducting measurement of locomotion of a living snake.

II. Biped Robots That Have Biarticular Muscles and Their Dynamic Locomotion

A. Overview

Bi-articular muscles

Biarticular muscles that drive not only one joint but also multi joints play an important role for realizing synergistic motion of the animal's body. They also provide redundancy that can be utilized for controlling complex body system. This redundancy can be utilized for roll sharing and cooperation between low and high control layers. In this report, we shortly introduce a monopod and b biped with biarticular muscles which are developed last year, and investigate jumping and running behavior.

B. 2D monopod with biarticular muscles

A 2D monopod with biarticular muscles is developed to investigate their roles on dynamic locomotion (Figure 1).

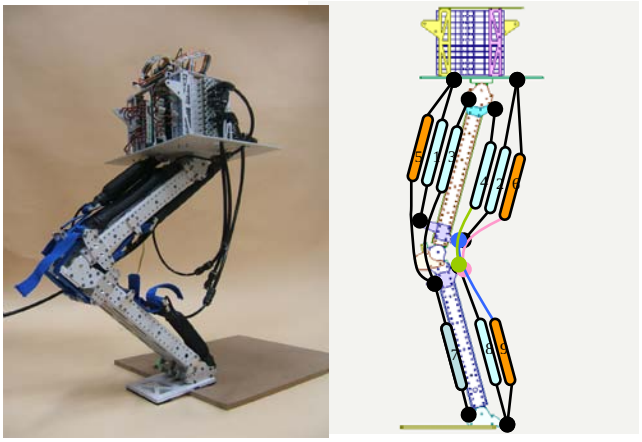

Figure 1: A 2D monopod with biarticular muscles

The robot consists of a body, a thigh, a shank and a foot. Three joints are driven by 6 (3 pairs) monoarticular and 3 biarticular McKibben artificial pneumatic muscles. These muscles are controlled based on the information observed by pressure sensors equipped in the artificial muscles and gyro sensor on the body. We conducted (1) jumping experiment from standstill, (2) landing experiment, and (3) bouncing experiment to investigate the role of the biarticular muscles. In this report, we show an experimental result on the jumping experiment.

C. Investigation on functions of biarticular muscles

The robot is equipped with 3 biarticular muscles: Rectus fomiris, Hanstrings, and Gastrocnemius. Each of them regulates the coordination between knee and hip joints and the one between knee and ankle joints. Since the system has these

muscles, it can realize coordinated movement between joints. When only the knee is driven by monoarticular muscles, extension of the knee drives ankle joint through the gastrocnemius and hip joint through hamstrings. The synergistic motion depends on designing parameters such as moment arm of the muscles, and in the case of the monopod shown in the figure, such coordinated movement occurs when the biarticular muscles are excited. As a result, the rotation of the robot is suppressed. This is shown in the experimental results (figure 2). The relation between angles of touch down and taking off is plotted in Figure 3. In these experimental results, we put a pre-determined set of air to the muscles, and let the robot fall. When it contacts with the ground, only the knee monoarticular muscle is driven. We can see that the rotating movement of the robot is suppressed when we increase the air to the gastrocinemius.

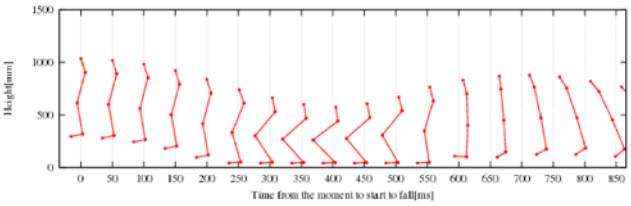

(a) air supply to gastrocinemius :0ms

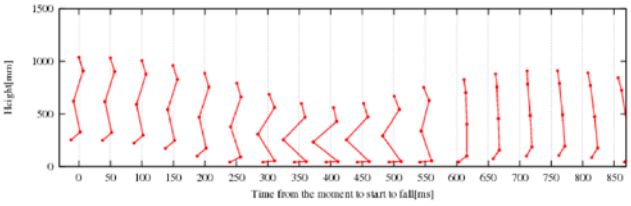

(b) air supply to gastrocinemius :10ms

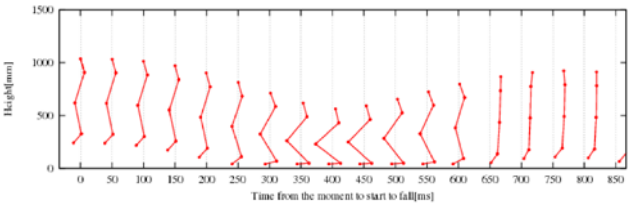

(c) air supply to gastrocinemius :150ms

Figure 2: bouncing behavior of the monopod when only the knee joint is activated at the contact.

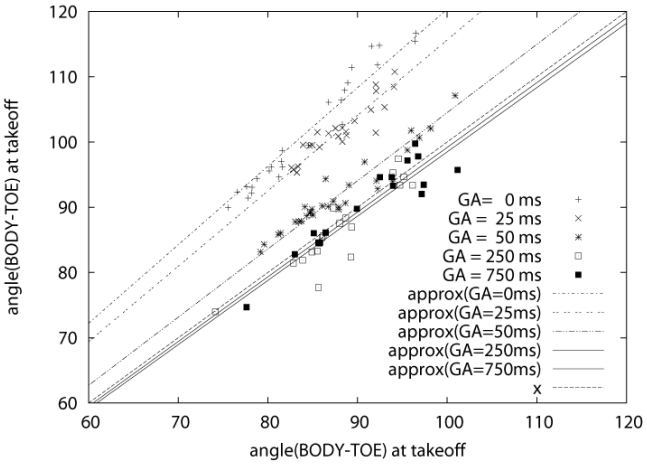

Figure 3: Relation between angles of touch down and taking off when the excitation of GA changes

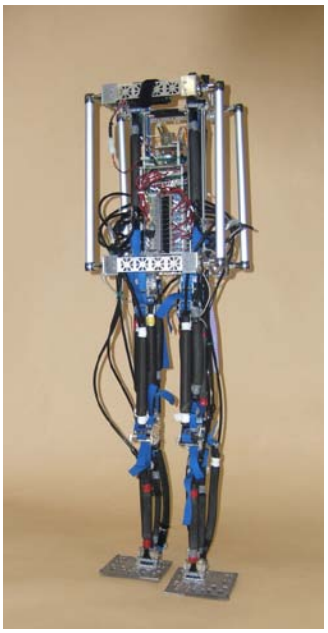

Figure 4: 3D biped robot with biarticular muscles

D. 3D biped robot with biarticular muscles

We also improved a 3D biped robot whose leg structure was almost the same as the jumping robot shown in the last section. (see Figure 4). We put additional parallel muscles to anti-gravity muscles; longer muscles increase the range of joint movement. We conducted experiments on walking, jumping, and running separately.

Comparing with the monopod that has smaller torso, this robot changes its behavior more sensitive to the activation of hip biarticular muscles, rectus and hamstrings. We demonstrated that the robot could walk and jump stably, and could run for several steps by experiments

III. A Feasibility Study on Stability of Gait Patterns with Changable Body Stiffness using Pneumatic Actuators in a Quadruped Robot

A. Overview

In this study, an oscillator-type gait controller for a quadruped robot with antagonistic pairs of pneumatic actuators is proposed. And by using the controller, a feasibility study on the stability of gait patterns with changeable body stiffness is reported. The periodic motions of the legs are generated and controlled by an oscillator network with state resetting. This type of controller has robustness in its gaits against variation of walking conditions or changes of environment. However, it sometimes loses robustness under conditions of actuation delay, decrease of actuator accuracy, etc. We investigated whether an oscillator-type controller with phase resetting is also effective under such conditions. The stability of locomotion also strongly depends on the mechanical properties of the body mechanism, especially the joint stiffness. In this report, the muscle tone of the robot on the pitching motion at the trunk is changeable by using the changeable elasticity of the pneumatic actuators. The stability of quadruped locomotion in walk and trot patterns with changeable body stiffness was evaluated with numerical simulations and hardware experiments.

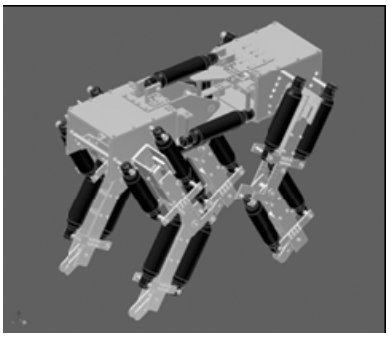

(a) CAD

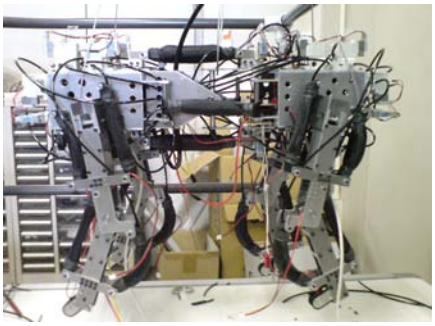

(b) real robot

Figure 5: A quadruped robot driven by pneumatic artificial muscles

B. Model and stability analysis

The model of the robot is shown in Figure 5. The stability of the limit cycle is examined in the following way.

First, eight variables were selected as state variables.

$$X = \left[\theta_1^{(0)} \quad \theta_2^{(0)} \quad \theta_p^{(B)} \quad \theta_y^{(B)} \quad \dot{\theta}_1^{(0)} \quad \dot{\theta}_2^{(0)} \quad \dot{\theta}_p^{(B)} \quad \dot{\theta}_y^{(B)}\right]^T$$

Variables $\theta_1^{(0)}$ and $\theta_2^{(0)}$ are the roll and pitch angles of the main body. $\theta_p^{(B)}$ and $\theta_y^{(B)}$ and are the pitch and yaw angles of the trunk.

The stability of the robot's locomotion is examined by checking eigenvalues $\lambda_k (k = 1, \cdots 8)$ of the Poincaré map in terms of variable

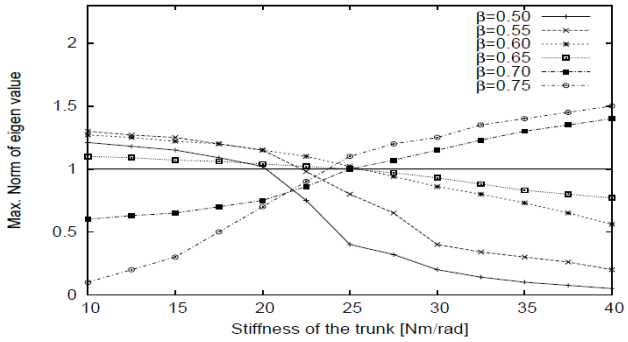

Figure 6 Maximum norm of Poincaré map's eigenvalue

C. Results

Figure 6 shows the maximum norm of the Poincaré map's eigenvalue at various duty ratio β and trunk joint stiffness K_{sp}. Note that when duty ratio β is around 0.75 (typical duty ratio for a walk pattern), the locomotion is stable at a low joint stiffness of the trunk. But when duty ratio β is around 0.50 (typical duty ratio for a trot pattern), the locomotion is stable at a high joint stiffness of the trunk. The midrange duty ratio and the joint stiffness are not suitable for stable locomotion. These facts may note that gait transition occurs from a stable attractor to another one by passing through the unstable parameter region. That remains as the future work to clarify.

We have developed a real quadruped robot driven by pneumatic artificial muscles, and conducted experiments. The robot could locomote stably both in walk and trot patterns although it is affected by unevenness of the floor. Therefore, we can conclude that the oscillatory network with phase resetting is effective for a quadruped robot driven by pneumatic artificial muscles, which leads to large time delay.

IV. Realization of Snake-like Locomotion, and Observation of a Real Snake

A. Overview

Snakes have long cord-shaped body and propel by winding its body to generate mechanical interaction with the environment (friction and pressure between abdomen or side of the body and the environment). This locomotion is essentially different from other legged animals. Based on this type of locomotion, living snakes exhibit highly adaptive behaviors in diverse environments such as rough ground, water, mud, sand, or tree branches. By investigating mobiligence of snakes underlying such adaptability, information about dependencies of intelligence to locomotion types can be obtained.

In this fiscal year, we developed several sensors required for adaptive locomotion of the snake-like robot, analyzed influence of viscoelasticity on locomotion performance, and conducted measurement of locomotion of a living snake.

B. Development of sensors for adaptation

In order to achieve and analyze environmentally adaptable locomotion on the snake-like robot that we have developed (Figure 7), we developed sensory systems to measure mechanical interaction during locomotion. This robot achieves animal-like viscoelasticity by the use of McKibben-type pneumatic actuators. The most essential sensory information in snake locomotion is status of each actuator and force acting between the robot body and the environment. Therefore, we developed an External Force Sensor (corresponding to sensory organs on the surface of the body) measuring lateral and normal force acting on the bottom of the robot and an Internal Force Sensor (corresponding to sensory organs in muscles: muscle spindle and tendon organ) that measures length (and extension speed) and tension of each pneumatic actuator. Up to now, we designed and developed a prototype of these sensors and conducted preliminary experiments.

C. Analysis of locomotive performance of the snake-like robot with pneumatic actuators

We conducted analysis and evaluation of contribution of viscoelasticity of the developed robot to locomotion control and locomotion performance.

One of the most important advantages of viscoelasticity is that complex body locomotion is controllable with simple controller. We verified if the robot can achieve smooth locomotion by simple control logic in which supply/expulsion modes of the high-pressure air valve are periodically switched at some specific timing in each cycle. As the result, such very simple control can exhibit three types of locomotion (lateral undulation, sidewinding, and rectilinear) smoothly.

Additionally, we compared locomotive performance of the robot with (a) electric motors and (b) pneumatic actuators on simulations. Results showed that the robot with pneumatic actuators has larger propulsive performance in narrow spaces (Figure 8).

D. Measurement of locomotion of a living snake

We conducted measurement of kinematics of a living snake (corn snake, *Elphe guttata*, Figure 9). Up to now, we installed a measurement system in which markers attached on the spine of the snake are tracked. Figure 10 shows a result of measurement of lateral undulation locomotion on a carpet environment. Up to the end of the fiscal year, we will investigate detailed body structure of a living snake using CT scanner and myoelectrical measurement with a specific adaptive locomotion by the real snake.

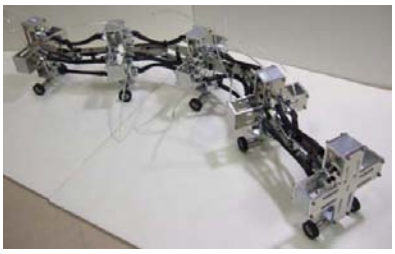

Figure 7 Snake-like robot with pneumatic actuators

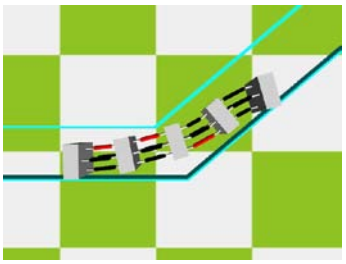

Fig. 8 Simulation of locomotion in narrow environment

Fig. 9 Experimental animal (*Elaphe guttata*)

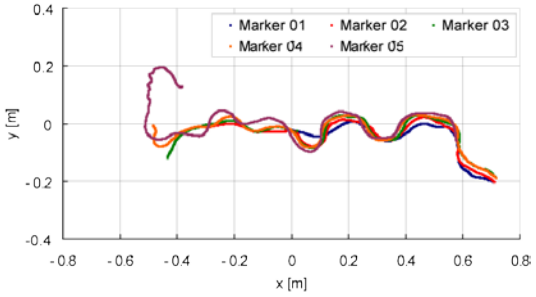

Figure 10 Kinematics of lateral undulation locomotion

Research on Modeling Reflex-Motion System for Assisting People with Walking Difficulties

Hiroshi YOKOI and Masatoshi TAKITA

Abstract – In our research, we aim at modeling reflex-motion system of people with walking difficulties, and develop walking assist devices functioning bio-feedback for them. Therefore, we focus on the following three topics: (1) motion-discrimination; (2) muscle assist; (3) bio-feedback system. This paper mainly reports development and verification experiments of our FES (functional Electrical Stimulator) using special reflex of people with walking difficulties.

I. INTRODUCTION

Disorder of nervous system causes paraplegic and panplegia, takes away human mobility, and decreases Quality of Life (QOL). This research aims at recovering mobility of people with walking difficulties, and try (1) to reveal the sensory-motor system of those people for assuming their motion intention and (2) to build function-recovery scheme. We take two approaches in parallel for solving those issues: a physiological approach to use animals and an engineering approach to build man-machine mutual adaptive system. As a final target, we focus on building a measurement/control system, which automatically adjust to human sensory-motor system. So, we use a functional electrical stimulator (FES), and examine responses of sensory-motor system in this paper.

II. PROPOSED FES SYSTEM: STIMULATION TO REFLEX AND MUSCLE

For enhancing the QOL of the people with walking difficulties, we use FES. The FES activates muscles and reflexes with electrical stimulations, and is effective to people who has functional peripheral nerves and muscles. That is, the FES functions as the central nerve system to actuate muscles.

However, there are various disorders of sensory-motor systems so that the system requires dynamical adaptability to the characteristics of their unique sensory system and usage environments. Thus, we propose our FES system, and the conceptual diagram is shown in fig.1. The main characteristics of this system are to stimulate two different types of targets: muscle and reflex. Therefore, it is necessary to implement assist scheme for its user: that is, we need to reveal the relationship between ways to stimulate and joint movements.

The FES device is shown in Fig.2 (a). It consists of a 16bit microchip controller and analogue switches. The user receives electrical stimulations through electrode pads (shown in Fig.2b), which are attached near target muscles or nerves.

The FES generates low-frequent and bipolar-square waves as shown in Fig.3. The user adjusts the following parameters: its amplitude, career frequency, burst frequency, and duty rate, Those parameters are adjustable by its user.

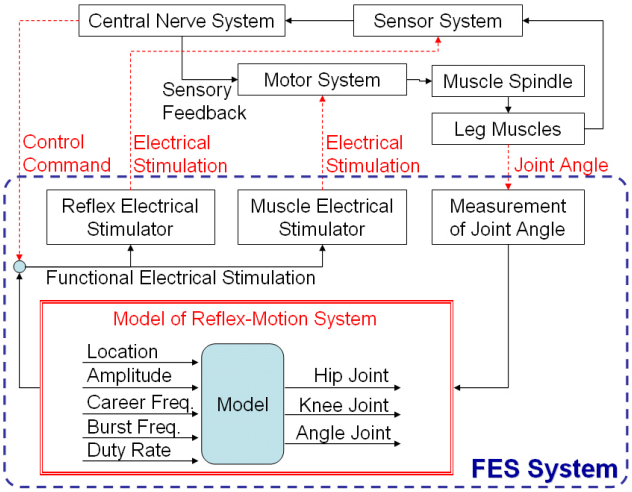

Fig.1. Conceptual Diagram of Proposed FES System

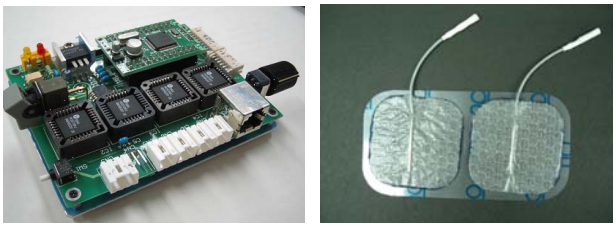

(a) Developed Device (b) Surface Electrode

Fig.2. Proposed FES System

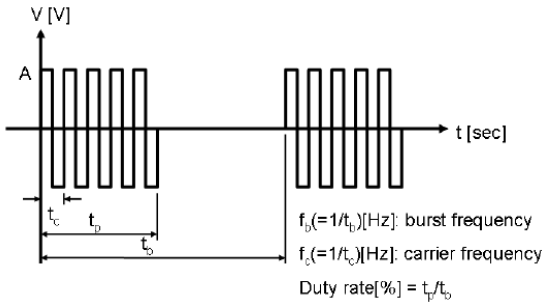

Fig.3. Wave Form of Functional Electric Stimulation

III.EXPERIMENTS

For generating target motions on a leg-paralysis person with the FES device, we need to reveal the relationship among muscle motions, signal types and locations of the electrical stimulation.

Hiroshi YOKOI: Dept. of Precision Engineering, The University of Tokyo, Tel:03-5841-8549, Email:hyokoi@robot.t.u-tokyo.ac.jp
Masatoshi TAKITA: Cognition and Action Research Group
Institute for Human Science and Biomedical Engineering, AIST, Tel:029-861-6632, FAX:029-861-6633, E-mail:takita.m@aist.go.jp

III-a. Responses to Amplitudes

As the first step, we focus on the stimulus part, which actuate the left ankle joint, and investigate its responses to 6 different stimulus amplitudes of electrical signals. Table 1 and Fig.4 show the results: muscle responses to the amplitudes of the electrical stimulation. Vrms and Irms indicate RMS values of the electrical stimulation, and Rrms is the value that Vrms is divided by Irms. As for the ankle motion, the patient does not feel the stimulation and does not generate any motion at the ankle joint when the amplitude is 5 [v]. Then, the patient starts feeling the stimulation at the amplitude 10 [v], bends the foot fingers at the amplitude 15 [v], and bend the ankle joint at the amplitude 17.5 [v]. However, the patient could voluntarily move its fingers and ankle under the amplitude 17.5 [v], and could rarely move at the amplitude 20[v], and could not move at the amplitude 22.5[v].

Table 1. Relationship between stimulus amplitude and ankle joint

Amp[V]	5.	10.	15.	17.5	20.0	22.5
Vrms[V]	0.63	1.14	1.63	1.49	1.55	1.50
Irms[mA]	0.76	1.59	2.46	2.88	3.30	3.60
Rrms[Ω]	0.82	0.71	0.66	0.48	0.46	0.41
Ankle Movement	-	-	-	Y	Y	Y
Stimulus Sensing	N	Y	Y	Y	Y	Y
Voluntary Control	Y	Y	Y	Y	N	N
Time to accomplish	-	-	-	5.0	1.5	0.5

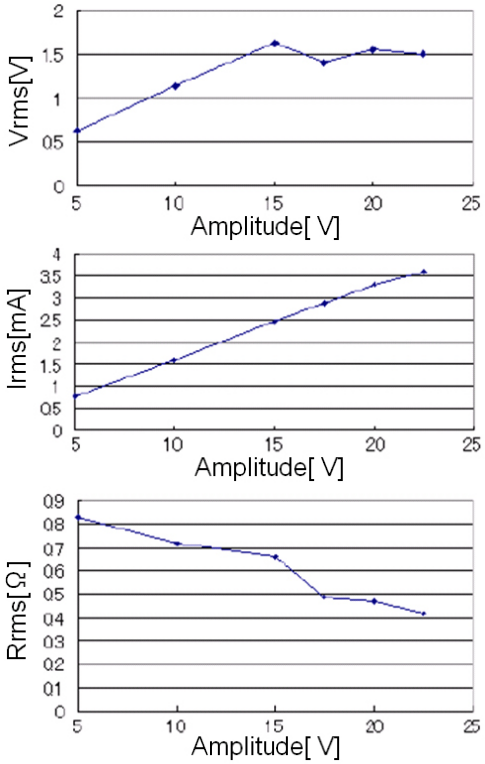

Fig.4. Relationship of strength of electric stimulus

III-b. Responses to Career Frequencies

Secondly, we investigate responses to career frequencies. We select 2 stimulus parts as shown in Fig.5 and career frequencies at the range from 1 [kHz] to 7 [kHz]. Table 2 and Table 3 show the results: muscle responses to the career frequencies. As for ID1, the patient does not move its leg at 1 [kHz], bends the ankle joint at 2 [kHz], bends the hip and knee joints at 3 to 5 [kHz]. We assume that the activation of the anterior tibial muscles require the career frequency 2 [kHz] at least. As for ID2, the leg does not move at 2 [kHz] but the leg moves stably at 4 to 5 [kHz]. Whereas, the leg moves little at 7 [kHz]. That is, it is necessary to reveal appropriate range of career frequencies for activating stable movements.

Moreover, we confirm that, the FES device consumes current 40 [mA] when the leg does not move in the both case of ID1 and ID2. Meanwhile, the FES devises consumes current 50 [mA when the leg moves stably. We assume that the career frequency relates to stimulus depth.

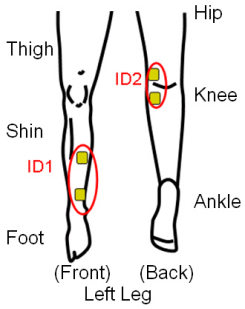

Fig.5 Stimulus part on the left leg.

Table 2. Result: Stimulus to ID1

Career Freq. [kHz]	Current [mA]	Joint Movement
1.0	40	No
2.0	50	Ankle
3.0	50	Hip and knee
4.0	50	Hip and knee
5.0	50	Hip and knee

Table 3. Result: Stimulus to ID2

Career Freq. [kHz]	Current [mA]	Joint Movement
2.0	35	No
3.0	50	Ankle (weak)
4.0	50	Ankle (stable)
5.0	50	Ankle (stable)
6.0	50	Ankle (stable)
7.0	50	Ankle (weak)

III-c. Modeling of Reflex-Motion System

For revealing reflex-motion system of a leg paralysis patient, we conducted the FES experiments again. The stimulus parameters are the same as the parameters in the previous experiment and we change the stimulus locations as shown in Fig.6. Table 4 lists the relationship between dominant nerves and leg muscles.

As a result of stimulus to ID3, the knee joint smoothly move. We assumed that the stimulus part should be the tendon of the rectus femoris muscle. Therefore, the receptor in the tendon is stimulated by the FES signal, the stimulus causes reflex, and the rectus femoris muscle strongly moved. For the patient, it was easier to achieve the knee extension with the direct stimulus to the rectus femoris muscle than with the stimulus to the tendon of the rectus femoris muscle. In short, we confirmed the possibility to generate faster joint movement with stimulus to reflexes. Thereby, it indicates the combination of muscle stimulus and reflex stimulus achieves efficient walking assistance.

Table 4. Relationship between dominant nerves and leg muscles

	Hip Joint		Knee Joint		Ankle Joint		dominant nerve
	Flex	Ext	Flex	Ext	Flex	Ext	
biceps femoris muscle		Y	Y				ischiadic nerve
semimembranosus muscle		Y	Y				ischiadic nerve
semitendinosus muscle		Y	Y				ischiadic nerve
rectus femoris muscle	Y			Y			femoral nerve
sartorius muscle	Y		Y				femoral nerve
pectineal muscle	Y						femoral nerve
iliopsoas muscle	Y						femoral nerve, lumbar nerves
tensor fascia lata muscle	Y						tibial nerve
gastrocnemial muscle		Y				Y	tibial nerve
soleus muscle						Y	superficial fibular nerve
long fibular muscle						Y	superficial fibular nerve
peroneus brevis muscle						Y	deep fibular nerve
peroneus tertius muscle					Y		deep fibular nerve
extensor digitorum longus muscle					Y		deep fibular nerve
extensor hallucis longus muscle					Y		deep fibular nerve
anterior tibial muscle					Y		deep fibular nerve

The results of the stimulus to ID1 and ID2 are shown in Fig.7. The angle transitions of hip, knee, and ankle are shown in Fig.8. As for ID2, the hip and knee joints extended, and the ankle joint bent. Those movements are corresponding to the standing-up leg motion and, it seems that, effective to assist the motion. As for ID1, the hip flexion in ID1 is different from the one in ID2. The main difference is the gap of stimulus location: the gap is 0.050 [m]. It tells that we need to choose carefully stimulus locations. Moreover, the stimulus to ID5 and ID6 causes bending the hip and knee joints. That is, the movement is corresponding to a part of the walking movement. It also contributes to walking assistance. Therefore, we reveal the relationship between stimulus locations and joint movements, and implemented its model. Then, the model is applied for the walking assist scheme in the proposed FES system.

Fig.6. Functional Electric Stimulation for Reflex Motion

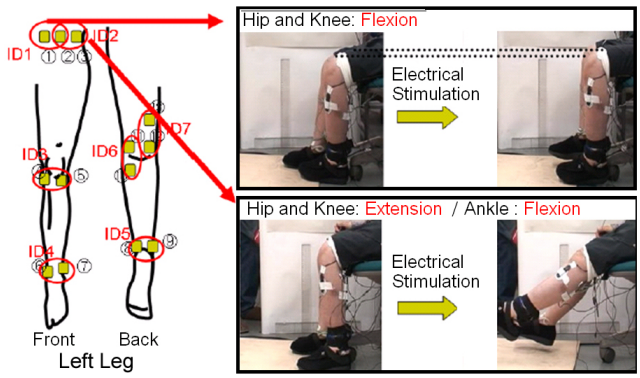

Fig.7. Stimulation effects of ID1 and ID2

Those joint movements stimulated by the reflexes are generated only on leg-paralysis patients but normal persons. Moreover, each patient has different relationship between stimulus locations and joint movements so that the FES system requires to examine the relationship to each user.

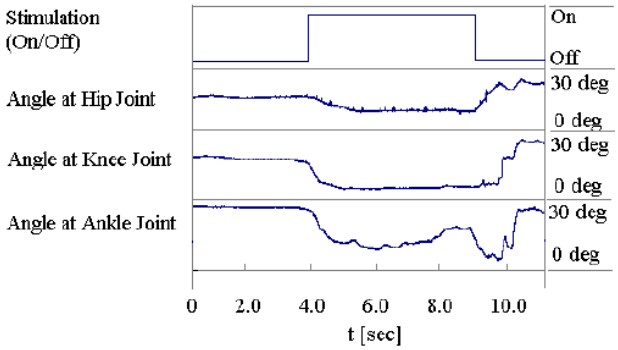

Fig.8. Stimulus timing for lower leg angle concerning on ID2

III-d. Multiple-Channel FES

It is known that the multiple-channel FES gives different effects from the single-channel FES to its patient. In this chapter, we investigate joint-motion responses to 1, 2, and 3 channels respectively. The locations and signal types of the electrical stimulations are shown in Fig.9.

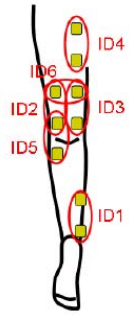

Table 5. Stimulus Parameters

Parameter	Value
Career Freq. [kHz]	4
Burst Freq. [Hz]	100
Duty Rate [%]	10
Distance between Electrodes [m]	0.1

Fig.9. Position and parameters on multi –functional electric stimulation

Table.6. 1ch stimulation (F: Flexion, E: Extension, →: Movement, 0 to 5 : Strength degree of joint movement)

	Joint Movement		
	Hip	Knee	Ankle
ID1	F4	F3	F2 → E2
ID2	F1 to F2	F1 to F2	F2
ID3	F1 to F2	F1 to F2	F2
ID4	F1 to F2	F1 to F2	F2
ID5	F1 to F2	F1 to F2	F2
ID6	F1 to F2	F1 to F2	F2

Table.7. 2ch stimulation (F: Flexion, E: Extension, →: Movement, 0 to 5 : Strength degree of joint movement)

		Joint Movement		
		Hip	Knee	Ankle
ID1	ID2	F2 to F3	F0 to F3	F2 → E2
ID2	ID3	F2 to F3	F0 to F3	F2
ID1	ID4	F2 to F3	F0 to F3	F2
ID1	ID5	F0 to F1	F1 to F1	F2
ID1	ID6	F1 to F3	F0 to F3	F2

Table 8. 3ch stimulation (F: Flexion, E: Extension, →: Movement, 0 to 5 : Strength degree of joint movement)

			Joint Movement		
			Hip	Knee	Ankle
ID1	ID2	ID3	F1 to F3	F0 to F2	F2
ID1	ID2	ID4	F3	F3	F2 → E2
ID1	ID3	ID4	F3	F3	F2 → E2

For the patients, it takes 5.0 [s] to stand up without the FES, meanwhile, it takes 5.4 [s] to stand up with the FES. That is, the FES assist improve the motion speed 7%. The transitions of joint angles with/without the FES are shown in Fig. It is clear that the joint motion with the FES is more smooth than the joint motion without the FES from 1.8 [s] to 5.0 [s].

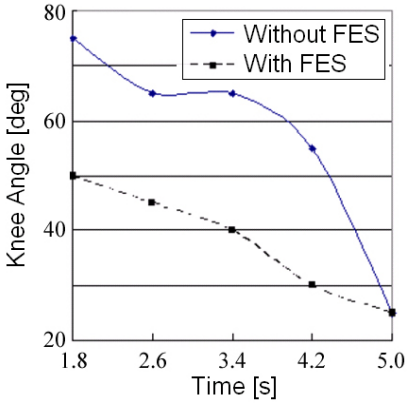

Fig.10. Time series data of knee angle of standing up motion

We apply the FES for walking assist. For the patient, it is necessary to prevent from scuffing. That is, we aim at bend knee and hip joints during swing phase on the left leg with the FES.

Based on the relationship between multiple-channel electrical stimulations and muscle motions is shown in table 1, 6, 7, and 8. The combination of the direct muscle stimulation and the reflex stimulation are applied for the walk assistance. The muscle stimulation was in charge of actuating the ankle joint and the reflex stimulation was in charge of actuating the knee and hip joints. We confirm that the FES assistance controls the walking speed of the patient. The maximum of the walking speed was similar to the speed of the normal person (Fig.11). Moreover, the patient demonstrated to climb up and down steps with the FES. The paralyzed leg did not scuff the steps as shown in Fig.12.

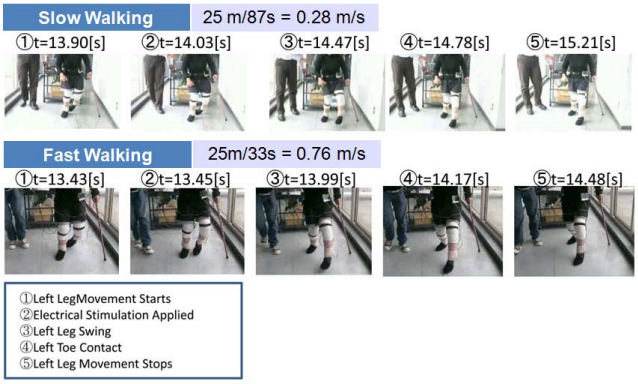

Fig.11. Reflex walking assist for arbitrary speed

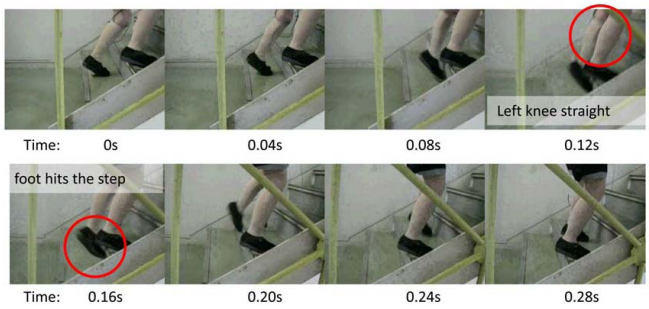

Fig.12. Reflex walking assist for climbing up steps.

IV. CONCLUSION

For leg paralysis persons caused with disorders of nervous system, we proposed our FES system: the combinations of reflex stimulus and direct muscle stimulus assist some parts of a patient's movements, and achieve walking. Therefore at first, we reveal movement segments generated by two stimulus-motion system (i.e., reflex-to-muscle and direct-muscle), and modeled those system. Then, the movements appropriately fit into the unique sensory-motor system of the patient for enhance the mobility. Eventually, the proposed approach is applied for a leg-paralysis patient, and the patients achieved better walking and step-climbing.

ACKNOWLEDGMENT

Grant-in-Aid for Scientific Research on Priority Areas "Emergence of Adaptive Motor Function through Interaction between Body, Brain and Environment - Understanding of Mobiligence by Constructive Approach -" from the Japanese Ministry of Education, Culture, Sports, Science and Technology.

REFERENCES

[1] Alejandro Hernandez Arieta, Kato Ryu, Hiroshi Yokoi, Takashi Ohnishi, and Tamio Arai An fMRI Study on the Effects of Electrical Stimulation as Biofeedback. Proceedings of the 2006 IEEE/RSJ International Conference on Intelligent Robots and Systems (IROS), 1-4244-0259-X/06/$20.00 ©2006 IEEE, pp 4336-4342, (2006)

Study on brain adaptation using rat-machine fusion systems and multi functional neural electrodes

Takafumi Suzuki*, Kunihiko Mabuchi*

Abstract— **The goal of our research project is to elucidate the brain adaptation function using rat-machine fusion systems and multi functional neural electrodes. To achieve this goal, we have developed fundamental techniques. These techniques include A) automatic adaptation of vehicle controller to time-varying neural signals recorded in these rat-machine fusion systems, and B) elemental techniques for long-term stable neural recording using devices such as flexible neural probes with micro fluidic channels for injection (or measurement) of medicines.**

I. Introduction

The goal of our research project is to elucidate the ability of the brain (especially the motor center) to adapt to a variable body environment by using a rat-machine fusion system in which the body's environmental conditions are changeable and also by using multi functional neural electrodes. We plan to construct a "rat car" vehicle system in which the car is controlled by neural signals in the motor cortices of rats. The system allows us to change the relationship between the motor command signals and the effectors (the muscles or the vehicle) arbitrarily. By using multi-channel recordings of neural signals together with injection and recording of certain medicines into the system, we plan to elucidate the brain property mentioned above.

We have been engaged in developing fundamental techniques to achieve this goal. The techniques includes A) automatic adaptation of vehicle controller to time-varying neural signals recorded in these rat-machine fusion systems, and B) elemental techniques for long-term stable neural recording using devices such as flexible neural probes with micro fluidic channels for injection (or measurement) of medicines.

II. Results

A) RatCar system[1, 4, 5]

A-I. Introduction

In this section, the outline of the "RatCar system" will be explained, and then the introduction and the potential of automatic adaptation of vehicle controller to time-varying neural signals will be shown.

We have developed a rat-machine fusion system in the form of a small vehicle BMI system, which we call the 'RatCar'. A unique point of our RatCar system is that a neural signal source (i.e., a rat) is mounted on the vehicle body and the two components move around as a unit. The rat is therefore provided with somatosensory feedback as the vehicle moves. This enables the rat to realize that its desire to move has been satisfied through the vehicle movement. We expect this condition to increase the ability of the rat to adapt to the system. Our ultimate goat is to illude the rat into recognizing the vehicle as corresponding to its own original limbs, and this will enable use of the RatCar as a platform for future neuroscience research. In addition, the movement of the vehicle system causes electromagnetic noise and artifacts in the recorded signals, an inevitable problem for real applications in hospitals and day to day society. The development of the RatCar system will help us investigate and solve these problems.

Although a simple linear model that we proposed in our former report[1] estimated an abstract locomotion velocity of a rat according to its neural firing rates, the results with too rough fluctuations were not suitable to control the RatCar vehicle. The model was divided into two sections; a section to correlate rat's locomotion velocity with each neural firing and another to estimate locomotion velocity compiling the whole pattern of neural firings. It enabled stable control of the vehicle even though the model precision had been inadequate. In addition, changing states both in the brain and the machine were observed through the model parameters.

A-II. Methods

Preparation

First, electrodes made of tungsten wires (40 μm in diameter) coated with parylene-c polymer (5 μm thick) were implanted in the motor cortex and basal ganglia regions which were determined according to a stereotaxic atlas of the rat brain[3].

As the rat ran inside the wheel-formed device, those electrodes transmitted neural spikes to the outside of the body followed by amplifier (5,000 times) and band-pass filter (300 Hz - 5 kHz).

Those spikes were then sampled (25 kHz) and sorted to calculate firing rates $s(t) = (s_1(t) \cdots s_n(t))$ in every 100 ms bin for each neuron. Finally, the principal component analysis normalized and whitened variances of those firing rates;

*Department of Information Physics and Computing, Graduate School of Information Science and Technology, The University of Tokyo

$$\boldsymbol{y}(t) = RL^{1/2}(\boldsymbol{s}(t) - \boldsymbol{\mu}) \quad (1)$$

$$\boldsymbol{\mu} = \mathrm{E}\{\boldsymbol{s}(t)\} \quad (2)$$

$$\mathrm{E}\left\{(\boldsymbol{s}(t) - \boldsymbol{\mu})(\boldsymbol{s}(t) - \boldsymbol{\mu})^{\mathrm{T}}\right\} = RLR^{\mathrm{T}} \quad (3)$$

$$(L : \text{diagonal})$$

Meanwhile, the actual locomotion velocity v(t) recorded as a rotating speed of the wheel was applied to identify or evaluate the model.

Estimation of Locomotion Velocity

Our model to estimate locomotion velocity of a rat has a state space representation described as,

$$\boldsymbol{x}(t+1) = F\boldsymbol{x}(t) + G\boldsymbol{\xi}(t) \quad (4)$$

$$\boldsymbol{y}(t) - \sum_{i=1}^{p} a_{n,i}\boldsymbol{y}(t-i) = H\boldsymbol{x}(t) + \boldsymbol{\eta}(t), \quad (5)$$

where

$$\boldsymbol{x}(t) \equiv \begin{pmatrix} v(t) \\ (v(t) - v(t-1))/\Delta t \\ (v(t) - 2v(t-1) + v(t-2))/\Delta t^2 \end{pmatrix}$$

$$F \equiv \begin{pmatrix} 1 & \Delta t & 0 \\ 0 & 1 & \Delta t \\ 0 & 0 & 0 \end{pmatrix}$$

$G \equiv I$

Δt = 100ms (bin size)

$\boldsymbol{\xi}$: model transition error (initially **0**)

$\boldsymbol{\eta}$: model output error (initially **0**).

In the algorithm, the equation (4) describes an update of internal states consist of the rat's locomotion velocity and its periodic differences. Meanwhile, the equation (5) correlates a combination of neural firings to the locomotion velocity with an output matrix H. Note that the neural firings were given as residuals of an auto-regression process (defined by parameters $a_{n,i}$) applied to neural firing rates.

To solve the model (i.e., to acquire $v(t)$,H, $a_{n,i}$), two sections were applied as follows. First, $H = (\boldsymbol{h}_1, \cdots, \boldsymbol{h}_n)$ and $a_{n,i}$ were identified by another state space representation for each neuron as actual locomotion velocity array x(t) was given:

$$\boldsymbol{u}_n(t+1) = \boldsymbol{u}_n(t) \quad (6)$$

$$\boldsymbol{y}_n(t) = \begin{pmatrix} \boldsymbol{h}_n & a_{n,1} & \cdots & a_{n,p} \end{pmatrix} \boldsymbol{u}(t), \quad (7)$$

where

$$\boldsymbol{u}_n(t) \equiv \begin{pmatrix} \boldsymbol{x}(t) & y_n(t-1) & \cdots & y_n(t-p) \end{pmatrix}^{\mathrm{T}}.$$

The measurement update algorithm from Kalman filter[2] were applied to identify $u_n(t)$ and therefore $a_{n,i}$ and $\boldsymbol{h}_n$.

Kalman filter algorithms (the time update and the measurement update) were then applied to the former state space model (4,5) to estimate locomotion velocity $v(t)$. Note that the algorithms were able to continue the estimation of the locomotion velocity $v(t)$ as the parameters $a_{n,i}$ and H were updated.

Experimental Condition

Six male Wistar rats were used as subjects. They were trained to walk inside the wheel-formed device described above after two days after the implant surgery. Although they had electrodes implanted both in motor cortex and basal ganglia, we focused only on the motor cortex in this experiment. The recording trials were divided into approximately 1 minute periods to prevent a rat from getting tangled in recording cables. While the first trial was used to identify the model and to observe varying parameters, the rest trials (typically 2; 120 s) evaluated a precision of the model.

A-III. Results

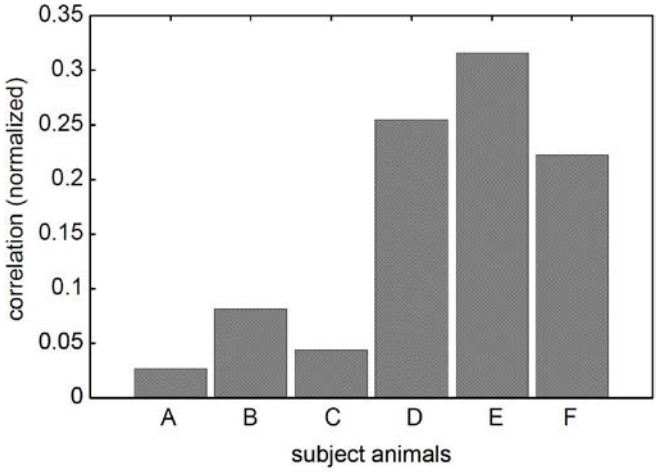

Fig.1 Correlation of actual and estimated locomotion velocity 2 days after the implant.

Figure 1 shows a correlation between actual and estimated locomotion velocity during the open estimation. Although these trials contained other movements unrelated to locomotion, rats D, E and F gave a high correlation over 0.2.

More detailed estimation for rat E, which showed a highest correlation, is presented in figure 2(E). While estimated value by our presented algorithm well followed start, stop and drastic changes of actual locomotion, it tended to be 3 – 4 times larger in amplitude. On the other hand, figure 2(C) partially shows a precise estimation around 100 – 110 s period. As a whole for rat C, however, the estimated velocity often failed to follow the actual one which resulted in the low correlation.

Next, figure 3 shows varying covariance components $h_{n,1}$ ($n = 1, \cdots, N$) during identification trials. They represent covariances between locomotion velocity and a firing rate of each neuron n. Those for rat E were hardly updated for the first 25 seconds since the rat kept still at the bottom of the wheel. Then, drastic changes of the value started around 30 seconds as the rat started moving and they converged in 10 seconds. In the case of rat C, changes immediately started after the trial had started. Although the components converged once at least in less than 10 seconds, they gradually kept

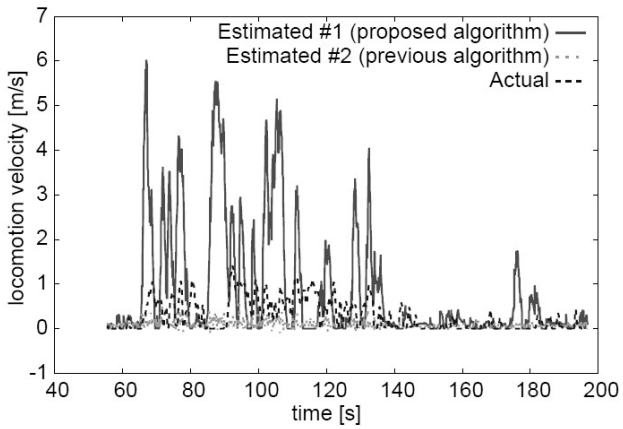

(rat E)

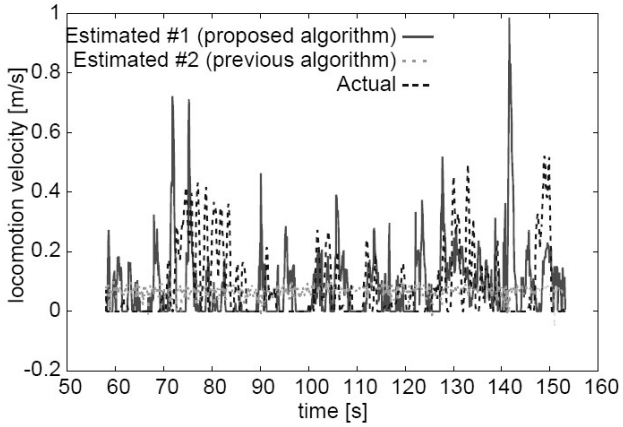

(rat C)

Fig. 2. Estimated (presented algorithm using state space representation and previous algorithm using least mean square estimation[1]) and actual locomotion velocity of rat E and C; 2 days after the implant.

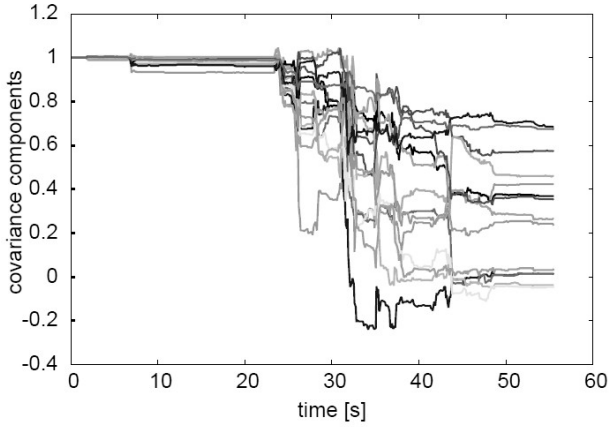

(rat E)

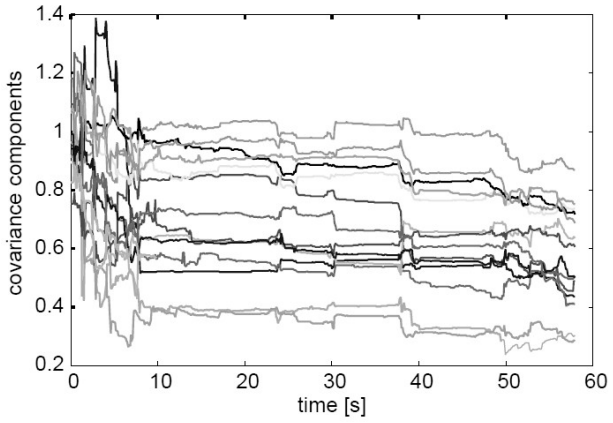

(rat C)

Fig. 3. Covariance components for the velocity $v(t)$; $h_{n,1}$ (n = 1, $\cdots$,N) during the adaptation of the model (rat E and C).

changing with several jumps.

A-IV. DISCUSSION & CONCLUSION

The results showed that the first 10 – 15 seconds period of the identification trial converged the initial covariance components to achieve a basic estimation of locomotion velocity. As long as these values stayed constant, the model well estimated locomotion velocity especially for drastic changes. On the other hand, some of them gradually changed after the initial identification period had passed in the case of rat C, some, which resulted in a weaker correlation with velocity.

These changes were caused either by plasticity of the brain, modification in recording condition (e.g., changes in alignment of neural electrodes), or dynamics in brain activity that our model did not take into account. It is not able to clearly distinguish them with our methods by themselves since our current results show phenomenological correlations between each neural firing and the locomotion velocity. Our results, however, still suggest that those changes were caused by some sort of state transition in the brain. Under an assumption that the recorded neural activities are stationary processes without plastic changes of the brain function or electrodes drifting, these parameters are supposed to converge and hold still as time elapse. This is obviously incorrect from our results. A more detailed comparison of these parameters between (a) the case that a rat is mounted on the vehicle, and (b) the case that a rat is freely moving without the vehicle. Functional changes in the brain to adapt to the vehicle are expected on the case (a), while functional and structural changing of the recording condition may equally occur in both cases.

In this research subject, a model to estimate locomotion velocity was improved to divide its function to two sections; a section to correlate rat's locomotion velocity with each neural firing and another to estimate locomotion velocity to achieve smooth control of the vehicle.While the former enabled us to monitor changes both in the brain and the machine, the latter stabilized the estimation results preventing rough fluctuation. Forfuture studies, continuous recording for long hours with a

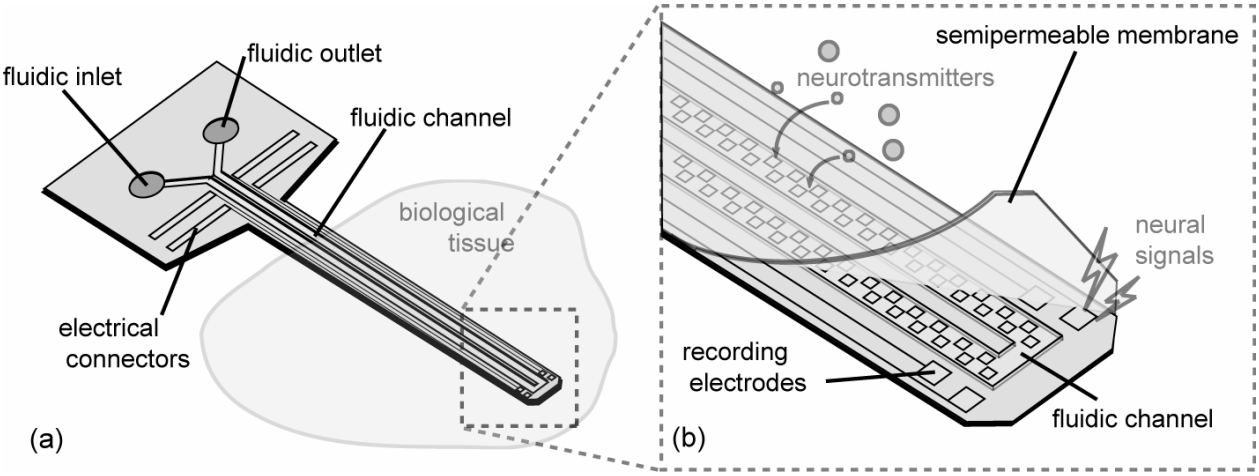

Fig. 4. Conceptual illustration of a probe. (a) Overview image of the probe. The probe is inserted into biological tissue. (b) Tip of the probe with recording electrodes and a fluidic channel. The fluidic channel is covered with a semipermeable membrane. When the probe is inserted into the brain, the microelectrodes record neural signals, and the fluidic channel collects neurotransmitter from the extracellular fluids around the point of interest.

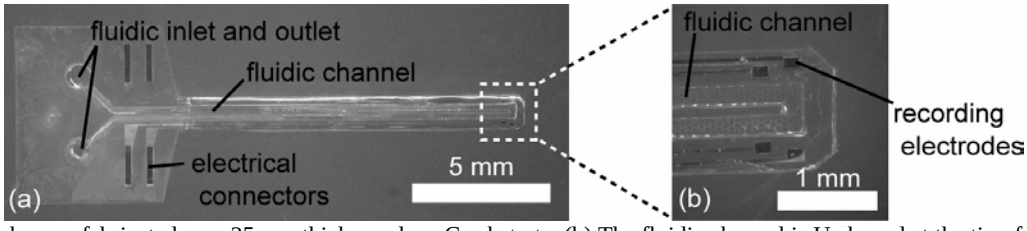

Fig.5 The probe was fabricated on a 25-μm-thick parylene C substrate. (b) The fluidic channel is U-shaped at the tip of the probe.

rat mounted on the vehicle will suggest quantitative results on dynamical changes and plasticity of the brain as connected to BMI system.

B) Multi-functional neural electrode

In this section, flexible probes to record both neuroelectrical and neurochemical activities (Figure 4, 5) are shown as an example of the multi-functional neural electrodes we have developed. These probes have four microelectrodes for neural recording and a fluidic channel covered with a semipermeable membrane; the membrane is used for microdialysis in the brain. We measured impedance of the electrodes, and examined the leakage of dialysate from the fluidic channel in vitro[6].

III Conclusion

We report the results of this project such as A) automatic adaptation of vehicle controller to time-varying neural signals recorded in these rat-machine fusion systems, and B) elemental techniques for long-term stable neural recording using devices such as flexible neural probes with micro fluidic channels for injection (or measurement) of medicines.

IV References

[1] O. Fukayama, N. Taniguchi, T. Suzuki, K. Mabuchi, Control of a vehicle-formed BMI system for rats by neural signals recorded in the motor cortex, *Proc. 3rd International IEEE EMBS Conf. on Neural Eng.*, 2007, pp. 394 – 397.

[2] R. E. Kalman and R. S. Bucy, New Results in Linear Filtering and Prediction Theory, *Trans. ASME, J. Basic Eng.*, Vol. 83D, No. 1, 1961, pp. 95 – 108.

[3] G. Paxinos and C. Watson, The Rat Brain in Stereotaxic Coordinates, Compact Third Edition, 1997, Academic Press.

[4] O. Fukayama, N. Taniguchi, T. Suzuki, K. Mabuchi: Automatic Adaptation of Vehicle Controller to Time-Varying Neural Signals Recorded in RatCar System; A Vehicle-formed BMI, Proc. of Joint 4th International Conference on Soft Computing and Intelligent Systems and 9th International Symposium on Advanced Intelligent Systems, 253-256 (2008)

[5] O. Fukayama, N. Taniguchi, T. Suzuki, K. Mabuchi: RatCar system for estimating locomotion states using neural signals with parameter monitoring: Vehicle-formed brain-machine interfaces for rat, Proc. of 30th Annual International Conference of the IEEE EMBS, 5322-5325 (2008)

[6] N. Kotake, T. Suzuki, K. Mabuchi, S. Takeuchi: A flexible parylene neural probe combined with a microdialysis membrane, Proc. of microTAS 2008, 1687-1689 (2008)

Analysis of relation between neuronal coding and body movement using BMI

Yoshio Sakurai
Graduate School of Letters, Kyoto University

Abstract — The present study is analyzing how body movement is involved in neuronal coding (representation) using multineuronal recording and a brain-machine interface (BMI). We report here that neuronal firing frequencies of neuronal population remarkably changed when they were working as neuronal codes for BMI to operate external device. Firing synchrony also changed especially in the hippocampus. We present a preliminarily result of experiment employing a target-operation task using BMI. The hippocampal neuronal firing increased when it operated the target device to approach to the rat.

I. INTRODUCTION

Recognition and detection of valid information in the environments are must for animals to behave adaptively, that necessarily require neural coding in the brain. Recent neuroscience studies have suggested that neural coding is based on activity of functional groups of neurons, i. e., cell assembly (Fig. 1), as the famous psychologist D.O.Hebb suggested. However, as the other famous psychologist J.J.Gibson indicated, recognition and detection of valid information need action to and interaction with the environments of much information. This suggests that real features of neuronal coding could be experimentally uncovered by investigating how body movements are involved in neural activity of coding in the working brains.

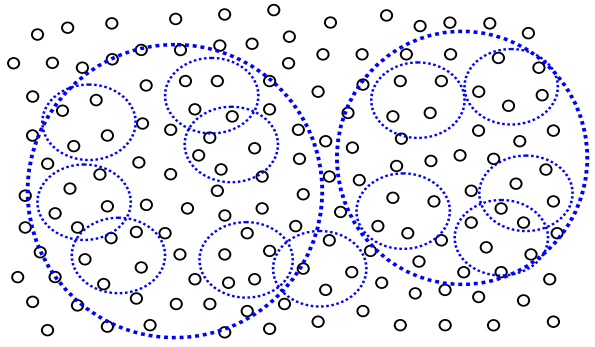

Fig. 1: Concept of cell assembly. Activity synchrony of individual neurons (○) dynamically causes various sizes of functional groups of neurons.

Ⅱ. PURPOSE

As in the previous year, the present study is detecting, with multineuronal recording and brain-machine interfaces (BMI), how body movements are involved in neural coding in the brain. For that, we establish behavioral learning tasks for rats and develope a BMI system with long-term multineuronal recording. The main brain regions are hippocampal-cortical systems.

Ⅲ. ORIGINALITY

The present study rejects the classical neuroscience framework, i.e., recognizing the brain as a simple device which passively percepts and processes incoming information in the environments. Instead, we focus on interactions between neural coding and body movements and aim to experimentally investigate them. To establish the BMI system for the present study, developing and integrating new hardwires and software and collaboration between psychological behavior experiments and neurophysiological recording experiments are required. That is surely a new multidisciplinary project among different fields of science.

Ⅳ. METHODS

We have already constructed a novel system consisting of automatic and real-time spike sorting with independent component analysis (ICA) in combination with a newly developed multi-electrodes for long-term recording from multi-sites of the brain. We are connecting the system with appropriate behavioral tasks for rats and look for valid neuronal activity and synchrony, which can be used as neuronal codes to work the BMI system. We especially focus on changes of

firing rates and firing synchrony in the neuronal groups.

Fig. 2 is the BMI system for a free-response task (free-operant task). When the rat uses its body movement, it pokes the nose to a hole (nose-poke behavior) and get reward of pellet. In the BMI task, a transparent panel is set just in front of the hole and some specific neuronal activity instead of behavior can deliver the reward.

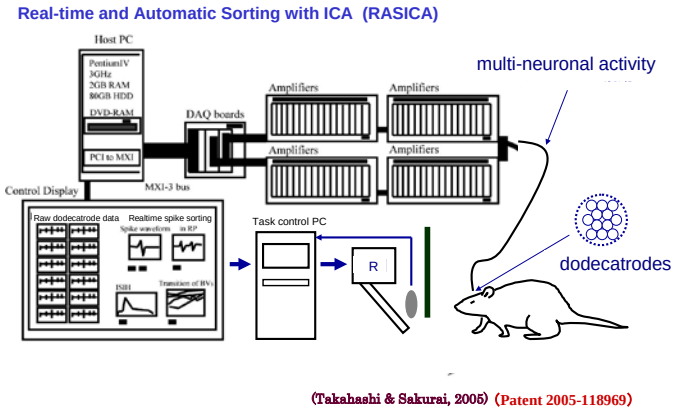

Fig. 2 : BMI system for the free response task. It consists of multineuronal recording from the dodecatrodes and real-time spike sorting with ICA (RASICA).

We can use various specific patterns of neuronal activity to control the pellet dispenser instead of behavior and call it "neuronal code". The neuronal code is firing frequency or synchrony of neurons, which can be selected from any of the recorded neurons. When the RASICA system detects specific neuronal codes, it transmits signals to a computer that controls the behavioral tasks and the reward dispenser. Then the specific neuronal codes effect the behavioral tasks and deliver the reward instead of the animal's behavior. Figure 3 is a schematic drawings of detection of the neuronal codes. In the upper panel, multineuronal spikes from plural neurons are recorded by the dodecatrode and automatically separated into individual neuronal spikes by ICA. Then the spike frequency of the neurons can be detected and work as a neuronal code. In the lower panel, plural neurons fire synchronously and an overlapped waveform is recorded by the dodecatrode but is automatically separated to individual neuronal spikes by ICA. Then spike synchrony of the neurons can be detected and work as a neuronal code. Fig. 4 is the computer displays of the BMI system with RASICA.

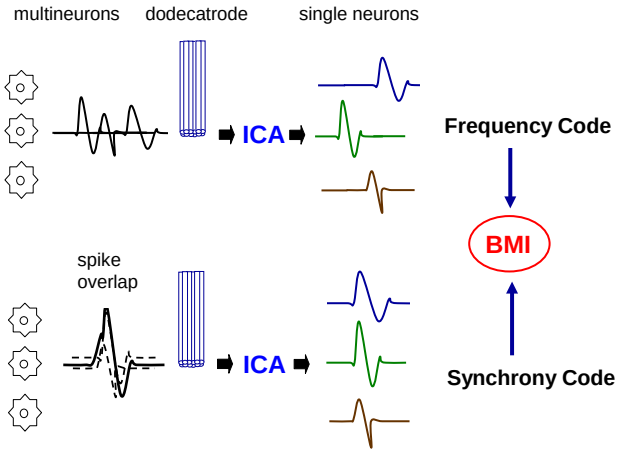

Fig. 3: Two types of neuronal codes detected by RASICA. Upper panel, neuronal code of spike frequency of the neurons. Lower panel, neuronal code of spike synchrony of the neurons.

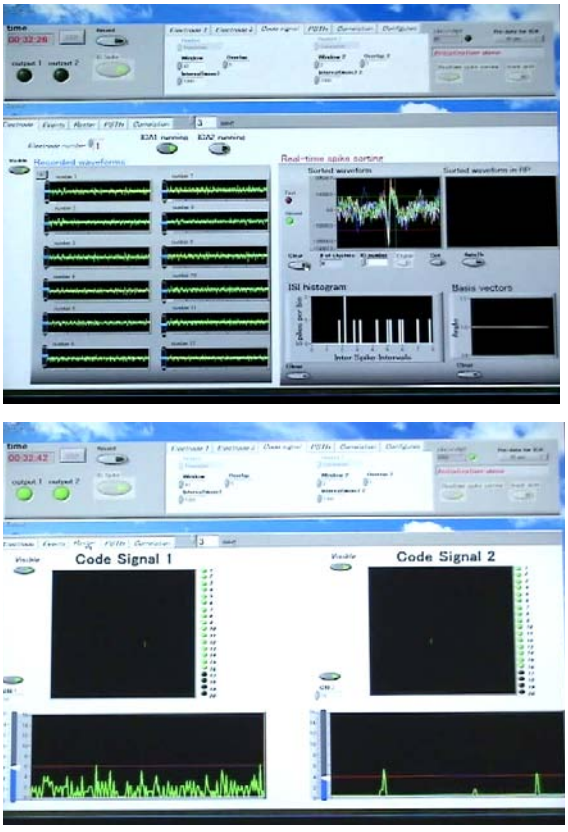

Fig. 4: Computer displays of the BMI system with RASICA. Upper display, Neuronal spikes on 12 microwires of the dodecatrode (left) and waveforms of separated individual neurons (right). Lower display, Firing frequency (left low) and synchrony (right low) of the separated 16 neurons

V. RESULTS

We report, following the last year, clear dynamic changes of neuronal activity in the free-reponse task. In the behavioral task, every nose-poke behavior caused delivery of a food pellet. In the BMI task, multineuronal activity was recorded from the neocortex (somatosensory) and hippocampal CA1. The neuronal codes that deputized for the nose-poke behavior were higher spike frequency than 2 spikes in a 40 ms window (frequency code) and spike synchrony among more than 2 neurons in a 2 ms window (synchrony code). Fig. 5 shows mean numbers of rewards delivered as a result of the nose-poke behavior and the neuronal codes in the free response task. The data were obtained from 3 dodecatrodes implanted in the neocortices of 3 rats. On the first day (behavioral task), only the nose-poke behavior could induce the delivery of food pellets, and the rats obtained the reward constantly during the 30 min session. On the 2nd day (BMI task), only the neuronal code of spike frequency could induce the delivery of the reward. The rats soon learned to frequently generate the neuronal code and obtained more rewards than by performing the behavior in the previous session. On the 3rd day (BMI task), the neuronal code was changed to the precise spike synchrony among the neurons. Contrary to the neuronal code on the second day, the rats could not increase the synchrony code.

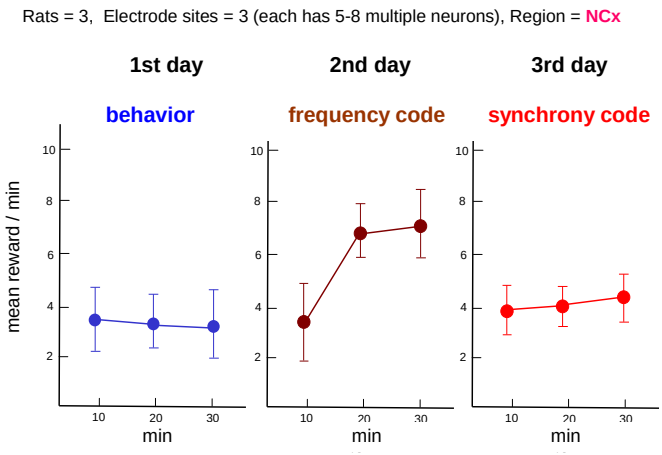

Fig. 5: Mean numbers of rewards delivered by behavior (1st day) and neuronal codes (2nd and 3rd days) in the free-response task. The data were obtained from 3 dodecatrodes implanted in the neocortices of 3 rats.

The data in Fig. 6 were obtained from 4 dodecatrodes implanted in hippocampal CA1 of 4 rats. By performing the nose-poke behavior on the first day, the rats obtained the reward constantly during the 30 min session. The spike frequency code on the second day rapidly increased, and the increment was slightly greater than in the neocortex (Fig. 5). On the third day, the neuronal code was changed to precise spike synchrony among the neurons. In contrast to the neocortical neurons (Fig. 5), the synchrony code of the HPC showed an increment and the rats obtained more reward than by performing the behavior.

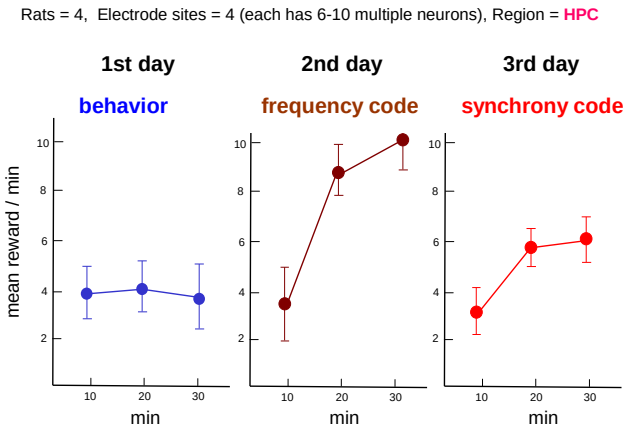

Fig. 6. Mean numbers of rewards delivered by behavior (1st day) and neuronal codes (2nd and 3rd days) in the free-response task. The data were obtained from 4 dodecatrodes implanted in hippocampal CA1 of 4 rats.

We have developed a target-approach task and a target-operation task with BMI. Fig. 7 is a schematic drawing of the target-operation task. Fig. 8 is a rat performing the target-approach task and the target-operation task.

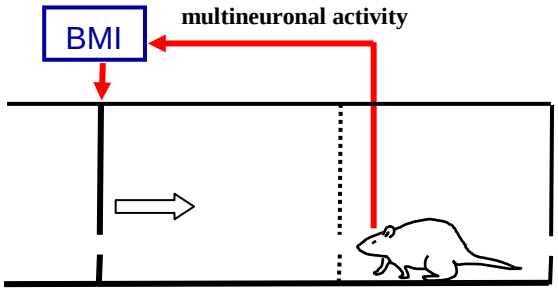

Fig. 7: Schematic drawing of the target-operation task. The target (the hole on the left wall) is being operated to approach to the rat by neuronal codes.

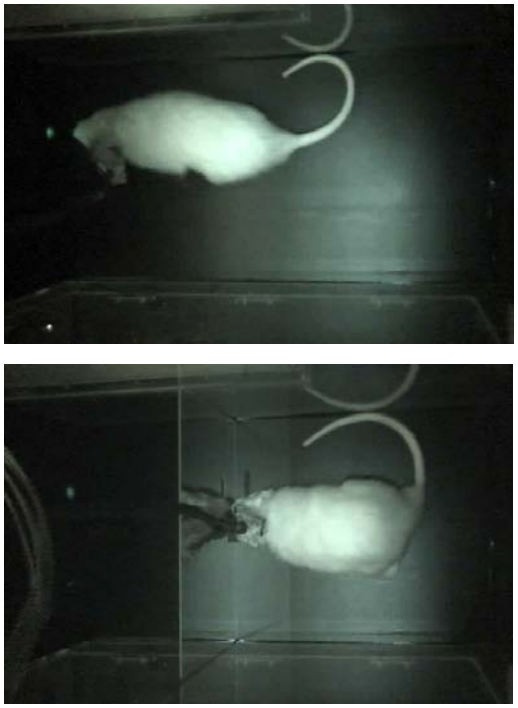

Fig. 8: Upper photo, A rat performing the target-approach task. It is locomotion from the right-side to the left wall to make a nose-poke response to the illuminated hole. Lower photo, The same rat performing the target-operation task with BMI. The target (the hole on the left wall) is being operated to approach to the rat by neuronal codes.

We analyzed activity of hippocampal CA1 neurons when the rat was performing the target-approach task and target-operation task. In the former task, the neuronal activity was just recorded. In the latter task, the frequency code (Figs. 5 and 6) from the hippocampal neurons made the left wall approach to the rat. Fig. 9 is a preliminary data showing changes of firing frequencies of the neurons during the 2 days of training of the tasks.

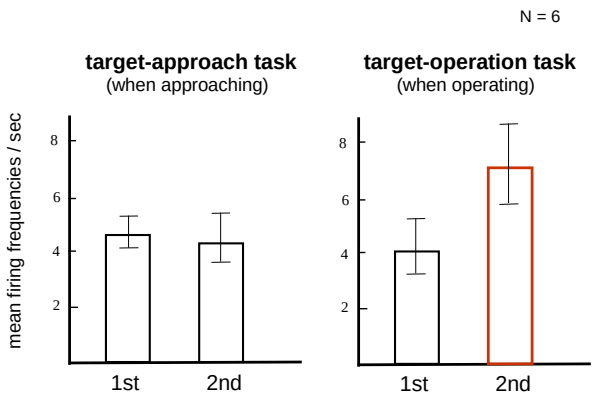

Fig. 9: Mean firing frequencies of the hippocampal CA1 neurons during the 2 days of training of the target-approach task and target-operation task.

ACKNOWLEGEMENTS

The author thanks Dr. Susumu Takahashi (Kyoto Sangyo University), Dr. Toshio Aoyagi (Kyoto University) and Dr. Masaki Nomura (Japan Science and Technology Agency) for their collaborating.

REFERENCES

(1) Sakurai, Y. and Takahashi, S.(2008) Dynamic synchrony of local cell assembly. *Reviews in the Neurosciences*, 19, 425-440.

(2) Sakurai, Y. (2008) Present states and future problems of invasive BMI. *Journal of the Japan Society of Mechanical Engineers*, 111, 916-919 (In Japanese).

(3) Hirokawa, J., Bosch, M., Sakata, S., Sakurai, Y. and Yamamori, T. (2008) Functional role of the secondary visual cortex in multisensory facilitation in rats. *Neuroscience*, 153, 1402-1417.

(4) Sakurai, Y. (2008) *Search for Representation in the Brain,* Kyoto University Press. (In Japanese)

(5) Takahashi, S. and Sakurai, Y. (2008) Hippocampal neuronal ensembles act as comparator during delayed non-matching to sample performance in rats. *38th Society for Neuroscience Annual Meeting Abstract,* November 16th.

(6) Hirokawa, J., Sadakane, O., Sakata, S., Bosch, M., Sakurai, Y. and Yamamori, T. (2008) Superior colliculus differently mediates behavioral facilitations of speed and accuracy by audiovisual integration. *38th Society for Neuroscience Annual Meeting Abstract,* November 16.

(7) Sakurai, Y. and Takahashi, S. (2008) Dynamic neuronal plasticity revealed by invasive brain-machine interfaces. *Neuroscience Research*, 61, s30.

(8) Iijima, T., Hirose, H., Choi, K., Ttsutsui, K., Sakurai, Y. and Koike, Y. (2008) A brain-machine interface for realizing both target-rearching movement and target-holding posture. *Neuroscience Research*, 61, s30.

(9) Takahashi, S. and Sakurai, Y. (2008) Hippocampal neuronal ensembles act as comparator during delayed non-maching to sample performance. *Neuroscience Research*, 61, s60.

(10) Aoyagi, T., Sakurai, Y. and Nomura, M. (2008) Estimation of neuronal functional connectivity of cultured neuronal networks. *Neuroscience Research*, 61, s236.

(11) Nomura, M., Hara, K., Sakurai, Y. and Aoyagi, T.(2008) Estimation of neuronal functional connectivity of rats' hippocampus CA1 during a conditional discrimination task. *Neuroscience Research*, 61, s251.

Exploring reinforcement learning and motivation

Yasushi Kobayashi
Graduate School of Frontier Biosciences, Osaka University

***Abstract*—We are addressing the role of neuronal activity in the pathways of the brainstem-midbrain circuit in reward and the basis for believing that this circuit provides advantages over previous reinforcement learning theory. Several lines of evidence support the reward based learning theory proposing that midbrain dopamine (DA) neurons send a teaching signal (the reward prediction error signal) to control synaptic plasticity of the projection area. However, the underling mechanism of where and how the reward prediction error signal is computed still remains unclear. Since the pedunculopontine tegmental nucleus (PPTN) in the brainstem is one of the strongest excitatory input sources to DA neurons, we hypothesized that the PPTN may play an important role in activating DA neurons and reinforcement learning by relaying necessary signals for reward prediction error computation to DA neurons. To investigate the involvement of the PPTN neurons in computation of reward prediction error, we used a visually guided saccade task during recording of neuronal activity in monkeys. Here, we predict that PPTN neurons may relay the excitatory component of tonic reward prediction and phasic primary reward signals, and derive a new computational theory of the reward prediction error in DA neurons.**

1. Introduction

In the older literature, the pedunculopontine tegmental nucleus (PPTN) in the brainstem is thought to be the central part of the reticular activating system, which provides background excitation for several sensory and motor systems essential for perception [1] and cognitive processes [2]. The PPTN contains both cholinergic and glutamatergic neurons [3], and is one of the major sources of cholinergic projections in the brainstem. The cholinergic system is one of the most important modulatory neurotransmitter systems in the brain, and controls neuronal activity that depends on selective attention, and anatomical and physiological evidence supports the idea of a 'cholinergic component' of conscious awareness [4]. The PPTN has reciprocal connections with the basal ganglia: the subthalamic nucleus (STN), the globus pallidus, and the substantia nigra [5], and recently, PPTN has been as argued to form a part of the basal ganglia [6]. Further, the PPTN also has reciprocal connections with catecholaminergic systems in the brainstem: the locus coeruleus (LC; noradrenergic) and the dorsal raphe nucleus (DRN; serotonergic) [7].

This basal ganglia-PPTN-catecholaminergic complex has been proposed to play an important role in gating movement and controlling several forms of attentional behavior [8]. Despite these abundant anatomical findings, however, the functional importance of the PPTN is not yet fully understood.

Recent lesion and drug administration studies using rodents have indicated that the PPTN is involved in various reinforcement processes [9]. According to a physiological study in cats, the PPTN is thought to relay either a reward signal or a salient event in a fully conditioned situation [10]. Anatomically, the PPTN receives reward input from the lateral hypothalamus [11] and the limbic cortex [12]. Conversely, the PPTN abundantly projects to midbrain dopamine (DA) neurons of the substantia nigra pars compacta (SNc) [13], which encode a reward prediction error signal for reinforcement learning [14]. For DA neurons, the PPTN is one of the strongest excitatory input sources [15]. The PPTN neurons release glutamate and acetylcholine to target neurons, and glutamatergic and cholinergic inputs from the PPTN make synaptic connections with DA neurons [16, 17], and electrical stimulation of the PPTN induces a time-locked burst in DA neurons in the rat [18]. Thus, PPTN activity and acetylcholine provided by the PPTN can facilitate the DA neuron's burst firing and appear to do so via muscarinic [19] and nicotinic [20] receptor activation. Furthermore, midbrain DA neurons are dysfunctional following excitotoxic lesioning of the PPTN [21]. A number of studies have found impairments in learning following excitotoxic lesions of the PPTN [22].

Humans and animals can learn to predict upcoming rewards. After learning, DA neurons respond to cues that predict reward, and also suppress responses to predicted rewards [14]. Therefore, the reward response of DA neuron corresponds to a discrepancy between the prediction of reward and the reward actually delivered. Since this activation of DA neurons also acts as a learning signal (termed the reward prediction error signal) in the striatum and other projection areas [23], it has been suggested to play a key role in reinforcement learning. One of the most critical issues in reinforcement learning involving the basal ganglia is where and how to compute the reward prediction error signal between actual reward and the prediction of an upcoming reward [24]. However, because of the poor physiological information regarding the input signals to DA neurons, this issue has remained controversial. The PPTN is one of the strongest afferent pathways for DA neurons, and in the PPTN, acetylcholine and glutamate have strong excitatory effects on DA neurons [21, 25]. Interestingly, one recent computational theory [26] predicts the PPTN to be a major input source of the excitatory signal to DA neurons and possibly an important component of reinforcement learning, but its functional role is still unclear. In this study, we hypothesize that the PPTN plays an important role in the computation of reward prediction error signals in DA neurons.

2. Experimental Procedures

To address the PPTN contribution to the reward prediction error, we analyzed neuronal activity of the PPTN during a visually guided saccade task (VGST) for monkeys. Most of data have been published previously [27]. For each trial of a VGST, initially the monkey was required to direct and maintain its gaze at a central fixation target (FT). The monkey then had to make a correct saccade to a peripheral saccade target (ST), and received a reward at the end of a trial (Fig. 1A). Here, we will show the preliminary results [28] when we controlled motivation or reward prediction of the monkey by altering the reward size across a block of trials (Fig. 1B).

All experimental procedures in this article were performed in accordance with the NIH Guidelines for the Care and Use of Laboratory Animals, and approved by the Committee for Animal Experiment at Okazaki National Institutes and Osaka University. The details of the surgical and data acquisition methods were published previously [27].

3. Results

Effect of reward prediction on behavior and neuronal activity of PPTN

In our experiment, the monkeys performed VGST in which they were required to make saccades toward a ST after extinction of the FT (Fig. 1A). To control the level of motivation (reward expectation

or prediction) for the task, the reward size was changed across a block of trials (i.e. initially rewarded trials, and then zero reward trials, shown in Figure 1B). As a result of reward control, the decreased level of reward prediction increased the error rate (Fig. 1B). This indicates that we could control the level of motivation (i.e. the prediction of reward for the task) of the monkeys by a reward control.

Next, we will show that the neuronal activity of the PPTN varied with motivational level of the animal. Many of the recorded neurons responded reliably to the onset of the FT, and a half of these neurons exhibited reliable sustained activity during execution of the task as reported previously [27]. As shown in Figure 1B, for the representative neuron, responses to the FT were stronger when the motivation of the monkeys was higher. During rewarded trials (the monkey could get a predicted reward on successful trials), the discharge increased gradually after onset of the FT, remained elevated for the duration of the fixation period, and was sustained until reward delivery (Fig. 1B, upper rasters). On the other hand, during reward omission trials (reward was not delivered for the successful trial), there was a decrease in the spike rate after the FT, as compared with rewarded trials (Fig. 1B, top and middle rastergrams). Yet, despite the decrease, the sustained activity remained above baseline until the end of trial, consistent with the fact that the monkey successfully completed the reward omission trials (low motivation) (Fig. 1B, middle). In this sense, we can expect that error trials where monkeys canceled the trial with the least motivation would show the least activity. In Figure 1C, activities after FT onset were plotted for rewarded, reward omission and error trials. As we predicted, the activity was the lowest for the error trials. Thus, higher success rate (high motivation or a high level of prediction of upcoming reward for the task) was associated with enhanced neural activity of the PPTN in response to the FT (initial target to direct gaze for executing the VGST) [28].

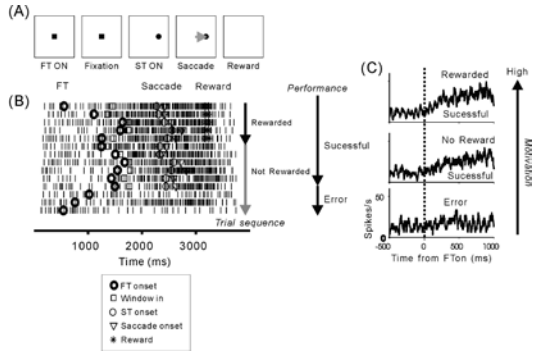

Figure 1. Neuronal activity of PPTN during VGST (**A**) The temporal sequence of the visually guided saccade task (VGST) showing the screen in front of the monkey during successive epochs of a single trial for the VGST. A fixation target (FT) appears at the center of the screen and the monkey achieves foveal fixation. After a fixation period (400-1000 ms), the FT is turned off and a peripheral saccade target (ST) appears at the left or the right with 10° eccentricity. The monkey is required to make a saccade directly to the target. The arrow indicates the direction of eye movement. After maintaining fixation on the target, the target stimulus is turned off, and the monkey receives the juice reward. (**B**) Each horizontal raster represents one trial. Trials are shown in order of presentation from top to bottom and each tick represents a neuronal impulse. Trials were changed from rewarded to reward omission. (**C**) Neural discrimination of task performance. Averages of responses to onset of FT for rewarded, reward omission and error trials are shown. The firing rates are aligned on FT appearance.

Tonic performance-related activity to the fixation target

To investigate the temporal dynamics of the output of the PPTN neurons elicited by FT appearance, we examined the time course of this effect. The two illustrated neurons in Figure 1C shows a higher FT response for successful trials than for error trials (Fig. 1C), as shown in the previous section. The temporal activation pattern for FT appearance varied among neurons. Figure 1 shows the sustained tonic type response for one representative neuron. For the sustained tonic responses, most of the sustained activity was maintained until the reward was delivered.

Interestingly, a substantial number of short latency responses to FT (possibly the most salient stimulus in the task) was observed, as compared to the cue stimulus response of DA neurons [29]. For the neurons, the activity latency for FT was less than 100 ms (Fig. 1C).

Neural activity elicited by the reward outcome in the fully learned condition

In addition to the motivational or reward prediction activity to FT appearance, we examined responses to the reward outcome. The PPTN neurons showed an abrupt increase in their firing in response to an unpredicted free reward delivered outside the task (Fig. 2A). This response was consistent with our previous observation [27]. The latency of the reward response (about 100 ms) was slightly shorter than that of reported DA neurons (mean 113 ms [30]). Most of the neurons that exhibited this reward response to free reward showed responses to reward during the fully learned task trials (Fig. 2B). These results are also consistent with our previous findings [27]. During continuous saccade task, we did not observe adaptive suppression [27], which is a remarkable feature of the reward response of the DA neuron.

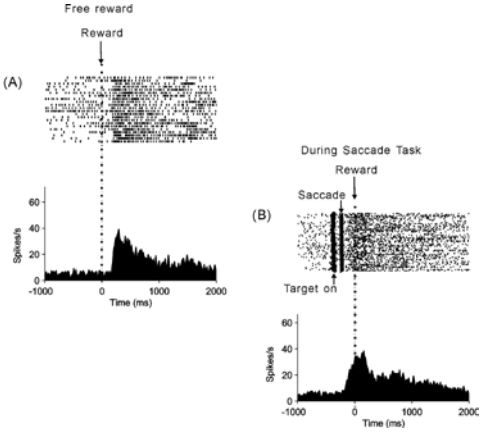

Figure 2. Neuronal activity for actual reward Rastergrams and histograms of activity from a single PPTN neuron when (**A**) a free reward delivery outside task and (**B**) when the reward was delivered during VGST. Monkeys could predict upcoming reward during the saccade task. This figure is modified from Kobayashi et al, (2002) [27].

4. Discussion

Possible reward prediction signal in PPTN

We demonstrated neuronal activity of PPTN in response to FT appearance, and the responses are predictive of an animal's performance on the task (Fig. 1) [27]. It is possible that the activity of PPTN to FT appearance is related to motivation level, reward prediction for the task and the sensory response to be conditioned. The result is consistent with a previous study of cats showing that activity in PPTN neurons was elicited during classical conditioning tasks in response to the conditioned stimulus [10]. Our result further suggests that the salience of the conditioned stimulus in this task (i.e. FT onset in the VGST) was influenced by motivation for the task. Thus, PPTN neurons may comprise a substrate whose role is to transform a sensory cue into a behavioral action. If this hypothesis is

correct, it is quite reasonable to expect that the cue responses of the same neuron in a cue-reward association task would be modulated by the magnitude of the expected reward.

From where does the PPTN receive this motivational or reward prediction signal? First, we propose that the excitatory signals travel via the ventral striatum-ventral pallidum pathway, which receives input mainly from the limbic cortex [31]. This pathway quite possibly includes limbic information, but it uses inhibitory connections from the GABAergic (gamma-amino butyric acid) pallidum pathway. There, excitation of PPTN is elicited by a double inhibition mechanism. Second, other possible excitatory sources may include the amygdala and STN [11]. Third, the activity may originate from the cerebral cortex. Recently, Matsumura has emphasized the functional role of cortical input to the PPTN in the integration mechanism of limbic-motor control [15].

Possible primary reward signal in the PPTN

In the PPTN, we observed phasic reward responses for free reward and reward during the task. It is possible that the reward signal comes from the lateral hypothalamus [32]. This pathway directly excites the PPTN [11], which fires a brief burst and then accommodates or habituates [10, 33]. This brief burst directly excites the SNc via cholinergic and glutamatergic projections [34] and thereby causes a phasic burst in DA neurons projecting to the striatum [35] for unexpected reward. In future work, we will examine whether the response properties of the PPTN fulfill the necessary features of a primary reward signal; i.e. the activity is related to reward occurrence, to value coding, and the activity has no adaptation under a fully leaned condition.

Computation of reward prediction error signal in DA neurons

As described above, DA neurons have unique firing patterns related to the predicted volume and actual times of reward [14]. Recent computational models [36, 37] of DA firing have noted similarities between the response pattern of DA neurons and well-known learning algorithms, especially temporal difference (TD) models [36]. In the TD model, a sustained tonic reward prediction pulse originating from the striatum is temporally differentiated to produce an onset burst followed by an offset suppression. The TD model uses fast-sustained excitatory reward prediction and delayed slow-sustained inhibitory pulse signals in DA neurons. In that model the neurons in the striatum (the striosome) provide a significant source of GABAergic inhibition to DA neurons [35], and the fast excitatory reward-predicting signals are derived via a double inhibition mechanism to DA neurons (matriosome-pallidum-DA neuron pathway [37]). Thus, the polysynaptic double inhibition pathway and monosynaptic direct inhibition may provide temporal differentiation of reward prediction in DA neurons. However, the model may not be realistic because it is assumed that (1) the polysynaptic net excitatory signal is faster than the inhibitory signal via the monosynaptic pathway to DA neuron, and (2) the double inhibition pathway is required to strongly excite burst activity of DA neuron to a conditioned cue.

A significant difference between our new model, derived from our present findings, and the previous model is the source of excitation for DA neurons [38]. It is possible that the excitatory PPTN neurons may send both a tonic reward prediction signal (Fig.1) and a phasic reward signal (Fig. 2) to DA neurons. Thus, interestingly the PPTN may relay both predictive and actual reward information to DA neurons.

Since we found sustained tonic excitatory PPTN input to DA neuron, we predict that a sustained inhibitory input from the striatum prevents DA neuron's tonic activation through the excitatory input from the PPTN after learning. With regard to the delayed and slow inhibition of DA neurons, Houk and colleagues [37] proposed that the connection of the striosome-DA neurons provides a prolonged inhibition of DA neurons, which persists from the time of the reward-prediction signal to the time when the reward occurs. Here, computation between a fast-sustained excitatory input and a delayed slow inhibition occurs in DA neurons. If the fast-sustained excitatory signals from the PPTN appear shortly before the slow-sustained inhibitory inputs from the striosome, the time lag results in a phasic activation in DA neuronal activity. The fast excitatory and slow inhibitory activation maintains an equivalent level of activity in DA neurons from after cue related phasic activation to just before reward delivery. If the excitatory signals from the PPTN disappear shortly before reward delivery, then the remaining inhibitory inputs should suppress the DA neuron at the time of reward. Thus, when expected rewards are not received, sustained-slow striosomal inhibition of DA neurons, unopposed by excitation, results in a phasic drop in DA neuronal activity. We need to further test PPTN neuronal involvement in the prediction of the timing of reward delivery with a classical conditioning task, as conducted by Schultz's group [14].

References

[1] D. B. Lindsley, "The reticular system and perceptual discrimination.," *In The reticular formation of the brain.*, vol. Boston, pp. Little, Brown & Co.:513-534, 1958.

[2] T. Steckler, W. Inglis, P. Winn, and A. Sahgal, "The pedunculopontine tegmental nucleus: a role in cognitive processes?," *Brain Res Brain Res Rev*, vol. 19, pp. 298-318, 1994.

[3] A. E. Hallanger and B. H. Wainer, "Ascending projections from the pedunculopontine tegmental nucleus and the adjacent mesopontine tegmentum in the rat," *J Comp Neurol*, vol. 274, pp. 483-515, 1988.

[4] E. Perry, M. Walker, J. Grace, and R. Perry, "Acetylcholine in mind: a neurotransmitter correlate of consciousness?," *Trends Neurosci*, vol. 22, pp. 273-80, 1999.

[5] S. M. Edley and A. M. Graybiel, "The afferent and efferent connections of the feline nucleus tegmenti pedunculopontinus, pars compacta," *J Comp Neurol*, vol. 217, pp. 187-215, 1983.

[6] J. Mena-Segovia, J. P. Bolam, and P. J. Magill, "Pedunculopontine nucleus and basal ganglia: distant relatives or part of the same family?," *Trends Neurosci*, vol. 27, pp. 585-8, Oct 2004.

[7] Y. Koyama and Y. Kayama, "Mutual interactions among cholinergic, noradrenergic and serotonergic neurons studied by ionophoresis of these transmitters in rat brainstem nuclei," *Neuroscience*, vol. 55, pp. 1117-26, 1993.

[8] E. Garcia-Rill, "The pedunculopontine nucleus," *Prog Neurobiol*, vol. 36, pp. 363-89, 1991.

[9] H. L. Alderson and P. Winn, "The pedunculopontine and reinforcement," *The Basal Ganglia VIII*, vol. 56, pp. 523-32, 2005.

[10] J. F. Dormont, H. Conde, and D. Farin, "The role of the pedunculopontine tegmental nucleus in relation to conditioned motor performance in the cat. I. Context-dependent and reinforcement-related single unit activity," *Exp Brain Res*, vol. 121, pp. 401-10, 1998.

[11] K. Semba and H. C. Fibiger, "Afferent connections of the laterodorsal and the pedunculopontine tegmental nuclei in the rat: a retro- and antero-grade transport and immunohistochemical study," *J Comp Neurol*, vol. 323, pp. 387-410, 1992.

[12] T. Chiba, T. Kayahara, and K. Nakano, "Efferent projections of infralimbic and prelimbic areas of the medial prefrontal cortex in the Japanese monkey, Macaca fuscata," *Brain Res*, vol. 888, pp. 83-101, 2001.

[13] M. Beninato and R. F. Spencer, "The cholinergic innervation of the rat substantia nigra: a light and electron microscopic

immunohistochemical study," *Exp Brain Res*, vol. 72, pp. 178-84, 1988.

[14] W. Schultz, "Predictive reward signal of dopamine neurons," *J Neurophysiol*, vol. 80, pp. 1-27, 1998.

[15] M. Matsumura, "The pedunculopontine tegmental nucleus and experimental parkinsonism A review," *J Neurol*, vol. 252 Suppl 4, pp. iv5-iv12, Oct 2005.

[16] T. Futami, K. Takakusaki, and S. T. Kitai, "Glutamatergic and cholinergic inputs from the pedunculopontine tegmental nucleus to dopamine neurons in the substantia nigra pars compacta," *Neurosci Res*, vol. 21, pp. 331-42, 1995.

[17] K. Takakusaki, T. Shiroyama, T. Yamamoto, and S. T. Kitai, "Cholinergic and noncholinergic tegmental pedunculopontine projection neurons in rats revealed by intracellular labeling," *J Comp Neurol*, vol. 371, pp. 345-61, 1996.

[18] S. J. Lokwan, P. G. Overton, M. S. Berry, and D. Clark, "Stimulation of the pedunculopontine tegmental nucleus in the rat produces burst firing in A9 dopaminergic neurons," *Neuroscience*, vol. 92, pp. 245-54, 1999.

[19] R. S. Scroggs, C. G. Cardenas, J. A. Whittaker, and S. T. Kitai, "Muscarine reduces calcium-dependent electrical activity in substantia nigra dopaminergic neurons," *J Neurophysiol*, vol. 86, pp. 2966-72, Dec 2001.

[20] T. Yamashita and T. Isa, "Fulfenamic acid sensitive, Ca(2+)-dependent inward current induced by nicotinic acetylcholine receptors in dopamine neurons," *Neurosci Res*, vol. 46, pp. 463-73, Aug 2003.

[21] C. D. Blaha and P. Winn, "Modulation of dopamine efflux in the striatum following cholinergic stimulation of the substantia nigra in intact and pedunculopontine tegmental nucleus-lesioned rats," *J Neurosci*, vol. 13, pp. 1035-44, 1993.

[22] W. L. Inglis, M. C. Olmstead, and T. W. Robbins, "Pedunculopontine tegmental nucleus lesions impair stimulus-reward learning in autoshaping and conditioned reinforcement paradigms," *Behav Neurosci*, vol. 114, pp. 285-94, Apr 2000.

[23] J. R. Wickens, R. Kotter, and M. E. Alexander, "Effects of local connectivity on striatal function: stimulation and analysis of a model," *Synapse*, vol. 20, pp. 281-98, Aug 1995.

[24] K. Doya, "Metalearning and neuromodulation," *Neural Networks*, vol. 15, pp. 495-506, 2002/// 2002.

[25] C. D. Blaha, L. F. Allen, S. Das, W. L. Inglis, M. P. Latimer, S. R. Vincent, and P. Winn, "Modulation of dopamine efflux in the nucleus accumbens after cholinergic stimulation of the ventral tegmental area in intact, pedunculopontine tegmental nucleus-lesioned, and laterodorsal tegmental nucleus-lesioned rats," *J Neurosci*, vol. 16, pp. 714-22, 1996.

[26] J. Brown, D. Bullock, and S. Grossberg, "How the basal ganglia use parallel excitatory and inhibitory learning pathways to selectively respond to unexpected rewarding cues," *J Neurosci*, vol. 19, pp. 10502-11, 1999.

[27] Y. Kobayashi, Y. Inoue, M. Yamamoto, T. Isa, and H. Aizawa, "Contribution of pedunculopontine tegmental nucleus neurons to performance of visually guided saccade tasks in monkeys," *J Neurophysiol*, vol. 88, pp. 715-31, Aug 2002.

[28] Y. Kobayashi, K. Okada, Y. Inoue, and T. Isa, "Reward-predicting activity of pedunculopontine tegmental nucleus neurons during visually guided saccade tasks," *Soc. Neurosci Abstract*, 2005.

[29] R. Romo and W. Schultz, "Role of primate basal ganglia and frontal cortex in the internal generation of movements. III. Neuronal activity in the supplementary motor area," *Exp Brain Res*, vol. 91, pp. 396-407, 1992.

[30] J. Mirenowicz and W. Schultz, "Importance of unpredictability for reward responses in primate dopamine neurons," *J Neurophysiol*, vol. 72, pp. 1024-7, 1994.

[31] W. Schultz, P. Apicella, E. Scarnati, and T. Ljungberg, "Neuronal activity in monkey ventral striatum related to the expectation of reward," *J Neurosci*, vol. 12, pp. 4595-610, Dec 1992.

[32] K. Nakamura and T. Ono, "Lateral hypothalamus neuron involvement in integration of natural and artificial rewards and cue signals," *J Neurophysiol*, vol. 55, pp. 163-81, Jan 1986.

[33] K. Takakusaki, T. Shiroyama, and S. T. Kitai, "Two types of cholinergic neurons in the rat tegmental pedunculopontine nucleus: electrophysiological and morphological characterization," *Neuroscience*, vol. 79, pp. 1089-109, 1997.

[34] H. Conde, "Organization and physiology of the substantia nigra," *Exp Brain Res*, vol. 88, pp. 233-48, 1992.

[35] C. R. Gerfen, "The neostriatal mosaic: multiple levels of compartmental organization," *Trends Neurosci*, vol. 15, pp. 133-9, 1992.

[36] W. Schultz, P. Dayan, and P. R. Montague, "A neural substrate of prediction and reward," *Science*, vol. 275, pp. 1593-9, 1997.

[37] J. C. Houk, J. L. Adams, and A. G. Barto, "A model of how the basal ganglia generate and use neural signals that predict reinforcement," in *Models of Information Processing in the Basal Ganglia* New York: The MIT Press, 1995, pp. 249-270.

[38] J. L. Contreras-Vidal, S. Grossberg, and D. Bullock, "A neural model of cerebellar learning for arm movement control: cortico-spino-cerebellar dynamics," *Learn Mem*, vol. 3, pp. 475-502, 1997.

Spinal control of grasping movement in primate

Tomohiko Takei, Kazuhiko SEKI (National Institute for Physiological Sciences, Okazaki, Japan)

I. Introduction

More than a half century ago A.N. Bernstein observed that "dexterity" residing in human limb motion emerges from accumulated involvement of multi-joint movements in surplus DOF [1]. Grasping movment is a typical multi-joint movement that require to control 39 different intrinsic or extrinsic hand muscles. Functional muscle synergy has bee proposed for the regulation of these redundant DOF, but the neural correlate that generate this synergy is not well established. In this study, we examined the potential involvement of spinal cord neurons for generating synergistic activity of hand muscles during grasping movement in non-human primates.

II. Methods

Behavioral task

A monkey was trained to sit in a chair with its right and left elbow restrained whilst it performed a precision grip task using a custom-made manipulandum (modified from Lemon et al. (Lemon et al. 1986)) (Fig.1A,B). The monkey inserted its thumb and index finger through separate holes in a horizontal plate to access the levers of the manipulandum. Fingers 3-5 were inserted through another hole. The manipulandum comprised two spring-loaded levers (10 cm length), each with a potentiometer (Model 357, Vishay Spectrol) fitted to its pivot point to report lever position and a touch sensor (D5C-1DA0, Omron, 30-100 pF) to measure thumb and index finger contact with the levers. The binary state of both touch sensors was constantly monitored throughout the experiments to determine when the signal from potentiometer represented thumb and index finger positions (i.e. when thumb and index finger were both in contact with the levers). A trial would not begin until both touch sensors were activated and would abort immediately upon loss of contact with either lever. Strain gage was attached to each lever for measuring the force exerted by both fingers.

Thumb and index finger positions were continuously presented to the monkey via the positions of two rectangle cursors displayed on a screen in front of monkey (Fig.1C). Two target boxes were also displayed and the monkey was required to keep each cursor inside its target box during a trial.

Each trial began with the presentation of two target boxes positioned so that the thumb and index finger were 3.0 cm apart ('Trial Start', Fig.1C). After 1.0-2.0 sec, the "out" targets disappeared and two "center" targets appeared simultaneously, signaling monkey to flex its thumb and index finger ('GO') to bring the cursors into the center targets. The required displacement of both fingers was 0.7-1.3 cm (monkey A) and 0.3-0.8 cm (monkey U), which corresponded to a force of 0.9-1.1 N and 0.4-0.6 N, respectively. The monkey was required to maintain the lever positions within the center targets for 1.0-2.0 sec then release them back into the out targets once the center targets disappeared ('GO2'). Successful completion of a trial was rewarded with a drop of applesauce. On average, ca 1500 successful trials/recording session with the success rate of ca 80% were performed by both monkeys.

Surgical operations

After behavioral training was complete, three

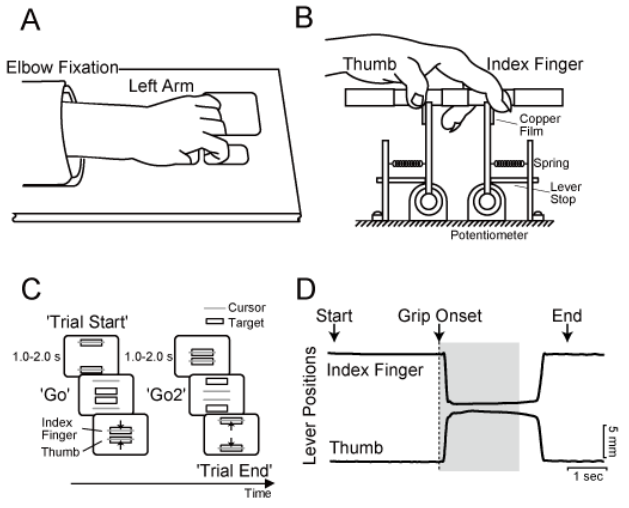

Figure 1.

Experimental setup. A,B: diagrams of the custom-made manipulandum for the precision grip task in top view (A) and lateral view (B). C: Sequence of a trial. Lever positions were reported to the monkey as two visual cursor signals on the computer display (gray bars). Two target boxes were also displayed (black rectangles). D: Example of finger movements during a single trial. Upper arrows indicate the time point of each task event. Two traces show lever positions (upper: index finger, lower: thumb). Shaded area indicates the time range where frequency analyses were performed (from 0 to 2.048 sec after 'Grip Onset').

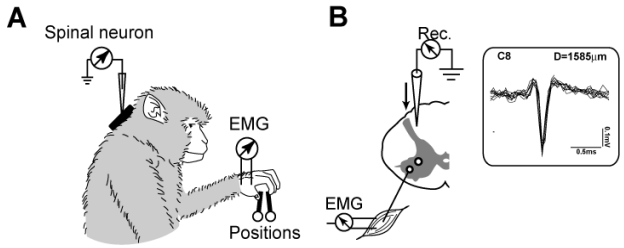

Figure 2 - *A*: Experimental setup for extracellular recording of spinal neurons from a monkey performing a precision grip task. The monkey squeezed spring-loaded levers with his index finger and thumb. Lever positions were recorded with muscular activities of hand/finger muscules and spinal neurons. *B*: Schematic diagram of recording procedure. A grass-insulated tungsten microelectrode was inserted into spinal cord by a hydraulic microdrive. Signal from the microelectrode was amplified and recorded, while EMG signals were simultaneously recorded. Inset: sample record of spinal neuron action potential (10 traces overlayed). Consistant waveform indicates the stable recording of action potentials. D, distance from the depth where the first neural activity were recorded in single penetration.

separate surgeries were performed to implant a head restraint, a recording chamber over the cervical spinal cord, and EMG wire electrodes into multiple forelimb muscles. All surgeries were performed on different days using isoflurane (1.0-2.0 % in 2:1 O2:N2O) or sevoflurane anesthesia (1.5–3.0% in 2:1 O2:N2O) and aseptic conditions. During the head restraint and spinal recording chamber surgeries the monkey was immobilized with intravenous pancuronium bromide (Mioblock, Organon, 0.05mg/kg every hour) and artificially respired. Respiration rate was adjusted to keep EtCO2 within 20–25 mmHg. Two head restraints (plastic tubes) were fixed to the skull with titanium screws and dental acrylic. An oval-shaped spinal recording chamber (Perlmutter et al. 1998) was implanted over the lower cervical spinal cord. C3-T2 vertebrae were exposed bilaterally and titanium screws were inserted into the lateral mass of each vertebra. After performing a unilateral laminectomy of C3-C7 vertebrae, the recording chamber was positioned over the laminectomy and cemented in place with dental acrylic. For recording EMGs, pairs of stainless steel wires (AS632, Cooner wire) were implanted subcutaneously in 19 muscles of monkey A, including four hand muscles (first dorsal interosseous (FDI), adductor pollicis (ADP), abductor pollicis brevis (AbPB), Abductor digiti minimi (AbDM)), fourteen forearm muscles (flexor digitorum superficialis (FDS), radial and ulnar parts of flexor digitorum profundus (FDPr and FDPu), flexor carpi radialis (FCR), flexor carpi ulnaris (FCU), palmaris longus (PL), extensor digitorum-2,3 (ED23), extensor digitorum communis (EDC), extensor digitorum-4,5 (ED45), extensor carpi radialis longus and brevis (ECRl and ECRb), extensor carpi ulnaris (ECU), brachioradialis (BRD), pronator teres (PT)), and one upper arm muscle (biceps brachii (B)). For monkey U, EMG wires were acutely inserted percutaneously in 2 muscles (FDI and AbDM) on each experimental day. The location of each EMG implant was confirmed by evoking joint- and muscle movement using low-intensity electrical stimulations applied through the wire electrodes during and after surgery.

Recording procedure

During each recording session, the monkey's head was fixed to the chair with plastic rods and a glass-insulated tungsten microelectrode (impedance 1 to 2 MΩ at 1 kHz) was inserted into cervical spinal cord (Fig.2). The position of the electrode was controlled by using a hydraulic microdrive (MO-951, Narishige Scientific Instrument) and a custom-made X-Y stage, both of which were mounted on the recording chamber. A silver-ball electrode was also inserted into spinal chamber as a reference electrode and placed on the scar tissue overlying the cord surface. In addition, output from the amplifier was high-pass filtered (0.3 kHz – 10 kHz) for monitoring action potentials from single spinal neurons.

Due to difficulties in locating recording sites using conventional histological methods following chronic spinal recordings, we used the depth of the electrode tip below the point at which single-unit activity was first recorded in each penetration. EMGs were amplified and filtered using a multichannel differential amplifier (SS-6110, Nihon Kohden, x3000-25000, 5 Hz - 3 kHz) and digitized at 5 kHz (Fig.3). Signals from potentiometers, strain gages, and touch sensors

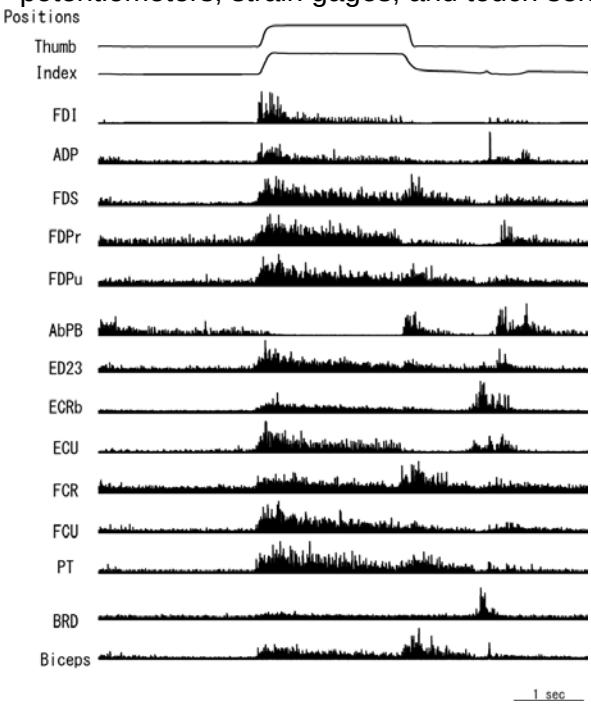

Fig.3. EMG recordings during precision grip task

were digitized at 1 kHz. All subsequent analyses were performed offline using MATLAB (Mathworks Inc.).

Data Analysis

Firing pattern of each recorded neuron was categorized due to the timing when their maximal firing rate was occurred. Then, Spike-triggered averaging (STAs) of each recorded EMGs [2] was performed using individual action potentials as a trigger. Post-spike effect of each STA was used to identify the recorded neuron in term of their connectivity with motoneuron pools.

III. Results

Among 199 neurons recorded from cervical spinal cord (C6-T1), a majority of the neurons (160 neurons, 80%) showed movement-related modulations of their firing rate during grip (138/199, 69%), hold (81/199, 41%), and release period (125/199, 63%). We compiled STAs of rectified EMGs for the 196 neurons (3920 neuron–muscle pairs), after careful rejection of motoneuron recordings. Among them, thirty neurons produced 56 significant STA effects (51 facilitations and 5 suppressions) in hand and arm muscles. The STA effects generated by electrical cross-talk of EMG signals were excluded from data pool. To discriminate pure post-spike effect from other synchrony effects [3], we used two criteria – onset latency and peak width at half maximum (PWHM). STA effects that have (1) a longer onset latency than the possible earliest latency estimated with intra-spinal microstimulation (single pulse, <30uV, 4.7ms for hand muscles and 3.5ms arm muscles), and (2) a narrower PWHM less than 7ms were determined as pure post-spike effects [4]. Using these criteria, 48 STA effects produced by 21 neurons were determined as pure post-spike effects from premotor interneurons (PreM-INs).

The majority of these 21 PreM-INs (13 neurons, 62%) produced post-spike effects in multiple muscles rather than an effect on single muscle. The size of muscle field (i.e. number of muscles on which single neuron had pure post-spike effects) was 2.3±1.4 in average. The type of post-spike effects was mainly facilitative (19 neurons) and only two neurons had suppressive effects. No neuron simultaneously had both of facilitative and suppressive effects. The muscle fields of single neuron were frequently observed within intrinsic hand muscles (6/13 neurons, 46%) and between intrinsic and extrinsic hand flexor (4/13 neurons, 31%), which were synergistically activated during the precision grip task. These results indicate that single spinal INs can produce co-activation of synergistic muscles.

IV. Discussion

Aims in this year was to elucidate the pattern of firing activity of spinal interneurons during precision grip performed by primate, and characterize the “muscle field” of each spinal neurons by means of spike-triggered averaging of EMG signals. We believe the result described above meets these objective in term of four points.

1. More than 80% of spinal neurons recorded showed a task-dependent activity during precision grip. This is a first study that successfully recorded an activity of spinal neuron in monkeys performing grasping movements. We found it possible to make a stable recording of spinal interneurons in monkeys behaving relatively unrestricted movement (c.f. [5,6]). The finding that a majority of neurons showed a task-related firing activity may suggest that spinal neurons may be involved in a various aspect of grasping control system, not only modulating an activity of single muscle/ joints.
2. Muscle field of spinal interneurons were restricted within an intrinsic hand muscle or extrinsic hand muscles. This results may suggest that spinal cord may be involved in the organization of synergistic movement between the muscles that is essential for generating grasping force. As a next step, it is essential to examine the functional significance of spinal muscle field by examining the correlations between firing characteristics and their muscle field of the last-order spinal interneurons.
3. Spinal last-order interneurons showed a muscle field with 2 to 3 finger muscles. It seems that the spinal muscle field is wider in the grasping movement than that in the wrist movement [5]. This may suggest that spinal neuron has a greater contribution for creating muscle synergy of hand muscle than that of wrist muscles. To confirm this hypothesis, it is important to compare the size of muscle field of spinal interneurons in single monkeys performing both wrist and finger movements.
4. Majority of last-order INs showed post-spike facilitation. One may suggest that the muscle synergy created by spinal neurons mainly induced by spinal excitatory last-order interneurons. However, relative strength or number between excitatory and inhibitory interneurons is difficult to estimate by STA method applied in this study. Rather, it is also likely that the inhibitory last-order interneuons may optimize the synergistic pattern generated by excitatory last-order interneurons

corresponding to different requirement of different movement epochs.

V. Future direction

In this study, we found that spinal cord may have a significant contribution for the generation of synergistic muscle activities of hand muscle in monkeys performing grasping movement. On the other hand, it is well known that the premotor interneuron in the primary motor cortex in primates also has a muscle field in hand muscle [7-9]. It would be of great interest to compare the size of muscle field between motor cortex and spinal cord. This comparison may give us a clue to understand the functional significance of spinally generated muscle synergy. One hypothesis is illustrated in Figure 4. Two contrasting strategy for generating muscle synergy are described in top and bottom. In the first strategy (top) , individual premotor neuron has no muscle field, so a number of premotor neuron needed to involve for generating synergistic movement. On the other hand, in the second strategy (bottom) each premotor neuron has a muscle field that is functionally relevant for voluntary movement, so the hand synergy can be constructed by a fewer premotor neurons. One possibility is that the second strategy involves spinal last-order interneuons, and the first strategy could be used by cerebral cortex for enabling precision control of finger force, not for generating hand synergy. Ongoing experiment in our laboratory may confirm the validity of this hypothesis.

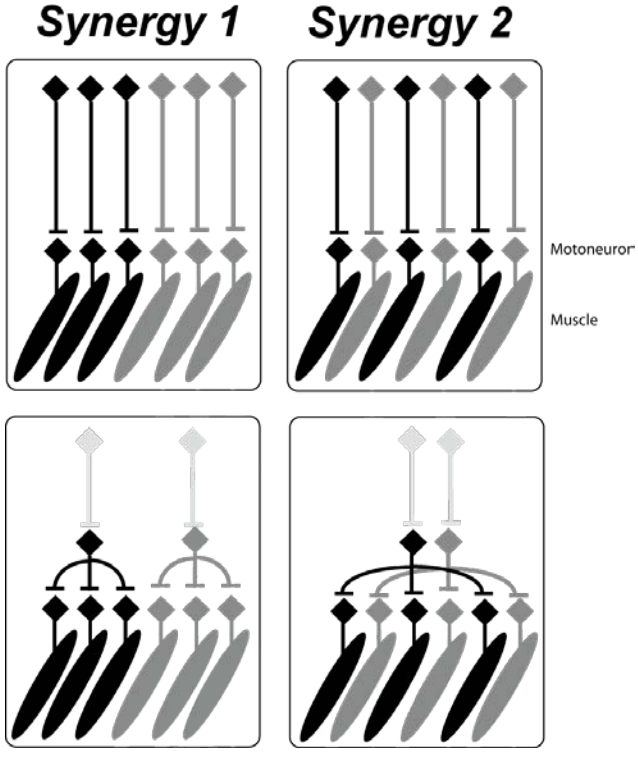

Fig.4. Independent and synergistic control of muscle activity

VI. References

1) Bernstein N. (1967) The co-ordination and regulation of movements. Oxford:Pargamon.

2) Fetz EE and Cheney PD (1980) Postspike facilitation of forelimb muscle activity by primate corticomotoneuronal cells. J Neurophysiol v44 pp751-72

3) Buys EJ, Lemon RN, Mantel GW and Muir RB (1986) Selective facilitation of different hand muscles by single corticospinal neurones in the conscious monkey. J Physiol v381 pp529-49

4) Schieber MH and Rivlis GJ (2005) A spectrum from pure post-spike effects to synchrony effects in spike-triggered averages of electromyographic activity during skilled finger movements. Neurophysiol v94 pp3325-41

5) Perlmutter SI, Maier MA and Fetz EE (1998) Activity of spinal interneurons and their effects on forearm muscles during voluntary wrist movements in the monkey. J Neurophysiol v80 pp2475-94

6) Maier MA, Perlmutter SI, Fetz EE (1998) Response patterns and force relations of monkey spinal interneurons during active wrist movement. J Neurophysiol v80 pp2495-513

7) Porter R and Lemon R. (1993) Corticospinal function and voluntary movement. Oxford University Press,

8) Muir RB and Lemon RN (1983) Corticospinal neurons with a special role in precision grip. Brain Res v261 pp312-6

9) Castiello U (2005) The neuroscience of grasping. Nat Rev Neurosci v6 pp726-36

Understanding the Functions of the Basal Ganglia through a Mouse Model of Dystonia

Atsushi Nambu

***Abstract*—Dystonia is a neurological disorder characterized by sustained or repetitive involuntary muscle contractions and abnormal postures. To understand the pathophysiology of dystonia, neurophysiological analyses were performed on hyperkinetic transgenic mice generated as a model of DYT1 dystonia. Abnormal muscle activity, such as co-activation of agonist and antagonist muscles and sustained muscle activation, was frequently observed in these mice. Recording of neuronal activity in awake state revealed reduced spontaneous activity with bursts and pauses in both the external and internal segments of the globus pallidus. Motor cortical stimulation evoked responses composed of excitation and subsequent long-lasting inhibition in both pallidal segments, which were never observed in the normal mice. In addition, the somatotopic arrangements in both pallidal segments were disorganized. Long-lasting inhibition induced by cortical inputs in the internal pallidal segment may disinhibit thalamic and cortical activity, resulting in the motor hyperactivity observed in dystonia. By way of temporal and spatial inputs thorough the cortico-basal ganglia loop, only the selected motor program is executed at the selected time, and other competing motor programs are cancelled in normal states.**

I. Introduction

DYSTONIA is a neurological disorder characterized by sustained or repetitive involuntary muscle contractions and abnormal postures. The pathophysiology of dystonia is poorly understood, and no consistent histopathological or biochemical changes have yet been detected. On the other hand, the internal (GPi) and external (GPe) segments of the globus pallidus have been discovered to exhibit decreased and bursting activity during stereotaxic surgery for deep brain stimulation.

Early-onset torsion dystonia, the most common type of primary generalized dystonia, is inherited in an autosomal dominant manner with a penetrance of 30-40%. This dystonia is caused by a three-base pair (GAG) deletion in the DYT1 gene on chromosome 9q34, resulting in loss of a glutamic acid residue (ΔE) in the torsinA protein. Recently, Shashidharan et al. (2005) generated a transgenic mouse model by overexpression of human ΔE-torsinA. These transgenic mice developed hyperkinesia and rapid bidirectional circling. They also exhibited abnormal involuntary movements with dystonic-appearing self-clasping of limbs and head-shaking.

Atsushi Nambu is with Division of System Neurophysiology, National Institute for Physiological Sciences and Department of Physiological Sciences, Graduate University for Advanced Studies, Myodaiji, Okazaki 444-8585, Japan Phone: +81-564-55-7771; fax, +81-564-52-7913; e-mail: nambu@nips.ac.jp).

Neuronal activity in the basal ganglia of this model were examined by electrophysiological methods in the present study. The functions of the basal ganglia will be discussed based on these electrophysiological findings.

II. Methods

Transgenic mice overexpressing human ΔE-torsin (Shashidharan et al., 2005) were used in the present study. Neuronal activity was recorded in the awake state to exclude effects of general anesthesia on neuronal firing rates and patterns. The experimental protocols were approved by the Animal Care and Use Committees of the Mount Sinai School of Medicine and the Okazaki Organization of National Institutes, and all experiments were conducted according to the guidelines of the National Institutes of Health Guide for Care and Use of Laboratory Animals. Prior to experiments, the mice were trained daily to acquaint them with handling by humans.

Each mouse was anesthetized. The skull was widely exposed and completely covered with transparent acrylic resin, and then a small U-frame made of acetal resin for head fixation was mounted and fixed on the head of the mouse. Two pairs of bipolar stimulating electrodes were inserted into the motor cortex, one into the caudal forelimb region and the other into the orofacial region.

After full recovery from the surgery, the mouse was positioned in a stereotaxic apparatus with its head restrained painlessly using the U-frame head holder in the awake state (Fig. 1 left). For single unit recording of GPi and GPe neurons (classically termed the entopeduncular nucleus and globus pallidus in rodents, respectively), a glass-coated Elgiloy-alloy microelectrode was inserted perpendicularly into the brain through the dura mater using a hydraulic microdrive (Fig. 1

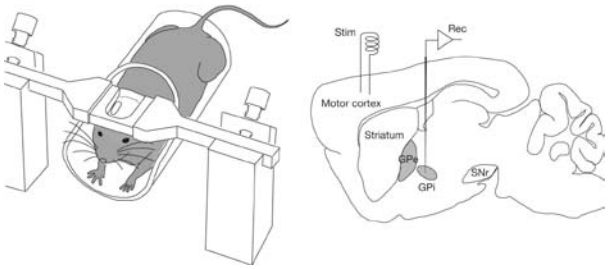

Fig 1 Experimental setup
GPe, external segment of the globus pallidus; GPi, internal segment of the globus pallidus; SNr, substantia nigra pars reticulata.

right). As GPi and GPe neurons showed similar changes, activity of GPi neurons was mainly described. Bipolar wire electrodes were also implanted in the triceps and biceps brachii muscles to record the electromyogram (EMG).

III. EMG Activity

The activities of the triceps and biceps brachii muscles, the extensor and flexor muscles of the forelimb, were simultaneously recorded in normal and transgenic mice (Fig. 2). Patterns of EMG activity during voluntary forelimb movements in the transgenic mice did not appear to differ from those in the normal mice during most of the time of recording (Fig. 2A, B). In all transgenic mice, however, the triceps and biceps muscles were sometimes co-activated during forelimb movements (Fig. 2C). Sharp EMG activities in the triceps and biceps muscles in these mice were synchronized with each other (Fig. 2C); such synchronization was never observed in the normal mice. Moreover, sustained muscle activity that lasted more than 10 s was frequently observed when the transgenic mice stopped movement (Fig. 2D). The sustained muscle activity was sometimes accompanied by co-activation of the triceps and biceps muscles (Fig. 2D). Co-activation of agonist and antagonist muscles is common to various types of dystonia. Sustained muscle activity is another important sign of dystonia. These observations suggest that the transgenic mice we examined exhibit EMG activity similar to that observed in human patients with dystonia.

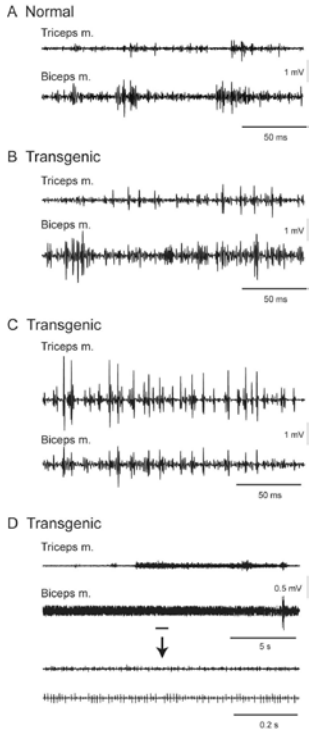

Fig. 2. Electromyographic (EMG) activity of triceps and biceps brachii muscles. **A,** EMG activity in a normal mouse during voluntary forelimb movements. **B-D,** EMG activity in a transgenic mouse.

IV. Spontaneous Neuronal Activity

The spontaneous activity of GPi and GPe neurons in normal and transgenic mice was recorded. GPi and GPe neurons in the normal mice fired continuously at high discharge rate above 50 Hz, as shown in traces of digitized spikes (Fig. 3A, C). On the other hand, GPi and GPe neurons in the transgenic mice fired at low frequency (Fig. 3B, C). Discharge patterns also differed in the transgenic mice. Bursts (indicated by thick black lines in Fig. 3B) and pauses (indicated by thick white lines) were frequently observed in GPi and GPe neurons of the transgenic mice.

Decreased discharge rates and irregularly grouped discharges with intermittent pauses in GPi and GPe neurons have also been observed in patients with generalized dystonia. These findings suggest that the transgenic mice may share neurological abnormalities with dystonia patients.

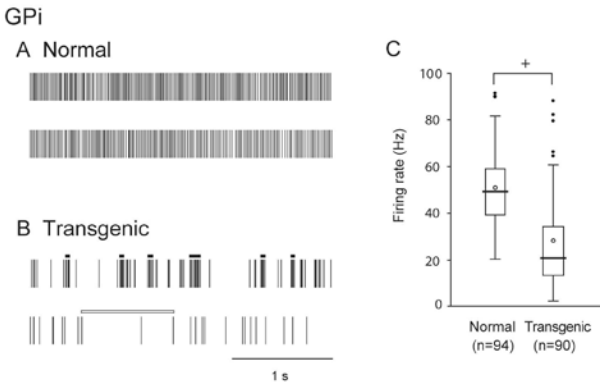

Fig. 3. Spontaneous activity of neurons in the internal segments of the globus pallidus (GPi). **A, B** Spikes are shown as digital signals in the normal (**A**) and transgenic mice (**B**). Bursts and pauses in the digital signals are indicated by horizontal black thick lines and horizontal white thick lines, respectively. **C** Box plots of firing rates in the normal (left) and transgenic mice (right).

V. Responses to Cortical Stimulation

Stimulation of the forelimb and/or orofacial region of the motor cortex typically induces triphasic responses composed of early excitation, inhibition, and late excitation in GPi and GPe neurons of normal monkeys and rodents (Fig. 4A). The origin of each component has been identified, with amplitudes and durations reflecting activity of the corresponding basal ganglia pathways and nuclei.

In contrast, cortical stimulation induced different responses patterns in the transgenic mice. The most common response pattern of GPi and GPe neurons in the transgenic mice was short-latency monophasic or biphasic excitation followed by long-lasting inhibition (Fig. 4B), a pattern never observed in the normal mice.

Neurons could be classified into four groups, those with forelimb inputs, those with orofacial inputs, those with convergent inputs from both forelimb and orofacial regions, and those with no responses, based on the responses evoked

by cortical stimulation. In the normal mice, small number of GPi and GPe neurons responded to stimulation of both forelimb and orofacial regions (Fig. 5A). In the transgenic mice, the number of neurons with convergent inputs from two regions was significantly increased.

The locations of recorded GPi neurons are plotted using

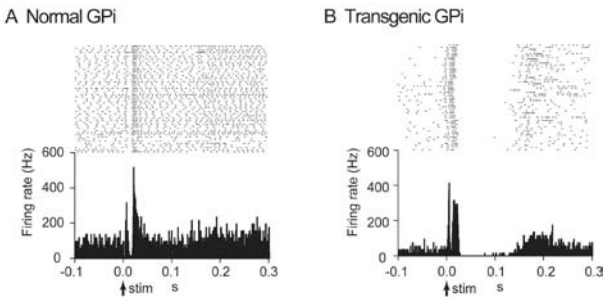

Fig. 4. Responses of GPi neurons to cortical stimulation. **A,** Raster and peristimulus time histogram (PSTH) for the normal mice. Cortical stimuli were delivered at time 0 (arrows). **B**, Raster and PSTH for the transgenic mice. Abnormal responses with long-lasting inhibition were observed.

symbols based on cortical inputs in Fig. 5B. In the GPi of the normal mice, the neurons with forelimb inputs were distributed over a wide area of the GPi, though not in the most medial portion of it (Fig. 5B top). A few neurons with

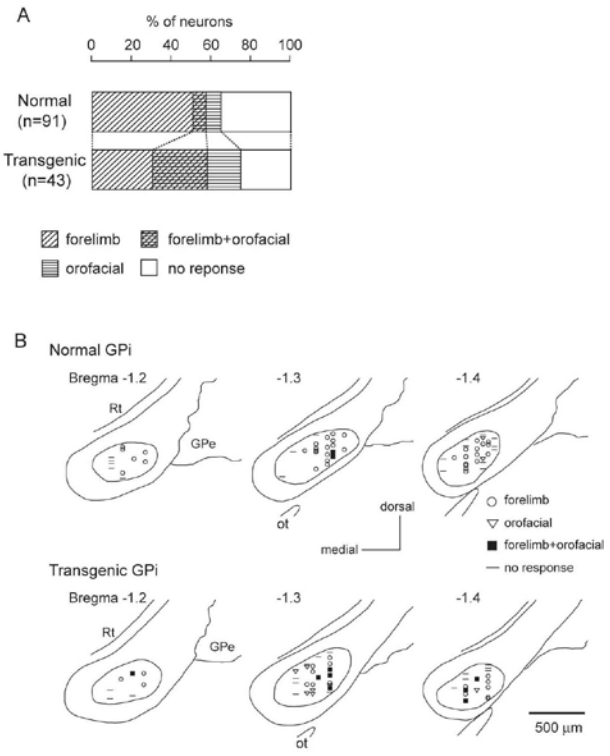

Fig. 5. Somatotopic organization in the GPi. **A,** Proportions of neurons classified based on cortical inputs in the normal (top) and transgenic (bottom) mice. **B,** Distribution of recorded GPi neurons indicated by symbols based on cortical inputs. Data from normal (top) and transgenic (bottom) mice are shown in frontal sections. Figures in the left upper corner represent distance from bregma. Rt, reticular thalamic nucleus; Ot, optic tract.

orofacial inputs and with convergent inputs were found in the lateral portion of the GPi. In the transgenic mice, this segregation was not observed (Fig. 5B bottom). The number of GPi neurons with orofacial inputs and those with convergent inputs increased, and they intruded into the central portion of the GPi, although the most medial portion remained unresponsive.

VI. Discussion

The present study characterized the electrophysiological properties of transgenic mice developed to express human ΔE-torsinA. These mice exhibited: 1) co-activation of agonist and antagonist muscles and sustained muscle activation, 2) decreased GPi and GPe activity with bursts and pauses, 3) cortically-evoked long inhibition in the GPi and GPe, and 4) somatotopic disorganization in the GPi and GPe. These neuronal abnormalities may be responsible for the behavioral abnormalities exhibited by these mice.

The mechanisms responsible for decreased firing rates may include: 1) alteration of membrane properties of GPi and GPe neurons, 2) increased inhibitory inputs to the GPi and GPe, such as GABAergic inputs from the striatum, and/or 3) decreased excitatory inputs to the GPi and GPe, such as glutamatergic inputs from the subthalamic nucleus (STN).

To investigate the mechanism of abnormal firing of GPi and GPe neurons in the transgenic mice further, responses evoked by cortical stimulation were observed. In the normal mice, cortical stimulation typically induced triphasic responses composed of early excitation, inhibition, and late excitation in GPi and GPeneurons. The origin of each component has been intensively studied. Early excitation is mediated by the cortico-STN-GPi *hyperdirect* pathway, while inhibition and late excitation are mediated by the cortico-striato-GPi *direct* and cortico-striato-GPe-STN-GPi *indirect* pathways, respectively. On the other hand, in the transgenic mice, cortical stimulation induced early excitation followed by late long-lasting inhibition in GPi neurons. These abnormal patterns of response may be generated through the cortico-basal ganglia pathways. The early excitation may, at least its early phase, be mediated by the cortico-STN-GPi pathway, as in the normal mice, since the latency of the early excitation in the transgenic mice was short and similar to that in the normal mice. These observations also suggest that the activity of STN neurons is unchanged in the transgenic mice. The origin of the late long-lasting inhibition may be 1) increased inhibitory input via the striato-GPi pathway, or 2) decreased excitatory input via the STN-GPi pathway. The latter explanation seems less likely to be correct, since activity along the cortico-STN-GPi pathway appeared to be unchanged, as discussed above. The above observations also suggest that spontaneous excitation in the cortex is transmitted to the GPi through the cortico-basal ganglia pathways, and induces short-latency excitation and long-lasting inhibition, which might be the origins of bursts and pauses, respectively.

Motor territories in the GPi of monkeys are somatotopically organized, as indicated by their

somatosensory inputs, activity during voluntary movements, and cortically-evoked responses. The present study confirmed the somatotopic organization in the normal mice. In the transgenic mice, on the other hand, somatotopic disorganization was observed, and many GPi neurons received convergent inputs from both forelimb and orofacial regions. Widened somatosensory receptive fields in pallidal neurons have been reported in patients with generalized and focal dystonia. Information-crossing may have occurred through the cortico-basal ganglia pathways. One explanation for this is that single GPi neurons receive inputs from more striatal neurons in the transgenic mice than in the normal mice (Fig. 6). This explanation agrees well with the assumption of increased inhibitory input via the striato-GPi pathway.

The GPi, an output nucleus of the basal ganglia, is composed of GABAergic inhibitory neurons and fires at high frequency in normal states. Its target structures, such as the thalamus and frontal cortex, are thus continuously inhibited. Striatal inputs reduce GPi activity in temporal fashion, excite thalamic and cortical neurons via disinhibition, and finally release appropriate movements with appropriate timing (Fig. 6A). On the other hand, in the transgenic mice, cortical excitation induced long-lasting inhibition in the GPi, suggesting that even tiny amounts of neuronal activity originating in the cortex are transmitted through the cortico-basal ganglia pathways and finally induce strong and long-lasting inhibition in the GPi (Fig. 6B). Moreover, somatotopic disorganization was noted in the GPi and cortical activation induced inhibition over a wide area of this region. Wide areas of the thalamus and cortex are thus activated in uncontrollable fashion, resulting in the motor hyperactivity and involuntary muscle contractions observed in the transgenic mice. A similar mechanism may underlie the symptoms of human dystonia. This may also explain the motor overflow in dystonia, which results in unintentional muscle contraction during voluntary movements. Activation of the forelimb region in motor cortex, for example, may inhibit large areas of the GPi and finally induce involuntary movements of multiple body parts.

Finally functions of the basal ganglia in normal states can be considered as follows; by way of temporal and spatial inputs to the target structure through the *hyperdirect, direct* and *indirect* pathways, only the selected motor program is executed at the selected time, and other competing motor programs are cancelled.

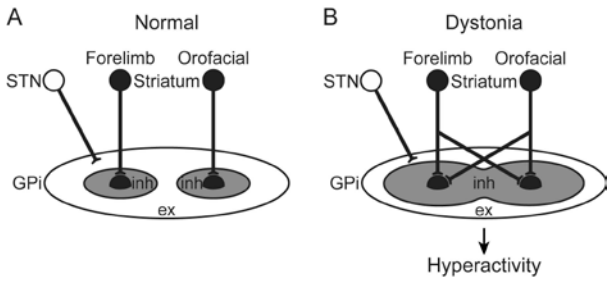

Fig. 6. Schematic diagrams showing information processing through the basal ganglia in normal condition (***A***) and dystonia (***B***). In dystonia, cortical activation induces strong inhibition over wide areas of the GPi, as well as strong excitation in the thalamus and cortex as a result of disinhibition, resulting in the motor hyperactivity and involuntary muscle contractions. STN, subthalamic nucleus.

REFERENCES

[1] Chiken S, Shashidharan P, Nambu A (2008) Cortically evoked long-lasting inhibition of pallidal neurons in a transgenic mouse model of dystonia. J Neurosci 28: 13967-13977

[2] Shashidharan P, Sandu D, Potla U, Armata IA, Walker RH, McNaught KS, Weisz D, Sreenath T, Brin MF, Olanow CW (2005) Transgenic mouse model of early-onset DYT1 dystonia. Hum Mol Genet 14: 125-133.

Quantitative Evaluation of Movement Disorders in Neurological Diseases based on EMG Signals

Shinji Kakei, Jongho Lee and Yasuhiro Kagamihara

***Abstract*—In this paper, we propose a new method to make a quantitative evaluation for movement disorders. Based on the EMG signals, we analyzed the movement disorders for cerebellar patients at the motor command level. As an experimental task, we asked subjects to perform step-tracking wrist movements with a manipulandum, and simultaneously recorded wrist joint movements and muscle activities of four wrist prime movers with surface electrodes. In order to quantitatively evaluate the correspondence between the movement kinematics and the activities of the four muscles, we approximated the relationship between the wrist joint torque calculated from the kinematics and the four EMG signals using a dynamics model of wrist joint. Our surprising observation was that there was very high correlation between the wrist joint torque and the EMG signals. In fact, we identified causal abnormality of muscle activities for movement disorders of cerebellar patients, confirming effectiveness of our proposed method for analysis of movement disorders at the level of the motor command.**

I. Introduction

RECENTLY, some researchers tried to make quantitative evaluation of the motor function for the arm movement [1]-[2]. They captured some features of movement disorders in patients with neurological diseases such as Parkinson's disease or cerebellar atrophy. However, their analysis was limited to the movement kinematics (i.e. the description of movement trajectories). The problem here is that the movement kinematics cannot specify its causal muscle activities or motor commands, due to the redundancy of the musculo-skeletal system. Thus, in order to understand central mechanisms for generation of the movement disorders, it is essential to capture anomaly of the motor command directly, rather than to observe the resultant movement indirectly [3],[4]. Hence, in our previous study, we developed a system for quantitative evaluation of the motor function using wrist movements [5]. We found that there were enough information in the activities of the four muscles to estimate the position, speed and acceleration (i.e. kinematics) of the wrist joint. However, there remained two problems with the system: 1) relatively poor estimation of extreme movement, such as jerky movements of the cerebellar patients; 2) ignorance of nonlinear properties of the wrist joint.

Therefore, in this study, we propose a new technique to analyze movement disorders based on Electromyography (EMG) signals. In order to verify our proposed method, we analyzed specifically the jerky movement of cerebellar patients.

This work has been partially supported by a Grants-in-Aid for Scientific Research on Priority Areas "Emergence of Adaptive Motor Function through Interaction between Body, Brain and Environment"from the Japanese Ministry of Education, Culture, Sports, Science and Technology (SK). This work was also supported by the Tokyo Metropolitan Organization for Medical Research (SK) and MEXT KAKENHI 18700202 (JL).

Shinji Kakei & Jongho Lee @Department of the Behavioral Physiology, Tokyo Metropolitan Institute for Neuroscience, 2-6 Musashidai, Fuchu, Tokyo 183-8526, Japan (e-mail:kakei-sj@igakuken.or.jp).

Yasuhiro Kagamihara @Tokyo Metropolitan Neurological Hospital, 2-6-1 Musashidai, Fuchu, Tokyo 183-0042, Japan.

II. Experimental Method

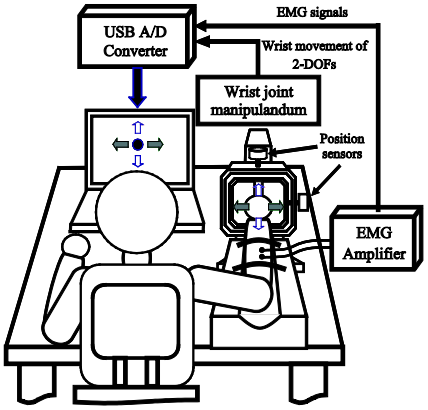

Fig. 1. Outline of the experimental setup.

A. Subject and Experimental Setup

Eight patients clinically diagnosed as cerebellar disorders (average age was 59.5, seven patients were diagnosed as spinocerebellar degeneration and one patient as multiple sclerosis) and eight normal controls who had no history of neurological disorders (average age was 50.9) participated as the subjects. All participants gave an informed written consent, and the local ethical committees approved this study.

Fig.1 shows the outline of the experimental setup. Subjects sat on a chair and grasped a manipulandum with his/her right hand. The forearm was comfortably supported with an armrest. As an experimental task, we asked subjects to perform step-tracking wrist movements for 8 directions [6]. The subjects were required to move the computer cursor immediately to the target as rapidly and accurately as possible. During the task, four channels of EMG signals and two degree of freedom wrist movements were simultaneously sampled and recorded at 2 kHz. The EMG signals were recorded with

Ag-AgCl surface electrodes and then amplified differentially. The EMG signals were recorded from four wrist prime movers: *extensor carpi radialis* (ECR), *extensor carpi ulnaris* (ECU), *flexor carpi ulnaris* (FCU) and *flexor carpi radialis* (FCR). Fig. 2 shows the approximate positions of the recording electrodes. The position of each electrode was adjusted for each subject to maximize EMG signals for a specific movement of each muscle. In a few healthy control volunteers, we confirmed effectiveness of the adjustment with high correlation between the surface EMG signals and the corresponding EMG signals recorded with needle electrodes from the *same* muscles identified with evoked-twitches.

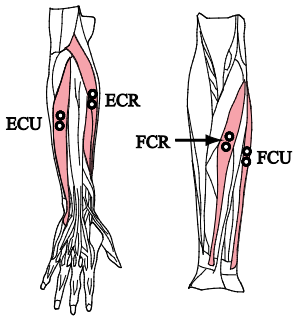

Fig. 2. Muscles related to the wrist joint and the approximate positions of the recording electrode. The four wrist prime movers whose activities were recorded: extensor carpi radialis (ECR), extensor carpi ulnaris (ECU), flexor carpi ulnaris (FCU) and flexor carpi radialis (FCR). We did not distinguish extensor carpi radialis longus (ECRL) and extensor carpi radialis brevis (ECRB), because they have quite similar actions on the wrist and their activities are indistinguishable

B. Normalization of EMG Signals

It is well known that EMG signals are closely correlated with activities of α motor neurons, which represent the final motor commands from the CNS. These motor commands generate muscle contraction, which results in muscle tension. It is established that a second order, low-pass filter is sufficient for estimating muscle tension from the raw EMG signal [7]. In this study, the measured EMG signals were first digitally rectified. Then, the muscle tension was obtained by filtering the rectified EMG signals with a Butterworth low-pass filter of a second order with cut-off frequency of 4Hz. Though the filtered EMG signal is proportional to muscle tension, the proportional constant varies due to variability of skin resistance or electrode position on the muscle. Therefore, for a quantitative analysis, we normalized EMG signals based on the muscular activity while the subject was generating wrist joint torque during isometric contraction for the preferred direction (PD) of each muscle [6]. Namely, for each muscle, we set the filtered EMG signals for 0.8 Nm of isometric wrist joint torque as 1. The normalized EMG signals were used as the motor commands in estimation of the relationship between the wrist kinematics and the four EMG signals.

C. Dynamics Model of Wrist Joint

The equations of the wrist joint torque calculated from the wrist joint kinematics (angle, angular velocity, angular acceleration) can be decomposed into the X-axis component and Y-axis component as follows.

$$I\ddot{\theta}_x(t) + \eta\dot{\theta}_x(t) + k\theta_x(t) = f_x(t) \quad (1)$$

$$I\ddot{\theta}_y(t) + \eta\dot{\theta}_y(t) + k\theta_y(t) + mgc\cos\theta_y(t) = f_y(t) \quad (2)$$

Where, $\theta_x(t)$ and $\theta_y(t)$ represent X-axis component and Y-axis component of the wrist joint angle. $\dot{\theta}_x(t)$, $\dot{\theta}_y(t)$, $\ddot{\theta}_x(t)$, and $\ddot{\theta}_y(t)$ indicate X-axis component and Y-axis component for angular velocity and angular acceleration of the wrist joint respectively. I is an inertial parameter and we calculated this parameter for each subject by measuring volume of the hand. η and k represent viscous coefficient and elastic coefficient. We set these coefficients as 0.03Nms/rad and 0.2Nm/rad for the step-tracking movement, based on the previous studies [6],[8]. m and c are the mass and center of mass for the hand, and we calculated these parameters for each subject by measuring volume of the hand. g is acceleration of gravity (g=9.8m/s^2). $f_x(t)$ and $f_y(t)$ denote X-axis component and Y-axis component of the wrist joint torque calculated from the wrist joint kinematics (in short, *wrist joint torque*).

We assumed that the wrist joint torque were proportional to the linear sum of the four normalized EMG signals. That is, considering the pulling direction of each muscle shown in [6], the relationship between the wrist joint torque and the four normalized EMG signals are formalized as follows:

$$a_{1x}e_1(t) + a_{2x}e_2(t) - a_{3x}e_3(t) - a_{4x}e_4(t) = g_x(t) \quad (3)$$

$$a_{1y}e_1(t) - a_{2y}e_2(t) - a_{3y}e_3(t) + a_{4y}e_4(t) = g_y(t) \quad (4)$$

Where, $e_1(t)$, $e_2(t)$, $e_3(t)$, and $e_4(t)$ represent the normalized EMG signals of the ECR, ECU, FCU, and FCR muscles, respectively. $g_x(t)$ and $g_y(t)$ represent X-axis component and Y-axis component of the wrist joint torque estimated from the four EMG signals, respectively. a_{1x}-a_{4x} (>0) and a_{1y}-a_{4y} (>0) denote the parameters that convert the normalized EMG activities into the wrist joint torque. It should be noted that the sign of each parameter works as a constraint to limit the pulling direction of each muscle.

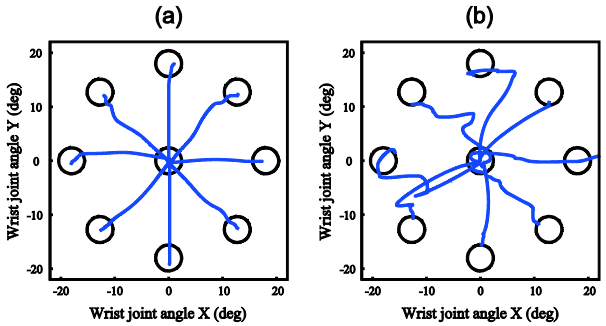

Fig. 3. Trajectories of step-tracking wrist movements. (a) example of a normal control, (b) example of a cerebellar patient.

By optimizing match between the wrist joint torque and the

linear sum of four EMG signals with the two equations (3) and (4) using the least squares method, we obtained these parameters for the musculo-skeletal system of the wrist joint. As a result, these parameters allowed us to estimate the wrist joint torque from the four normalized EMG signals.

III. Results

A. Analysis of the Kinematics for the Movement Disorder

Fig. 3 shows examples of step-tracking wrist movements. As shown in Fig. 3(a), the trajectories of a normal control were almost straight lines from the center to the targets. But, in the case of a cerebellar patient (Fig. 3(b)), irregularity of the trajectories was so intense that the wrist frequently moved away from the targets from the beginning. First, we made quantitative analysis of the wrist movements of the cerebellar patients, in terms of accuracy and directional deviation, velocity components of wrist movements, and compared with the normal controls (Fig. 4).

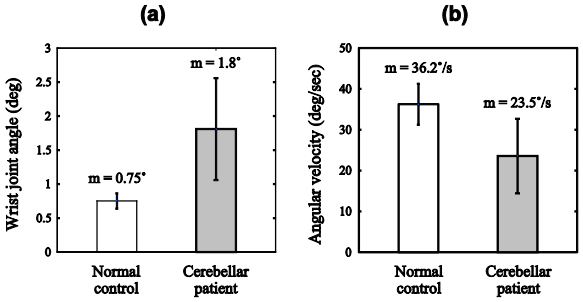

Fig. 4. Analysis of the kinematics in the cerebellar patients and the normal control. (a) accuracy of wrist movement, (b) mean velocity.

1) Accuracy: Accuracy of wrist movements was calculated as mean distance of the observed trajectory from the ideal straight trajectory from the center to the target. As shown in Fig. 4(a), the mean value of the accuracy for the cerebellar patients (1.8˚) were significantly different from that for the normal controls (0.75˚)(p<0.005).

2) Mean Velocity: The mean velocity of the wrist movement for the cerebellar patients (36.2˚/s) was significantly lower than that of the normal controls (23.5˚/s) (p<0.005) (Fig. 4(b)).

B. Analysis of Causal Motor Commands for the Movement Disorder

Fig. 5 shows an example of the relationship between the wrist joint torque calculated from the wrist joint kinematics (*blue line*) and the linear sum of the four EMG signals (*red line*) for a normal control (a) and a cerebellar patient (b). As clearly seen in Fig. 5 and Table 1, there were very high correlations between the wrist joint torque and the four normalized EMG signals for both the cerebellar patients and the normal controls (R for normal controls = 0.81±0.08 (X-axis), 0.84±0.05 (Y-axis); R for cerebellar patients = 0.81±0.09 (X-axis), 0.81±0.05 (Y-axis)). The result strongly suggested that it is possible to identify causal anomaly of the muscle activities for each abnormal movement. Therefore, it should be possible to analyze the jerky movement of the cerebellar patients at the level of the motor command.

In fact, Fig. 6 demonstrates a typical example of one-to-one correlation between the muscle activities and the concomitant movement for the downward movement in Fig. 5(b). This figure summarizes relationship between the muscle activities (i.e.motor commands) and the jerky wrist movement of a cerebellar patient for every 100msec. For instance, the initial

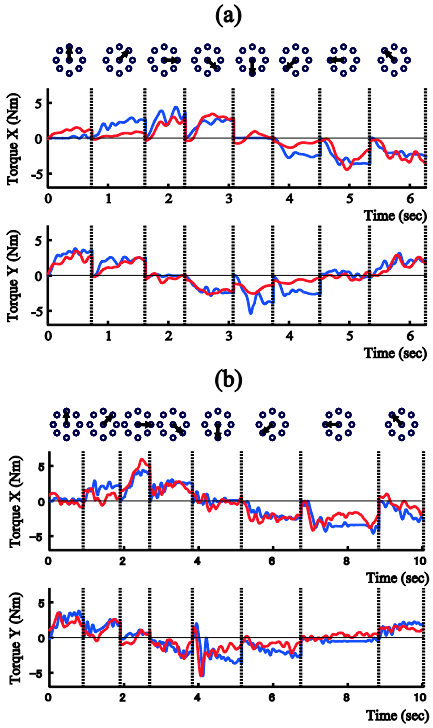

Fig. 5. Relationship between the wrist joint torque calculated from the wrist movement (blue line) and the linear sum of four EMG signals (red line) for a normal control (a) and a cerebellar patient (b). Figures of top trace indicate the direction of wrist movement.

movement (0msec) was away from the down target (i.e. upward) due to the excess activities of ECR that pulls the wrist upward. Then the wrist was redirected toward the down target due to the desirable predominance of the activities of FCU (100-300msec). However, 400msec after the movement onset, inadvertent activities of FCR pulled the wrist leftward, again, away from the target. In this way, it is possible with our new method to determine the anomalous motor command for the movement disorder of the cerebellar patients.

TABLE I
Correlation between Wrist Joint Torque and Muscle Activities

	Correlation R of normal control	Correlation R of cerebellar patient
Torque X	0.81±0.08	0.81±0.09
Torque Y	0.84±0.05	0.81±0.05

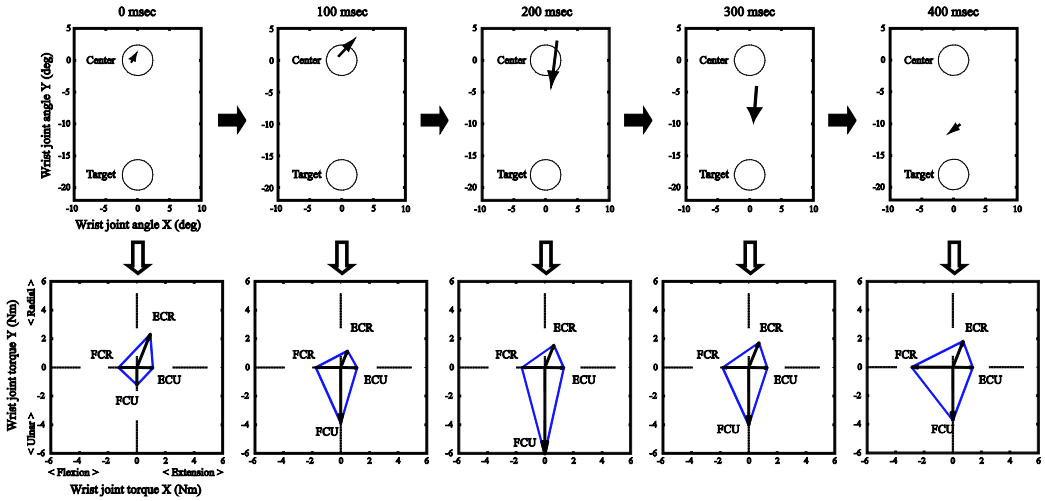

Fig. 5. Causal relationship between the muscle activities (i.e.motor commands) and the jerky wrist movement of a cerebellar patient. Top panels show directions of the wrist movement for every 100msec. 0msec indicates the movement onset. Bottom panels show activities of the four muscles for the corresponding time window. Muscle activities are represented as vectors.

IV. Discussion

In this study, we made a quantitative evaluation for the wrist movements. Especially, we proposed a new method to make a quantitative evaluation for movement disorders based on the EMG signals. In the following discussion, we will focus on two points: 1) Why it is essential to analyze muscle activities for evaluation of movement disorders; 2) How effective our proposed method is.

Some researchers tried to make quantitative evaluation of the motor function for the arm movement [1],[2]. However, their analysis was limited to the movement kinematics. Unfortunately, the movement kinematics cannot specify its causal muscle activities due to the redundancy of the musculo-skeletal system. Thus, in order to make more fundamental evaluation of the movement disorders, it is necessary to identify the causal muscle activities directly, rather than to observe the resultant movement indirectly [3],[4]. Therefore, it is necessary to examine muscle activities to make more fundamental evaluation of movement disorders.

In this paper, we analyzed the movement disorders for cerebellar patients based on the EMG signals. The cerebellar patients have various movement disorders, including: 1) slow to start and slow movement, 2) inaccuracy in achieving a target (dysmetria), 3) intention tremor, and 4) extreme movement such as jerky movement, and so on [1],[2]. In this paper, we verified our proposed method by analyzing these movement disorders for the cerebellar patients based on EMG signals. Above all, we resolved two problems found in our previous study: 1) relatively poor estimation of extreme movement, such as jerky movements of the cerebellar patients; 2) ignorance of nonlinear properties of the wrist joint.

The reason of the first problem was mainly due to the property of the filter used in estimating muscle tension from EMG signals. The filter was originally designed to be optimal to transform muscle activities to joint torques for the elbow and shoulder joints. Thus, it had limited performance for the wrist joint that has different dynamics suitable for finer movements. Hence, in order to make better estimation of the wrist joint torque, we used a new filter optimal for the wrist joint (the Butterworth low-pass filter of a second order with cut-off frequency of 4Hz). As a result of the verification at the torque level of wrist joint (Fig. 5 and Table 1), we found that the new filter was optimal for the wrist joint. For the second problem, as shown in the equations (3) and (4), we calculated the parameters of the musculo-skeletal system, considering the nonlinear properties of the wrist joint [8]. Finally, we confirmed the effectiveness of our proposed methods, identifying the causal abnormality of muscle activities for movement disorders of the cerebellar patients with high accuracy (Fig. 6).

References

[1] R. Nakanishi, H. Yamanaga, C. Okumura, N. Murayama, and T. Ideta, "A quantitative analysis of ataxia in the upper limbs," *Clinical neurology*, 1992, pp. 251-258.

[2] V. Sanguineti et al., "Cerebellar ataxia: Quantitative assessment and cybernetic interpretation," *Hum Mov Sci.*, 2003, pp. 189-205.

[3] M. Manto, "Pathoplysiology of Cerebellar dysmetria: The imbalance between the agonist and the antagonist electromyographic activities," *European Neurology*, 1996, pp. 333-337.

[4] P. Brown, DM. Corcos, and JC. Rothwell, "Does parkinsonian action tremor contribute to muscle weakness in Parkinson's disease?," *Brain*, 1997, pp. 401-408.

[5] J. Lee, Y. Kagamihara, and S. Kakei, "Development of a quantitative evaluation system for motor control using wrist movements—an analysis of movement disorders in patients with cerebellar diseases." *Rinsho Byori*, 2007, pp. 912-921.

[6] M. Haruno and DM. Wolpert, "Optimal control of redundant muscles in step-tracking wrist movements," *J. Neurophysiol.*, 2005, pp.4244-4255.A. Mannard and R. Stein, "Determination of the frequency response of isometric soleus muscle in the cat using random nerve stimulation," *Journal of Physiology*, 1973, pp. 275-296.

[7] GL. Gielen and JC. Houk, "Nonlinear viscosity of human wrist," *Journal of Neurophysiology*, 1984, pp. 553-569.

A study on adaptive mechanisms of human gait by means of multidimensional neuroimaging and computational approaches: Annual Report 2008

Takashi Hanakawa, Satoshi Tanaka, and Rieko Osu

SUMMARY : (1) For the better understanding of brain activity during motor tasks, we developed a system allowing for simultaneous recording of transcranial magnetic stimulation (TMS), electromyography and functional magnetic resonance imaging (fMRI). With this system, stimulus-response relationship was examined between brain activity and intensity of single-pulse TMS to the hand representation of the primary motor cortex (M1). TMS pulses induced a non-linear pattern of stimulus-response relationship in not only the directly stimulated M1 but also remote motor areas such as the supplementary motor areas. (2) A preliminary investigation was conducted to test whether transcranial direct current stimulation (tDCS) could enhance motor functions of the legs. A promising result was obtained. The usefulness of tDCS for neurorehabilitation of gait disturbance will be tested in the near future.

I. Introduction

Bipedal gait is a rather unstable locomotion system. Falling tendency is increased dramatically in association with aging or disease processes. Falling could cause femoral neck fracture, leading to an increased bed-ridden rate in the elderly. Even in this modern era, a measure to prevent senior citizens or patients from falling still heavily depends on labor of caretakers. In preparation for the aging of society in Japan where shortage of caretakers is foreseen, we must develop proactive and effective measures for preventing people from falling. Disappointingly, however, we only have insufficient understanding of mechanisms of gait and balance disturbance in the elderly. Lack of basic knowledge would hinder the development of effective anti-falling measures. The present study aims at: (1) measuring brain activity as well as conventional gait parameters relevant to neural control of gait, (2) understanding of gait and balance problems in the elderly, (3) modeling of neural control of gait by using computational approach, and (4) developing a new method such as brain stimulation or brain machine/computer interface (BMI/BCI) for restoring disturbed gait functions.

A precursory series of studies included the following researches in 2006-2007. First, we performed a neuroimaging study that demonstrated the roles of non-primary motor areas such as the premotor cortex (PMC) in observation and imagining of gait movement [1]. Second, a combined gait analysis and blood flow study examined pathophysiology underlying gait disturbance in age-related white matter changes. As compared with patients without gait disturbance, gait-disturbed patients revealed decreased gait-induced activity in the supplementary motor areas (SMA) and thalamus along with compensatory activity in the right PMC (in submission). Third, we developed a simultaneous recoding system of functional magnetic resonance imaging (fMRI), surface electromyography (sEMG), and transcranial magnetic stimulation (TMS) so that we can try to discriminate neural activity for voluntary movement, generation of movement, and analysis of sensory afferents resulting from movement.

In this Annual Report 2008, we describe a study using the simultaneous TMS-sEMG-fMRI system and also a preliminary study aiming at enhancing motor performance of the legs by means of transcranial direct current stimulation (tDCS).

II. Stimulus-Response Profile during Single-Pulse TMS to the Primary Motor Cortex

A. Background

When brain activity is measured during motor tasks by neuroimaging technique, brain activity reflects voluntary aspects of motor control, generation of movement, and analysis of sensory afferents from muscles and joints. To use information from brain activity in the computational approach, these components must be dissected. Here, a step toward this direction was taken by investigating brain activity during single-pulse TMS to the M1 with a wide range of intensity that induced or did not induce movement [2].

B. Method

1） Subjects: Nineteen healthy volunteers (mean age, 31 years) without any history of neuro-psychiatric disorders, especially epilepsy, participated in the study after giving written informed consent.

This work was in part supported by the Grant-in-Aid for the Priority Areas (“Emergence of adaptive motor function through interaction among body, brain and environment”; area 454) from the Ministry of Education, Science, Sports and Culture of Japan.

Takashi Hanakawa (National Institute of Neuroscience, National Center of Neurology and Psychiatry、4-1-1 Ogawahigash, Kodaira, Tokyo 187-8502, TEL 042-341-2711、FAX 042-346-1748、hanakawa@ncnp.go.jp）

Satoshi Tanaka (Research Center for Advanced Science and Technology, University of Tokyo, 4-6-1 Komaba, Meguro, Tokyo 153-8904）

Rieko Osu (Computational Neuroscience Laboratories, Advanced Telecommunication Research Institute, 2-2 Hikaridai, Seika, Kyoto 619-0288)

2） Simultaneous TMS-sEMG-fMRI: An MRI compatible figure-of-eight TMS coil with an outer wing of 70 mm (Magstim) was attached to a Magstim Rapid stimulator situated outside of the MRI scanner room. Prior to the scanning, sEMG was monitored from the right abductor pollicis brevis with Ag-AgCl electrodes and a commercial amplifier (SynAmp, Neuroscan) at a sampling rate of 1 kHz, and motor evoked potentials (MEPs) were checked during application of TMS pulses to the left M1. We first identified a scalp site where MEPs were maximized and then fixed the coil to the scanner bed by using a custom-made device. A resting motor threshold (rMT) was determined under MEP monitoring in the MRI room. A 3-T MRI (Siemens Trio) equipped with a standard transmitter-receiver coil was utilized for acquisition of fMRI data. T2*-weighted, gradient-echo, echo planar imaging was modified so that scanning noises on sEMG during MRI acquisition were reduced (stepping stone sampling) [3]. Trans-axial MRI slices were acquired to cover the whole brain with the following parameters (TR/TE = 2700/30 ms, acquisition delay = 200 ms, flip angle = 90 degrees, 3×3×3.75-mm voxel size, 30 slices). During a single fMRI run lasted for 3 min 9 sec, 20 single TMS pulses were delivered with the same intensity at a frequency of 0.07-0.125 Hz. Stimulus intensity was varied across fMRI runs between 30% and 95% of machine output (30-110% of original machine output in 7 subjects for whom a special booster was available) at 5 or 10% steps. Each subject underwent 16-21 fMRI runs

3） Data analysis: sEMG data were analyzed with Scan4 software (Neuroscan), which yielded mean MEP amplitude for each stimulus intensity in each subject. FMRI data were analyzed with SPM2 and MATLAB. Preprocessing included slice timing correction, realignment, spatial normalization to the standard anatomical template, and spatial smoothing with a 6-mm three-dimensional Gaussian filter. The TMS trials were regarded as events, and were modeled with a series of delta functions convolved with a hemodynamic response function. This model was used as an explanatory variable in the statistical analysis based on the general linear model. A summary image in each individual was generated by using the contrast between the maximum stimulation and the minimal stimulation conditions. These images were fed into a second-stage, population-level analysis, which produced a statistical parametric mapping of t-statistics. The relationship between TMS intensity and fMRI signals was based on regions of interest (ROI), and both physical intensity (% of machine output) and physiological intensity (% of rMT) of the stimulus were considered.

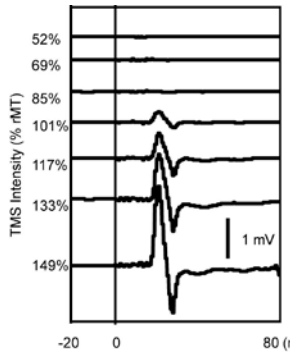

Figure 1: Stimulus-response relationship between MEP and intensity of single TMS pulses during simultaneous TMS-sEMG-fMRI. The data are from a representative subject. Modified from [2].

C. Results

1） MEPs: Stimulus-response relationship between MEPs and single pulse TMS intensity (Figure 1) was consistent with the one reported previously [4].

2） Distribution of brain activity: Three subjects out of 19 were excluded from the study due to insufficient quality of data. Brain activity evoked by suprathreshold single pulse TMS was observed in motor-related regions including the left M1 (directly stimulated), primary somatosensory cortex, ventral part of the SMA extending into the caudal cingulate zone (SMAv/CCZ), bilateral PMC, second somatosensory cortex, thalamus, and cerebellum as well as in the cognitive/affective regions including the auditory cortex, prefrontal cortex, and temporal cortex (Figure 2).

3） Stimulus-response profile: Brain activity was extracted from representative ROI and was analyzed with regard to intensity of single TMS pulses. Data from the directly stimulated left M1 and those from the remote SMAv/CCZ are shown in Figure 3. Stimulus-response profile in both regions showed a non-linear component. The evoked brain responses were abruptly increased at the level of rMT in the M1 and gradually increased below the rMT in the SMAv/CCZ.

D. Discussion

The present study for the first time identified multiple sources of non-linear brain responses evoked by single TMS pulses. Sensory components cannot explain all of the signal increases at the rMT level in the M1 since muscle twitches evoked by peripheral nerve stimulation were reported to induce only minimal activity in the M1. It is possible that non-linear recruitment of a population of neurons whose membrane excitability is distributed normally around the rMT resulted in non-linearly induced brain activity around the rMT. As reported previously [5], remote motor areas such as the SMA/CCZ showed increases in brain activity at weaker levels of stimulation than did the directly stimulated M1. This finding might be explained by an idea that remote area activity would be caused by physiological mechanisms involving neurotransmitter releases while neurons in the M1 would be partially activated by eletctromagnetic energy given externally. These differences may indicate different degrees of energy demands and oxygen consumption across the regions and could explain paradoxical behaviors of M1 and SMA activity in response to TMS with the same intensity.

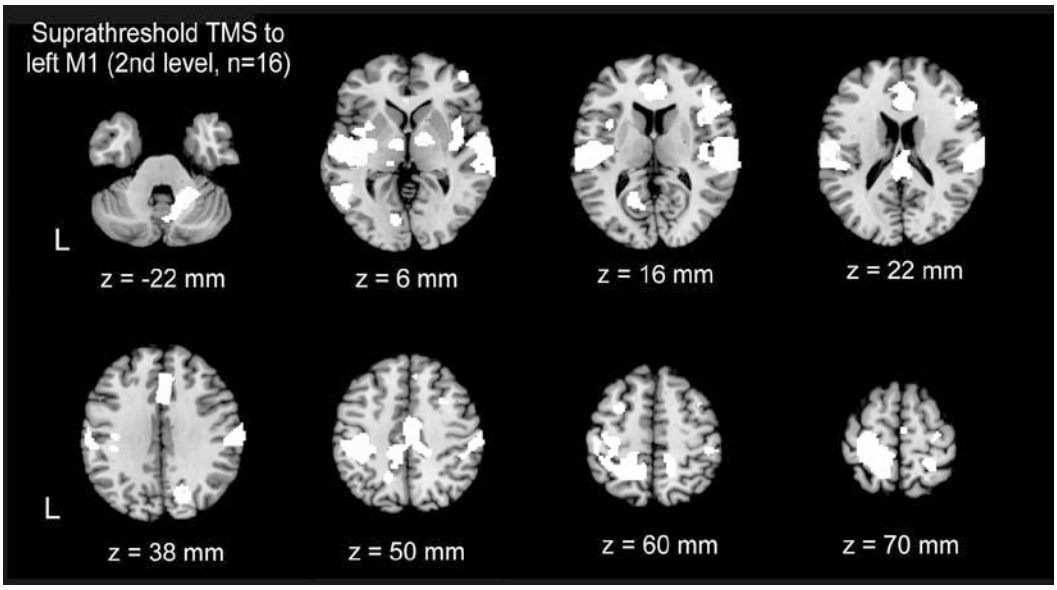

Figure 2. Second-level contrast images between the maximum stimulation (95-110% machine output) and the weakest stimulation (30% machine output). Activity induced by suprathreshold single TMS pulses is observed in the directly stimulated left M1 as well as remote areas including the supplementary motor areas, cingulate motor areas, lateral premotor areas, thalamus, second somatosensory areas, auditory areas and cerebellum. Modified from [2].

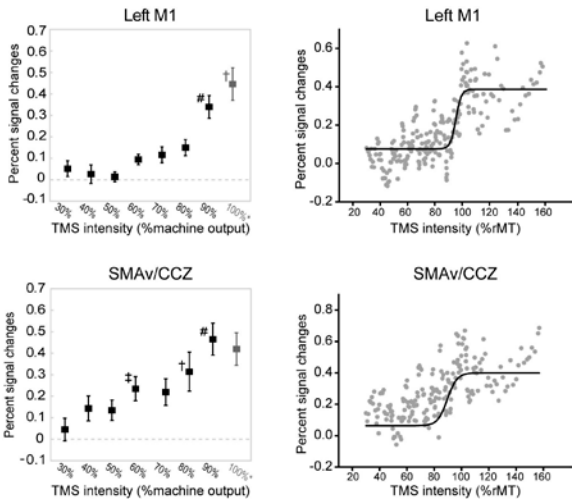

Figure 3: Intensity-dependent changes of fMRI signals sampled from the left primary motor cortex (M1) and ventral supplementary motor area-caudal cingulate motor zone (SMAv/CCZ). TMS intensity is expressed as percentage of the default machine output (left panels). Compared with stimulation with the 30% machine output, only the suprathreshold stimulation conditions revealed significant increases in fMRI signals in the M1, but activity in the SMAv/CCZ showed significant effects already at the subthreshold stimulation levels (†P < 0.05, ‡P<0.01, # P<0.001). These findings were supported by an analysis reformatting the stimulus-response relationship with regard to physiological intensity (% of rMT) of TMS (right panels; a gray dot represents each data point). Black lines represent results from non-linear fitting with Boltzmans

III. Enhancement of Leg Motor Functions by Transcranial Direct Current Stimulation

A. Background

tDCS is a recently proposed non-invasive brain stimulation technique in which weak direct current (~1 mA) is delivered to the brain through the intact scalp and skull. Similar to repetitive TMS techniques, tDCS is reported to be able to modulate brain excitability beneath the electrodes [6, 7]. However, tDCS has several advantages over the repetitive TMS as an interventional tool for modulating brain functions. First, depending on the polarity of the stimulating electrode, tDCS can either enhance (anodal tDCS) or inhibit (cathodal tDCS) brain functions beneath the electrode. Thus far, no significant adverse effects (such as convulsions) were reported in association with tDCS. Only weak tingling sensation can be perceived for several tens of seconds after the beginning of tDCS. Unpleasantness of tDCS is estimated to be half as much as that of repetitive TMS. Thus, controlled blinded trials for studying clinical effects can be much easily designed with tDCS than with TMS. Moreover, tDCS is a compact device allowing for easy mobility, and is less expensive than TMS. Because of these features, tDCS can be a really useful tool for daily rehabilitation in hospitals.

Previous studies with tDCS have shown that tDCS can enhance motor performance of the upper limbs. For example, when tDCS was applied to the M1 at intensity of 1 mA for 20 min, performance of standard upper limb motor tests was temporarily improved in both healthy volunteers and stroke patients [8, 9, 10]. Although these studies suggest the potential usefulness of tDCS for improving gait functions, no studies have ever addressed this issue. However, before jumping into such studies, we first need to consider the possibility that the lower limb representations of the M1 may be less easily excited by tDCS than the upper limb representations of the M1. In the present study, we hence used tDCS to test if it could improve performance of simple motor tasks of the lower limbs in healthy subjects.

B. Methods

Seven healthy volunteers participated in the study after giving written informed consent. They performed motor tasks before, during, and after (30 and 60 min) the application of tDCS. tDCS was delivered for 10 min at intensity of 2 mA. Sponge-type electrodes (surface area = 35 cm^2) were placed over the leg representation of the M1 in the right hemisphere and over the contralateral forehead. The motor tasks included a pinch force task and a reaction time task. The subjects performed each type of tasks with the left leg and also with the left hand.

For the pinch force task with the left leg, pinch force was measured between the great toe and the 2nd toe of the left leg (SHINKIKAKU SHUPPAN, Sokushi Checker, Tokyo, JAPAN). For the pinch force task with the hand, pinch force was measured between the thumb and the 2nd finger of the left hand (BASELINE Hydraulic Hand Dynamometer, Irvington, USA). Pinch force was measured three times, and the maximum force was used as a representative measure. For the reaction time task with the leg, the subjects were asked to release a pedal under the left leg as soon as they perceived a GO signal (red color) on a computer screen. For the reaction time task with the hand, they were required to release a button beneath the left hand in response to the same stimulus.

We employed three stimulus conditions including anode tDCS, cathode tDCS, and sham stimulation. In the sham condition, tDCS was delivered only during the first 10 sec after beginning of tDCS. An interval between successive sessions was about a one week.

C. Results

The pinch force of the leg was significantly increased during the anodal tDCS in comparison with the baseline force measured before the intervention (Figure 4). This effect was only temporarily observed; the force returned to the baseline level 60 min after the intervention. Neither the cathode tDCS nor the sham stimulation produced statistically significant effects. No effect was observed for the hand pinch force, either. None of the stimulation conditions modulated reaction times in either the leg task or the hand task.

D. Discussion

Although this is a preliminary result from a small number of subjects, the present study for the first time demonstrated application of the anodal tDCS to the leg representation of the M1 temporarily enhanced pinch force of the leg. Negative effects of tDCS on pinch force of the hand indicate that the anodal tDCS with the present stimulation parameters showed somatotopically specific effects. It is suggested that pinch force of the toes is one of the important factors that influence falling tendency. It may thus be promising to apply tDCS to patients with gait disturbance to see if tDCS is effective in preventing them from falling. We want to address this issue after concluding the present study with a larger number of subjects.

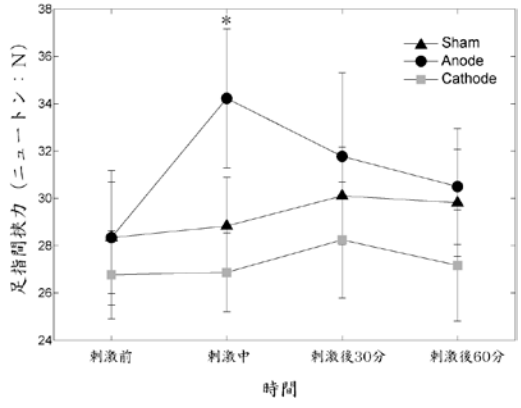

Figure 4：Effects of tDCS on pinch force in the leg. Anodal tDCS significantly enhanced the pinch force during its application *p<05

IV. Conclusion

It is possible that at least portions of motor area activity during motor tasks reflect processing of sensory inputs as a result of movement. To address this issue, we are now studying brain activity during voluntary movement and also during evoked movement by TMS and peripheral nerve stimulation. Knowledge from these studies should refine the interpretation of brain activity during motor tasks including gait. As a preliminary study with tDCS has suggested the usefulness of tDCS for enhancing recovery from gait/balance disturbance, we will positively seek this possibility in the coming years.

REFERENCES

[1] K. Iseki, T. Hanakawa, J. Shinozaki, M. Nankaku, H. Fukuyama. "Neural mechanisms involved in observation and imagery of gait movement" *Neuroimage*, vol. 41, no. 3, pp. 1021-1031, July 2008.

[2] T. Hanakawa, T. Mima, R. Matsumoto, M. Abe, M. Inouchi, S. Urayama, K. Anami, M. Honda, H. Fukuyama. "Stimulus-response profile during single-pulse transcranial magnetic stimulation to the primary motor cortex" Cerebral Cortex (in press)

[3] T. Anami, T. Mori, F. Tanaka, Y. Kawagoe, J. Okamoto, M. Yarita, T. Ohnishi, M. Yumoto, H. Matsuda, O. Saitoh. "Stepping stone sampling for retrieving artifact-free electroencephalogram during functional magnetic resonance imaging," Neuroimage, vol. 19, no. 2, pp. 281-295, Jun 2003.

[4] M. C. Ridding, J. C. Rothwell. "Stimulus/response curves as a method of measuring motor cortical excitability in man," Electroencephalogr Clin Neurophysiol, vol. 105, no. 5, pp. 340-344, Dec 1997.

[5] S. Bestmann, J. Baudewig, H. R. Siebner, J. C. Rothwell, J. Frahm. "Subthreshold high-frequency TMS of human primary motor cortex modulates interconnected frontal motor areas as detected by interleaved fMRI-TMS," Neuroimage, vol. 20, no. 3, pp. 1685-1696, Nov 2003.

[6] M. A. Nitsche, W. Paulus. "Excitability changes induced in the human motor cortex by weak transcranial direct current stimulation" J Physiol vol. 527, no. 3, pp. 633-639, Sep 2000.

[7] S. Tanaka, K. Watanabe. "Transcranial direct current stimulation: A new tool for human cognitive neuroscience." Brain Nerve. vol. 61, no. 1, pp. 53-64, Jan 2009.

[8] F. Hummel., P. Celnik, P. Giraux, A. Floel., W. H. Wu, C. Gerloff, L. G. Cohen. "Effects of non-invasive cortical stimulation on skilled motor function in chronic stroke" Brain vol. 128, no. 3, pp. 490-499, Jan 2005.

[9] F. C. Hummel, B. Voller, P. Celnik, A. Floel., P. Giraux, C. Gerloff, L. G. Cohen. "Effects of brain polarization on reaction times and pinch force in chronic stroke." BMC Neurosci vol. 7, pp. 73, Jan 2006

[10] P. S. Boggio, L. O. Castro, E. A. Savagim, R. Braite,, V. C. Cruz, R. R. Rocha, S. P. Rigonatti, M. T. Silva, F. Fregni. "Enhancement of non-dominant hand motor function by anodal transcranial direct current stimulation." Neurosci Lett vol. 404, no. 1-2, pp. 232-236, Aug 2006

Group C: Social Adaptation

Hitoshi Aonuma, Research Institute for Electronic Science, Hokkaido University

I. Introduction

ANIMALS acquired the capability to behave adaptively throughout their long history of evolution. In the group C, we consider a society, a population of individuals, as one of the environmental factors and try to elucidate the mechanisms of social adaptation in various animals. Especially, we focused on the mechanisms underlying expeditious social adaptive behavior and social structure formation. To promote these studies, we have employed the following two methodologies, "synthetic neuroethology" and "brain-machine hybrid system". In the method of synthetic neuroethology, a dynamical model is constructed based on the physiological knowledge, and in the method of brain-machine hybrid system, an integrated model as a combination of biological elements and the artificial devices is constructed. Performances of these models are analyzed, and the adequacies of the models are tested by the behavioral studies using real animals.

The basic mechanisms of social adaptation, such as the dominance-subordinance hierarchy based on the inter-individual competition, communication among individuals, and formation and maintenance of the society, have been studied using insects as materials. The higher functions for social adaptation, such as discrimination and understanding others, and the mechanisms underlying impairment of social adjustment have been studied using vertebrates including humans. We are aiming at constructing a multi-scale model combining our results obtained throughout these studies about the social adaptation mechanisms on various scales.

II. Contents and overviews

Insects are very useful materials for studying the basic mechanisms of social adaptation. We are especially focusing on some specific social behaviors observed in solitary insects, such as crickets and silkworm moths, and the social insects, such as honeybees, ants and termites. An insect has small central nervous system consisted of only 10^5 neurons, which is less than 10^{-6} compared with those of mammals. Using crickets and silkworm moths, the motivation of behavior, dominance-subordinance hierarchy formation based on the fighting behavior, and the neural mechanisms of courtship behavior have been investigated. The mechanisms of information propagation and sharing within a social group, and the mechanisms of caste formation and the social order have been investigated using the social insects, especially focusing on the molecular and physiological functions. Moreover, some dynamical models have been constructed based on the biological knowledge obtained throughout these studies, and refined by comparing the simulation results with the biological data. Taking this approach, the adaptation mechanism in insects, as a distributed autonomous system, could be expected to apply into developing a new artificial system.

Most vertebrates such as birds and mammals construct and maintain highly organized society based on the individual recognition and inter-individual communication. Affectivity, inter-individual communication, understanding others etc. are very important topics for understanding social adaptive behavior. Songbirds have been used for studying acquisition processes of social adaptive behavior based on the vocal communication, and Japanese monkeys have been used for studying brain mechanisms underlying behavioral decisions based on the social hierarchy. Furthermore, the study of understanding others, one of the important factors of adaptation in the human society, is expected to lead to the elucidation of development process of social adjustment impairments, such as integration disorder syndrome.

In the Group C, planned and subscribed research groups, and/or biological and engineering groups work together closely in the process of each study.

Aonuma *et al.*, Ota *et al.*, planned research groups, and Nagao *et al.*, a subscribed research group, are aiming at understanding the mechanism of behavioral selection based on the social experiences in crickets by combining the knowledge in different scales, such as neurons, individuals and groups. A dynamical behavioral model and a neurophysiological model have been proposed based on the behavioral and physiological data of the plastically changing motivation behind the aggressive behavior depending on the experiences and the social factors during the developmental processes. The model proposed in the last year has been refined by comparing the simulation results and the biological data. A closed-loop model with a multiple feedback pathway, which is a neurophysiological model concerning neuroactive substances in the brain, such as nitric oxide and biogenic amines, has been constructed. Using this model, behaviors of the crickets could have been well mimicked. They are now proceeding both bottom-up and top-down modeling procedures to understand the whole system. Kurabayashi *et al.*, a planned research group, are trying to clarify the adaptation mechanisms developed through the interaction among the body, brain and

environment by both behavioral and neuronal experiments. It has been suggested that a functional network crucial to adaptive behavior is existed in the brain. They have investigated the information processing functions in the brain and attempted to reconstruct such a network technologically. Moreover, the information processing mechanisms by the group of relatively small number of neurons, and the network functions resulted from the interaction between the body and the environment have been investigated, mainly by combining the experiments using a insect- or insect-brain-controlled robot and the molecular genetic and/or physiological techniques. Taking these approaches, it is expected that the relationship between the body-brain-environment interaction and the adaptation capability.

Mainly by the subscribed research groups, the mechanisms of colony (social group) construction and maintenance, based on the labor division, trophallaxis, caste differenciation etc., have been studied using honeybees, termites and ants.

Ito *et al.* is focusing on the waggle dance of the honeybee, one of the social insect species. They have studied the mechanisms on the maintaining the colony, sharing information, and accumulating information by communicating between individuals. They regard the waggle dance as a good model of the 'propagation and sharing of knowledge' that maintains a society, and are attempting to reveal the effects of the waggle dance in terms of the colony's benefit and adaptability to environmental changes using mathematical models and computer simulation based on parameters from observations of the bee behavior and environmental changes.

Miura *et al.* have focused on the labor division and communication among each caste in the colony of the social insect, which is referred to as a 'super-organism' and proposed a systematic control mechanism of the caste differentiation suited to the colony situation. They have constructed a model of the colony organization in the termites based on the knowledge of morphology formation, behavior differentiation, physiological function and gene expression. They have also tried to clarify the mechanisms of the social behavior by studying the neural specificity in the each caste neuroethologically. Takeuchi *et al.* have studied the schooling behavior in the killifish. They are trying to identify the brain functions (genes, neural networks and brain region) crucial for the schooling behavior and estimate an information-processing pathway in the brain for the schooling behavior by taking a constructive approach.

Tsuji *et al.* have studied the mechanisms underlying the very sophisticated functions of the group of ants. They have shown that the appropriate regulation of the group behavior in the ants could be achieved by 'self-organizing' system for the whole society by intrinsic feedback mechanisms. They are now investigating the chemical ecological basis and the self-organizing system of the colony size recognition and the appropriate behavioral switching mechanisms in the ants, and discussing the evolutionary dynamics by which these systems are evolved. In addition, they are also testing this regulation mechanism using a model simulation and robots. By comparing the three systems, the expected system evolved by the natural selection, the system of the ants and the system of the robots, they are aiming at elucidating the 'design principle of the nature' by which the regulation mechanisms of the society are evolved.

Oka *et al.* have studied the mechanism of individual recognition from the various neural levels, molecular to behavior. They have studied male-female communication in the zebra finch, especially focused on the mechanisms of the female brain to recognize the males' tweet. They have succeeded to detect neural activities in the hippocampal formation by the catFISH method. Because there have not been enough anatomical knowledge of the hippocampal formation, they have tried to analyze the neural networks in the hipocampal formation exhaustively by the following two newly developed visualization techniques of the neurons, 1) visualization of the neural networks responsible to the males' tweet by pH imaging and 2) visualization of the neurons using a gene gun and liposoluble fluorescence dyes. They are now investigating the information processing mechanisms of the males' tweet in the hippocampal formation.

Fujii is focusing on the brain mechanism underlying appropriate recognition of one's surroundings and involuntary behavioral selection to satisfy one's desires maximally. They have discussed that the individual recognizes and manipulates the environment and optimizes its behavior through the virtual space in the brain linked directly to the real world. They are aiming at cutting into an as-yet-undiscovered brain function, the social brain function, which is one of the fundamental functions of the brain determining our behavior.

Kato *et al.* are attempting to prove the importance of understanding the others' visual lines and faces for recognition of the social signal. They have applied the studies on the patients with schizophrenic disorder to construct a machine and interface with the social adaptability. They have innovated the ability to recognize the humans' action, which is necessary for social cognitive artifacts. They have also studied a cognitive model to mimic the dissonance between the intention and the action, and proposed a forward model.

That is the brief description of the contents of the project. Each group leader in the following chapter summarizes detailed results of each research group, respectively.

Systematic understanding of neuronal mechanisms for adaptive behavior in changing environment

Hitoshi Aonuma, Research Institute for Electronic Science, Hokkaido University

Abstract: **Animals alter their behavior in order to respond to the demands of changing environments. Society and crowd are also one of the dynamic environments. We have investigated the design principle of neuronal mechanisms for social adaptation in animals, by focusing on how animals select their behavior depending on previous social interactions or social experiments. Insect pheromone behaviors provide a good model system to elucidate the mechanisms of social adaptation. We have focused on cricket agonistic behavior that is released by cuticle pheromones. Our biologist group mainly concentrated on revealing behavioral and physiological aspects of socially adaptive behaviors. Nitric oxide NO) system and octopamine (OA) system in the cricket brain could mediate aggressive behavior of the crickets. Based on our results, we collaborate with engineering groups to establish dynamic behavior models and neurophysiological models.**

I. Introduction

Animals have evolved nervous systems to adapt dynamically changing environment. Insects have rather simple and identical nervous systems than mammalian brain. Thus insects must be good model animals to investigate neuronal mechanisms underlying adaptive behavior. Insects have rather simple and identical nervous systems. Mammalian brain has about 10^{12} neurons. On the other hand, an insect nervous system has about 10^{6} neurons. Such insect brains allow us to access each neuron easily, which accelerate us to investigate how animals show socially adaptive behavior from cellular level to behavioral level analysis. They perceive lots of signals as stimulation from environment and they adjust their behavior. They do not always respond same way to the same external stimuli. The state of central nervous system must be dependent on their experiences as well as internal and/or external conditions. These factors would mediate threshold of releasing a behavior or behavioral pattern. Insect neuroethology has already provided valuable insight into how nervous systems organize and generate sophisticated behavior. It has made important contributions to brain research, expanding our overall understanding of sensory and motor systems. However, thousands of mechanisms to understand how adaptive behavior emerges have been still remained unclear.

We have here investigated the neuronal mechanisms underlying socially adaptive behaviors that are emerged from individual interactions among animals. We have combined neuroethological approaches and system engineering approaches to understand how animals form social communities, how they learn and retain previous experiences and how they alter their behavior depending on dynamic environments, which will help us to unravel the universal design of central nervous systems.

II. Aims

The aim of our research is to elucidate the neuronal mechanism of socially adaptive behavior. To understand mobiligence of social adaptation, we have focused on neuronal mechanisms that animals alter their behaviors in order to respond to the demands of changing social environment. To understand the neuronal function underlying behavior selection of animals including human being, it is necessary to elucidate internal states that introduce animal adaptive behaviors.

Insects provide us a good model system to investigate neuronal mechanisms of adaptive behavior, since they have rather simple and identical nervous systems. Communication behavior using pheromones in insects must be one of the greatest model systems to investigate neuronal mechanisms of animal adaptive behavior. Most of pheromone-induced behaviors in insects have been thought to be hard-wired: a behavior that could be turn on and off but with no plasticity. However, some of pheromone behaviors are revealed to be modified by their previous experiences. Cricket aggressive behavior is an example of such pheromone induced behaviors. The response of males to the pheromone can be modified by the previous fighting experiences [(1)]. The behavior of insects has been understood that internal states and external environments drastically mediate threshold of releasing behavior or releasing behavioral pattern. Previous social interaction such as mating and agonistic interaction mediates following behavior. In this study, we have focused on the aggressive behavior of crickets.

III. Achievements

Insects can adapt to various environments and emerge adaptive behaviors using their simple nervous system. We have investigated neuronal mechanisms of behavior selection after agonistic interaction among cricket (*Gryllus bimaculatus*). We here performed behavioral work to elucidate functional role of contact-chemo receptive information from antennae, performed physiological and biochemical analysis to elucidate functional role of neuroactivators such as NO and biogenic amines, and performed anatomical research to elucidate information

processing pathway in the cricket brain. In order to understand the neuronal mechanisms underlying social adaptive behavior in the crickets, we have constructed dynamic models for behavior of animals and role of NO/OA system in the brain by collaborating with engineering researchers.

3-1 Neuronal processing pathway for aggressive behavior releasing pheromone

Male crickets *Gryllus bimaculatus* show intensive aggressive behaviors when they encounter another male and detect conspecific male cuticular pheromone (Fig. 1). When two male crickets engage in combat, the loser cricket will refuse to fight again. The cricket battle starts out slowly and then escalates into a fierce struggle. Therefore, the previous agonistic interactions between male crickets had influence over the following behavior of subordinate males. Once dominant hierarchy was established between male crickets, the dominant cricket showed aggressive behavior when it encountered the opponent cricket whereas subordinate cricket would not attack again against the opponent but showed avoidance behavior. We have focused on loser cricket (subordinate) behavior to understand how animals alter their behavior dependent on social interaction [(1)]. The cuticular pheromones that introduce aggressive behavior have not identified. Then collaborating with Prof. Yamaoka's group, we are identifying the substance and its structure. We are also synthesizing putative component of hydrocarbons that work as aggressive pheromones. After behavior assay using them, we will determine which chemical substance can work as aggressive pheromone.

Fig 1. Fighting between male crickets. The aggressive behavior is released by cuticular pheromones and the crickets' battle starts out slowly and then escalates into a fierce

In order to develop neurophysiological research of the cricket agonistic behavior, as a first step, we have performed anatomical research of the cricket brain. The cuticular substances release the agonistic behavior of the cricket as a tactile chemical stimulus. Therefore, the processing pathway for tactile chemical signals from antennae was investigated. The antennal lobe is the primary center for the chemical processing. It is composed of 49 glomeruli. The tactile signals, on the other hand, are processed at ventral area of flagellar afferents (VFA). Innervating pathway of the projection neurons from AL and VFA was examined. Ten tracts were originated from the AL, whereas eight tracts from the VFA. The tracts from the AL and the VFA shared several projection tracts, but their termination areas were segregated in the lateral protocererbrum [(2)]. Using synthesized substance we are identifying aggressive pheromone processing pathway in the cricket brain.

3-2 Effects of multimodal inputs on fighting experience dependent behavior selection

Aggressive behavior is released when male crickets detect cuticular substances on the body surface of another male by the antennae. However the neural mechanism underlying fighting behavior is still unknown. Here we test the effect of contact chemical information (antennae information) and of visual information on releasing aggressive behavior.

In order to examine if antennae are necessary to release aggressive behavior of male crickets, the behavior to another male were observed 1 hr after antennal legions. Over 90 % of intact crickets showed aggressive behavior, such as antennal fencing and/or threat posture, and start to fight with the other male. On the other hand, the percentage of aggressive crickets was significantly reduced when the whole antennae were cut. The crickets, whose maxillary palpi were removed as a sham operation, showed aggressive behavior to the other male as well as intact crickets. These results suggest that the male crickets use the sensory information from the antennae to perform correctly to other crickets, i.e. the aggressive behavior to males or the courtship behavior to females [(3)].

Although the males without the antennae did not show clear aggressiveness to another male with the same operation, they could fight against another intact male. When they faced to the intact male, the percentage of the aggressive males became significantly higher than that to the males without the antennae. The level of the fighting between the intact male and the male without the antennae was not significantly different compared with those between intact males and males without the maxillary palpi. These results indicate that the input from the antennae is necessary to start fighting to another male but not to fight against an aggressive male. The fact that the males without the antennae could fight against the intact males under the dark conditions suggests that there are at least two parallel pathways to elicit the male aggressive behavior, 1) one mediated by the sensory input from the antennae, and 2) the other one mediated by the mechanical input from the body surface.

In order to examine the effects of visual cue on releasing aggressive behavior in male crickets, compound eyes were painted with enamel or behavior experiments were performed under red light. Interestingly, the duration of

fighting increased significantly if visual cue was blocked. Cricket fighting is terminated if one of male give up continues attack and escape from the opponent. If their visual cue were blocked, they might not notice if opponent recognize lose each other. Then they would continue fighting.

Using these results of behavior experiments, we collaborate with Ota's group to build a dynamic model explaining the effects of multi modal information on releasing aggressive behavior.

3-3 Effective time window of NO in the aggressive behavior

Effect of NO/cGMP signaling on aggressive behavior has been examined by pharmacological and behavioral experiment. Inhibition of NO/cGMP signaling cascade impaired the behavioral selection in losers, and thus it is suggested that the NO/cGMP signaling cascade plays a crucial role to the behavioral selection in losers. The behavior of loser cricket whose antennae were removed was similar to the behavior of loser crickets whose NO/cGMP signaling pathway was inhibited. This suggests that NO/cGMP signaling pathway in the antennal sensory information-processing pathway participate with the neuronal mechanism underlying behavior selection.

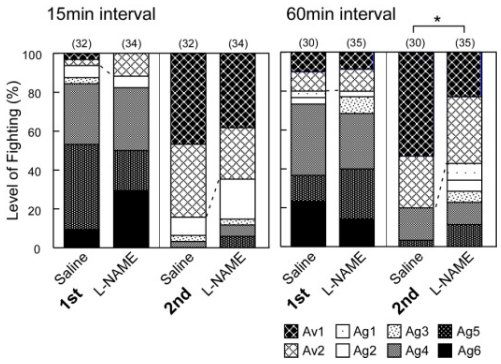

Fig. 2. Effect of NOS inhibitor L-NAME on aggressive behavior. One hour after injection of L-NAME, behavior in the first encounter was observed. After fighting was settled, they were isolated for 15nim and then behavior of the second encounter was observed. In other experiments, Twenty min after injection of L-NAME, behavior of the first encounter was observed. After fighting was settled, they were isolated for 1 hr and then behavior of the second

In order to examine the effective timing of NO/cGMP signaling on behavior selection, we inhibited NO synthase (NOS) activity using an inhibitor L-NAME. L-NAME was injected into the brain of the cricket prior to the first engagement between males (Fig. 2). One hour after the head injection of L-NAME, 2 males were encountered and observed ther behavior. For contral cricket saline were injected. In the first encounter, there are no significant change between control pairs and L-NAME injected pairs. After fighting was settled, they were isolated for 15nim and then behavior of loser in the second encounter was observed. The loser seemed to be rather aggressive but it was not significant. Next experiment, L-NAME was injected 20 min before first encounter. After the fighting in the first encounter was settled, they were isolated for 1 hr and then observed the behavior of loser crickets in the second encounter. The losers became more aggressive than control animals.

NO is generated by activating NOS and diffuses about100 μm/sec through cell membrane of the target cells. It activates soluble guanylyl cyclase to increase cGMP level. The functional concentration of NO is thought to be 10-100 nM in the nervous system [4]. The lifetime of NO in the tissue is very short. These natures of NO suggest that effective time window must be necessary. To examine the effective time window, we next inhibited NOS activities using L-NMAE just after the first fighting (Fig. 3).

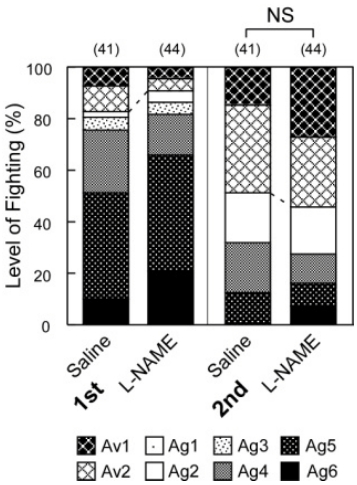

Fig. 3. L-NAME was injected just after fighting was settled in the first encounter. Behavior of loser cricket in the second encounter was observed after 80 min of L-NAME injection. NS: no significance, Mann-Whitney U-test

A NOS inhibitor L-NAME was injected into the brain of crickets that were loser in the first fighting. For control cricket saline was injected in the brain. After 80 min of injection, losers were encountered with previous winners. Most of losers avoided fighting soon after they notice previous winners. There are no significance between control and L-NAME injected losers. Our previous results indicate that NO deceases biogenic amines in the cricket brain. These results indicate that it is necessary for losers to generate NO in the brain before or during the first encounter to introduce avoidance behavior in the second encounter. The timing of NO release and decrease of biogenic amine must be also important factor. We need further investigation how NO/biogenic amine system works in the brain to select and decide behavior in the crickets.

3-4 Effect of octopamine on aggressiveness of male crickets

We have demonstrated that biogenic amine in particular octopamine (OA) level in the brain decrease just after the fighting. Our behavior experiments showed that loser crickets wouldn't elicit aggressive behavior against conspecific males for more than 1 hour after the fighting. Nitric oxide (NO) system is also shown to regulate aggressive behavior. NO system decrease biogenic amine levels in the brain. Since NO is free radical substance in the tissue, it must be oxidized quickly. Therefore biogenic amines can be one of the candidates to regulate aggressive behavior. We examined the changes of biogenic amine levels in the brain after aggressive behavior. We found decreased OA level gradually restored to the original level after the aggressive behavior. It took about 1 hour.

Then we examined the effects of OA antagonists on aggressive behavior between male crickets. We here use 2 kinds of OA antagonists Epinastine and Mianserin. These antagonists were head-injected 1 hr before behavior experiments. Both antagonist decreased aggressiveness in the crickets. This result suggests that OA regulates aggressiveness of crickets. The effect of OA antagonist must mimic decrease in OA level in the brain. Thus NO/OA system must be important factor for neuronal mechanisms underlying aggressive behavior.

We now need to examine the combination effects of NO and OA antagonist, or NOS inhibitor and OA agonist to clarify role of NO/OA system for aggressive behavior.

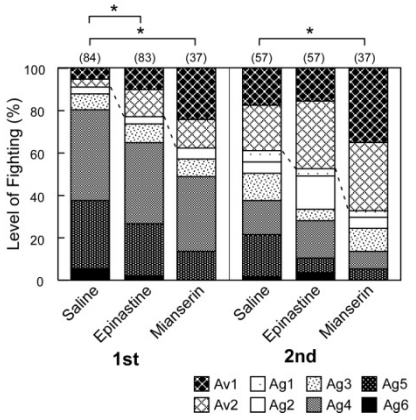

Fig. 4. Effect of antagonist of octopamine on aggressiveness of male crickets. Antagonist of OA was head injected 1 hr before behavior experiments. Six hours after the first fighting, the behavior of second encounter was observed. *: $P<0.05$, Kruskal-Wallis test

IV. Conclusion and future plan

We have investigated neuronal mechanisms underlying behavior selection dependent on fighting experience in the crickets. We have focused on role of NO/cGMP/OA system in the brain. Based on our biological experiments, we built dynamic behavior models and neurophysiology model with Ota's group. In the behavior model, we included internal state. We are thinking this internal state could be neuromodulatory function in the brain and be NO system and OA system.

The behavior model well demonstrated the cricket behavior dependent on population density. In order to examine the simulation of this model, we removed dominant agent from the group of artificial crickets. Then measured how long it takes to reconstruct dominance-subordinance relationship. It was less than 10 min. Then we tried the same experiments using animals. We placed several males in a arena. Cricket usually starts fighting and one of them becomes a dominant. Then we remove the dominant from the group and observed the behavior of rest crickets. One of subordinate crickets becomes dominant if dominant animal is disappeared. Interestingly, it was also within 10 min. This indicates that internal state is modified by individual interactions among crickets. Now we are investigating neuronal mechanism underlying

Neurophysiolagy model demonstrated that multiple feed back loops are necessary to explain cricket behavior in high-density group. The behavior model and cricket behavior experiments also demonstrated that social interactions improve internal state of animals. Thus this hypothesis must be examined by biological experiment. We will carry on investigating the detail of neuronal function underlying behavior selection from cellular level to behavior level and carry on collaboration with engineering research group to understand systematically by constructing dynamic models.

REFERENCES

1. Aonuma H, Nagao T, Ota J, Kawabata K, Asama H (2007) Modeling of socially adaptive behavior and its application – Lesson from agonistic behavior in the cricket–. J. Socie. Instr. Contr. Engin. 46: 903-909.
2. Yoritsune A and Aonuma H (2007) 3-D atras of the cricket antennal lobe. Proc. International Symp. Mobiligence, 2: 187-190
3. Sakura M, Yoritsune A, and Aonuma H (2007) Fighting experiences modulate aggressive and avoidance behaviors in crickets against male cuticular substances. Proc. International Symp. Mobiligence, 2: 243-246
4. Aonuma H., Kitamura Y., Niwa K., Ogawa H. and Oka K. (2008) Nitric oxide-cGMP signaling in the local circuit of the cricket abdominal nervous system. *Neuroscience.*157: 749-761.

Three Models of Fighting Behavior in Crickets

Jun OTA, Hajime ASAMA, The Univ. of Tokyo, Kuniaki KAWABATA, RIKEN

Abstract: Three models are proposed as for group behavior of crickets, individual interaction among crickets, physiological findings of a cricket. Simulation results indicate the effectiveness of the proposed models.

Keywords: crickets, adaptive behavior, multi-agent systems

1. Introduction

Our group studies adaptation mechanisms of crickets to other individuals and environments, through analyzing fighting behaviors among crickets and the effect of social population.

Our aim is to clarify the mechanisms embedded in animates to adapt to other animates and environments. In our study, we apply a system engineering approach with mathematical models focusing on the crickets to clarify its mechanisms of adaptation. As shown in Fig.1, three models are proposed: the top-down model, the bottom-up model, and growth model.

Behavior modeling of crickets is made connecting cricket individual fighting behavior and the effect of social population in Section 2. In Section 3, simulated swarm behavior is discussed based on proposed neuronal circuit model of the cricket and advanced modeling approaches. In Section 4, growth modeling of cricket is described considering growing environment including other crickets. We conclude the paper in Section 5.

2. Behavior modeling of crickets[1]

Establishing social status in the crickets was observed. Since fighting behavior in crickets can be treated as a two-body problem, we examined individual discrimination in male crickets by behavior experiment using two crickets' battle.

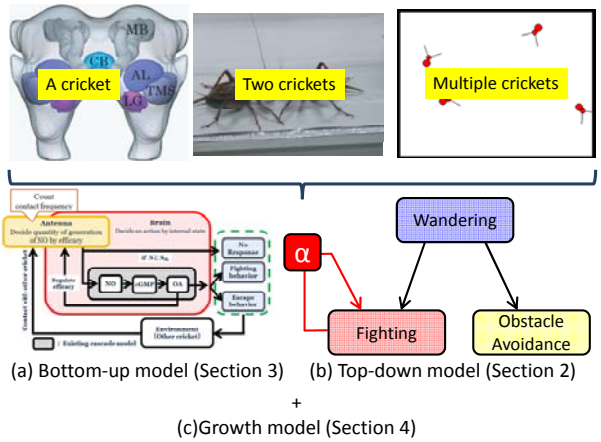

Fig. 1 The proposed three models

2.1 Experimental method

We examined whether crickets discriminate former opponents after the fighting by observing the behavior of subordinate cricket in the following encounter with conspecific males. Each loser cricket in the first battle was placed in the arena and familiar dominant (a), unfamiliar dominant (b), naïve (c), and subordinate (d) were encountered respectively. Two naïve crickets were set in the arena to keep isolated for 15 min using the partitions. Then the behavior of first encounter was observed after removing the partition. After 30 s from the settle of the fighting, we placed the partition again at the center of the arena to keep each cricket isolated. The pairs which did not show aggressive behavior were excluded from the analysis in this study. The winner cricket was removed from the arena, and then the opponent against the loser was changed to observe the behavior of subordinate animals in

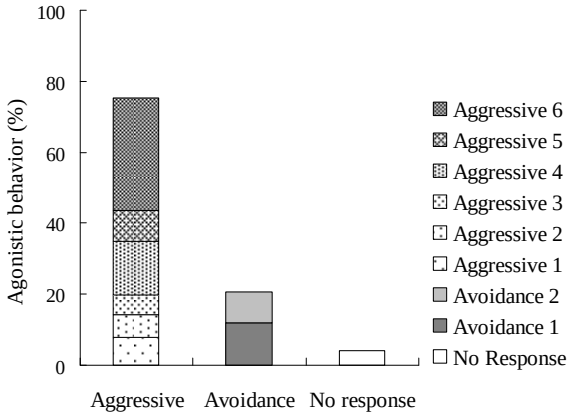

Fig. 2 Behavior of the male crickets in the first encounter with conspecific males

the second engagements.

Figure 3 shows the behavior at the first contact (n=126). The pairs of 75% showed aggressive behavior, but the pairs of 21% showed avoidance behavior. Other pairs of 4% showed no response.

Figure 8 shows the behavior at the second fighting.

(a) vs. Familiar dominant (n=17)

At the pairs of 82%, the cricket that had experienced losing showed avoidance behavior (Fig. 7(a)). At the pair of 12%, the cricket that experienced losing showed aggressive behavior again. Other pairs of 4% showed no response.

(b) vs. Unfamiliar dominant (n=22)

At pairs of 59%, the cricket that had experienced losing showed avoidance behavior (Fig. 7(b)). At the pair of 27%, the cricket that had experienced losing showed aggressive behavior again. Other pairs of 14% showed no response.

(c) vs. Naïve (n=10)

At pairs of 80%, the cricket that had experienced losing showed avoidance behavior (Fig. 7(c)). At the pair of 20%, the cricket that had experienced losing showed aggressive behavior again.

(d) vs. subordinate (n=14)

At pairs of 86%, the cricket that had experienced losing showed avoidance behavior (Fig. 7(a)). At the pair of 14%, the cricket that had experienced losing showed aggressive behavior again.

No significant difference was found between (a) vs. Familiar dominant and (b) vs. Unfamiliar dominant (a–b: P=0.169). This result demonstrates that crickets did not select behavior depending on the previous fighting experience. However, no significant differences were found between (b) vs. Unfamiliar dominant, (c) vs. Naïve, and (d) Subordinate (b–c: P=0.425, b–d: P=0.142, c–d: P=1.000). These results suggest that would not select behavior depending on dominant status.

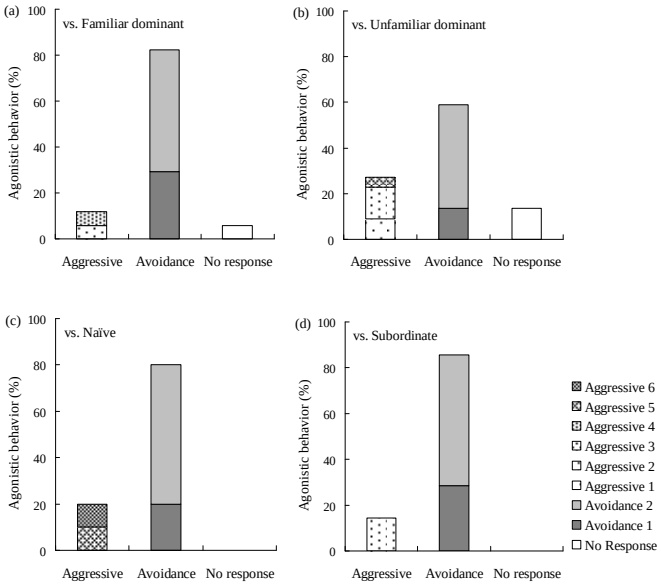

Fig. 3 Behavior responses of subordinate crickets in the second encounter.

3. Neuronal circuit modeling of crickets

In this year, we constructed an advanced neuromodulation model with interaction effect and run multi-individual simulations utilizing the model.

Constructed model with interaction effect introduce a new state value S to previous neuromodulation model. Here, S means the efficacy to sensory input (pheromone). Equation (1) shows the property of the efficacy.

$$\frac{dS}{dt} = -\rho S + aA - bF_{in} \quad (S \geq 1.0) \qquad (1)$$

Here, A indicates the amount of OA and F_{in} is a step -form function which expresses sensory input (pheromone). It is set as that single input state is kept for 15 [sec] after each antennal contact. In order to realize the behavior of previous proposed neuromodulation model, each coefficient (ρ, a, b) is tuned based on biological knowledge (ρ=0.8, a=2.0, b=1.0). Figure 4 shows transition of internal state and efficacy value (sensitivity) of a simulated cricket with S. It shows similar behavior to our

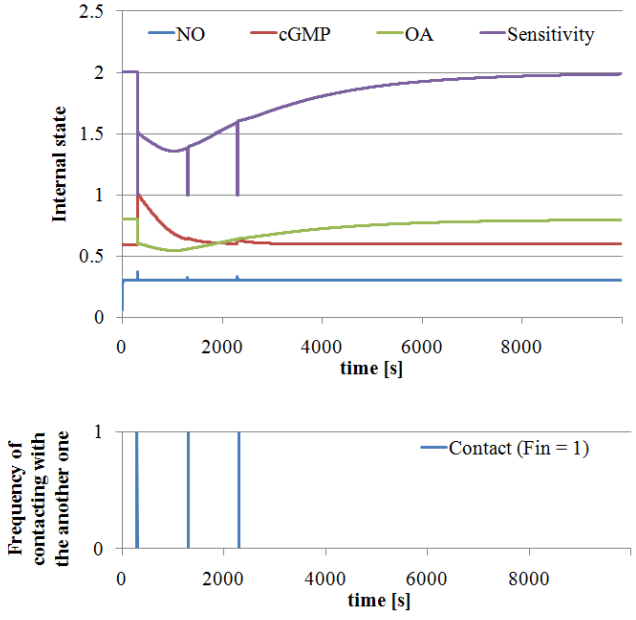

Fig. 4 Simulated transition of internal states and efficacy (sensitivity) in case of low frequent stimulation

previous model. Here, when pheromone input exists, F_{in} takes value 1. F_{in}=0 means no contact. Figure 5 also shows the result in case of high frequent (50 times with 15 seconds interval) pheromone stimulation after time=300 [sec].
As the result, simulated crickets can not become aggressive state because of the efficacy S is lowered by high frequent pheromone stimulation even if the OA level is high.

Next, in order to observe swarm behavior which is emerged by advanced model, we run simulations using four simulated crickets. Here, the simulation is done for 4000[sec] and the number of aggressive one under each environment is counted. Figure 6 shows the results of the simulations. Number of trials under same size of environment is 50 times.

As the results, all individuals did not take aggressive state in high-density environment and 0 or 1 individual became aggressive in middle-density environment. Also, in low-density environment, 1 or 2 individual(s) took aggressive state. It shows that the number of aggressive ones changes depending on the population density. It is similar tendency to ecological observation knowledge.

Since these simulation results, it is considered that proposed neuromodulation model with interaction effect (frequency of pheromone stimulus) can realize both of fighting behavior between individuals and adaptive swarm behavior according to the population density, simultaneously.

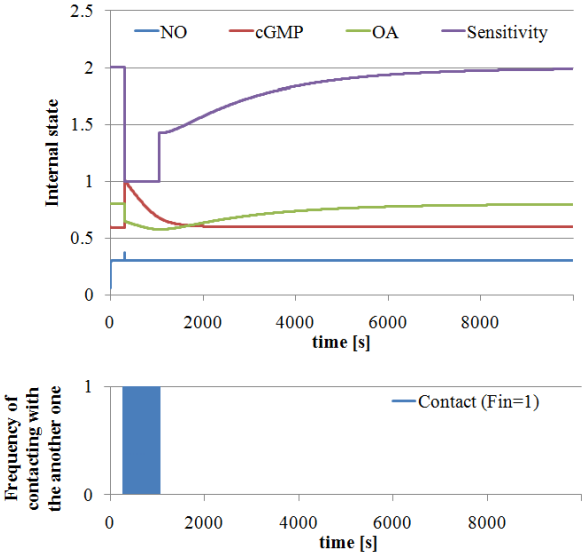

Fig.5 Simulated transition of internal states and efficacy (sensitivity) in case of high frequent stimulation

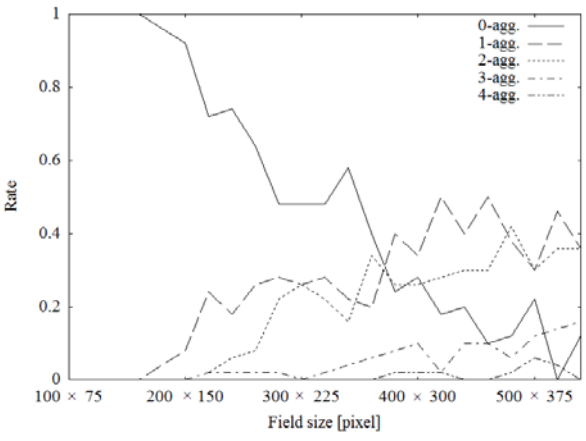

Fig. 6 Simulation result for swarm behavior

4. Growth modeling of crickets

It has been reported that many of vertebrate and invertebrate species show overdevelopment of aggressive behavior increased by social isolation. Of course, human is no exception. The study of this has been done with a few vertebrates: rat, mouse, monkey and so on. On the other hand, studies with invertebrates have benefits that nerve system of invertebrates is simple and has a little individual difference. So, study with cricket would be contributory to elucidate the interspecific nerve system of aggression.

Aggressive behavior is necessary for

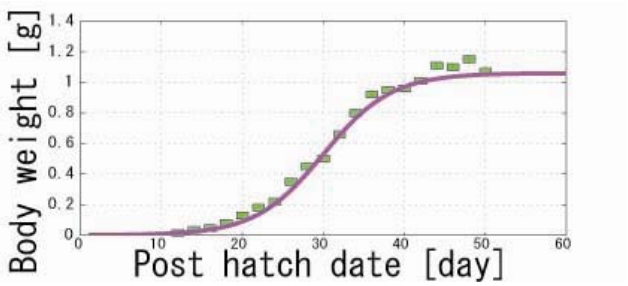

Fig.7 Solid line: body weight growth function without interaction [2]

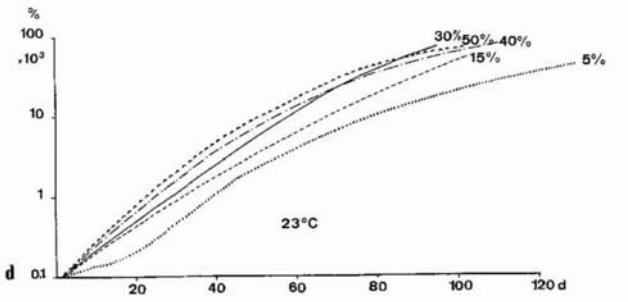

Fig.8 Body weight growth curve with interaction [3]

competition for survival, so time variation of aggression is reflected in growth function of body weight cause of its foraging competition. So we focused the growth function of body weight with larval cricket. At first, we constructed the body weight growth function negated interaction effect which reflects isolated condition. The growth function is well described with logistic function (Fig. 7). The case of crowded growth condition there exists interaction effect: the growth curve shows slower and lighter growth than isolated condition (Fig. 8).

Social competition model is well studied by Eric Bonabeau et al. and we extended this model. In Bonabeau's model, there are variable h which shows individual's degree of fighting and individual who has higher h tends to win. h comes to $h+1$ by winning and $h-F$ by losing, so it means ratio between winning and losing is $1:F$. Decreasing rate of h is calculated by experiments (Fig. 9). Individual who has higher h tends to keep high foraging efficiency (Fig. 10). We analyzed these models qualitatively about $1:F$. Fig.11 shows distribution of imaginary body weight of isolated and crowded conditions. The distribution of crowded condition shows larger variance value and smaller mean value than that of isolated condition. Figs. 12, 13 show simulation results of model equations under condition of $F = 0.5$ and $F = 2$. These results and analytical proof shows that $F > 1$ is necessary for corresponding biological data. It means crickets give greater importance on losing than winning. It is proposed to make F to dynamical function which represents development of aggressive behavior and evaluate modulus quantitatively.

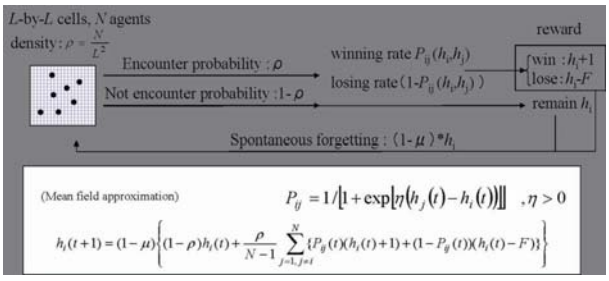

Fig.9 Equation systems

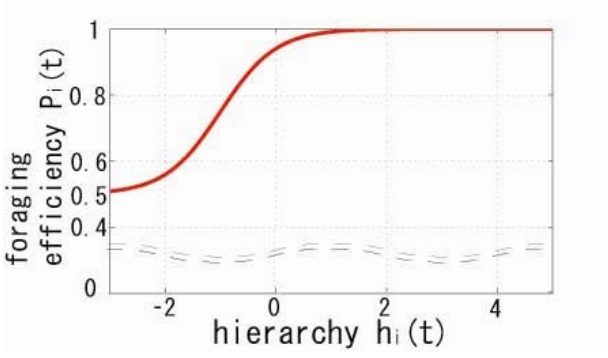

Fig.10 Relation between degree of fighting h and foraging efficiency [Wilson 75]

5. Conclusion

Cricket models are created and are shown to be effective through simulation results.

References

[1] M. Ashikaga, et al., Advanced Robotics, to appear, (2009).
[2] M. Iba et al., Zoological science, 12, 6, 695/702, (1995).
[3] G. Merkel, , Oecologia, 30, 2, 129/140 (1977).
[4] E.O. Wilson, Harvard University Press, (1975).

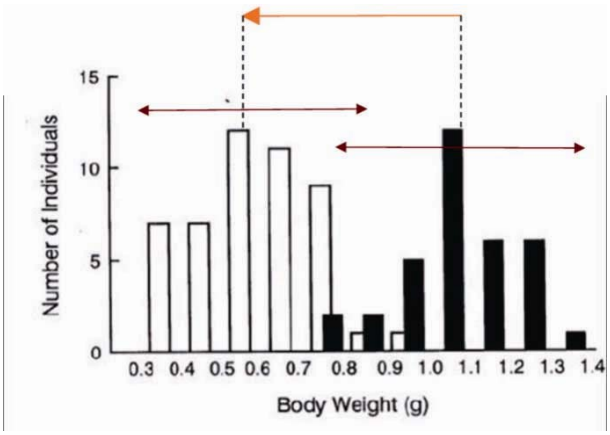

Fig. 11 White bar : final body weight of crowded condition. Black bar : final body weight of isolated condition[Iba 95]

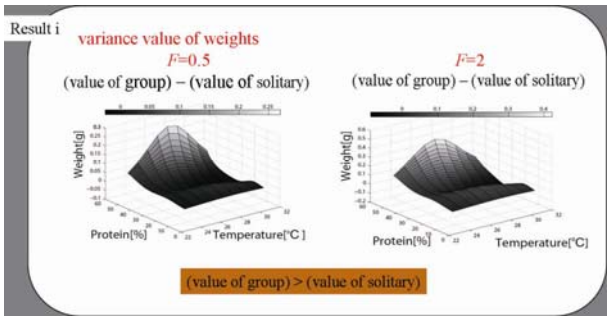

Fig.12 "Variance values of crowded - that of isolated" (F=0.5 or 2), (x-axis: Temperature y-axis : Quality of foods)

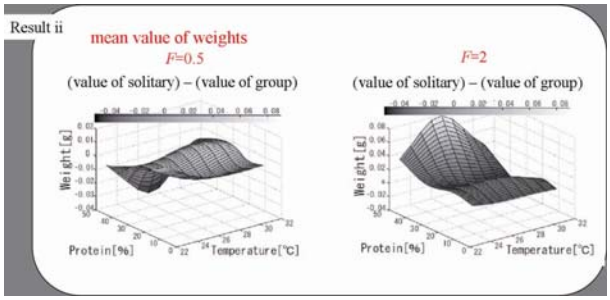

Fig.13 "Mean values of isolated - that of crowded " (F=0.5 or 2)

Adaptive behaviors emerged by functional structures in intearction networks

C01-03 Daisuke Kurabayashi Ryohei Kanzaki

Abstract– Insects have only a little brain but the behavior is highly adaptive. We consider that physical structure of the interaction network works on the creation of the brain function and model the behavioral processor that controlled by its structural disposition. In this research, we investigate mechanisms for intelligent behaviors through novel approach called bio-machine hybrid systems. We focus on (i) insect-driven robot to see adaptabilities, (ii) cyborg contained by insect-brain and mechanical body, and (iii) network property to expose long-lasting excitation.

Key Words: Bio-machine hybrid system, network, *bombyx mori*

1 Introduction

In this study, we investigate adaptive behavior switching mechanism.

A moving individual obtains many types of information through interactions with other individuals and environments. Creatures can adaptively feed back conditions around it to adaptive behaviors. Robots, artificial products can work perfectly only in limited environment. Insects have high adaptability with limited resources. So, we have focused on the aspect of network property in some levels observed in creatures.

In our research project, we try to make the difference clear between artificial intelligence (AI) and a living brain. By using same body and environment, we can observe the difference (Fig. 1). This will make possible to build novel network model to exhibit adaptability like a silkworm moth does.

We consider that physical structure of the interaction network works on the creation of the brain function and model the behavioral processor that controlled by its structural disposition. In this research, we investigate mechanisms for intelligent behaviors through novel approach called bio-machine hybrid systems. We focus on (i) insect-driven robot to see adaptabilities, (ii) cyborg contained by insect-brain and mechanical body, and (iii) network property to expose long-lasting excitations.

In this study, we focus on a small insect, silkworm moth *Bombyx mori*. A female moth distributes special chemicals, called pheromones. A male moth moves toward to the female by sensing the pheromones. For the purpose, it makes a typical sequential motion: straight, zigzag, and turn [1] (Fig. 2). There are many biological researches on neurochemical behaviors[1)-5)].

2 Insect-controlled robot

In this section, we describe an experiment system by which we can observe walking motion of a silkworm moth directly and we can manipulate correspondence between actual motion and walking pattern. The experimental system, named "insect-controlled robot", is composed of walking monitoring system with a living silkworm moth and robot body with two driving wheels. We have already analyzed adaptability of a silkworm moth against manipulation of gains to drive motors, and discovered importance of visual inputs for adaptability. In this year, we have make analysis of adaptability against time lag (delay) to drive motors on the robot body, and then consider about fusion system of odor and visual inputs.

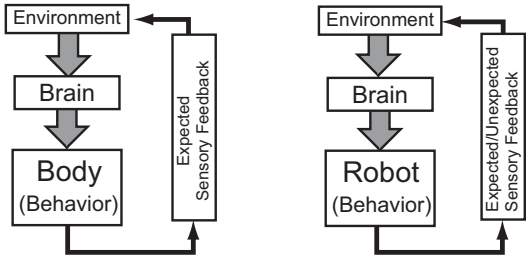

(a) Interaction among brain-body and environment. (b) Replacement of the body by a robot.

Fig. 1: Bio-machine hybrid system

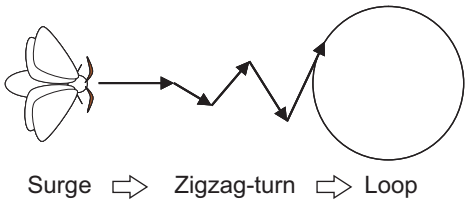

Fig. 2: Motion sequence of a silkworm moth.

2.1 Experiments with time lag of driving motors

Figure 3(a) shows the developed insect-controlled robot[3)]. A silkworm moth, tethered on its back, walks on a ball. A light sensor reads movements of the ball,

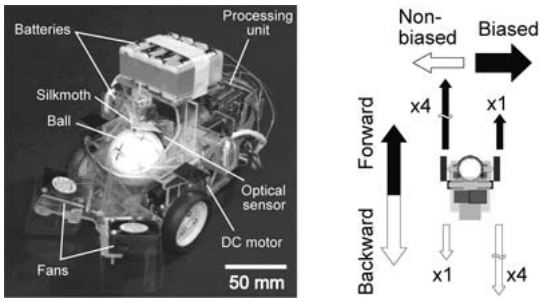

(a) Overview (b) Gain setting

Fig. 3: Experimental setup of insect-controlled robot.

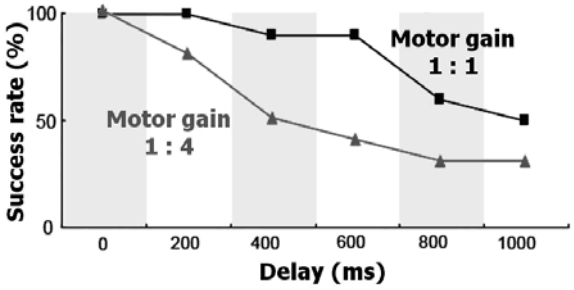

Fig. 4: Relationship between success rate and delay of motor control.

then a microcomputer on the robot body translate movements of the moth into motion commands for electric motors. Therefore, robot body moves just like the moth does.

We investigate feasibility of the strategy of a silkworm moth's behavior by setting time lag to drive the electric motors. We set 0-1000 [ms] delays, and carried out experiments to reach pheromone source. We also make experiments under uneven gains to drive electric motors indicated in Fig. 3(b). We apply 10 moths, and carried out an experiment for each condition. We evaluate success ratio to achieve the pheromone source.

Figure 4 illustrates the success ratio to the time delay. When the robot has equal driving gain (1:1), the success ratio was very high, for example, even if we set 600 [ms] delay, it was 80%, and when we set 1000 [ms] delay, 50% trials achieved the goal. In the contrast, when the robot has uneven driving gain (1:4), the success ratio significantly decreases, for example, only 50% success to 400 [ms] delay.

2.2 Adaptability of a moth

When the driving gain is balanced (1:1), the behavior of a silkworm moth is quite robust against time delay. This result suggests that real-time feedback is not so important to achieve pheromone source. Because pheromone molecule forms plumes, it is quite difficult to follow density of pheromone in the atmosphere by continuous feedback. Thus, the experimental results strongly support a hypothesis that the motion

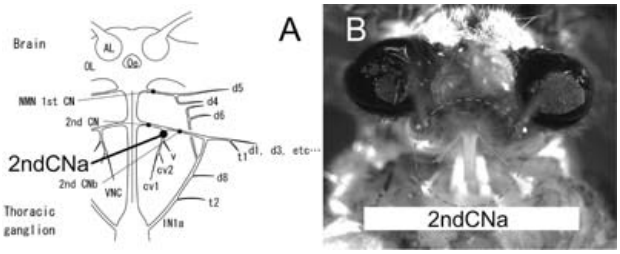

Fig. 5: Silkworm moth's nerves and 2ndCNa.

sequence of a silkworm moth to achieve pheromone source is a fixed instinctive behavior.

In the contrast, when we set unbalanced gain (1:4), the success ratio significantly decreases. We consider that a real-time feedback works hard to arrange behaviors. By our previous researches, we think that a silkworm moth arranges unbalanced motion based on visual information. Thus, the results support a hypothesis that visual inputs modulate behaviors quickly as reflex actions.

By the results including those of former studies, we can say that a silkworm moth combines both fixed instinctive behavior and reflex of visual feedback in order to realize robust and effective achievement of a pheromone source.

2.3 Future work

We have already investigated a "hard-wired" adaptability that we find in pheromone source finding behavior of male silkworm moth. We are going to challenge to reveal adaptability based on plasticity of neural system in a micro brain. We are building experimental setups to understand learning mechanisms by using the insect controlled robot.

3 Cyborg: novel tool for analysis of dynamical brain systems

In this section, we describe a novel tool for analysis of dynamical brain systems. It is so-called "cyborg" that has living brain of an insect, computer to translate neural signals into motion commands, and driving motors on a robotic body. We have realized decoding motion commands in neural fibers and observed sequences of odor-source searching.

3.1 Decoding neural signals

We observe motion commands from a brain through 2ndCNa of neck motor neurons. Left and right 2ndCNas consist of five neural fibers each, and are connected to left and right neck muscles, respectively(Fig. 5:A). We cut fibers sending return signals from body to the brain, because we regard that the external inputs are more important than the feedback signals.

We remove all legs, wings, and an abdomen, then mount the moth on a wax chamber ventral-side up.

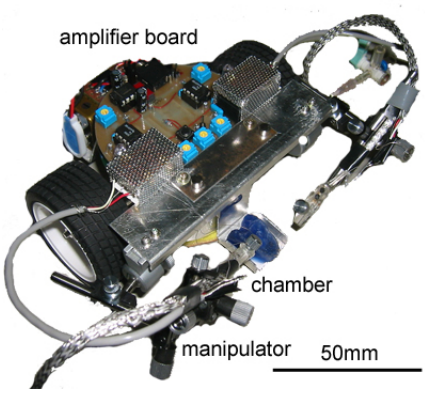

Fig. 6: Overview of the brain-machine hybrid system

Left and right 2nd CNas of exposed NMNs are suctioned into the glass microelectrodes. The silkworm moth is anesthetized by cooling at 4 centigrade 30 minutes. We dipped the fibers into physiological saline, and exposed NMNs are suctioned into the glass microelectrodes.

To translate neural activities into motion commands, we refer to behavioral researches[6] that measures responses to one-shot stimuli of pheromone. We regards motions of a silkworm moth as follows; averaged rotational speed is about $\pi/9$[rad/s], maximum $\pi/3$[rad/s], averaged running speed is about 25[mm/s], maximum 80[mm/s].

Our preliminary experiments shows that the rotational speed of the body axis highly correlates with those of the neck angle, and both of them take few discrete states, almost left, right or zero. Thus, we express motions of the body angle as $\dot{\theta} = a\phi + C$, where θ denotes the body axisϕ shows the angle of the neck, and $a \parallel$ nd C are static coefficients.

Let us formulate a translation from neural signals to motion commands. Let ϕ_{max} be the maximum angle of the neck, n_l and n_r are counted pulse signals during 0.1[s]. Based on the preliminary experiments, we formulate simple dynamics of ϕ as (1), where h is a fixed threshold, and $n_d \triangleq n_l - n_r$.

$$\phi = \begin{cases} \mathrm{sig}(n_d) * \phi_{max} & (\text{if} \quad |n_d| > h) \\ n_d * \phi_{max} & (\text{otherwise}) \end{cases} . \qquad (1)$$

3.2 Experimental system of insect-brain-driven robot

We have built a hardware of a cyborg, insect-brain-driven robot. This is a complete autonomous robot contains a brain, electrodes, amplifiers, microcontroller, motors and Bluetooth communication system (Fig. 6).

We have carried out pheromone-source-tracking experiments in a wind tunnel that is 840[mm] width, 1500[mm] length and 240[mm] hight. We observe 15 trials. Figure 7 illustrate a typical trajectory of the cyborg, where we put fan on the rightside of the figure, and the initial position of the cyborg was leftside.

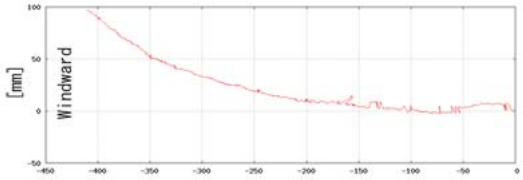

Fig. 7: An example of trajectory of the moth-borg.

Figure 8 illustrates a transition of angular velocity of the body axis. Notice that, in the figure, we have already removed drift-effect from original data. Like a silkworm moth, the cyborg exhibits zigzag motion to reach the pheromone source. We regard that we successfully reconstruct behaviors of a silkworm moth on the robotic body.

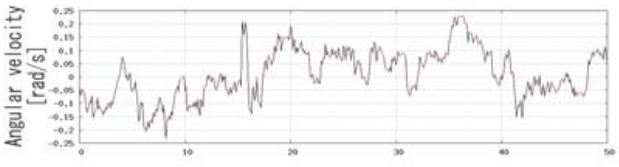

Fig. 8: The angle of body axis.

3.3 Future plans

At this moment, we do not have many numbers of experiments yet. We are going to carry out many experiments and make analysis with mathematical formulations to understand emergence of the intelligence in a micro brain.

4 Functional structure to exhibit long-lasting excitation

Like the zigzag motion trigged by pheromone, a creature can exhibit considerably slower transitions than those of the elements in its brain. To understand a functional structure to generate such effect, we formulate a simple model and construct a network to exhibit long-lasting excitation (LLE) trigged by external inputs.

Neural circuits often are modeled by oscillator networks because neurons fire in a vibrating manner. We employ phase oscillators as the simplest element in a network. Let ϕ_i be a state of oscillator i and $f(\phi_i)$ be its output function. We define $f(\phi_j) = \cos^{20}(\frac{\phi_j}{2})$ to make impulse-like signal.

Let F を (2) be a summarized output of a network, where N is the number of elements.

$$F(\boldsymbol{\phi}) = \frac{1}{N}\sum_{i=1}^{N} f(\phi_i) \ , \ \boldsymbol{\phi} = [\phi_1, \phi_2, \cdots, \phi_N]^T \qquad (2)$$

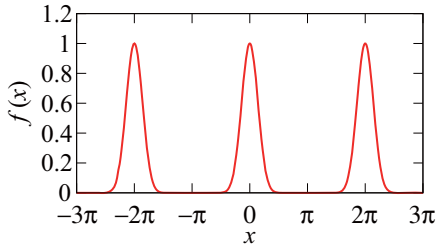

Fig. 9: An example of a 2π-periodic, single-peaked, non-negative function

We design a dynamics of an element as (3), where a_{ij} becomes 1 when i and j are connected.

$$\dot{\phi}_i = \omega + \frac{\kappa}{N_i}\sum_{j=1}^{N} a_{ij} f(\phi_j) g(\phi_i) + \alpha_i + \beta_i \qquad (3)$$

In the model, $g(\phi_i) = \sin(\phi_i)$ represents sensitiveness, and α_i and β_i show ignition and breaking switch, respectively.

Figure 10(a) illustrates a transition of the system. As an initial state, all phases of oscillators are the same. The time development of F_p, the envelop of F, reduces slowly. Here, let us suppose the following approximations.

$$\begin{aligned}\dot{\phi}_i &\approx \omega + \tfrac{\kappa}{2\pi N_i}\textstyle\sum_{j=1}^{N} a_{ij}\sin(\phi_i - \phi_j) \\ &\approx \omega + \tfrac{\kappa}{2\pi N_i}\textstyle\sum_{j=1}^{N} a_{ij}(\phi_i - \phi_j) \qquad (4)\end{aligned}$$

Then, we can express the dynamics of the system by using graph Laplacian L as (5), where $\mathbf{1}_N = [1, 1, \cdots, 1]^T$.

$$\dot{\boldsymbol{\phi}} = \omega \mathbf{1}_N + \frac{\kappa}{2\pi} L\boldsymbol{\phi} \qquad (5)$$

Because we can regard the phase gap as ψ_i in (6),

$$\psi_i = \phi_i - \frac{1}{N}\mathbf{1}_N^T \boldsymbol{\phi} \qquad (6)$$

Then, the dynamics can be formulated as (7), where the behavior is independent from original frequency ω. The response just depends on L.

$$\dot{\boldsymbol{\psi}} = \frac{\kappa}{2\pi}\hat{L}\boldsymbol{\psi}\ ,\ \hat{L} \equiv (I - \frac{1}{N}\mathbf{1}_N\mathbf{1}_N^T)L \qquad (7)$$

Based on the above formulations, we can build control systems to trigged by α_i and stopped by β_i, and make analysis of duration of the response. Figure 10(b) illustrates an example to start and stop active oscillations by the external triggers.

5 Conclusions

We have already built the novel experimental systems called bio-machine hybrid system, and have gotten some results. Our future plan includes analysis of functional structure in a micro brain by using multi-aspect experiments and constructive approach of mathematical formulations.

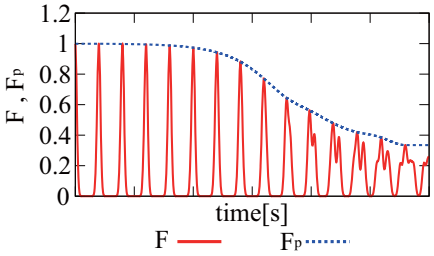

(a) Time development

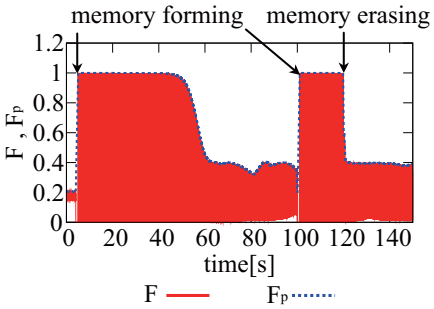

(b) Switching by external inputs

Fig. 10: Transitions of F and F_p

References

1) R. Kanzaki, N. Sugi, and T. Shibuya: "Self-generated zigzag turning of *Bombyx mori* males during pheromone-mediated upwind walking", Zool. Sci., vol.9, pp.515-527, 1992.

2) L. Gatellier and R. Kanzaki: "Short and long term habituation of the male silkmoth to female sex pheromone", In Abstracts of the 14th International Symposium on Olfaction and Taste, Kyoto, Japan, P-247, 2004.

3) S. Emoto, N. Ando, H. Takahashi, R. Kanzaki: "Insect- Controlled Robot -Evaluation of Adaptation Ability" - J. Robotics and Mechatronics, Vol. 19, pp. 436-443, 2007.

4) T. Mishima, R. Kanzaki. "Coordination of flipflopping neural signals and head turning during pheromone-mediated walking in a make silkworm moth *Bombyx mori*", J. Comp. Physiol. A, vol. 183, pp. 273-282, 1998.

5) S. Wada, R. Kanzaki "Neural control mechanisms of the pheromone-triggered programmed behavior in male silkmoths revealed by double-labeling of descending interneurons and the motor neuron", J. Neurol., vol.484, pp.168-182, 2005.

6) Ryohei Kanzaki and Tatsuya Mishima,"Pheromone-Triggered 'Flipflopping' Neural Signals Correlate with Activities of Neck Motor Neurons of a Male Moth,*Bombyx mori*",*ZOOLOGICAL SCIENCE*,**13**,(1996),pp.79-87.

Mobiligence Studies on the Physiological Systems that Control Social Behavior in Animals

Toru Miura[1], Hideaki Takeuchi[2], Yuki Ishikawa[1], Akiko Hattori[1], Haruka Imada[2], Yuji Suehiro[2], Yusuke Ikemoto[3], Ken Sasaki[4], Hitoshi Aonuma[5], Hajime Asama[3]

[1]Graduate School of Environmental Science, Hokkaido University, [2]Graduate School of Science, The University of Tokyo, [3]Research into Artifacts, Center for Engineering, The University of Tokyo, [4] Kanazawa Institute of Technology, Hokkaido University, [5]Research Institute for Electronic Science, Hokkaido University

***Abstract*—In colonies of social insects like termites, there are various castes, among which tasks are allocated. As the results, we can see the elaborate social behavior in those insects. Social interactions also play important roles in the schooling behavior that is seen in fishes like medakas. Through various approaches, we are investigating the molecular and neurophysiological basis of organized behavior in animals, to understand the mechanisms and evolution of sociality, and to find out new concepts in relation to the autonomous decentralized systems.**

INTRODUCTION

There are diverse systems, which are recognized as self-organization systems or complex systems. Also in animals, lots of examples of interactions among individuals constructing social systems have been reported, although the underlying mechanisms that control such social behavior are largely unknown. In our project, two subthemes are now ongoing; one is on the social behavior in termites and the other is on the schooling behavior in fishes. Here, we report our recent progresses on the mobiligence studies on the projects.

SUBPROJECT I: REGULATIONS OF SOCIAL BEHAVIOR AND CASTE DIFFERENTIATION IN THE DAMP-WOOD TERMITE

Social Insects organize colonies, live together with their related individuals, and perform elaborate social behavior [1]. In the colonies, there are reproductive and sterile individuals, and those sterile ones are helpers that are engaged in altruistic tasks such as foraging, defense, etc. Those types of individuals that specialize in certain tasks are called 'castes'. Although there are diverse research subjects in the studies of social insects, one of the fundamental questions is that what mechanisms underlie the caste differentiation, and what types of neural modifications are required in the caste-specific behavior. Here, we summarize the recent progresses in our studies on the mechanisms regulating social behavior in the damp-wood termite *Hodotermopsis sjostedti*.

The termite social behavior is organized elaborately by task allocation and cooperation. In order to accomplish the social behavior, there must be at least two intrinsic mechanisms in termites. The first mechanism is that all individuals possess a set of genes (a genome) that enable them to differentiate into any castes. Similar mechanism is seen in the cell differentiation of multicellular organisms, in which all of the cells include the genomic information that is required for any cells constituting the organismal body. The second mechanism is to regulate the caste ratio in a colony. If all of the individuals differentiate into soldiers, the colony should be destroyed because they lack reproductive options. For this reason, they have flexible options that can change the caste fate during their developmental processes. Namely, each individual can change the physiological status in response to the environmental factors, followed by the change of developmental pathways. Thus, by means of mechanism of "polyphenism" and "feedback", termites can realize the appropriate caste ratio under a certain environment [2].

<Differentiation of biogenic-amine systems in the soldier differentiation>

In the studies of social insects, there are lots of unraveled mechanisms underlying behavioral differentiation among castes. Our previous study showed that the nervous system of soldiers is specialized in the differentiation process [3]. This year, we analyzed how biogenic amine systems are involved in the behavioral specializations in soldiers. Firstly, concentrations of dopamine (DA), serotonin (5HT), octopamine (OA) and tyramine (TA) in brain and suboesophageal ganglion (SOG) were quantified by HPLC. Unexpectedly, no differences of amine titers between soldiers and workers were detected (Fig. 1), although soldiers tended to have relatively higher titer of tyramine that is a precursor of octopamine.

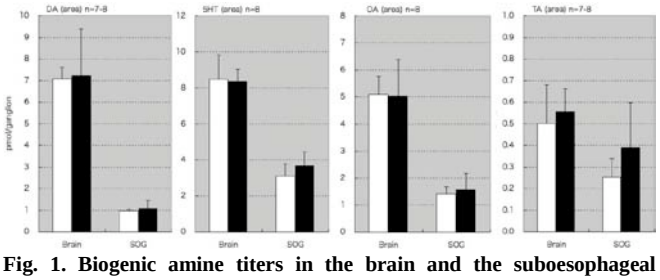

Fig. 1. Biogenic amine titers in the brain and the suboesophageal ganglion (SOG) in soldiers and workers of the damp-wood termite. No significant differences were detected between the two castes.

It is generally known that neuroregulators including biogenic amines

work locally at the site of secretion to regulate the sensitivity of adjacent synapses. Such locally regulated differences between castes could not be detected in the measurements of whole brains. Therefore, in order to detect such local differences, we tried to visualize neurons producing amines by means of antibodies against them. In this observation, we first focsued on octopamine, which is known to involve in aggression. The results of immunostains showed that there were 11 clusters of octopamine-producing neurons. The comparison between soldiers and workers revealed that two largest neurons (DUM1-L and DUM2-L) in the DUM1 and DUM2 clusters were more enlarged in soldiers than in workers (Fig. 2A). Other OA immunoreactive neurons showed no size differences. The intracellular staining of DUM1-L and DUM2-L neurons revealed that the projection sites of DUM1-L and DUM2-L neurons included tritocerebrum and mandibular muscles (Fig. 2B), suggesting that the these neurons secrete octopamine to these target sites to promote the soldier-specific behavioral changes. In the future studies, further analyses on target sites of these neurons in addition to the functional analyses using antagonists and/or agonists will unravel the functions of biogenic amines in the behavioral caste differentiation in termites.

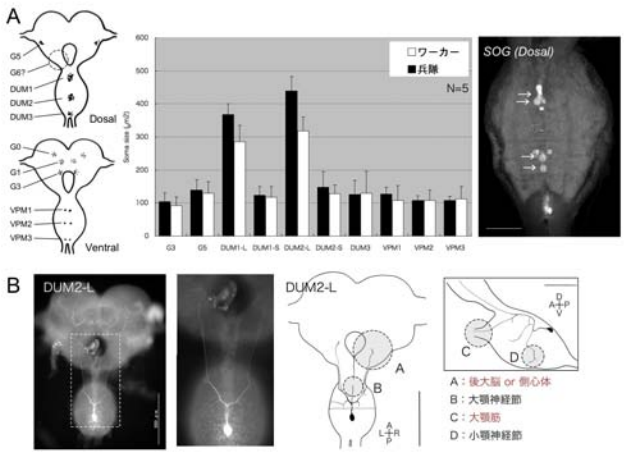

Fig. 2. Among OA-producing neurons, DUM1-L and DUM2-L neurons are enlarged in soldiers. The projection sites include tritocerebrum and mandibular muscles.

<Screening of genes expressed in CNS during the soldier differeneiation>

Genes related to behavioral differentiations in social insects have been focused by many researchers, although there are lots of unrevealed mechanisms. So far, we found that the soldier-specific features seen in the nervous system appeared during the soldier differentiation [3]. These results indicate that not only changes in substances regulating response thresholds but also changes in neural networks play important roles in the behavioral differentiations in termites. Since genes that control these neuronal changes should be the key factors to understand the behavioral differentiation, we tried to identify genes that were specifically expressed in brain and SOG during the soldier differentiation. Screening by differential display identified 11 gene candidates that were up-regulated in the process. Those included a signal molecule called “14-3-3 epsilon” that relates neuronal migrations, “Ciboulot” that regulates the polymerization of actin filaments, and ß-tubulin which is a component of cytoskeleton. All of these factors are known to relate to morphological modifications of neurons, suggesting that these factors may control the neural modifications in the soldier differentiation and contribute to the behavioral differentiation in soldiers. In the further works, we would like to reveal the functional significances of these factors in the soldier differentiation processes.

<Soldier morphogenesis regulated by the insulin signaling>

In the focal termite species, head capsules and mandibles are elongated in the course of soldier differentiation. Histological analyses of *H. sjostedti* during the soldier differentiation show that new epidermis is produced prior to molt into presoldiers [4]. In this study, therefore, the insulin-signaling pathway that regulates organ sizes were focused. As the relative expression patterns of *InR*, *PKB/Akt* and *FOXO* in mandibles were quantified by real-time quantitative RT-PCR, it was suggested that the insulin-signaling pathway is activated just prior to the presoldier molt. Furthermore, the RNA interference of *HsjInR* produced presoldiers with smaller mandibles, suggesting that the activation of insulin signaling in mandibles results in the morphological specialization of soldier caste. The above results revealed the insulin signaling pathway coordinates the soldier differentiation through several developmental/physiological cascades.

Fig. 3. The experiments using RNA interference of InR gene showed the relative inhibition of mandibular exaggeration in the course of soldier differentiation. This indicates that the insulin signaling pathway plays some important roles in the morphogenetic processes in termite soldier differentiation.

＜Mathematical modeling of morphological alteration in caste differentiation＞

Lots of physiological factors control developmental pathways and determine the caste specific morphologies and behavioral patterns in the process of caste differentiation. An approach with multi-level model, integrating endocrine system, individual behavior, and swarm behavior, seems effective methodology to elucidate the mechanisms underlying caste development. So far, it has been known that the juvenile hormone (JH) titer operates the differentiation pathway, so that we modeled the dynamics of JH level determining individual’s internal state, and simulated to understand the mechanism of caste differentiation involving morphological changes. As a simulation results, the patterns of JH titer transitions almost corresponded to the empirical data [5]. Additionally, resultant morphological patterns corresponded to the pattern obtained by the JH-induction experiments [6]. Thus, the adequacy of proposed model was evaluated and the results suggested

the role of JH as a mediator between environmental factors and internal state.

Although more evidences are needed in future studies because of non-negligible assumptions in the model, the results are useful to understand the complicated phenomenon like caste determination. Currently, we are developing more realistic models to approach the general principles for evolution of polyphenism

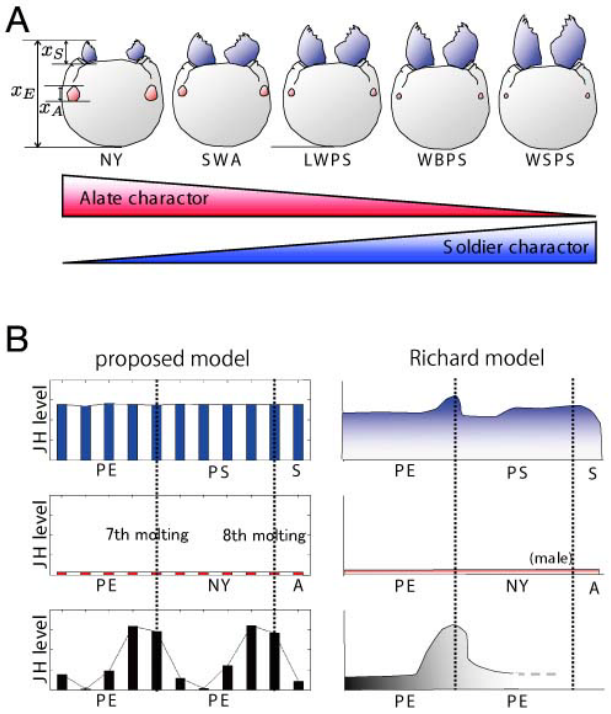

Fig.4. Computer simulations representing caste differentiation patterns under the endocrine systems. The results accurately reproduce the actual patterns observed in nature. (A) JH-dependent morphological changes of mandibular traits seen in various types of soldiers. (B) Caste-specific patterns of internal JH titer simulated in our model (left), compared with empirical data (right).

SUBPROJECT II: ANALYSIS OF MOLECULAR / NEURAL BASIS UNDERLYING SCHOOLING BEHAVIOR OF SMALL FISH (MEDAKA) BY MATHEMATICAL AND MOLECULAR BIOLOGICAL APPROACH

To clarify both molecular/neural basis and brain information processing underlying social interactions in vertebrates, we have focused on Medaka fish and established a novel behavior system to induce Medaka schooling behavior. Using this system, we are planning to identify internal factors (gene, neural network, brain regions) essential for Medaka schooling behavior. On the other hand, to estimate brain information processing underlying schooling behavior, we developed a mathematical modeling, which could explain actual fish movement.

<A novel system for medaka schooling behavior >

In our study, we established a novel system for medaka schooling behavior by inducing optomotor response (OMR). In the OMR, animals follow a moving visual pattern to maintain a constant visual field. Under natural conditions, fish exhibit an OMR to maintain a stable position in a flowing stream. The apparatus consisted of a fixed cylindrical tank (14-cm diameter) and striped cylinder (20-cm diameter) (Fig.1A). The tank in which the fish could swim freely was surrounded by a striped cylinder placed on a rotating disk, which could be controlled by an electric motor. The behavior of fish was monitored from above by a CCD camera and recorded on the harddisk drive of a personal computer (Fig.1A, B). In the present study, we demonstrated that two adult fish tend to swim maintaining a distance (2-3 cm) to each other, under a condition where the two fish exhibited OMR simultaneously (Fig.1C). The behavior was observed selectively in conspecific pairs. Considering that members in fish school can swim coordinately maintaining a distance between them [7,8], analysis of the behavior might help us to understand neural basis of fish schooling behavior.

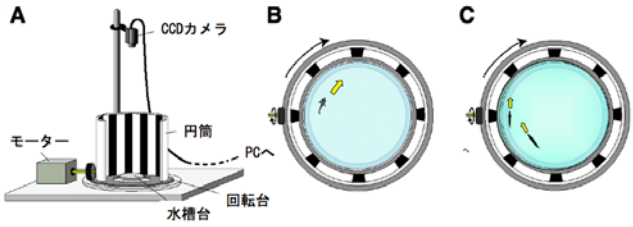

Fig. 1. (A) Apparatus for measuring the OMR. (B) Schematic view of the OMR. The striped cylinder rotates clockwise (shown by arrows) around the fish tank fixed on the pedestal. The fish swims to maintain a constant visual field. (C) The distance between the two fish was stable (2-3cm).

<Neuropeptides in the medaka brain >

To identify candidate genes involved in medaka social interactions, we searched for neuropeptides in the medaka brain and identified genes encoding neuropeptides for the future genetic research. We focused on neuropeptides in the telencephalon as the brain region is proposed to be homologous to a mammalian cerebrum [10]. The telencephalon receives sensory information from different modalities in the fish brain [11]. Analysis of the brain structures in Lake Tanganyikan cichlid fish indicates that the development of the telencephalon tends to correlate with the social parameters of these fish [12]. Here, we used direct matrix-assisted laser desorption/ionization with time-of-fligh mass spectrometry (MALDI-TOF MS) and detect the presence of 16 neuropeptides from telencephalon and other brain regions [9]. We also detect its expression of gamma-prepro-tachykinin gene encoding a neuropeptide, Substance P in both the telencephalon and hypothalamus (Fig.2). Using advanced genetic methods in medaka, it will be possible to analyze the function of genes generating knockout strains or transgenic lines, in which the expression of exogenous genes is modulated in a brain region-specific manner i.e., a telencephalic and/or hypothalamic-specific manner.

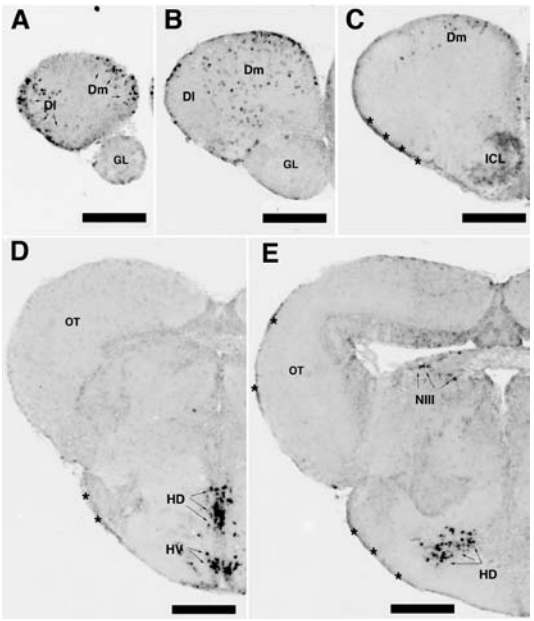

Fig. 2. Gamma-*PPT*-expression in the adult medaka brain analyzed by *in situ* hybridization. (A-E) Transverse sections of the medaka brain from anterior to posterior. Signals were detected in the telencephalon. (Dl and Dm, in panels A-C), ICL (panel C), and the two zones in the hypothalamus (HD and HV in panels D and E), but not in the OT (panels D and E). Dl and Dm, telencephali; ICL, internal cellular layer of the olfactory bulb; HT and HV, hypothalamus NIII, nucleus of nervus oculomotorius; OT, tectum optium [9].

<Mathematical modeling of a single fish OMR>

At the initial step of the mathematical modeling of brain information processing underlying schooling behavior, we used a single fish exhibiting the OMR and analyzed relation between visual input (what a fish can see) and output (how the fish behaves) and develop a mathematical modeling, which could explain some features of OMR [13].

To estimate how each internal factor (gene or brain-region) is involved in our model, we will generate a transgenic fish and analyze the behavioral disorder mathematically. If the similar disorder can be expressed in a simulation by modulating the algorithm, we can assume that the modulated part in the algorithm may be involved in the defected internal factor (gene or brain-region).

PERSPECTIVES

In this article, we introduced our studies on the mechanical basis underlying elaborate social life in termites and fishes. This year, the lots of experimental results were obtained on the physiological, neuronal and morphogenetic regulations in termites, in addition to the establishment of experimental systems on the schooling behavior in the medaka fishes.

Based on these studies on social regulation in these animals, we will understand the elaborate systems of social organization in animals, and will obtain some clues to find out new concepts of autonomous decentralized systems that can be applied to the area of robotics.

REFERENCES

[1]Wilson EO (1971) Insect Societies. Harvard.

[2] Miura T (2005) Developmental regulation of caste-specific characters in social-insect polyphenism. *Evol Dev* 7: 122-129.

[3] Ishikawa Y, Koshikawa S, Miura T (2007) Differences in mechanosensory hairs among castes of the damp-wood termite Hodotermopsis sjostedti (Isoptera: Termopsidae). Sociobiol 50: 895-907.

[4] Koshikawa S, Matsumoto T, Miura T (2003) Mandibular morphogenesis during soldier differentiation in the damp-wood termite Hodotermopsis sjostedti (Isoptera: Termopsidae). Naturewissenschaften 90: 180-184.

[5] Cornette R, Gotoh H, Koshikawa S, Miura T (2008) Juvenile hormone titers and caste differentiation in the damp-wood termite Hodotermopsis sjostedti (Isoptera, Termopsidae). J Insect Physiol 54: 992-930.

[6] Miura T, Koshikawa S, Matsumoto T (2003) Winged presoldiers induced by a juvenile hormone analogue kin Zootermopsis nevadensis: implications for plasticity and evolution of caste differentiation in termites. J Morphol 258: 22-32.

[7] Partridge BL, Pitcher TJ.(1979) Evidence against a hydrodynamic function for fish schools. *Nature* 279: 418-419.

[8] Partridge BL, Pitcher TJ, Cullen JM, Wilson J (1980) The three-dimensional structure of fish schools. *Behav. Ecol. Sociobiol.* 6: 277-288.

[9] Suehiro Y, Yasuda A, Okuyama, Imada H, Kuroyanagi, Y, Kubo T, Takeuchi H†(2009) Mass spectrometric map of neuropeptide expression and analysis of the gamma-prepro-tachykinin gene expression in the medaka (Oryzias latipes) brain. *Gen. Comp. Endocrinol*.in press.

[10] Yamamoto N, Ishikawa Y, Yoshimoto M, Xue H-G, Bahaxar N, Sawai N, Yang CY, Ozawa H, Ito H (2007) A new interpretation on the homology of the teleostean telencephalon based on hodology and a new eversion model. *Brain Behav. Evol.* 69: 96-104.

[11] Finger TE. (1980) Nonolfactory sensory pathway to the telencephalon in a teleost fish. *Science* 210:671-673.

[12] Pollen AA, Dobberfuhl AP, Scace J, Igulu MM, Renn SC, Shumway CA, Hofmann HA. (2007) Environmental complexity and social organization sculpt the brain in Lake Tanganyikan cichlid fish. *Brain Behav. Evol.* 70:21-39.

[13] Suehiro Y, Imada H, Okuyama T, Kubo T, and Takeuchi H. (2007) Analysis of adaptive behaviors of small fishes by using combination of mathematical modeling and molecular biological approach. Proceeding of the Second International Symposium on Mobiligence. p219-222.

The evolution of decentralized control systems in social insects

Kazuki TSUJI（University of the Ryukyus), Ryohei YAMAOKA(Kyoto Institute of Technology).
Ken SUGAWARA(Tohoku Gakuin University)

Summary: We investigated the evolutionary mechanisms of decentralized control and self-regulated dynamics of adaptive behavior in social insect colonies. We focused mainly on colony-size dependent regulation of division of labor in ants, wasps and bees. The underlying intracolonial evolutionary conflict was investigated both theoretically.

Major evolutionary transitions are the formation of the biological hierarchy (Maynard Smith and Szathmáry 1995). The question is how resolution of conflicts among the lower-level units was achieved to form the higher unit. Modern evolutionary theories predict various conflicts in hymenopteran societies. Pamilo (1991) classified them into three major categories: (1) sex allocation conflict, i.e. the conflict over the decision how resources are allocated to male and female reproductive offspring (2) male parentage conflict, i.e. the conflict over who will directly produce males and (3) reproductive allocation conflict, i.e. the conflict over reproduction (production of reproductive offspring) versus colony maintenance (production of workers). However, so far, no theory has tackled the evolution of worker policing, when a colony faces these three conflicts simultaneously. Here we develop a dynamic game model involving workers and the queen and study interactions of these conflicts simultaneously operating (for details see Ohtsuki and Tsuji 2009).

The Model

Let us assume a monogynous (single-queened) colony with an annual life cycle. Workers are assumed to lack mating ability but can directly produce males. The colony starts at time t = 0, with a queen and a minimal number of workers, W_0, that are daughters of the queen. Note that we do not necessarily assume dependent colony founding or swarming. We ignore the developmental time of the individual brood from the egg to the adult stages; therefore, eggs laid by the independently founding queen at time t = 0 immediately become the initial cohort of workers or her reproductive offspring. The life span of the colony is given by T (fixed). We assume that each individual knows perfectly the time t and T. Throughout the colony's life span, the queen neither dies nor is replaced by others. Mortality of workers is set to zero, so the colony size never diminishes. The mating frequency of the queen is denoted by k. The demographic variable, W = W(t), represents the number of workers in the colony at t.

Each worker i has a life-history strategy that is described as a set of si(t) and pi(t) across time.
First, si(t) represents her social strategy [$0 \le s_i(t) \le 1$]. It prescribes the allocation of her effort into two different purposes: colonial work and personal reproduction. As the cost of worker reproduction is known, we assume that these two are in a tradeoff. At a given time, t, worker i allocates a proportion of si(t) of her total effort to work such as nursing, and the rest [1 − si(t)] she allocates to her own male-offspring production.

Second, pi(t) represents her policing strategy [$0 \le p_i(t) \le 1$], which represents the intensity of policing direct reproduction of other nestmate workers. In our current model the value of p is itself adjustable from no policing (average p = 0) to perfect policing (average p = 1) with no constraint that is a novel assumption. We assume that policing behavior incurs no direct cost to the policers.

The queen can lay sufficient numbers of eggs, both diploid and haploid, that will be reared to adulthood by workers and will become three different castes: workers, gynes, and males. We assume that each of these three castes is equally costly to produce, but the production cost of each egg is negligibly low. The resource allocation ratio to each caste is described by two parameters. First, f describes the proportion of resources invested in the production of females, and the rest (1 − f) is invested in males. Second, w describes the proportion of female-production resources invested in the production of workers, and the rest (1 − w) goes to the production of gynes. In summary, workers, gynes, and males receive the respective proportions of fw, f(1 − w), and (1 − f) of resources. Variables f and w change over time. The question is who controls those parameters. Regarding f(t), we assume that the queen controls the primary sex ratio of her eggs, either by laying only diploid eggs, only haploid eggs, or both types. Let r(t) denote the queen's resource allocation strategy, which takes the value "diploid," "haploid," or "both." If the queen chooses r(t) = diploid, she lays only diploid eggs at time t; as a result we automatically have f(t) = 1. If she chooses r(t) = haploid, she lays only haploid eggs, resulting in f(t) = 0. If she chooses r(t) = both, she supplies a sufficient number of eggs of both sexes. In this last case, workers control secondary sex ratio of queen-produced eggs. Let fi(t) [$0 \le f_i(t) \le 1$] be a resource allocation strategy of worker i. We assume that the colony average of fi(t) realizes the actual ratio of investment in each sex, f(t), when r(t) = both.

We assume that w(t) is fully controlled by workers. Let wi(t) [$0 \le w_i(t) \le 1$] be another resource allocation strategy of worker i. Then the proportion of female eggs that grow into new workers, w(t), is given by the colony average of wi(t). To summarize the strategy, the queen has life-history strategy r(t), and worker i has a life-history strategy, $v_i(t) = [s_i(t), p_i(t), f_i(t), w_i(t)]$.

The workers' effort affects how many eggs grow into adulthood. We assume that the number of eggs that become adults is proportional to the total colonial work force at that time. We call this the breeding capacity, which is given by $\sigma = \beta \sum_i s_i$, where β is a constant (note that hereafter we sometimes omit t for simplicity).

If all workers work at 100% for the colony (si = 1), the queen can produce σ offspring. However, if some workers are engaged in self-reproduction, σ is partitioned among all egg-layers. We assume a simple egg raffling; the more fertile an egg-layer is, the more she shares the breeding capacity. The share is assumed to be proportional to one's fertility.

The queen's relative fertility is given by q, which is relative to that of a worker ovipositing at her maximum speed. Worker i's realized fertility is given by (1 − si)(1 − p-i), where p-i is the average policing level in the colony over all workers except worker i. The term (1 − p-i) represents the decline of worker i's relative fertility in response to worker policing. We do not assume queen policing.

Taking f and w into account, we have the following population dynamics:

$$\frac{d}{dt} W(t) = \left(\frac{q}{C}\sigma\right) \cdot fw, \quad (1a)$$

$$\frac{d}{dt} G(t) = \left(\frac{q}{C}\sigma\right) \cdot f(1-w), \quad (1b)$$

$$\frac{d}{dt} M(t) = \left(\frac{q}{C}\sigma\right) \cdot (1-f), \quad (1c)$$

$$\frac{d}{dt} m_i(t) = \frac{(1-s_i)(1-p_{-i})}{C}\sigma, \quad \text{(1d)}$$

where W(t) is the number of workers. G(t), M(t), and mi(t) are the total number of gynes, queen-derived males, and worker i–derived males produced until time t. C is a normalization constant.

The queen and the workers try to maximize their own inclusive fitness independently. They gain reproductive success directly and/or indirectly through gynes, queen-derived males, and worker-derived males. The relative values of these castes are variable, because colony members can be differently related to each caste (Ohtsuki and Tsuji 2009 for details). This situation represents a dynamic game. The objective functions to maximize for the queen and worker i are their inclusive fitnesses, which are respectively given by

$$\phi^Q = V_G^Q G(T) + V_M^Q M(T) + \sum V_{m_j}^Q m_j(T) \quad \text{(2a)}$$

$$\phi^{W_i} = V_G^{W_i} G(T) + V_M^{W_i} M(T) + \sum_j V_{m_j}^{W_i} m_j(T), \quad (i=1,2,\ldots) \quad \text{(2b)}$$

where is a kin value (Ohtsuki and Tsuji 2009), which describes the inclusive fitness return to per capita production of the caste A (= G, gynes; M, males produced by the queen; mj, males produced by worker j) for the individual B (= Q, queen; Wi, worker i), which is measured at the last moment of colony life. Inclusive fitnesses in eqs.(2) are not the relative effect of individuals on the gene pool (which can be either positive or negative), but the absolute effect on the total number of copies of genes that one can pass to future generations. For simplicity, we assume that all sexually reproductive offspring produced in a colony are simultaneously released at the end of the colony life.

We solve the dynamic game defined above to obtain the homogeneous Nash equilibrium. We use k = 1 (the queen is monandrous) and q = 1 (the queen is as fertile as a worker). For demographic parameters such as sex ratio in the population, X:Y, we assume that they are at the equilibrium.

Results

Figures 1show the solution of our dynamic game. We observe a phase transition at t = 33.4. Figure 1 illustrates the strategies of workers and the queen at the Nash equilibrium. Until t = 33.4 all workers invest all their efforts into working (s = 1 in Fig. 1ad), the queen lays only diploid eggs (r = diploid and f = 1 in Fig. 1c), and those diploid eggs are raised by workers to be new workers (w = 1, in Fig. 1cd). Because the level of worker policing is the highest (p = 1, in Fig. 1b), if reproduction by workers were to occur, then the laying workers and/or the worker-derived eggs would suffer from the severest punishment by other nestmate workers, although the model does not predict any actual attempts of oviposition by workers (i.e., s = 1 in Fig. 1a). In contrast, after the phase transition the model predicts that 85.7% of workers' efforts are invested in colonial work, with the remaining 14.3% invested in workers' self-reproduction (s = 0.857 in Fig. 1a). The queen continues to lay only diploid eggs at this phase (r = diploid and f = 1 in Fig. 1c), but workers rear these diploid eggs into gynes (w = 0 in Fig. 1c). As a result, we predict that the colony produces workers' sons and gynes (derived from the queen) at this phase. Worker policing at this stage is incomplete (p = 0.933 in Fig. 1b). Although this reduction in the average policing level is small (p = 1.000 to 0.933), this imperfect policing leads to the survival of many worker-derived males to adulthood in the colony as a whole, because many workers start to lay eggs. As explained later, however, the policing behavior at this stage is not true worker policing but simple reproductive competition among workers.

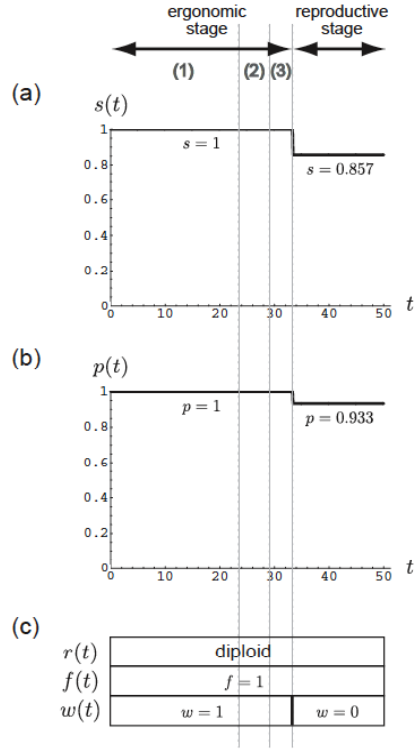

Figure 1. Solution of the dynamic game. Each figure shows the value of strategies and demographic parameters at a Nash equilibrium. The horizontal axis in each table represents time, t. The colony season is defined as . We observe dramatic change at t=33.4. For the sake of our explanation, we call the phase before t=33.4 the "ergonomic stage" and the one after t=33.4 the "reproductive stage". Additionally we divide the ergonomic stage into three substages as follows: (stage one) t<23.4, (stage two) 23.4<t<29.2, and (stage three) 29.2<t<33.4.
(a) The population average of social strategy of workers, s(t), at the Nash equilibrium. In the ergonomic stage all workers invest all their effort into colonial work (s=1). In the reproductive stage, 85.7% of workers' effort is invested into colonial work while 14.3% is into personal reproduction.
(b) The population average of policing strategy of workers, p(t). In the ergonomic stage the policing level is the highest (p=1). In the reproductive stage worker policing is incomplete (p=0.933). About 6.7% of worker-derived eggs escape policing.
(c) Resource allocation to each caste. At the Nash equilibrium the queen always lays diploid eggs both in the ergonomic and the reproductive stages (r="diploid"). As a result the queen produces female only (f=1). In the ergonomic stage workers rear female eggs into new workers (w=1). In the reproductive stage workers rear them into gynes (w=0).

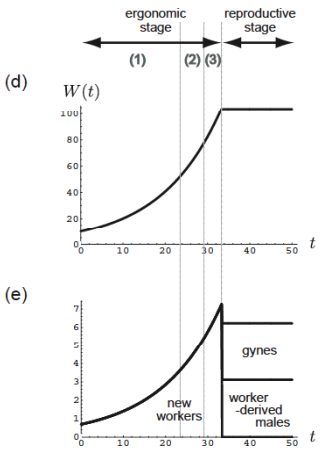

Figure 1 (continued). Demographic parameters at a Nash equilibrium. The horizontal axis in each table represents time t. (d) The number of workers in the colony, W(t), over time. W(t) increases exponentially in the ergonomic stage, whereas it remains constant in the reproductive stage. (e) The content of castes produced from the colony. The vertical axis represents the rate of production per unit time. New workers are produced in the ergonomic stage. In the reproductive stage gynes and worker-derived males are produced. The model predicts that the equilibrium sex ratio is approximately 1:1 (0.501:0.499 female to male).

Discussion

This paper presents the first use of dynamic game modeling to examine the interaction among the three evolutionary conflicts in social Hymenoptera. While based on certain assumptions, our model provides several novel predictions. The most important one is that worker policing can exist even in the monandrous and monogynous social Hymenoptera. Given that polyandry is a phylogenetically derived condition in social Hymenoptera from the ancestral state of monogyny and monandry and that the prevalence of worker policing behavior also in monandrous and monogynous species, an important conclusion might be possible from our model's analysis. Unlike commonly believed (e.g. Ratnieks et al. 2006) worker policing has originally evolved not because of relatedness asymmetries, but instead due to ergonomic benefits at the level of the colony. Later this behavior might have converted to the use to settle conflicts among workers caused by queen multiple mating and relatedness asymmetry.

.

References

Maynard Smith, J. and E. Szathmáry. 1995. The major transitions in evolution. W. H. Freeman, Oxford.

Pamilo, P. 1991a. Evolution of colony characteristics in social insects. 1. Sex allocation. The American Naturalist 137:83-107.

Ratnieks, F. L. W., K. R. Foster, and T. Wenseleers. 2006. Conflict resolution in insect societies. Annual Review of Entomology 51:581-608.

Ohtsuki, H., Tsuji, K. 2009. Adaptive reproduction schedule as a cause of worker policing in social Hymenoptera: a dynamic game analysis. The American Naturalist (in press).

Hippocampal Neural Mechanisms for Discrimination of Bird Songs in Zebra Finch

Kotaro Oka, Akira Fujimura, Fumihiro Takayama, Mai Iwasaki, Masafumi Hagiwara and Ei-ichi Izawa

***Abstract*— For understanding the neural mechanisms in the female zebra finch, we applied a combinational approach between bio-imaging and modeling. We have investigated the neural activity in the hippocampal formation (HF) with immediate early gene expression and pH imaging, and found that HF is a candidate as a key region for song discrimination in the female brain. To clarify this finding for quantitative modeling, we have to know the cytoarchitecture in the HF. We, therefore, start the exhaustive investigation of cytoarchitecture in male and female zebra finch brains with several fluorescent imaging techniques. We also found the propagation of the neural activity in the surface of the HF with pH imaging. These new findings will be valuable information for constructing neural models in the HF of female zebra finch.**

I. Introduction

Communication with songs is important for Zebra finches. For understanding the song communication, information processing in the female brains is crucial. However, the neural network for the information processing in female brains has been poorly understood. From our previous study using retrograde labeling by fluorescent dye, we found the neural connection between Hippocampal Formation (HF) and auditory cortices; caudomedial nidopallium (NCM), caudomedial mesopallium (CMM), robust nucleus of the arcopallimu (RA) cup (unpublished data). We also found the neuronal activity propagation form the posterior to the anterior in HF, and this observation is consisted with recent anatomical findings.

Recently, we used catFISH (cellular compartment analysis of temporal activity by fluorescence in situ hybridization) technique for *Arc* (activity-regulated cytoskeletal-associated protein) mRNA to visualize the active neurons [1], and found that CMM and HF were candidates for song discrimination. This finding is useful for understanding the neural coding in female brains.

However, there are few numbers of studies for female brains. To understand the neural basis of the song discrimination in female zebra finches, one of the solid strategies is to investigate the neural architecture in HF and neural connection around HF regions. We adopted the usual neuro-anatomical approach for multi-color staining: DAPI for nucleus, Nissl for neurons, and FluoroMyelin for neural axons covered with myelin. Using this method, we succeeded to visualize the neural architecture in the whole male and female brains. To investigate the cytoarchitecture in HF in detail, we adopted the shot-gun like technique. The gene gun is usually used for the gene transfer to cells, but we used this technique to deliver the different types of lipophilic fluorescent dyes to the neurons by chance [3]. We succeeded to visualize each neuron with this method, and this technique enables us to exhaustive investigation of cytoarchitecture in HF. Finally, we continued to neuronal activity imaging with a pH sensitive dye, Neutral Red, with the minor modification of the experimental setup.

Kotaro Oka is with Department of Biosciences and Informatics, Keio University, 3-14-1 Hiyoshi, Kohoku-ku, Yokohama, Kanagawa 223-8522, Japan (phone: 045-566-1728; fax: 045-564-5095; e-mail: oka@bio.keio.ac.jp).

Akira Fujimura is with Department of Biosciences and Informatics, Keio University, 3-14-1 Hiyoshi, Kohoku-ku, Yokohama, Kanagawa 223-8522, Japan.

Fumihiro Takayama is with Department of Biosciences and Informatics, Keio University, 3-14-1 Hiyoshi, Kohoku-ku, Yokohama, Kanagawa 223-8522, Japan.

Mai Iwasaki is with Department of Biosciences and Informatics, Keio University, 3-14-1 Hiyoshi, Kohoku-ku, Yokohama, Kanagawa 223-8522, Japan.

Masafumi Hagaiwara is with Department of Information Engineering, Keio University, 3-14-1 Hiyoshi, Kohoku-ku, Yokohama, Kanagawa 223-8522, Japan

Ei-ichi Izawa is with The Graduate School of Human Relations, Keio University, 2-15-45 Mita, Minato-ku, Tokyo 108-8345, Japan

II. Experimental Method

A. Animal Preparation

We described this in our last annual report in detail. Experiments were performed on adult female or male zebra finches (> 90 days old). All subjects were treated under Keio University's Animal Use Guidelines.

The bird was anesthetized and supplemental doses were administered as necessary. The bird was placed on a platform attached to a stereotaxic head holder (David Kopf Instruments, USA), and the cranium and the dura were removed. We made the small window for observation of HF for pH imaging.

B. Whole Brain Staining

We used the BrainStain Imaging Kit (Molecular Probes, Cat#34650) recently developed by Molecular Probes which uses FluoroMyelin Green (excitation/emission maxima ~479/598 nm) to selectively label myelin, DAPI (excitation/emission maxima ~358/461 nm) to stain nuclei and Neurotrace 530/615 (excitation/emission maxima ~530/615 nm) to stain neuron cell bodies (Nissl substance).
The procedure of this experiment is as follows. We used 10 zebra finches (coronal section: 2 males, 4 females, saggital section: 2 males, 2 females) in this experiment. Birds were anaesthetised with a dose of ketamin/xylazine (40 mg/kg, 8

mg/kg) via intramuscular injection and intracardially perfused with a fixative containing 4% paraformaldehyde in 0.1M phosphate buffer, pH 7.4. The brains were dissected out and immersed in the fixative, cryoprotected by equilibration in a 30% sucrose solution, frozen on dry-ice, included in embedding medium (Tissue-Tek; Sakura Finetek), cut on a cryostat (Leica CM 1850, Japan) (12 μm thick sections), mounted on MAS-coated glass slides (Matsunami), and dried at 37 C.

The staining protocol was followed by instructions from the manufacture with some modifications. Slides were immersed in 0.01M PBS and hydrated for 30 min at room temperature. We prepared the three-color staining solution by diluting each stock solution (DAPI: 300-fold, FluoroMyelin Green and Neurotrace 530/615: 150-fold) into PBS in a single vial and flood the sections with staining solution and stain them for 20 minutes at room temperature. When staining was complete, the solution was removed, and the sections were rinsed with PBS, washed 3 times for 10 minutes each with PBS, and mounted with ProLong Gold Antifade Reagent (Molecular Probes). The images were obtained by a fluorescence microscope BZ-9000 with GFP-BP, Texas Red, DAPI filters (Keyence).

C. Lipophilic-dye application by the gene gun

We prepared the "bullets" referred to Gan's paper [3], which were gold particles coated with lipophilic dyes, DiI, DiO, or DiD (Molecular Probes, catalog numbers D-282, D-275, and D-307). Stock solutions were prepared for each dye by dissolving 15 mg of DiI, DiO, or DiD in 200 ml methylene chloride. Using these stock solutions, we made seven different combinations which were various volumetric proportions of different dyes. The proportions are as follows: (1) DiI, (2) DiO, (3) DiD, (4) 1 DiI:1 DiO, (5) 1 DiO:1 DiD, (6) 1 DiI:1DiD, and (7) 1 DiI:1 DiO:1 DiD (Fig. 2). The final concentration of each combination was 3 mg of dye in 100 ml methylene chloride. A small amount (15 mg) of gold particles (1.0 μm diameter, Bio-Rad) was added to each dye solution and mixed well. As methylene chloride evaporated quickly, each dye combination precipitated onto the gold particles. The dye coated particles were resuspended in 1 ml of distilled water and well-mixed to prevent the formation of large clusters of particles. The "bullets" were prepared with individual colors or a mixture of different color particles and stored at room temperature for future use.

Dye-coated particles were delivered to the preparation (slice preparation, see below) using a commercially available biolistic device (PDS-1000/He System, Bio-Rad). A membrane filter with a 3 μm pore size and $8.0x10^5$ pores/cm^2 density (Becton Dickinson Labware, Cat# [35]3096) and a 10 μm pore size (millipore, Cat# NY1004700) were placed on the stopping screen to prevent clusters of large particles from landing on the tissue. Density of labeling was controlled by using various gas pressures (450–2200 psi helium gas) or by changing the setting positions of the micro-carrier launch assembly and the target shelf. Lower gas pressures and larger distance between the rapture disk and the micro-carrier launch assembly, or between the micro-carrier launch assembly and target shelf lead to lower labeling densities.

For slice preparation, birds were deeply anesthetized by ketamin/xylazine via intramuscular injection and decapitated. The brain was removed and then mounted in a 2.5% low-melting point agarose gel (nacalai) prepared with Tyrode's solution (in mM: 134 NaCl, 3 KCl, 10 HEPES, 4 NaOH, 2 $CaCl_2$, 1 $MgCl_2$). Slices were made in ice-cold artificial cerebrospinal fluid (ACSF) containing (in mM: 85 NaCl, 75 Sucrose, 2.5 KCl, 1.25 $NaH_2PO4 \cdot 2H_2O$, 4 $MgSO_4$, 0.5 $CaCl_2$, 25 $NaHCO_3$, and 25 Glucose). Coronal slices (400 μm) were cut with a microslicer (D.S.K., DTK-1000). The preparation images were obtained by confocal laser scanning microscope FV1000 (Olympus).

D. Optical imaging with pH sensitive dye, neutral red

After anesthesia, the cranium and the dura were removed and a handmade plastic chamber was bonded on the skull with dental cement (GC Unifast II, GC, Japan). The brains were stained for 30-40 min by neutral red (10 mM, Sigma) in artificial cerebrospinal fluid (ACSF, in mM: NaCl 119.0, KCl 2.5, $MgCl_2$ 1.3, $CaCl_2$ 2.5, NaH_2PO_4 1.0, $NaHCO_3$ 26.2, glucose 11.0). Following wash the brain with ACSF, the surface was covered with ACSF. The camber was then held on with a handmade head positioner under an epifluorescent microscope (MZ-6, Leica, Japan) on a vibration isolator (AET0806-NC, Meiritsu, Japan).

The MiCAM01 optical imaging system (Brainvision, Japan) consists of an area sensor with 96 × 64 photodiodes and a data processing unit. The epifluorescent optics, consisting of two lenses, ×1.0 objective lens, ×0.63 light focusing lens (PLANAPO, Leica) and a dichroic mirror (575 nm) with absorption (590 nm) and excitation (530 nm) filters, were mounted above the brain. Each photodiode received signal from a 20 × 20 μm^2 sample area, thus creating a 2.0 × 1.3mm^2 entire imaging field. The experimental setup was shown in Fig.3. The data was collected 2730 sequential images (0.75 ms/frame). The ratio of the fractional change in fluorescence of voltage sensitive dye to the fluorescence of the background ($\Delta F/F_0$) was calculated and used as the optical signal.

III. RESULTS

A. Neuronal architecture in female zebra finch brain

We show that low magnitude images of the sagittal section of female zebra finch brain. Three staining was simultaneously presented: nuclei (dark blue; DAPI), myelinated-neuronal fibers (green; FluoroMyelin), and cell bodies of neurons (magenta; Nissl staining). In the deep regions in the brain, we can observe broad areas of myelinated-neuronal fibers, and clear regional differences are observed in the cerebellum cortex. A little higher magnification image reveals cytoarchitecture in HF (Fig. 1B).

In HF, there is a V-shaped region with low density of DAPI staining. This kind of staining region was reported in the pigeon HF, and that region corresponds to the dentate gyrus in mammalian HF [2]. Furthermore, we investigated the cytoarchitecture of HF in detail (Fig. 1C). At the surface of the HF, there are myelinated-fibers. The direction of this fiber is from anterior to posterior. This structure is almost the same to the parallel fibers on the cerebral surface. In the following section, we report the spontaneous propagation of active areas in HF, and this propagation may concern to the direction of these myelinated-fibers.

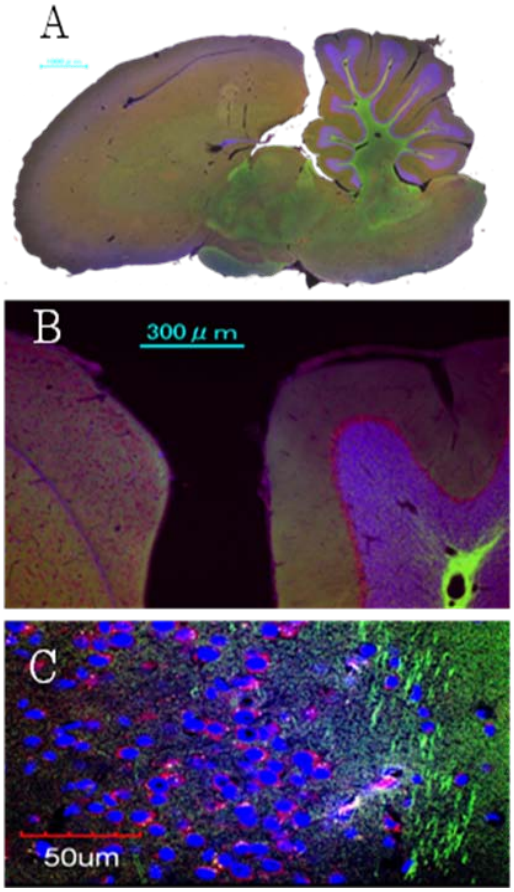

Fig. 1 Fluorescent images of the brain in female zebra finch with low (A), middle (B) and high (C) power magnification.

To elucidate the neuronal connection in HF, Golgi staining is one choice. Golgi staining visualizes the morphology of single neurons in detail, however, the staining is by chance and it is hard to determine the neuronal connectivity by this method because of its "black and white" staining image. We, therefore, applied a new staining technique with the gene gun and several types of lipophilic fluorescent dyes (see Materials and Methods). This method enables us to stain the number of neurons in different fluorescent colors by chance, and also check the neuronal connectivity between stained neurons (Fig. 2B). We can observe beautiful fluorescent color neurons in 30 min after dyes are applied to the slice preparation of brains. Fig. 2B is a stacked image from z-sections by the confocal laser scanning microscope, and the thickness of the stacked section is about 90 μm. There are several numbers of different shapes of neurons; some of them have long dendrites with a lot of spines, and some of them have short dendrites.

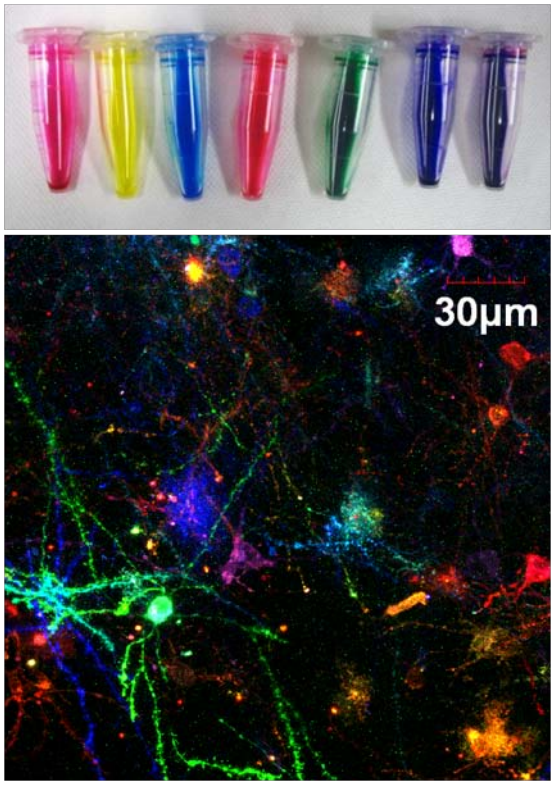

Fig. 2 Lipophilic fluorescent dyes (upper panel) and confocal image of HF (lower panel).

B. Activity dependent pH imaging in HF

One of the interesting findings form pH imaging is the spontaneous neuronal activity and its propagation in HF. The amplitude of this response is 3 to 6 % of $\Delta F/F$, and it corresponds to acidification from pH7.4 to 7.3. Finally, we visualized the propagation direction in several areas in HF (Fig. 3). We can observe the specific regions with same direction of propagation in HF. Some of them along anterior to posterior axis, that is corresponds to the direction of myelinated-axons observed specific fluorescent dye staining (Fig. 1B). The velocity of propagation is 44.9 ± 25.4 μm/sec, and it is much slower than the action potential propagation along the neuronal axon (~ m/sec).

We applied the several types of sound to female birds including white noise, call, pure song, reversed-song, combinatorial song. We reported that some of the songs induced neuronal activities in HF (last year mobiligence annual report). We found two types of neuronal activities: one is no latency and another one with long latency. Neuronal activities with no latency frequently show the propagation of active regions in HF (Fig. 4).

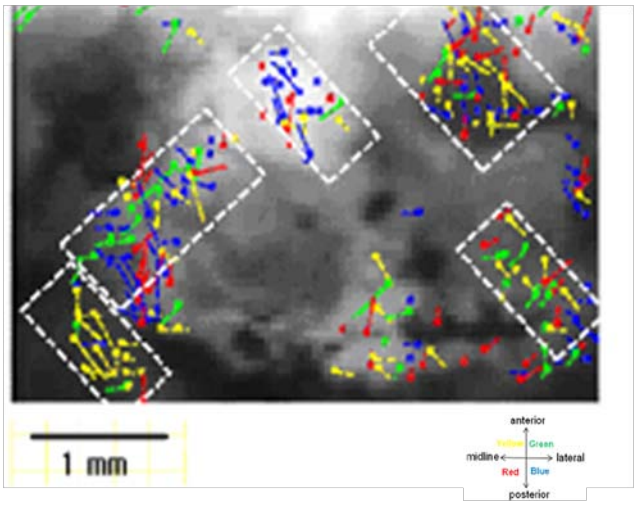

Fig. 3 Spontaneous neuronal activity and its propagation in HF. The directions of propagation are represented in 4 different colors.

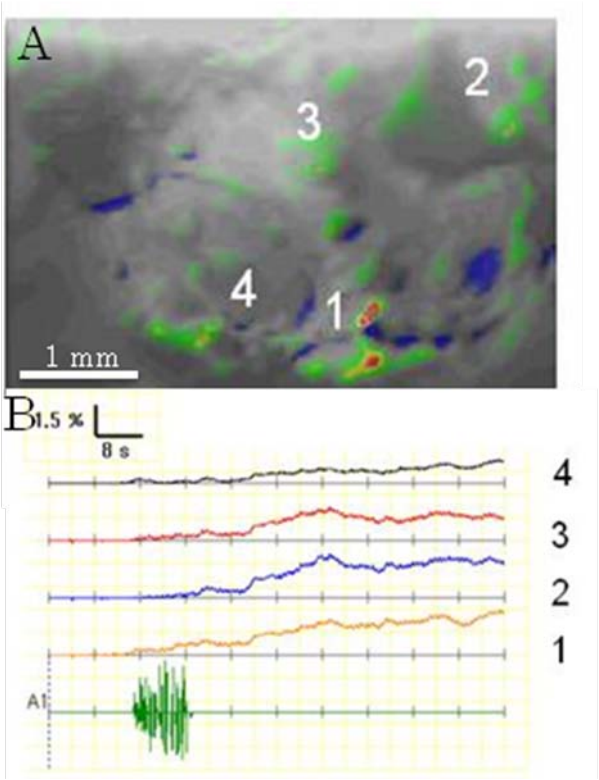

Fig. 4 Song-induced neural activity changes in female HF. The lower trace indicates the timing of stimulation.

IV. Discussion

To understand the neural mechanisms in the female HF, static and dynamic information is prerequisite for describing the detailed computational model. The static information is for the knowledge to the neuronal architecture in HF: number and types of neurons, location of excitatory and inhibitory synaptic connections, input and output of information flows among HF and also around HF areas including hearing systems. The dynamic information is complement for the static one, and it is the spatial and temporal activity of neurons. However, very little knowledge exits in HF of zebra finches. Only one exception is the cytoarchitecture study in pigeon HF region [2].

We, therefore, acquired the static and dynamic information concerning HF from zebra finches with several fluorescent imaging techniques. The static fluorescent imaging by DAPI, FluoMyelin, and Nissl staining reveals the global cytoarchitecture in the whole brain. We visualized sagittal and coronal sections of male and female brains of zebra finches, and it will be accessible by the internet in the near future. We also found the precise brain cytoarchitecture in HF with the combination technique of lipophilic fluorescent dyes and the gene gun. This technique is very powerful to investigate the neuronal connections in the narrow areas in HF, and we observed several types of neurons in this region. A possibility to cytoarchitecture in the brain is to find the higher structure with several numbers and types of neurons. One of the examples is the hyper column in the cortex of the mammalian brain. Finding of these neuronal architectures is helpful to understand neuronal information processing in HF.

We have also developed the imaging system for visualizing neuronal activities in HF with the pH indicator. Construction of a small chamber on the skull and its tight fixation decrease the signal to noise ration dramatically, and we can observe the small neuronal activity from HF in the resting. One of the interesting findings is the propagation of neuronal activities on the surface of HF. The velocity of this propagation is very slow compared to the one of the action potential propagation. The area of propagation is very restricted, and the function and meaning of this propagation is unknown. We have to understand this propagation with the relationships between the song recognition and cytoarchitectures in HF in the near future for construction of the information processing model for song recognition.

V. Conclusion

Using a combination of fluorescent imaging techniques, we succeeded to visualize the cytoarchitecture of HF. We found that several numbers of sub-regions in HF and massive myelined-fiber on the surface of HF. From the pH imaging, activity of the neurons was observed during the resting and also presentation of songs. The areas for these activities propagate on the surface of HF. These anatomical and pH imaging results are useful to construct the quantitative model for song discrimination in HF.

References

[1] Fujimura A, Hotta K, Oka K. 2007. Proceedings of the 2nd international symposium on mobiligence 215-218.

[2] Atoji Y, Wild MJ. 2007 .Limbic systems in birds: morphological basis ◦ Watanabe S, Hofman MA (eds.) Integration of comparative neuroanatomy and cognitive. 97-123, Keio Univ.

[3] Gan WB, Grutzendler J, Wong WT, Wong RO, Lichtman JW. 2000. Multicolor "DiOlistic" labeling of the nervous system using lipophilic dye combinations. Neuron. 27(2):219-25.

The Effect of Gaze as Central Cue on Horizontal Distribution of Attentional Field

Motoichiro Kato, Shuhei Nakamoto, Mihoko Otake, Hajime Asama

Abstract — Eyes catch our attention. A paradigm to test the implicated role of eyes in orienting attention toward relevant target is the spatial cueing task using cues such as gaze and arrow direction. However, in the previous studies on this effect, the distance between the central cue and target was constant. In the present paper, by changing the distances, we examined the strength of attentional field elicited by central cues. We also compared the effects of seven cues (without cue, left/neutral/right arrow cues, and left/neutral/right gaze cues). The results showed two main findings; gaze cues enhance the attention more than arrow cues as a whole, and the appearance effect of the cues decreases as the increased distance from the fixation point, while the inducing effect by cues is independent of the distance.

1 Introduction

Eyes are crucial for human interactions as social signals. They attract our attention because they provide us with information about feelings and intentions. For example, eye gaze tells us whether other person looks at us.

A experimental paradigm to test the implicated role of eyes in orienting attention toward relevant stimuli, is the spatial cueing task using cues such as gaze and arrow direction (Friesen and Kingstone, 1998; Tipples , 2002). In these tasks, where central gaze/arrow is used to trigger attentional orienting, normal subjects have repeatedly demonstrated faster reaction times in detecting peripheral targets presented congruently to the cue direction, opposed to incongruently presented targets.

It has been reported that patients with a lesion in the amygdala or the superior temporal sulcus (STS) showed different results from normal subjects (Akiyama et al, 2006a, 2006b, and 2007) In the gaze condition,
patients with a lesion in the amygdale showed smaller congruency effects in the gaze condition, and patients with a lesion in the STS had difficulty discriminating the direction of gazes. However, both patients made less difference from normal subjects in the arrow condition. Therefore, gaze information, that is biological signal, appears to be processed in the amygdala and the STS, while arrow information, that is non-biological signal, in different regions of the brain. Besides, people with schizophrenia, who are thought to have lesions in these regions, showed similar results (Akiyama et al, 2008). Therefore, researches on gaze recognition are important as clues to understand the pathology of these disorders and to elucidate the human interaction.

However, to date, there are few experiments on the changes of the visual attentional field elicited by arrow or gaze cues. For example, Handy (1996) showed enhanced attention within about 2.5 °from the direction of the cue. Handy's study, however, didn't take into account the distance between the target and the cue.

We therefore expand the measurement range in order to investigate the strength of the attentional field elicited by gaze and allow cues. Moreover, experiments are designed to separate the appearance or inducing effect from overall results.

2. Method for measuring the attentional Field elicited by gaze and allow

Eight elderly adults and ten students participated in the experiment.

There were three conditions of seven cue types (without cue, left/neutral/right arrow, and left/neutral/right gaze). In the no-cue condition, we can examine the normal attentional field when the fixation point was at the center of the monitor. In the arrow or gaze condition, we can find out the effects of cue directionality. The difference between arrow and gaze cues is whether they are biological or not.

The factor affecting reaction times (RTs) is not only the inducing effect caused by directionality of arrows or gazes but also the appearance effect caused by the target onset.

Therefore in this experiment, cues were designed in order to separate these effects.

The RT difference between neutral condition and left and right condition represents inducing effects of the cues. The RT difference between the no-cue condition and neutral arrow condition represents the effect caused by the onset of figure (appearance effect of figure), while the difference between the neutral gaze condition and neutral arrow condition represents the effect caused by biological factors (appearance effect of face).

Trial sequence is illustrated in Figure 1. Trials began with the onset of a fixation figure. The fixation figure is a cross in the no-cue condition, a horizontally long cross in the arrow condition, and a face with blank eyes in the gaze condition. After 675 ms, the left/neutral/right cue was presented on the monitor. Then, after 100, 300 or 700 msec (stimulus onset asynchrony; SOA), the target appeared at the randomized point on the horizontal line. Subjects were instructed to press the space bar as quickly and accurately as possible when the target appeared. The range of target locations is ±16.1 °in the no-cue condition and -16.1 °～-2.0 °or 2.0 °～ 16.1 ° in the arrow/gaze condition.

Figure 1 : Flow of experiment

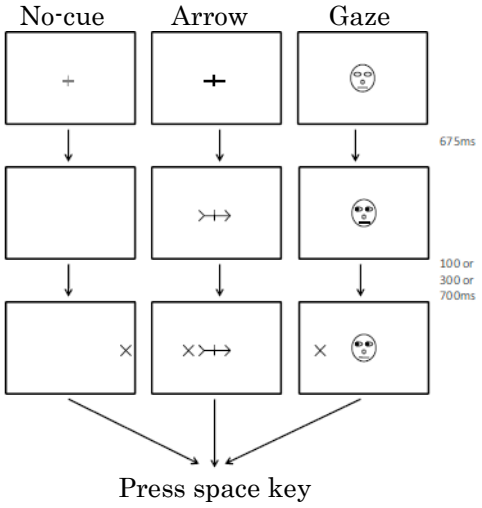

3. Results

An ANOVA with cue type (without cue, arrow, and gaze) and cue direction (left, neutral, right) and t-test were conducted. Errors, defined as anticipations (RTs < 100 ms) or incorrect responses (RTs > 800ms) were excluded from further analysis. These errors accounted for 1.2% of all the trials. Then, trials at the 100 ms SOAs are also excluded because they had less inducing effect (details are given in "Difference between SOAs"). In analysis, we divided the range into six sec- tions (−16.1◦ - −11.6◦, −11.6◦ - −7.0◦, −7.0◦ - −2.0◦, 2.0◦ - 7.0◦, 7.0◦ - 11.6◦, 11.6◦ - 16.1◦), and RTs within each section were averaged. Note that the vertical axis was inverted so that we can see quickness as strength of attention.

The main effect of cue type was significant [$F(2, 6711) = 41.24$, $p < 0.001$]. In the no-cue condition, RTs within the section near the fixation point (0◦) were shorter than those near the edge (Figure 2). The average RT in the arrow condition was 19 ms longer than that in the no-cue condition [$t(4447) = -8.46$, $p < 0.001$] (Figure 3). In the neutral arrow condition, there was no significant difference between visual fields [$t(659) = 0.18$, $p = 0.86$]. In the left arrow cue condition, the average RT in the LVF was 14 ms shorter [$t(784) = -2.69$, $p < 0.01$]. In the right arrow cue condition, the average RT in the RVF was 11ms shorter while one of the RTs was longer than that in the LVF [$t(784) = 1.98$, $p = 0.048$]. The attention had a tendency to decrease as the distance from the fixation point increased. The comparison between cue directions showed no significant difference (left arrow:342 ms, neutral arrow:343 ms, right arrow:344 ms)[$F(2, 2268) = 0.16$, $p = 0.86$]. The average RT in the gaze condition was 6 ms longer than that in the no-cue condition [$t(4341) = -3.04$, $p < 0.01$] (Figure 4). In the right gaze condition, the average RT in the RVF was 8 ms shorter [$t(797) = 1.82$, $p = 0.07$]. In the same way as in the arrow condition, the attention had a tendency to decrease, and the comparison between cue directions showed no significant difference [$F(2, 2251) = 0.89$, $p = 0.41$].

Figure 2

Reaction time without cue

(Error bars show 95% confidence range)

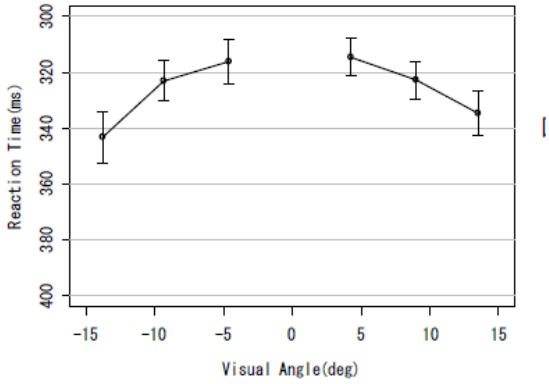

Figure 3

Reaction time to arrow cues

(Error bars show 95% confidence range)

○: left arrow, △: neutral arrow, +: right arrow

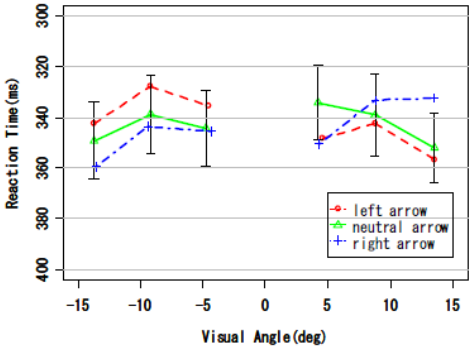

Figure 4

Reaction time to gaze cues

(Error bars show 95% confidence range)

○:left gaze, △:neutral gaze, +:right gaze

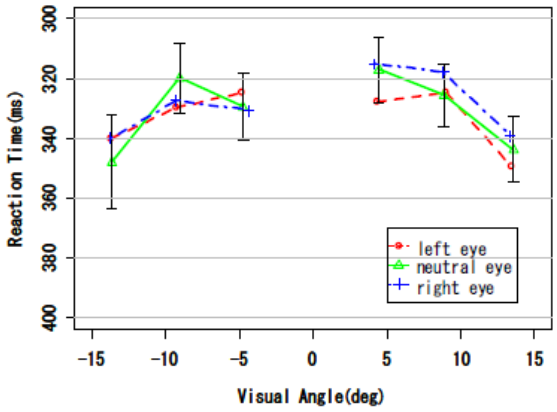

3.1 Appearance effect

The effect of the target onset (appearance effect of figure) obtained by subtracting the RT in the no-cue condition from that in the neutral arrow condition resulted in the 17 ms (delay). As the distance from the fixation point increased, the appearance effect of figure decreased in the LVF but not in the RVF. The effect of the face target(appearance effect of face) obtained by subtracting the RT in the neutral arrow condition from that in the neutral gaze condition resulted in the -12 ms in the LVF and -13 ms in the RVF (facilitation). The appearance effect of face decreased in both of the visual fields.

3.2. Inducing effect

We investigated the inducing effect of the cues by subtracting the RTs in the left or right cues from those in the neutral cues. The inducing effect of the left arrow cue resulted in -9 ms (facilitation) in the LVF and 8ms (delay) in the RVF (Figure 11). On the other hand, the inducing effect of the right arrow cue resulted in 6 ms in the LVF and the facilitation by -3 ms in the RVF. In contrast to the appearance effect, there was no remarkable decrease in the LVF and, there was some increase in the RVF. The inducing effect of the left gaze cue resulted in -1 ms in the LVF and 5 ms in the RVF. Likewise, the inducing effect of the right gaze cue resulted in 0 ms in the LVF and -5 ms in the RVF. As well as in the arrow cues, there was no remarkable decrease in both the visual fields.

4. Conclusion

The attention without cue was the highest near the fixation point and decreased as the distance from the center increased.

In the left and right arrow and right gaze condition, there were significant cueing effects, which had been repeatedly observed since Friesen and Kingstone (1998).

In the arrow and gaze condition, the strength of attentional field decreased as well as in the no-cue condition. This result may be

affected strongly by the attentional feature of humans, which was evident in the no-cue condition.

The appearance effect of figure (the decrease of attention by the cue onset) is possibly a kind of gap effect. This term refers to faster responses to a peripheral target in the condition with offset of the fixation stimulus than with the condition where the fixation point remains visible (Dorris & Munoz, 1995) (Senju & Hasegawa, 2005).

The gaze cues which have biological features, facilitated RT by -12 ms (appearance effect of face). Probably, this resulted from stronger interest in the human face and boredom with the arrow cues. Although similar effects were apparent in some studies(Akiyama et al., 2006b), they didn't pay much attention to the effects of face because what has been discussed was the difference between congruent and incongruent condition.

The inducing effect calculated by subtracting the RTs in the neutral condition from those in left and right condition showed the benefit in the congruent condition. It is notable that the left gaze condition, which didn't have the benefit in "overall results", showed the inducing effect in the LVF. The inducing effect didn't decrease and sometimes increased at the edge of the monitor. This result indicates that an arrow and a gaze has the information about direction (e.g. likely to appear to the left), but not about distance (e.g. likely to appear at ○ cm from the center). This coincides with Calder and Young's model(Calder &Young, 2005), which separates between the recognition of facial identity and facial expression (gaze direction).

In summary, the present study expand the target area in the visual filed, and revealed the strength of attentional field (distribution of attention) elicited by arrow or gaze cues. The results supported previous observations and revealed several new findings;

(1) In the arrow and gaze condition, attentional curve has its peak near the center and decrease monotonically toward the edge.
(2) Gaze cues facilitate attention more than arrow cues.
(3) The appearance effect decreases toward the edge.
(4) The inducing effect doesn't decrease toward the edge.

References

Akiyama, T., Kato, M. et al (2008). Gaze-triggered orienting is reduced in chronic schizophrenia.. *Psychiatry Research*, 158,287–296.

Akiyama, T., Kato, M. et al (2006a). A deficit in discriminating gaze direction in a case with right superior temporal gyrus lesion. *Neuropsychologia*,44, 161–170.

Akiyama, T., Kato, M. et al (2006b). Gaze but not arrows: A dissociative impairment after right superior temporal gyrusdamage.*Neuropsychologia*,44,1804–1810.

Akiyama, T., Kato, M. et al (2007).Unilateral Amygdala Lesions Hamper Attentional Orienting Triggered by Gaze Direction.*Cerebral Cortex*, 17, 2593–2600.

Barbara,A et al (1994). Visual attention mechanisms show a center-surround organization. *Vision Research*,35, 1859–1869.

Calder, A. et al (2005). Understanding the recognition of facial identity and facial expression.*Nature reviews Neuroscience*, 6, 641–651.

Dorris,M.C.&Munoz,D.P. (1995). A neural correlate for the gap effect on saccadic reaction times in monkey. *Journal of neurophysiology*, 73, 2258–2562.

Driver, J. et al (1999). Gaze Perception Triggers Reflexive Visuospatial Orienting. *Visual Cognition*, 6, 509–540.

Friesen, C. K. & Kingstone, A. (1998). The eyes have it! Reflexive orienting is triggered by nonpredictive gaze. Psychonomic bulletin & review, 5, 490–495.

Friesen, C. K. & Kingstone, A. (2003). Covert and overt orienting to gaze direction cues and the effects of fixation offset. *Neuroreport*, 14, 489–493.

Handy, T. et al (1996). Spatial distribution of visual attention: Perceptual sensitivity and response latency. Perception & Psychophysics, 58, 613–627.

Okada, T et al (2006). Right hemispheric dominance in gaze-triggered reflexive shift of attention in humans. *Brain and Cognition*, 62, 128–133.

Posner,M.I. (1980). Orienting of attention. *Journal of Experimental Psychology*, 32, 3–25.

Senju, A. & Hasegawa, T. (2005). Direct gaze captures visuospatial attention. *Visual Cognition*, 12, 127–144.

Tipples, J. (2002). Eye gaze is not unique: Automatic orienting in response to uninformative arrows. Psychonomic Bulletin & Review,9, 314–318.

Artificial target toxin eliminating specific octopamine-interacting cells as a new tool for studying the cricket's aggressive behavior

Akio Kishigami, Ken Sasaki, Yoshihide Tamori, Takashi Nagao

***Abstract*—Male crickets *Gryllus bimaculatus* exhibit vigorous stereotyped aggressive behavior when they encounter the conspecific males. This aggressive behavior is under modulation by octopamine which acts as a neurohormone, a neuromodulator, and a neurotransmitter through octopamine receptors belonging to the family of G-protein coupled receptor. Further studies for the relation between octopamine and aggressiveness should give deeper insight into modulation of peripheral and sense organ and within central nervous system in cricket. Therefore we designed to make a specific toxin to target and eliminate cells including octopamine-interacting protein on their surface.**

I. Aggressive Behavior

Aggressive behavior is a complex social interaction influenced by numerous internal and external factors. Aggressiveness is widespread in the animal kingdom. Aggressive interaction between conspecifics are a common phenomenon throughout the animal kingdom, having been described in the lowest metazoans and of course in humans [1]-[3]. In mammals, noradrenaline is a key modulator of aggression [4]. For example dopamine β-hydroxylase knockout mice lacking noradrenaline hardly show any aggressive behavior [5]. The effect of noradrenaline is suggested to be biphasic: Slight increase in noradlrenaline level lead to enhanced aggressive behavior, whereas strong elevations suppress aggression. In arthropods, Octopamine, a closely related biogenic amine to noradrenaline, has been proposed to have a similar function to noradrenaline in mammals [6]. As in insects, their aggressive behaviors have been studied to relate with octopamine-mediated neuromodulation, they are experimental models to understand the physiological basis of complex and plastic behavior [7], [8].

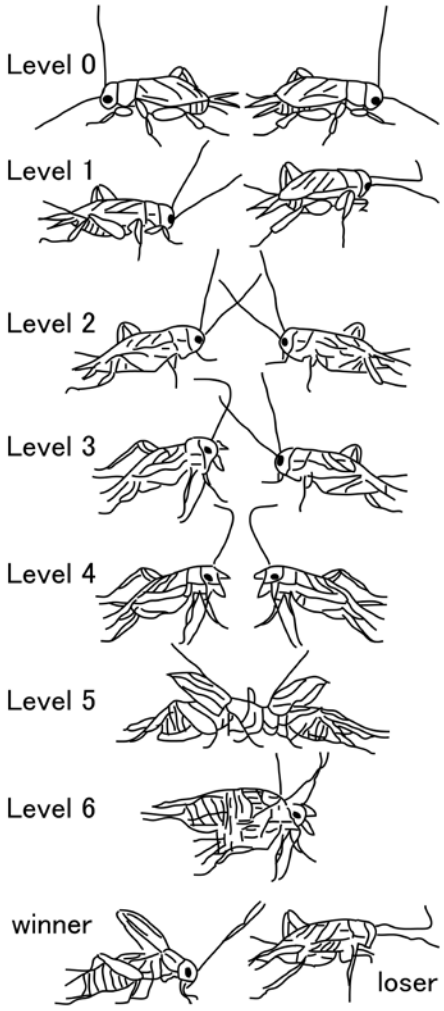

Fig.1. The stereotyped esalating sequence of motor perfomances (level 0-6) characteristic for aggressive encounters between male crickets

Authors are with Kanazawa Institute of Technology, 3-1 Yakkaho, Hakusan, Ishikawa 924-0838, Japan (corresponding author to provide phone: 076-274-8264; fax: 076-274-8251; e-mail: nagao@ his.kanazawa-it.ac.jp).

II. Aggression in Crickets

In crickets, aggressive and escape behaviors have been analyzed the relation with biogenic amines [9]-[11]. When two previously isolated adult male crickets meet they exhibit a highly stereotyped, escalating sequence of motor acts that culminates in combat [12]. The stages denoting the level of aggression are distinguished as in Fig.1 [9], [12], [13]. Level 0 applies to interactions where both crickets avoid each other and show no indication of aggressive behavior. Level 1 describes a situation of clearly preestablished dominance, in which one animal retreats from an approaching potential aggressor. At level 2, the antennae of the two contestants make contact and lash each other in a fashion only expressed during agonistic encounters. This is followed by level 3, in which one of the crickets faces its opponent with broadly spread mandibles and then level 4 where both crickets display their spread mandibles. Mandible spreading is only exhibited during agonistic encounters between conspecifics. At level 5, the spread mandibles of the two combatants engage, each animal pushing forward by stemming both hind legs in the ground. At level 6 the animals enter a stage of all-out combat, during which the contestants mandibles may disengage and reengage several times, with intermittent sallies by each cricket to attack and bite the other. A fight can be concluded at any level by one animal retreating, and this establishes a clear winner and a clear loser. The established winner typically produces the rival song together with characteristic body-jerking movements.

This aggressiveness of crickets is reduced after depleting octopamine and dopamine from central nervous system but is unaffected by serotonin depletion [10]. By pharmacological approach for the octopamine

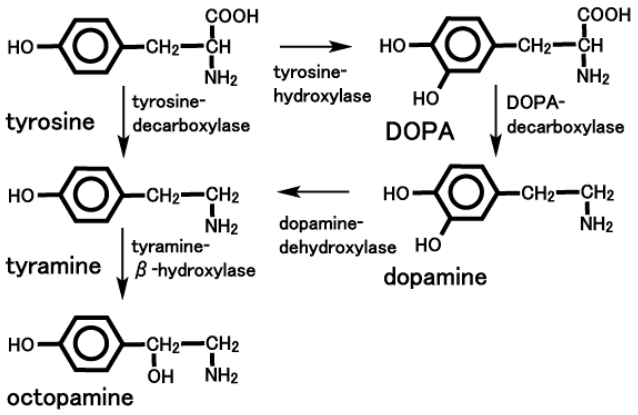

Fig.2 Metabolic pathway of octopamine

receptor in brain, octopamine has been suggested to act as a central neuromodulator that enhances aggressiveness by raising a cricket's threshold to retreat from an opponent, so that it escalates further and fights longer [8], [10].

III. Octopamine and Its Receptors in Insect

Octopamine, p-hydoxyethanolamine was first discovered in the salivary glands of *octopus vulugaris* [14]. Octopamine can be distinguished from noradrenaline by the absence of a hydroxyl group at position 3 of the phenol ring (Fig.2). Both phenolamines have functional significance in the central and peripheral nervous systems of invertebrates and vertebrates. Based on similarities in their action, it has been suggested that noradrenergic system in vertebrates [7]. Octopamine is present in high concentration in the peripheral nervous system, central nervous system and various other insect tissues [15]. Octopamine serves as a neurotransmitter and neuromodulator in both peripheral and central nervous systems and also functions as a circulating neurohormone in insects. In the peripheral nervous system, octopamine modulates the activity of flight muscles, peripheral organs (such as fat body, oviduct, and hemocytes), and almost all sense organs. In the

central nervous system, octopamine is essential for regulation of motivation, desensitization of sensory inputs, initiation, and maintenance of various rhythmic behaviors and complex behaviors including learning and memory. Octopaminergic system is mainly functional in invertebrate because its receptors are not found in vertebrates. Collective evidence strongly suggests that octopamine plays a major neuromodulatory role in insect behaviors [7], [8], [15].

Octopamine exerts its effects by binding to specific proteins that belong to the superfamily of G protein-coupled receptors (GPCR) and share the structure motif of seven transmembrane domains [8]. They are octopamine receptors. Insect octopamine receptors are classified into three main classes based on similarities in structural and signaling properties of cloned fruit fly *D.melaogaster* octopamine receptors with vertebrate adrenergic receptors. Interaction of octopamine with its specific receptors leads to a cellular signal transduction cascade involving different second messenger systems [16]. These second messengers include adenosine 3',5'-cyclic mono- phosphate, Calcium, inositol-1,4,5-tris- phosphate and diacylglycerol. Octopamine-mediated generation of these second messengers is associated with changes in cellular response affecting insect behaviors [17], [18]. Generally, agonist activation of a GPCR like octopamine receptors not only results in the G protein-dependent activation of effector systems, but also sets receptor internalization by endocytosis and receptor trafficking to regulate the temporal and spatial aspects of GPCR signaling. Endocytosis is the process by which cells internalize portions of their cell membrane along with embedded proteins. These membrane proteins can be recycled back to the plasma membrane from the endosomal compartments to be reused or, alternatively, follow a degradative pathway to the lysosomes [19].

IV. Immunotoxin

Ribosome inactivating proteins (RIPs) are a family of highly potent protein toxins that bring about inhibition of protein synthesis by directly interacting with and inactivating the ribosomes or by modification of factors involved in translation, usually the elongation step. These toxins are known to be produced by a wide variety of plants. Examples of plant RIPs include abrin, ricin, gelonin, momordin, saporin, etc. [20]-[23]. Type I RIPs are made up of the toxic subunit (A-chain) alone, while type II RIPs consist of a toxic A-chain and a lectin like subunit (B-chain) linked together by a disulfide bond. The toxicity of A-chain is due to its RNA-N-glycosidase activity, by which it brings about depurination of adenine at position 4324 in the 28 S rRNA. This activity prevents the formation of a critical stem−loop configuration, to which the elongation factor is known to bind during the translocation step of translation. The end result of this activity is complete inhibition of cellular translation. The role of the B-chain is to help in the transport of RIPs into the cells by binding to specific sugar residues of glycoproteins or glycolipids on the plasma membrane and internalization by endocytosis. After the binding of RIPs on the cell surface, endocytosis processes direct the molecules to endosomal vesicles to be sorted for further routing in membrane traffic system. These RIPs appear to be guided to the Golgi apparatus and from there to the endoplasmic reticulum (ER). The RIPs molecule or at least its active chain must then enter the cytosol to gain access to the ribosomal substrate. The translocation of ricin to the cytosol was demonstrated to occur in the ER.

As soon as it was realized that some RIPs consist of two parts with different roles in the intoxication process, the idea appeared that the receptor-binding part might be replaced by another binding moiety, such as an antibody directed against a cell surface antigen. In particular, chimeric proteins consisting of an antibody linked to a toxin, which are called as immunotoxin, have been used to eliminate tumor cells, autoimmune cells, and virus-infected cells [23]-[25]. Also other binding molecules, such as hormones and growth factors have been used to direct toxins to cells of interest.

V. PERSPECTIVE

It is expected that a study by molecular targeting in combination with behavior physiology analysis, may help in shedding more light on the underlying molecular mechanisms of octopamine-mediated neuromodulation on aggressive behaviors in crickets. We attempted to develop a toxin direeting to cells including octopamine-interacting proteins on their surface, helping to study by manipulation disrupting cells with either specific octopamine receptors or proteins in cricket nervous system. We prepared biotin-labeled octopamine and avidin-conjugated saporin. After mixing with them, the specific toxin was purified by column chromatography. The toxin will examine to estimate effective concentration and injection region in cricket. Antibodies to specific octopamine receptors and transporters are candidates to conjugate with saporin. Future studies by using them will contribute to demonstrate the spatial and temporal regulation by octopamine relating to the escalation of aggressive behavior in cricket.

References

[1] R.C.Brace and J.Purvey, "Size-dependent dominance hirearchy in the anemone Actinia equina." Nature, 273, pp752-753,1978.

[2] I.Eibl-Eibesfeld, "Aggression in the Iko-bushmen." Aggression, vol.52, pp1-20, 1974.

[3] D.J.Albert, M.L.Walsh, and R.H.Jonik, "Aggression in humans: what is its biological foundations?" Neurosci. Behav. Rev. vol.17, pp405-425, 1993.

[4] J.Haller, G.B.Makara and M.R.Kruk, "Catecholaminergic involvement in the control of aggression: hormones, the peripheral sympathetic and central noradrenergic systems." Neurosci. Behav. Rev., vol.22, pp85-97, 1998.

[5] M.D.Marino, B.N.Bourdelat-Parks, L.L.Cameron, and D.Weinshenker, "Genetic Reduction of noradrenergic function alters social memory and reduces aggression in mice." Behav. Brain Res. vol.161, pp197-203, 2005.

[6] E.A.Kravitz and R.Hurber, "Aggression in invertebrates." Cur. Opin. Neurobiol. vol.13, pp736-743, 2003.

[7] T.Toeder, "Octopamine in invertebrate." Prog.Neurobiol. vol.59, pp533-561, 1999.

[8] T.Farooqui, "Octopamine-mediated neuromodulation of insect senses." Neurochem.Res. vol.32, pp1511-1529, 2007.

[9] P.S.Stevenson, H.A.Hofmann, K.Schoch, and K.Schildberger, "The fight and flight responses of crickets depleted of biogenic amines." J.Neurobiol. vol.43, pp107-120, 2000.

[10] P.A.Stevenson, V.Dyakonova, J.Rillich, and K.Schildberger, "Octopamine and experience-dependent modulation of aggression in crickets." J.Neurosci. vol.25, pp1431-1441, 2005.

[11] S.A.Adamo, C.E.Linn, and R.R.Hoy, "The role of neurohormonal octopamine during `fight or flight' behavior in the field cricket *Gryllus bimaculatus*." J.Exp.Biol. vol.198, pp1691-1700, 1995.

[12] R.D.Alexander, "Aggressiveness, territoriality, and sexual behavior in field crickets (Orthoptera: Gryllidae)." Behavior, vol.17, pp130-223, 1961.

[13] H.Hofman, P.A.Stevenson, "Flight restores fight in crickets." Nature, vol.403, pp613, 2000.

[14] V.Erspamer, and G.Boretti, "Identification and characterization by paper chromatography of enteramine, octopamine, tyramine, histamine, and allied substances in extracts of posterior salivary glands of octopoda and in other tissue extracts of vertebrates and invertebrates." Arch. Int. Pharmacodyn. Ther. vol.88, pp296-332, 1951.

[15] J.Axelrod, and J.M.Saaverdra, "Octopamine" Nature, vol.265, pp501-504, 1977.

[16] P.D.Evans, and B.Maqueria, "Insect octopamine receptors: a new classification scheme based on studies of cloned Drosophila G-protein coupled receptors." Invert. Neurosci. vol.5 pp111-118, 2005.

[17] W.Blenau, and A.Baoumann, "Molecular and pharmacological properties of insect biogenic amine receptors: lessons from *Drosophila melanogaster* and *Apis mellifera*." Arch. Insect Biochem. Physiol. vol.48, pp13-38, 2001.

[18] W.Blenau, and A.Baoumann, "Aminergic signal transduction in invertebrates: focus on tyramine and octopamine receptors." Recent Res. Dev. Neurochem. vol.6, pp225-240, 2003.

[19] A.C.Hanyalogu, and M.von Zastrow, "Regulation of GPCRs by endocytotic membrane trafficking and its potential implications." Annu. Rev. Pharmacol. Toxicol. vol.48, pp537-568, 2008.

[20] F.Stirpe, "Ribosome-inactivating proteins." Toxicon vol.44, pp371-383, 2004.

[21] M.R.Hartley, and J.M.Lord, "Cytotoxic ribosome inactivating lectins from plants." Biochim. Biophys. Acta., 1701, pp1–14. 2004.

[22] S.Narayanan, K.Surendranath, N.Bora, A.Surolia, A.A.Karande, "Ribosome inactivating proteins and apoptosis." FEBS Let. vol.579 pp1324–1331, 2005.

[23] F.Stripe and M.G.Battelli, "Ribosome-inactivating proteins: progress and problem." Cell.Mol.Life Sci. vol.63, pp1850-1866, 2006.

[24] O.W.Press, "Immunotoxins." Biotherapy, vol.3, pp65-76, 1991.

[25] V.Ghetie, and E.S.Vitetta, "Chemical construction of immunotoxins." Mol.Biotech. vol.18. pp251-268, 2001.

Mechanism of social adaptive foraging behavior in the honeybee

Etsuro Ito[1], Hidetoshi Ikeno[2], Mizue Ohashi[2], Toshifumi Kimura[2], and Ryuichi Okada[1]

[1]Tokushima Bunri University and [2]University of Hyogo

Abstract—A honeybee informs her nestmates of the location of a flower she has visited by a unique behavior called a "waggle dance." We regard the waggle dance as a good model of the "propagation and sharing of knowledge" that maintains a society, and thus we are attempting to reveal the effects of the waggle dance in terms of the colony's benefit using mathematical models and computer simulation based on parameters from observations of the bee behavior. This past year, we improved our mathematical model and observed honeybee behavior in the field to obtain detailed biological parameters of the waggle dance. Video analysis showed that most dance followers that listen to the waggle dance left the dancer after one or two sessions of listening. A follower attended to multiple dancers before her flight. Furthermore, we found most bees in the hive did not walk for long distance. In parallel to biological experiments, we also developed an automatic bee-tracking system by using a vector-quantization method, and a continuously automatic measuring system of environmental factors such as CO_2, humidity, temperature etc. These will bring us better understanding of the effects of the waggle dance on the colony.

I. Introduction

HIGHLY developed societies such as those of human beings require communication between individuals. The honeybee (*Apis mellifera*), one of the social insect species, is well known to have the ability to communicate with its nestmates, using the so-called "waggle dance" to inform them of the location of a food source (Fig. 1, [1]-[4]). In the waggle dance, the dancer moves in a straight line with her wings beating (waggle run), then circles back to the starting point without wing-beating (the return run). On a vertical comb, the direction of the waggle run (during which the dancer wags her body from side to side and emits sounds) relative to gravity indicates the direction to the food source relative to the sun's azimuth in the field. The duration of the waggle run depends on the distance to the food source. A few follower bees keep close contact with the dancer, and these bees may be recruited to visit the flower the dancer is locating for her nestmates.

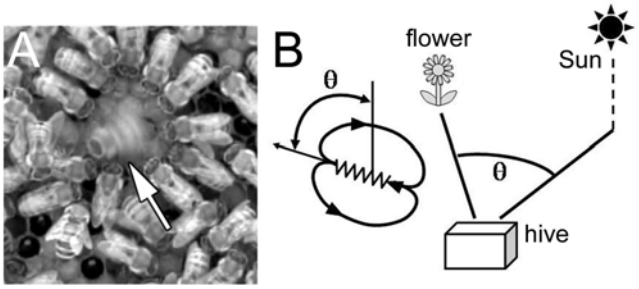

Fig. 1 Waggle dance (left panel) and the relationship between the dance orientation and food source (right panel).

We regard the waggle dance as a good model of the "propagation and sharing of knowledge" that maintains a society, and are attempting to reveal the effect of the waggle dance in terms of its benefits to the colony using mathematical models and computer simulation based on parameters from observations of the bee behavior [5, 6, 7].

Here we will report that we (1) developed our mathematical model based on biological data we have obtained so far, (2) continued the biological experiments of behavioral patterns of dance followers and locomotion patterns of bees in the hive, (3) developed an automatic tracking system for bee behavior in the hive [8], (4) built a continuous data collection system for hive environments of inside/outside of the hive [9].

II. Results

2-1 Results of observation of dance behavior

Behavioral studies were done in the campus of Hokkaido University (Sapporo, Japan) from 8:30 am to 4 pm on several days between August and October, 2006 and 2007 (temperature: 25-36 ˚C in most experiments). Honeybees, *Apis mellifera*, were kept in the beekeeping box with a queen. Bee behavior on the vertical comb was monitored by a video camera (JVC, GR-HD1), stored on a digital video tape (30 frames/sec), and then analyzed off-line frame by frame.

2-1-1 Behavioral patterns of dance followers

Followers go out to forage after listening to several sessions of waggle runs. Detailed observations of dance followers revealed that 80% of 355 bees (for 4 dancers) turned away from the dancer after one or two sessions of waggle runs and that only 4 % of bees followed more than 5 consecutive runs.

Tracing a single follower for 5 minute, we found that a follower attended to dances performed by multiple dancers before flight (Fig. 2). Moreover, a follower bee followed

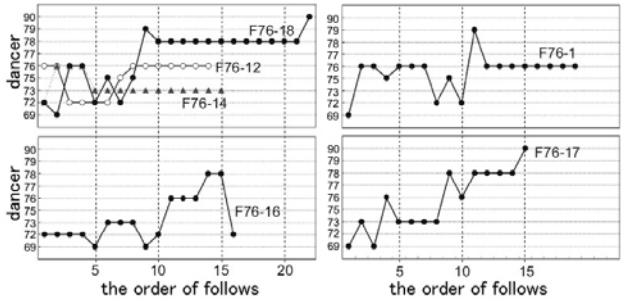

Fig. 2 Dancers a follower bee followed. One follower bee attended to waggle runs performed by multiple dancers before her flight. Numbers in the ordinate indicate dancer identity numbers and the abscissa is the order of waggle runs that a follower followed.

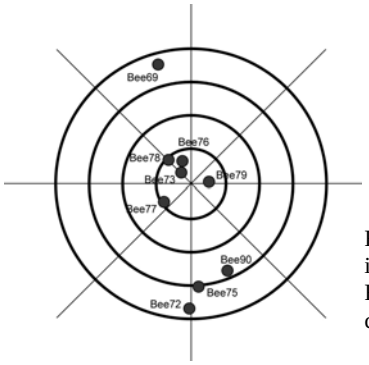

Fig. 3 Relative positions indicated by dancers in Figure 2. The nest is on the center.

dancers that have advertised completely different food sources (Fig. 3). It would be interesting to reveal how a follower makes her decision to visit a food source among food sources multiple dancers had shown. We will continue to analyze to obtain more parameters about dance followers for our mathematical model.

2-1-2 Locomotion of bees in the hive

We analyzed the locomotion patterns of bees in the hive, which is necessary for modeling basic bee behaviors. Tracing trajectories of locomotion for 10 sec from all analyzable 753 bees on a side of a comb (sampling rate = 1 Hz), we found that walk distance for 1 sec is less than 0.4 cm in about 80% of 7530 walks. We classified bees into 4 groups depending on their behavior, dancers (n = 4), followers (n = 25), movers that moved more than 2.5 mm in 10 sec (n = 492), and stayer that moved up to 2.5 mm in 10 sec (n = 232). 2.5 mm was the spatial resolution of our video system. We counted the number of "move" during 10 sec whether or not a bee moved more than 2.5 mm in 1 sec. The results showed that a few movers keep locomotion whole 10 sec but majority of movers showed less than 5 times.

We also found no clear preference for the destination in orientation after long time (10 sec) although there was a weak tendency that bees move forward in a short time (1 sec).

2-2 Model and simulations

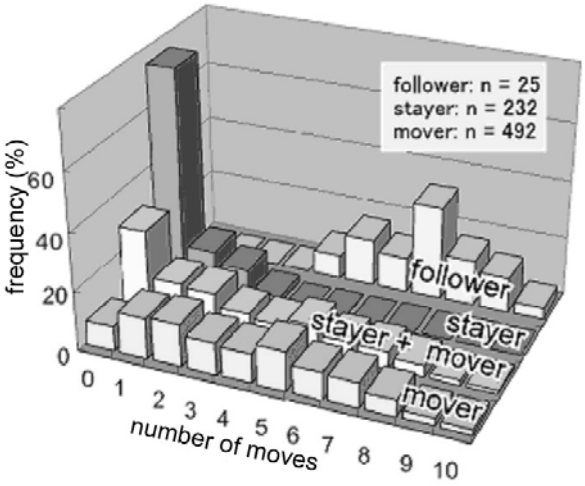

Fig. 4 Distributions of frequencies of "move" during 10 sec in four groups. Even movers rarely keep moving during 10 sec. They did often stay rather than move.

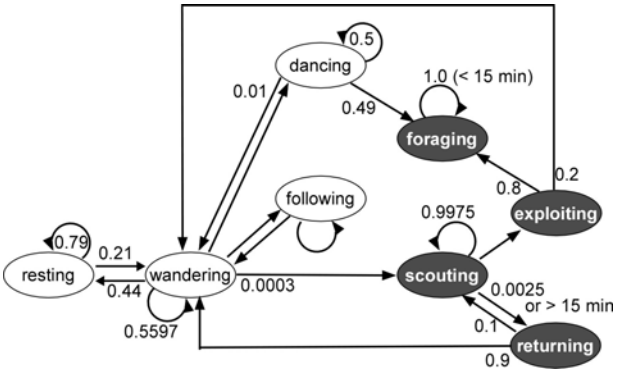

Fig. 5 Transition probabilities of our mathematical model. Bee behaviors were classified into 8 categories possibly relating to dance communication or foraging. Our old model had only three states (resting, wandering, exploiting).

In our old model, to evaluate the effect of the waggle dance, we constructed a foraging model by assuming that honeybee foraging behavior is the result of decision-making after a transition through 3 states: 1) resting, 2) wandering in the hive, and 3) foraging. And we showed importance of dance for the efficient foraging [6, 7]. This past year we improved our model by re-classifying behavioral states into eight states: resting in the hive (resting), walking in the hive (wandering), flying for searching for a food source (scouting), success in finding a food source (exploiting), failure in finding a food source (returning), flying to a known food source (foraging), dancing, and following (Fig. 5). A bee will fly out from the hive by these transition probabilities. We used our own data for wandering patterns in the hive. Parameters for flights were used from the literature [10]. The comparison between a colony that honeybees can memorize the location of food source and a colony that honeybees cannot memorize showed that memory colony succeeded 1.8 times in the number of visits at food sources as the

non-memory colony. We will continue to make behavioral experiments and video analysis for obtaining of additional parameters to construct a better model.

2-3 Tracking system of multiple honeybee behaviors

It is important to describe detailed movements of honeybees and obtain essential parameters of behaviors when constructing a mathematical model and performing simulation experiments. In general, bee behaviors were analyzed manually after recording by a video camera. Those analyses require large amounts of time and labors. We, thus, have attempted to develop a computer-aided automatic system for identifying and tracking behaviors of multiple honeybees [8].

The developed system consists of the following three processes: 1) extraction of the putative regions including honeybee (honeybee body region) from the whole hive image, 2) detection of individual bees from the honeybee body regions by the body size and the shape of a honeybee, 3) identifying and tracking of honeybee movements by temporal and spatial contextual information of individuals.

We used 10-second movie (30 fps) for analysis and found that more than 500 bees (72 %) were successfully identified in all three tested frames that were randomly chosen from an original movie (Fig. 6). Next, our system succeeded in tracking more than 50 % of honeybees simultaneously and tracing their trajectories (Fig. 7). In the coming year, we will improve this system to extract automatically the necessary parameters for a mathematical model and simulation experiments.

2-4 Observation system of the hive environment

The bee foraging behavior is adaptively modulated against changes in an environment both inside and outside of the hive, i.e., CO_2 concentration, temperature, and humidity. This year we developed an automatic measurement system of them to know their adaptability to the environments.

A honeybee colony was reared in a custom-made two-frame observation hive (Fig. 8). The inside of the hive was partitioned vertically into two rooms using a porous metal plate. Honeybees were in one room and the temperature, humidity and CO_2 sensors were in the other room. The outside air temperature and humidity were also monitored at 1 m away from the hive. The weight of the observation hive was measured by a platform scale. The behavior and coming/going conditions of honeybees were monitored by a CCD camera and a photo interrupter, respectively. All data were acquired with particular sampling rates [9].

Figures 9 and 10 indicate typical changes of the hive environment in August 2008. The hive mass decreased in the morning and increased in the afternoon. The temperature within the hive increased during the day and decreased at night. At night, the hive temperature was higher than outside by about 3 °C. While outside humidity increased at night and

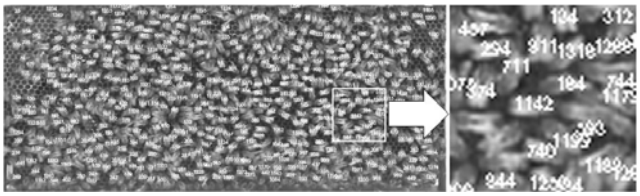

Fig. 6 Identifying unmarked honeybees in a hive. The area surrounded by the rectangle in the left image is shown in the right image

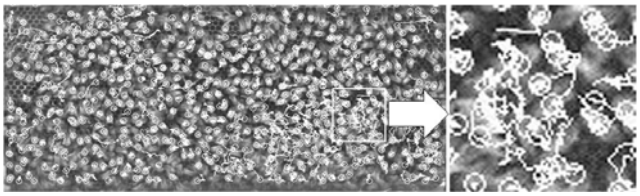

Fig. 7 The trajectories of tracked individuals simultaneously. The area surrounded by the rectangle in the left image is shown in the right image.

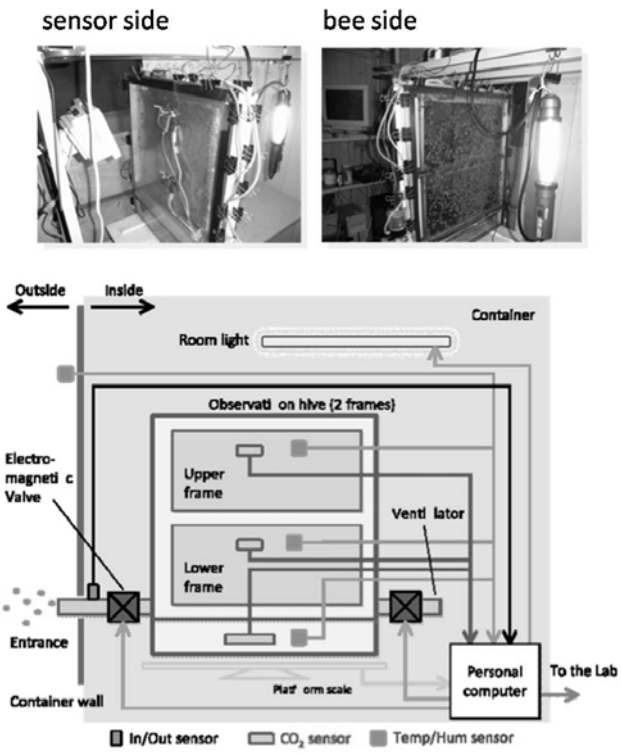

Fig. 8 Observation system. Temperature, humidity and CO_2 concentration in the hive were measured. Hive weight, CO_2 production and coming/going conditions were also recorded on a personal computer. All data were automatically acquired with particular sampling rates and recorded in a PC.

decreased during the day, the humidity within the hive was stable and higher than ambient all day. The different daily patterns between humidity and temperature suggest that honeybees might control these two factors with different mechanisms.

The hive CO_2 concentration had two peaks in a day in summer; a higher peak in the early morning and a lower peak

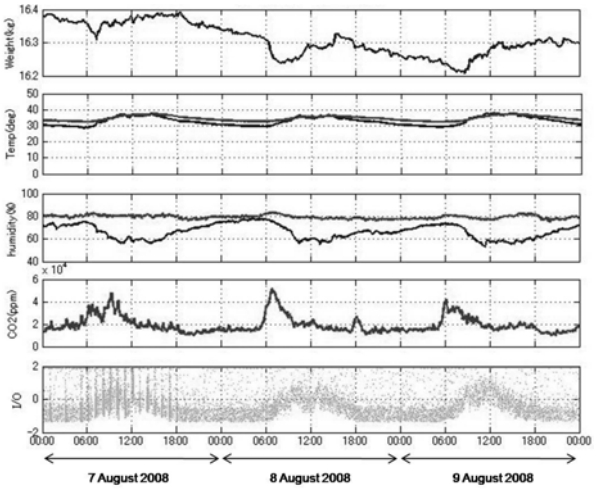

Fig. 9 Hive weight, temperature, humidity, and CO_2 concentration on 7–9 August 2008. The daily cycle of the hive weight was revealed. The temperature in the hive changed synchronously with the ambient temperature. The humidity in the hive was kept constant. A prominent increase in the CO_2 concentration was observed around 6 am.

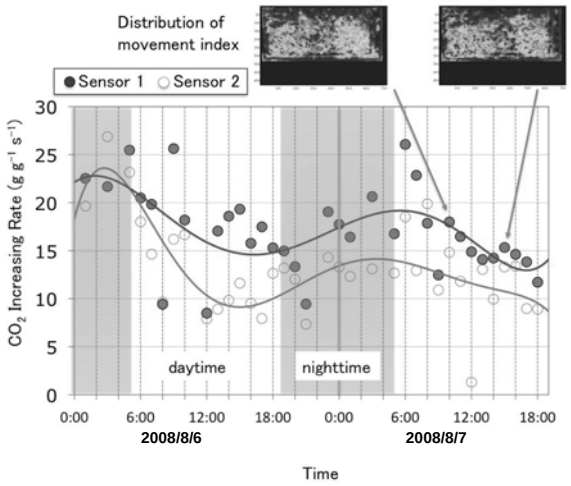

Fig. 10 CO_2 production and colony activity in summer. The CO_2 production rate increased in the morning. Honeybee activities at 10 am and at 15 pm are shown by a grayscale image.

in the evening. This might be caused by a circadian activity of honeybees. CO_2 production in the hive was high in the early morning and low in the afternoon, which corresponded with changes in colony activities (Fig. 10). The rapid decrease in the hive weight following the increases in hive CO_2 production and CO_2 concentration suggests that foragers have flown from the hive to forage. Long-term experiments by this system will increase our understandings of the mechanisms of the social behaviors of the bee, such as controls of hive environment as well as dance behavior.

III. Future Plan

We found that 1) most follower bees turned away from dancers after one or two consecutive sessions of attendances of dances, 2) one follower attended to multiple dancers before the flight, and 3) most honeybees did not walk in her hive. It is expected that the probability of the failure foraging is high because of the small number of chance to listen to such dance information as “ambiguous” information about the location of the food source. However, even if the number of listening of each individual is small, the colony itself would obtain averaged information, if the number of honeybees that fly out for foraging is large. Bee colonies may overcome this problem caused from impression information in this manner. This possibility is an opposite direction of the design for engineering products that are never allowed to fail.

This coming year, we will incorporate biological parameters into our model that will be obtained by continuing behavioral experiments and by our two automatic measuring systems. We hope to propose mechanisms of adaptive behaviors that honeybees perform in their foraging.

We believe that our research is not merely a topic for biology, and that the mechanisms for maintaining a society by the sharing of information will have useful applications to practical utility, such as, optimization and control of robots under a multi-agent environment.

IV. References

[1] K. von Frisch, *The dance language and orientation of bee.* Harvard University Press, Cambridge, Massachusetts, London, 1993

[2] J. M. Gould and C. G. Gould, *The honey bee.* Scientific American Library, New York, 1988

[3] A. Michelsen, “The transfer of information in the dance language of honeybees: progress and problems”, *J Comp Physiol* vol. 173, pp. 135-141, 1993

[4] A. Michelsen, “Signals and flexibility in the dance communication of honeybees”, *J Comp Physiol* vol. 189, pp. 165-174, 2003

[5] R. Okada, H. Ikeno, N. Sasayama, H. Aonuma, D. Kurabayashi, and E. Ito “The dance of the honeybee: how do honeybees dance to transfer food information effectively?”, *Acta Biol Hung*, vol. 59 (suppl), pp. 157-162, 2008

[6] H. Ikeno, N. Sasayama, R. Okada, E Ito “Behavioral analysis of honeybee waggle dance and its effect on foraging”, 2nd International Symposium on Mobiligence in Awaji, 223-226, 2007

[7] R. Okada, H. Ikeno, H. Aonuma, and E. Ito “Biological insights into robotics: honeybee foraging behavior by waggle dance”, *Adv Robotics* vol. 22, pp. 1665-1681, 2008.

[8] T. Kimura, H. Ikeno, R. Okada, E. Ito. “A Study for identification and behavioral tracking of honeybees in the observation hive using vector quantization method”, Proc Measuring Behavior 2008, pp. 165-166, 2008.

[9] M. Ohashi, R. Okada, T. Kimura, H. Ikeno. “Observation system for the control of hive environment by the honeybee (*Apis mellifera*)”, *Behav Res Methods, in press*, 2009.

[10] M. Beekman, RL Fathke, and TD Seeley. “How does an informed minority of scouts guide a honeybee swarm as it flies to its new home?”,*Anim Behav* vol. 71, pp. 161-171, 2006.

Social risk representation in primate caudate nucleus

Gustavo S Santos[1], Yasuo Nagasaka[4], Kazuhito Takenaka[3], Atsushi Iriki[2], Hiroyuki Nakahara[1,5] and Naotaka Fujii[4]

***Abstract*—Research in reward-oriented behavior has focused on nonsocial contexts. However, social life often requires the suppression of reward-oriented behavior when competing with a dominant peer. We address this issue by examining the neural activities of Japanese macaque in two tasks: (1) the human sits beside the monkey and at times competes for baits placed within their reach; (2) a monkey is handed food by a dominant human who may: let the monkey take the bait; deny it by closing his hand; or drop it out of reach. We recorded fro m the prefrontal cortex (PFC), caudate nucleus (CN) and the parietal cortex, and analyzed the activity during the preparatory period. In all three areas, the induced social state is an important modulating factor during the reward-oriented behavior. At least 1/3 of the modulated neurons overlap across t asks, suggesting that some neurons recognize social cues independently of the setting.**

I. INTRODUCTION

Our outstanding intelligence compared with other species is thought to be evolutionally acquired through strategic communication with other individuals in the society. The intelligence is called social intelligence that enables us complex social behaviors, i.e. making and breaking alliance, rules, promises, misleading, misdirection, lying and truth-telling. Those behaviors are intentionally selected depending on circumstance and performed at the right moment when it becomes the performance the most effective.

However, our daily social behavior does not always require strategic view but requires more tactical view. What is the most essential social brain function is social decision function. Since, social brain function aims to obtain maximal reward while avoiding social conflict with other, deciding whether triggering certain action or not is primarily important. But the neural mechanism of the function remains unknown.

In past few years, we have devoted developing new experimental environment for revealing social brain function in monkeys. The technique, called multi-dimensional recording technique (MDR) combines multi-electrode recording technique and motion capture system that allow recording neural activity from multiple sites of brain and kinematic motion of monkeys and human experimenter simultaneously. By using MDR technique, we have found that parietal cortex and prefrontal cortex modulate neural activity depending on social context at the time.[1-3] Parietal cortex changed response pattern of self and other's motion. In contrast, prefrontal cortex modulated baseline activity depending on social behavioral manner, whether if the monkey was behaving as dominant or submissive one. These preliminary studies forced us to reveal further mechanism of social decision-making.

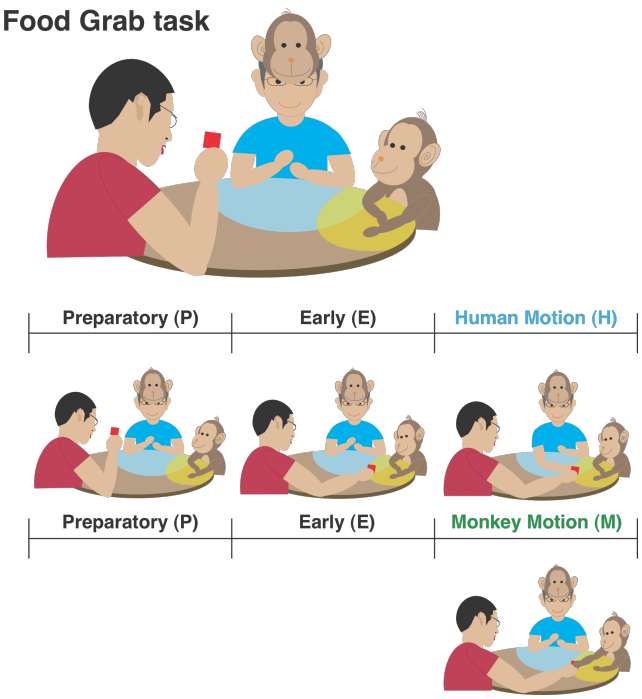

Fig 1. Monkey and human competitors sit side-by-side and get baits placed by experimenter. The human competes for the baits between himself and the monkey. Trials are segmented into 3 Periods according to the motion of experimenter, human and monkey.

Research in reward-oriented behavior has been conducted primarily in nonsocial contexts. However, animals that form social hierarchies commonly suppress their reward-oriented behavior when competing with a dominant. The neural mechanism for this social suppression remains elusive. We begin to address this issue by examining the neural activities of Japanese macaque in a task of simulated competition.

II. METHOD

Two Japanese monkeys were used for entire experiment. Before recording, we chronically implanted tungsten thin

1Integrated Theoretical Neuroscience Lab, RIKEN BSI, Japan, 2 Symbolic Cognitive Development Lab, RIKEN BSI, Japan 3 ISI, School of Info. Science and Tech., U. of Tokyo, Japan, 4 Adaptive Intelligence Lab, RIKEN BSI, Japan,5 Comp Intelli and Syst Sci., Tokyo Inst. of Tech., Japan

electrodes into brain that aim recording neural activity from prefrontal cortex (PFC) and caudate nucleus (CN). Neural activity was recorded from PFC and CN, when monkey was performing tasks, Food Grab task and GO, No-GO task. (Figure 1 and 2)

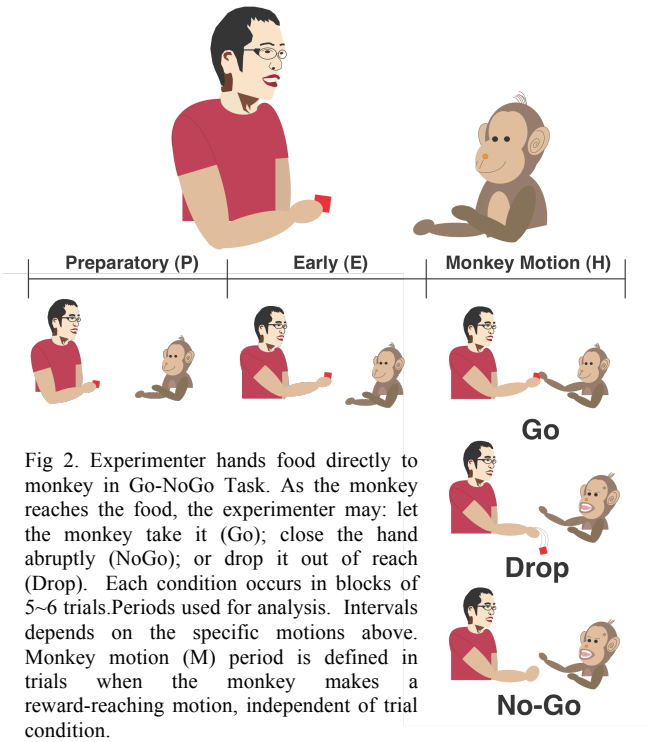

Fig 2. Experimenter hands food directly to monkey in Go-NoGo Task. As the monkey reaches the food, the experimenter may: let the monkey take it (Go); close the hand abruptly (NoGo); or drop it out of reach (Drop). Each condition occurs in blocks of 5~6 trials.Periods used for analysis. Intervals depends on the specific motions above. Monkey motion (M) period is defined in trials when the monkey makes a reward-reaching motion, independent of trial condition.

Food Grab task (Figure 1) used in this experiment is similar to the one used in previous studies. In previous studies, two monkeys shared social environment. If their peri-personal spaces were overlapped, there was a conflict occurred between animals to get reward. Under such condition, dominant monkey always took reward placed at conflict area, and submissive rarely received reward because of social suppression. In the current study, human subject joined the task by showing two alternative roles, one is dominant and the other is submissive. When the subject was pretending as dominant monkey, he always showed eagerness to take reward in conflict space. If the subject showed aggressive behavior, monkey seemed to take the behavior as dominancy, thus suppressed to take reward in the space under such condition. In contrast, if the subject showed less interest to take reward, monkey took the behavior as submissiveness, so that monkey altered behavioral mode into dominant monkey and started to take all of reachable reward. They always get baits placed in the noncompetitive space.

In, GO and No-GO task (Figure 2), there was no competition like Food Grab task. In each trial experimenter took a reward and tried to pass the reward to monkey. In GO trial, experimenter passed the reward to monkey. In No-GO trial, experimenter moved his hand toward monkey as if he was going to pass reward. But at the end of the motion, experimenter closed his palm and denied to pass reward. In Drop task, experimenter moved his hand toward monkey as if he was going to pass reward to monkey, but dropped the reward through fingers just before monkey reached to the reward. These three conditions were separated by block.

Recorded Area	Monkey A	Monkey B
PFC (Area 46)	75 (51)	53 (46)
Parietal (Area 5)	72 (59)	38 (34)
CN	118 (73)	59 (35)

TABLE 1

III. RESULTS

We recorded neural activity from PFC (n=128), Parietal cortex (n=110) and CN (n=177) in two monkeys (Table 1) and analyzed the activity in intervals before ('pre-motion intervals') and during ('motion intervals') the reward-reaching motions of both human and monkey.

During the motion intervals, the spiking activity in many CN and parietal neurons is enhanced as the human stops

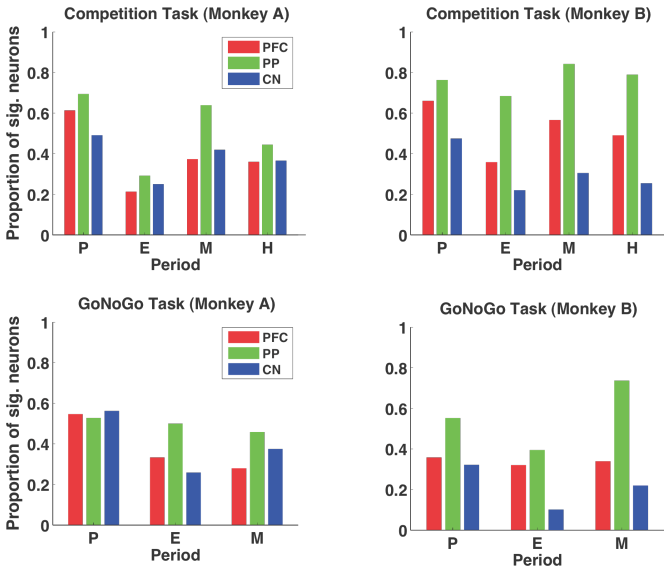

Fig 3. A sizeable ratio from all areas had significant activity relative to Inter-Trial Intervals (ITI) over all periods and tasks. Frames of significant motion were excluded from ITI.

competing and the monkey reaches the baits in the shared space, irrespectively of laterality. Reaching for baits in the noncompetitive space also causes excitation, though less strongly both at the population and individual neuronal level. The difference in the excitatory effect between reaching in the shared space versus the noncompetitive space is largest in the caudate neurons.

In contrast, the activity of PFC neurons during the motion intervals take a different nature. Activity of several PFC neurons is enhanced during the human's competitive motion

on the contralateral side, and is inhibited during the monkey's reward-reaching motion on the ipsilateral side.

During the pre-motion intervals, both parietal and CN neurons exhibit contralateral preference for the bait placement location. Caudate neurons furthermore have a contralateral preference for the human's position. This preference is maintained even during the active competition blocks. We suggest that the pre-motion activity in the CN neurons expresses the social constraints for the reward-reaching motion, but is not by itself predictive of the monkey's motion.

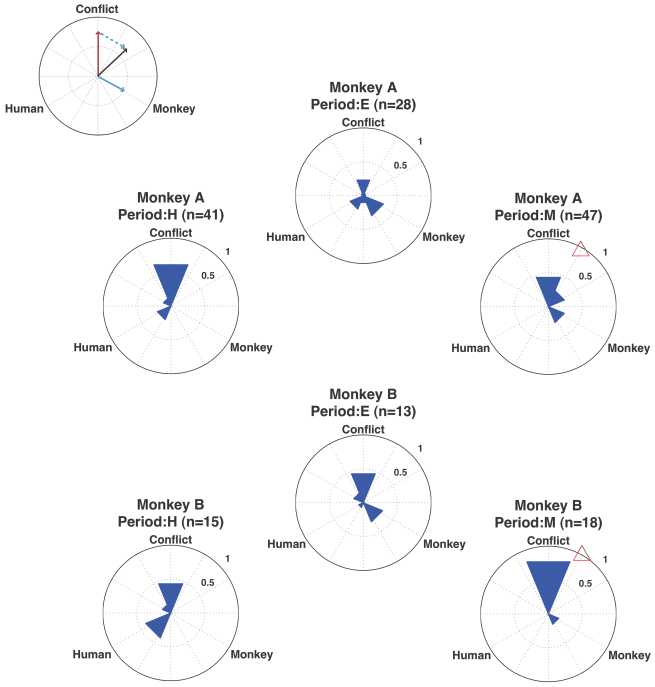

Fig 4. Histogram of net preference vectors for Food Location in Competition task. Note strong preference for Conflict location during Period M (indicated by △).

Then we have tested if neurons have preference to specific task condition in terms of social context and found it only in CN not in PFC and parietal cortex. Figure 4 is showing that CN neurons presented preference to conflict condition not to other non-conflict condition. The tendency became significant during M and H period but not significant during E period. And it was common in both monkeys. The result suggested that CN neurons are more sensitive to conflict in space regardless of monkey's social hierarchical status.

The finding guided us to see if these CN neurons are responding to social pressure or loosing reward. To compare contribution of those factors, we compared neural response between GO, No-GO and Drop condition. Figure 5 shows that CN neurons have preference to NO-GO trial compared to Go and Drop trial. This finding together with preference to conflict space in Figure 4 is suggesting that CN neuron are responding more when social pressure is present. But

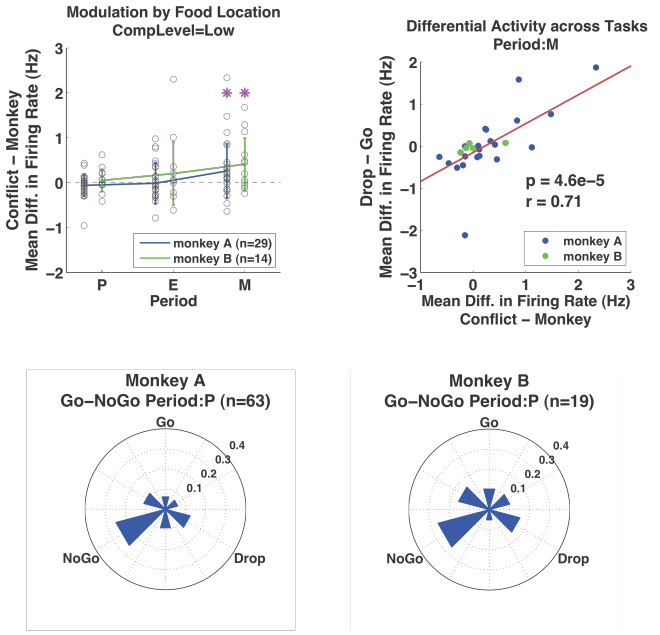

Fig 5. A) Differential activity of the neurons from Fig. 4 over different periods. Population preference for Conflict location becomes significant only in Period M. B) Relation between modulation in Period M of Fig. 4 and modulation between Drop and Go trials in Period M of Go-NoGo task. The strong correlation suggests a common function for the CN neurons across tasks. C) Strong CN neuron preference for NoGo condition during period P.

these neurons did not show response to Drop and GO condition. It is suggesting that CN is more conflict sensitive. Thus, we plotted correlation in firing rate between conflict trial in Food Grab task and No-GO task. Figure 5B indicates significant correlation between these factors. (r=0.71)

Overall, we detected strong and varied modulations in the neural activity in all recorded areas due to the presence of the competing human, even as the monkey's behavior is not altered during noncompetitive trials. We shall discuss that the observed modulations are related to the computation of adequate and desirable behavior in social context, and suggest possible roles for each area.

IV. Discussion

We performed two tasks to investigate the interaction between social and reward-oriented behaviors in two monkeys, while examining the activity in three brain areas: PFC, PP and CN. Sizeable ratios of neurons in all areas have significant task-related activity in every period. CN neurons are strongly modulated by human and monkey motion during Conflict trials relative to similar motions during non-Conflict trials. Comparison across tasks suggests that CN neurons could indicate a general risk or uncertainty. The uncertainty may be related to the expected reward (Go-Drop modulation in Go-NoGo task), as well as to the social risk (Conflict-Monkey modulation in Competition task, and NoGo-Drop modulation in GoNoGo task).

These results suggest that CN is involved in uncertainty cognition related to unpredictable social environment for making socially correct behavior.

REFERENCE

[1] Fujii N, Hihara S and Iriki A Social cognition in premotor and parietal cortex, *Social Neurosci*. 3(3-4):250-60, 2008

[2] Fujii N, Hihara S and Iriki A. Dynamic Social Adaptation of Motion Related Neuorns in Primate Parietal Cortex, *PLoS ONE* Apr 25;2:e397, 2007

[3] Fujii N, Hihara S, Nagasaka Y and Iriki A Social state representation in prefrontal cortex, *Social Neurosci*. May 23:1-12. 2009

Group D: On Common Principle of Mobiligence

Koichi Osuka, Kobe University

1.Intruduction

A common principle of Mobiligence observed in various living things is considered in Group D. To do so, we should explain the principle as objective as possible. That is, we try to express various phenomena in living thing by mathematical or physical way. Now, some hypotheses are going to propose in Group D. Multi-Layer, Multi-Feedback, Multi-Optimality of Prediction Mechanism are the examples. We expect that one of the common principles of Mobiligence is understood if these are expressible unitedly in the word of the mathematic. In this note, we report the results in Group D in 2008.

2.Structure of Group D

In Fig.1, we show the hypothesis in Group D and the relation between each hypothesis and the member of Group D.

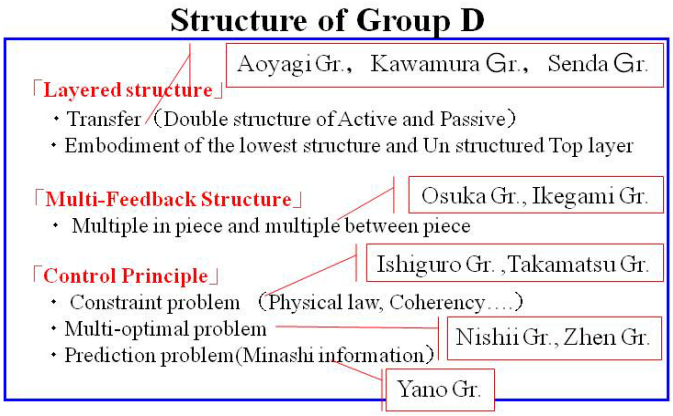

Fig.1 Structure of Mobiligence, and research allotment

D01-01 Voluntary movements controlled by "Mi-Nashi" created in the motor cortices (Leader:Masafumi Yano, Tohoku University)

A voluntary movement is an action that the biological system makes for carrying out an aim with adapting unpredictable environments. The aim of the movement can be acquired by the system having "Mi-Nashi". As a higher constraint for resolving the ill-posedness in motor control, "Mi-Nashi" has to set practical constraints in various levels of control mechanisms in real time. Here, we focused attentions on the reaching movement and addressed the following two issues.

(1) We analyzed our adaptive, autonomous decentralized model for arm reaching motion, in which a joint command is determined through mobility-based interactions among joints. It was clarified that the model includes two different type controllers, i.e., spring/accurate ones, and they are switched in real-time depending on difference of mobility among joints.

(2) For investigating characteristics of the arm reaching movement, we developed a manipulandum system, which is composed of a lightly- and compactly-designed two-link unit that measures the hand position and applies an arbitrary force to the hand, and two sliders that move the two-link unit in 2 dimensional space. Using the manipulandum system, we examined how the human arm control system would adapt to an unpredictable environment. Fig.2.

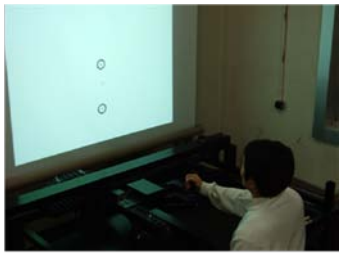

Fig.2 Manipulandum system

D01-02 Discovery and development of dynamical common principle of mobiligence (Leader: Koichi Osuka, Kobe University)

We started to think of Mobiligence from motion control function, formulated a problem named "Problem of inseparability between controlled object and control law". Then we clarified the existence of Embedded control law, and claimed that the passive dynamic walking problem is a example of solving the problem.

D01-03 Understanding Mobiligence from Coupled Oscillators with Simple Motile Function (Leader: Akio Ishiguro, Tohoku University)

In this year, we have been aiming at designing the hardware of Slimebot. Since the experimental study is still in the early stage, this paper deals with the locomotion of Slimebot consisting of only several real physical modules. The obtained results, however, strongly suggest that this hardware enables highly scalable adaptive locomotion (see Fig.3).

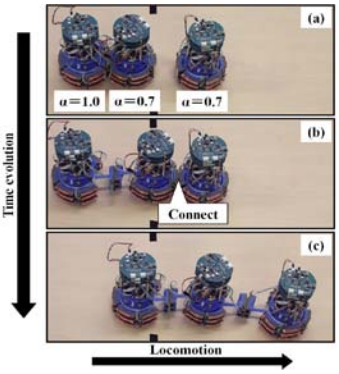

Fig.3 Slimebot

D01-11 Studying autonomous robots and explorative behaviors of flies to understand biological autonomy (Leader: Takashi Ikegami, The University of Tokyo)

In order to see the mechanisms of biological/artificial autonomy, we studied explorative behavior of a housefly and a simple vehicle-like robot MIURO. A main discovery was that 1) chaotic itinerant behaviors in both cases, 2) anomalous diffusion in a fly motion and 3) inventing the third robot time scale to reconcile autonomy and meaningful behavior.

D01-12 Emergence of mobiligence by environment-generation in flapping flight of butterfly (Leader: Kei Senda, Kyoto University)

A.Biological Approach: An experimental system with a low-speed wind tunnel is constructed. The motion and aerodynamic forces of actual butterflies are measured quantitatively. Moreover, their musculoskeletal structure has been analyzed by using micro-XCT image to clarify their possible active motion.

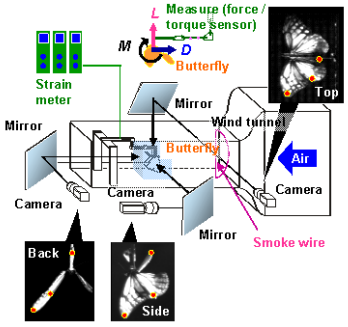

Fig.4 Experimental system

B. Technological approach: A two- dimensional mathematical model is developed to achieve steady flight by focusing on butterfly's attitude. The recovery motion after a large perturbation has been investigated (Figure 4), and the state transition ability will be analyzed. Moreover, three-dimensional mathematical model has been constructed. Its validity and accuracy are examined by comparing with the experimental data.

D01-13 A study on adaptation to environments in a network of dynamical elements (Leader: Toshio Aoyagi, Kyoto University)

We first investigate co-evolving dynamics in a weighted network of phase oscillators. It is found that this system exhibits three kinds of asymptotic behavior: a two-cluster state, a coherent state with a fixed phase relation, and a chaotic state with frustration. Next, to clarify a mechanism of episodic memory formation in the hippocampus, we made a model for the hippocampal CA3 and CA1. We obtained, for the model CA3, a successive association of stored patterns, which can be regulated by emergent chaotic activity of neural networks. We found in the model CA1 a Cantor set in the membrane potentials of CA1 neurons, and clarified the functional significance of this set in relation to episodic memory. On the basis of these findings, we will explore the essential mechanisms of neuronal systems for emergence of adaptation through interaction among the body, brain and environment.

D01-14 Basic strategy for trajectory planning in living movements (Leader: Jun Nishii, Yamaguchi University)

We studied the following two topics: (1) how living bodies constrain and utilize their redundancy during usual movements, and (2) how they efficiently acquire the ability to manipulate their redundant bodies.(1) Authors have shown that typical leg swing trajectories during human walking is similar to the optimal one which minimizes energy cost. Furthermore, our recent result has shown that swing trajectories of backward walking and monkey's biped walking are also similar to those minimizing energy cost. These results suggest that the minimization of the energy cost is an basic strategy for legged locomotion. On the other hand, movement trajectories of living bodies often show variability. We found that the variability of joint trajectories during monkey biped-walking are constrained so as to suppress the variability of the foot position in the end of swing phase (Fig.5). (2) Bernstein pointed out that human freezes their redundant actuators in the beginning of learning and acquires the ability to manipulate them by freeing the frozen degrees of freedom as learning proceeds. We took a simulation experiment of learning control of a redundant arm in order to confirm the validity of the Bernstein's hypothesis, and the result have suggested that efficient learning can be realized by freezing and freeing of wrist stiffness.

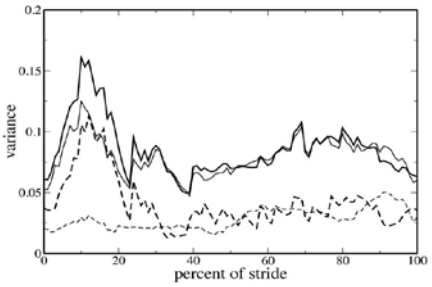

Fig. 5 Time profile of variability of joint angle during biped walking of Japanese monkey.

D01-15 Adaptive behavior and emergence of biological function by environment dependent tube networks in plasmodial slime mold（Leader: Atsuko Takamatsu, Waseda university）

Plasmodium of true slime mold is a giant multi-nucleated unicellular organism. It crawls on environment by oscillating the cell thickness and conduct itself through the morphological change emerged by environmental signal. The plasmodium forms nutrient transportation network with tubes to maintain the giant cell body. We have analyzed the network topology depending on environment. In H. 20 fiscal year, we analyzed the structure of growing network by obtaining precise information on node dynamics and links and obtained the characteristics of the structure in attractive/repulsive environment. Our goal is to abstract an algorithm of adaptive behavior by dynamical network morphology using a both-side analysis of experiment and theory.Fig.6.

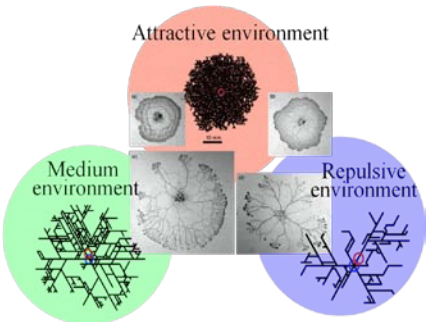

Fig.6 Network morphology

D01-16 Measurement and Modeling of Human Movement Mastery Process (Leader: Sadao Kawamura, Ritsumei-kan University)

The aim of this research is to clarify the movement mastery process of humans. For this, we have the following two approaches.

[1] Mathematical model approach

①We have proposed a new method which minimizes the energy of actuators by using adaptive mechanical stiffness control. It will be confirmed that a biped locomotion robot can go up a slope and stairs with minimum energy consumption by using Passive Active Combination.

②On a two DOF mechanism with six muscles, we will clarify the nonlinear mapping from a task space to a muscle space. Next, the characteristics of the internal forces among the muscles will be investigated. For this purpose, we have realized a numerical simulator which can show motions of the two DOF mechanism with six muscles. It has been revealed that the mapping from a task space to a muscle space can become linear.

[2]Living body measurement approach

We have developed a measurement system which makes inertia or elastic load. In the developed system, the process that subjects learn a desired motion is measured through the EMG of six muscles(Fig.7).

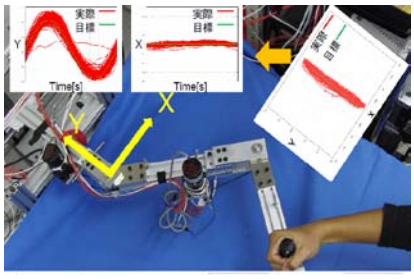

Fig 7 Measurement system

3. Conclusion

In this report, we described the image of of Mobiligence which will be constructed in Group D. And we also showed the abstract of the results from the members. The point of our policy is to describe the common principle of Mobiligence by using a kind of terminology of mathematics or physics.

Voluntary Movements Controlled by "Mi-Nashi" Created in the Motor Cortices.

Masafumi Yano, *Research Institute of Electrical Communication, Tohoku University*

1. INTRODUCTION

A voluntary movement is an action that the biological system makes for carrying out an aim with adapting unpredictable environments. The aim of the movement can be acquired by the system having "Mi-Nashi". As a higher constraint for resolving the ill-posedness in motor control, "Mi-Nashi" has to set practical constraints in various levels of control mechanisms in real time. Furthermore, for adapting unpredictable changes in conditions of the system and the environment, "Mi-Nashi" should emerge from the system itself depending on interactions between the system and the environment, and the system have to evaluate whether the emerged "Mi-Nashi" would be satisfied every moments. These are computational problems that the motor control system, i.e., the motor cortices, has to solve during the voluntary movement control in the real world. Here, we focused on the arm reaching movement and addressed the following two issues: i) mathematical analyses of the autonomous decentralized controller that we proposed; ii) development of the manipulandum system for analyzing human arm reaching movements.

2. ANALYSIS OF ADAPTABILITY OF THE AUTONOMOUS DECENTRALIZED ARM REACHING MODEL

As a multi-joint manipulator, human arm is redundant: the number of degrees of freedom granted by the joint is greater than that of the hand position. The redundancy of the arm allows the system to adapt to unpredictable changes of environment and body-conditions. To control the movement of the redundant arm, the controller must solve the following ill-posed transformation problems: (TF1) determining a desirable hand velocity based on the target hand position; (TF2) determining desirable angular velocities of joints based on the desirable hand velocity. For solving these problems, the system needs to have respective transformation matrices that are appropriately determined depending on the situations. So far, we have proposed a model of the arm reaching movement that solves the two transformation problems autonomously in decentralized manner [1].

In our model, a respective controller was allocated for each joint, which evaluated mobility of the joint, and communicated with other joints' controllers transferring the mobility information. Through this mobility based autonomous decentralized interactions, a hand motion was coordinated in which a more mobile joint worked dominantly and immobile ones cooperatively. Because such joint-level motion patterns were determined on-line, it was confirmed that the model was capable in keeping a hand motion robustly even when various environmental changes occurred unexpectedly.

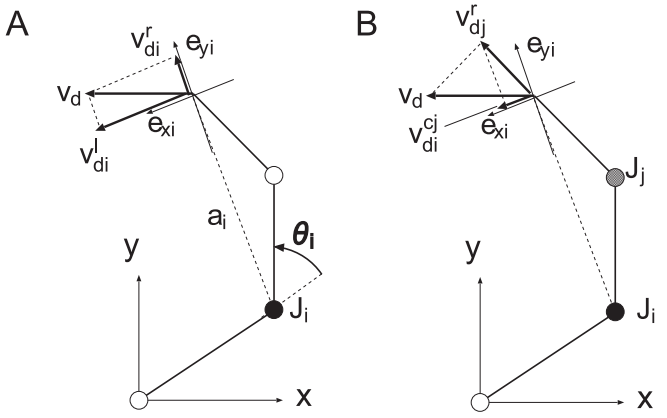

Fig. 1. Three-joint arm model. A: Definition of local vector for joint i and its residual vector. B: Definition of coupling vector relating joint j and joint i.

The robust performance of our model suggests that the transformation matrix might be created proficiently depending on the situations, but its mechanism is still unclear because the original controllers were described in a distributed manner. Here, we transform the description of the autonomous decentralized controllers into matrix-form description, and mathematically clarify the adaptive mechanism of the decentralized controllers as a whole system [2].

2.1. Autonomous decentralized model

For controlling planar m joints arm, our autonomous decentralized model was implemented as follows. First, to carry out the ill-posed transformation (TF1), a real-time hand command, termed as a desired hand velocity, $\boldsymbol{v}_d$, is calculated as:

$$\boldsymbol{v}_d = G_t(\boldsymbol{x}_d - \boldsymbol{x}), \tag{1}$$

where, $\boldsymbol{x}_d$, G_t, $\boldsymbol{x}$ are a desired hand position, a gain factor, and a current hand position, respectively.

Second, a command for a joint i, $\tilde{\boldsymbol{v}_{di}}$, is determined by a following autonomous decentralized network:

$$\tilde{\boldsymbol{v}_{di}} = \Pi^m_{j\neq i}(1-k_j)\boldsymbol{v}^l_{di} + \Sigma^m_{j\neq i} k_j \boldsymbol{v}^{cj}_{di}, \tag{2}$$

where, $\boldsymbol{v}^l_{di}$ is a component of $\boldsymbol{v}_d$ that the joint i can generate by its own rotation (we termed as a local vector, Fig.1 A), and $\boldsymbol{v}^{ci}_{dj}$ is a residual component of $\boldsymbol{v}_d$, which a joint j requests the joint i to generate (we termed as a coupling

vector, Fig.1 B). k_i is a "mobility measure" calculated from sensory information representing how the joint i is currently mobile. The mobility measure is defined as:

$$k_i = \exp[-4\ln 2(\|\boldsymbol{v}_{di}^l - \boldsymbol{v}_i\|^2 + \epsilon_1)/(\|\boldsymbol{v}_{di}^l\|^2 + \epsilon_2)], \tag{3}$$

where, $\boldsymbol{v}_i$ is a velocity resulted by a rotation of the joint i. ϵ_1 and ϵ_2 are tiny terms. When the joint i is mobile/immobile, it approaches to 1/0.

Finally, using a simple inverse kinematics and a velocity feedback, a desired angular speed, $\dot{\theta}_{di}$, and a desired joint torque, τ_{di}, for the joint i are calculated as:

$$\dot{\theta}_{di} = \tilde{\boldsymbol{v}_{di}} \cdot \boldsymbol{e}_{xi}/\|\boldsymbol{a}_i\|, \tag{4}$$

$$\tau_{di} = G_i(\dot{\theta}_{di} - \dot{\theta}_i), \tag{5}$$

where, G_i is a feedback gain factor. As a result, Eq. (5) represents the controller for each joint in autonomous decentralized form.

2.2. Matrix form transformation of the proposed model

To clarify the adaptive mechanism of our decentralized model, we transform the autonomous decentralized form of Eqs. (4) and (5) into combined matrix forms as follows:

$$\dot{\boldsymbol{\theta}}_d = \left[\boldsymbol{K}_l\boldsymbol{D}^{-1}\boldsymbol{J}^T + \boldsymbol{D}^{-1}\boldsymbol{J}_\perp{}^T\boldsymbol{J}\boldsymbol{D}^{-1}\boldsymbol{K}_c\boldsymbol{J}_\perp{}^T\right]\boldsymbol{v}_d, \tag{6}$$

$$\boldsymbol{\tau}_d = \tilde{\boldsymbol{J}}(\boldsymbol{\theta},\dot{\boldsymbol{\theta}})^T G_t(\boldsymbol{x}_d - \boldsymbol{x}) - \boldsymbol{G}\dot{\boldsymbol{\theta}}, \tag{7}$$

where, $\dot{\boldsymbol{\theta}}_d = [\dot{\theta}_{d1},\cdots,\dot{\theta}_{dm}]^T$, $\boldsymbol{\tau}_d = [\tau_{d1},\cdots,\tau_{dm}]^T$, $\boldsymbol{G}$ =diag$[G_1,\cdots,G_m]$, $\boldsymbol{J} = \partial\boldsymbol{x}/\partial\boldsymbol{\theta}$, $\boldsymbol{J}_\perp = R_{90}\boldsymbol{J}$($R_{90}$: a rotation matrix), and $\boldsymbol{D}$ = diag$(\boldsymbol{J}^T\boldsymbol{J})$. $\tilde{\boldsymbol{J}}(\boldsymbol{\theta},\dot{\boldsymbol{\theta}})$ is defined as:

$$\tilde{\boldsymbol{J}}(\boldsymbol{\theta},\dot{\boldsymbol{\theta}}) \equiv \left[\boldsymbol{G}\boldsymbol{K}_l\boldsymbol{D}^{-1}\boldsymbol{J}^T + \boldsymbol{G}\boldsymbol{D}^{-1}\boldsymbol{J}_\perp{}^T\boldsymbol{J}\boldsymbol{D}^{-1}\boldsymbol{K}_c\boldsymbol{J}_\perp{}^T\right]^T. \tag{8}$$

Eq. (8) varies depending on k_i in real-time, and it transforms the desired hand velocity into the joint torque. Thus, we termed Eq. (8) as a variable Jacobian matrix.

2.3. Characteristic property of the variable Jacobian matrix

It is obvious that the variable Jacobian matrix, $\tilde{\boldsymbol{J}}(\boldsymbol{\theta},\dot{\boldsymbol{\theta}})$, plays an important role in adaptability of our controller as a whole system. Following mathematical analysis of the matrix in the case of the all mobility measures as zero or one helped us to understand the qualitative characteristics intuitively.

1) In case that the mobility measures are all zero: When all mobility measures are zero, $\boldsymbol{K}_l$ and $\boldsymbol{K}_c$ in Eq. (8) turns out to be an identity matrix and a zero matrix, respectively. Thus, Eq. (8) can be written as a following simple expression:

$$\tilde{\boldsymbol{J}}(\boldsymbol{\theta},\dot{\boldsymbol{\theta}}) = [\boldsymbol{G}\boldsymbol{D}^{-1}\boldsymbol{J}^T]^T. \tag{9}$$

Thus, the controller (7) can be described as:

$$\boldsymbol{\tau}_d = \boldsymbol{G}\boldsymbol{D}^{-1}\boldsymbol{J}^T\boldsymbol{G}_t(\boldsymbol{x}_d - \boldsymbol{x}) - \boldsymbol{G}\dot{\boldsymbol{\theta}}. \tag{10}$$

The term $\boldsymbol{D}^{-1}\boldsymbol{J}^T\boldsymbol{G}_t(\boldsymbol{x}_d - \boldsymbol{x})$ is an angular velocity vector. Each component of the term is a desired angular speed of respective joint, which corresponds to the signed norm of the local vector of the desired hand velocity divided by each moment-arm. Thus Eq. (10) implies that all the joints moves independently only based on the target position and current hand position, and consequently the hand moves spring-like toward the target position. According to this characteristic of (10), we term Eq. (9) as a spring-like matrix.

2) In case that the mobility measures are all one: When the mobility measures are all one, $\boldsymbol{K}_l$ and $\boldsymbol{K}_c$ in (8) results in a zero and an identity matrix, respectively. Thus, Eq. (8) can be written as:

$$\tilde{\boldsymbol{J}}(\boldsymbol{\theta},\dot{\boldsymbol{\theta}}) = [\boldsymbol{G}\boldsymbol{D}^{-1}\boldsymbol{J}_\perp{}^T\boldsymbol{J}\boldsymbol{D}^{-1}\boldsymbol{J}_\perp{}^T]^T \tag{11}$$

Thus, the controller (7) turns out to be:

$$\boldsymbol{\tau}_d = \boldsymbol{G}\boldsymbol{D}^{-1}\boldsymbol{J}_\perp{}^T\boldsymbol{J}\boldsymbol{D}^{-1}\boldsymbol{J}_\perp{}^T\boldsymbol{G}_t(\boldsymbol{x}_d - \boldsymbol{x}) - \boldsymbol{G}\dot{\boldsymbol{\theta}}. \tag{12}$$

For the matrix $(\boldsymbol{D}^{-1}\boldsymbol{J}_\perp{}^T\boldsymbol{J}\boldsymbol{D}^{-1}\boldsymbol{J}_\perp{}^T)$ in (12), a following equation holds:

$$\angle[\boldsymbol{J}(\boldsymbol{D}^{-1}\boldsymbol{J}_\perp{}^T\boldsymbol{J}\boldsymbol{D}^{-1}\boldsymbol{J}_\perp{}^T\boldsymbol{v}_d)] = \angle\boldsymbol{v}_d. \tag{13}$$

From Eq. (13), the hand moves in a direction of $\boldsymbol{v}_d$ accurately, when the joints controlled by Eq. (12). According to this, we termed Eq. (11) as a directional matrix.

3) Emergent property of the transformation matrix: These analyses in the two extreme cases reveal that the variable Jacobian matrix can work in two different control modes, i.e., spring-like and accurate directional ones. We can now see the qualitative property of the variable Jacobian matrix during movement, in which the mobility measures of each joint have different values (between 0 and 1). For instance, suppose the mobility measure of joint i is larger than those of the other joints. Because the (i,i) component of $\boldsymbol{K}_l$ becomes the largest, we see that the joint i is dominantly controlled by the spring like matrix, (9), while the others by the directional matrix, (11). Thus, it is clarified that the variable Jacobian matrix, or our controller, has an autonomous and flexible function, assigning two contrasting strategies, spring-like and directional ones, to mobile and immobile joints respectively, depending on the value of mobility measures.

With this autonomous and flexible function, our controller acquires an adaptability to unexpected changes, such as sudden target shift, configuration change during motion, and partial malfunction of a joint.

In previous approaches to arm reaching movements, the transformation matrices for (TF1) and (TF2) were considered to be given a priori or to be learned through repetitive try and errors. In our approach, on the other hand, mathematical analysis shows that our controller enables to create the transformation matrix with the adaptive function in real-time based on sensory information. Thus, we conclude that our autonomous decentralized approach is effective in solving the ill-posed problems in human movement control adaptively in the real environment.

3. Design and development of Manipulandum

3.1. Design of manipulandum

In unpredictably changing environment, biological systems set movement goals and carry out them flexibly. Voluntary movements can be defined as such goal-oriented movements. Visually guided arm reaching movement is one of important voluntary movements. In our daily life, we make the reaching movement in various situations, e.g., grasping an object while walking or running, grasping a moving object while sitting, and etc. In such situations, visual information of the target changes during movement execution. Thus, according to such changes, the system must create control commands in real time to successfully carry out movement goals.

To present various dynamical environments to subjects during arm movements, manipulators that are called " manipulandums "have been developed, and using them, mechanisms adapting to environmental changes have been investigated. So far, it has been thought that the control system would adapt to the environmental changes by modifying and adjusting its internal model of the environment trial by trial, and consequently each sub-system for planning, feed-forward and feed-back in the controller system would adapt to the environment progressively. In this scheme, however, it is difficult to understand an ability to adapt to dynamically changing environments.

The aim of our study is to examine how we adapt ourselves to a newly environment in one trial. We hypothesize that it is possible to understand an adaptation process in the early, middle, and late stages of the reaching movements, distinctively, by measuring reaching movements under various visual and mechanical perturbations. So, we developed a new manipulandum system for analysing human arm reaching movement. This system allows subjects to execute reaching movements with lower mechanical or cognitive load. It includes two independent mechanical servo systems, position and force one. When a subject moves the servo-driven grip, frictional force that a subject feels is small (only few newtons) and subjects can move their hand natullary. Manipulandum has the visual stimulation system using a half mirror. There is no discrepancy between vision and body coordinate systems.

3.2. Manipulandum setup

The manipulandum (Fig.2) includes 1) a manipulator-slider mechanism to present a force to a subject's hand and to measure its position, and 2) an apparatus for presenting visual stimuli to subjects.

1) Manipulator-slider mechanism: The manipulator-slider mechanism (Fig.3) includes a servo driven grip, a 2-joints manipulator, and two servo-driven sliders.

The servo-driven grip is fixed on a tip of a 2-joints robot manipulator each driven by two DC motors. They can be programmed so that the robot manipulator generates an arbitrary force to the grip. So, holding the serve driven grip, subjects can experience a newly force field environment.

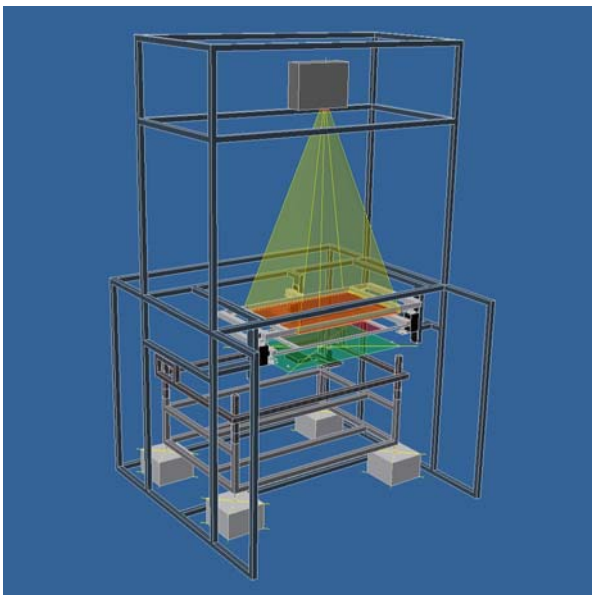

Fig. 2. Manipulandum setup.

TABLE I
MANIPULANDUM SPECIFICATION

Strokes	$X = 1000\text{mm}, Y = 600\text{mm}$
Maximum hand speed	2m/s
Maximum hand acceleration	6m/s^2
Positional resolution	12.5μm/count
Hand force sensor	$\pm$60N(10%)
Hand force application range	$\pm$20N($\pm 5\%$)

To study adaptation processes in such newly force environment, it is desirable that subjects can execute motions in a large workspace in as natural as possible especially when any force field is not applied to the hand (i.e., null field). To realize this, we produced the robot manipulator as light and short as possible. Also, to compensate for the inertia of the manipulator and to make the workspace extensive, we designed a manipulator mounter movable; the mounter is on two orthogonal servo-sliders in X and Y directions. The servo-driven grip is on a base plate which is connected to the mounter. The servo-sliders are programmed to control so that the position of the servo-driven grip is always at the center of the base plate. When the subject moves the servo-driven grip, the sliders are controlled so that the base plate tracks the subject's hand.

This control allows the manipulator to keep unchanged configuration relative to the base plate, so that the subject is not forced to move the manipulator mechanisms (i.e., inertia compensation). Also, it helps to make the hand workspace wide-range which covers almost all area that the human arm can reach ($1000\text{mm} \times 600\text{mm}$). In addition, because the manipulator configuration is unchanged, programming force field is easy because the hand force ellipse is almost unchanged. Specification of the manipulator-slider mechanism is summarized in TABLE I.

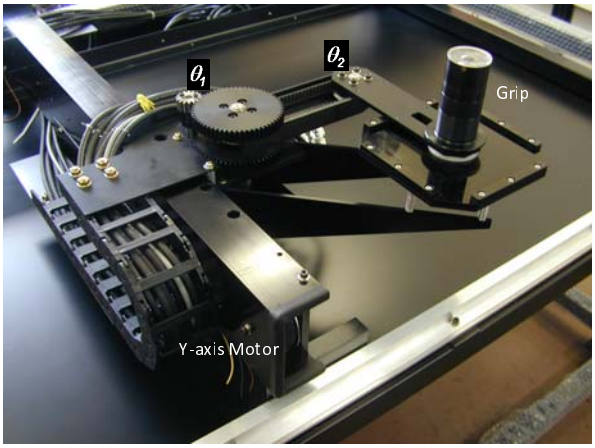

Fig. 3. Manipulator-slider mechanism.

2) Apparatus for presenting visual stimuli: The apparatus for presenting visual stimuli consists of a LCD projector, a frosted glass as a screen, and a half-mirror (Fig.2). The half-mirror reflects visual stimuli projected on the frosted glass, whereas it transmits images of the hand and the grip of the manipulandum. So, subjects sitting in front of the manipulandum can see the visual stimuli projected on the screen as they are on the plane where the hand and the grip are movable. Since this situation is very close to the natural situation, our stimulus-presentation method does not demand subjects to learn or acquire an apparatus-specific visuomotor map, and consequently allows subject to participate in arm reaching experiments without any particular training.

3.3. Measuring arm reaching movements

Using the developed manipulandum, we measured the arm reaching movements when visual information of the hand position was rotationally transformed at various degrees from the original hand position (visuomotor discrepancy). The hand position measured by the manipulandum was projected to the upright screen (Fig.4A). Subjects were instructed to move the hand position from a starting point to a goal point on the screen. The starting point was fixed (red circle in Fig.4A) and, in each trial, the target point was randomly selected from eight points around the starting point (blue circles in Fig. 3A). As visuomotor discrepancy, the hand position on the screen was rotated around the starting point. In each trial, the rotation was randomly selected from eight conditions (0, 45, 90, 135, 180, 225, 270 and 315 deg). The number of trials in one session was 64 (eight targets×eight rotations). Fig.4B-D shows typical results of the experiment, indicating that the rotation conditions would strongly affect the profiles of hand-trajectory and hand-velocity. To clarify how the human arm control system would adapt to an unpredictable environment, we are going to obtain the reaching data in various rotation conditions and various session conditions.

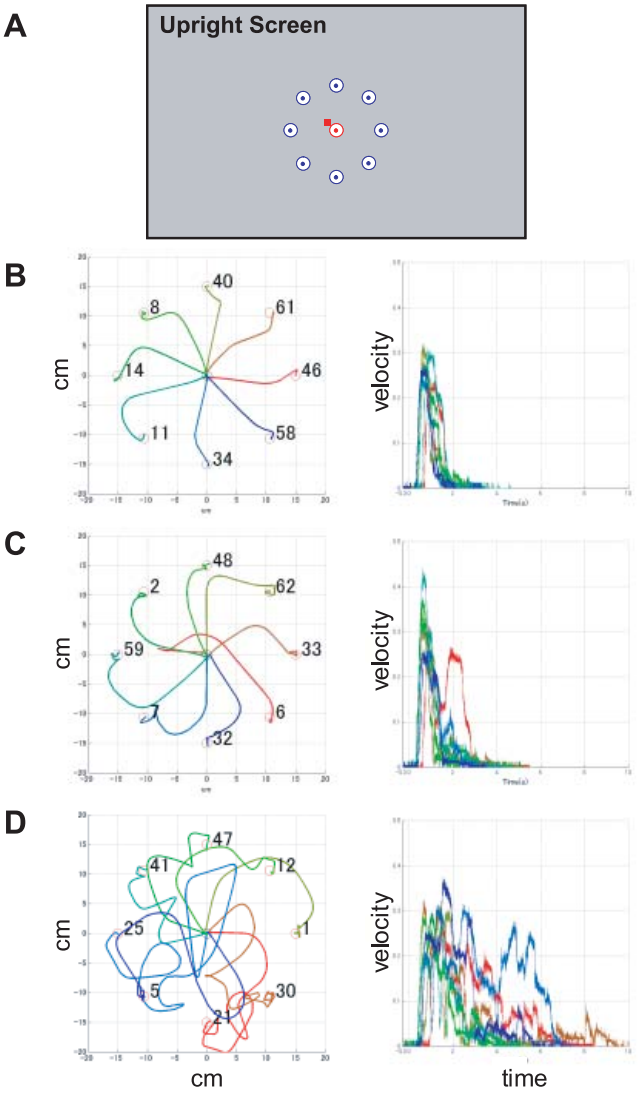

Fig. 4. Measurements of the arm reaching movements. A: Visual information. The starting point, the target position and the hand positions are presented on the upright screen. Red circle, starting point; blue circles, eight target positions; red square, hand position. B-C: Typical experimental results under three rotation conditions, 0 deg in B, 45 deg in C, and 90 deg in D. The trajectories and velocity profiles to the eight targets are shown in left and right panels respectively. Each color indicate the data obtained from respective target position.

REFERENCES

[1] Yoshihara Y, Tomita N, Makino Y, & Yano M (2007) Journal of Robotics and Mechatronics, 19, 4, 448-458

[2] Yoshihara Y, Tomita N, Makino Y, & Yano M (2009) Proceedings of 21st SICE-DAS, 123-128 (in Japanese)

Discovery and Development of Dynamical Common Principle of Mobiligence
－ Common Understanding of Artificial Thing and Living Thing －

Koichi Osuka(Kobe Univ.), Akio Ishiguro(Tohoku Univ.), Xin-Zhi Zheng(ASTEM)
Kuninari Ohgane(Kyusyu Univ.), Jiro Adachi(Hokkaido Univ.), Dai Owaki(Tohoku Univ.)

Abstract－In this note, we discuss the stand point of research of passive dynamic walking in the research of Mobiligence. Concretely speaking, we formulate Embedding problem. This problem says that there is a possibility of existence of implicit control law in the dynamics of controlled object. To solve the problem, we introduce a problem of inseparability and a closed loop problem and show a way to solve the two problems.

Key Words: Passive dynamic locomotion, Mobiligence, Embedding problem, Implicit control law

1. Introduction

In this report, the role that the research of passive dynamic walking pays in Mobiligence research is considered.

The phenomenon of passive dynamic walking is well known[1]. This is a phenomenon that a kind of walking machine without actuator walks down on the slight slope. This walking machine is so called Passive Dynamic Walker : PDW. See Fig.1[2)~5)] .

Fig.1 Passive Dynamic Walkers

PDW is an opposite existence from current most robots walking with two legs which perform ZMP standard walking, active walking by the entire body full control. And though it is stable as a walking phenomenon, the walking principles (stabilization principle) has not been completely clarified yet. To understand walking movement completely, a principle of passive dynamic walking should be understood to the same degree as actively- walking, but the goal has not been achieved yet. In this situation, the current situation of[6)~9)] has been gradually becoming clear that stabilization control law (additionally adaptive function) which has generated by walking vehicle (controlled object) and incline (environment) interference is embedded in PDW by experiments, simulations or theoretical analysis. We call this Implicit Feedback Structure[7)9)].

In contrast, organism has "Mobiligence" and the study on understanding and application of the mechanism is now proceeded[10]. Regarding the ability, an existence of locomotion ability is premise, so it should be considered that the ability is based on "motion control function". That is to say, to get closer to Mobiligence, it is necessary to start with seeking the mechanism of "motion control function". That is to say, it is necessary to do system analysis on organisms as control system. However, when trying to start to think of this problem, (stated in chapter 2.) "embedding problem "appears which is difficult to be clarified by 2 essential problems of "indivisible problem" and "closed loop problem". That is to say, to understand "Mobiligence", it reaches to the thought that first, clarification of "embedding problem " is necessary.

In this report, 2 essential problems are avoided and then it shows that "passive locomotion" is treated as a rare example of toehold for solving "embedding problem ". And we try to give a suggestion on understanding of Mobiligence with its toehold.

2. Control System of Mobiligence System

As stated in the previous chapter, to understand Mobiligence, organisms should be taken as control system and " clarify control law" in it is necessary. In this chapter, to do this, the necessity to consider problem, " embedding problem " which exists more deeply is stated.

Then, as Fig.2, considering a general structure of control system which can seen in control engineering, and the factors are applied to this figure for various organisms.

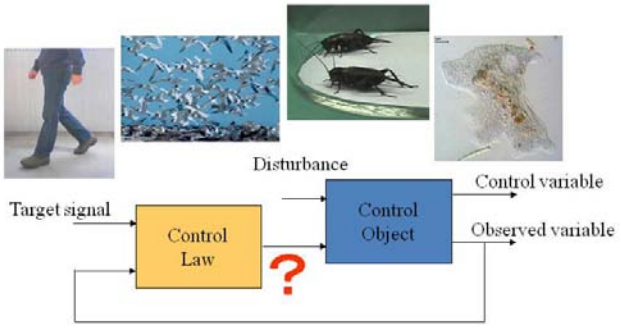

Fig.2 Traditional expression of control system

Then easily the following questions come out.

[Q1] When seeing individual, which is controlled object and which is control law in it ?

[Q2] Can boundary of controlled object and control law, or discrimination against environment be clarified?

Such questions deepen more by seeing an experiment of a cat whose brain has been removed shown in Fig.3. The cerebrum has been removed in this cat. (that is to say, there is no control law in a simple meaning.) In spite of this, walking pattern changes depending on speed of treadmill. CPG (central pattern generator) remains as the factors

in residual nervous system and an analogy that it generates pattern change is general. However, recently simulation that four-legged passive dynamic walking vehicle makes walking pattern change depending on change of inclined surface has been reported [5]. This indicates in some ways that walking is feasible even without control law. In contrast, a meaningful movement is performed, so it can be also considered that some sort of control law exists.

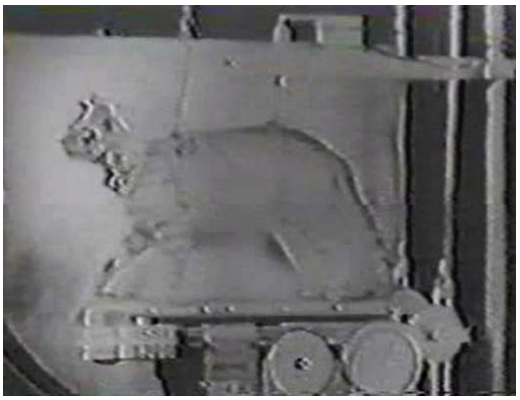

Fig.3 Decerebrate cat

Based on the above consideration, if venturing to describe organisms as control system, it can be drawn like Fig.4. This figure is a conceptual diagram, but by drawing such a picture, it can be rediscovered that to understand control law, the existence of the part which controlled object and control law appears to be overlapped should be clarified. That is to say, the following problem will be conscious clearly.

[Embedding problem] the problem of considering possibility that a part of control law is embedded in controlled object （Clarifying if control law is embedded in controlled object and furthermore, if so, what kind of thing is embedded）. □

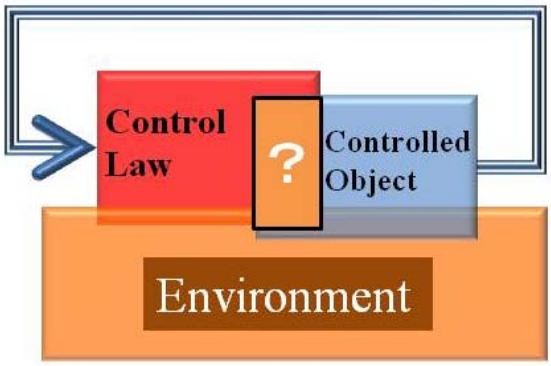

Fig.4 Realistic expression of control system in living thing

Therefore, eventually, a conclusion is drawn that an unequivocal answer for this embedding problem should be gotten to truly understand Mobiligence. Refer to Fig.5.

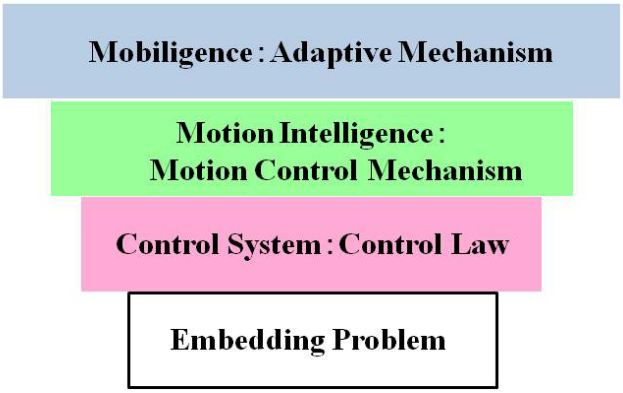

Fig.5 Structure of our question

Problems to be covered in this study will be summarized as follows.

[Problem] On the following hypothesis, proceeding to the goal.

[Hypothesis] There are many structures such as Fig.4 in Mobiligence system. That is to say, the problem structure which “embedding problem“ is considered is the common composition on thinking of Mobiligence.

[Goal] After clearing up ”embedding problem “, ”control law” is clarified.

3. Problem Avoidance Method

As factors which make the problem difficult to find the cause of “embedding problem “, the following 2 factors can be cited.

[Indivisible problem] In the motion control system of organisms, control law and controlled object is combined harmoniously and boundary or division of roles of the both is not always clear. □

[Closed loop problem] Originally it is closed loop system, so control law or controlled object itself can not be understood（identification）in principle by internal signal analysis. □

In this chapter, measures of avoiding ” indivisible problem” and ” closed loop problem” is considered.

First, as shown in Fig.4, regarding that overlapping of control law and controlled object（additionally environment）can be seen, 2 possibilities of the cases are considered. ; 1) there is a true intersection and 2) they are appearing to intersect by observation. If so, as the result that some sort of the axis of rotation （movement of corresponding point of sight）as shown in Fig.6 left figure can be assumed and a certain angle can be rotated around the axis, in the case that can be seen as shown in Fig.6 right figure, obscureness for this overlapping will disappear. That is to say, “decoupling “ can be achieved. Furthermore, though such a things have realized, in the case that it is found that a certain control law is still embedded in controlled object, we will call it ” Implicit Control Law”. And we will call （red）control law which has been separated as shown in the Figure as “Explicit Control Law” for the future.

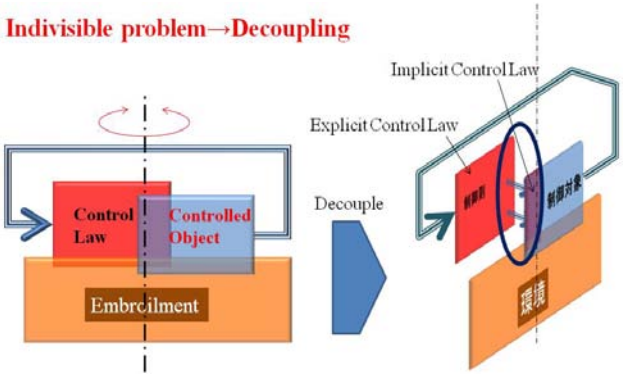

Fig.6 Transformation of problem: Decoupling

Next, we consider to avoid closed loop problem. To do this, loop should be cut by some sort of method. Refer to Fig.7. In this cut, there are possibilities of a method of cutting physically（anatomic level） and method of discreating loop by movement selection.

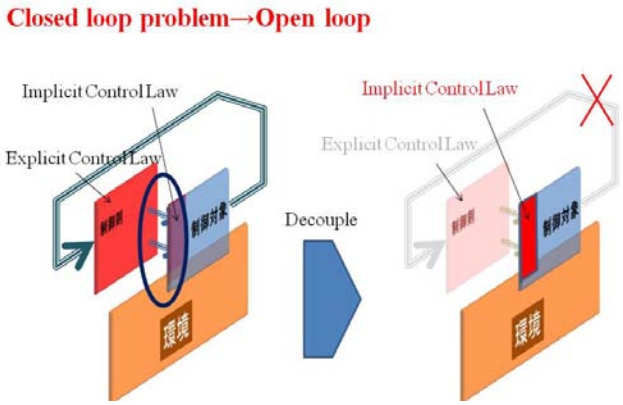

Fig.7 Closed loop to Open loop

In any event, if operations of Fig.6～Fig.7 can be performed, it becomes easy to think of embedding problem. The method can be two steps or simultaneous one.(Refer to Fig.8).

However, as for level of difficulty of approach for embedding problem, it can be expected to depend on which object/ movement will be the attention paid and it is parted into the following levels.

[Level A] Noninteracting closed looping can be performed without decomposing an object or performing anatomic operation to an object, by executing meaningful movement on some sort of environment.

[Level B] If decomposing an object or performing anatomic operation to an object, noninteracting closed looping can be performed.

[Level C] Decomposing an object or anatomic operation can't be performed to an object, so no interacting closed looping can't be performed.

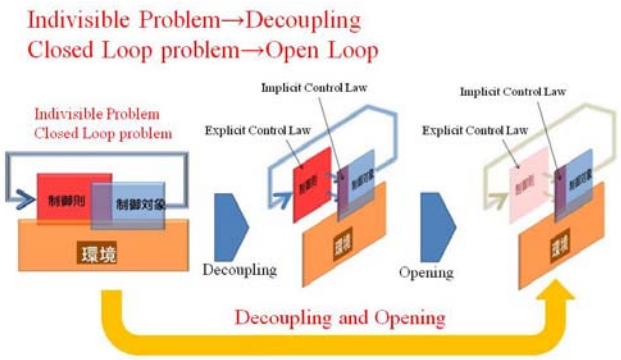

Fig.8 One-shot transformation

4. Passive Dynamic Locomotion

In this chapter, on considering embedding problem, （as the first step） Level A which is the most simple in the above 3 levels is considered. For this, it is necessary to find one meeting the following conditions out of various movements （conditions）.

[C1] It should be meaningful movement which can be performed under a certain condition.

[C2] The movement itself is stable.

This is not necessary only one, but at least one example should be found. As the result of consideration, writers think that "passive locomotion" is a rare example which meets the conditions and suggest the following proposition.

[Proposition] Passive locomotion avoids noninteracting closed loop problem and simplified model of a movement example which can show clearly embedding problem （Level A problem）. □

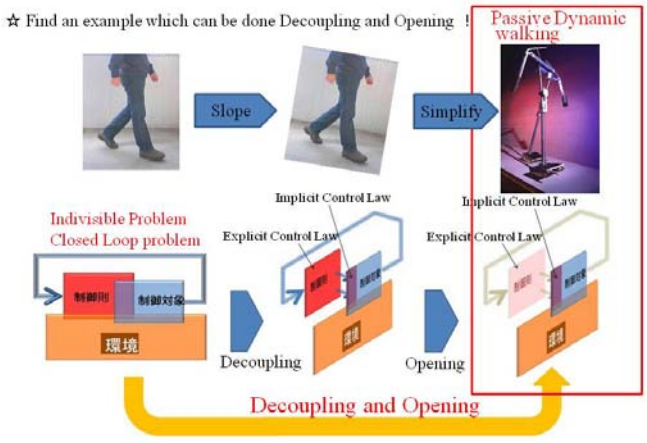

Fig.9 An example of the transformations

Then, candidates of "implicit control law" regarding walking which were found from the previous studies on passive dynamic walking are shown diagrammatically.（Fig.10）. Due to space limitation, details will be omitted here, but C1)～C3)[6)-9)] are theoretical finding s based on mathematical model about passive dynamic walking or passive running. And regarding C4)5)C5)[11)], the existence of implicit control law on four-legged PDW is suggested by simulations or experiments, and theoretical study about these is an issue in the future.

Fig.10 Candidates of Implicit Control Laws

5. Conclusion

In this note, we described the viewpoint that the meaning of research of passive dynamic walking is deeply related to the core of Mobiligence research. The followings are discussions.

At first, we discussed the existence of implicit control law through studying the passive dynamic walking as an example. We think that though the internal of the implicit control law is different if the target Mobiligence is different, such a embedding problem is common.

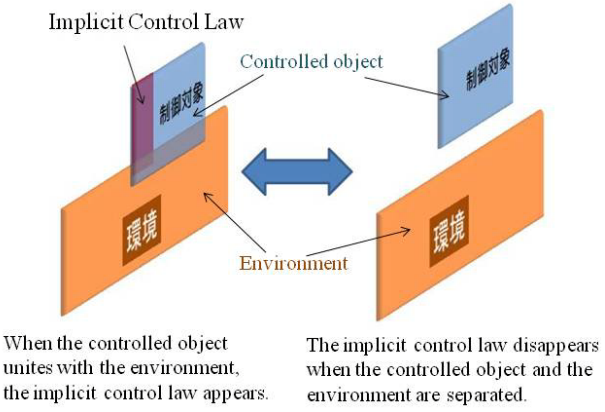

Fig.11 Appearance of Implicit Control Law

In this note, we use the terminology “Control law embedded in the controlled object”, more precisely speaking, we should say “Control law that arises by contact of controlled object and environment”. That is, as shown in the left of Fig.11, generally speaking, control law does not appear in the controlled object itself, we can only recognize only if the controlled object and environment become one system. Therefore, depending on the situation or task, the same controlled object gives the deferent implicit control law.

Next, we show the three future works. 1) At first, after becoming clear the implicit control law, we should find the way for constructing the explicit control law. And, it is necessary to verify that such a structure can be seen in the living thing. Secondarily, it is necessary to think how to handle the problem of Lebel B and Lebel C though the problem of Lebel A was considered in this report. Thirdly, it is necessary to handle the top layer in addition to advance to the whole of Mobiligence though the control rule of the bottom of the heap was considered here. That is, this means that a kind of “intelligent law” That is, there is a possibility that "embedding problem" exists also in this intelligence law and the control law, and it will be necessary to handle "Multiple embedding problem" in the future though it is necessary to think about "Intelligence law" in a certain meaning.

Finally, we want to clarify the following. Firstly, we do not want to say that understanding the implicit control law is equal to the understanding the Mobiligence. I want to clarify the insistence on "It is necessary to understand a implicit control law clearly to understand Mobiligence".

In the future, I want to analyze the individual results which had been obtained through such a viewpoint for a current Mobiligence research again though the implicit control rule have not become yet completely obviously.

References

1) T.McGeer : Passive Dynamic Walking, Int. J. of Robotics Research, 9-2, pp.62-82, 1990.
2) K.Osuka, T.Fujitani and T.Ono: Passive Walking of 8-legged Passive Dynamic Walking Robot, Proc. of Robotics Mechatronics Conference 1998, CD-ROM, 2CIII-6, 1998.
3) K.Osuka and K.Kirihara: Motion Analysis and Experiment of Passive Walking Robot Quartet II, Journal of the Robotics Society of Japan, Vol.18, No.5, pp.737- 742, 2000.
4) K.Osuka and Y.Saruta: Walking Control of Legged Robot QUARTET-III based on Passive Dynamic Walking, Proc. of The 8th Symposium on Control Technology, pp.355-360, 2000.
5) K.Osuka, T.Akazawa and K.Nakatani: On Multi-legged Passive Dynamic Walking, Proc. of The 51st Annual Conf. on The Institute of Systems, Control and Information Engineers, pp.281-282, 2007.
6) K.Hirata and E.Kokame: Periodic Solutions of Linear Systems with State Jump, —Modeling of Compass Walking, Stability Analysis and Feedback Control, Trans. of the Institute of Systems, Control and Information Engineers, Vol.17, No.12, pp. 553- 560, 2004.
7) Y.Sugimoto and K.Osuk: Stability Analysis of Passive Dynamic Walking — An Approach via Interpretation of Poincare Map's Structure, Trans. of the Institute of Systems, Control and Information Engineers, Vol.18, No.7, pp.255-260, 2005.
8) K.Hirata: On Stabilizing Mechanism in Passive Dynamic Walking, Proc. of The 8th Control Division Conference, 2008.
9) D.Owaki, K.Osuka and A.Ishiguro: Understanding of the Stabilization Mechanism underlying Passive Dynamic Running, Proc. of The 26th Annual Conference on Robotics Society of Japan, 3B1-09, 2008.
10) http://www.arai.pe.u-tokyo.ac.jp/Mobiligence/
11) M.Iribe and K.Osuka: Passive dyamic walking robot with an adaptive gait stabilize function, Proc. of the 13rd Robotics Symposia, pp.358-363, 2008.

Understanding Mobiligence from Coupled Oscillators with Simple Motile Function

∼Design of a Real Physical Amoeboid Robot∼

Akio Ishiguro, Masahiro Shimizu, and Kazutoshi Gohara

Abstract— **This paper discusses experimental verifications of a two-dimensional modular robot called "Slimebot", consisting of many identical modules, each of which has simple motile functions. We have so far investigated a fully decentralized algorithm able to control the morphology of the modular robot in real-time according to the environment encountered. One of the most significant features of our approach is that we explicitly exploit "emergent phenomena" stemming from the interplay between control and mechanical systems. In order to verify our proposed cotrol scheme, we have constructed real physical Slimebot. Preliminary experiments suggest that this robot enables real-time reconfiguration.**

I. INTRODUCTION

Mobiligence is a form of intelligence through locomotive function induced from the tight interplay between brain-nervous system(control system), body(mechanical system) and environment[1]. While there are so many types of locomotion in nature, we have focused on amoeboid locomotion, which is one of the most primitive locomotive functions, in order to capture the common principles of mobiligence effectively. To this end, we have particularly focused on true slime mold since it exhibits significantly supple locomotion only with a purely decentralized control mechanism. Thus, in this study, we intend to deal with a reconfigurable robotic system as a model of an amoeboid locomotive function.

In the research area of robotics, various types of modular robots have developed so far[2]-[7]. These robots, however, have the following two issues: first, modules are normally connected mechanically and/or electromagnetically by highly rigid mechanisms; second, morphological alteration is usually resolved by turning into a module rearrangement problem in a centralized-planning manner. These issues lead to the absence of adaptivity in the traditional modular robots.

In light of these facts, this study is intended to deal with an emergent control method which enables a modular robot to change its morphology in real time according to the situation encountered without the use of any global information as well as without losing the coherence of the entire system. Based on this consideration, we have so far developed a two-dimensional modular robot, called *Slimebot*[8]. In order to realize an emergent control method, the coupling between the control and mechanical systems of Slimebot has been carefully designed as follows: we have particularly focused on a *functional material*, *i.e.*, a genderless *Velcro strap*, and *mutual entrainment* between nonlinear oscillators, the former of which is used as a spontaneous connectivity control mechanism between the modules, and the latter of which acts as the core control mechanism for the generation of locomotion and ensures the scalability. Simulation results indicate that the proposed method can induce amoeboid locomotion, which allows us to successfully control the morphology of the modular robot in real time according to the situation without losing the coherence of the entire system.

To verify the feasibility of our proposed method, experiments with a real physical Slimebot are also significantly important. Therefore, in this year, we have been aiming at designing the hardware of Slimebot. Since the experimental study is still in the early stage, this paper deals with the locomotion of Slimebot consisting of only several real physical modules. The obtained results, however, strongly suggest that this hardware enables highly scalable adaptive locomotion.

II. DESIGN STRATEGIES

So far, we have confirmed real-time adaptive reconfiguration under the simulations(see Fig. 1). In what follows, the design strategies introduced in this study are explained.

A. The Mechanical Structure

A two-dimensional Slimebot has been developed, consisting of many identical modules, each of which has a mechanical structure like the one shown in Fig. 2 and 3. Figure 4 shows schematic representation of the control system for the real physical Slimebot. Each module is equipped with telescopic arms, a ground friction control mechanism, and an omnidirectional light-detecting sensor. Note that the module is covered with a functional material. More specifically, we used a genderless Velcro strap as a practical example, since this intrinsically has interesting properties: when two halves of Velcro contact each other, they are connected easily; and when a force greater than the yield strength is applied, the halves will come apart automatically. Exploiting the property of this material itself as a spontaneous connectivity control mechanism, we can expect not only to reduce the computational cost required for the connection control dramatically, but also to induce

A. Ishiguro is with the Deptartment of Electrical and Communication Engineering, Tohoku University, 6-6-05 Aoba, Aramaki, Aoba-ku, Sendai 980-8579, Japan ishiguro@ecei.tohoku.ac.jp

M. Shimizu is with the Deptartment of Electrical and Communication Engineering, Tohoku University, 6-6-05 Aoba, Aramaki, Aoba-ku, Sendai 980-8579, Japan shimizu@cmplx.ecei.tohoku.ac.jp

K. Gohara is with the Department of Applied Physics, Hokkaido University, Sapporo 060-8628, Japan gohara@eng.hokudai.ac.jp

emergent properties in morphology control. The property of the connectivity control mechanism is mainly specified by the yield stress of Velcro employed: connection between the modules is established spontaneously where the arms of each module make contact; disconnection occurs if the disconnection stress exceeds the Velcro's yield stress. We also assume that local communication between the connected modules is possible(see Fig. 5), which will be used to create phase gradient inside the modular robot (discussed below). In this study, each module is moved by the telescopic actions of the arms and by ground friction. Note that each module itself does not have any mobility but can move only by the collaboration with other modules.

B. The Control Algorithm

Under the above mechanical structure, now we consider how we can generate stable and continuous locomotion. To this end, a nonlinear oscillator is implemented onto each module, allowing us to generate rhythmic and coherent locomotion through the *mutual entrainment* among the oscillators. In the following, we will give a detailed explanation of this algorithm.

Active Mode and Passive Mode: Each module in the Slimebot can take one of two exclusive modes at any time: *active mode* and *passive mode*. A module in the active mode actively contracts/extends the connected arms, and simultaneously reduces the ground friction. In contrast, a module in the passive mode increases the ground friction, and returns its arms to their original length. Note that a module in the passive mode does not move itself but serves as a *supporting point* for efficient movement of the module group in the active mode.

Creating the Phase Gradient through Mutual Entrainment: In order to generate rhythmic and coherent locomotion, the mode alternation in each module should be controlled appropriately. Of course, this control should be done in a *decentralized* manner, and its algorithm should not depend on the number of the modules and the morphology of the Slimebot. To do so, we have focused on the *phase gradient* created through the mutual entrainment among locally-interacting nonlinear oscillators in the Slimebot, exploiting this as a key information for the mode alternation. Therefore, the configuration of the resulting phase gradient is extremely important. In the following, we will explain this in more detail.

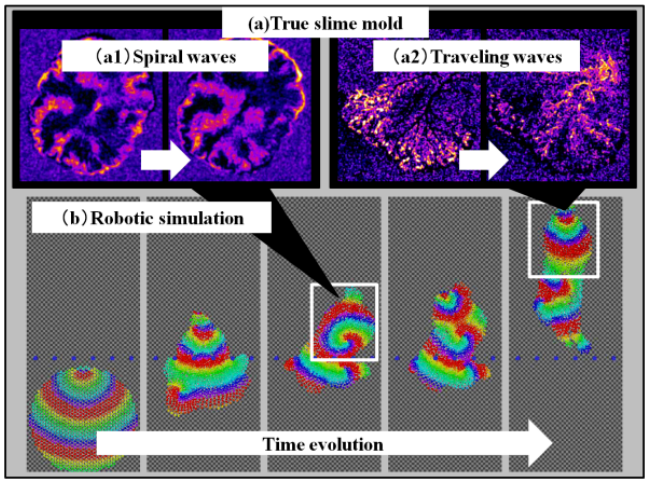

Fig. 1. : Representative data of qualitative agreements between the Slimebot and rhythmic protoplasmic movement in the true slime mold.

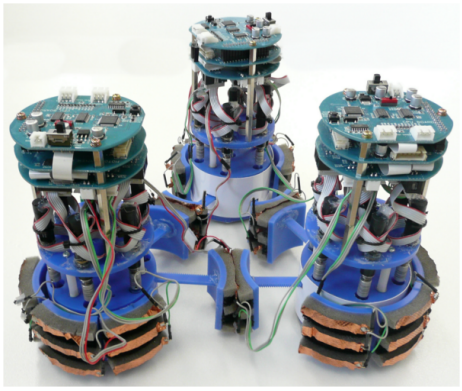

Fig. 2. : Real physical Slimebot consisting of 3 modules.

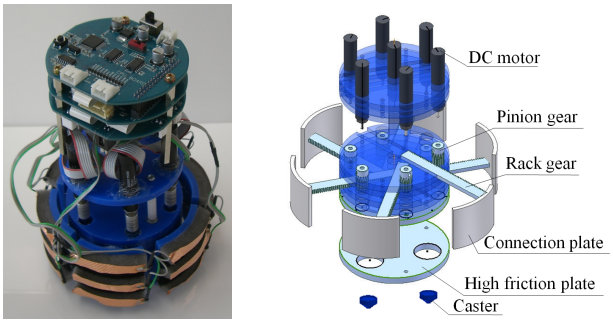

(a) Oblique view (b) 3D CAD

Fig. 3. : (a)Photo of the improved real physical module. (b)3D CAD data of the same module. The module has 7 DC motors. 6 motors of which are for extension/contraction of the arms, and the rest is for the ground friction control mechanism.

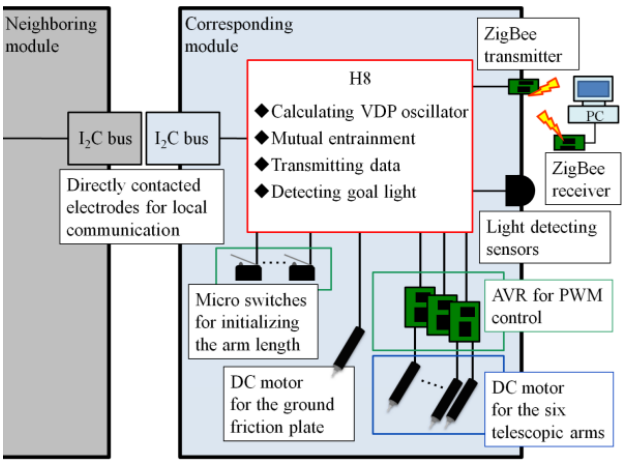

Fig. 4. : Schematic representation of the control system for the real physical Slimebot.

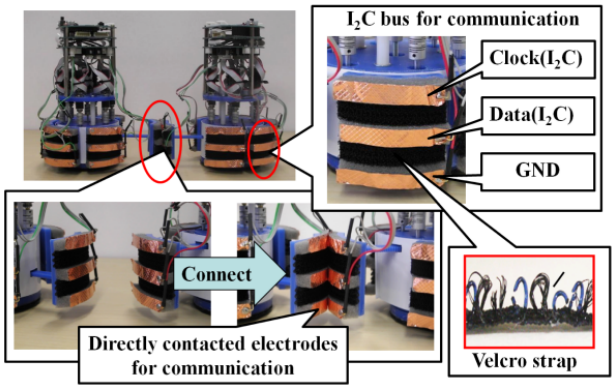

Fig. 5. : The physical connection control mechanism by exploiting genderless velcro straps.

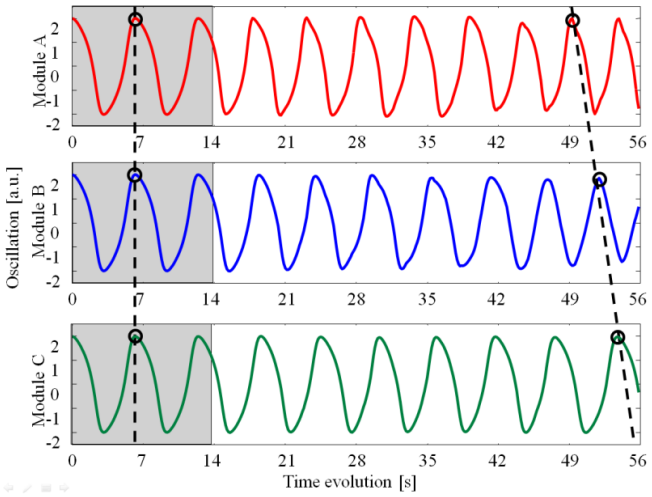

Fig. 6. : A verification of mutual entrainment among the VDP oscillators embedded into the modules.

As a model of a nonlinear oscillator, the *van der Pol oscillator* (hereinafter VDP oscillator) was employed, since this oscillator model has been well-analyzed and widely used for its significant entrainment property. The equation of VDP oscillator implemented on module i is given by

$$\alpha_i \ddot{x}_i \quad \beta_i(1 \quad x_i^2)\dot{x}_i + x_i = 0, \tag{1}$$

where the parameter α_i specifies the frequency of the oscillation. β_i corresponds to the convergence rate to the limit cycle.

The local communication among the physically connected modules is done by the local interaction among the VDP oscillators of these modules, which is expressed as:

$$x_i = x_i^{\mathrm{tmp}} + \varepsilon \left\{ \frac{1}{N_i(t)} \sum_{j=1}^{N_i(t)} x_j^{\mathrm{tmp}} \quad x_i^{\mathrm{tmp}} \right\}, \tag{2}$$

where x_i^{tmp} and $N_i(t)$ represent the state before the local interaction, and the number of modules neighboring module i at time t, respectively. The parameter ε specifies the strength of the interaction. Note that this local interaction acts like a *diffusion*.

When VDP oscillators interact according to Equation (2), significant phase distribution can be created effectively by varying the value of α_i in Equation (1) for some of the oscillators. In order to create an equiphase surface effective for generating locomotion, we set the value of α_i as:

$$\alpha_i \quad = \quad \begin{cases} 0.7 & \text{if the goal light is detected} \\ 1.3 & \text{if the module is outer surface} \\ 1.0 & \text{otherwise} \end{cases} \tag{3}$$

Note that except the modules detecting the goal light, the modules on the boundary, *i.e.*, the outer surface, have the value of $\alpha_i = 1.3$. This allows us to introduce a kind of effect of *surface tension*, which is indispensable to maintain the coherence of the entire system.

Generating Locomotion: Here, we consider a control algorithm exploiting the phase distribution created from the aforementioned mutual entrainment among the VDP oscillators. To do so, the two possible modes, *i.e.*, the active and passive modes, of each module should be appropriately altered according to the phase distribution that emerges. The timings of the mode alternation are propagated from the front to the rear inside the modular robot as traveling waves. In this study, the extension/contraction of each arm of module i in the active mode is determined according to the phase difference with its corresponding neighboring module. Due to this, the degree of arm extension/contraction of each module will become most significant along the phase gradient, enabling the entire system to move toward the goal light while maintaining its coherency.

III. EXPERIMENTAL VERIFICATIONS

Mutual Entrainment between Real Physical Modules: Here, we have carried out the verification of mutual entrainment between 3 modules arranged so as to form a string-like shape. Figure 6 shows the experimental result. As the figures explain, in the gray region, each module is set to $\alpha = 1.0$, thus all the oscillators will be synchronized. On the other hand, in the white region, only module *A* is allowed to detect goal light($\alpha = 0.7$), thus the phase gradient will be occurred.

Connection and Disconnection between Real Physical Modules: We have verified the mechanism for mutual entrainment with two modules. As Fig. 7 shows, the oscilloators of these modules can successfully exhibit mutual entrainment.

Locomotion Generated under Different Morphology: Figure 8 shows an experimental verification of locomotion under the change in morphology. In this experiment, we changed the number of modules from two to three. As the figure explains, the Slimebot exhibits highly scalable adaptive locomotion.

IV. CONCLUSION AND FUTURE WORK

In this study, we have developed a real physical modular robot that enables to control its morphology in real time by explicitly exploiting emergent phenomena stemming from

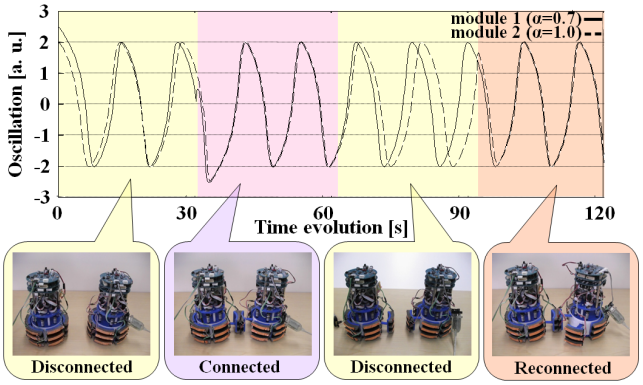

Fig. 7. : A verification of connection mechanism.

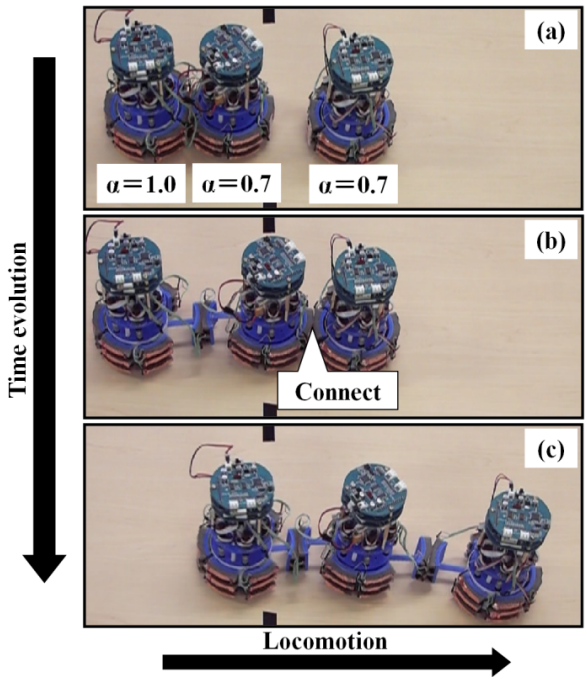

Fig. 8. : Experimental verification of locomotion with the change in the number of modules. See from (a) to (c).

the interplay between the control and mechanical systems. To this end, we have implemented a functional material (*i.e.*, genderless Velcro strap) and a locally-interacting nonlinear oscillator (*i.e.*, VDP oscillators) into each module, the former of which was utilized as a spontaneous connectivity control mechanism and the latter of which as a core mechanism for generating locomotion.

The experiments conducted suggest that our modular robot Slimebot is highly promising, which can be summarized as: (1) while each module is simply controlled with the VDP oscillator, adaptive reconfiguration can be self-organized according to the situation encountered; and (2) the spontaneous connectivity control mechanism provided by the functional material was fully exploited.

In this paper, we have proposed another real physical Slimebot module driven by DC motors. However, a few new modules have been constructed by now. On the other hand, we have so far found an interesting phenomenon through the simulations: the Slimebot exhibits significant cohesive force inside effective to maintain the coherence of the entire system as the number of the modules exceeds a certain *critical number*; and this critical number exists around 10 modules. Considering this fact, experiments conducted with more than 10 real physical modules are extremely important. This is currently under investigation.

REFERENCES

[1] H. Asama, et al.: "System Principle on Emergence of Mobiligence and Its Engineering Realization", in Proc. of the 2003 IEEE/RSJ International Conference on Intelligent Robots and Systems, pp.1715–1720, 2003.

[2] T. Fukuda and Y. Kawauchi, *Cellular Robotic System (CEBOT) as One of the Realization of Self-Organizing Intelligent Universal Manipulators*, in Proc. of IEEE ICRA, pp.662–667, 1990.

[3] A. Kamimura, S. Murata, E. Yoshida, H. Kurokawa, K. Tomita, and S. Kokaji, *Self-Reconfigurable Modular Robot – Experiments on Reconfiguration and Locomotion –*, in Proc. of 2001 IEEE/RSJ IROS, pp.590–597, 2001.

[4] M. Dorigo, et al., *Evolving Self-Organizing Behaviors for a Swarm-bot*, Autonomous Robots, pp.223-245, 2004.

[5] M. W. Jorgensen, E. H. Ostergaard and H. H. Lund, *Modular ATRON: Modules for a Self-Reconfigurable Robot*, in Proc. of 2004 IEEE/RSJ IROS, pp.2068–2073, 2004.

[6] M. Yim, C. Eldershaw, Y. Zhang, and D. Duff, *Self-reconfigurable Robot Systems: PolyBot*, Journal of the Robotics Society of Japan, Vol.21, No.8, pp.851-854, 2003.

[7] H. Yokoi, T. Nagai, T. Ishida, M. Fujii, and T. Iida, *Amoeba-like Robots in the Perspective of Control Architecture and Morphology/Materials*, Morpho-functional Machines: The New Species, Springer, pp.99–129, 2003.

[8] A. Ishiguro, M. Shimizu, and T. Kawakatsu, *Don't Try to Control Everything!: An Emergent Morphology Control of a Modular Robot*, in Proc. of 2004 IEEE/RSJ IROS, pp.981-985, 2004.

Studying Artificial and Biological Autonomy

Ikegami Takashi and Shimada Masakazu
Graduate School of Arts and Sci. University of Tokyo,
Komaba Campus, Tokyo 153-8902

Abstract: By designing a robot and analyzing behaviors of a housefly, we discuss the meaning of autonomy in artificial and natural systems. This project is an experiment-oriented research study based on our theoretical ideas of autonomous systems. Three findings are reported in the experiments: 1) anomalous diffusion and 2) chaotic itinerancy are observed in the exploration motion of flies [4], and an intermediate third time-scale is introduced for a robot manipulation[1].

1 A New Principle

A difference between living and non-living is the presence of autonomy. Autonomy is necessary for agents to take actions and become cognitive. Whereas a complex machine cannot create its own motivation or behavior without being controlled from outside by a designer, simple organisms can decide what to do and see spontaneously. In this sense, living systems are autonomous compared to systems made up of nonliving matter. Understanding autonomy is thus important in perceiving differences between living and non-living.

Over the last 20 years, people have studied autonomy through the design of autonomous robots. For example, R. Brooks proposed a "subsumption architecture" as a design principle and created several artificial creatures. R. Pfeiffer also created new kinds of autonomous robots including a distributed tile system. In Japan, Yasuo Kuniyoshi is studying human development through the design of a baby robot, and Jun Tani has been exploring autonomous navigation robots controlled by a recurrent neural net. In the field of experimental biology, Greenspan et al. studied the electro-physiology of flies, and Kristan studied the autonomous behavior of leeches. Nevertheless, we still have almost no design principles for producing autonomous behaviors. This project seeks new principles for understanding autonomy in living systems.

In previous studies, we proposed two guiding principles for simulating autonomy from artificial life studies. One is a form of self-tuning sensoricoupling referred to as "autonomous coupling" (AC) [7], and the other is chaotic itinerancy induced by self-movement, referred to as "Embodied Chaotic Itinerancy" (ECI) [6]. AC tunes the strength of the connections between sensors and internal neural states. Using this mechanism, we designed an agent to distinguish between different blinking frequencies of light sources. We also designed an ECI mobile agent with the FitzHugh Nagumo equation to demonstrate spontaneous motion switching from one style to another, with corresponding

changes in internal dynamics. An agent receives its input from the environment when its internal state is chaotic and behaves independently from the environment when the internal state is periodic. We say that ECI realizes AC by the self-organized chaotic dynamics.

Based on these ideas, we develop the idea of autonomy in both natural and artificial systems, which is the aim of this project. Autonomy is no more mere randomness driven by a chaotic dynamics. Our concern should be with embodiment that mediates autonomy. Embodiment does not simply mean possessing a physical body, but must also incorporate the coordinated self-organization of behavior structures. This project will use a robotic experiment and a fly experiment to test this idea. Specifically, we are carrying out two experiments.

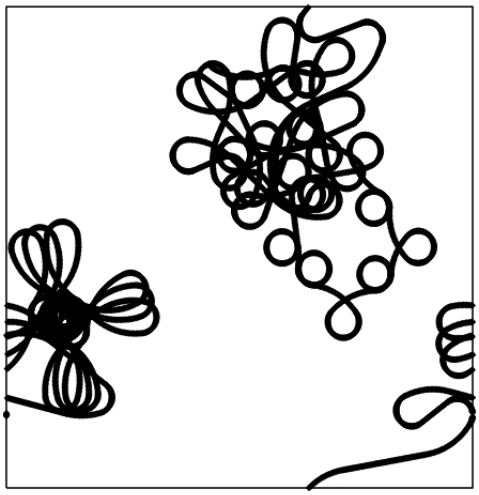

Figure 1: ECI trajectory in this time step the agent indicating [6]

2 Methodology

ECI was tested with an agent on the 2dimensional grid pattern (fig.1). As we see in the figure, the agent switches from one style to another. We applied the idea of ECI to a commercial robot called MIURO, who plays music from an ipod on its top and synthesizes dance styles (Fig 2) . In order to examine the ECI idea in a natural system, we analyzed the explorative behavior of a fly in a shallow closed cage (Fig. 3).

For our first year plan: 1) We use a robot (MIURO) to study how a robot generates autonomous movement. Miuro plays music and its movement pattern is controlled by a remote PC. We have designed the program that generates ECI with MIURO. 2) We conduct animal experiments using the Drosophila and the housefly in a cage. Sugar drops are placed in several places in a cage and we quantitatively study the exploration patterns of the flies. Using a Drosophila mutant with a different memory capacity, we analyze the relationship between movement and memory capacity. We also examine the effect of communication between two flies on their respective exploratory patterns.

3 results

3.1 Experimental Robotics

Miuro is a robot with a circular body and two wheels, and speakers on either side. Murio generates "Dancing" patterns in response to the music played. In addition, visual information is available by CCD camera and the robot also has four IR sensors equipped with tactile sensors. A remote PC controls the robot, altering its dancing style in response to the music [1, 2].

Figure 2: Appearance of the robot MIURO [1]

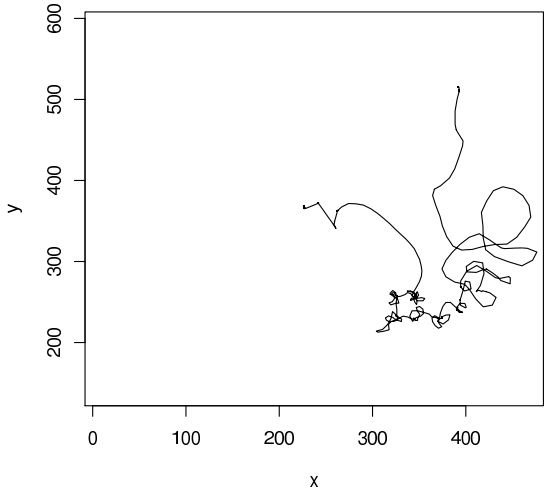

Figure 3: A trajectory of a house fly in a cage [4]

We introduced a third time scale in the robot. Whereas the time scale of the transition period of the neural network is set at around 5msec, the robot and computer need about 100 msec to communicate. Directly connecting these two time scales would not allow for any correlation between music and movement. Thus about 30 msec is needed to sample the state of the neural network and use this state to create a movement. We also generate dynamics of creating and breaking the relationship between dance and music, which is chaotic itinerancy. We also plan to use the mutual information metric to characterize this chaotic itinerancy [2].

This internal time scale issue was critical for detecting agency from an external (observer) point of view. This third time scale, artificially introduced to the system, can thus be considered an important ingredient in design agency. Actually, we have tried different sampling rates and found that the dancing behavior is highly sensitive to this time scale.

3.2 Experimental flies

Exploration activities of a fly were observed with video systems in the experiment using flies and a glass cage. The cage (47cm square, depth 2cm) is used and fly walks around the cage. We take a video recording and analyze it with R software for statistical analysis using the Autoregression (AR) method. By using this method, we are able to explore changes in the number of degrees of freedom of movement, and discovered anomalous diffusion in the fly's walking pattern. Also, using a mutant of Drosophila with a smaller storage capacity, we studied how movement pattern changes, but the memory capacity did not alter the pattern [3]. Also, the flies show anomalous diffusion with or without food [4]. Surprisingly,

the exploration pattern is not altered if there is another fly in the cage. This point will be further pursued in the next year.

4 Future directions

In addition to the above findings, we also developed a study of active perception [8, 9] through the creation of artificial tactile sensors, and the study of organizing processes of autonomy in an evolutionary context, for example through the design of behavioral adjustment between body and environment in the study of homeodynamic vehicles [5]. We also studied the effect of body shape in organizing primitive perception [10].

Regarding directions of future research, the following are noteworthy:

1) In natural and artificial systems, we study "robustness" in order to consider and discuss the meaning of action as coordination dynamics to the environment.

2) In natural and artificial systems, we consider "online learning " by considering a more open environment, to discuss the meaning of the act as an adjustment between a body and the environment.

References

[1] Aucouturier, J.-J. and Ogai, Y. and Ikegami Using chaos to trade-off synchronization and autonomy in a dancing robot, Trends and Controversies, IEEE Intelligent Systems 2 3 2 74-85 2008.

[2] Aucoutier,J-J., Ogai, Y and Ikegami, T., Making a robot dance to music using chaotic itinerancy in a network of FitzHugh-Nagumo neurons, LNCS 4985 (Part II), 2007, pp. 647-656.

[3] Horibe, N, "Adaptive Strategy of Memory and Learning :" (Master thesis, University of Tokyo, 2008).

[4] Takahashi, H., Horibe, N., Shimada, M. and Ikegami, T., Analyzing the House Fly's Exploratory Behavior with Autoregression Methods ,J. Phys. Soc. Japan.77 84802 2008

[5] Ikegami, T and Suzuki, K From Homeostatic to Homeodynamic Self, BioSystems 91 388-400 2008

[6] Ikegami, T., Simulating Active Perception and Mental Imagery with Embodied Chaotic Itinerancy, Journal of Consciousness Studies Vol.14 (2007) pp.111-125.

[7] Iizuka, H. and T.Ikegami Simulated autonomous coupling in discrimination of light frequencies, Connection Science, 17 (2004) pp.283-299.

[8] Ogai, Y., Ikegami, T Microslip as a Simulated Artificial Mind Adaptive Behavior 16 2-3 129-147 2008

[9] Ogai, Y. and Ikegami, T, "Mathematical studies on Microslips as Complex Systems", Ecological Psychology Volume 4, Number 1, 39-50, 2009

[10] Suzuki, K and Ikegami, T. Shape and Self-movements in Protocell Systems Atrtificial Life15 (2009) 59-70.

Emergence of mobiligence by environment-generation in flapping flight of butterfly

Kei Senda, Makoto Iima, and Norio Hirai

I. Introduction

A. Objective

The flapping flight of butterfly is an example of Mobiligence in which the environment is the generated flowfield. Actually, it essentially has the same structure with other Mobiligence subjects, e.g., (a) to emerge the mobiligence from the interaction of the nervous system, body, and environment, (b) to utilize the dynamic nonlinearity of the interaction between body and environment, and so on. This research analyzes the mechanism to emerge butterfly's Mobiligence, i.e., the adaptive function in flapping flight of butterfly, from the viewpoint where the environment as the flowfield with vortex street induced by the flapping effects on the stability and/or maneuverability. This study aims for contributions to clarify a dynamics principle of Mobiligence in common with other various subjects and to create a new area of Mobiligence by the environment-generation. Concretely, this study investigates the following two issues by the biological analysis through experimental observations of living butterflies and by the systems engineering or synthetic approach: (1) relation between the sensor input and the body response, and (2) effects of the environment (flowfield) to the control mechanism that achieves the stable flight and maneuver. The above is the target during the period of this study.

B. Summary

This research project has carried out the following items, where "A" and "B" are the biological approach and engineering approach, respectively. Relating achievements are listed in references [1]-[16].

A1. Breeding In order to provide the butterflies, *Parantica sita niphonica*, ordinarily, it is established that to breed from eggs to imagoes by the breeding equipment of Osaka Prefecture University, where the eggs are collected from the outdoors female imagoes.

Kei Senda is a Professor of Department of Aeronautics and Astronautics, Graduate School of Engineering, Kyoto University, Yoshida-Honmachi, Sakyo-ku, Kyoto 606-8501, JAPAN (phone: +81-774-38-3960; fax: +81-774-38-3962; e-mail: senda@kuaero.kyoto-u.ac.jp).

Makoto Iima is an assistant professor of Research Institute for Electronic Sciences, Hokkaido University, Sapporo, Hokkaido 001-0020, JAPAN.

Norio Hirai is an assistant professor of Entomological Laboratory, Graduate School of Life and Environmental Sciences, Osaka Prefecture University, Sakai, Osaka 599-8531, JAPAN.

A2. Experimental observation An experimental system with a low-speed wind tunnel is constructed to measure the motion and aerodynamic forces of actual butterflies quantitatively. The acquired experimental data are used to evaluate the accuracy of numerical simulations.

A3. Anatomical observation Anatomical understanding is advanced by using micro-XCT images to clarify their possible active motion.

B1. Analysis using 2D mathematical model A 2D (two-dimensional) mathematical model is developed to achieve steady flight by focusing on butterfly's attitude. The recovery motion after a large perturbation has been investigated, and the state transition ability, maneuverability, will be analyzed.

B2. Construction of 3D mathematical model A 3D mathematical model is constructed to analyze the stability of actual free-flying butterflies and so on. Its validity and accuracy are examined by comparing with the obtained experimental data.

II. Experimental Observation of Flapping Butterfly

An experimental system with a low-speed wind tunnel (Figure 1) is constructed. The motion and aerodynamic forces of actual butterflies, *Parantica sita niphonica*, are measured

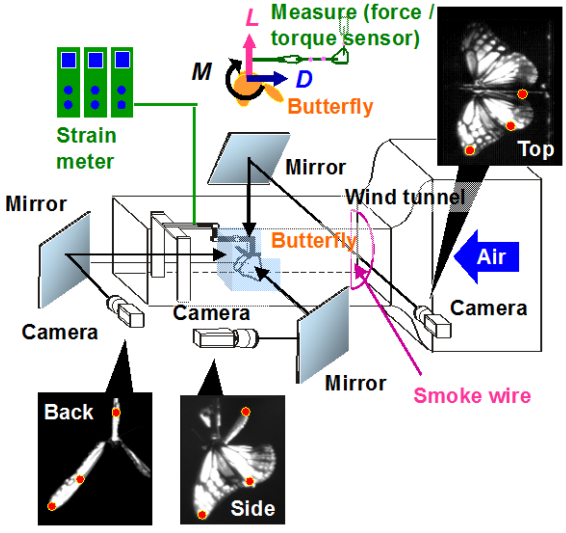

Figure 1: Experimental system

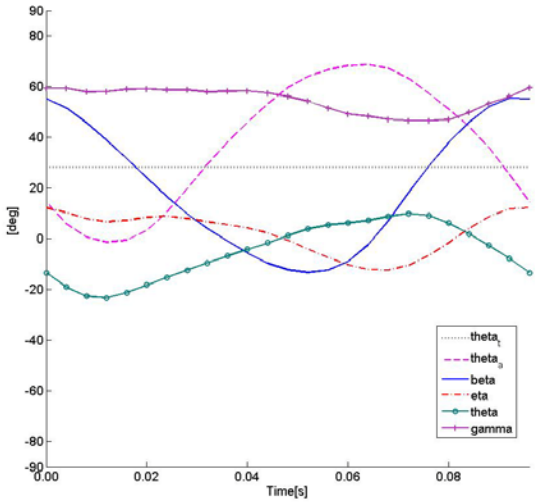

Figure 2: Measured motion of flapping butterfly (mainstream 1.5m/s, attack angle 30 degrees)

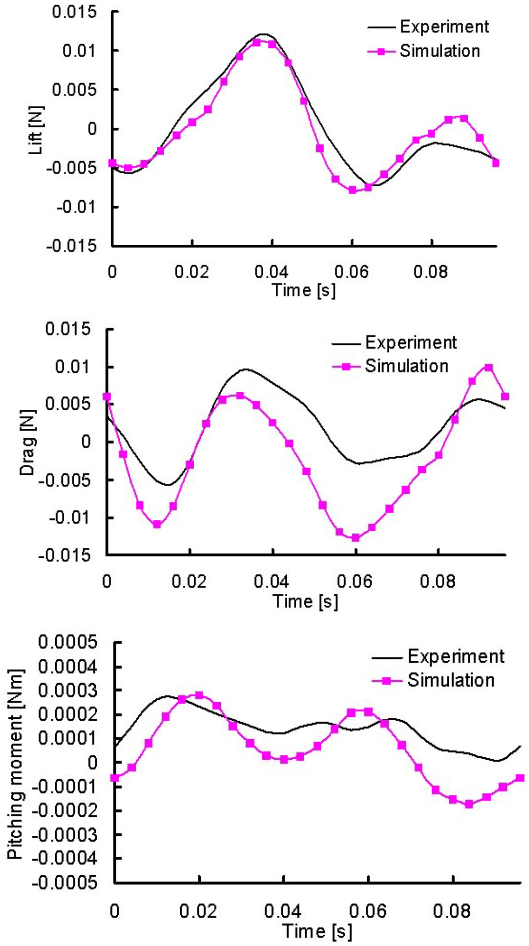

Figure 3: Measured aerodynamic forces of flapping (mainstream 1.5m/s, attack angle 30 degrees)

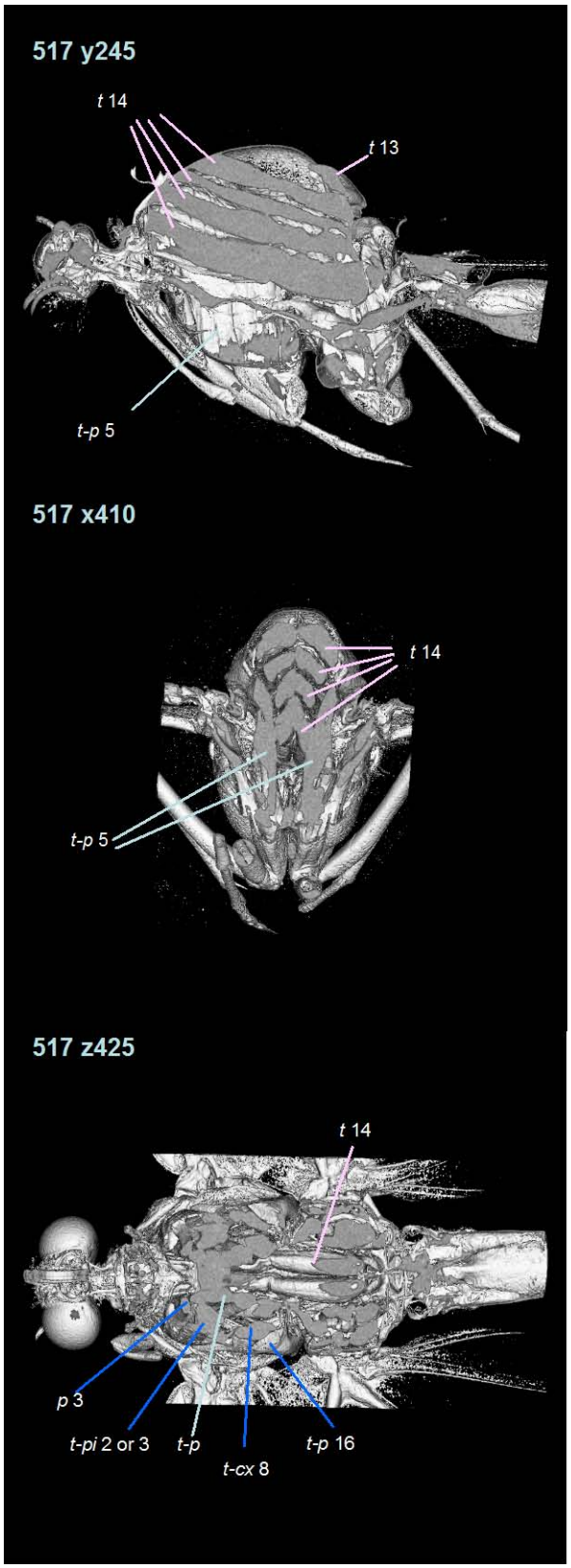

Figure 4: 3D images reconstructed with micro-XCT images of *Parantica sita niphonica*

quantitatively (Figures 2 and 3). The butterfly is put into the wind tunnel, and the flapping-of-wings motion in the flow is captured by three high-speed video cameras. The joint angles of butterfly are calculated from the measured positions of typical points on the body in video images. Simultaneously,

the forces applied to the butterfly, i.e. lift *L*, drag *D* and pitching moment *M*, are sensed by the measure. There is a smoke wire for airflow visualization.

Figures 2 and 3 show the motion and forces for one flapping cycle. The butterfly repeats this cyclic motion in a constant period when it continues the periodic flapping motion. Measured aerodynamic forces are also cyclic during the motion. The flapping angle is a cosine-like curve. The abdomen angle is also a sinusoidal curve, but is out of phase to the flapping angle. Even if we change the experimental condition and/or the individual, they keep similar smooth cosine curves. On the other hand, there are some data changed by the experimental conditions. It indicates that they change their motion to control actively.

III. Anatomical Observation of Butterfly

To clarify the possible flight movements, morphology of thoracic muscles of a danaid butterfly, *Parantica sita niphonica* are investigated using the micro-XCT (Comscantecno ScanXmate-A080S). The x-ray tube voltage, the tube current, and the minimum resolution (i.e. slice width and pitch) are adjusted 70 kV, 90 mA, and 18 μm, respectively. Three-dimensional images are obtained by the software, Analyze. The images are examined and muscles observed are identified referring to the published thoracic skeletal structure and musculature of a papilionid butterfly, *Luehdorfia japonica* (Emoto, 1983). As a result, major indirect flight muscles including dorsal longitudinal muscles and dorso-ventral muscles of this species are identified (Figure 4). Some direct flight muscles such as basalar muscles and subalar muscles are also observed. Further observations of muscles around the basalar sclerite are needed to understand the detailed wing manipulation.

IV. Discussion using 2D Model

We constructed two-dimensional models to analyze flight stabilization and maneuverability. These results will be useful for further analysis.

Insects create the environment due to vortices generated by flapping wings. They fly freely by interaction between wings and such environment, which is a characteristic for the insect's flight. Understanding such properties of such environment will be of great use. We proposed a theory of flapping flight using vortices [3][7][8].

A simple model described by ordinary differential equations was analyzed to obtain candidates of appropriate solution for flapping flight. A bifurcation-tracking software was used, and we tried to determine the solution from a trivial solution obtained at a different parameter. Currently this approach is not successful because we found too many bifurcation processes before we reach to the solution. In the case of analysis for strong interaction between convection cells [5], several techniques were shown effective, that is, focusing on the qualitative change under parameter change or

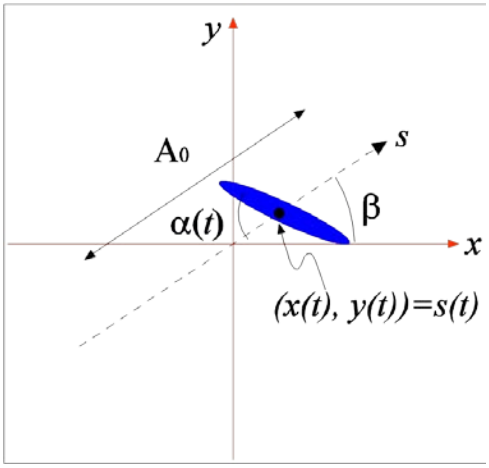

Figure 5: Two-dimensional flapping model. Angle $\alpha(t)$ is a given function of time. Position of the center of the wing (x, y) moves according to the equations of motion under the hydrodynamic force.

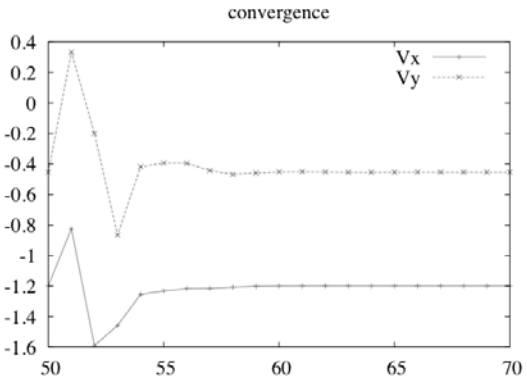

Figure 6: An example of the recovery from a perturbed state to the steady state. Velocities of the center-of-mass are shown as a function of the time measured by the flapping periods. A quick recovery is observed.

imposing symmetry on the phase space.

Based on this knowledge, we constructed another model with a restriction to achieve stable flight. The constructed model achieves stable flight in wide ranges of parameters. Therefore, maneuverability analysis in terms of the role of environment will be possible.

Currently we are studying the recovery process from the state in which a large perturbation is added at some time. An immediate recovery from the perturbed state is observed with the help of the vortices. We will tune the model parameter to compare the experimental results.

V. Discussion using 3D Model

The 3D mathematical model using a panel method has been constructed, where the panel method is a kind of vortex

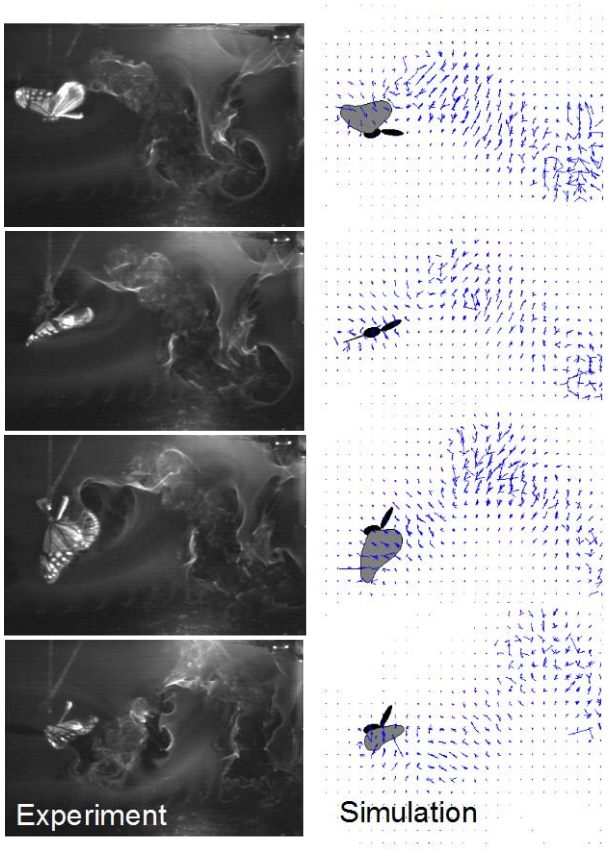

Figure 7: Experimentally visualized flow of flapping *Parantica sita niphonica* (left) and numerical simulation using 3D mathematical model (right)

methods. Its arithmetic precision has been improved by modification in the computer code because there was a situation in which the precision decreases.

The motion of the actual butterfly in Figure 2 is substituted into the mathematical model of the butterfly. Its aerodynamic forces are illustrated in Figure 3 with the experimental result. The numerical simulation result is comparatively in agreement with the experimental data. The improvement is to be continued because the error in drag is larger than that in lift.

Figure 7 shows video images of the flow around a butterfly visualized by a smoke wire. Figure 7 also shows the flowfield calculated by the 3D model. It is understood that the complex flowfield is formed by the flapping-induced free vortex in wakes from the experimental result. The numerical simulation almost catches the flowfield of the experiment.

ACKNOWLEDGMENT

The authors would like to express sincere thanks to Dr. Naomichi Ogihara of Kyoto University for the help of making XCT images of a butterfly.

REFERENCES

[1] K. Senda, M. Sawamoto, M. Kitamura, T. Obara, Towards Realization of Stable Flapping-of-Wings Flight of Butterfly, International Symposium on Adaptive Motion in Animals and Machines, 2008, pp. 62-63.

[2] K. Senda, M. Sawamoto, M. Kitamura, T. Obara, Effects of Flexibly Torsional Wings in Flapping-of-Wings Flight of Butterfly, World Automation Congress, 2008, pp. 1-6.

[3] M. Iima, A paradox of hovering insect in two-dimensional space, Journal of Fluid Mechanics, vol. 617, 2008, pp. 207-229.

[4] M. Iima and A. S. Mikhailov, Propulsion hydrodynamics of a butterfly micro-swimmer, Europhysics Letters, 2009. (accepted)

[5] M. Iima and Y. Nishiura, Unstable periodic solution controlling collision of localized convection cells in binary fluid mixture, Physica D, vol. 238, 2009, pp. 449-460.

[6] M. Iima, Mathematical analysis of flapping flight, Section 8, Chapter 1, Part 3 in Insect Mimetics, NTS, Tokyo, Japan, 2008, pp. 672-277. (in Japanese)

[7] M. Iima, Mathematical Structures in flapping flight, Bulletin of the Japan Society for Industrial and Applied Mathematics, vol. 18, no. 4, 2008, pp. 39-51. (in Japanese)

[8] M. Iima, Force acting on flapping wing in two-dimensional fluid and its application to insects flight, Annual Meeting of the Japan Society of Fluid Mechanics, 2008. (in Japanese)

[9] M. Iima, Fluid Dynamics of Flapping Flight, Butsuri (Physical Society of Japan), vol. 63, no. 4, 2008, pp. 629-633. (in Japanese)

[10] M. Iima, Robustness of an insect's hovering: a transition of flapping free-flight, ICTAM 2008, 2008.

[11] M. Ishii, N. Hirai and T. Hirowatari, The occurrence of an endangered lycaenid, Zizina emelina (de l'Orza), in the Osaka International Airport, central Japan, Trans. lepid. Soc. Japan, vol. 59, 2008, pp. 78-82.

[12] M. Yago, N. Hirai, M. Kondo, T. Tanikawa, M. Ishii, M. Wang, M. Williams, R. Ueshima, Molecular systematics and biogeography of the genus Zizina (Lepidoptera: Lycaenidae), Zootaxa, vol. 1746, 2008, pp. 15-38.

[13] N. Iwata, N. Akieda, N. Hirai and M. Ishii, Seasonal prevalence of a migratory dragonfly, *Pantala flavescens*, in Sakai City, Osaka Prefecture, central Japan, Tombo, 2009. (in press) (in Japanese with English summary)

[14] S. Kuroda, N. Hirai, M. Ishii, Effects of host instar at the time of parasitization on the development of *Apanteles baoris* (Hymenoptera: Braconidae), a larval parasitoid of *Parnara guttata guttata* (Lepidoptera: Hesperiidae) Jpn. J. Appl. Entomol. Zool., 2009. (in press) (in Japanese with English summary)

[15] N. Hirai, Distributional expansion of two lepidopterans, *Chilades pandava* and *Asota ficus*., Nature and Insects, vol. 43, no. 12, 2008, pp.13-16. (in Japanese)

[16] S. Yokota, N. Hirai, A record of Hypolimnas bolina from Ikeda City, Osaka Prefecture, central Japan, Nature and Insects, vol. 44, no. 1, 2009, p. 30.

A study on adaptation to environments in a network of dynamical elements

Toshio Aoyagi, Graduate School of Informatics, Kyoto University
Ichiro Tsuda, Research Institute for Electronic Science, Hokkaido University

***Abstract*— To realize high adaptability to the environment for the survival, the animal has to decide the optimal action, for example, to walk to the better environment. The central nervous system is an extremely efficient information processing device for this purpose. Therefore, we need to clarify the essence of the underlying mechanisms. The key feature is that the state of neurons at the nodes and the synaptic weights interact with each other via learning mechanisms. As such a system, we first investigate co-evolving dynamics in a weighted network of phase oscillators. It is found that this system exhibits three kinds of asymptotic behavior: a two-cluster state, a coherent state with a fixed phase relation, and a chaotic state with frustration. Next, to clarify a mechanism of episodic memory formation in the hippocampus, we made a model for the hippocampal CA3 and CA1. We obtained, for the model CA3, a successive association of stored patterns, which can be regulated by emergent chaotic activity of neural networks. We found in the model CA1 a Cantor set in the membrane potentials of CA1 neurons, and clarified the functional significance of this set in relation to episodic memory. On the basis of these findings, we will explore the essential mechanisms of neuronal systems for emergence of adaptation through interaction among the body, brain and environment.**

I. INTRODUCTION

The central nervous system is an extremely efficient information processing device to realize high adaptability to the environment for the survival. As the underlying mechanisms, the synaptic plasticity such as Hebbian learning is very important[1], [2]. This activity-dependent synaptic plasticity is based on the memory function. In this context, we have mainly studied two closely related subjects.

The first one is to elucidate the types of behaviors that can emerge in neuronal systems with various leaning rules and the functional role played by the evolution of the synaptic weights. Among many typical types of behavior, limit-cycle oscillation is widely observed in real neuronal systems, and coupled limit-cycle systems often generate a rich variety of collective behavior. Furthermore, limit-cycle oscillation is structurally stable, and it can be described by a simple model of phase oscillator that is mathematically tractable. Therefore, it is reasonable to first consider a limit-cycle oscillator as the dynamical unit in the neuronal network1.

The other is to clarify a neural representation of input temporal sequence of spatial patterns in the hippocampus. For this purpose, we have tried to extract a dynamical law embedded in the neural dynamics. In the model CA3, chaotic itinerancy plays a role in producing a sequence of memory patterns. In the model CA1, such a sequence can be encoded into a Cantor set, being regulated by self-organization of affine transformations. To substantiate these things, we also conducted an experiment, using rat hippocampal slices, collaborated with Tsukada's laboratory in Tamagawa university. The experiment proved the presence of affine transformations and a hierarchical clustering of responsive membrane potentials, indicating the creation of Cantor sets. In the following, we describe attractors which can be a basis of chaotic itinerancy, and show an example of chaotic itinerancy in neural networks. We further describe dynamic behaviors of CA1.

II. CO-EVOLUTION OF PHASES AND CONNECTION STRENGTHS IN A NETWORK OF PHASE OSCILLATORS

We first investigate the co-evolving dynamics in a weighted network of phase oscillators, in which the phases of the oscillators at the nodes and the weights of the links interact with each other. Depending on the nature of the evolution of the coupling weights, this system can exhibit three distinct types of dynamical behavior: a two-cluster state, a coherent state with a fixed phase relation, and a chaotic state with frustration(See figure 1). This system exhibits a two-cluster state and a coherent state with a fixed phase relation when the dynamics of the weights are qualitatively similar to typical learning rules in neural network specified by the Hebbian and the spike-timing dependent plasticity rules, respectively. A chaotic state is realized in the

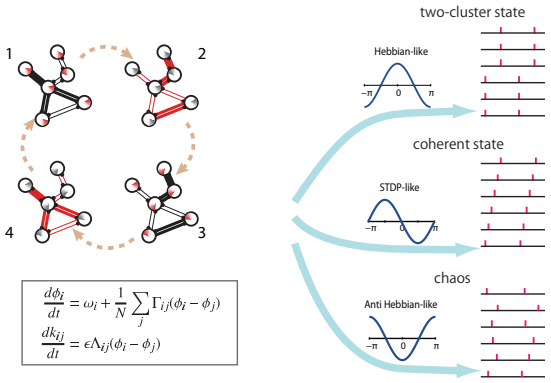

Fig. 1. A schematic illustration of co-evolution of both phase oscillators and network connections. 1. The phase pattern causes the structure of the weighted network to change. 2. The change undergone by the weights causes a new phase pattern to appear. 3. The change of the phase pattern results in further modulation of the weights of the network. 4. This process repeats. Note that in the actual process the phases and connections co-evolve simultaneously, not in a step-by-step manner.

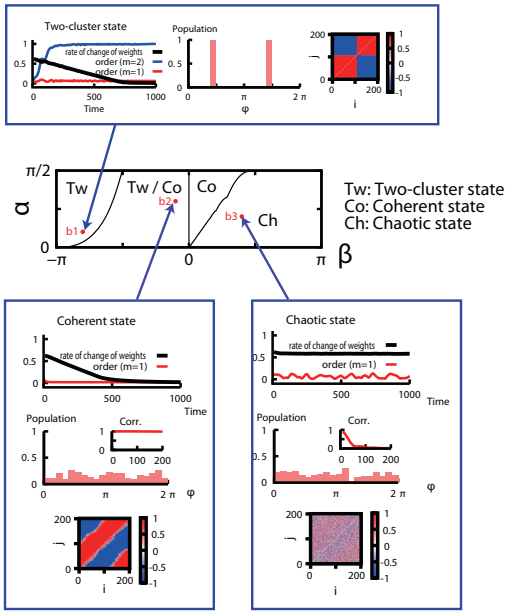

Fig. 2. Phase diagram of an N oscillators system (N=200). The asymptotic states appearing in the regions depicted are a two-cluster state, a coherent state with a fixed phase relation, and a chaotic state with frustration. For three typical simulation results, the time evolution of the order parameters and the normalized rate of change averaged over all weights, the distribution of the phase ϕ_i at t = 1000 (The inset displays the auto-correlation function of the phase pattern), the weight matrix k_{ij} in the final state (t=1000) are shown. The indices i and j of oscillators are arranged in order of increasing phase. The parameter value is ε=0.005, and the initial conditions for k_{ij} were chosen randomly from a uniform distribution on $[-1, 1]$.

case that the dynamics of the weights and phases are frustrated(See figure 2). A more complete characterization of these three states is provided by the mutual information between the initial and final phase patterns and the entropy of final phase pattern. As a result, the mutual information is largest for the coherent state. Because the mutual information is the information that the initial and final states share, the initial phase relationship among the oscillators is most easily inferred from the final one in the case of the coherent state. This suggests that the coherent state can be interpreted as representing a memory of the phase pattern. In context of neural networks, which represent a typical example of the type of co-evolving system to which our model may be applicable, such sequential neural activity embedded in a network organized under STDP learning, has been studied both theoretically and experimentally with regard to the temporal neural coding. For the two-cluster state, the situation is qualitatively similar, except that the entropy is much smaller. This is because the allowed states of an oscillator belonging to the two clusters is restricted to only two possibilities. Therefore, this state is capable of representing a memory of binary data. As stated above, this state is organized under a kind of like-and-like rule. For the chaotic state, the fact that the mutual information vanishes implies that the information regarding the initial state is lost with time, and the fact that entropy is close to maximal suggests that the system wanders over all or nearly all possible phase patterns. Even though at the present time we cannot give an example of this kind of chaotic state observed in real systems, we believe that such chaotic behavior will be seen in some type of co-evolving systems when compared with our model.

III. CA1 MODEL AND CANTOR CODING

A. *The definition of attractors*

First, we introduce a conventional definition of attractor.

a) : **Definition (Geometric attractor)**

Let M be a compact smooth manifold. Let $f : M \to M$ be a continuous map on M. A trapping region is defined as a subset N of M, satisfying $f(N) \subset inter(N)$, where $inter(N)$ is an interior of N. For the trapping region N of M like this, $A = \cap_{n=0}^{\infty} f^{(n)}(N)$ defines an attracting set. A geometric attractor is a minimal attracting set, that is, an attracting set satisfying topological transitivity is a geometric attractor, which is simply called an attractor.

b) : However, the above definition of attractor cannot be applied to some class of dynamical behavior, which is typically produced by the following dynamical

system. This dynamical system is essentially the same as that provided by Milnor, i.e. a dynamical system producing a different attractor from a geometric attractor [7].

c) : **Criticality to intermittency** [6]

Let f be at least a C^1 map on R, $f : R \to R$. We use the following map, f, defined on the unit interval in R.

$$x_{n+1} = f(x_n) \mod 1 \quad (x_n \in [0,1), \forall n \geq 0), \quad (1)$$

$$f(x) = x - \omega \cos(2\pi x) + \omega, \quad \omega = \frac{1}{2}. \quad (2)$$

The stability of the fixed points of the map is neutral, i.e. indifferent, which is a typical nonhyperbolic dynamical system. That is, a perturbed system in neighborhoods of these fixed points begins from the second order. In this example, there is no trapping region of the fixed points because there are orbits departing from the fixed points in these neighborhoods. Thus, the fixed points are not geometric attractors. The orbits starting from the points $x_0 \in [0,1)$ are eventually absorbed in either fixed point. Therefore, it is plausible to think that the fixed point like this is an attractor in a different sense from the conventional one. In this way, the concept of attractor must be extended to include a measure-theoretic concept. The direction that Milnor showed is this type of conceptualization. A Milnor attractor [**?**], [7] is defined as follows.

d) : **Definition (Milnor attractor)**

Let M be a phase space, and B a set. A basin-like region of B is defined as follows: $\rho(B) = \{x | \omega(x) = B, x \in M\}$. A Milnor attractor is defined as a set B satisfying the following two conditions.

1. $\mu(\rho(B)) > 0$, where μ is a measure equivalent to the Lesbegue measure.

2. There is no true subset B' of B such that $\mu(\rho(B) \backslash \rho(B')) = 0$.

e) : In this way, the condition that all orbits in a neighborhood of the attractor should be absorbed into it is not necessarily demanded. A positive measure of orbits converging onto an attractor is demanded. This implies that there could be orbits leaving an attractor. Thus, a geometric attractor is a Milnor attractor, but not vice versa.

B. Chaotic itinerancy in neural systems

We have also proposed a simple neuron model with two variables, the μ- model [8].

μ-model: (class I)*

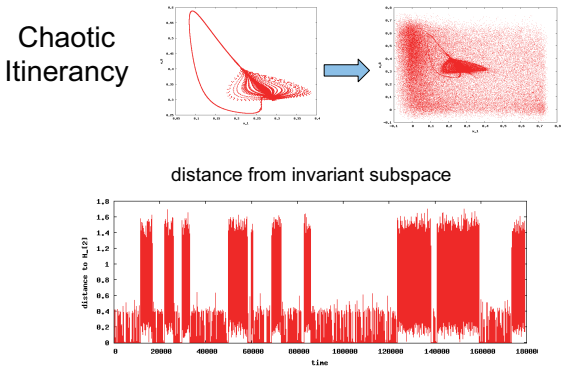

Fig. 3. A typical chaotic transition between synchronized and desynchronized states in the gap junction-coupled μ-model.Top-left:on-off intermittency, Top-right: chaotic itinerancy. Bottom:Random transition between on-off intermittency and fully developed chaos.

$$\begin{cases} \dfrac{dx}{dt} = -y - \mu x^2 (x - \dfrac{3}{2}) + I \\ \dfrac{dy}{dt} = -y + \mu x^2. \end{cases} \quad (3)$$

We found a chaotic transition between synchronized and desynchronized states in the gap junction-coupled μ-model that has similar symmetry to the one mentioned above, that is, the whole synchronized state constitutes an invariant subspace (See figure 3). Based on numerical studies, we have further proposed a hypothesis that this transition can be described as CI.

C. Cantor coding in CA1

We studied an abstract CA1 model and found the Cantor coding [10]. Furthermore, to investigate the biological plausibility of this idea, we investigated a biology-oriented model that represents the physiological neural networks of CA1. For a single neuron model, we used a two-compartment model proposed by Pinsky and Rinzel [9], which produces quite similar dynamics for the membrane potentials of an actual hippocampal neuron. The input consists of a given number of spatial patterns. We investigated the dynamic behavior of membrane potentials produced by the model CA1 neurons. In both subthreshold and superthreshold dynamics, we found Cantor sets. Furthermore, the distribution of membrane potentials for the model CA1 neurons obeys a bimodal distribution whose minimum corresponds to the neuron's threshold. This result may indicate the possibility of decoding the information embedded into Cantor sets by means of a pulse train output from pyramidal cells.

At the next stage, we investigated a mechanism of the production of Cantor sets in the membranes? We observed a set of affine transformations, by taking return maps of the membrane potentials of neurons whenever each elementary pattern in input time series appears. Thus, if we find a set of affine transformations as a basis of IFS in experiment, this can be an evidence of the presence of Cantor coding.

To substantiate these things, we conducted an experiment, where we investigated whether Cantor coding can be realized in the actual neural system of the hippocampal CA1. We used rat hippocampal slices and presented electric stimuli to the Shaffer collaterals of pyramidal cells in CA3, with these collaterals making synaptic contacts with pyramidal cells in CA1. The electric stimuli used consisted of random time series of spatial patterns. We observed a set of contractive affine transformations in a return map [14], as well as a hierarchical clustering of the membrane potentials of a CA1 neuron [13], which apparently indicate the production of Cantor sets in CA1 neurons.

IV. CONCLUSIONS AND FUTURE WORKS

In summary, we have first investigated co-evolving dynamics in a weighted network of phase oscillators in which phase oscillators at the nodes and the weights of their links interact and co-evolve. We found that this system exhibits three distinct types of dynamical patterns: a two-cluster state, a coherent state with a fixed phase relation, and a chaotic state with frustration. Because of its structural stability, it is believed that our model captures the essential characteristics of a class of neural networks. Next, to clarify a mechanism of episodic memory formation in the hippocampus, we made a model for the hippocampal CA3 and CA1. We obtained, for the model CA3, a successive association of stored patterns, which can be regulated by emergent chaotic activity of neural networks, i.e. chaotic itinerancy. In the model CA1, we found a Cantor set and affine transformations in the membrane potentials of CA1 neurons. We also conducted an experiment, using the rat hippocampal slices, and observed the Cantor-like sets as well as affine transformations. On the basis of the above findings, using the novel experimental methods such as brain machine interface and cultured neural systems, we will study the adaptation mechanism through the interaction between environments and neuronal systems in the near future.

V. ACKNOWLEDGMENTS

We would like to thank T. Tanaka, M. Nomura and T. Aoki who participated in the first study. We also would like to express our special thanks to H. Fujii, M. Tsukada, K. Aihara, and S. Nara, for continual and invaluable discussions about the second study.

REFERENCES

[1] D. O. Hebb, *The Organization of behavior: A Neuropsychological Theory*. Wiley, New York, 1949.

[2] G. Q. Bi and M. M. Poo, "Synaptic modifications in cultured hippocampal neurons: dependence on spike timing, synaptic strength, and postsynaptic cell type," *J. Neurosci.*, vol. 18, pp. 10 464–10 472, Dec. 1998.

[3] H. Cateau and T. Fukai, "Local synchrony formed by spike-timing-dependent plasticity working on asynchrony-favoring neurons," *Neurosci. Res.*, vol. 58, p. S53, 2007.

[4] T. Aoki and T. Aoyagi, "Co-evolution of phases and connection strengths in a network of phase oscillators," *Phys.Rev.Lett.* in press.

[5] Kaneko, K. and Tsuda, I., eds.: *Focus Issue on Chaotic Itinerancy*. *Chaos* **13**: 926-1164, 2003.

[6] Tsuda, I. and Umemura, T., Chaotic itinerancy generated by coupling of Milnor attractors. *Chaos* **13** (3) (2003) 937-946.

[7] Milnor, J.: On the concept of attractor. *Comm. Math. Phys.* **99**: 177-195, 1985.

[8] Tsuda, I.,Fujii, H., Tadokoro, S., Yasuoka, T., and Yamaguti, Y. Chaotic Itinerancy as a Mechanism of Irregular Changes between Synchronization and Desynchronization in a Neural Network. *J. of Integrative Neuroscience* **3**(2004) 159-182.

[9] Pinsky, P. F. and Rinzel, J., Intrinsic and network rhythmogenesis in a reduced traub model for CA3 neurons. *J. Comput. Neurosci. 1* (1994), 39-60.

[10] Tsuda, I. and Kuroda, S.: Cantor coding in the hippocampus. *Japan J. Indust. Appl. Math.* **18**: 249-258, 2001.

[11] Tsuda,I.: Towards an interpretation of dynamic neural activity in terms of chaotic dynamical systems. *Behav. Brain Sci.* **24**: 793-847, 2001.

[12] Yamaguti Y., et al. in preparation, 2008.

[13] Fukushima, Y., Tsukada, M., Tsuda, I., Yamaguti, Y., and Kuroda, S., Spatial clustering property and its self-similarity in membrane potentials of hippocampal CA1 pyramidal neurons for a spatio-temporal input sequence. *J. Cogn. Neurodynamics* **1** (2007) 305-316.

[14] Kuroda, S., *et al*, submitted to J. Cogn. Neurodynamics, 2008.

Basic strategy for trajectory planning in human movements

Jun NISHII
Yamaguchi University

***Abstract*— Many living bodies have actuators with redundant degrees of freedom. In order to understand the design of animal movements that exploit such redundancy, we have studied the following three topics: (1) how living bodies (1) constrain and (2) utilize their redundancy during usual movements, and (3) how they efficiently acquire the ability to manipulate their redundant bodies.

Concerning to the first topic, authors have shown that typical leg swing trajectories during human walking is similar to the optimal one which minimizes energy cost. Furthermore, our recent results have shown that swing trajectories of backward walking and monkey's biped walking, and arm reaching trajectories are also similar to those minimizing energy cost. These results suggest that the minimization of the energy cost would be an basic strategy in the design of animal movements. On the other hand, movement trajectories of living bodies often show variability. We found that the variability of joint trajectories during monkey biped-walking are constrained, in other word synergy of joint movements are observed, so as to suppress the variability of the foot position at the end of swing phase. Concerning to the second topic, we took a simulation experiment of learning control of a redundant system in order to confirm the validity of the Bernstein's hypothesis of freezing and freeing which suggests that joint stiffness might be decreased as learning proceeds and our result have suggested that efficient learning can be realized by the idea of freezing and freeing.

I. INTRODUCTION

Bernstein argued that human skill is to manipulate redundant degrees of freedom of our body. In order to understand the underlying mechanism to manipulate the redundancy, authors have studied (1) how living bodies constrain and (2) utilize their redundancy during usual movements, and (3) how they efficiently acquire the ability to manipulate their redundant bodies.

The first problem is about what kind of criterion living bodies are using in the selection of a trajectory from infinite number of possible ones which can accomplish a given task. This question also ask what is the goal of learning, which would be an important view point to know the learning mechanism of living bodies.

The graduate school of science and engineering, Yamaguchi University, 1677-1 Yoshida, 753-8512 Yamaguchi, JAPAN, nishii@sci.yamaguchi-u.ac.jp

The second one is related to an episode told by Bernstein "skilled smith's hammer hits a given target correctly but his joint trajectories are not constant but show variability". Such variability would be a cue to understand how our brain constrain and utilize the multiple degrees of freedom of our body in order to accomplish a task.

The third problem is about the learning process to acquire an ability to manipulate redundant system, Bernstein suggested that human freezes some degrees of freedom by increasing joint stiffness in the beginning of learning and then freeing them as learning proceeds. Following sections summarize some results concerning these problems.

II. CONSTRAINT ON DEGREES OF FREEDOM

A. Trajectory planning of leg swing trajectory during walking

We have obtained some results which indicate that the leg swing trajectory during walking might be optimized on energy cost [1]. This year, we examined whether leg swing trajectory of human backward walking and monkey biped locomotion can be explained by the same criteria. Grasso et al. reported that backward walking is a kind of reverse motion of leg kinematics of forward walking [2]. However, the results of our measurement experiments of backward walking show some difference from the reverse of forward walking. On the other hand, the optimal swing trajectory minimizing energy cost well coincident with the measured one (Fig.1). This result indicate that backward walking would be an optimized movement rather than a simple reversal motion of forward walking. We also confirmed that such optimization is observed not only in human walking but also in biped walking by a Japanese monkey (Fig. 2).

Many experimental and theoretical studies have suggested that locomotor pattern is optimized on energy cost. Above results also support the hypothesis that locomotor pattern is optimized on energy cost.

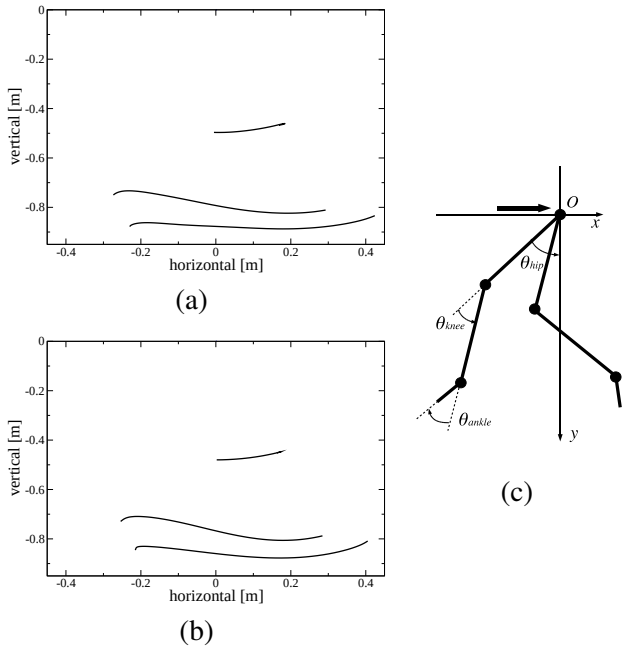

Fig. 1. Horizontal view of the measured and optimal leg swing trajectories of human backward walking. (a) shows the measured trajectory and (b) shows the optimal one minimizing energy cost. In each figure, the upper, middle and lower lines show the position of knee joint, ankle joint and toe. The origin is the location of the hip joint (see (c)). Right side is the walking direction.

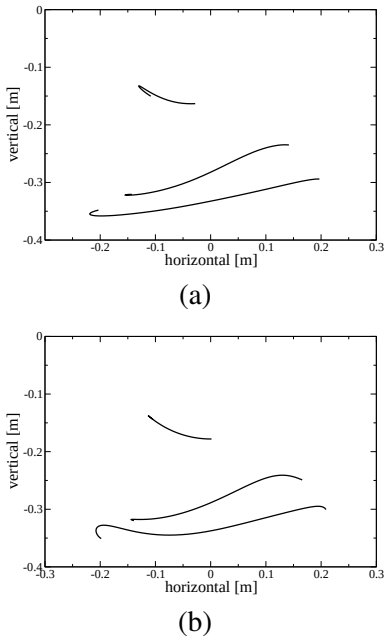

Fig. 2. Horizontal view of the measured and optimal leg swing trajectories of biped-locomotion of a Japanese monkey. (a) shows the measured trajectory and (b) shows the optimal one minimizing energy cost. In each figure, the upper, middle and lower lines show the position of knee joint, ankle joint and toe joint. The origin is the location of the hip joint (see Fig.1(c)). Left side is the walking direction.

B. Trajectory planning of human arm reaching

As noted in the previous section, many studies have suggested that locomotor pattern is optimized on energy cost. On the other hand, reaching movements of human upper-limb have been explained by other criterion.

We computed the optimum reaching trajectory minimizing the expected value of energy cost when motor command is affected by noise [3]. The speed profile of the optimal trajectory showed a bell-shaped curve like human data when movement duration is short, however, showed a collapsed shape when the duration is long. In order to examine the speed profile of human arm reaching with long duration, we took an experiment and confirmed that speed profile took collapsed shape when the movement duration is over about 1.5 [s] even after one week practice. Theis result suggests that the criteria of minimization of the expected value of energy cost explains not only the characteristics of usual reaching movements but also those for slow movements.

III. Exploitation of degrees of freedom

Even for skilled tasks, human movements show variability at every trial. Fig. 3 is the joint trajectories of biped locomotion of a Japanese monkey that is nine years old and have trained biped walking for eight

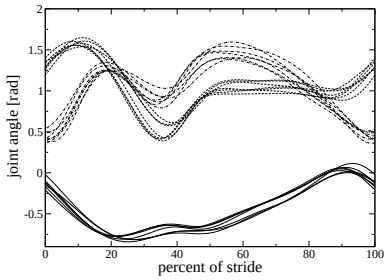

Fig. 3. Joint trajectories of biped locomotion of a Japanese monkey. Solid, broken and chain lines show hip angle, knee angle, and ankle angle respectively.

years. Although the monkey shows skilled biped walking, the figure shows that joint trajectories take different path each time. Scholz and Schöner proposed the idea of Uncontrolled Manifold (UCM) by respecting such variability [4]. The UCM is defined as a manifold that express a combination of the task variables, such as joint angles, which can accomplish a given task (Fig.4). For instance, there are infinite number of possible leg joint angles in order to realize a given hip height except its maximum height, and the space which is composed of the possible angles is called as the UCM. Latash et al. suggested that motor control by living body would

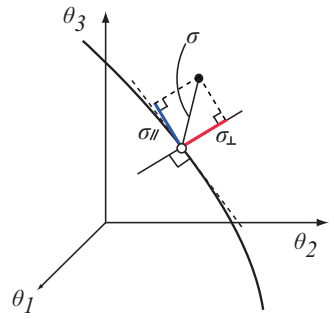

Fig. 4. Analysis of variability from the view point of the UCM. In the analysis of the leg trajectory of a Japanese monkey, axes show joint angles, open circle shows the average of joint angles at a specific time in a waking cycle, and curved line is the UCM that shows the possible solutions to realize the same toe position. $\sigma_{\parallel}$ and $\sigma_{\perp}$ show the parallel and orthogonal components of the deviation to the UCM. The former deviation does not affect the toe position but the latter does.

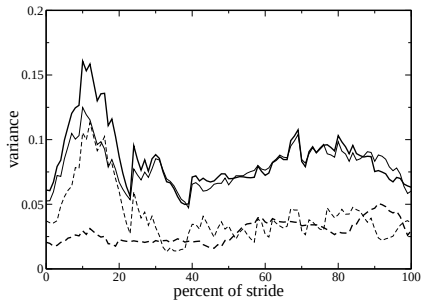

Fig. 5. Time profile of variability of joint angles during biped walking of a Japanese monkey. 0% of stride is the start of swing phase, 37% and 100% of stride shows the start and the end of stance phase, respectively. Thin and thick solid lines show $\sigma^x_{\parallel}$ and $\sigma^y_{\parallel}$, respectively, and thin and thick broken lines show $\sigma^x_{\perp}$ and $\sigma^y_{\perp}$, respectively.

permit variability on the UCM at some extent and stabilize the UCM [5].

Fig. 5 shows the variability of joint angles during biped-walking of the Japanese monkey of which leg trajectory was shown in Fig. 3. $\sigma^x_{\parallel}$ and $\sigma^x_{\perp}$ show the parallel and orthogonal components of the standard deviation to the UCM which keep the x value of the foot position relative to the hip position constant (see Fig. 1(c) about the axis), respectively (see Fig.4 about the geometrical meaning of them), and $\sigma^y_{\parallel}$ and $\sigma^y_{\perp}$ show the parallel component and orthogonal components of the standard deviation to the UCM which keep the y value of the relative foot position constant, respectively. Over the stride period, $\sigma^y_{\perp}$ is low, but $\sigma^y_{\parallel}$ takes much larger value than $\sigma^y_{\perp}$. This implies that coordination between joints, synergy, works so as to suppress the variance of the foot height. During the middle of swing (10-20% stride) all standard deviations except $\sigma^y_{\perp}$ are large, which means that variance which does not affect the foot height increases, however, in the end of swing (30-37% stride), $\sigma^x_{\perp}$ decreases, which means that coordination of joints works so as to tune the foot position precisely for grounding.

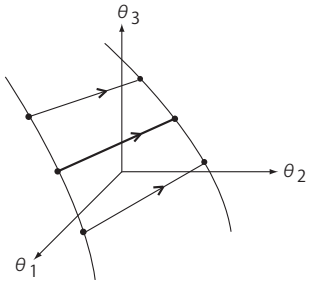

Fig. 6. Reaching movement between two points by a redundant arm is expressed as a movement between two manifolds. One of the most important factors of mastery is to know the wider range of the UCM.

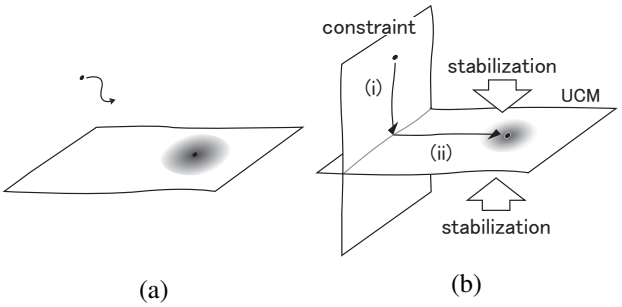

Fig. 7. Schematic view of learning process. Each figure shows the space of control variables, such as joint angles, planes show the UCM, the point on the UCM is the optimal solution and shaded area shows the permitted deviation from optimal point. Most learning technique searches the optimal point from the beginning of learning (a), however, Learning process of human might be composed of two phases; the first is to find a solution to realize a given task by preparing a constraint adequate (see (i) in (b)) and the second is to explore on the UCM and find an optimal solution ((ii) in (b)).

IV. Freezing and Freeing of Degrees of Freedom

From the view point of the UCM, learning is a process to find and acquire the UCM to accomplish a given task. Redundant number of actuators enlarge the dimension and range of the UCM. If nervous system acquires wider range of the UCM, the knowledge would contribute to manipulate redundant actuators and improve robustness. On the other hand, larger number of actuators require longer time for learning. Bernstein pointed out that human freezes their redundant actuators in the beginning of learning and acquires

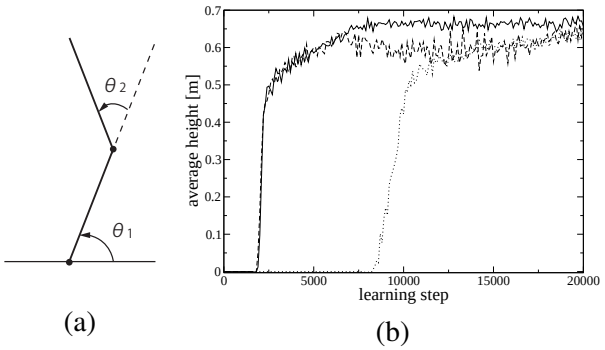

Fig. 8. Learning simulation of two-joint inverted pendulum. (a) Inverted pendulum. (b) Simulation result. Every learning steps, control signal to the pendulum was learned by TD learning from random initial position. Every 100 learning step, 100 test simulations were performed from random initial positions and the final height at the end of each test was recorded. The lines show the average height of such 10 simulations. Solid, dotted, and broken lines show the results when the stiffness of knee joint is high (frozen), low (freed), and from high to low (from frozen to freed), respectively. The maximum height of the pendulum is 0.7.

the ability to manipulate them by freeing the frozen degrees of freedom as learning proceeds. From these considerations, learning process might be composed of following four phases.

1) **Reaching UCM:** Sub-goal in the beginning of learning would be to find a point on the UCM for a given task.
2) **Acquiring UCM:** After finding a point on the UCM, next sub-goal is to know many other possible solutions to accomplish a task by acquiring the shape of the UCM (Fig.6).
3) **Stabilizing UCM:** Acquired UCM must be stabilized by some control mechanism, so as to reach a point on the UCM which is near from given initial state (Fig.7).
4) **Finding optimal solution on UCM:** Final phase would be to know better solution on the UCM in some meaning, e.g., finding a solution to accomplish a task with minimum energy cost.

Bernstein's idea of freezing would be effective during the first phase and freeing would be necessary from 2nd to 4th phase.

We took a simulation experiment of learning control of a redundant arm in order to confirm the validity of the Bernstein's hypothesis of freezing and freeing. Fig.8 shows a results of learning simulation of stand up straight of a two-joint inverted pendulum and shows that when knee joint stiffness decreases with the improvement of the performance, the average height of the pendulum increases in earlier stage than the results when knee stiffness is low from the beginning of the learning. This result indicate that freezing and freeing would be effective to accomplish a task in early stage and then acquire the ability to utilize more degrees of freedom as Bernstein suggested

V. Conclusion

We have studied how living bodies constrain and exploit the redundant degrees of freedom of their body. Our results suggest that minimization of energy cost would be an important strategy to constrain the DOFs on skilled movements. On the other hand, even for skilled tasks living bodies show variability on their movements. Our analysis of the variability of the biped locomotion of a Japanese monkey have suggested that leg posture for grounding is precisely controlled by a coordination of joints. Such analysis of variance would be an effective method to know how living bodies control their movements in order to increase robustness. We are planning to analyze human movements by the same method to know the control strategy and learning mechanism of human from view points of the UCM and "freezing and freeing".

Acknowledgement

The data of biped locomotion of the Japanese monkey analyzed in this article is provided by Dr. Naomichi Ogihara at Kyoto University. I would like to express my gratitude for the cooperation.

References

[1] A. Fujii, H. Suenaga, Y. Hashizume, and J. Nishii, "Variability of leg swing trajectories and their optimality," *Proc of 4th International Symposium on Adaptive Motion in Animals and Machines*, pp. 173–174, 2008.

[2] R. Grasso, L. Bianchi, and F. Lacquaniti, "Motor patterns for human gait: backward versus forward locomotion," *J Neurophysiol*, vol. 80, no. 4, pp. 1868–1885, 1998.

[3] Y. Taniai and J. Nishii, "Optimality of reaching movements based on energetic cost under the influence of signal-dependent noise," *Neural Information Processing, Lecture Notes in Computer Science*, vol. 4984, pp. 1091–1099, 2008.

[4] J. P. Scholz and G. Schöner, "The uncontrolled manifold concept: Identifying control variables for a functional task," *Exp Brain Res*, vol. 126, pp. 289–306, 1999.

[5] M. L. Latash, J. P. Scholz, and G. Schöner, "Motor control strategies revealed in the structure of motor variability," *Motor control and motor variability*, vol. 31, no. 1, pp. 26–31, 2002.

Adaptation and emergence of biological function by environment-dependent-dynamical network in plasmodium of *Physarum polycephalum*

A. Takamatsu*[1], M. Ito[1], R. Okamoto[1], T. Gomi[1],
S. Arafune[1], S. Watanabe[1], A. Tero[2], T. Nakagaki[2]
[1] Department of Electrical Engineering and Bioscience, Waseda University,
3-4-1, Okubo, Shinjuku-ku, Tokyo, 168-8555, Japan
[2] Research Institute for Electronic Science, Hokaido University,
Kita 12 Nishi 6, Kita-ku, Sapporo 060-0812, Japan

***Abstract*— Plasmodium of true slime mold, *Physarum polycephalum*, is multinucleated unicellular amoeba-like organism. It crawls on environment with cell-thickness oscillation. Although the plasmodium seems to be peculiar, it is one of the ideal model organisms from viewpoint of "mobiligence."**

Even when the plasmodium is divided into parts, each part behaves as a single oscillating cell without losing biological funcition. Therefore the plasmodium can be considered as a collective of units, i.e., coupled oscillators. On the other hand, the cell forms a network of tubular structure, inside which protoplasmic streaming is observed. The streaming act as interaction among the units. Interestingly, the morphology of the plasmodial network depends on environmental condition, as well as oscillation frequency. This suggests that the network morphology could affect the biological function to adapt to environment.

Currently, we focus only on the topology of the tubular network and have been analyzed the network structure for each environment. In this study, we will step into analyzing the relation between the dynamical network and biological function with considering interaction between the plasmodium and the environment to capture an algorithm of adaptation by dynamical network morphology.

I. Introduction

Most of biological organism have transportation network to distribute oxygen, neutrient and etc., into whole body. Animals including human have blood vessels network. Plants have leaf veins and vessels [1]. By expanding this to population, trail pattern by ant-foraging [2], road grid constructed by human [3], and power grid as man-made structures can be included as some of examples for transportation networks. The morphology of the networks depends on species and environment, which could affect each biological function. In this study, we investigate adaptation by transportation network morphology by using plasmodium of true slime mold, *Physarum polycephalum*.

II. Plasmodium of true slime mold as model organism

The cell size of plasmodium of true slime mold ranges from 10μ m to 1 m. Even if the single cell is divided into multiple parts, each part can be alive. On the other hand, multiple cells can fuse into a single cell to behave as a single individual. Ability of the cut & paste manipulation in the plasmodium results from unusual cell system, i.e., in which the plasmodium is multinucleated unicellular organism including thousands of nucleus in a single cell.

To maintain such a large cell body, the plasmodium developed a peculiar system in which the cell itself is a transportation network consisting of tubular structure. The tubular network is formed when the cell body spread into environment by oscillating cell thickness and crawling. The protoplasmic streaming observed inside the tubes transports nutrients, oxygen, organella, and etc., all aver the cell body.

The morphology of the plasmodium changes depend on environment [4]. It shows thin sheet with meshed thin tube network when the environment is nutrient-rich or the substratum is stiff (attractive condition; Fig.1(a,b)). In contrast, it shows dendritic network with thick tubes when the environment contains harmful chemicals or the substratum is soft(repulsive condition; Fig.1(d)).

The network morphology continuously changes depending on culture condition such as concentration of nutrient, repellents, substratum stiffness. At neutral condition with substratum of intermediate stiffness without chemicals, the plasmodium shows intermixture morphology between attractive and repulsive conditions, namely, meshed in center and dendritic network in outer region (Fig.1(c)).

Our goal is to elucidate (1) what the physical mechanism for the environment-dependent morphology is, and (2) how effective and functional the strategy of the environment-dependent morphology is as biological system . For this, synthetic and systematic approach will be effective; We should discuss functionality and efficiency of those various networks based on mathematical model. To obtain information for construction of mathematical model, we first quantify the growing process of the network morphology in §III, §IV, then investigate the efficiency of each network in §V, last introduce application examples for the artificial system §VI.

*atsuko_ta@waseda.jp

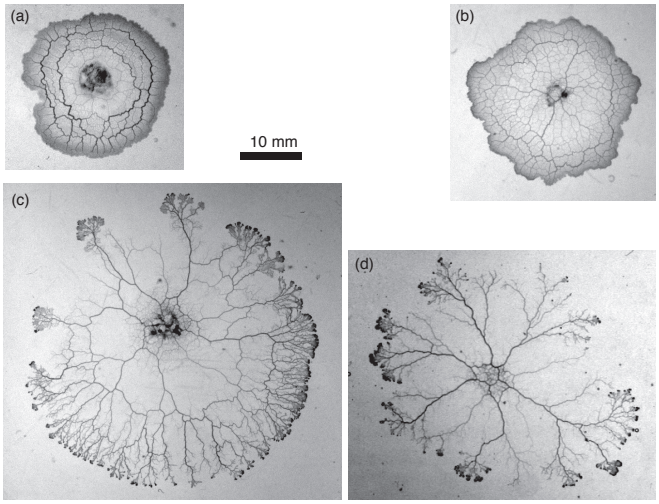

Fig. 1. Environment dependent morphology.(a) Concentric network, (b) mesh, (c) mixture of mesh and tree, (d) tree network. All plasmodia were cultured on 0.9 w/v% agar media including 10 w/v% oat meal extract (a, b), 10mM KCl (d). Pictures were taken at 470 min (a), 690 min (b), 710 min (c), 465 min (d) after sample set up.

III. Analysis on network topology (Ito and Takamatsu)

We only focus on network topology of tubular structure in this section. Vertices in the network were defined at bifurcation points or meeting point of protoplasmic flow in the tubes. Edges were defined in the tubes connecting the both ends, i.e., the vertices. Then the connection relations were examined (Fig.2(c), [9]).

From the information on vertices and edges, we calculated number of vertices n, mean degree $< k >$ (k is number of edges the regarding vertex has), clustering coefficient C, mean path length L as usually considered to analyze complex networks [6]. In addition to this, we also estimated meshedness coefficient M [7], which is useful to evaluate how densely the network has circle structure in two-dimensional network such as plasmodial network. Significant examples are shown in Fig.3 for plasmodial networks in attractive condition and repulsive condition.

The mean shortest distance between any two vertices L indicates how widely the network spread. Fig.3(a) shows n-L plot. L increases slowly depending on n in attractive condition, while it increases drastically at $n = 2000$ in repulsive condition.

In general, two dimensional lattice shows the relation $L \propto \sqrt{n}$, while tree-graph network shows the relation $L \propto \log n$. We analyzed which model can be applied to networks in each condition by cross-validation method [8] by including a linear relation. The networks in attractive conditions tend to follow the lattice model, while the networks in repulsive conditions tend to follow the tree-graph model (except the drastically increased part).

The meshedness M indicate density of cycle structure consisting of a polygon. It can be calculated as $M = f/f_{max}$ using Euler's theorem $f = 1 \quad n + m$, where n, m, f are

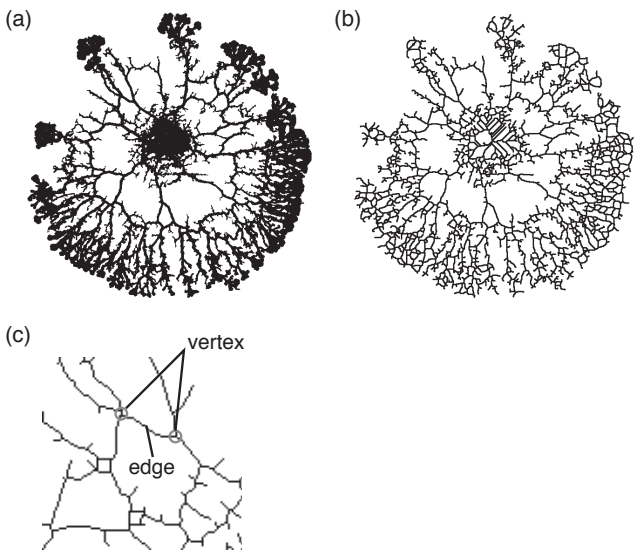

Fig. 2. Method for the network analysis.(a) Binary image of 1(c). (b) Skeletonized image of (a). Note that the thickness of the skeletons was dilated here for presentation. (c) Magnified picture of (b). The picture is original skeletonized one not but dilated one. All image processing were performed by a image processing software Image J [5]

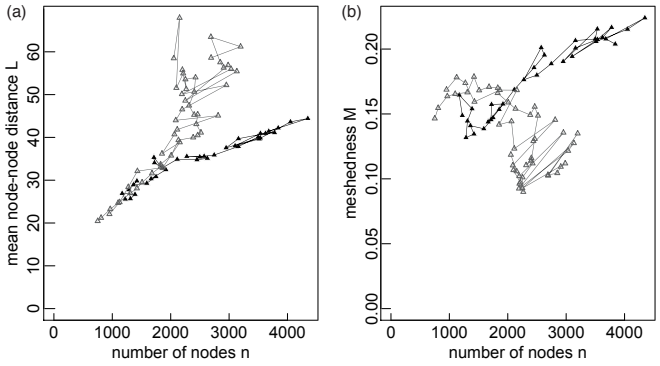

Fig. 3. Mean path length and meshedness.(a)n-L plot. (b)n-M plot. Closed triangles and open triangles denote the data for 1.5 w/v% agra medium with 10 w/v% oat extract and 0.3 w/v % agar medium with 10 mM KCl, respectively. Lines are connected in order of time.

number of vertices, edges, faces, respectively [7]. Maximum number of f, f_{max}, can be calculated as $f_{max} = 2n \quad 5$ under fixed n.

Fig.3(b) shows n-M plot. The meshedness coefficient M increases up to 0.20 in attractive condition, while down to 0.05–0.10 in repulsive condition. M is useful for estimation of number of edges in polygons composing the network. For example, the values are calculated as $M = 0$ in tree graph, 0.15–0.25 in hexagonal-lattice, 0.3–0.5 in tetragonal lattice, and 0.65–1.00 in trigonal lattice. The plasmodial network would be close to hexagonal lattice in attractive condition and tree-graph network in repulsive condition.

IV. Network morphology (Okamoto and Takamatsu)

To consider the biological function such as transport efficiency in the networks, it would be important to obtain

information on tube diameter and length. Fig.4 shows examples of distribution of tube diameters in each network. Under attractive condition, the distributions were broad and exponential-like at early stage (after 3h from cultivation start) then the continuous distribution was maintained even though a few samples showed a peak at 0.2–0.3 mm at late stage. Under repulsive condition, the distributions of most of samples were with peaks at around 0.3 mm at early stage, and all samples had peaks at 0.3–0.4 mm at late stage. Thicker tubes formed at earlier stages under repulsive condition comparing with attractive condition.

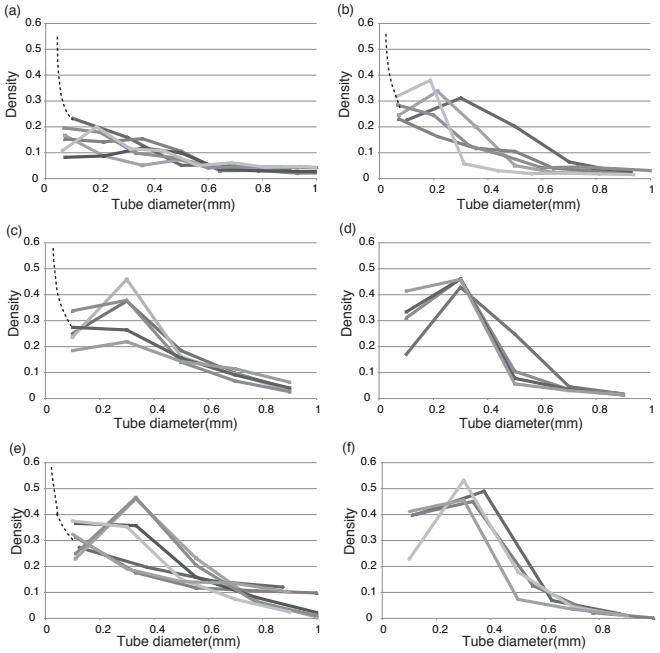

Fig. 4. Distribution of tube thickness in networks. (a,b) Conditions were 1.5 w/v% agra medium with 10 w/v% oat extract. (c,d) Conditions were 1.5 w/v% agra medium without chemicals. (e,f) Conditions were 0.3 w/v % agar medium with 10 mM KCl. (a,c,d) After 5-hr-clutivation. (b,d,f) After 11-hr-cultivation. Each line was obtained from single sample. 5–7 samples were tested for each condition. Dashed lines denote undetected extremely thin tubes by the image processing method illustrated in Fig.2.

V. Energy consumption (Gomi and Takamatsu)

The plasmodium show tree-like network with thick tubes under repulsive condition, while lattice network with thin tubes and thin sheet structure under attractive condition. The difference of network morphology could affect energy efficiency to maintain the biological body and transportation of protoplasm. We measured oxygen consumption per unit time which indicates energy consumption as shown in Fig.5. The results suggests energy consumption is lager in attractive condition than repulsive condition. We need more analysis whether the energy consumption is controlled by only the network morphology or accompanied by other biochemical reason.

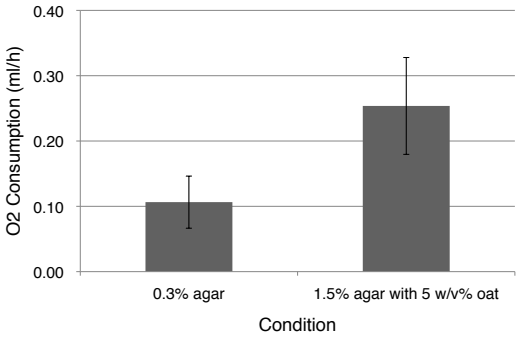

Fig. 5. Oxygen consumption in tree-structured plasmodium (0.3 % agar medium) and mesh-structured plasmodium (1.5 % with 5 w/v % oatmeal extract). Weights of plasmodium are 0.10 ± 0.01 (g).The value $p = 0.028 < 0.05$ in two sample one sided t-test and $p = 0.027 < 0.05$ in Wilcoxon rank sum one sided test. Variances were evaluated as equal by F-test (p-value $= 0.15 > 0.05$).

VI. Applications of plasmodial network algorithm

In above sections, we see importance of morphology of transportation networks. At this moment, mathematical models based on environment dependent morphology have been incomplete. Here we introduce some possibility of the plasmodial network based algorithm as applications.

A. Analysis on reaction to a task–toward to an application of amoeba-robot– (Arafune and Takamatsu; Collaboration with Shimizu, M., Kato, T., and Ishiguro, A. Tohoku University)

Ishiguro and Shimizu [10] developed amoeba-mimic robot consisting of oscillator modules. The oscillator modules are coupled in their neighborhood. The amoeba robots move toward light stimulus with generating progressive waves. It was shown by their simulation that the wave patterns changes to spiral ones when the robot passing through the obstacle and moving speed drastically decreases. We applied similar task to real plasmodium and the result is shown in Fig.6. The real plasmodium moves without slowdown even though the obstacle is lager and the spiral waves are observed. This could be derived by the plasmodium maintaining thick tubular structure. Other experimental result shows that the plasmodium without thick tubes and showed spiral waves cannot move faster (data not shown here). The tubular structure which generate long-distance interaction could help to pass through obstacles effectively.

B. Optimization of rail grid by a slime path finding algorythm [11](Watabane, Tero, Takamatsu, Nakagaki)

Tero et al. developed path finding algorithm mimicking plasmodium where shortest path connecting food site is calculated by flux of protoplasmic streaming [11]. We applied this algorithm to JR lines in Tokyo area to optimize amount of transportation. The result showed almost good agreement to real rail line networks as shown in Fig.7. We need to investigate whether this algorithm can be applied to the environment-dependent-network formation.

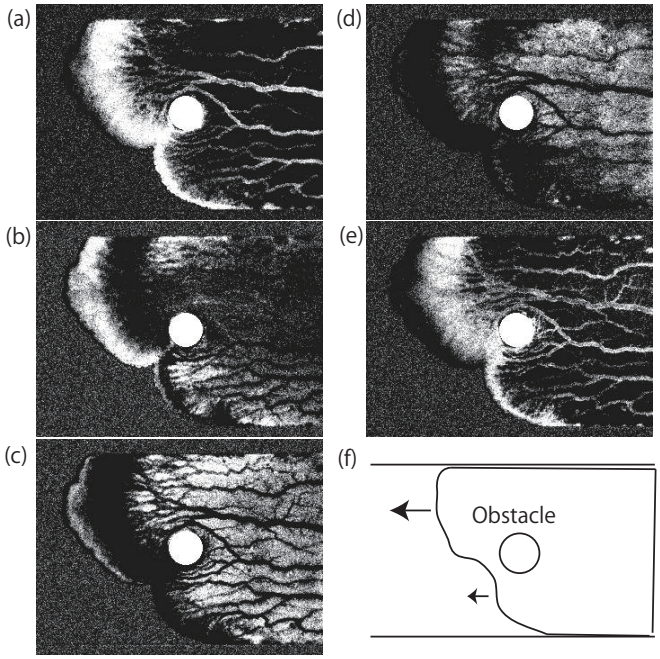

Fig. 6. Plasmodium passing through an obstacle and spiral waves. (a–e) Time-differential images. White/black image indicates decreasing/increasing thickness, respectively. Time intervals are 8 sec. Spiral waves are observed couterclockwisely. (f) Schematic diagram of experimental condition. Pass width is 15 mm, diameter of obstacle is 2.8 mm. Culture medium was 1.5w/v% agar and culture condition was 25°C, RH85%

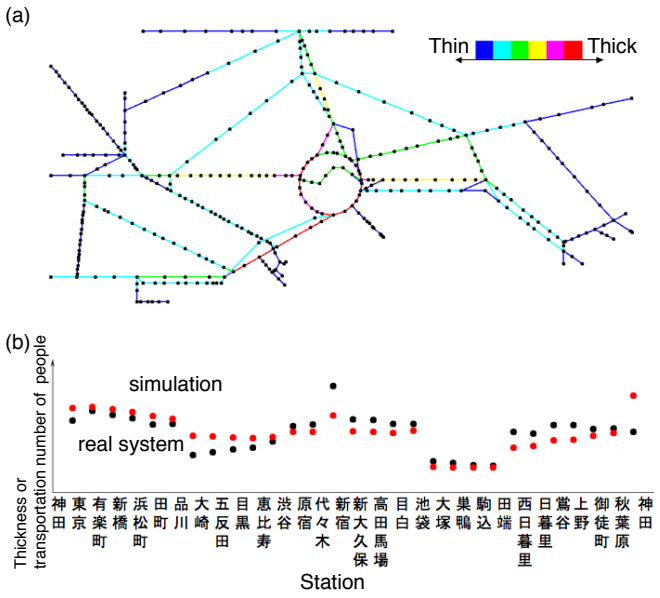

Fig. 7. Optimum thickness distribution in JR-line network calculated with a path finding algorithm by true slime mold [11]. (a) Simulation result. Dots denote stations and lines denote railroads. (b) Calculated thickness of transportation lines and transportation number of people in real system.

VII. Summary and Future Works

We analyzed the network topology depending on environmental conditions. We elucidate that the plasmodium shows hexagonal lattice under attractive condition. However the network under repulsive condition is not simple tree-graph network but with processes of generation/degeneration of edges.

To achieve the goal mentions in §II, (1) to elucidate the mechanism of environment-dependento morphology, (2) to investigate functionality and efficiency of each network, we quantified the network growth process and obtained some hint concerned in the rules. In respect to adaptation behavior of plasmodia, we could discuss some speculation; The most efficient morphology for the plasmodia in repulsive condition could be tree-graph to escape faster from bad environment to find better one with limited resources by using generation/degeneration process; On the other hand, the most efficient morphology for the attractive condition could be dense network with thin tubes to absorb much more nutrient. To discuss more quantitatively, we still have left several subjects to examine, e.g., how are the efficiencies of migration, nutrient absorption, transportation of protoplasm, finding probability of better environment, and etc.

References

[1] Nelson, T. and Dengler N., Leaf cascular pattern formation. The Plant Cell, 9, 1121-1135 (1997).
[2] Burton J. L., and Franks, N. R., The foraging ecology of the army ant *Ection rapax* An Ergonomic enigrama? Ecol. Entomol. 10, 131-141 (1985)
[3] Barthélemy, M. and Flammini A., Modeling urban street patterns. Phys. Rev. Lett, 100, 138702 (2008).
[4] Takamatsu, A., Takaba, E. and Takizawa,G., Environment-dependent morphology in plasmodium of true slime mold *Physarum polycephalum* and a network growth model. J. theor. biol. , 256, 29-44 (2009).
[5] Rasband, W. S., 1997–2008. ImageJ, U. S. National Institutes of Health, Bethesda, Maryland, USA, http://rsb.info.nih.gov/ij/ .
[6] Newman M. E. J., The Structure and Function of Complex Networks, SIAM Review, 45, 167-256 (2003)
[7] Buhl, J., Gautrais, J., Solé, R. V., Kuntz, P., Valverde, S., Deneubourg, J.L., Theraulaz, G. Efficiency and robustness in ant networks of galleries. Eur. Phys. J. B 42, 123-129 (2004).
[8] Stone, M., Cross-validatory choice and assessment of statistical predictions, J. Roy. Stat. Soc. B, 36, 111-147 (1974).
[9] Ito, M and Takamatsu, A. Analysis on adaptation mechanism of biological transportation network. Proceedings of 51th Joint Conference on Automatic Control, 336-340 (2008). (in Japanese)
[10] Ishiguro, A. and Shimizu, M., On the task distribution between control and mechanical systems., in 50 years of AI, Festschrift, LNAI 4850, Lungarella et al. Eds. pp. 144-153, Springer-Verlag Berlin Heidelberg (2007).
[11] Tero, A., Kobayashi, R., Nakagaki, T., A mathematical model for adaptive transport network in path finding by true slime mold., J. theor. Biol. 244, 553-564 (2007).

Measurement and Modeling of Human Movement Mastery Process

Sadao Kawamura, Takashi Mitsuda, Mitsunori Uemura, Masahiro Sekimoto, and Tadao Isaka
(Ritsumeinkan University)

I. INTRODUCTION

The aim of this research is to clarify the movement mastery process of humans. In particular, we focus on the human ability to reduce the total energy of human muscles in the process of master of skillful motions. In most of sports or martial arts, relaxation of muscles is extremely important to generate high speed and precise motions. In order to clarify the mastery process, we have the following two approaches. It is expected that the results of the two approaches make synergy effects.

(1) Mathematical model approach

In this approach, the human motor control system is boldly simplified to clarify the essential parts of the movement mastery process of humans and to make a mathematical model of the human motor learning. To simplify the human complex motor control system, we have a hypothesis that humans do not have the exact information on kinematics and dynamics. A biped locomotion model and an arm model with 2-DOF 6-muscles are investigated.

(2) Living body measurement approach

The human movement mastery process is directly measured through physiological data. For his purpose, we have developed a measurement system which changes inertia or elastic load. In the developed system, the process that subjects learn a desired motion is measured through the EMG of six muscles (triceps brachii Caput laterale, pectoralis major, brachioradialis, deltoideus, biceps brachii caput longum, triceps brachii caput longum)

II. MATHEMATICAL MODEL APPROACH

A. Biped Locomotion Model

(1) Adaptive Adjustment of Joint Stiffness and Motion

Dynamics of multi-joint structure, such as human beings or robotic systems, has multi degree of freedom and is nonlinear. In this case, complex numerical techniques are generally utilized to solve problems of motion generation with torque minimization. This kind of numerical solution requires precise modeling of dynamics and huge numerical calculations. However, if we want robotic systems to adapt to environments, such numerical calculation may disable the adaptation.

On the other hand, in the field of robotics, some researchers have proposed control methods that utilize properties of the multi-joint robots [1]. In spite of the nonlinearity and multi degree of freedom, this kind of control method requires neither exact parameter values of the multi-joint structures nor huge numerical calculations in order to obtain the good control performance. Therefore, to utilize properties of dynamics seems to be essential for adaptive robotic systems and understanding human skillful movements.

In this study, we have discovered one property of the multi-joint structures which can generate periodic motions with minimum actuator torque by linear state feedback of angular velocity. Based on this property, we propose a new controller that adaptively adjusts joint stiffness and motion patterns for biped locomotion.

(2) Problem Formulation

Here we consider a biped locomotion robot. When the robot swings a leg, dynamics is given by

$$\mathbf{R}(\mathbf{q})\ddot{\mathbf{q}} + \left\{\frac{1}{2}\dot{\mathbf{R}}(\mathbf{q}) + \mathbf{S}(\mathbf{q},\dot{\mathbf{q}}) + \mathbf{D}\right\}\dot{\mathbf{q}} + \mathbf{g}(\mathbf{q}) - \mathbf{K}(\mathbf{q}-\mathbf{q}_e) = \boldsymbol{\tau} \quad (2A\text{-}1)$$

In this study, we try to minimize actuator torque while generating periodic motions. A cost function can be given by

$$J = b\int_0^{T^-} \boldsymbol{\tau}^T \mathbf{A}^{-1}\boldsymbol{\tau}\mathrm{d}t \quad (2A\text{-}2)$$

(3) Optimal Actuator Torque

We have analytically derived that optimal actuator torque $\boldsymbol{\tau}_{\mathbf{opt}}$ can be described linear state feedback of velocity $\dot{\mathbf{q}}$.

$$\boldsymbol{\tau}_{\mathbf{opt}} = \mathbf{A}\dot{\mathbf{q}} \quad (2A\text{-}3)$$

This relationship is clarified using energy-based analysis or the Hamilton-Jacobi equation. This result is the same as conventional resonance in the sense of generating periodic motions by linear velocity feedback with using minimum actuator torque. Therefore, our proposed concept can be regarded as a kind of extension of conventional resonance to multi-joint structures.

(4) Control Method

This study proposes the following control method.

$$\boldsymbol{\tau} = -\mathbf{K}_{\mathbf{v}}\left(\dot{\mathbf{q}} - \dot{\mathbf{q}}_{\mathbf{d}}\right) + \hat{b}\mathbf{A}\dot{\mathbf{q}} \quad (2\text{-}4)$$

$$\dot{\hat{b}} = -\gamma_a \dot{\mathbf{q}}^T\left(\dot{\mathbf{q}} - \dot{\mathbf{q}}_{\mathbf{d}}\right) \quad (2\text{-}5)$$

$$\dot{\mathbf{q}}_{\mathbf{d}}(t) = (1-\alpha)\dot{\mathbf{q}}_{\mathbf{d}}(t-T) - \alpha\dot{\mathbf{q}}(t-T) \quad (2\text{-}6)$$

$$\dot{\mathbf{k}} = \boldsymbol{\Gamma}\mathbf{Q}\left(\dot{\mathbf{q}} - \dot{\mathbf{q}}_{\mathbf{d}}\right) \quad (2\text{-}7)$$

The term of $-\mathbf{K}_v(\dot{\mathbf{q}}-\dot{\mathbf{q}}_d)$ in Eq.(2A-4) means velocity error feedback. The desired motion is adjusted by Eq.(2A-6). This structure is the same as delayed feedback control [2]. It has been pointed out that delayed feedback control can realize convergence of state variables to unknown periodic equilibriums. When the motions will converge to the desired ones $\dot{\mathbf{q}} \to \dot{\mathbf{q}}_d$, the actuator torque will be the same as optimal actuator torque of Eq.(2A-3). We also use adaptive parameter adjustment of Eq.(2A-5) and Eq.(2A-7). We have proved that the structure of the Eq.(2A-7) can optimize joint stiffness [3]. Therefore, we can expect that the proposed controller can adaptively generate optimal periodic motions.

(5) Simulation

We conducted a numerical simulation to verify the effectiveness of the proposed controller. We used the walking model as shown in the Fig.1. We assumed that falling down phenomena will not occur in this simulation.

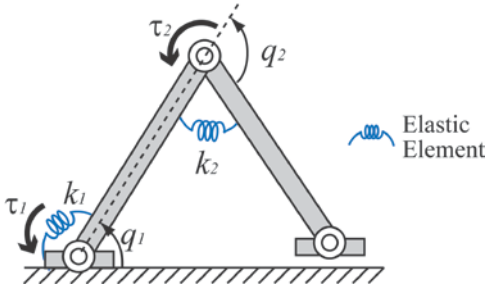

Fig.1 Simulation Model

Simulation results showed that the proposed controller could generate periodic motion and the actuator torque converge to the optimal condition of Eq.(2A-3). Therefore, it has been verified that the proposed controller can generate periodic motions that require minimum actuator torque.

B. An Arm Model with 2-DOF and 6-muscles

An arm model with 2-DOF and 6-muscles shown in Fig.2 is investigated. A final goal is to make a model which can explain the process of master of human skillful motions. For this, it is very important to consider how the feedback control scheme can be constructed from some sensor signals. This report presents the following two topics. One is the linear characteristics of the mapping from task-oriented coordinates to the muscle coordinates. In the second topics, a robust controller for the arm model is proposed and the stability condition is revealed.

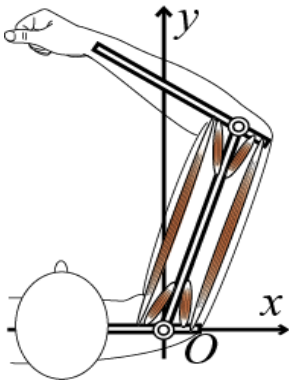

Fig.2 Arm Model

(1) Linearity in mapping from hand coordinates to muscle length

The mapping from visual information to motor command is an important issue in the study of voluntary arm movement. Planning of reaching movement to a visual target is generally based on the inverse kinematics, which is the mapping from the hand position in Cartesian coordinates to the joint angles of the arm. This mapping is non-linear.

On the other hand, it is reported that the mapping from the hand position described in binocular visual coordinates to the joint angles of the arm is approximated by a linear function [4]. The linear mapping simplifies the control system. This study examined the linearity of the mapping from the hand position to the muscle length.

Binocular visual space is defined as the vergence angle and the horizontal direction. The kinematic model of the arm consists of two links and two joints. The elbow joint and the shoulder joint have 1 d.o.f. and the arm moves on the horizontal plane.

The muscle lengths were determined by the use of the following three models.

model 1: Pulley model (Fig.3(a))

The moment arms are constant. This model is used frequently in many papers.

model 2: A model where muscles are fixed on the links directly.(Fig.3(b))

model 3. An anatomical model proposed by Pigeon[5]

The length of mono-articular muscle determined in model 1 is proportional to the joint angle, thus the muscle length is proportional to the hand position in binocular visual coordinates. The length of mono-articular muscle determined in model 2 and model 3 are nearly proportional to the joint angles except the singular posture. Moreover the muscle length of biceps brachii is proportional to the distance of hand position from the head. These results imply the linear approximation of musculoskeletal model of human being on task oriented coordinates. Applying the linear model in three dimensional coordinates is a future subject.

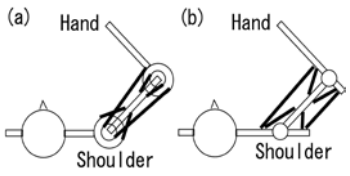

Fig.3 Muscle Model

(2) Robust Sensory Feedback Motion Control

On the arm model shown in Fig.2, the relation between the joint torque $\boldsymbol{\tau}$ (2x1) and the muscle tension α (6x1) is given by

$$\boldsymbol{\tau} = \mathbf{W}(\mathbf{q})\,\boldsymbol{\alpha} \qquad (2B\text{-}1)$$

where $\mathbf{W}(\mathbf{q})$: a matrix (2x6) and $\mathbf{q}$ (2x1): a joint angle coordinates vector.

Here, we propose a robust sensory feedback motion control scheme given by

$$\boldsymbol{\alpha} = \mathbf{M}\,\{\,\mathbf{K}_p\,(\mathbf{x}_d - \mathbf{x}) - \mathbf{K}_v\,\dot{\mathbf{x}}\,\} \qquad (2B\text{–}2)$$

where **M**: appropriate matrix (2x6), $\mathbf{K_p}$: potion feedback gain matrix (2x2), $\mathbf{K_p}=k_p\mathbf{I}$, k_p: feedback gain, **I**: unit matrix, $\mathbf{K_v}$: velocity feedback gain matrix (2x2), $\mathbf{K_v}=k_v\mathbf{I}$, k_v: feedback gain, $\mathbf{x}(t)$: position vector in the task-oriented coordinates (2x1), $\mathbf{x_d}$: desired position vector in the task-oriented coordinates (2x1), and $\dot{\mathbf{x}}$: velocity vector. Here, we do not consider gravity to simplify the problem.

If the kinematics parameters are exactly given, the matrix **M** is easily set

$$\mathbf{M} = \mathbf{W}^{+}\mathbf{J}^{\mathbf{T}} \tag{2B-3}$$

where $\mathbf{W}^{+} = \mathbf{W}^{\mathrm{T}}(\mathbf{W}\mathbf{W}^{\mathrm{T}})^{-1}$: pseudo-inverse matrix (6x2) and **J**: Jacobian matrix from joint angle coordinates to task oriented coordinates (2x2). As the results, the stability to the desired point $\mathbf{x_d}$ can be guaranteed as seen in [6]. However, it will be occurred that the sensor coordinates or the force directions contains the parameter errors. Therefore, the robustness on the parameter error is crucially important in making a model of human motor control. In this research, the condition on the robustness has been obtained as follows:

$$\mathbf{WMJ} > \mathbf{0}. \tag{2B-4}$$

The details of stability proof are omitted because of the limitation of this report. From some simulation results, we have already confirmed that a matrix **M** whose all elements are constant can make stable motions. In this simulation, the matrix **M** is set

$$\mathbf{M} = \mathbf{W_c}\,\mathbf{J}(\mathbf{q_d}) \tag{2B-5}$$

where $\mathbf{J}(\mathbf{q_d})$: Jacocian matrix at the desired point and

$$\mathbf{W_c} = \begin{bmatrix} -1 & 1 & 0 & 0 & -1 & 1 \\ 0 & 0 & -1 & 1 & -1 & 1 \end{bmatrix}^{T}. \tag{2B-6}$$

The motion converges to the desired point and appropriate internal forces among muscles are generated. In this simulation, the muscle force is set zero if the value of the muscle force calculated by Eq.(2B-1) is negative.

The previous subsection implies linear mapping between the muscle coordinates and the binocular visual coordinates. It suggests that there can be a constant matrix **M** which satisfies the stability condition given by Eq.(2B-4) in wide work space.

III. LIVING BODY MEASUREMENT APPROACH

A. Biometrical Study

In order to construct a control model for a system with a musculoskeletal body to acquire skilled motions, we investigate some human upper-arm movement and activities of a group of muscles in a learning process. Several papers have reported the qualitative characteristics arising in iterative tasks under an elastic or viscose force field [7]. However, the analysis of the mechanism from the viewpoint of mechanics is still lack. Hence, we carried out pilot experiments on human upper-arm movement under an elastic force field in order to gain a physical insight into coordination among a group of muscles in iterative tasks.

This report focuses on planar movement of a human upper arm as shown in Fig.4. In order to give the subject's hand an external force by an elastic force field and to measure the hand position of the subject, a robotic arm (manipulandum) with two joints which moves in a plane was developed. The height of the robot arm was adjusted in advance so that the subject can move his arm comfortably and smoothly. The subject grasps a grip attached to the endpoint of the robot arm and the subject' hand is subject to the external load generated by springs (Spring constant: 4.52N/mm) attached to the joints of the robot arm during movements. The endpoint position of the subject is calculated from information of rotary encoders attached to the joints of the robot and kinematic information of the robot. The calculated end-position is illustrated, together with the target, on the display real-time. The subject endpoint on the display is colored with red if it is within a radius of 4[cm] from the target or with blue otherwise, and the subject can confirm the color real-time during movement. Further, we measured electromyography (EMG) signals of six muscles (Biceps brachii, Triceps brachii lateral head, Brachioradialis, Pectoralis major, Deltoideus posterior, and Deltoideus posteriror), using the EMG device (ML880 PowerLab 16/30 (made by AD instruments), DL-141(made by S&ME)). The EMG signals were sampled at 4k Hz.

The subject was requested so as to accurately track the target point appearing on the display real-time which travels periodically at a distance of 0.2[m] and a speed of 2[s] per cycle. Each cycle was counted as a trial and the subject performed 196 trials totally. In the experiment, the subject had 7-8 breaks to avoid fatiguing.

Fig.5 shows transient responses of endpoint position of the subject in the x and y directions (red line) together with the desired trajectory (green line). Fig.6 shows alteration of the EMG signals of a group of muscles according to increase of trials. After full-wave rectified, the EMG signals were

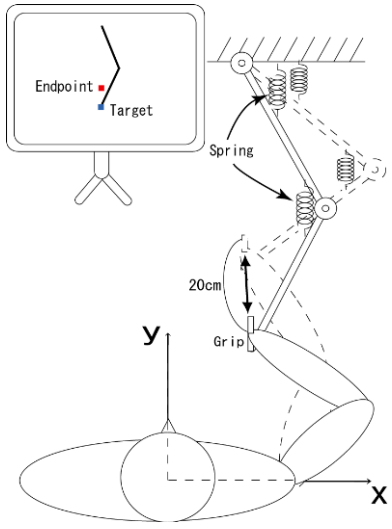

Fig. 4. An experimental setup

smoothed through the band-pass filter of 5 to 1k Hz and were integrated in time at each trial. These results show that the integral EMG values concerning the biceps brachii, the tricepts brachii lateral head, and the brachioradialis tend to increase according to increase of trials. While, those concerning the deltoideus posterior tend to decrease. Since the obtained results are not yet enough to construct a model, we will continue to investigate the EMG activities of muscles in a learning process in different tasks. Then, we will construct a model of muscle control in a learning process in future work.

IV. Conclusion

We could prepare two basic mathematical models. One is a motion skill model for energy saving and the other is a motion control model for muscular redundant mechanisms. Both of them, there are gaps to reveal biological models. The comparison with the EMG data given in the chapter 3 is future work from now.

References

[1] Suguru Arimoto, ” Control Theory of Nonlinear Mechanical Systems: A Passivity-based and Circuit-theoretic Approach”, Oxford University Press, 1996

[2] K. Pyragas, ”Continuous Control of Chaos by Self-Controlling Feedback”, Physics Letters A, Vol.170, No.6, pp.412-428, 1992.

[3] M. Uemura, K. Kanaoka, S. Kawamura, ”A New Control Method Utilizing Stiffness Adjustment of Mechanical Elastic Elements for Serial Link Systems”, IEEE International Conference on Robotics and Automation 2007, pp.1437-1442, 2007.

[4] T.Mitsuda et al. “Binocular visual servoing based on linear time-invariant mapping” , Advanved Robotics, Vol.11, No.5, pp.429-443, 1997

[5] Pascale Pigeon, L’Hocine Yahia and Anatol G. Feldman, “Moment arms and lengths of human upper limb muscle as functions of joint angles”, J.Biomechanics, Vol.29, No.10, pp.1365-1370, 1996

[6] Kenji Tahara and Zhi-Wei Luo,“On Dynamic Control Meahcnisms of Redundant Human Musculo-Skeletal System“ pp.217-247 Advances in Robot Control, Springer 2006 (Editor S. Kawamura and M. Svinin)

[7] T. Kondo and K. Ito, "Modeling of Intra-cerebral Mechanisms for Motor Adaptation to Unknown environment," the 2007 Annual Report for Mobiligence, pp.11-14, 2007.

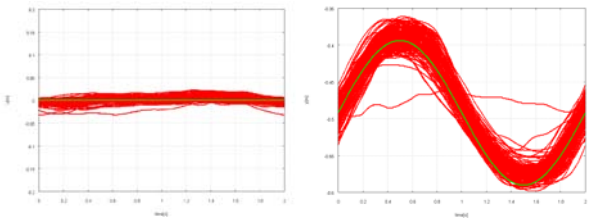

(a) x-component (b) y - component

Fig. 5. Transient responses of endpoint position of the subject

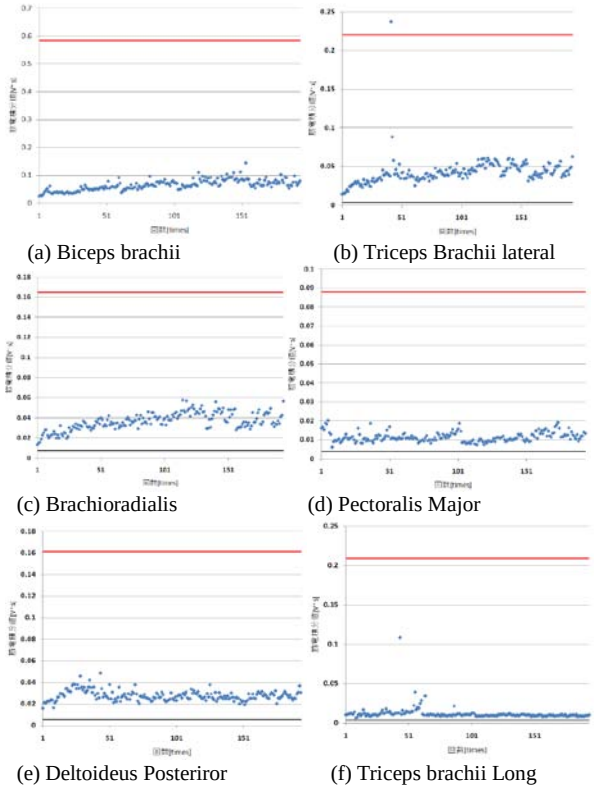

(a) Biceps brachii (b) Triceps Brachii lateral

(c) Brachioradialis (d) Pectoralis Major

(e) Deltoideus Posteriror (f) Triceps brachii Long

Fig. 6. Alteration of the EMG values for the six muscles according to increase of trials

Member List

■=Director ■=Planned Research Groups ■=Subscribed Research Groups

	Name	Organization	
Director	Hajime Asama	The University of Tokyo	■
A01-01	Koji Ito	Tokyo Institute of Technology	■
A01-01	Manabu Gouko	Tokyo Institute of Technology	■
A01-01	Hiroyuki Nakahara	RIKEN	■
A01-02	Toshiyuki Kondo	Tokyo Institute of Technology	■
B01-01	Kaoru Takakusaki	Asahikawa Medical College	■
B01-01	Masahiko Inase	Kinki University	■
B01-01	Shigeru Kitazawa	Juntendo University	■
B01-01	Taizo Nakazato	Juntendo University	■
B01-01	Kenji Yoshimi	Juntendo University	■
B01-01	Katsumi Nakajima	Kinki University	■
B01-01	Futoshi Mori	Yamaguchi University	■
B01-01	Dai Yanagihara	The University of Tokyo	■
B01-01	Kiyoji Matsuyama	Sapporo Medical University	■
B01-01	Yoshimasa Koyama	Fukushima University	■
B01-01	Toshikatsu Okumura	Asahikawa Medical College	■
B01-02	Naomichi Ogihara	Kyoto University	■
B01-02	Kazuo Tsuchiya	Doshisha University	■
B01-02	Yasuhiro Sugimoto	Kobe University	■
B01-02	Shinya Aoi	Kyoto University	■
B01-02	Masato Nakatsukasa	Kyoto University	■
B01-03	Koh Hosoda	Osaka University	■
B01-03	Kousuke Inoue	Ibaraki University	■
B01-03	Hiroshi Kimura	Kyoto Institute of Technology	■
B01-03	Katsuyoshi Tsujita	Osaka Institute of Technology	■
B01-03	Takashi Takuma	Osaka Institute of Technology	■
C01-01	Hitoshi Aonuma	Hokkaido University	■
C01-02	Jun Ota	The University of Tokyo	■
C01-02	Hajime Asama	The University of Tokyo	■

C01-02	Kuniaki Kawabata	RIKEN	■
C01-02	Ryosuke Chiba	Tokyo Metropolitan University	■
C01-03	Daisuke Kurabayashi	Tokyo Institute of Technology	■
C01-03	Ryohei Kanzaki	The University of Tokyo	■
D01-01	Masafumi Yano	Tohoku University	■
D01-01	Kazuhiro Sakamoto	Tohoku University	■
D01-01	Yoshinari Makino	Tohoku University	■
D01-02	Koichi Osuka	Kobe University	■
D01-02	Xin-Zhi Zheng	ASTEM	■
D01-02	Jiro Adachi	Hokkaido University	■
D01-02	Kunishige Ohgane	National Center for Geriatrics and Gerontology	■
D01-03	Akio Ishiguro	Tohoku University	■
D01-03	Masahiro Shimizu	Tohoku University	■
D01-03	Kazutoshi Gohara	Hokkaido University	■
Evaluation	Shinzo Kitamura	Hyogo Assistive Technology Research and Design Institute	■
Evaluation	Ryoji Suzuki	Kanazawa Institute of Technology	■
Evaluation	Shigemi Mori	National Institute for Physiological Sciences	■
Evaluation	Rolf Pfeifer	University of Zurich	■
Evaluation	Sten Grillner	Karolinska Institutet	■
Evaluation	Avis H. Cohen	University of Maryland	■
A01-11	Toshiya Matsushima	Hokkaido University	■
A01-12	Yasuharu Koike	Tokyo Institute of Technlogy	■
A01-12	Jiro Okuda	Kyoto Sangyo University	■
A01-12	Hiroyuki Kambara	Tokyo Institute of Technlogy	■
A01-12	Tetsuya Matsuda	Tamagawa University	■
A01-13	Tadashi Ogawa	Kyoto University	■
A01-13	Takatsune Kumada	Advanced Industrial Science and Technology	■
A01-14	Yasuji Sawada	Tohoku Institute of Technology	■
A01-15	Akira Murata	Kinki University	■
A01-16	Tetsunari Inamura	National Institute of Imformatics	■
A01-17	Jun Tani	RIKEN	■

A01-17	Hiroaki Arie	RIKEN	■
A01-17	Shigeki Sugano	Waseda University	■
B01-11	Hiroshi Yokoi	The University of Tokyo	■
B01-11	Masatoshi Takita	Advanced Industrial Science and Technology	■
B01-12	Takafumi Suzuki	The University of Tokyo	■
B01-12	Kunihiko Mabuchi	The University of Tokyo	■
B01-13	Yoshio Sakurai	Kyoto Universty	■
B01-14	Yasushi Kobayashi	Osaka Universty	■
B01-15	Kazuhiko Seki	National Institute for Physiological Problems	■
B01-16	Atsushi Nambu	National Institute for Physiological Problems	■
B01-17	Shinji Kakei	Tokyo Metropolitan Institute for Neuroscience	■
B01-17	Saeka Tomatsu	Tokyo Metropolitan Institute for Neuroscience	■
B01-17	Jongho Lee	Tokyo Metropolitan Institute for Neuroscience	■
B01-18	Takashi Hanakawa	National Center of Neurology and Psychiatry	■
B01-18	Rieko Osu	Advanced Telecommunications Research Institute International	■
C01-11	Toru Miura	Hokkaido University	■
C01-11	Hideaki Takeuchi	The University of Tokyo	■
C01-11	Hajime Asama	The University of Tokyo	■
C01-11	Hitoshi Aonuma	Hokkaido University	■
C01-12	Mizuki (Kazuki) Tsuji	University of Ryukyus	■
C01-12	Ryohei Yamaoka	Kyoto Institute of Technology	■
C01-12	Ken Sugawara	Tohoku Gakuin University	■
C01-13	Kotaro Oka	Keio University	■
C01-13	Masafumi Hagiwara	Keio University	■
C01-13	Eiichi Izawa	Keio University	■
C01-14	Motoichiro Kato	Keio University	■
C01-14	Mihoko Otake	The University of Tokyo	■
C01-15	Takashi Nagao	Kanazawa Institute of Technology	■
C01-15	Yoshihide Tamori	Kanazawa Institute of Technology	■
C01-15	Akio Kishigami	Kanazawa Institute of Technology	■

C01-15	Ken Sasaki	Kanazawa Institute of Technology	
C01-16	Etsuro Ito	Tokushima Bunri University	
C01-16	Hidetoshi Ikeno	University of Hyogo	
C01-16	Mizue Ohashi	University of Hyogo	
C01-16	Toshifumi Kimura	University of Hyogo	
C01-17	Naotaka Fujii	RIKEN	
D01-11	Takashi Ikegami	The University of Tokyo	
D01-11	Masakazu Shimada	Kanazawa University	
D01-12	Kei Senda	The University of Tokyo	
D01-12	Makoto Iima	Hokkaido University	
D01-12	Norio Hirai	Osaka Prefecture University	
D01-13	Toshio Aoyagi	Kyoto University	
D01-13	Ichiro Tsuda	Hokkaido University	
D01-14	Jun Nishii	Yamaguchi University	
D01-15	Atsuko Takamatsu	Waseda University	
D01-15	Toshiyuki Nakagaki	Hokkaido University	
D01-16	Sadao Kawamura	Ritsumeikan University	
D01-16	Takashi Mitsuda	Ritsumeikan University	
D01-16	Masahiro Sekimoto	Ritsumeikan University	
D01-16	Tadao Isaka	Ritsumeikan University	
D01-16	Mitsunori Uemura	Ritsumeikan University	

Publications, Awards, Patent

Publications

1. Plessy, C., Fagiolini, M., Wagatsuma, A., Harasawa, N., Kuji, T., Asaka-Obam, A., Kanzaki, Y., Fujishima, S., Waki, K., Nakahara, H., Hensch, T, K., & Caminci, P., A Resource for Transcriptomic Analysis in the Mouse Brain, PLoS ONE, 3, 8, 2008
2. Nakahara, H., Shimono, M., Uchida, G & Tanifuji, M., Stimulus-induved pairwise interaction can be revealed by information geometric approach, Springer Lecture Notes, in press, 2008
3. Bissmark, F., Nakahara, H., Doya, K., & Hikosaka, O., Combining modalities with different latencies for optimal motor control, Journal of Cognitive Neuroscience, 20, 11, 1966-1979, 2008
4. Santos, G, S., Nagasaka, Y., Takenaka, K., Iriki, A., Fujii, N., & Nakahara, H., Social modulation of the prefrontal cortex, parietal cortex, and caudate activity for reward-oriented behavior, Neuroscience Meeting Planner. Society for Neuroscience, Online., Program No. 93.11.TT40, 2008
5. Takeshi Sakurada, Hiroaki Gomi, Koji Ito, Extrinsic reference frame during bilateral finger coordination, Neuroscience 2008, 2008
6. Manabu Gouko, Koji Ito, Action generation model for multiple tasks based on the ecological approach, Proceedings of the 2nd IEEE International Conference on Self-Adaptive and Self-Organizing Systems (SASO2008), 457-458, 2008
7. Naoki Tomi, Manabu Gouko, Koji Ito, Inaccuracy of internal models in force fields and complementary use of impedance control, Proceedings of the 2008 IEEE International Conference on Intelligent Robots and Systems (IROS 2008), 393-398, 2008
8. Naoki Tomi, Manabu Gouko, Koji Ito, Impedance control complements incomplete internal models under complex external dynamics, Proceedings of The 30th Annual International Conference of the IEEE Engineering in Medicine and Biology Society (EMBC2008), 5354-5357, 2008
9. Mitsuru Takahashi, Manabu Gouko, Koji Ito, Electroencephalogram (EEG) and Functional Electrical Stimulation (FES) System for Rehabilitation of Stroke Patients, Proceedings of The 21th IEEE International Symposium on Computer-Based Medical Systems (CBMS 2008), 53-58, 2008
10. Kaveri, S, R., Nakahara, H., Uncertainty and discounting of rewards for dopamine activity by dissociating internal and physical times, Neuroscience Meeting Planner. Society for Neuroscience, Online., Program No. 98.2.UU32., 2008
11. Santos, G, S., Nagasaka, Y., Takenaka, K., Iriki, A., Fujii, N., & Nakahara, H., Social Reward-Oriented Behavior in the PFC, CN, and Parietal Cortex, The 31st Annual Meeting of the Japan Neuroscience Society (Neuroscience 2008), P2-r07, 2008
12. Kaveri, S, R., Nakahara, H., Timing in Temporal Difference Models of Dopamine, The 31st Annual Meeting of the Japan Neuroscience Society (Neuroscience 2008), P3-q12, 2008
13. Nakahara, H., Analyzing neural dynamics by considering higher-order interaction and, also, the effect of time on reward prediction, EPSRC Workshop on Computational Neuroscience, 2008
14. Nakahara, H., Effects of internal time and context representation on dopamine activity and value-based decision making, Open Problems in Neuroscience of Decision Making, 2008
15. Nakahara, H., Computational modeling of Basal Ganglia, The 3rd APCTP-KAIST Summer School for Brain Dynamics, 2008
16. Toshiyuki Kondo, Daisuke Hirakawa, Takayuki Nozawa, Sustainability and Predictability in a Lasting Human-Agent Interaction, Proc. of the Eight International Conference on Intelligent Virtual Agents (IVA08), 505-506, 2008
17. Takayuki Nozawa, Toshiyuki Kondo, Information-theoretic characterization of relative and fluctuating system-environment distinction, Proc. of Artificial Life XI, 791, 2008
18. Toshiyuki Kondo, Yuya Kobayashi, Takayuki Nozawa, Effect of Successive Experiences on Simultaneous Learning of Conflicting Visuomotor Rotations, IROS2008 Full Day Workshop, 2008
19. Toshiyuki Kondo, Osamu Amagi, Takayuki Nozawa, Proposal of Anticipatory Pattern Recognition for EMG Prosthetic Hand Control, Proc. of the 2008 IEEE International Conference on Systems, Man, and Cybernetics (SMC 2008), 897-902, 2008
20. Yuki Orii, Takayuki Nozawa, Toshiyuki Kondo, Web-based Intelligent Photo Browser for Flood of Personal Digital Photographs, Proc. of International Workshop on Web Intelligence (IWI08), 127-130, 2008
21. Matsushima, T., Kawamori, A., and Bem-Sojka T., Neuro-economics in chicks: foraging choices based on delay, cost and risk, Brain Research Bulletin, 76, 245-252, 2008
22. Yamaguchi, S., Fujii-Taira, I., Katagiri, S., Izawa, E.-I., Fujimoto, Y., Takeuchi, H., Takano, T., Matsushima, T., and Homma, K.J., Gene expression profile in cerebrum in the filial imprinting of domestic chicks (Gallus gallus domesticus), Brain Research Bulletin, 76, 275-281, 2008
23. Yamaguchi, S., Fujii-Taira, I., Murakami, A., Hirose, N., Aoki, N., Izawa, E.-I., Fujimoto, Y., Takano, T., Matsushima, T., and Homma, K.J., Upregulation of microtubule-associated protein 2 accompanied by the filial imprinting of domestic chicks (Gallus gallus domesticus), Brain Research Bulletin, 76, 282-288, 2008
24. Kawamori A, Matsushima T, Distinct patterns of risk sensitivity for amount and delay in foraging choices of week-old domestic chicks., Animal Cognition (in revision), 2009
25. Matsushima T, Ecology meets neuroscience: neural mechanisms of profitability-based choices in the domestic chicks, International symposium on Evolutionary studies in behavioral neuroscience, June 26, 2008, Hayama, Japan, 2008
26. Matsushima T, Ecology meets neuroscience: rationality of profitability-based choices in the domestic chicks, (invited seminar at the Department of Psychology), September 19, 2008, University of Otago, Dunedin, New Zealand, 2008
27. Amita H, Matsunami S, Matsushima T, Impulsive choice in chicks: effects of competitive foraging and SSRI (fluvoxamine), The 31th Japan Neuroscience Meeting (Neuro2008), July 9-11, Tokyo, Japan, 2008
28. Matsunami S, Amita H, Matsushima T, SSRI (fluvoxamine) elongates food-patch residence time in chicks, The 31th Japan Neuroscience Meeting (Neuro2008), July 9-11, Tokyo, Japan, 2008
29. Kawamori A, Matsushima T, Risk-sensitive choice in chick, The 31th Japan Neuroscience Meeting (Neuro2008), July 9-11, Tokyo, Japan, 2008
30. Toshihiro KAWASE, Kazuo KURASHIGE, Masato WATANABE, Hiroyuki KAMBARA, Yasuharu, KOIKE, Controller of Ultrasonic Motor for Rehabilitation Robot, ISEK2008, CD-ROM, 2008
31. T. Ogawa, H. Komatsu, Condition-dependent and condition-independent target selection in macaque posterior parietal cortex, Journal of Neurophysiology, 2, in press, 2009
32. Murata A, Ishida H, Consciousness of body and mirror neuron system, Acta Medica Kinki University, 33, 1, 2, 9-21, 2009
33. Hiroaki Ishida, Kasumi Nakajima, Masahiko Inase, Akira Murata, Shared mapping of own and others' bodies in visuo-tactile bimodal area of the monkey parietal cortex, Journal of Cognitive Neuroscience (in press), 2009
34. Sakata H, Murata A, Tsutsui K, Visual space representation for action, In: Encyclopedia of Neuroscience (C. Binder MD, Hirokawa N, Windhorst U, Hirsch MC,

eds) （Springer-Verlag Berlin and Heidelberg）, 2008
35. Akira Murata, Hiroaki Ishida, Other's body representation referred to self body in the brain, The tenth international conference on the simulation of adaptive behavior SAB2008 Osaka, Japan, 2008
36. Ishida H, Inase M, Murata A., Shared representation of self ad other's body parts in visuo-tactile bimodal area of the monkey parietal cortex, The 6th Forum of European Neuroscience. 2008 Geneva Switzerland, 4, 020.8, 2008
37. Tetsunari Inamura and Keisuke Okuno, Adaptive acquisition of mimesis model based on communication between humanoid robots, International workshop on Imitation and Coaching in Humanoid Robots, 2008
38. Tetsunari Inamura, Multimodal Sensorimotor Integration and Behavior Induction Between Other and Self Based on Mirror Neuron Model, First France-Japan Research Workshop on Human-Robot Interaction, 2008
39. J. Tani, R. Nishimoto, J. Namikawa, M. Ito, Codevelopmental learning between human and humanoid robot using a dynamic neural-network model, IEEE Trans. on Syst. Man and Cybern. Part B-Cybernetics, 38, 1, 43-59, 2008
40. R. Nishimoto, J. Namikawa, J. Tani, Learning Multiple Goal-Directed Actions Through Self-Organization of a Dynamic Neural Network Model: A Humanoid Robot Experiment, Adaptive Behavior, 16, 2/3, 166-181, 2008
41. J. Tani, R. Nishimoto, R.W. Paine, Achieving 'organic compositionality' through self-organization: Reviews on brain-inspired robotics experiments, Neural Networks, 21, 584-603, 2008
42. Y. Yamashita, J. Tani, Emergence of functional hierarchy in a multiple timescale neural network model: a humanoid robot experiment, PLoS Computational Biology, 4, 11, e1000220, 2008
43. M. Maniadakis, J. Tani, Acquiring rules for rules: neuro-dynamical systems account for meta-cognition, Adaptive Behavior, accepted
44. H. Arie, T. Endo, T. Arakaki, S. Sugano, J. Tani, Creating novel goal-directed actions at criticality: a neuro-robotic experiment, New Mathematics and Natural Computation, in press
45. R. Nishimoto, J. Tani, Development process of functional hierarchy for actions and motor imagery: a constructivist view from synthetic neuro-robotics study, Psychological Research, accepted
46. Bando Y, Takakusaki K, Ito S, Terayama R, Kashiwayanagi M, Yoshida S., Differential changes in axonal conduction following CNS demyelination in two mouse models, European Journal of Neuroscience, 28, 1731-1742, 2008
47. Kumei S, Motomura W, Yoshizaki T, Takakusaki K, Okumura T., Troglitazone increases expression of E-cadherin and claudin 4 in human pancreatic cancer cells, Biochemical and Biophysical Research Communications (in press)
48. Takakusaki K, Tomita N, Yano M., Substrates for normal gait and pathophysiology of gait disturbances with respect to the basal ganglia dysfunction., Journal of Neurology, 255, suppl 4, 19-29, 2008
49. Takakusaki K, Forebrain control of locomotor behaviors, Brain Research Review, 57, 192-198, 2008
50. Okumura T, Takakusaki K, Role of orexin in central regulation of gastrointestinal functions, Journal of Gastroenterology, 43, 652-660, 2008
51. Takakusaki K, Okumura T, Neurobiological Basis of Controlling Posture and Locomotion, Advanced Robotics, 22, 1629-1663, 2008
52. Adachi M, Nonaka S, Katada A, Arakawa T, Ota R, Harada H, Takakusaki K, Harabuchi Y, Carbachol injection into the pontine reticular formation depresses laryngeal muscle activities and airway reflexes in decerebrate cats, Neuroscience Research (in press)
53. Takakusaki K, Substrates for execution for gait performance with respect to the basal ganglia function, IROS2008 Full day Workshop, September 26th 2008, Nice, France
54. Takakusaki K, Basal ganglia efferents to the brainstem control postural muscle tone by modulating the activity of cholinergic PPN neurons via GABAA-receptors in cats, ＳＦＮ 2008
55. An Qi, Ikemoto Y, Asama H, Matsuoka H, Chugo D, Takakusaki K, Extraction of Behavior Primitives in Human Standing-up Motion for Development of Power Assisting Machine, ROBIO 2008
56. Takakusaki K, Background excitability of spinal reflex arcs are modulated by muscle tone inhibitory system, Neuroscience 2008
57. Atsushi Chiba, Ken-ichi Oshio and Masahiko Inase, Striatal Neurons Encoded Temporal Information in Duration Discrimination Task, Experimental Brain Research, 186, 671-676, 2008
58. Ken-ichi Oshio, Atsushi Chiba and Masahiko Inase, Temporal Filtering by Prefrontal Neurons in Duration Discrimination, European Journal of Neuroscience, 28, 11, 2333-2343, 2008
59. Atsushi Chiba, Ken-ichi Oshio and Masahiko Inase, Effects of Isotonic Contraction Excised vas Deferens of Guinea-Pigs under Pain-Related Drugs, 16th International Conference on Biomagnetism, 275-277, 2008
60. N. Wada, F. Mori, et al, Investigation and characterization of rat bipedal walking models established by a training program, Brain Research, 1243, 70-77, 2008
61. T. Hosoido, F. Mori, et al, Characteristics of H- and M-waves recorded from rat forelimbs, Neuroscience Letters, 450, 239-241, 2009
62. F. Mori, K. Nakajima and S. Aoi, Cortical motor areas in the postural and locomotor control, XXV Barany Society Meeting, 2008
63. Shogo Endo, Fumihiro Shutoh, Tung Le Dinh, Takehito Okamoto, Toshio Ikeda, Michiyuki Suzuki, Shigenori Kawahar|, Dai Yanagihara, Yamato Sato, Kazuyuki Yamada, Yutaka Kirino, Nicholas A. Hartell, Kazuhiko Yamaguchi, Shigeyoshi Itohara, Angus Naim, Paul Greengard, Soichi Nagao, and Masao Ito, Dual involvement of G-substrate in motor learning revealed by gene deletion, Proceedings of the National Academy of Sciences of the United States of America, in press, 2009
64. Kiyoji Matsuyama, Kaoru Takakusaki, Organizing Principles of Axonal Projections of the Long Descending Reticulospinal Pathways and Their Targets' Spinal Commissural Neurons: With Special Reference to the Locomotor Function, Handbook on White Matter: Structure, Function and Changes (Editors: Westland T.B., Calton R.N.), in press, 2009
65. Onuma Boonyarom, Naoki Kozuka, Kiyoji Matsuyama, Shinji Murakami, Effect of Electrical Stimulation to Prevent Muscle Atrophy on Morphological and Histological Properties of Hindlimb Suspended Rat Hindlimb Muscles, American Journal of Physical Medicine & Rehabilitation, 88, in press, 2009
66. Kiyoji Matsuyama, Masanori Ishiguro, Mamoru Aoki, Roles of supraspinal signals and sensory feedbacks in generation of coordinated quadrupedal locomotion in rabbits, Journal of Physiological Sciences, 58, Suppl, S195, 2008
67. Natori, S., Yoshimi, K., Takahashi, T., Kagohashi, M, Oyama, G., Shimo, Y., Hattori, N, Kitazawa, S., Subsecond reward-related dopamine release in the mouse dorsal striatum, Neuroscience Research (in press), 2008
68. Ono, F., & Kitazawa, S., The effect of marker size on the perception of an empty interval., Psychonomic Bulletin & Review, 16, 1, 182-189, 2009
69. G. Oyama, K. Yoshimi, S. Natori, Y. Chikaoka, Y. Shimo, S. Kitazawa, R.Takahashi, N. Hattori., Reduced dopamine release in the striatum of Parkin knockout mouse., Movement Disorder Society Annual meeting, 2008

70. Kitazawa S, Endo Y, Yamane M, Takahashi M., Temporo-spatial gaze patterns in autistic children., 38th Annual Meeting, Society for Neuroscience, 2008
71. G. Oyama, K. Yoshimi, S. Natori, Y. Chikaoka, Y. Shimo, S. Kitazawa, R. Takahashi, N. Hattori., Reduced dopamine release in the striatum of Parkin knockout mouse., 38th Annual Meeting, Society for Neuroscience, 2008
72. Shihoko Natori, Kenji Yoshimi, Genko Oyama, Yasushi Shimo, Nobutaka, Hattori, Shigeru Kitazawa., Reward-associated dopamine release in the striatum of behaving mice., 38th Annual Meeting, Society for Neuroscience, 2008
73. Shihoko Natori, Kenji Yoshimi, Maki Kagohashi, Genko Oyama, Yasushi Shimo, Nobutaka Hattori, Shigeru Kitazawa. , Reward-associated dopamine release in the striatum of behaving mice., 第31回神経科学会, 2008
74. Kitazawa S. & Nishida S., Adaptive anomalies in conscious time perception., Tutorial workshop in the 12th Annual Meeting of the Association for the Scientific Study of Consciousness., 2008
75. Juan Carlos Toledo Salas, Hiroshi Iwasaki, Eiichi Jodo, Markus H. Schmidt, Akihiro Kawauchi, Tsuneharu Miki, Yukihiko Kayama, Manabu Otsuki, Yoshimasa Koyama, Penile erection and micturition events triggered by electrical stimulation of the mesopontine tegmental area, American Journal of Physiology, 292, R102-R111, 2008
76. Gulia KK, Jodo E, Kawauchi A, Miki T, Kayama Y, Mallick HN, Koyama Y., The septal area, site for the central regulation of penile erection during waking and REM sleep in rats : a stimulation study, Neuroscience, 156, 4, 1064-1073, 2008
77. Motomura W, Yoshizaki T, Ohtani K, Okumura T, Fukuda M, Fukuzawa J, Mori K, Jang S-J, Nomura N, Yoshida I, Suzuki Y, Kohgo Y, Wakamiya N, Tissue distribution of a collectin CL-K1 in murine tissues., J Histchem Cytochem, 56, 243-252, 2008
78. Yamazaki M, Nakamura K, Mizukami Y, Ii M, Sasajima J, Sugiyama Y, Nishikawa T, Nakano Y, Yanagawa N, Sato K, Maemoto A, Tanno S, Okumura T, Karasaki H, Kono T, Fujiya M, Ashida T, Chung DC, Kohgo Y., Sonic hedgehog derived from human pancreatic cancer cells augments angiogenic function of endothelial progenitor cells, Cancer Sci, 99, 1131-1138, 2008
79. Tanno S, Nakano Y, Nishikawa T, Nakamura K, Sasajima J, Minoguchi M, Mizukami Y, Yanagawa N, Fujii T, Obara T, Okumura T, Kohgo Y., Natural History of Branch Duct Intraductal Papillary-Mucinous Neoplasms of the Pancreas without Mural Nodules: Long-term Follow-up Results, Gut, 57, 339-343, 2008
80. Okumura T, Takakusaki K, Role of orexin in central regulation of gastrointestinal functions, J Gastroenterol, 43, 652-660, 2008
81. Kumei S, Motomura W, Yoshizaki T, Takakusaki K, Okumura T, Troglitazone increases expression of E-cadherin and claudin 4 in human pancreatic cancer cells., Biochem Biophys Res Coomun (in press)
82. Ogihara, N., Makishima, H., Aoi, S., Sugimoto, Y., Tsuchiya, K., Nakatsukasa, M., Development of an Anatomically Based Whole-Body Musculoskeletal Model of the Japanese Macaque (Macaca fuscata), American Journal of Physical Anthropology, in press
83. Aoi, S., Ogihara, N., Sugimoto, Y., Tsuchiya, K., Simulating adaptive human bipedal locomotion based on phase resetting using foot-contact information, Advanced Robotics, 22, 1697-1713, 2008
84. Oishi, M., Ogihara, N., Endo, H., Asari, M, Muscle architecture of the upper limb in the orangutan, Primates, 49, 204-209, 2008
85. Kagaya, M., Ogihara, N., Nakatsukasa, M., Morphological study of the anthropoid thoracic cage: scaling of thoracic width and analysis of rib curvature, Primates, 49, 89-99, 2008
86. S. Aoi, Y. Sato, and K. Tsuchiya, Arc Feet Effects on Stability Based on a Simple Oscillator-Driven Walking Model, Journal of Robotics and Mechatronics, 20, 5, 709-718, 2008
87. Yasuhiro Sugimoto, Koichi Osuka, Hierarchical Implicit Feedback Structure in Passive Dynamic Walking, Journal of Robotics and Mechatronics, 20, 4, 559-566, 2008
88. Yasuhiro Sugimoto, Shinya Aoi, Naomichi Ogihara, Kazuo Tsuchiya, The Stabilizing function of musculoskeletal system for periodic motion, Advanced Robotics, in press
89. Kazuhiko Nakatani, Yasuhiro Sugimoto, Koichi Osuka, Demonstration and Analysis of Quadrupedal Passive Dynamic Walking, Advanced Robotics, in press
90. Ogihara, N., Aoi, S., Sugimoto, Y., Nakatsukasa, M., Tsuchiya, K, Computer simulation of locomotion in the Japanese monkey: A constructive approach towards understanding adaptive mechanism in primate locomotion, IEEE/RSJ 2008 International Conference on Intelligent Robots and Systems Workshop, Nice, France, 2008
91. Ogihara, N., Nakatsukasa, M., A computer simulation study of precision grip in human and chimpanzee based on an anatomically realistic hand musculoskeletal model, IPS Post-Congress Symposium on Comparative Functional Morphology in Primates, Durham, UK, 2008
92. Kagaya, M., Ogihara, N., Nakatsukasa, M., Clavicular length of hominoids: a comparison with the thoracic cage width, IPS Post-Congress Symposium on Comparative Functional Morphology in Primates, Durham, UK, 2008
93. Ogihara, N., Hirasaki, E., Nakatsukasa, M., Experimental and computational studies of bipedal locomotion in the bipedally-trained Japanese monkey, The International Primatological Society XXII Congress, Edinburgh, UK, 2008
94. Kagaya, M., Ogihara, N., Nakatsukasa, M., Morphological Study of the anthropoid thoracic cage: Rib orientation and its implication for orthograde postural behavior, The International Primatological Society XXII Congress, Edinburgh, UK, 2008
95. Ogihara, N., Aoi, S., Sugimoto, Y., Nakatsukasa, M., Tsuchiya, K, Synthetic study of quadrupedal/bipedal locomotion in the Japanese monkey, 4th International Symposium on Adaptive Motions of Animals and Machines, Cleveland, OH, USA, 2008
96. S. Aoi, N. Ogihara, Y. Sugimoto, and K. Tsuchiya, Computer Simulation of Adaptive Human Bipedal Locomotion Based on Phase Resetting Using Foot Contact Information, 4th Int. Symp. on Adaptive Motion of Animals and Machines, 64-65, 2008
97. S. Aoi, Y. Sato, and K. Tsuchiya, Stability Characteristics in Walking Behavior with Two Different Oscillatory Elements: Roles of Arc Foot and Internal Oscillator, Proc. IEEE/RSJ Int. Conf. on Intell. Robots Syst., 3414-3419, 2008
98. Y.Sugimoto, S. Aoi, N. Ogihara, K. Tsuchiya, The role of the force-velocity relationship of muscle for the stability of periodic motions, 4th Int. Symp. on Adaptive Motion of Animals and Machines, 2008
99. K. Hosoda, T. Takuma, A. Nakamoto, S. Hayashi, Biped Robot Design Powered by Antagonistic Pneumatic Actuators for Multi-Modal Locomotion, Robotics and Autonomous Systems, 56, 1, 46-53, 2008
100. K.Tsujita, T.Kobayashi and T.Masuda, A Feasibility Study on Stability of Gait Patterns with Changable Body Stiffness using Pneumatic Actuators in Quadruped Robot, Advanced Robotics, 23, 5, to appear, 2009
101. K.Tsujita, T.Inoura, T.Kobayashi and T.Masuda, A Study on Locomotion Stability by Controling Joint Stiffness of Biped Robot with Pneumatic Actuators, Motion and Vibration Control, 305-314, 2008
102. T.Takuma, S.Hayashi, K.Hosoda, 3D Biped Robot for Multi-modal Locomotion Driven by Antagonistic Pneumatic Actuators, Fourth International Symposium on Adaptive Motion of Animals and Machines, CD-ROM, 2008
103. Koh Hosoda, Hitoshi Takayama, and Takashi Takuma, Jumping of an Anthropomorphic Robot Equipped with Biarticular Muscles, Fourth International Symposium on

Adaptive Motion of Animals and Machines, CD-ROM, 2008

104. T.Takuma, S.Hayashi, K.Hosoda, 3D Bipedal Robot with Tunable Leg Compliance Mechanism for Multi-modal Locomotion, IEEE/RSJ 2008 International Conference on Intelligent Robots and Systems, 1097-1102, 2008
105. K.Hosoda, H.Takayama, T.Takuma, Bouncing Monopod with Bio-mimetic Muscular-Skeleton System, IEEE/RSJ 2008 International Conference on Intelligent Robots and Systems, 3083-3088, 2008
106. K.Tsujita, T.Kobayashi, T.Inoura and T.Masuda, Gait Transition by Tuning Muscle Tones using Pneumatic Actuators in Quadruped Locomotion, Proc. of IEEE/RSJ IROS2008, 2453-2458, 2008
107. K.Tsujita, T.Inoura, T.Kobayashi and T.Masuda, A Study on Locomotion Stability by Controling Joint Stiffness of Biped Robot with Pneumatic Actuators, CD-ROM Proc. of Int. Conf. of Motion and Vibration Control, RO1-1195, 2008
108. K.Tsujita, T.Kobayashi, T.Inoura and T.Masuda, A study on adaptive gait transition of quadruped locomotion by changing muscle tone, Proc. of SICE Annual Conference 2008, 2489-2494, 2008
109. K.Tsujita, T.Inoura, T.Kobayashi and T.Masuda, A Study on Locomotion Stability at the Variance of Joint Stiffness, Proc. of Int. Symp. on Adaptive Motion of Animals and Machines(AMAM) 2008, 58-59, 2008
110. C. Maufroy, H. Kimura and K. Takase, Towards a general neural controller for quadrupedal locomotion,NEURAL NETWORKS, 21, 4, 667-681, 2008
111. C. Maufroy, H. Kimura and K. Takase, Towards a general neural controller for 3D quadrupedal locomotion, Proc. of SICE Annual Conference 2008, 2495-2500, 2008
112. T. Masuda, H. Kimura and K. Takase, Emergenceof a Quadrupedal Bound Gait as Interaction among the Brain, Body and Environment, Proc. of SICE Annual Conference 2008, 2501-2506, 2008
113. Y. Otoda, H. Kimura and K. Takase, Adaptive Walking of a 2D Biped Robot during Splitbelt Treadmill, Proc. of SICE Annual Conference 2008, 2507-2512, 2008
114. H. Kimura, Robotics as a Tool for Gait AND Posture Study, Fourth International Symposium on Adaptive Motion of Animals and Machines, CD-ROM, 2008
115. C. Maufroy and H. Kimura, Towards a general neural controller for 3D quadrupedal locomotion, Proc. of 20th Autonomous Distributed System Symposium, 251-256, 2008
116. K. Nakamura, W. Yoshinaga, K.inoue, Development of a Biomimetic control system for a Snake-like Robot with Pneumatic Actuators, 4th International Student Conference at Ibaraki University, 66-72, 2008
117. Yoshinori Izaki, Masatoshi Takita and Tatsuo Akema, Specific role of the posterior dorsal hippocampus-prefrontal cortex in short-term working memory, European Journal of Neuroscience, 27, 3029-3034, 2008
118. Takeshi Uejima, Toshiyuki Fujii, Hiroshi Yokoi Masatoshi Takita, Motion Classification by Epidural Potential Measurement of Rat for Low-Invasive Brain-Machine Interface, Proceedings of 2008 IEEE International Conference of Robotics and Biomimetics, 2009
119. Kojiro Matsushita, Hiroshi Yokoi, and Tamio Arai, Robotic Education for Human-Robot Interaction: Proposal of Two Robotic Developmental Kits that Bring Creativity, 2008 IEEE/RSJ International Conference on Intelligent Robots and Systems (IROS), Workshop Teaching Human-Robot Interaction to Humans, 2008
120. Hiroshi Yokoi and Kojiro Matsushita, Self-regulatory Hardware: Evolutionary Design for Mechanical Passivity on a Pseudo Passive Dynamic Walker, Artificial Life Models in Hardware (Ed. Andrew Adamatzky and Maciej Komosinski), Springer-Verlag, 2009
121. Kojiro Matsushita and Hiroshi Yokoi, Embodiment of Legged Robots Emerged in Evolutionary Design: Pseudo Passive Dynamic Walker, Frontiers in Evolutionary Robotics (Ed. Aleksandar Lazinica), I-Tech Education and Publishing, ISBN: 978-3-902613-19-6., 311-326, 2008
122. Naoki Kotake, Takafumi Suzuki, Kunihiko Mabuchi, Shoji Takeuchi, A flexible parylene neural probe combined with a microdialysis membrane, Proc. of microTAS 2008, 1687-1689, 2008
123. Osamu Fukayama, Noriyuki Taniguchi, Takafumi Suzuki, Kunihiko Mabuchi, Automatic Adaptation of Vehicle Controller to Time-Varying Neural Signals Recorded in RatCar System; A Vehicle-formed BMI, Proc. of Joint 4th International Conference on Soft Computing and Intelligent Systems and 9th International Symposium on Advanced Intelligent Systems, 253-256, 2008
124. Osamu Fukayama, Noriyuki Taniguchi, Takafumi Suzuki, Kunihiko Mabuchi, RatCar system for estimating locomotion states using neural signals with parameter monitoring: Vehicle-formed brain-machine interfaces for rat, Proc. of 30th Annual International Conference of the IEEE EMBS, 5322-5325, 2008
125. Takafumi Suzuki, Development of flexible neural probes and their applications to neuroprostheses, EDIS 2008 satellite symposium GCOE global seminar Advances in Neuroengineering, 2008
126. Noriyuki Taniguchi, Osamu Fukayama, Tatsuo Okubo, Takafumi Suzuki, Kunihiko Mabuchi, RatCar System: A vehicle-formed BMI system by neural signals recorded with implantable electrodes, Proc. of International Symposium on Biological and Physiological Engineering, 173-174, 2008
127. Sakurai, Y., Takahashi, S., Dynamic synchrony of local cell assembly, Reviews in the Neuroscience, 16, In press, 2008
128. Hirokawa, J., Bosch, M., Sakata, S., Sakurai, Y. and Yamamori, T., Functional role of the secondary visual cortex in multisensory facilitation in rats., Neuroscience, 153, 1402-1417, 2008
129. Takahashi, S., Sakurai, Y., Hippocampal neuronal ensembles act as comparator during delayed non-matching to sample performance in rats., 38th Society for Neuroscience Annual Meeting. ,
130. Hirokawa, J., Sadakane, O., Sakata, S., Bosch, M., Sakurai, Y., Yamamori, T., Superior colliculus differently mediates behavioral facilitations of speed and accuracy by audiovisual integration, 38th Society for Neuroscience Annual Meeting. , USA. Nov., 2008
131. Yasushi Kobayashi, Ken-ichi Okada, Different Pedunculopontine Tegmental Neurons Signal Predicted and Actual Task Rewards., The XXV Barany Society Meeting, Satellite symposium, Neural mechanism in control of eye, head and limb movements, P11, 2008
132. Yasushi Kobayashi, Pedunculopontine Tegmental Nucleus Neurons Signal Predicted and Actual Reward for Reinforcement Learning., 12th Annual meeting, Association for the Scientific Study of Consciousness , 121, 2008
133. Yasushi Kobayashi, Motivation and reward prediction error computation in the midbrain., Open Problems in Neuroscience of Decision Making OIST symposium, 2008
134. Ken-ichi Okada, Yasushi Kobayashi, Neural correlates of task performance of the visually guided saccade tasks in the primate pedunculopontine tegmental nucleus., Society for Neuroscience Abstarct, 88.8, 2008
135. Ken-ichi Okada, Yasushi Kobayashi, Neural correlates of task performance in the primate pedunculopontine tegmental nucleus., Neruscience Research, 61, Suppl 1, S60, 2008
136. Yuri Kitamura, Koshiro Maruyama, Ken-ichi Okada, Yasushi Kobayashi, Yuji Yahata, Syoji Kobashi, Ikuko Mohri, Masako Taniike, Using eye-movements as a research tool in children with autistic spectrum disorders., Neruscience Research, 61, Suppl 1, S131, 2008
137. Tomohiko Takei, Kazuhiko Seki, Spinomuscular coherence in monkey performing a precision grip task., Journal of Neurophysiology, 99, 4, 2012-2020, 2008
138. Kazuhiko Seki, Tomohiko Takei, Activity of spinal interneurons mediationg afferent inputs from forearm muscles in monkeys performing volunary wrist movement, The 38th annual meeting of the Society for the Neuroscience, 860.20, 2008

139. Jackson, A., Baker, SN., Isa, T., Seki, K., Motor networks in the primate cervical spinal cord explored using intraspinal microstimulation, The 38th annual meeting of the Society for the Neuroscience, 860.19, 2008
140. Tomohiko Takei, Kazuhiko Seki, Spinomuscular coherence in monkey performing a precision grip task., The 38th annual meeting of the Society for the Neuroscience, 77.17, 2008
141. Chiken S, Shashidharan P, Nambu A, Cortically evoked long-lasting inhibition of pallidal neurons in a transgenic mouse model of dystonia. , Journal of Neuroscience, 28, 51, 13967-13977, 2008
142. Tachibana Y, Kita H, Chiken S, Takada M, Nambu A, Motor cortical control of internal pallidal activity through glutamatergic and GABAergic inputs in awake monkeys., European Journal of Neuroscience, 27, 1, 238-253, 2008
143. Hatanaka N, Tokuno H, Nambu A, Takada M, Transdural doppler ultrasonography monitors cerebral blood flow changes in relation to motor tasks. , Cerebral Cortex, in press, 2009
144. Nambu A, Seven problems on the basal ganglia. , Current Opinion in Neurobiology, 18, in press, 2008
145. Nambu A, Basal ganglia: physiological circuits., Encyclopedia of Neuroscience, 2, 111-117, 2009
146. S. Tomatsu, Y. Someya, Y.W. Sung, S. Ogawa S, S. Kakei, Temporal features of BOLD responses varies with temporal patterns of movement., Neurosci Res, 62, 160-167, 2008
147. Y. Tsunoda, S. Kakei, Reaction time changes with the hazard rate for a behaviorally relevant event when monkeys perform a delayed wrist movement task., Neurosci Lett, 433, 152-157, 2008
148. J.H. Lee, Y. Kagamihara, S. Kakei, Quantitative Evaluation of Movement Disorders in Neurological Diseases based on EMG Signals., Conf Proc IEEE Eng Med Biol Soc, 1, 181-184, 2008
149. J.H. Lee, Y. Kagamihara, S. Kakei, Quantitative Evaluation of Cerebellar Ataxia based on EMG signals., The second IEEE RAS / EMBS International Conference on Biomedical Robotics and Biomechatronics, in press, in press, 2009
150. J.A. Ting, A. D'Souza, K. Yamamoto, T. Yoshioka, D.S. Hoffman DS, S. Kakei, Variational Bayesian least squares: An application to brain-machine interface data., Neural Netw, 21, 1121-1131, 2008
151. S. Kakei, Cerebellar mossy fibers provide precise copies of cortical motor commands., XXV Barany Society Meeting, Kyoto, April 2008, 2008
152. S. Kakei, Gain modulation and wrist motor control: from agonist selection to sensorimotor transformation., Neuroscience Seminar, Johns Hopkins University, Baltimore MD, Nov. 2008, 2008
153. S. Tomatsu, Y. Tsunoda, S. Kakei, Temporal patterns of Golgi cell activities for execution of wrist movements in monkeys., 38th Annual Meeting of the Society for Neuroscience, Washington DC, Nov. 2008
154. Y. Tsunoda, S. Kakei, Reaction time reflects anticipation of events in a simple reaction time task in the monkey., 38th Annual Meeting of the Society for Neuroscience, Washington DC, Nov., 2008
155. Hanakawa T, Dimyan MA, Hallett M, The representation of blinking movement in cingulate motor areas: a functional magnetic resonance imaging study., Cerebral Cortex, 18, 4, 930-937, 2008
156. Iseki K, Hanakawa T, Shinozaki J, Nankaku M, Fukuyama H, Neural mechanisms involved in observation and imagery of gait movement., Neuroimage, 41, 3, 1021-1031, 2008
157. Hanakawa T, Dimyan MA, Hallett M, Motor planning, imagery and execution: a time-course study with functional MRI., Cerebral Cortex, 18, 12, 2775-2788, 2008
158. Namiki C, Yamada M, Yoshida H, Hanakawa T, Fukuyama H, Murai T, High resolution MRI revealed small orbitofrontal traumatic lesions responsible for behavioral changes, Neurocase, 14, 6, 474-479, 2008
159. Yamamoto T, Takahashi S, Hanakawa T, Urayama S, Fukuyama H, Ejima Y, The stereokinetic effect reveals different roles of the lateral occipito-temporal and parietal cortex for 3-D perception from motion: An fMRI study, Journal of Vision, 8, 10:14, 1-17, 2008
160. Lerner A, Bagic A, Hanakawa T, Boudreau EA, Pagan F, Mari Z, Bara-Jimenez W, Aksu M, Sato S, Murphy DL, Hallett M, Is the insula responsible for suppression of natural urges?, Cerebral Cortex, 19, 1, 218-223, 2009
161. Matsumoto R, Okada T, Mikuni N, Mitsueda T, Taki J, Sawamoto N, Hanakawa T, Miki Y, Ikeda A, Hashimoto N, Fukuyama H, Takahashi R, Hemispheric asymmetry of the arcuate fasciculus in patients with unilateral language dominancy defined by Wada test, Journal of Neurology, 255, 11, 1703-11, 2008
162. Tsubomi H, Ikeda T, Hanakawa T, Hirose N, Fukuyama H, Osaka N, Parieto-occipital connectivity predicts top-down attentional effect in visual masking: an fMRI study with individual differences approach, Neuroimage, in press
163. Toda H, Sawamoto N, Hanakawa T, Saiki H, Matsumoto S, Okumura R, M, Ishikawa M, Fukuyama H, Hashimoto N, A novel composite targeting method using high-field magnetic resonance imaging for subthalamic nucleus deep brain stimulation, Journal of Neurosurgery, in press
164. Abe M, Hanakawa T, Functional coupling underlying motor and cognitive functions of the dorsal premotor cortex, Behavioural Brain Research, 198, 1, 13-23, 2009
165. Hanakawa T, Mima T, Matsumoto R, Abe M, Inouchi M, Urayama S, Anami K, Honda M, Fukuyama H, Stimulus-response profile during single-pulse transcranial magnetic stimulation to the primary motor cortex, Cerebral Cortex, in press
166. Hanakawa T, Hallett M, Parallel basal ganglia-frontal cortical loops for the control of motor and cognitive agility, Neuroscience 2008, Online, 2008
167. Shitara H, Hanakawa T, Shinozaki T, Takagishi K, Honda M, Simultaneous measurement of fMRI, TMS and EMG with stepping stone sampling method, 14th Annual Meeting of the Organization for Human Brain Mapping, Online, 2008
168. Tanaka S, Honda M, Hanakawa T, Cohen LG, Consolidation of motor memories encoded by different practice schedules, 14th Annual Meeting of the Organization for Human Brain Mapping, Online, 2008
169. HanakawaT, Hosoda C, Honda M., Does mental rotation of hands and feet involve somatotopically organized brain regions?, 14th Annual Meeting of the Organization for Human Brain Mapping, Online, 2008
170. Hosoda C, Hanakawa T, Nariai T, Ohno K, Honda M, Substrates of Switching of Phonology between the First and Second Languages, 14th Annual Meeting of the Organization for Human Brain Mapping, Online, 2008
171. Matsumoto R, Sawamoto N, Urayama S, Mikuni N, Hanakawa T, Behrens T, Ikeda A, Takahashi R, Fukuyama H, In vivo tract tracing of cortico-cortical connections in humans: a combined study of CCEP and probabilistic diffusion tractography, 14th Annual Meeting of the Organization for Human Brain Mapping, Online, 2008
172. Ashikaga M., Sakura M., Kikuchi M., Hiraguchi T., Chiba R., Aonuma H. and Ota J., Establishment of social status without individual discrimination in the cricket, Adv. Robotics., in press, 2009
173. Aonuma H., Kitamura Y., Niwa K., Ogawa H. and Oka K., Nitric oxide-cGMP signaling in the local circuit of the cricket abdominal nervous system, Neuroscience, 157, 749-761, 2008

174. Okada R., Ikeno H., Aonuma H. and Ito E., Biological insights into robotics: Honeybee foraging behavior by waggle dance, Adv. Robotics., 22, 1665-1681, 2008
175. Ishikawa Y., Aonuma H. and Miura T., Soldier-specific modification of the mandibular motor neurons in termites, PLoS ONE, 3, 7, e2617:1-8, 2008
176. Yono O. and Aonuma H., Cholinergic neurotransmission from mechanosensory afferents to giant interneurons in the terminal abdominal ganglion of the cricket, Gryllus bimaculatus, Zool. Sci., 25, 517-525, 2008
177. Funato T., Kurabayashi D., Nara M. and Aonuma H., Switching mechanism of sensor-motor coordination through oscillator network model, IEEE Trans. Systems, Man and Cybernetics - Part B, 38, 3, 764-770, 2008
178. Okada R., Ikeno H., Sasayama N., Aonuma H., Kurabayashi D., and Ito E., The dance of the honeybee: how do they dance to transfer the food information effectively?, Acta Biol. Hung., 59, 157-162, 2008
179. Sakura M., Hiraguchi T., Ohkawara K., and Aonuma H., The Compartment structures of the antennal lobe in the ant Aphaenogaster smythiesi japonica, Acta Biol. Hung., 59, 183-187, 2008
180. Ikeno H., Kanzaki R., Aonuma H., Takahata M., Mizunami M., Yasuyama K., Matsui N., Yokohari F. and Usui S., Development of invertebrate brain platform: Management of research resources for invertebrate neuroscience and neuroethology, Proceedings of 14th International Conference on Neural Information Processing 2007: Part II, LNCS 4985, (Eds. Ishikawa M. et al.) Springer-Verlag Berlin Heidelberg, 905-914, 2008
181. Aonuma H., Modelling of social interaction dependent behavior selection in the cricket, Workshop on Dynamical Circuits in the Brain, 2008
182. Ota J., Aonuma H., Asama H., Kawabata K. and Ashikaga M., Multidisciplinary contributions from neuroethology and engineering-Understanding experience dependent behavior selection in crickets, IROS2008, 54-59, 2008
183. Aonuma H., Experience dependent behavior selection in the cricket, International Seminar: Evolutionary Studies in Behavioral Neuroscience, 2008
184. Aonuma H. and Ota J., Synthetic neuronethological approach to understand experience dependent adaptive behavior in the cricket, The 4th International Symposium on Adaptive Motion of Animals and Machines, 2008
185. Aonuma H., Murakami J. and Nagao T., Nitric oxide mediated biogenic amine system underlying agonistic behavior in the crickets, FENS2008, 2008
186. Ashikaga M., Sakura M., Kikuchi M., Hiraguchi T., Chiba R., Ota J. and Aonuma H., Modeling of adaptive behavior of crickets in crowd, FENS2008, 2008
187. K. Kawabata, T. Fujiki, T. Fujii, H. Aonuma, Y. Ikemoto, M. Ashikaga, J. Ota, T. Suzuki, H. Asama, Towards Synthetic Understanding of Neural System, of Adaptive Behavior Selection in the Fighting Behavior of Male Crickets, 6th Forum of European Neuroscience Abstr, 4, 226.7, 2008
188. Aonuma H., Modelling of experience dependent behavior - Fighting among male crickets, International Conference for Nonlinear Sciences SAPPORO WINTER SCHOOL, 2009
189. Norisuke Fujii and Jun Ota, Rearrangement Task by Multiple Mobile Robots with Efficient Calculation of Task Constraints, Advanced Robotics, 22, 2-3, 191-213, 2008
190. Kenji Terabayashi, Natsuki Miyata and Jun Ota, Grasp Strategy when Experiencing Hands of Various Sizes, International Journal on Human-Computer Interaction, I, 4, 55-74, 2008
191. K. Nakajima, S. Morishita, T. Kazawa, R. Kanzaki, K. Kawabata, H. Asama, T. Mishima, Interpolation of binarized CLSM images for extraction of premotor neuron branch structures in silkworm moth, Sensor Review, in printing, 2008
192. Yusuke Ikemoto, Shingo Suzuki, Hiroyuki Okamoto, Hiroki Murakami, Hajime Asama, Soichiro Morishita, Taketoshi Mishima, Xin Lin, Hideo Itoh, Force sensor system for structural health monitoring using passive RFID tags, Sensor Review, in printing, 2009
193. J. Ota, H. Aonuma, H. Asama, K. Kawabata, Modeling of Adaptive Mechanism in Crickets by Means of Constructive Approach, Workshop/Tutorial Proceedings of International Conference on Intelligent Robots and Systems, 5, 988-991, 2008
194. Yewguan Soo, Masao Sugi, Hiroshi Yokoi, Tamio Arai, Tatsuhiro Nakamura, Rulin Du and Jun Ota, The Relationship between Changes in Amplitute and Instantaneous Mean Frequency at Low and High Frequency Bands during Dynamic Contraction, Proceedings of the 2nd Int. Conference on Bioinformatics and Biomedical Engineering, 02-06-04, 1-4, 2008
195. Yewguan Soo, Masao Sugi, Hiroshi Yokoi, Tamio Arai, Rulin Du and Jun Ota, Simultaneous Measurement of Force and Muscle Fatigue using Frequency-band Wavelet Analysis, Proceedings of 30th Annual International Conference of the IEEE Engineering in Medicine and Biology Society, 5045-5048, 2008
196. Hitoshi Aonuma, Modori Sakura, Mika Kikuchi, Masatoshi Ashikaga and Jun Ota, Synthetic neuroethological approach of understanding neuronal mechanisms of social adaptive behavior of crickets, Prepr. 10th RIES-Hokudai International Symposium on aya, 71-72, 2008
197. M. Otake, T. Takagi, H. Asama, Open Brain Simulator Estimating Internal State of Human through External Observation towards Human Biomechatronics, Proc. 2008 IEEE International Conference on Robotics and Automation, 2008
198. M. Murabayashi, Y. Ikemoto, M. Otake, T. Maeda, M. Kato, H. Asama, Analysis of the Sense of Agency using a Tactile Device, 17th CISM-IFToMM Symposium on Robot Design, Dynamics, and Control, 2008
199. Y. Ikemoto, S. Suzuki, H. Okamoto, H. Murakami, X. Lin, H. Itoh, H. Asama, Monitoring using Passive RFID Tags for Structural Health Monitoring, 2nd IEEE International Interdisciplinary Conference on Portable Information Devices, 2008
200. M. Ikeda, Y. Ikemoto, T. Miura, H. Asama, A Termite Internal State Model for Elucidating Caste Differentiation, 2008 SICE Annual Conference, 142-145, 2008
201. K. Nakajima, S. Morishita, T. Kazawa, R. Kanzaki, H. Asama, T. Mishima, Interpolation of the Cross-sectional Area of a Premotor Neuron in a Silkworm Moth Brain using the Ellipse Model, 2008 IEEE International Conference on Multisensor Fusion and Integration for Intelligent Systems, 2008
202. S. Yano, Y. Ikemoto, H. Aonuma, T. Nagao, H. Asama, Modeling of self-organized competition hierarchy with body weight development in larval cricket, Gryllus bimaculatus, Preprints 9th International Symposium on Distributed Autonomous Robotic Systems, 2008
203. Q. An, Y. Ikemoto, H. Asama, H. Matsuoka, D. Chugo, K. Takakusaki, Extraction of Behavior Primitives in Human Standing-Up Motion for Development of Power Assisting Machine, 2008 IEEE International Conference on Robotics and Biomimetics, 2009
204. Tetsuro Funato, Daisuke Kurabayashi, Network Structure for Control of Coupled Multiple Non-Linear Oscillators, IEEE Transactions on Systems, Man and Cybernetics - Part B, 38, 3, 675-681, 2008
205. Herianto, Toshiki Sakakibara, Tomoaki Koiwa, Daisuke Kurabayashi, Realization of Pheromone Potential Field for Autonomous Navigation by Radio Frequency Identification, Advanced Robotics, 22, 1461-1478, 2008
206. Tomoki Kazawa, Hidetoshi Ikeno, Ryohei Kanzaki, Development and application of a neuroinformatics environment for neuroscience and neuroethology, Neural Networks, 21, 8, 1047-1055, 2008
207. Kanako Nakajima, Taketoshi Mishima, Soichiro Morishita, Hajime Asama, Tomoki Kazawa, Ryohei Kanzaki, Kuniaki Kawabata, Interpolation of binarized images for form reconstruction of a neuron, Sensor Review, in press
208. Tomoko Yamagata, Takeshi Sakurai, Keiro Uchino, Hideki Sezutsu, Toshiki Tamura, Ryohei Kanzaki, GFP labeling of neurosecretory cells with the GAL4/UAS system in the silkmoth brain enables selective intracellular staining of neurons, Zoological Science, 25, 5, 509-516, 2008

209. Shigehiro Namiki, Ryohei Kanzaki, Reconstructing the population activity of olfactory output neurons that innervate identifiable processing units, Frontiers in Neural Circuits 2:1, 2, 1, 1-11, 2008
210. Shigehiro Namiki, Satoshi Iwabuchi, Ryohei Kanzaki, Representation of a mixture of pheromone and host plant odor by antennal lobe interneurons of the silkmoth Bombyx mori, Journal of Comparative physiology A, 194, 501-515, 2008
211. Tomoki Kazawa, Shigehiro Namiki, Ryota Fukushima, Mitsuhiro Terada, Kajin Soo, Ryohei Kanzaki, Constancy and variability of glomerular organization in the antennal lobe of the silkmoth, Cell and Tissue Research, accepted, accepted
212. Ryota Fukushima, Ryohei Kanzaki, Modular subdivision of mushroom bodies by kenyon cells in the silkmoth, Journal of Comparative Neurology, 513, 315-330, 2008
213. Masaaki Iwano, Evan S. Hill, Akio Mori, Tatsuya Mishima, Tsuneko Kumagai, Kei Ito, Ryohei Kanzaki, Generation mechanism of flip-flop activity in the lateral accessory lobe and ventral protocerebrum of the insect brain, Journal of Comparative Neurology, accepted
214. Ryohei Kanzaki, Noriyasu Ando, Takeshi Sakurai, Tomoki Kazawa, Understanding and reconstruction of the mobiligence of insects employing multiscale biological approaches and robotics, Advanced Robotics, 22, 1605-1628, 2008
215. Takuro Moriyama and Daisuke Kurabayashi, An Oscillator Network with a Temporary Memory Function, IEEE International Conference on Robotics and Biomimetics (accepted, to be appeared), 2009
216. Daisuke Kurabayashi, Tatsuki Choh, Jia Cheng, Tetsuro Funato, Adaptive Formation Transition among a Mobile Robot Group based on Phase Gradient, IEEE International Conference on Robotics and Biomimetics (accepted, to be appeared), 2009
217. Herianto, Toshiki Sakakibara, Daisuke Kurabayashi, Realization of an Artificial Pheromone System by using Random Data Carriers for Navigation of Autonomous Robots, 5th International Conference on Uniquitous Robots and Ambient Intelligence, 329-334, 2008
218. Ryohei Kanzaki, Insect-Machine Hybrid System for Understanding and Evaluating the Motor Control by Sex Pheromone in Bombyx mori, Janelia Farm Conference, 2008
219. Ryohei Kanzaki, Insect-Machine Hybrid System for Understanding an Adaptive behavior, The 10th International Conference on the Simulation of Adaptive Behavior (SAB'08), 2008
220. Kamiura N, Urata H, Saitoh A, Isokawa T, Ikeno H, Matsui N, Seki Y, Kanzaki R, On-map basaed classification of insect neurons using three-dimensional quantification, SMC 2008, 2008
221. Nakajima K, Asama H, Kanzaki R, Mishima T, Interpolation of the cross-sectional surface of a single neuron using the ellipse model, IAS10, 2008
222. Kurabayashi D, Kanzaki R, Minegishi R, Takashima A, Toriihara S, Bio-machine fusion system: novel synthetic methodology to investigate adaptive behaviors of insects, IROS Workshop, 2008
223. Noriyasu Ando, Shuhei Emoto, Hirokazu Takahashi, Ryohei Kanzaki, Adaptability of pheromone tracking behavior of the silkmoth revealed by the insect-controlled robot, AMAM 2008 conference abstract, 60-61, 2008
224. Ryo Minegishi, Shigeru Toriihara, Daisuke Kurabayashi, Ryohei Kanzaki, Construction of a brain-machine fusion system to evaluate adaptability in an insect, AMAM 2008 conference abstract, 131-132, 2008
225. Ryohei Kanzaki, Insect-Machine Hybrid System for Understanding an Adaptive Control in Biological Systems, AMAM 2008 conference abstract, 24-25, 2008
226. Takeshi Sakurai, Hidefumi Mitsuno, Keiro Uchino, Hideki Sezutsu, Toshiki Tamura, Fumio Yokohari, Takaaki Nishioka, Ryohei Kanzaki, Activation of bombykol receptor neurons by ectopically expressed olfactory receptor triggers pheromone searching behavior in male silkmoths, ISOT2008 conference abstrascts, 189, 2008
227. Ryota Fukushima, Takeshi Sakurai, Keiro Uchino, Hideki Sezutsu, Toshiki Tamura, Ryohei Kanzaki, Anatomical and functional organization of Kenyon cells in the mushroom bodies of male Bombyx mori, ISOT2008 conference abstract, 95, 2008
228. Ikuko Nishikawa, Masayoshi Nakamura, Yoshiki Igarashi, Tomoki Kazawa, Hidetoshi Ikeno, Ryohei Kanzaki, Neural network model of the lateral accessory lobe and ventral protocerebrum of Bombyx mori to generate the flip-flop activity, BMC Neuroscience, 9, Suppl 1, 23, 2008
229. Suehiro Y*, Yasuda A*, Okuyama, Imada H, Kuroyanagi, Y, Kubo T, Takeuchi H.†(2009) †corresponding author. *equal contribution, Mass spectrometric map of neuropeptide expression and analysis of the g-prepro-tachykinin gene expression in the medaka (Oryzias latipes) brain, Gen. Comp. Endocrinol., in press, 2008
230. Nakaoka T, Takeuchi H† and Kubo T. †corresponding author., Laying workers in queenless honeybee (Apis mellifera L.) colonies have a physiologic state similar to that of nurse bees but opposite that of foragers, J. Insect. Physiol., 54, 806-812, 2008
231. Cornette R, Koshikawa S, Miura T, Histology of the hormone-producing glands in the damp-wood termite Hodotermopsis sjostedti (Isoptera, Termopsidae): A focus on soldier differentiation., Insectes Sociaux, 55, 2008
232. Goto H, Cornette R, Koshikawa S, Miura T, Effects of precocenes on the corpora allata and the JH titer in the damp-wood termite Hodotermopsis sjostedti (Isoptera: Termopsidae)., Sociobiology, 52, 345-356, 2008
233. Koshikawa S, Miyazaki S, Cornette R, Matsumoto T, Miura T, Genome size of termites (Insecta, Dictyoptera, Isoptera) and wood roaches (Insecta, Dictyoptera, Cryptocercidae)., Naturwissenschaften, 95, 859-867, 2008
234. Maekawa K, Mizuno S, Koshikawa S, Miura T, Compound eye development during caste differentiation of the termite Reticulitermes speratus (Isoptera: Rhinotermitidae)., Zoological Science, 25, 699-705, 2008
235. Cornette R, Gotoh H, Koshikawa S, Miura T, Juvenile hormone titers and caste differentiation in the damp-wood termite Hodotermopsis sjostedti (Isoptera, Termopsidae)., Journal of Insect Physiology, 54, 922-930, 2008
236. Ishikawa A, Hongo S, Miura T, Morphological and histological examination of polyphenic wing formation in the pea aphid Acyrthosiphon pisum (Hemiptera, Hexapoda)., Zoomorphology, 127, 121-133, 2008
237. Fujita A, Miura T, Matsumoto T, Differences in cellulose digestive systems among castes in two termite lineages., Physiological Entomology, 33, 73-82, 2008
238. Takeuchi H., "Analysis of Social Interactions Using Adult Medaka Fish", Common Themes and New Concepts in Sensory Formation, The 18th CDB Meeting., 2009
239. Takeuchi H., Analysis of Social Interactions Using Adult Medaka Fish, The 54th NIBB Conference, New Frontiers for the Medaka Model, Genome, Bioresources and Biology, 2008
240. Suehiro Y, Okuyama T, Imada H, Shimada A, Nakuru K, Takeda H, Kubo T and Takeuchi H, Modeling and molecular genetic analysis of neural mechanism for the optomotor response of the medaka fish, The 38th annual meeting of the Society for Neuroscience (Washington, DC), 2008
241. Okuyama T, Suehiro Y, Imada H, Shimada A, Naruse K, Takeda H, Kubo T and Takeuchi H., Analysis of the molecular and neural bases that underlie sexual preference in the small Medaka fish, UCSF Neuroscience retreat （Asilomar Conference Grounds）, 2008
242. Okuyama T, Suehiro Y, Imada H, Shimada A, Naruse K, Takeda H, Kubo T and Takeuchi H., Analysis of the molecular and neural bases that underlie sexual preference in the small Medaka fish, NASA Ames Research Center, Seminar（Lynn Rothschild Lab., NASA Ames Research Center ）, 2008
243. Okuyama T, Suehiro Y, Imada H, Shimada A, Naruse K, Takeda H, Kubo T and Takeuchi H., Modulation of Female mating receptiveness depending on visual information, using small fish medaka, Society for Neuroscience 2008 meeting（Washington D. C.）, 2008

244. Miura T, Social evolution by gene duplication: soldier-specific lipocalin proteins and social communication in termites., Evolution 09, 67
245. Miura T, Okumura Y, Nakagawa Y, Ishikawa A, Regulations of polyphenic wing development in the vetch aphid Megoura crassicauda: morphogenesis, tradeoffs and gene expressions., Pea Aphid Genome Annotation Workshop I: Workshop Program, 32
246. Miura T, Ishikawa A, Brisson J, Jaubert S, Rispe C, Tagu D, Walsh T, Gene annotation for the endocrinological factors in the pea aphid Acyrthosiphon pisum., Pea Aphid Genome Annotation Workshop I: Workshop Program, 32
247. Okada Y., Tsuji K. and Miura T., Molecular and physiological aspects of behavioral-caste differentiation in the ponerine ant Diacamma sp., Proceedings of 4th European Meeting of IUSSI, 166
248. Yoshikatsu Hayashi, Mai Yuki, Ken Sugawara, Tomonori Kikuchi and Kazuki Tsuji, Analysis and modeling of ants' behavior from single to multi-body, Journal of Artificial Life and Robotics, 120-123, 2008
249. Kikuchi, T, Miuazaki, S., Ohnishi, S., Takahashi, J., Nakajima, Y., Tsuji, K, Small queens and big headed workers in a monomorphic ponerine ant, Naturwissensaften, 95, 10, 963-968, 2008
250. Suwabe, M., Ohnishi, H., Kikuchi, T., Tsuji, K., Seasonal and daily activity patterns of tramp and endemic ants in the northern forest of Okinawa Island, Ecological Research, doi:10.1007/s11284-008-0534-9, 2008
251. Kikuchi, T., Nakagawa, T., Tsuji, K., Changes in relative importance of multiple social regulatory forces with colony size in the ant Diacamma sp. from Japan, Animal Behaviour, 76, 6, 2069-2077, 2008
252. Dobata, S., Sasaki, T., Mori, H., Hasegawa, E., Shimada, M., Tsuji, K, Cheater genotypes in the parthenogenetic ant Pristomyrmex punctatus, Proceedings of the Royal Society of London, Series B, 276, 2, 567-574, 2009
253. Ohtsuki, H., Tsuji, K., Adaptive reproduction schedule as a cause of worker policing in social Hymenoptera: a dynamic game analysis., The American Naturalist, in press, 2009
254. Mai Yuki, Yoshikatsu Hayashi, Ken Sugawara, Analysis and Modeling of Diacamma workers' Behavior, Proc. of 14th Int. Symp. on Artificial Life and Robotics 2009, 2008
255. Ei-Ichi Izawa, Socio-cognitive ability of crows: an attempt cognitive neuroethology, International seminar 'Evolutionary studies in behavioural neuroscience', -, -, 33, 2008
256. Ei-Ichi Izawa, Chemical neuroanatomy of the crow: do they have large prefrontal cortex?, NeuroscienceResearch, 61, S1, S141, 2008
257. Toshiyuki Kurihara, Motoichiro Kato, Delays in seeking psychiatric care among patients with schizophrenia in Bali, Health Knowledge, Attitudes and Practices, eds by Patricia I. Eddington and Umberto V. Mastolli, Nova Biomedical Books, Nova Science Publishers, New York, 158-172, 2008
258. Tomoko Akiyama, Motoichiro Kato, Taro Muramatsu, Takaki Maeda, Tsunekatsu Hara, Haruo Kashima, Gaze-triggered orienting is reduced in chronic schizophrenia, Psychiatry Research, 158, 287-296, 2008
259. Hidehiko Takahashi, Masato Matsuura, Michihiko Koeda, Noriaki Yahata, Tetsuya Suhara, Motoichiro Kato, Yoshiro Okubo, Brain activations during judgments of positive self-conscious emotion and positive basic emotion: pride and joy, Cerebral Cortex, 18, 4, 898-903, 2008
260. Hidehiko Takahashi, Yota Fujimura, Mika Hayashi, Harumasa Takano, Motoichiro Kato, Hiroshi Ito, Tetsuya Suhara, Enhanced dopamine release by nicotine in cigarette smokers: a double-blind randomized, placebo-controlled pilot study, The International Journal of Neuropsychopharmacology , 11, 413-417, 2008
261. Ryosuke Arakawa, Hiroshi Ito, Akihiro Takano, Hidehiko Takahashi, Takuya Morimoto, Takeshi Sassa, Katsuya Ohta, Motoichiro Kato, Yoshiro Okubo, Tetsuya Suhara, Dose-finding study of paliperidone ER based on striatal and extrastriatal dopamine D2 receptor occupancy in patients with schizophrenia, Psychopharmacology, 197, 229-235, 2008
262. Hidehiko Takahashi, Tomohisa Shibuya, Motoichiro Kato, Masato Matsuura, Michihiko Koeda, Noriaki Yahata, Tetsuya Suhara, Yoshiro Okubo, Enhanced activation in the extrastriate body area by goal-directed actions., Psychiatry and Clinical Neurosciences, 62, 214-219, 2008
263. Hidehiko Takahashi, Motoichiro Kato, Masato Matsuura, Michihiko Koeda, Noriaki Yahata, Tetsuya Suhara, Yoshiro Okubo, Neural correlates of human virtue judgment., Cerebral Cortex, 18, 8, 1886-1891, 2008
264. Mika Hayashi, Motoichiro Kato, Kazue Igarashi, Haruo Kashima, Superior fluid intelligence in children with Asperger's disorder., Brain and Cognition, 66, 306-310, 2008
265. Sho Yagishita, Takamitsu Watanabe, Tomoki Asari, Hiroshi Ito, Motoichiro Kato, Hiroo Ikehira, Iwao Kanno, Tetsuya Suhara, Hideyuki Kikyo, Role of left superior temporal gyrus during name recall process: An event-related fMRI study, Neuroimage, 41, 1142-1153, 2008
266. Nobuyuki Matsuura, Yoshiyuki Shibukawa, Motoichiro Kato, Tatsuya Ichinohe, Takashi Suzuki and Yuzuru Kaneko, Ketamine, not fentanyl, suppresses pain-related magnetic fields associated with trigeminally innervated area following CO2 laser stimulation, Neuroscience Research, 62, 105-111, 2008
267. Hidehiko Takahashi, Motoichiro Kato, Harumasa Takano, Ryosuke Arakawa, Masaki Okumura, Tatsui Otsuka, Kodaka Fumitoshi, Mika Hayashi, Yoshiro Okubo, Hiroshi Ito, Tetsuya Suhara, Differential contributions of prefrontal and hippocampal dopamine D1 and D2 receptors in human cognitive functions, The Journal of Neuroscience, 28, 46, 12032-12038, 2008
268. Michitaka Funayama, Taro Muramatsu, Motoichiro Kato, Differential hand-neglect following a callosal lesion, Cognitive and Behavioral Neurology, 21, 4, 246-248, 2008
269. Akira Uno, Taeko N. Wydell, Motoichiro Kato, Kanae Itoh, Fumihiro Yoshino, Cognitive Neuropsychological and Regional Cerebral Blood Flow Study of a Japanese-English Bilingual Girl with Specific Language Impairment (SLI), Cortex, 45, 154-163, 2009
270. Hidehiko Takahashi, Motoichiro Kato, Sassa Takeshi, Michihiko Koeda, Noriaki Yahata, Tetsuya Suhara, Yoshiro Okubo, Diminished activation in the extrastriate body area during observation of sport-related actions in chronic schizophrenia, Schizophrenia Bulletin (in press)
271. Tatsuhiko Yagiashi, Motoichiro Kato, Kosuke Izumi, Rika Kosaki, Kaori Yago,
272. Kazuo Tsubota, Yuji Sato, Minoru Okubo, Goro Watanabe, Takao Takahashil, Kenjiro Kosaki, Adult Phenotype of Mulvihill-Smith Syndrome, American Journal of Medical Genietics Part A, 2008 (in press)
273. Shoko Nozaki, Motoichiro Kato, Harumasa Takano, Hiroshi Ito, Hidehiko Takahashi, Ryosuke Arakawa, Masaki Okumura, Yota Fujimura, Ryohei Matsumoto, Miho Ota, Fimihiko Yasuno, Akihiro Takano, Akihiko Otsuka, Yoshiro Okubo, Haruo Kashima, and Tetsuya Suhara, Regional Dopamine Synthesis in Patients with Schizophrenia using L-[β-11C]DOPA PET, Schizophrenia Research, 2008 (in press)
274. Hidehiko Takahashi, Motoichiro Kato, Masato Matsuura, Dean Mobbs, Tetsuya Suhara, Yoshiro Okubo, When your gain is my pain and your pain is my gain: Neural correlates of envy and Schadenfreude, Science (in press)
275. K. Harano, K. Sasaki, T. Nagao, M. Sasaki, Influence of age and juvenile hormone on brain dopamine level in male honeybee (Apis mellifera): association with reproductive maturation, Journal of Insect Physiology, 54, 848-853, 2008
276. K. Harano, M. Sasaki, T. Nagao, K. Sasaki, Dopamine influences locomotor activitiy in honeybee queens: implications for a behavioural change after mating, Physiological Entomology, 33, 395-399, 2008
277. K. Sasaki, Biogenic amines and division of reproduction in social insects, Insect Physiology: New Research, (Ed.) R.P. Maes, NOVA Science Publisher, Chapter 7, 2008
278. K. Sasaki, K. Yamasaki, K. Tsuchida, T. Nagao, Gonadotrophic effects of dopamine in isolated workers of the primitively eusocial wasp, Polistes chinensis,

Naturwissenschaften, 96, in press, 2009
279. Ogawa, H., Cummins, G. I., Jacobs, G. A., Oka, K., Dendritic design implements algorism for extraction of sensory information., Journal of Neuroscience, 28, 4592-4603, 2008
280. Aonuma, H., Kitamura, Y., Niwa, K., Ogawa, H., Oka, K., Nitric oxide-cyclic guanosine monophosphate signaling in the local cirtcuit of the cricket abdominal nervous system., Neuroscience, 157, 749-761, 2008
281. T. Nagao, S. Kishigami, K. Sasaki, H. Tamori, Neurohormonal control of development and motivation of instinctive behavior in male crickets, 6th Asian Biophysics Association Symposium and 27th Hong Kong Society of Neuroscience Annual Meeting, Hong Kong, PS2-29, 2008
282. Ogawa, H., Oka, K., In vivo calcium imaging of mushroom body calyx in the tethered cricket for odor-taste conditioning, 2008 Neuroscience Meeting Planner. Washington, DC: Society for Neuroscience, Program No. 362.20, 2008
283. Shindo, Y., Ogawa, H., Hotta, K. Oka, K., Alteration of Mg2+ transport during 1-methyl-4-phenyl-pyridinium ion (MPP+) induced cell death in PC12 cells., 2008 Neuroscience Meeting Planner. Washington, DC: Society for Neuroscience, Program No. 140.16, 2008
284. Watanabe, K., Hase, S., Shimoi, T., Ogawa, H., Hotta, K. Oka, K., Expression of cyclic AMP responsive element binding protein 1 (CREB1) in long-term memory formation in the earthworm Eisenia fetida., 2008 Neuroscience Meeting Planner. Washington, DC: Society for Neuroscience, Program No. 793.10, 2008
285. Ogawa, H., Oka, K., Directional-dependent plasticity in wind sensitivity of the cricket giant interneurons, Neuroscience Research, 60, S1, S183, 2008
286. Mizue Ohashi, Ryuichi Okada, Toshifumi Kimura, Hidetoshi Ikeno, Observation system for the control of the hive environment by the honeybee (Apis mellifera), Behav Res Methods, in press, 2009
287. Kanako Aono, Ayachika Fusada, Yorichika Fusada, Wataru Ishii, Yuji Kanaya, Mami Komuro, Kanae Matsui, Satoru Meguro, Ayumi Miyamae, Yurie Miyamae, Aya Murata, Shizuka Narita, Hiroe Nozaka, Wakana Saito, Ayumi Watanabe, Kaori Nishikata, Akira Kanazawa, Yutaka Fujito, Miki Yamagishi, Takashi Abe, Masafumi Nagayama, Tsutomu Uchida, Kazutoshi Gohara, Ken Lukowiak, Etsuro Ito, Upside-down gliding of Lymnaea, Biol. Bull, 215, 272-279, 2008
288. Mizue Ohashi, Hidetoshi Ikeno, Toshifumi Kimura, Tadaaki Akamatsu, Ryuichi Okada, Etsuro Ito, Control of hive environment by honeybee (Apis mellifera) in Japan., Proceedings of Measuring Behavior 2008, 243, 2008
289. Toshifumi Kimura, Hidetoshi Ikeno, Ryuichi Okada, Etsuro Ito, A Study for identification and behavioral tracking of honeybees in the observation hive using vector quantization method., Proceedings of Measuring Behavior 2008, 165-166, 2008
290. Ryuichi Okada, Foraging strategy of the honeybee colony by waggle dance., International Seminar on Current Issues in Social Insect Research -In Case of Honeybee and Ants-, 2008
291. Fujii N, Hihara S, Iriki S., Social cognition in premotor and parietal cortex., Soc Neurosci., 3, 3-4, 250-60, 2008
292. Fujii N, Hihara S, Nagasaka Y, Iriki A., Social state representation in prefrontal cortex., Soc Neurosci., 4, 1, 73-84, 2009
293. Y. NAGASAKA, T. NOTOYA, A. IRIKI, N. FUJII, Amygdala, anterior cingulate, and orbital frontal cortices activity in Japanese macaques while watching emotional expressions with social context, Program No.883.2. 2008 Neuroscience Meeting Planner. Washington, DC: Society for Neuroscience, 2008. Online, 2008
294. G. S. SANTOS, Y. NAGASAKA, K. TAKENAKA, A. IRIKI, N. FUJII, H. NAKAHARA, Social modulation of the prefrontal cortex, parietal cortex, and caudate activity for reward-oriented behavior, Program No.93.11. 2008 Neuroscience Meeting Planner. Washington, DC: Society for Neuroscience, 2008. Online, 2008
295. Masafumi Yano, Hospitality Technology : The Place of Culture Technology, (quarterly issue) iichiko, 101, 37-46, 2009
296. Kaoru Takakusaki, Nozomi Tomita, Masafumi Yano, Substrates for nomal gait and patholhysiology of gait disturbances with respect to the basal ganglia dysfunction, Journal or Neurology, 255, Suppl 4, 19-29, 2008
297. Sakamoto K, Mushiake H, Saito N, Aihara K, Yano M, Tanji J., Discharge synchrony during the transition of behavioral-goal representations encoded by discharge rates of prefrontal neurons., journal Cerebral Cortex, 18, 2036-2045, 2008
298. Hisanori Makinae, Yoshinari Makino, Tsukasa Obara, Masahumi Yano, Specific spatio-temporal activities in the cerebral ganglion of Incilaria fruhstorferi in response to superior and inferior tentacle nerve stimulation, Brain Research, 1231, 47-62, 2008
299. Kaoru Takakusaki, Nozomi Tomita, Masafumi Yano, Substrates for execution for normal gait performance with respect to the basal ganglia function, Proc. Of IEEE/RSJ 2008 International Conference on Intelligent Robots and Systems, September, 22-26, 2008
300. Yoshinari Makino, Makoto Yasuike, Yuki Naka, Haruki Miura & Masafumi Yano, A computational algorithm for odor representation using a spatiotemporal sequence, Neuroscience 2008, 2008
301. Y. Yoshihara, N. Tomita, Y. Makino, M. Yano, Autonomous Control for Voluntary Movement in the Real World －Online Load Estimation and Compensation using Two Parallel Redundant Actuators－, Tohoku University Global Brain Science 2008 Summer Retreat, 2008
302. Makino Y, Yasuike M, Naka Y, Miura H, Yano M, Principal characteristics in odor recognition naturally emerge from spatiotemporal coding., NEUROSCIENCE RESEARCH 61, S249, 2008
303. S.Sakai, M.Iida, K.Osuka, M.Umeda, Design and control of a heavy material handling manipulator for agricultural robots, Auton Robot, DOI 10.1007/s10514-008-9090-y, 2008
304. K.Ohgane, K.Ueda, Instability-induced hierarchy in bipedal locomotion, Phys. Rev., E, 77, 51915, 2008
305. K.Ohgane, S.Ei, H.Mahara, Neuron phase shift adaptive to time delay in locomotor control, Applied Mathematical Modelling, 33, pp.797-811, 2009
306. Akio Ishiguro, *Masahiro Shimizu, On the Task Distribution between Control and Mechanical Systems: A Case Study with an Amobeboid Modular Robot, 50 Years of Artificial Intelligence: Essays Dedicated to the 50th Anniversary of Artificial Intelligence（Eds. M. Lungarella, F. Iida, J. Bongard, and R. Pfeifer）, Springer, 144-153
307. Masahiro Shimizu, Takuma Kato, Max Lungarella, *Akio Ishiguro, Adaptive Modular Robots Through Heterogeneous Inter-Module Connections, Journal of Robotics and Mechatronics, 20, 3, 386-393
308. Takuya Umedachi, Taichi Kitamura, *Akio Ishiguro, An Amoeboid Locomotion That Exploits Real-Time Tunable Springs and Law of Conservation of Protoplasmic Mass, Journal of Robotics and Mechatronics, 20, 3, 449-455
309. Wataru Watanabe, Toshihiro Kawakatsu, *Akio Ishiguro, Rapid and Cheap Learning by Exploiting Biarticular Muscles - A Case Study With a Two-Dimensional Serpentine Robot, Advanced Robotics Special Issue on Mobiligence (1), 22, 15, 1683-1696
310. Masaki Nomura, Daisuke Ito, Hiroki Tamate, *Kazutoshi Gohara, Estimation of functional connectivity that causes burst-like population activities, FORMA
311. J. Nishikawa and *K. Gohara, Automata on Fractal Sets Observed in Hybrid Dynamical Systems, International Journal of Bifurcation and Chaos, 18, 12
312. J. Nishikawa and *K. Gohara, Anomaly of fractal dimensions observed in stochastically switched systems, Physical Review E, 77, 036210-1-8
313. Masahiro Shimizu, Takuma Kato, Max Lungarella, *Akio Ishiguro, Adaptive Reconfiguration of a Modular Robot through Heterogeneous Inter-Module Connections, 2008 IEEE International Conference on Robotics and Automation proceedings, 3527-3532

314. Dai Owaki, Koichi Osuka, *Akio Ishiguro, On the Embodiment That Enables Passive Dynamic Bipedal Running, 2008 IEEE International Conference on Robotics and Automation proceedings, 341-346
315. Takuya Umedachi, Taichi Kitamura, *Akio Ishiguro, A Fully Decentralized Control of an Amoeboid Robot by Exploiting the Law of Conservation of Protoplasmic Mass, 2008 IEEE International Conference on Robotics and Automation proceedings, 1144-1149
316. Wataru Watanabe, Takahide Sato, *Akio Ishiguro, An Efficient Decentralized Learning by Exploiting Biarticular Muscles, 2008 IEEE International Conference on Robotics and Automation proceedings, 3826-3831
317. *Akio Ishiguro, Masatoshi Koyama, Dai Owaki, Jun Nishii, Increasing Stability of Passive Dynamic Bipedal Walking by Exploiting Hyperextension of Knee Joints, the fourth meeting of Adaptive Motion of Animals and Machines (AMAM 2008) proceedings, 164
318. Dai Owaki, Koichi Osuka, *Akio Ishiguro, Adaptive Gait Transition between Passive Dynamic Walking and Running, the fourth meeting of Adaptive Motion of Animals and Machines (AMAM 2008) proceedings, 160-161
319. *Akio Ishiguro, Understanding Mobiligence Through Amoeboid Locomotion –– A Case Study with a Modular Robot –-, the fourth meeting of Adaptive Motion of Animals and Machines (AMAM 2008) proceedings, 20-21
320. Dai Owaki, Koichi Osuka, *Akio Ishiguro, Gait Transition between Passive Dynamic Walking and Running by Changing the Body Elasticity, SICE Annual Conference 2008, 2513-2518
321. *Akio Ishiguro, Takuya Umedachi, Taichi Kitamura, Toshiyuki Nakagaki, Ryo Kobayashi, A Fully Decentralized Morphology Control of an Amoeboid Robot by Exploiting the Law of Conservation of Protoplasmic Mass, IEEE/RSJ 2008 International Conference on Intelligent Robots and Systems
322. Wataru Watanabe, Takuya Umedachi and Dai Owaki, Investigation of the Design Principles for Adaptive Intelligence, Proc. of The 1st Student Organizing International Mini-Conference on Information Electronics Systems, 221 F5P-35
323. D. Ito, H. Tamate, M. Nomura, T. Aoyagi, and *K. Gohara, Immunocytochemstry in low-density culture of neurons on multielectrode arrayes is effective for identification of action-potential pathway, Proceedings of neuroscience 2008, 104948
324. D. Ito, H. Tamate, M. Nagayama, T. Uchida, and *K. Gohara, Multi-agent Robot Systems as Distributed Autonomous Systems, Proceedings of MEA Meeting 2008, 53-54
325. H. Tamate, D. Ito, M. Nagayama, T. Uchida, and *K. Gohara, Analysis of neural-network dynamics using multi-electrode array, Sup. Neuroscience Research, 25, S86
326. M. Nomura, D. Ito, H. Tamate, *K. Gohara, and T. Aoyagi, Estimation of neurronal functional connectivity of cultured neuronal networks, Sup. Neuroscience Research, 25, S90
327. Ono, N., Madina, D. and Ikegami, Origin of Life and Lattice Artificial Chemistry, Bridging Nonliving and Living Matter, edby S.Rasumussen, L.Chen, N.Packard, M.Bedau, D.Deamer, P.Stadler and D.Krakauer, MIT Press, 197-212, 2008
328. Ogai, Y., Ikegami, T, Microslip as a Simulated Artificial Mind, Adaptive Behavior, 16, 2-3, 129-147, 2008
329. Hiroshi C. Ito, Masakazu Shimada and Takashi Ikegami, Coevolutionary dynamics of adaptive radiation for food-webdevelopment, Population Ecology, 51, 65-81, 2009
330. Hisanao Takahashi, Naoto Horibe, Masakazu Shimada, and Takashi Ikegami, Analyzing the House Fly's Exploratory Behavior with Autoregression Methods, J. Phys. Soc. Japan., 77, 84802, 2008
331. Aucouturier, J.-J. and Ogai, Y. and Ikegami, Using chaos to trade-off synchronization and autonomy in a dancing robot, Trends and Controversies, IEEE Intelligent Systems, 23, 3, 74-85, 2008
332. Ishii Y. and Shimada M., Competitive exclusion between contest and scramble strategists in Callosobruchus seed beetle modeling., Population Ecology, 50, 197-205, 2008
333. Ikegami, T and Suzuki, K, From Homeostatic to Homeodynamic Self, BioSystems, 91, 388-400, 2008
334. Suzuki, K and Ikegami, T., Shape and Self-movements in Protocell Systems, Atrtificial Life, in press, 2008
335. Ishii Y. and Shimada M., Predator's learning and search image promoting persistence of the insect prey-predator experiment system., Population Ecology, in review
336. Ikegami, T, Artificial Life is Dead, International 10th Cncference on Artificial Life (Keynote), 2008
337. Ikegami, T, Organizer, Agency WorkshopSatelite workshop at SAB, 2008
338. Ikegami, T, Self-moving droplets as emergence of a life system, Japan-Slovenia Seminar on Nonlinear Science, 2008
339. Nakajima, K and Ikegami, T, Considering the reconfiguration process of subjective temporal order by using recurrent neural networks, International 10th Cncference on Artificial Life (Keynote), 2008
340. Shimada M., Rapid adaptation: the new dimension of evolutionary ecology.(Opening Address), 24th Society of Population Ecology, 2008
341. Iizuka, H and Ikegami, T, Simulating active touch with a simple embodied agent, International 10th Cncference on Artificial Life (Keynote), 2008
342. Suzuki, K. and Ikegami, T, Homeodynamics in the game of life, International 10th Cncference on Artificial Life (Keynote), 2008
343. Hanczyc, M. and Ikegami, T, Chemical basis for minimal cognition, International 10th Cncference on Artificial Life (Keynote), 2008
344. M. Iima, A paradox of hovering insect in two-dimensional space, Journal of Fluid Mechanics, 617, 207-229, 2008
345. M. Iima and A. S. Mikhailov, Propulsion hydrodynamics of a butterfly micro-swimmer, Europhysics Letters, accepted, 2009
346. M. Iima and Y. Nishiura, Unstable periodic solution controlling collision of localized convection cells in binary fluid mixture, Physica D, 238, 449-460, 2009
347. Ishii, M., N. Hirai and T. Hirowatari, The occurrence of an endangered lycaenid, Zizina emelina (de l'Orza), in the Osaka International Airport, central Japan. Trans. lepid. Soc. Japan, Trans. lepid. Soc. Japan, 59, 78-82, 2008
348. M. Yago, N. Hirai, M. Kondo, T. Tanikawa, M. Ishii, M. Wang, M. Williams, R. Ueshima., Molecular systematics and biogeography of the genus Zizina (Lepidoptera: Lycaenidae)., Zootaxa, 1746, 15-38, 2008
349. K. Senda, M. Sawamoto, M. Kitamura, T. Obara, Towards Realization of Stable Flapping-of-Wings Flight of Butterfly, International Symposium on Adaptive Motion in Animals and Machines, 62-63, 2008
350. K. Senda, M. Sawamoto, M. Kitamura, T. Obara, Effects of Flexibly Torsional Wings in Flapping-of-Wings Flight of Butterfly, World Automation Congress, 1?6, 2008
351. M. Iima, Robustness of an insect's hovering: a transition of flapping free-flight, ICTAM 2008, 2008
352. T. Aoki and T. Aoyagi, Co-evolution of phases and connection strengths in a network of phase oscillators, Physical Review Letters, in press
353. T. Tanaka, T. Aoyagi, Optimal weighted networks of phase oscillators for synchronization, Physical Review E, 78, 4, 046210-1～10, 2008
354. T. Tanaka, T. Kaneko, T. Aoyagi, Recurrent infomax generates cell assemblies, neuronal avalanches, and simple cell-like selectivity, Neural Computation, in press
355. T. Tanaka, T. Aoyagi, Weighted scale-free networks with variable power-law exponents, Physica D, 237, 7, 898-907, 2008
356. T. Aoki, K. Ota, K. Kurata, T. Aoyagi, Ordering Process of Self-Organizing Maps Improved by Asymmetric Neighborhood Function, Cognitive Neurodynamics, in press
357. X. Pan, K. Sawa, I. Tsuda, M. Tsukada and M. Sakagami, Reward prediction based on stimulus categorization in primate lateral prefrontal cortex., Nature (Neuroscience), 11, 703-712, 2008

358. I. Tsuda, Number Created by the Interaction Between Consciousness and Memory: A Mathematical Basis for Preafference, Integrative Psychological and Behavioral Science, 42, 153-156, 2008
359. I. Tsuda, Y. Yamaguti, S. Kuroda, Y. Fukushima and M. Tsukada, A Mathematical Model for the Hippocampus: Towards the Understanding of Episodic Memory and Imagination, Prog. Theor. Phys. Suppl., 173, 99-108, 2008
360. I. Tsuda, Hypotheses on the functional roles of chaotic transitory dynamics, Chaos, A Focus Issue on Chaos in immune and cognitive systems (ed. T. Arecchi) (accepted, Dec. 23, 2008), in press
361. K. Matsumoto, H. Diebner, I. Tsuda and Y. Hosoi, Application of chaos theory to engine systems, Proc. of Small Engine Technology Conference, Society of Automotive Engineers, 32-0010-0016, 2008
362. A. Ishiguro and M. Koyama and D. Owaki and J. Nishii, Increasing stability of passive dynamic bipedal walking by exploiting hyperextension of knee joints, Proc of 4th International Symposium on Adaptive Motion in Animals and Machines, 164-165, 2008
363. A. Fujii and H. Suenaga and Y. Hashizume and J. Nishii, Variability of leg swing trajectories and their optimality, Proc of 4th International Symposium on Adaptive Motion in Animals and Machines, 173-174, 2008
364. Y. Taniai and J. Nishii, Optimality of reaching movements based on energetic cost under the influence of signal-dependent noise, Neural Information Processing, Lecture Notes in Computer Science, 4984, 1091-1099, 2008
365. J. Nishii and Y. Taniai, Evaluation of trajectory planning models for arm reaching movements based on energy cost, Neural Computation, in press, 2009
366. A. Takamatsu, E. Takaba, G. Takizawa, Environment-dependent morphology in plasmodium of true slime mold Physarum polycephalum and a network growth model, Journal of Theoretical Biology, 256, 29-44, 2009
367. A. Takamatus, Evironment-dependent morphology in plasmodium of true slime mold Physarum polycephalum, Gordon research conference on theoretical biology & biomathematics 2008, 2008
368. M. Ito, A. Takamatsu, K. Yokotani, Analysis on transportation network in plasmodium of true slime mold, 6th Asian Biophysics Association Symposium, 114-115, 2009
369. Masahiro Sekimoto, Suguru Arimoto, Sadao Kawamura, Ji-Hun Bae, Skilled-Motion Plannings of Multi-Body Systems Based upon Riemannian Distance, Proc. of the 2008 IEEE International Conference on Robotics & Automation, Pasadena, CA, USA, May 19-23, 2008, 1233-1238, 2008
370. Mitsunori Uemura, Guangqiang Lu, Sadao Kawamura, Shugen Ma, Passive Periodic Motions of Multi-Joint Robots by Stiffness Adaptation and DFC for Energy Saving, Proc. of SICE Annual Conference 2008, The University Electro-Communications, Japan, August 20-22, 2008, 2853-2858, 2008

Awards

1. Hitoshi Aonuma, Zoological Science Award 2008, The Zoological Society of Japan「Tsuji E., Aonuma H., Yokohari F. and Nishikawa M. (2007) Serotonin-immunoreactive neurons in the antennal sensory system of the brain in the carpenter ant, Camponotus japonicus. Zool. Sci., 24: 836-849.」
2. Dai Owaki, Koichi Osuka and Akio Ishiguro： ICRA2008, IEEE Robotics and Automation Society Japan Chapter Young Award, “On the Embodiment That Enables Passive Dynamic Bipedal Running”, May 19-23, 2008, 2008 IEEE International Conference on Robotics and Automation proceedings, pp 341-346, 2008
3. Dai Owaki , Koichi Osuka , Akio Ishiguro: SICE Annual Conference Young Author's Award of the SICE2008, “Gait Transition between Passive Dynamic Walking and Running by Changing the Body Elasticity”, August 20-22, 2008, SICE Annual Conference 2008, pp 2513-2518, 2008
4. Dai Owaki , Koichi Osuka , Akio Ishiguro： Finalist in the SICE Annual Conference International Award, “Gait Transition between Passive Dynamic Walking and Running by Changing the Body Elasticity”, August 20-22, 2008, SICE Annual Conference 2008, pp 2513-2518, 2008
5. Toshiyuki Nakagaki, Hiroyasu Yamada, Ryo Kobayashi, Atsushi Tero, Akio Ishiguro, Ágotá Tóth： 2008 Ig Nobel Prize （Cognitive Science Prize）, For discovering that slime molds can solve puzzles, October 2, 2008
6. Masahiro Sekimoto, Suguru Arimoto, Sadao Kawamura, and Ji-Hun Bae: 2008 IEEE International Conference on Robotics and Automation (ICRA2008), Best Manipulation Paper Award Finalist, “Skilled-Motion Plannings of Multi-Body Systems Based upon Riemannian Distance,”Proc. of the ICRA2008, pp.1233-1238, Pasadena, CA, USA, May 19-23, 2008.

Patent

1. S. Kakei, J. Lee, Y. Kagamihara, international patent, applied, 2008.8.26, PCT/JP2008/053735

Activity Records

See the project homepage (http://www.robot.t.u-tokyo.ac.jp/mobiligence/act/index.html) for detailed information (in Japanese).

1	Time and Date:	2008/3/17 9:00-19:00
	Place:	National Institute for Physiological Science, JAPAN
	Subject:	5th research discussion and experiment
2	Time and Date:	2008/4/7 9:00-19:00
	Place:	National Institute for Physiological Science, JAPAN
	Subject:	6th research discussion and experiment
3	Time and Date:	2008/4/14-16
	Place:	Fukushima Medical University
	Subject:	Cooperative experiment to measure volume of discharge of GABA at PPN
4	Time and Date:	2008/4/15-16 10:00-17:00
	Place:	The University of Tokyo
	Subject:	D-group meeting
5	Time and Date:	2008/4/15-16 10:00-17:00
	Place:	Kanazawa University
	Subject:	Mobiligence seminar on butterflies
6	Time and Date:	2008/4/18-19
	Place:	School of Human Science and Environment, University of Hyogo
	Subject:	International Seminar on Social Insects
7	Time and Date:	2008/4/19 13:00-4/20 12:00
	Place:	Yamaguchi University
	Subject:	Seminar on CPG
8	Time and Date:	2008/4/25
	Place:	Auditorium, 11th bld., F.o.E., The University of Tokyo
	Subject:	Workshop on Mobiligence, "New Development of Mobiligence"
9	Time and Date:	2008/4/25 12:00-22:00
	Place:	School of Human Science and Environment, University of Hyogo
	Subject:	Research discussion
10	Time and Date:	2008/4/26 9:00-19:00
	Place:	School of Human Science and Environment, University of Hyogo
	Subject:	Cooperative preliminary experiment for measurement of CO2 density in nest box of hunnybees.
11	Time and Date:	2008/4/28 10:00-17:00
	Place:	The University of Tokyo
	Subject:	Workshop on Mobiligence
12	Time and Date:	2008/4/28 12:00-18:00
	Place:	Yamaoka Lab., Kyoto Institute of Technology
	Subject:	Research meeting on Crickets
13	Time and Date:	2008/5/12-15 9:00-17:00
	Place:	Asahikawa Medical College
	Subject:	Research discussion on how to record brainstem region in monkey walking
14	Time and Date:	2008/5/20-21 9:00-17:00
	Place:	Asahikawa Medical College
	Subject:	Research discussion on how to record brainstem region in monkey walking
15	Time and Date:	2008/6/3 8:30-19:30
	Place:	Case Western Reserve University, Creveland, Ohio, USA

	Subject:	OS "Mobiligence" at 4th International Symposium on Adaptive Motion of Animals and Machines
16	Time and Date:	2008/6/5 10:00-16:00
	Place:	Big Hat, Nagano, Japan
	Subject:	Mobiligence tutorial session: "From Cognition to Emergence of Locomotion and Behavior" in ROBOMEC2008
17	Time and Date:	2008/6/9 13:00-20:00
	Place:	Human Information System Laboratories, Kanazawa Institute of Technology
	Subject:	Research meeting on Crickets
18	Time and Date:	2008/6/13 12:00-13:00
	Place:	Lobby of Kyoto Station Hotel
	Subject:	7th Research disucussion
19	Time and Date:	2008/6/16 18:00-20:00
	Place:	Video discussion
	Subject:	Seminar
20	Time and Date:	2008/6/18-19 10:00-17:00
	Place:	Osaka Prefecture University, Kyoto University
	Subject:	Mobiligence Seminar on Butterflies and Photographing experiment
21	Time and Date:	2008/6/23 18:00-20:00
	Place:	Video discussion
	Subject:	Seminar
22	Time and Date:	2008/6/28 9:30～17:00
	Place:	Die Eidgenossische Technische Hochschule Zurich
	Subject:	International Workshop on "Control of locomotion: from animals to robotos"
23	Time and Date:	2008/6/30-7/5 13:00-19:00
	Place:	School of Human Science and Environment, University of Hyogo
	Subject:	Cooperative experiments on dancing behavior of hunnybees
24	Time and Date:	2008/7/4 18:00-20:00
	Place:	Video discussion
	Subject:	Seminar
25	Time and Date:	2008/7/11-12
	Place:	Kansai Seminar House, Kyoto
	Subject:	International Workshop on "Agency"
26	Time and Date:	2008/7/15 18:00-20:00
	Place:	Video discussion
	Subject:	Seminar
27	Time and Date:	2008/7/22-23 13:00-18:00
	Place:	Research Institute of Electronic Science, Hokkaido University
	Subject:	Collaborative group meeting
28	Time and Date:	2008/7/25 18:00-20:00
	Place:	Video discussion
	Subject:	Seminar
29	Time and Date:	2008/8/6-7 9:00-19:00
	Place:	School of Human Science and Environment, University of Hyogo
	Subject:	Cooperative experiment on hunnybee's behavior
30	Time and Date:	2008/8/6 16:00-17:30
	Place:	Seminar room, RACE, The University of Tokyo
	Subject:	Research meeting on Mobiligence
31	Time and Date:	2008/8/12 13:00-18:00
	Place:	Osaka University
	Subject:	Research discussion on how to record brainstem region in monkey walking
32	Time and Date:	2008/8/18 17:00-19:00
	Place:	University of Hyogo/Tokushima Bunri University (Video discussion)
	Subject:	Seimar and research discussion

33	Time and Date:	2008/8/21 13:15-15:15
	Place:	The University of Electro-Communication
	Subject:	SICE Annual Conference Organized Session OS "Biomimetic Approach on Robot Design and Control for Dynamic Locomotion"
34	Time and Date:	2008/8/22 10:00～16:00
	Place:	Body Motion Science Laboratory, The University of Tokyo
	Subject:	B-group meeting
35	Time and Date:	2008/8/24-26 12:00-17:00
	Place:	Asahikawa Medical College
	Subject:	1st research discussion on biped walking model
36	Time and Date:	2008/8/28 13:00-16:00
	Place:	Ishiguro laboratory, Tohoku University
	Subject:	Research discussion on self-assembly system
37	Time and Date:	2008/9/13 10:00-12:00
	Place:	University of Hyogo/Tokushima Bunri University (Video discussion)
	Subject:	Seimar and research discussion
38	Time and Date:	2008/9/10 12:30-14:30
	Place:	Faculty of Engineering, Kobe University
	Subject:	The 26th Annual Conference on Japan Robotics Society (RSJ2008), Session "Mobiligence"
39	Time and Date:	2008/9/15 14:30-2008/9/7 13:00
	Place:	Design gallery, Asahikawa KURAIMU
	Subject:	Research meeting on neurobiology on invertebrate
40	Time and Date:	2008/9/17
	Place:	Osaka University
	Subject:	B03 group meeting
41	Time and Date:	2008/9/20 13:00-15:00
	Place:	University of Hyogo/Tokushima Bunri University (Video discussion)
	Subject:	Seimar and research discussion
42	Time and Date:	2008/9/22 14:00～17:00
	Place:	National Rehabilitation Center for Persons with Disabilities
	Subject:	Seminar on Bipedal Walking Control
43	Time and Date:	2008/9/25-10/7 9:00-19:00
	Place:	School of Human Science and Environment, University of Hyogo
	Subject:	Cooperative experiment on hunnybee's behavior in the nest
44	Time and Date:	2008/9/25 11:00-14:00
	Place:	Ishiguro laboratory, Tohoku University
	Subject:	Research discussion on self-assembly system
45	Time and Date:	2008/9/25 19:30-21:00
	Place:	University of Hyogo/Tokushima Bunri University (Video discussion)
	Subject:	Seimar and research discussion
46	Time and Date:	2008/9/26 9:00-18:00
	Place:	Acropolis Convention Center, Nice, France
	Subject:	IROS2008 Full Day Workshop
47	Time and Date:	2008/10/1-2
	Place:	The University of Tokyo, Komaba Campus
	Subject:	Workshop on "Artificial Life: Half way through"
48	Time and Date:	2008/10/9-10 10:00-16:00, 10:00-14:00
	Place:	Asahikawa Medical College
	Subject:	2nd research discussion on biped walking model
49	Time and Date:	2008/10/10 13:30～18:00
	Place:	Wind-tunnel laboratory, Kyoto University

	Subject:	Bibliographic survey and discussion
50	Time and Date:	2008/10/14-16 9:00-19:00
	Place:	Fukushima Medical University
	Subject:	Cooperative experiment to measure volume of discharge of GABA at PPN
51	Time and Date:	2008/10/14 18:30-20:00
	Place:	University of Hyogo/Tokushima Bunri University (Video discussion)
	Subject:	Seimar and research discussion
52	Time and Date:	2008/10/15 9:30-12:00
	Place:	Kyoto Institute of Technology
	Subject:	Research discussion on collaborative research
53	Time and Date:	2008/10/17 13:30～18:00
	Place:	Kyotanabe Campus, Doshisha University
	Subject:	Research discussion
54	Time and Date:	2008/10/21 10:00-17:40
	Place:	RACE, The University of Tokyo
	Subject:	2nd Open Symposium on Mobiligence
55	Time and Date:	2008/10/22 9:30-16:00
	Place:	The University of Tokyo
	Subject:	D-group meeting
56	Time and Date:	2008/10/23 18:00-20:00
	Place:	University of Hyogo/Tokushima Bunri University (Video discussion)
	Subject:	Seimar and research discussion
57	Time and Date:	2008/10/24 13:00-17:00
	Place:	Tohoku University
	Subject:	Seminar on Passive Dynamic Walk
58	Time and Date:	2008/10/24 13:30～18:00
	Place:	Kyotanabe Campus, Doshisha University
	Subject:	Research discussion
59	Time and Date:	2008/10/30 13:30～18:00
	Place:	Kyotanabe Campus, Doshisha University
	Subject:	Research discussion
60	Time and Date:	2008/10/31 18:30-20:00
	Place:	University of Hyogo/Tokushima Bunri University (Video discussion)
	Subject:	Seimar and research discussion
61	Time and Date:	2008/11/6 13:00～18:00, 11/7 10:00～15:30
	Place:	National Institute of Informatics
	Subject:	2nd A-group meeting
62	Time and Date:	2008/11/8 15:00-17:00
	Place:	University of Hyogo/Tokushima Bunri University (Video discussion)
	Subject:	Seimar and research discussion
63	Time and Date:	2008/11/7 13:30～18:00
	Place:	Kyotanabe Campus, Doshisha University
	Subject:	Bibliographic survey and discussion
64	Time and Date:	2008/11/14-15 10:00-17:00
	Place:	Kyushu University
	Subject:	Mobiligence seminar on butterflies and Symposium of The Lapidopterological Society of Japan
65	Time and Date:	2008/11/14 13:30～18:00
	Place:	Kyotanabe Campus, Doshisha University
	Subject:	Bibliographic survey and discussion
66	Time and Date:	2008/11/14 17:00-19:00

	Place:	University of Hyogo/Tokushima Bunri University (Video discussion)
	Subject:	Seimar and research discussion
67	Time and Date:	2008/11/15 18:00-19:00
	Place:	Washington, D.C.
	Subject:	8th research discussion
68	Time and Date:	2008/11/17 15:15-16:45
	Place:	Tsukuba International Congress Center, Tsukuba, Ibaraki, Japan
	Subject:	OS "Mobiligence" at The 9th International Symposium on Distributed Autonomous Robotic Systems (DARS2008)
69	Time and Date:	2008/11/20 11:15-13:00
	Place:	Ishiguro laboratory, Tohoku University
	Subject:	Research discussion on self-assembly system
70	Time and Date:	2008/11/21 13:30～18:00
	Place:	Wind-tunnel laboratory, Kyoto University
	Subject:	Bibliographic survey and discussion
71	Time and Date:	2008/11/21 13:30-18:00
	Place:	Ishiguro laboratory, Tohoku University
	Subject:	Research discussion: scaling effect on adaptability of deformed body of slime mold
72	Time and Date:	2008/11/21 19:00-21:00
	Place:	University of Hyogo/Tokushima Bunri University (Video discussion)
	Subject:	Seimar and research discussion
73	Time and Date:	2008/11/26 15:15-17:20
	Place:	Himeji International Exchange Center
	Subject:	OS "Mobiligence" at SICE System & Information Division: Annual Conference
74	Time and Date:	2008/11/27 15:00-17:00
	Place:	Ishiguro laboratory, Tohoku University
	Subject:	Research discussion on self-assembly system
75	Time and Date:	2008/11/28 13:30～18:00
	Place:	Kyotanabe Campus, Doshisha University
	Subject:	Research discussion
76	Time and Date:	2008/12/1 18:00-20:00
	Place:	University of Hyogo/Tokushima Bunri University (Video discussion)
	Subject:	Seimar and research discussion
77	Time and Date:	2008/12/4 11:00-13:00
	Place:	Ishiguro laboratory, Tohoku University
	Subject:	Research discussion on self-assembly system
78	Time and Date:	2008/12/5 10:00-12:00
	Place:	Nagaragawa Convention Center
	Subject:	SICE SI2008, Organized session "Emergence of Adaptive Locomotive Function from Interaction of Body, Brain and Environment"
79	Time and Date:	2008/12/5 13:30～18:00
	Place:	Kyotanabe Campus, Doshisha University
	Subject:	Bibliographic survey and discussion
80	Time and Date:	2008/12/11 14:30-16:00
	Place:	Hongo, Tokyo
	Subject:	9th research discussion
81	Time and Date:	2008/12/15-16
	Place:	The University of Tokyo
	Subject:	Workshop on Informatics of Dynamical Systems
82	Time and Date:	2008/12/16-17 10:00-17:00
	Place:	Osaka Prefecture University

	Subject:	Mobiligence seminar on butterflies
83	Time and Date:	2008/12/18 10:00-17:00
	Place:	Tohoku University
	Subject:	Research discussion
84	Time and Date:	2008/12/18 13:00-20:00
	Place:	Laboratory of Physiological Chemistry, The University of Tokyo
	Subject:	Research survey and discussion on measurement of swarm behavior
85	Time and Date:	2008/12/18 14:00-12/19 12:00
	Place:	Research Institute of Electrical Communication, Tohoku University
	Subject:	Research meeting on RIEC Collaborative Project Research "Understanding and Engineering Application of Environmentally Harmonic Adaptive Systems in Living Things"
86	Time and Date:	2008/12/19 13:30-17:50
	Place:	Research Institute of Electrical Communication, Tohoku University
	Subject:	Debate session on locomotive control of animals
87	Time and Date:	2008/12/25-26 9:00-19:00
	Place:	Kagawa School of Phermaceutical Sciences, Tokushima Bunri University
	Subject:	Research discussion
88	Time and Date:	2008/12/25 13:00-15:00
	Place:	Ishiguro laboratory, Tohoku University
	Subject:	Research discussion on self-assembly system
89	Time and Date:	2008/12/26 13:00-18:00
	Place:	Takamatsu laboratory, Waseda University
	Subject:	Research discussion: scaling effect on adaptability of deformed body of slime mold
90	Time and Date:	2009/1/5 13:00-19:00
	Place:	Human Information System Laboratories, Kanazawa Institute of Technology
	Subject:	Research discussion on collaborative research
91	Time and Date:	2009/1/5 13:00-19:00
	Place:	Human Information System Laboratories, Kanazawa Institute of Technology
	Subject:	Research discussion on collaborative research
92	Time and Date:	2009/1/5 13:30-1/6 11:00
	Place:	Awaji Yumebutai, Convention Hall
	Subject:	Symposium on Walking
93	Time and Date:	2009/1/8 18:30-20:00
	Place:	University of Hyogo/Tokushima Bunri University (Video discussion)
	Subject:	Seimar and research discussion
94	Time and Date:	2009/1/9 13:30～18:00
	Place:	Kyotanabe campus, Doshisha University
	Subject:	Research discussion
95	Time and Date:	2009/1/12 13:00-17:00
	Place:	Concert hall, School of Human Science and Environment, University of Hyogo
	Subject:	Mobiligence seminar on "Ecological and Physiological Studies about Sociality of Insects"
96	Time and Date:	2009/1/13 9:30-18:00
	Place:	Concert hall, School of Human Science and Environment, University of Hyogo
	Subject:	C-group meeting
97	Time and Date:	2008/1/14 15:00-20:00
	Place:	Kagawa School of Phermeceutiacal Sciences, Tokushima Bunri University
	Subject:	Research discussion on collaborative research
98	Time and Date:	2009/1/16 13:30～18:00
	Place:	Kyotanabe campus, Doshisha University
	Subject:	Research discussion

99	Time and Date:	2009/1/20 16:00-20:00
	Place:	Faculty of Liberal Arts, Tohoku Gakuin University
	Subject:	Research discussion on self-assembly system
100	Time and Date:	2008/1/23 13:00-16:45
	Place:	Torigin Bunka Kaikan, Tottori, Japan
	Subject:	OS "Mobiligence" at 21st Symposium on Distributed Autonomous Systems
101	Time and Date:	2009/1/28 13:30～18:00
	Place:	Kyotanabe campus, Doshisha University
	Subject:	Research discussion
102	Time and Date:	2009/1/28 18:00-20:00
	Place:	University of Hyogo/Tokushima Bunri University (Video discussion)
	Subject:	Seimar and research discussion
103	Time and Date:	2009/2/03-04 10:00-17:00
	Place:	Hokkaido University
	Subject:	Mobiligence seminar on Butterflies
104	Time and Date:	2009/2/4
	Place:	Tokyo Institute of Technology
	Subject:	Review meeting on textbook publication
105	Time and Date:	2009/2/4 17:30-18:30
	Place:	The University of Tokyo, Komaba Campus
	Subject:	Seminar
106	Time and Date:	2009/2/7 13:00-15:00
	Place:	University of Hyogo/Tokushima Bunri University (Video discussion)
	Subject:	Seimar and research discussion
107	Time and Date:	2009/2/13-2/19 9:00-19:00
	Place:	Research Institute of Electronic Science, Hokkaido University
	Subject:	Invitation of foreign researcher and research discussion
108	Time and Date:	2009/2/13 13:30～18:00
	Place:	Kyotanabe campus, Doshisha University
	Subject:	Research discussion
109	Time and Date:	2009/2/13 17:00-19:00
	Place:	University of Hyogo/Tokushima Bunri University (Video discussion)
	Subject:	Seimar and research discussion
110	Time and Date:	2009/2/18 9:00-20:00
	Place:	National Institute for Physiological Science, JAPAN
	Subject:	10th research discussion and cooperative experiment
111	Time and Date:	2009/2/18
	Place:	Research Institute of Electronic Science, Hokkaido University
	Subject:	Invitation of foreign researcher and research discussion
112	Time and Date:	2008/2/19 10:30-13:30
	Place:	Ishiguro laboratory, Tohoku University
	Subject:	Research discussion on self-assembly system
113	Time and Date:	2009/3/2 13:40-3/4 12:00
	Place:	Hotel Matsushima Taikanso
	Subject:	4th Mobiligence Symposium
114	Time and Date:	2009/3/11 13:30-17:30
	Place:	Waseda University
	Subject:	6th collaborative seminar of SICE research group of "biological control system" and "mobiligence"